frontiers | Research Topics

Innate immunity and neurodegenerative diseases – triggers from self and non-self

Edited by
Kiran Bhaskar, Surojit Paul and Adam Bachstetter

Published in
Frontiers in Molecular Neuroscience

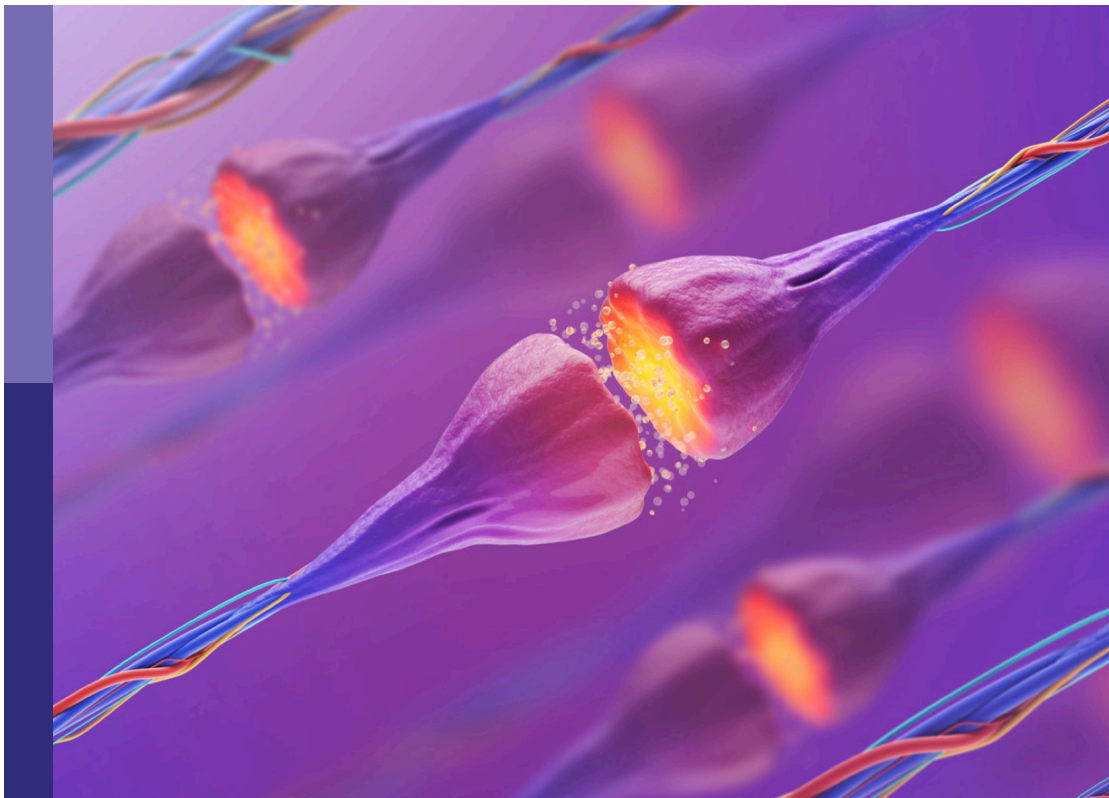

ISSN 1664-8714
ISBN 978-2-8325-2775-7
DOI 10.3389/978-2-8325-2775-7

About Frontiers

Frontiers is more than just an open access publisher of scholarly articles: it is a pioneering approach to the world of academia, radically improving the way scholarly research is managed. The grand vision of Frontiers is a world where all people have an equal opportunity to seek, share and generate knowledge. Frontiers provides immediate and permanent online open access to all its publications, but this alone is not enough to realize our grand goals.

Frontiers journal series

The Frontiers journal series is a multi-tier and interdisciplinary set of open-access, online journals, promising a paradigm shift from the current review, selection and dissemination processes in academic publishing. All Frontiers journals are driven by researchers for researchers; therefore, they constitute a service to the scholarly community. At the same time, the *Frontiers journal series* operates on a revolutionary invention, the tiered publishing system, initially addressing specific communities of scholars, and gradually climbing up to broader public understanding, thus serving the interests of the lay society, too.

Dedication to quality

Each Frontiers article is a landmark of the highest quality, thanks to genuinely collaborative interactions between authors and review editors, who include some of the world's best academicians. Research must be certified by peers before entering a stream of knowledge that may eventually reach the public - and shape society; therefore, Frontiers only applies the most rigorous and unbiased reviews. Frontiers revolutionizes research publishing by freely delivering the most outstanding research, evaluated with no bias from both the academic and social point of view. By applying the most advanced information technologies, Frontiers is catapulting scholarly publishing into a new generation.

What are Frontiers Research Topics?

Frontiers Research Topics are very popular trademarks of the *Frontiers journals series*: they are collections of at least ten articles, all centered on a particular subject. With their unique mix of varied contributions from Original Research to Review Articles, Frontiers Research Topics unify the most influential researchers, the latest key findings and historical advances in a hot research area.

Find out more on how to host your own Frontiers Research Topic or contribute to one as an author by contacting the Frontiers editorial office: frontiersin.org/about/contact

Innate immunity and neurodegenerative diseases – triggers from self and non-self

Topic editors

Kiran Bhaskar — University of New Mexico, United States
Surojit Paul — University of New Mexico, United States
Adam Bachstetter — University of Kentucky, United States

Citation

Bhaskar, K., Paul, S., Bachstetter, A., eds. (2023). *Innate immunity and neurodegenerative diseases – triggers from self and non-self*. Lausanne: Frontiers Media SA. doi: 10.3389/978-2-8325-2775-7

Table of contents

frontiers | Frontiers in Molecular Neuroscience

TYPE Editorial
PUBLISHED 07 June 2023
DOI 10.3389/fnmol.2023.1227896

OPEN ACCESS

EDITED AND REVIEWED BY
Detlev Boison,
Rutgers, The State University of New Jersey, United States

*CORRESPONDENCE
Kiran Bhaskar
✉ kbhaskar@salud.unm.edu

RECEIVED 23 May 2023
ACCEPTED 24 May 2023
PUBLISHED 07 June 2023

CITATION
Hulse J, Bachstetter A, Paul S and Bhaskar K (2023) Editorial: Innate immunity and neurodegenerative diseases – triggers from self and non-self. *Front. Mol. Neurosci.* 16:1227896. doi: 10.3389/fnmol.2023.1227896

Editorial: Innate immunity and neurodegenerative diseases – triggers from self and non-self

Jonathan Hulse[1], Adam Bachstetter[2], Surojit Paul[3] and Kiran Bhaskar[1,3]*

[1]Department of Molecular Genetics and Microbiology, University of New Mexico, Albuquerque, NM, United States, [2]Department of Neuroscience, Sanders-Brown Center on Aging, University of Kentucky, Lexington, KY, United States, [3]Department of Neurology, University of New Mexico, Albuquerque, NM, United States

KEYWORDS

neurodegenerative disease, innate immunity, neuroinflammation, neurological disease, blood-brain barrier disruption

Editorial on the Research Topic
Innate immunity and neurodegenerative diseases – triggers from self and non-self

While innate immune responses are typically short-lived, resolving upon clearance of the inciting pathogen or damage-associated molecular pattern, unresolved innate immune responses in the central nervous system (CNS) promote toxic inflammatory conditions that mediate neurodegenerative diseases. Understanding the cellular mechanisms that mediate the transition from neuroprotective immune responses to toxic chronic inflammatory responses in the CNS is a major area of ongoing research. Furthermore, neuroinflammatory signaling in neurological disease is a self-propagating process, worsening the disease state over time as additional immune cells are recruited and polarized toward inflammatory phenotypes, blood-brain barrier (BBB) function is disrupted, and neurodegeneration progresses. This Research Topic includes 14 peer-reviewed articles published in different Frontiers journals. Five are comprehensive reviews on the role of inflammatory alterations in neurological and neuropsychiatric diseases. The remaining nine articles are original research on innate immune activation in spinal cord injury, ischemia, and other neurological and neuroinflammatory conditions. This editorial summarizes these published reports and how they may advance our knowledge of innate immune activation driven by self- and non-self-triggers (Figure 1). Furthermore, we also attempt to identify gaps in knowledge so that future research can focus on these unexplored areas.

To start with, the nature of innate immune responses and the production of inflammatory cytokines is to recruit a more robust immune response from additional cells. This is highlighted by Sánchez et al. in their study on the effects of the innate immune molecules apoptosis-associated speck-like protein containing a CARD (ASC) and matrix metalloprotease 10 (MMP10) on inducing an inflammatory microglial phenotype and further upregulating inflammatory cytokine signaling. This study, and many others in this Research Topic demonstrate how innate inflammatory signaling molecules in the CNS contribute to pathological feed-forward processes in neurodegenerative diseases and identify many nodes for future therapeutic targeting.

Tissue injury in the CNS, such as mechanical trauma, environmental toxins, hypoxic insult, or hemorrhage, is a major instigator of innate immune processes, including toxic neuroinflammation, that worsens neurodegeneration. The role of innate immunity in response to each of these modes of CNS injury is explored in this Research Topic. Xue et al. demonstrate the role of innate immune processes in mechanical spinal cord injury for mediating allodynia, highlighting the role of the RIPK-NF-κB-NLRP3 pathway for triggering inflammatory signaling in response to cellular damage signals even at sites away from the primary site of mechanical tissue injury. Ramos et al. review the mechanism of ethanol toxicity-induced neurodegeneration, highlighting the role of ethanol reactive microglia (ERMs) and innate immune neuroinflammatory processes as a key mediators of ethanol-induced neurotoxicity with parallels to Alzheimer's disease (AD) and potential contributions to AD etiology. Wang et al. identify a novel cytokine, Tissue Non-specific Alkaline Phosphatase, that plays a substantial role in the NF-κB-mediated inflammatory processes in response to the hypoxic injury related to the development of Spastic Cerebral Palsy. Finally, Yang G. et al. provide a detailed review of the innate immune signaling mechanisms in microglia in response to intracerebral hemorrhage that confers protection, promote resolution and cleanup of toxic blood products, or drive neuroinflammation that worsens neurodegenerative processes after a hemorrhagic stroke.

The BBB is the primary interface between the CNS and the peripheral immune system. The neurovascular unit, which forms the BBB, comprises several cell types, including a monolayer of tightly sealed vascular endothelial cells with a basement membrane, surrounding pericytes, and a covering layer of astrocyte end feet. This selectively permeable barrier protects the CNS from circulating toxins, pathogens, and damaging immune cells and inflammatory mediators and was believed to maintain the CNS as an immune-privileged site. More recently, researchers have appreciated the importance of a coordinated cross-talk between the peripheral immune system and the CNS in health and disease.

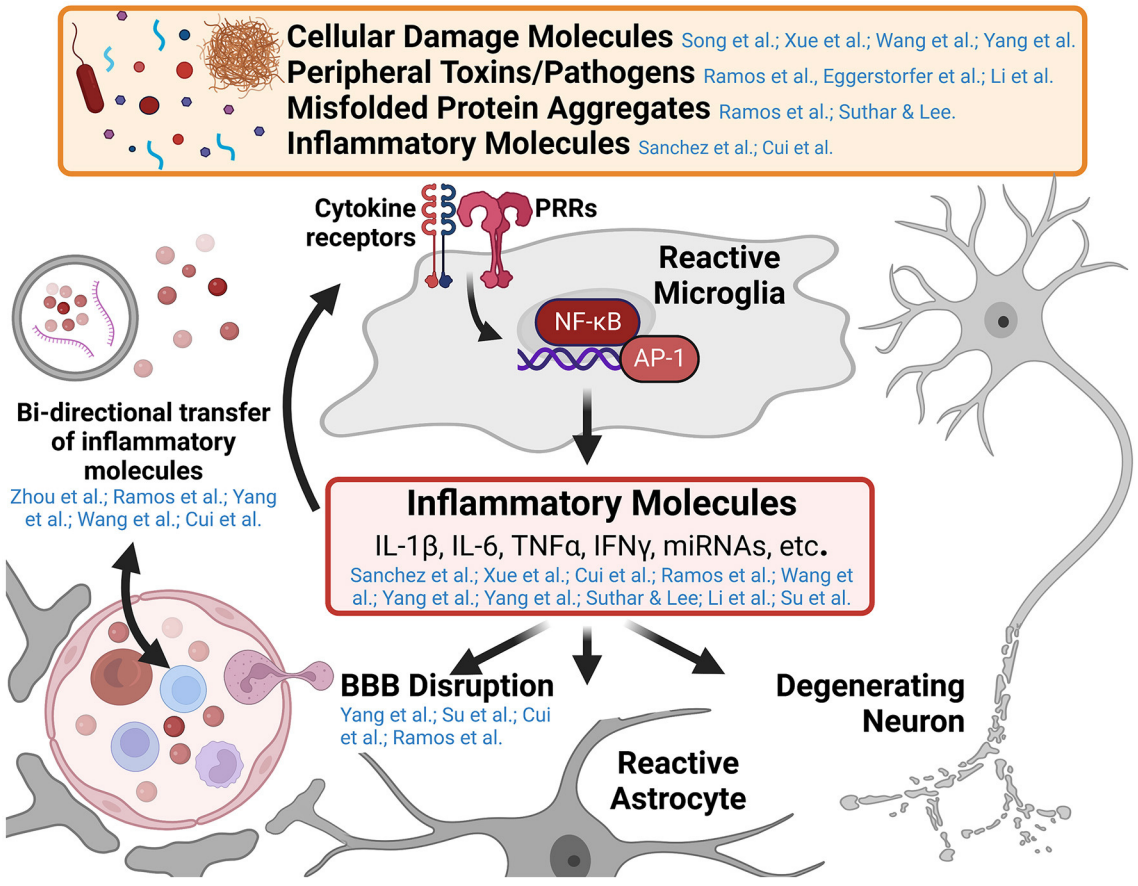

FIGURE 1
Graphical abstract of major concepts and themes explored in this Research Topic. Microglia are the primary innate immune cell of the central nervous system (CNS) and respond to numerous pathogen and damage associated molecular patterns in various neurological diseases. Pattern recognition receptors (PRRs) such as Toll-like receptors and Nod-like receptors, recognize the presence of a variety of inflammatory molecules such as cellular damage debris, peripheral toxins and pathogens (e.g., alcohol and bacterial lipopolysaccharide), and misfolded protein aggregates (e.g., amyloid-β, tau, and α-synuclein aggregates). These trigger signaling cascades resulting in the activation of inflammatory genes by transcription factors like nuclear factor kappa-B (NF-κB) and activating protein-1 (AP-1). The release of inflammatory molecules from reactive microglia effects numerous cell types within the CNS including enhancing inflammatory microglial responses, altering astrocyte function, promoting blood-brain barrier disruption and recruiting peripheral immune invasion, and promoting the degeneration and dysfunction of neurons (a central theme of this Research Topic). Several papers in this collection highlight the cross-talk between the innate immune system of the CNS and the peripheral immune system in the development of neuroinflammatory and neurodegenerative diseases. This figure was created using BioRender.com.

In this Research Topic, Su et al. assert that markers of increased BBB permeability and peripheral immune cell recruitment are signatures of normal aging across brain regions coinciding with increased molecular signatures of neuroinflammatory signaling. Disruption of the BBB with increased inflammatory infiltrate is a common pathological phenomenon in numerous disease states related to neurodegeneration. Interestingly, BBB disruption in response to inflammatory signaling is highlighted in Multiple Sclerosis (MS; Cui et al.), alcohol use disorder (AUD), and AD (Ramos et al.). In each of these disease states, the inflammatory cytokine interleukin-1β (IL-1β) is a key culprit in BBB dysfunction along with interleukin-6 (IL-6) and tumor necrosis factor-α (TNFα). These three critical inflammatory cytokine mediators of BBB disruption are explored in detail by Yang J. et al., highlighting the known molecular signaling mechanisms by which BBB integrity is disrupted, peripheral immune cells are recruited to the CNS, and inflammatory signaling in microglia and peripheral immune cells are upregulated.

Cross-talk between the peripheral immune system and the innate immune system of the CNS involving the transfer of inflammatory signaling molecules across the BBB is described throughout this Research Topic. Zhou et al. describe brain-derived small extracellular vesicles (sEVs) circulating in the plasma after acute cerebral ischemia containing brain-specific micro-ribonucleic acids (miRNAs). Temporal dynamics of these sEVs indicated that their presence in the peripheral circulation correlated with BBB disruption and could serve as a marker of disease staging and progression. Conversely, Ramos et al. describe the potential role of peripherally derived sEVs containing inflammatory cargo from liver in AUD that can modulate CNS neuroinflammatory processes. In many disease states, peripheral inflammation may accompany and contribute to neuroinflammation and vice versa. Increases in peripheral inflammatory molecules and immune cells in response to neuroinflammatory processes in the brain are discussed in the context of MS (Cui et al.), AUD and AD (Ramos et al.), Spastic Cerebral Palsy (Wang et al.), and intracerebral hemorrhage (Yang G. et al.). Eggerstorfer et al. and Li et al. both assert that peripheral inflammation, such as a peripheral bacterial lipopolysaccharide endotoxin (LPS) exposure in mice or during illness in humans, contributes to neuroinflammatory processes in the CNS that contribute to neuronal dysfunction.

Major Depressive Disorder (MDD) is the topic of two articles in this Research Topic (Eggerstorfer et al.; Li et al.). In a meta-analysis of eight separate imaging studies, Eggerstorfer et al. demonstrate that Translocator protein (TSPO), a marker of neuroinflammation, is elevated in several brain regions associated with disease symptoms in human patients assessed using positron emission tomography (PET). Li et al. dive into the mechanism of hypoxia-inducible factor 1 (HIF-1) and phosphoinositide 3 kinase (PI3K) signaling in response to LPS-induced peripheral inflammation for regulating depressive behaviors in rodent models. This study also demonstrated that repurposing of the FDA-approved HIF-1 stabilizing agent, FG-4592, could reduce depressive symptoms, neuroinflammation, and synaptic defects in rodents stimulated with LPS. These studies further support a new understanding of the role of neuroinflammation in mediating MDD, establishing a potential therapeutic target outside of monoamine neurotransmitter modulation that may yield improvements for many patients with MDD that are refractory to current pharmaceutical therapies.

While this editorial is not aimed to cover all 14 articles in this Research Topic, with some articles slightly outside the theme yet highly relevant to neuronal homeostasis, we express our gratitude to the many authors, reviewers, and editors around the world that contributed to this Research Topic to further our understanding of innate immunity in neurodegenerative diseases. We hope that readers will enjoy reading it.

Author contributions

JH reviewed the articles published on this Research Topic, drafted the manuscript, and created the figure. AB, SP, and KB read through published articles and edited the manuscript and figures. All authors contributed to the article and approved the submitted version.

Funding

This editorial was funded by the National Institute of Health: RF1NS083704.

Conflict of interest

The authors declare that the research was conducted in the absence of any commercial or financial relationships that could be construed as a potential conflict of interest.

Publisher's note

frontiers | Frontiers in Molecular Neuroscience

ORIGINAL RESEARCH
published: 19 April 2022
doi: 10.3389/fnmol.2022.861312

Receptor-Interacting Protein Kinase 3 Inhibition Relieves Mechanical Allodynia and Suppresses NLRP3 Inflammasome and NF-κB in a Rat Model of Spinal Cord Injury

Song Xue[1†], Zhen-xin Cao[2†], Jun-nan Wang[2], Qing-xiang Zhao[1], Jie Han[2], Wen-jie Yang[2] and Tao Sun[1,2]*

[1] Department of Pain Management, Shandong Provincial Hospital, Cheeloo College of Medicine, Shandong University, Jinan, China, [2] Departments of Pain Management, Shandong Provincial Hospital Affiliated to Shandong First Medical University, Jinan, China

Background: Neuroinflammation is critical in developing and maintaining neuropathic pain after spinal cord injury (SCI). The receptor-interacting protein kinase 3 (RIPK3) has been shown to promote inflammatory response by exerting its non-necroptotic functions. In this study, we explored the involvement of RIPK3 in neuropathic pain after SCI.

Methods: Thoracic (T10) SCI rat model was conducted, and the mechanical threshold in rats was measured. The expressions of RIPK3, nod-like receptor family pyrin domain-containing protein 3 (NLRP3), caspase-1, and nuclear factor-κB (NF-κB) were measured with western blotting analysis or quantitative real-time polymerase chain reaction (qRT-PCR). Double immunofluorescence staining was used to explore the colabeled NLRP3 with NeuN, glial fibrillary acidic protein (GFAP), and ionized calcium-binding adapter molecule 1 (IBA1). In addition, enzyme-linked immunosorbent assay (ELISA) was applied to analyze the levels of proinflammatory factors interleukin 1 beta (IL-1β), interleukin 18 (IL-18), and tumor necrosis factor alpha (TNF-α).

Results: The expression of RIPK3 was elevated from postoperative days 7–21, which was consistent with the development of mechanical allodynia. Intrathecal administration of RIPK3 inhibitor GSK872 could alleviate the mechanical allodynia in SCI rats and reduce the expression levels of RIPK3. The activation of NLRP3 inflammasome and NF-κB was attenuated by GSK872 treatment. Furthermore, immunofluorescence suggested that NLRP3 had colocalization with glial cells and neurons in the L4–L6 spinal dorsal horns. In addition, GSK872 treatment reduced the production of inflammatory cytokines.

Conclusion: Our findings indicated that RIPK3 was an important facilitated factor for SCI-induced mechanical allodynia. RIPK3 inhibition might relieve mechanical allodynia by inhibiting NLRP3 inflammasome, NF-κB, and the associated inflammation.

Keywords: neuropathic pain after spinal cord injury, receptor-interacting protein kinase 3, NLRP3 inflammasome, nuclear factor-kappa B (NF-κB), GSK872

OPEN ACCESS

Edited by:
Ildikó Rácz,
University Hospital Bonn, Germany

Reviewed by:
Xuhong Wei,
Sun Yat-sen University, China
Enrique Verdú,
University of Girona, Spain
Renjun Peng,
Central South University, China
Han-Rong Weng,
California Northstate University, United States
Sheu-Ran Choi,
Catholic Kwandong University, South Korea

****Correspondence:***
Tao Sun
suntaosdph@163.com

[†]These authors have contributed equally to this work and share first authorship

Specialty section:
This article was submitted to Pain Mechanisms and Modulators, a section of the journal Frontiers in Molecular Neuroscience

Received: *24 January 2022*
Accepted: *14 March 2022*
Published: *19 April 2022*

Citation:
Xue S, Cao Z-x, Wang J-n, Zhao Q-x, Han J, Yang W-j and Sun T (2022) Receptor-Interacting Protein Kinase 3 Inhibition Relieves Mechanical Allodynia and Suppresses NLRP3 Inflammasome and NF-κB in a Rat Model of Spinal Cord Injury. Front. Mol. Neurosci. 15:861312. doi: 10.3389/fnmol.2022.861312

INTRODUCTION

Neuropathic pain is a common complication after spinal cord injury (SCI) (Bryce et al., 2012; Sweis and Biller, 2017). The neuropathic pain after SCI is stubborn, severe, and protracted, which brings great pain and endless torture to the patients (Attal, 2021). The sense of helplessness and despair that pain brings to patients is even more harmful than the impact of dysfunction. Unfortunately, there is still a lack of effective treatment to control the progression of pain. Therefore, it is essential to explore the mechanisms of neuropathic pain after SCI to develop effective treatment programs or drugs.

The pathophysiological mechanism of neuropathic pain after SCI is complex. However, the previous research suggested that neuroinflammation in the remote spinal dorsal horn might play an especially critical role in the development course of neuropathic pain after SCI (Gwak and Hulsebosch, 2009). It was confirmed that activated glial cells and inflammatory factors in the remote spinal dorsal horns promoted the induction and maintenance of neuropathic pain after SCI by increasing neurons' excitability (Detloff et al., 2008; Sandhir et al., 2011; Gwak et al., 2012). However, the upstream kinases or signal pathways that promote neuroinflammation in remote spinal dorsal horns have not been well-studied.

Receptor-interacting protein kinase 3 (RIPK3) is a crucial threonine–serine protein kinase for necroptosis (Khan et al., 2014). Tumor necrosis factors, toll-like receptor agonists, oxidative stress, and virus infection could activate RIPK3 and trigger necroptosis (Kaczmarek et al., 2013). It is well-known that necroptosis is a highly inflammatory cell death that can trigger inflammatory responses due to the release of intracellular immunogenic contents. Interestingly, the recent studies demonstrate that activated RIPK3 may contribute to the inflammation by exerting its non-necroptotic functions, such as activating nuclear factor-κB (NF-κB) or nod-like receptor family pyrin domain-containing protein 3 (NLRP3) inflammasome (Moriwaki et al., 2014) (Moriwaki and Chan, 2017). Both NF-κB and NLRP3 inflammasome are the important pathways for promoting inflammatory. NF-κB is a transcriptional activator of inflammatory factor genes (Lawrence, 2009). NLRP3 inflammasome is a protein complex composed of NLRP3, the adaptor apoptosis-associated speck-like protein containing a CARD (ASC) and caspase-1 (Kelley et al., 2019). When stimulated by the endogenous and exogenous dangerous signals, the assembled NLRP3 inflammasome activates caspase-1, which converts the pro-IL-1β and pro-IL-18 into mature interleukin 1 beta (IL-1β) and interleukin 18 (IL-18) (Kelley et al., 2019).

The previous studies showed that RIPK3 might be involved in inflammatory bowel disease (Lee et al., 2020) and autoinflammatory disease (Speir and Lawlor, 2021). RIPK3 has also been studied in the rodent SCI model. A previous study showed that RIPK3 was highly expressed at the injured site for 21 days after SCI and localized in neurons, astrocytes, and oligodendrocytes (Kanno et al., 2015). Furthermore, the recent investigations have found that inhibiting RIPK3-mediated necroptosis helped to reduce neuroinflammation and the recovery of locomotion (Wang et al., 2019; Hongna et al., 2021). Nevertheless, a few studies investigated the expression of RIPK3 in the remote spinal cord after SCI, and whether RIPK3 inhibition could relieve neuropathic pain after SCI was also unclear.

To solve these problems, by establishing the thoracic SCI model, we studied the RIPK3 expression in the remote spinal dorsal horns and further explored its role in neuropathic pain after SCI. Furthermore, we examined the effect of RIPK3 inhibitor GSK872 on the expression of the NLRP3 inflammasome, NF-κB, and proinflammatory cytokines.

MATERIALS AND METHODS

Animals and Grouping

This experimental object was the male SD rats (6–7 weeks, 210–260 g) provided by the Shandong University Laboratory. All experimental rats were fed with a 12-h light/dark cycle at 25°C and had free access to rodent water and food. The Animal Care and Use Committee at Shandong University approved our experimental designs and operation procedures.

All rats were randomly divided into four groups ($n = 4$–7 per group for various analyses): sham group, SCI group, vehicle group, GSK872 group. In the sham group, only the vertebral lamina was removed without SCI; In the vehicle group, rats with SCI received an intrathecal injection of 10% dimethyl sulfoxide (DMSO) (Cell Signaling Technology, USA); In the GSK872 group, rats with SCI received an intrathecal injection of GSK872 (Med Chem Express, China). GSK872 was dissolved in DMSO.

SCI Model

Spinal cord injury model was made using modified Allen's method (Khan et al., 1999). Rats were anesthetized by intraperitoneal injection of 30 mg/kg of pentobarbital. The skin around the T10 segment in the back was disinfected and a longitudinal incision was made. The tendons and muscle tissue were separated to expose the T10 spinous processes and lamina, and then, the T10 lamina was removed, which exposes the corresponding spinal cord. A 10-g iron bar was used to cause SCI, vertically dropped from a height of 30 mm through a glass tube onto the exposed spinal cord. The hemostatic suture was performed using 3-0 silk thread, and antibiotics were then injected subcutaneously. Only the vertebral lamina was removed in the sham group without SCI. Rats were intramuscularly injected with 20×10^4 U/d penicillin for 5 days and received artificial micturition two times a day until the recovery of micturition function.

Intrathecal Injection and Drug Administration

The direct transcutaneous intrathecal injection was based on the method reported by Mestre et al. (1994). In brief, rats were anesthetized by inhaling enflurane, and then, the hip tubercle was touched to determine the L5 or L6. The 25-μl microinjection syringe (Shanghai Gaoge Industry and Trade Co., Ltd) was inserted into L5 or L6 intervertebral space vertically until the occurrence of tail-flick reflex, which indicated the tip of the

needle had reached the subarachnoid space. When the tail-flick reflex was observed, the needle insertion was stopped and injected 10 μl GSK872 (25 mmol/L) (Hou et al., 2018) or 10 μl of DMSO. Rats were injected with GSK872 or DMSO 30 min before the surgery, 1 day, and 2 days after the surgery.

Pain Behavior Assessment

A total of 50% paw withdrawal threshold (PWT) was used to assess the mechanical allodynia according to the previous reports (Chaplan et al., 1994). Observers were blinded to the experimental groups and recorded 50% PWT on the first day before surgery and on the 7th, 10th, 14th, 17th, and 21st days after the operation. Before each measurement, it was necessary to let the rats adapt to the watch box for at least 30 min until exploration activities disappeared.

A total of eight von Frey hairs (0.4, 0.6, 1, 2, 4, 6, 8, and 15.0 g, Stoelting, United States) were used to measure 50% PWT in rat hind paws according to the "Up-Down" method. The filament of 2 g was used first. Then, the intensity of the next filament was decreased when the animal reacted or increased when the animal did not respond. Withdrawal of claws, shaking or licking was considered a painful reaction. When the response change was observed for the first time, this procedure was continued for six stimuli. Fifty percentage PWT was calculated using the following formula: 50% PWT $= 10^{(Xf+\kappa\delta)}$ (Xf is the logarithm value of the last von Frey fiber, and K is the corresponding value of the sequence, $\delta = 0.224$). Bilateral rat hind paws were tested. Finally, the average of 50% PWT of bilateral hind paws was taken.

Tissue Sample Collection

To explore the protein and mRNA expression of RIPK3 at different time points after the operation, the rats in the SCI group were sacrificed by pentobarbital anesthesia (60 mg/kg, i.p) at postoperative days 7, 14, and 21 after conducting the pain behavior assessment. Rats in the sham group were euthanized on postoperative day 21. To study the effect of GSK872 on the expression of target molecules, all rats in each group (sham, SCI, vehicle, and GSK872 groups) were sacrificed at postoperative day 7. In double immunofluorescence staining, the rats were cardiac infused with 0.9% NaCl and 4% paraformaldehyde, and then, the L4–L6 spinal cord was separated from the rats and fixed with 4% paraformaldehyde. For other molecular detection, bilateral spinal dorsal horns (L4–L6) were collected, frozen in liquid nitrogen, and stored at −80°C until further analysis.

Western Blotting

Total proteins from tissues were extracted in RIPA lysis buffer (Solarbio, China), and a bicinchoninic acid (BCA) protein assay kit (Solarbio, China) was used for evaluating the protein concentration. The sample proteins were separated by sodium dodecyl sulfate–polyacrylamide gel electrophoresis and transferred onto polyvinylidene difluoride membranes. The membranes were blocked with 5% non-fat milk in TBST followed by incubating with primary antibody overnight. The primary antibodies were as follows: anti-RIPK3 (1:1,200; Novus Biologicals), anti-NLRP3 (1:400; Novus Biologicals), anti-caspase-1 (1:800; Novus Biologicals), anti- NF-κB/p65 (1:1,000; Cell Signaling Technology, CST), anti-β-actin (1:5,000; Proteintech Group, PTG), and anti-glyceraldehyde 3-phosphate dihydrogen (GAPDH) (1:5,000; Proteintech Group, PTG). After being washed with Tris Buffered Saline with Tween (TBST) , the membranes were incubated with goat anti-rabbit second antibody for 1.5 h. Finally, the enhanced chemiluminescence (ECL; Thermo Scientific) was used to visualize immunoblots, and the densities of the relative target proteins were measured using ImageJ. The GAPDH or β-actin was chosen as the internal reference control.

TABLE 1 | Sequences of primers.

Gene	Forward primer	Reverse primer
RIPK3	CTACTGCACCGGGACCTCAA	GTGGACAGGCCAAAGT CTGCTA
NLRP3	CTGAAGCATCTGCAACC	AACCAATGCGAGATCCTG ACAAC
caspase-1	ACTCGTACACGTCTTGCC CTCA	CTGGGCAGGCAGCAAA TTC
β-actin	GGAGATTACTGCCCTGGCT CCTA	GACTCATCGTACTCCTG CTTGCTG

ELISA

On the 7th postoperative, the bilateral spinal dorsal horns were ground to tissue homogenization and were centrifuged at 10,000 rpm at 4°C for 30 min. After the supernatant was collected, we used enzyme-linked immunosorbent assay (ELISA) kits (TNF-α: Westang, China; IL-1β: MultiSciences, China; IL-18: Westang, China) to detect the levels of TNF-α, IL-1β, and IL-18 according to the instructions of ELISA kits.

qRT-PCR

According to the instructions, total RNAs were extracted from the bilateral dorsal horns using RNAex Pro Reagent (AG21102, Accurate Biotechnology, Hunan, China). Complementary DNA (cDNA) was synthesized using Evo M-MLV RT Mix Kit (AG11728, Accurate Biotechnology, Hunan, China). Polymerase chain reaction (PCR) amplifications were conducted using SYBR® Green Premix Pro Taq HS qPCR kit (AG11701, Accurate Biotechnology, Hunan, China). Real-time fluorescent quantitative PCR was carried out using Light Cycler® 480 II (Roche, Switzerland). β-actin was served as the internal reference for normalization. The mRNA levels of RIPK3, NLRP3, and caspase-1 were calculated using the $2^{-\Delta\Delta CT}$ method. The primers for NLRP3, RIPK3, caspase-1, and β-actin are shown in **Table 1**.

Double Immunofluorescence Staining

On postoperative day 7, the L4–L6 spinal cord was harvested from rats ($n = 3$ for SCI group), embedded in paraffin, and cut into 20-μm-thick sections. These sections ($n = 3$ for each sample) were dewaxed, dehydrated by gradient alcohol, and repaired by antigen. Next, the sections were blocked with endogenous peroxidase and 10% donkey serum and then incubated with the following primary antibodies: NLRP3 (1:200; bs-6655R, Bioss),

GFAP (1:500; GB12096, Servicebio), IBA-1(1:500; GB12105, Servicebio), and NeuN (1:100; GB13138-1, Servicebio) overnight at 4°C. After the primary antibody incubation, the sections were incubated with the corresponding secondary antibodies conjugated with CY3 and FITC for 1 h in dark conditions at 37°C. Finally, the dorsal horns were observed and photographed under a fluorescence microscope (Olympus, Japan).

Statistical Analysis

SPSS 24.0 software (IBM, USA) was used to perform all the data analysis. All results were presented as mean ± SD. The Kolmogorov–Smirnov test was used to detect whether the data conformed to the normal distribution. For behavioral experiments, comparisons between multiple groups were conducted by repeated-measures analysis of variance and Tukey's *post-hoc* analysis. For quantitative real-time polymerase chain reaction (qRT-PCR), western blot, and ELISA, multiple-group comparisons were carried out by one-way ANOVA and Tukey's *post-hoc* analysis. When $p < 0.05$, we considered the difference between the two groups to be statistically significant.

RESULTS

Upregulation of RIPK3 Expression in the SCI Model

Mechanical allodynia was tested using 50% PWT (**Figure 1**). Compared with the rats in sham group, rats in the SCI group developed mechanical allodynia from 7 to 21 days after the surgery ($p < 0.05$), which indicated that the SCI model was established successfully.

Western blot analysis was carried out to detect the RIPK3 protein level at different time points postoperation (**Figure 2A**). Compared with the sham group, the protein expression of RIPK3 was significantly increased in SCI group from postoperative days 7–21 ($p < 0.05$). Meanwhile, similar results were verified using qRT-PCR ($p < 0.05$) (**Figure 2B**).

GSK872 Decreased RIPK3 Expression Level and Relieved Mechanical Allodynia Induced by SCI

To determine whether RIPK3 was involved in neuropathic pain after SCI, the effect of GSK872 on mechanical allodynia and the RIPK3 expression level were assessed. About 10 μl GSK872(25 mmol/L) was injected 30 min before the surgery, 1 day, and 2 days after the surgery. Western blot analysis was performed to evaluate RIPK3 expression level (**Figure 3A**). The protein expression of RIPK3 was upregulated in vehicle rats compared with those in the sham group ($p < 0.05$). The upregulation of RIPK3 was wholly reversed after GSK872 treatment ($p < 0.05$). In addition, the results from qRT-PCR were consistent with the western blot analysis ($p < 0.05$) (**Figure 3B**).

As shown in **Figure 1**, 50% PWT was significantly decreased in the vehicle group compared with the sham group ($p < 0.05$). After intrathecal injection of RIPK3 inhibitor GSK872, mechanical allodynia in rats who received SCI was relieved from 7 to 21 days postoperation ($p < 0.05$).

GSK872 Reduced the Production of Inflammatory Cytokines

To further investigate whether inhibition of RIPK3 could restrict neuroinflammation, ELISA was used to assess the levels of inflammatory cytokines (**Figures 4A–C**). The expressions of IL-1β ($p < 0.05$), IL-18 ($p < 0.05$), and TNF-α ($p < 0.05$) markedly ascended in the vehicle group compared with the sham group. The protein levels of TNF-α ($p < 0.05$), IL-1β ($p < 0.05$), and IL-18 ($p < 0.05$) were restricted in the GSK872 group compared with the vehicle group.

GSK872 Suppressed the Activation of NLRP3 Inflammasome in Glia and Neurons

To further explore the potential molecular mechanism of GSK872 in alleviating mechanical allodynia, the expression of NLRP3 inflammasome was investigated. The results from western blot showed that the protein levels of NLRP3 ($p < 0.05$) and caspase-1 ($p < 0.05$) were remarkably upregulated in the vehicle group compared with the sham group (**Figures 5A,B**). Rats treated with GSK872 exhibited lower protein levels of NLRP3 ($p < 0.05$) and caspase-1 ($p < 0.05$) compared with the rats in the vehicle group. We also found similar results by examining the mRNA expression of NLRP3 ($p < 0.05$) and caspase-1 ($p < 0.05$) (**Figures 5C,D**).

In addition, the cellular localization of NLRP3 in nerve cells of spinal dorsal horns was researched (**Figures 5E–P**). Double immunofluorescent staining revealed that NLRP3 was localized in the microglia, neurons, and astrocytes in the dorsal horn of SCI rats.

Effect of GSK872 on NF-κB p65

The western blot was conducted to evaluate the expression level of NF-κB p65 (**Figure 6**). Our data showed that NF-κB p65 was markedly upregulated in the vehicle group compared with the sham group ($p < 0.05$). Intrathecal delivery of GSK872 inhibited the protein level of NF-κB p65, as shown in the GSK872 group ($p < 0.05$).

DISCUSSION

The current work mainly explores whether RIPK3 is a potential target for alleviating neuropathic pain after SCI. We are the first to find an increased expression of RIPK3 in the lumbar spinal dorsal horns of rats with thoracic SCI. Significantly, RIPK3 inhibitor GSK872 inhibited the expression of RIPK3 and alleviated mechanical hyperalgesia. Furthermore, we showed that GSK872 treatment reduced the expression of NLRP3 inflammasome, NF-κB, and proinflammatory factors, which indicated that RIPK3 inhibition effectively relieved neuroinflammation in the lumbar spinal dorsal horns.

Thoracic spinal cord contusion in male rats is the most commonly used model for studying SCI pain because this model matches clinical characteristics quite well in terms of trauma type and gender (Kramer et al., 2017). Mechanical stimulation and thermal stimulation were used to evaluate the pain behavior of neuropathic pain models. However, heat response in SCI models

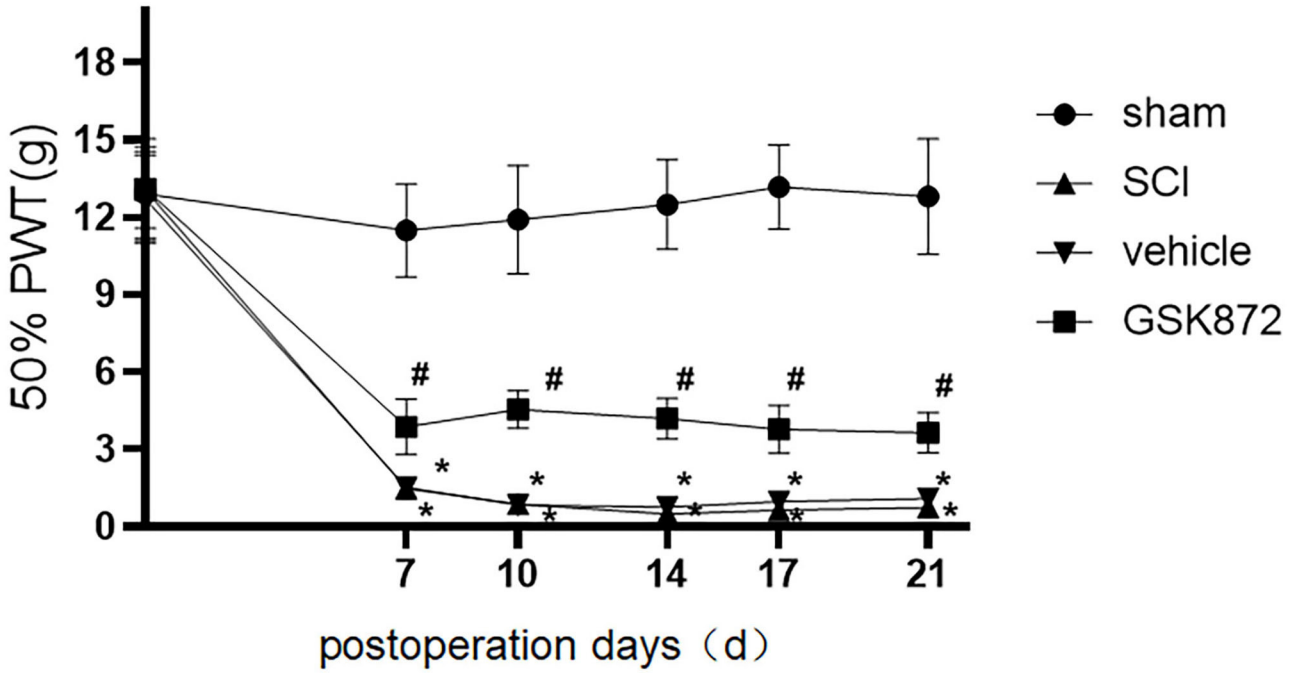

FIGURE 1 | Intrathecal administration of GSK872 (10 μl, 25 mmol/L) attenuated mechanical hypersensitivity induced by SCI ($n = 7$ for each group). All data were calculated as mean ± SD. $^{*}p < 0.05$ vs. the sham group; $^{\#}p < 0.05$ the vehicle group. Comparisons between multiple groups were conducted by repeated-measures analysis of variance and Turkey's *post-hoc* analysis SCI: spinal cord injury. 50% PWT, fifty percentage paw withdrawal threshold.

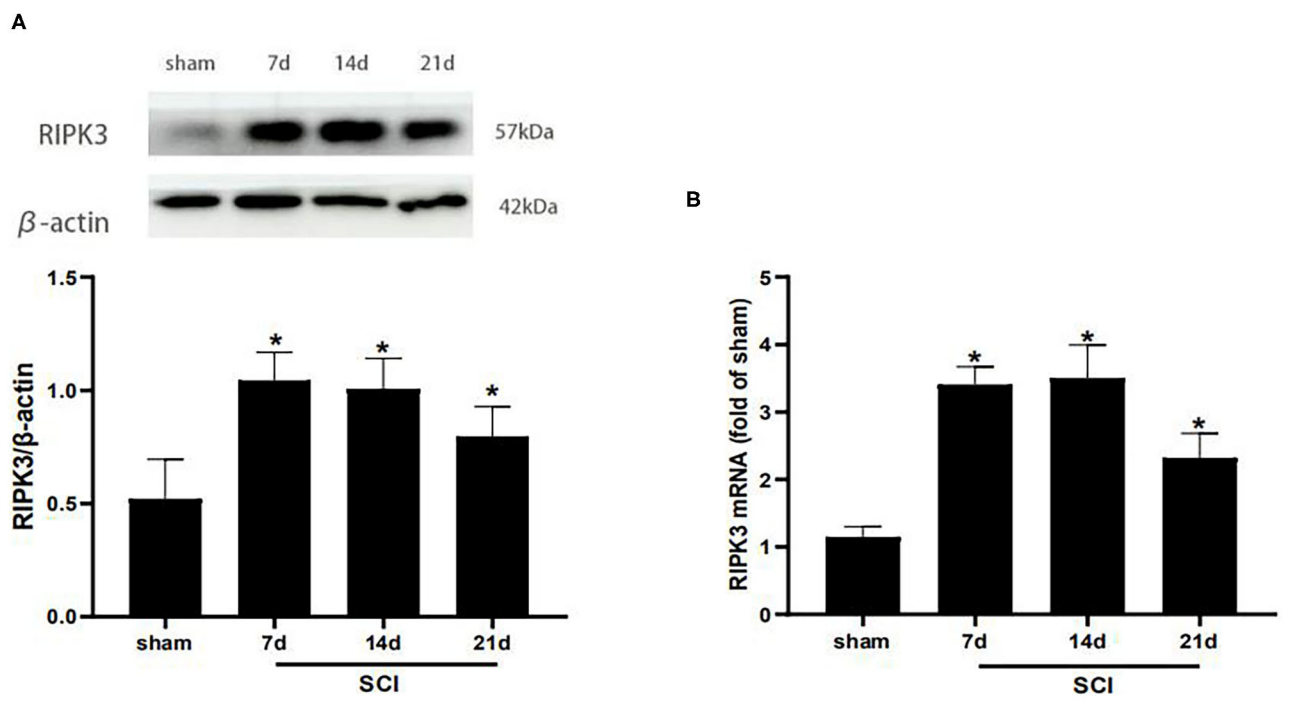

FIGURE 2 | RIPK3 was up-regulated in the dorsal horns after thoracic SCI. **(A)** The expression of RIPK3 in the SCI group was measured by western blot analysis on the 7th, 14th, 21th postoperative days ($n = 5$ for each group). **(B)** Quantitative analysis of the mRNA expression of RIPK3 in the sham group and SCI group on the 7th, 14th, 21th postoperative days ($n = 4$ for each group). All data were calculated as mean ± SD. $^{*}p < 0.05$, vs. the sham group. Comparisons between multiple groups were carried out by one-way ANOVA and Turkey's *post-hoc* analysis. RIPK3, receptor-interacting protein kinase 3.

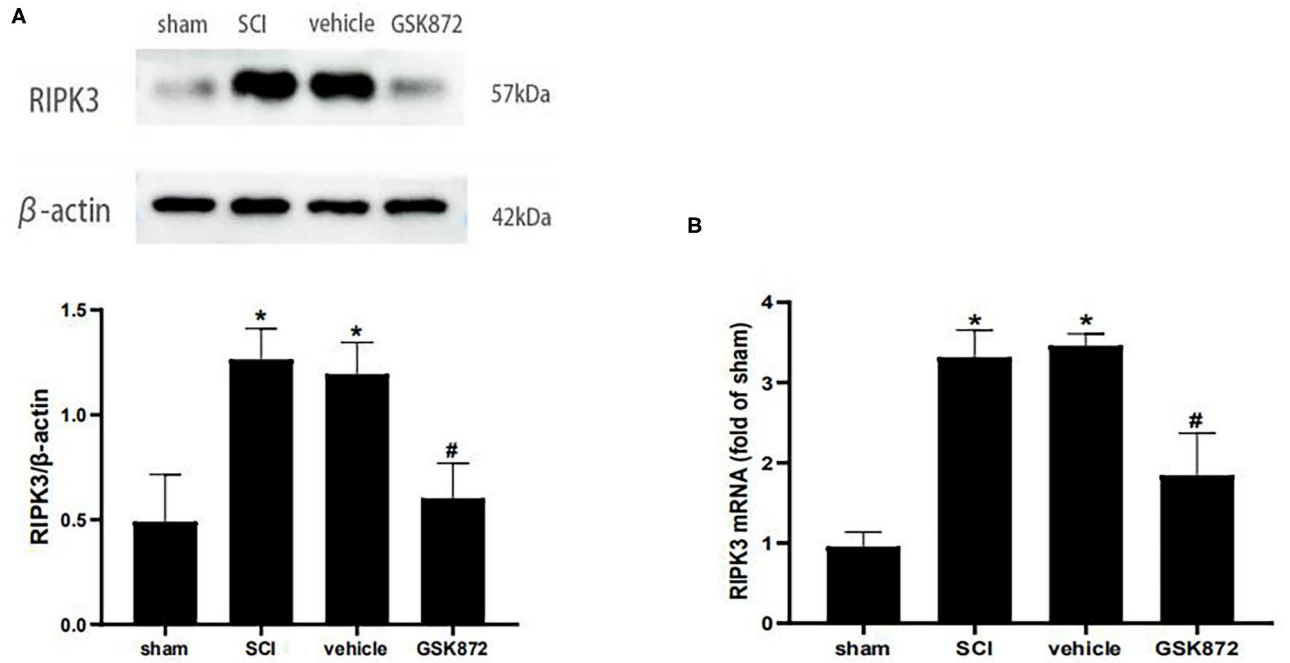

FIGURE 3 | GSK872 (10 μl, 25 mmol/L) reduced the expression levels of RIPK3 after SCI. **(A)** The expression of RIPK3 in different groups, including sham, SCI, vehicle and GSK872 group, was measured by western blot analysis ($n = 5$ for each group). **(B)** Quantitative analysis of the RIPK3 mRNA expressions in different groups including sham, SCI, vehicle and GSK872 group ($n = 4$ for each group). All data were calculated as mean ± SD. $^{*}p < 0.05$ vs. the sham group. $^{\#}p < 0.05$ vs. the vehicle group. Comparisons between multiple groups were carried out by one-way ANOVA and Turkey's *post-hoc* analysis.

could represent exaggerated spinal reflexes (Shiao and Lee-Kubli, 2018). It has been reported that patients with SCI have a low probability of thermal hyperalgesia (Finnerup et al., 2014). In addition, van Gorp et al. (2014) found that rats that received severe thoracic contusion did not show low thermal withdrawal latency. In this study, we studied mechanical hyperalgesia of male rats with SCI and found that rats that received thoracic spinal cord contusion showed lower PWT than rats in the sham group, which indicated that the SCI neuropathic pain model was established.

Recently, RIPK3 has been well-studied in the neuropathic pain model caused by peripheral nerve injury. For instance, investigators reported that RIPK3 was highly expressed in the spinal cord, dorsal root ganglia, and hippocampus of the chronic constriction injury (CCI) model (Pu et al., 2018). He et al. (2021) further found that RIPK3 played an important role in CCI-induced neuropathic pain, and inhibition of RIPK3 ameliorated neuropathic pain *via* suppressing JNK signaling. We were curious about the role of RIPK3 in neuropathic pain after SCI. Our results indicated that rats with thoracic SCI exhibited high expressions of RIPK3, accompanied by remarkable mechanical allodynia from 7 to 21 days postoperation. It has been reported that the death signal ligand TNF-α activated RIPK3 and caused necrosis by binding to the death receptor (Vandenabeele et al., 2010). Our results showed that SCI led to increased TNF-α expression. Therefore, we speculated that TNF-α might be an important factor for causing the increased expression of RIPK3. Our observation also showed that RIPK3-specific inhibitor GSK872 could relieve allodynia and downregulate the expression of RIPK3 in the dorsal horns. Taken together, it suggested that the high expression of RIPK3 in the spinal dorsal horn could contribute to the development of neuropathic pain after SCI.

Inflammatory factors are the essential components of neuroinflammation. It has been demonstrated that proinflammatory factor is involved in neuropathic pain progress. Proinflammatory factors, such as IL-18, IL-1β, and TNF-α, are the famous pain mediators (Kawasaki et al., 2008; Pilat et al., 2016). The previous studies have indicated that increased expressions of TNF-α and IL-1β were associated with pain-related behaviors in a rat model of SCI (Detloff et al., 2008). The proinflammatory factor could induce SCI rat hyperalgesia *via* upregulating the excitability of superficial dorsal horn neurons (Fakhri et al., 2021). RIPK3 is a key kinase in regulating inflammatory factors (Yabal et al., 2014). Moreover, one research found that RIPK3 inhibition relieved neuropathic pain induced by peripheral nerve injury by decreasing proinflammatory factors' expressions (Fang et al., 2021). In this study, the proinflammatory factors were significantly increased in the spinal dorsal horns in SCI rats, accompanied by a reduction in mechanical pain threshold. Meanwhile, after intrathecal administration of GSK872, the proinflammatory factors such as IL-18, IL-1β, and TNF-α levels descended, with the relief of mechanical pain in rats with SCI. These results suggested that

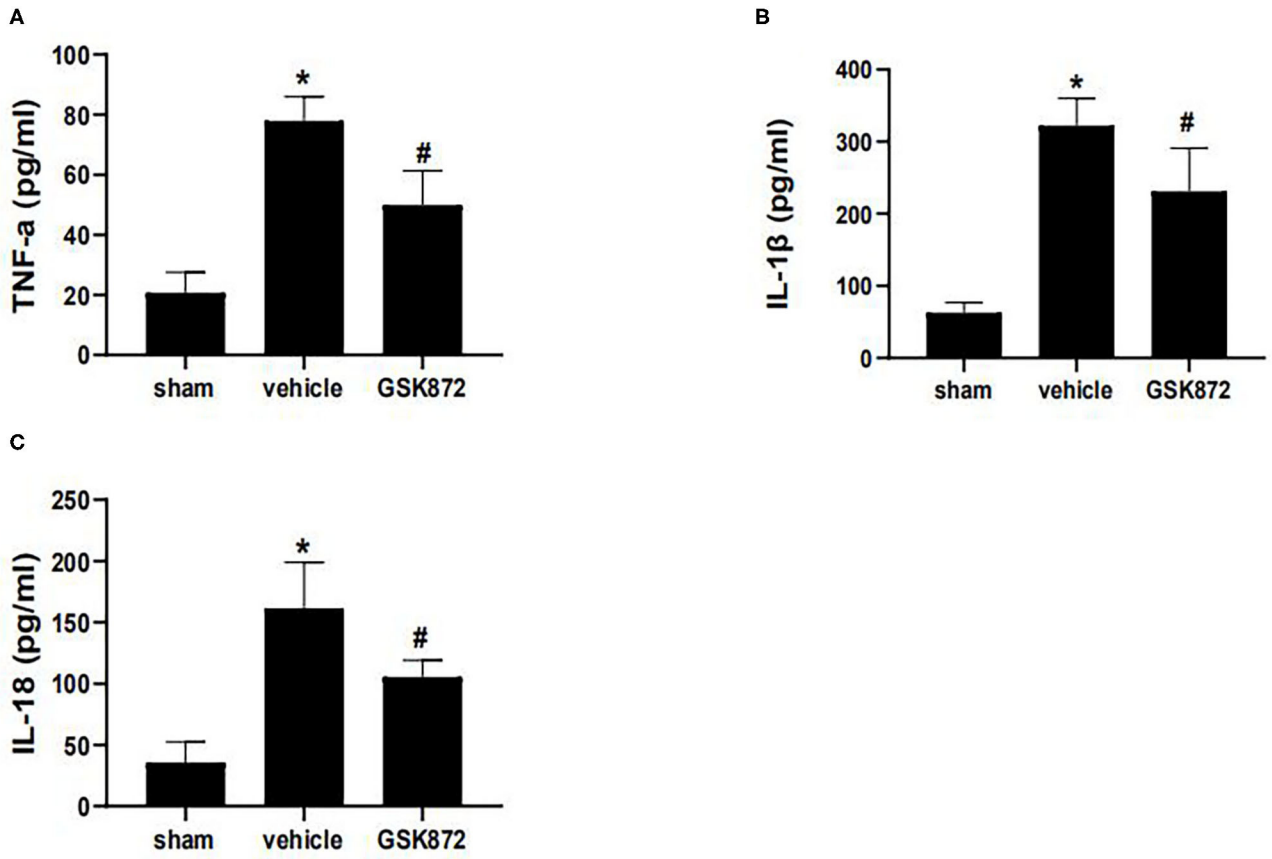

FIGURE 4 | Intrathecal injection of GSK872 (10 μl, 25 mmol/L) inhibited neuroinflammation in the lumbar spinal dorsal horns ($n = 4$ for each group). **(A–C)** The levels of TNF-α, IL-1β, and IL-18 in different groups, including sham, vehicle and GSK872 group, were investigated by ELISA. The protein level of TNF-α, IL-1β, and IL-18 were reduced after GSK872 treatment. All data were calculated as mean ± SD. $^{*}p < 0.05$ vs. the sham group. $^{\#}p < 0.05$ vs. the vehicle group. Comparisons between multiple groups were carried out by one-way ANOVA and Turkey's *post-hoc* analysis. IL, interleukin; TNF-α, tumor necrosis factor-α.

RIPK3 inhibition ameliorated mechanical allodynia possibly by reducing proinflammatory factors' expressions. However, the production mechanism of proinflammatory factors is not completely clear. We were curious about the upstream pathway of inflammatory factors.

Nod-like receptor family pyrin domain-containing protein 3 is a widely studied inflammasome that plays a vital role in the inflammatory immune response (Kelley et al., 2019). It has been reported that the dysregulation of the inflammasome is involved in a series of inflammatory diseases *via* promoting the secretion of inflammatory factors (Mangan et al., 2018). In the SCI model, we found that the expressions of NLRP3, caspase-1, and proinflammatory factors were increased in remote dorsal horns. In addition, immunofluorescence showed that NLRP3 was expressed in glial cells and neurons. These results indicated that NLRP3 inflammasome could contribute to the release of proinflammatory factors in glial and neurons, which also explain the potential mechanism of inflammatory factors released by the neurons and glial in remote dorsal horns. The growing evidence shows that NLRP3 may be a molecular target for neuropathic pain relief (Chen et al., 2021). For example, adenosine deaminase acting on RNA 3 (ADAR3) promoted pain relief in CCI rats by targeting NLRP3 inflammasome (Li et al., 2021). Our previous study also confirmed that caspase-1 inhibitor VX-765 could attenuate radicular pain *via* inhibiting NLRP3 inflammasome activation (Wang et al., 2020). In addition, D-β-hydroxybutyrate, one of the NLRP3 inflammasome inhibitors, effectively alleviated mechanical and thermal pain hypersensitivities in rats with SCI (Qian et al., 2017). The previous studies have confirmed that RIPK3 is a critical kinase regulating the NLRP3 inflammasome (Yabal et al., 2014). RIPK3 could contribute to NLRP3 inflammasome activation by producing ROS or potassium efflux (Moriwaki and Chan, 2017). The recent studies further suggested that RIPK3 is involved in the development of renal fibrosis (Shi et al., 2020), brain injury after subarachnoid hemorrhage (Zhou et al., 2017), and lung injury (Chen et al., 2018) by activating the NLRP3 inflammasome. Therefore, we speculated that the analgesic effect of RIPK3 inhibition might be connected with the reduction of proinflammatory cytokines by inhibiting the NLRP3 inflammasome. Intrathecal injection of GSK872 could significantly decrease the expressions of NLRP3, caspase-1, IL-1β,

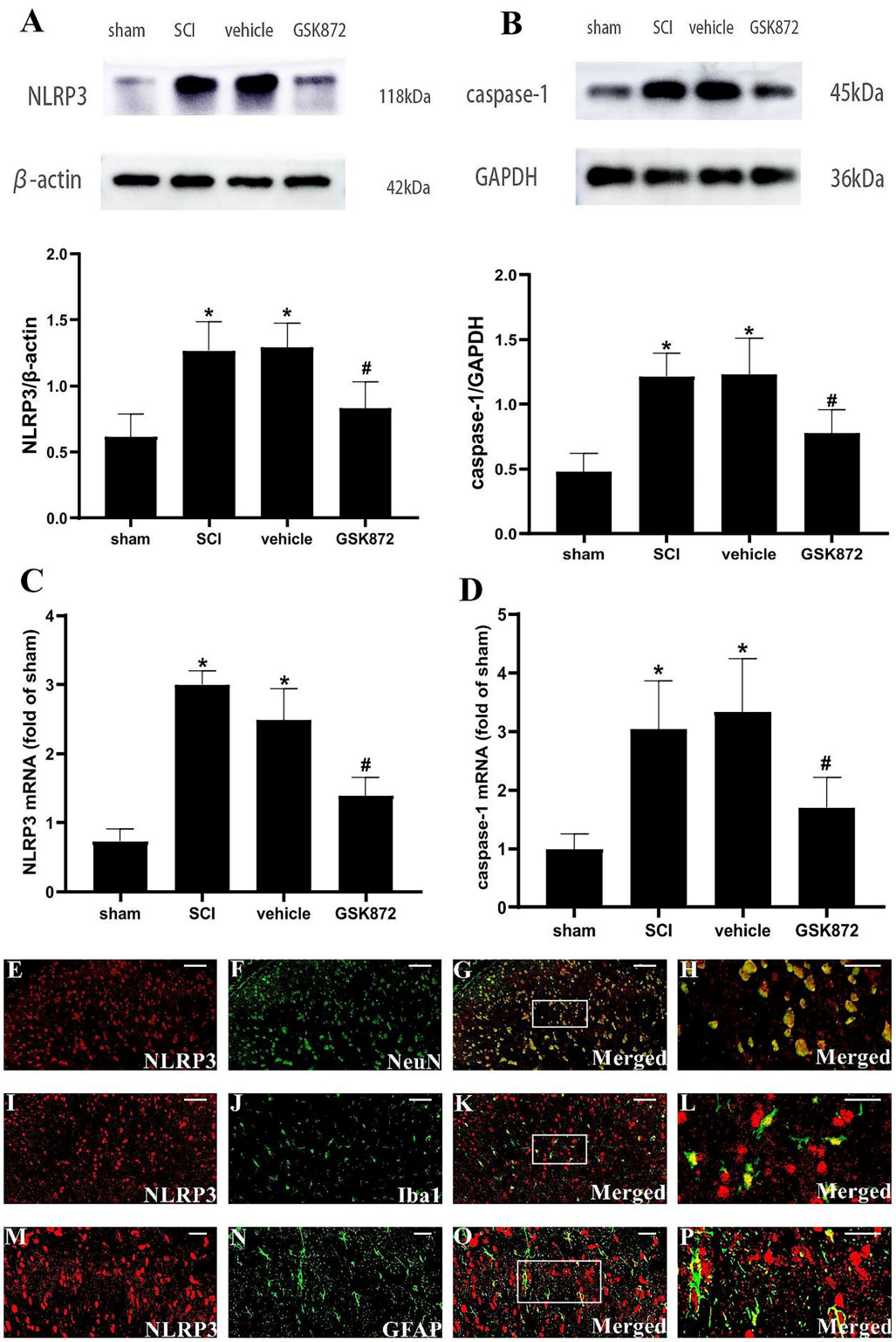

FIGURE 5 | GSK872 (10 μl, 25 mmol/L) suppressed the activation of NLRP3 inflammasome in glia and neurons. **(A,B)** The expressions of NLRP3 and caspase-1 in different groups, including sham, SCI, vehicle and GSK872 group, were measured by western blot analysis ($n = 5$ for each group). **(C,D)** Quantitative analysis of NLRP3 and caspase-1 mRNA expressions in different groups including sham, SCI, vehicle and GSK872 group ($n = 4$ for each group). **(E–P)** Immunofluorescence staining of NLRP3 (red) with NeuN, a neuronal marker (green); GFAP, an astrocyte marker (green); and Iba-1, a microglial marker (green) in the lumbar dorsal horns of SCI rats. Scale bar, 50 μm **(E–G,I–K)**. Scale bar, 25 μm **(M–O)**. Scale bar, 20 μm **(H,L,P)**. All data were calculated as mean ± SD. $^{*}p < 0.05$ vs. the sham group. $^{\#}p < 0.05$ vs. the vehicle group. Comparisons between multiple groups were carried out by one-way ANOVA and Turkey's *post-hoc* analysis.

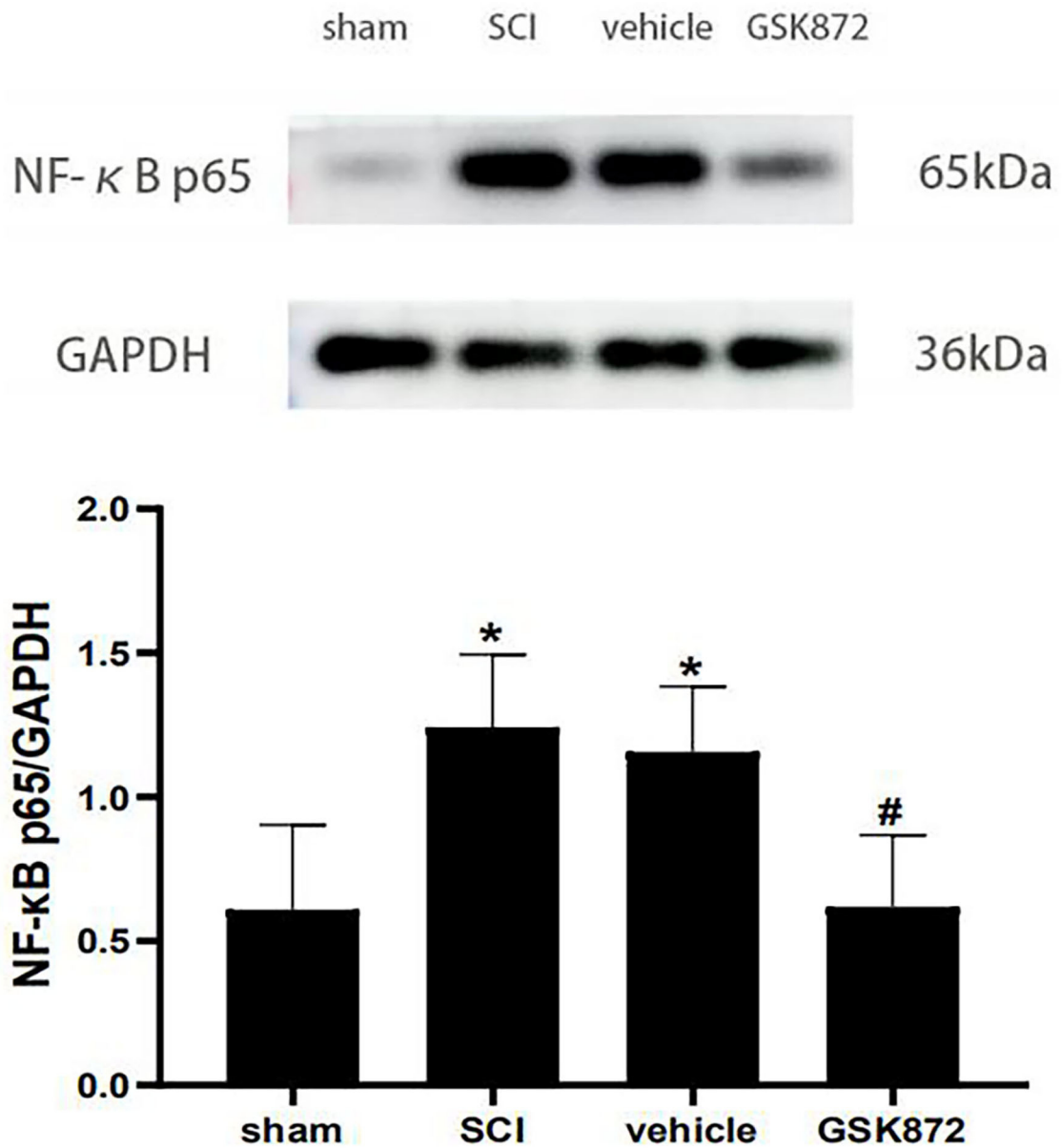

FIGURE 6 | Intrathecal injection of GSK872 (10 μl, 25 mmol/L) inhibited NF-κB p65 in the lumbar spinal dorsal horns ($n = 5$ for each group). The expression of NF-κB p65 in different groups, including sham, SCI, vehicle and GSK872 group, was measured by western blot analysis. All data were calculated as mean ± SD. $^{*}p < 0.05$ vs. the sham group. $^{\#}p < 0.05$ vs. the vehicle group. Comparisons between multiple groups were carried out by one-way ANOVA and Turkey's *post-hoc* analysis. NF-κB, nuclear factor-kappa B.

and IL-18 in the dorsal horns of model rats. These results further confirmed our conjecture.

The NF-κB p65, the main component of NF-κB pathways, is important in inflammatory and immune processes (Liu et al., 2017). When stimulated by external signals, NF-κB p65 separates from IκB and enters the nucleus to promote the transcription and expression of inflammatory genes related to pain (Mitchell and Carmody, 2018). NF-κB p65 has been shown to act as a contributor to neuropathic pain (Chu et al., 2020; Zhao et al., 2021). It has been reported that NF-κB inhibitor PDTC had a significant analgesic effect on CCI rats (Li et al., 2017). L-arginine, one of the NF-κB inhibitor, also relieved thermal pain hypersensitivity induced by SCI (Meng et al., 2017). An early investigation demonstrated that over-expression of RIPK3 could activate NF-κB signal (Kasof et al., 2000). The recent study further showed that RIPK3 inhibition could ameliorate osteoclastogenesis by regulating the NF-κB signaling pathway (Liang et al., 2020). Our experiments suggested that

the expression of NF-κB p65 was significantly increased after SCI. Intrathecal injection of GSK872 could inhibit NF-κB p65 protein expression in SCI rat models. These results preliminarily indicated that anti-inflammatory and analgesic effects of RIPK3 inhibition are also related to the regulation of NF-κB pathways.

The previous studies mainly discussed the role of RIPK3-mediated necroptosis in secondary SCI, but few studies further explored the effects of regulating RIPK3 on neuroinflammation and pain. Sugaya et al. (2019) found that RIPK3 modulation prevented necroptosis of various nerve cells at the lesion site and favored neuroprotection. Dabrafenib treatment, one of the RIPK3 inhibitors, also promoted the recovery of motor function and sensory function after SCI. In this study, we studied the effects of RIPK3 modulation on pain and neuroinflammation. Our results suggested that the RIPK3 inhibition may mediate an anti-nociceptive effect by alleviating dorsal horn neuroinflammation. This study further emphasized the role of RIPK3 inhibition, which can not only alleviate necroptosis in the injured spinal cord and favor neuroprotection, but also reduce neuroinflammation and neuropathic pain after SCI.

Our study has some limitations, which need to be solved in the future research. This study preliminarily proved that RIPK3 inhibition could relieve mechanical allodynia of SCI rats. We did not further explore the effect of GSK872 dose change on mechanical allodynia. In this study, it was also not clear whether the inhibition of RIPK3 contributes to alleviating the neuroinflammation at the injured spinal cord and promoting the recovery of motor function.

CONCLUSION

Our findings indicated that over-expressed RIPK3 developed mechanical allodynia in the SCI rat model. RIPK3 inhibition relieved mechanical allodynia possibly by suppressing NLRP3 inflammasome, NF-κB, and proinflammatory cytokines. Therefore, RIPK3 may be a potential target for treating neuropathic pain after SCI.

DATA AVAILABILITY STATEMENT

The original contributions presented in the study are included in the article/supplementary materials, further inquiries can be directed to the corresponding author.

ETHICS STATEMENT

The animal study was reviewed and approved by Ethical Committee of the Shandong University.

AUTHOR CONTRIBUTIONS

SX and Z-xC carried out the major part of the study for making SCI model, detecting molecular indicators, the statistical analyses, and writing the manuscript. J-nW helped to conduct behavioral tests. Q-xZ performed the part of the western blot study. JH was in charge of part of the ELISA study. W-jY conducted the part of qRT-PCR. TS designed the study and revised the manuscript. All authors read and approved the final manuscript.

FUNDING

This article was supported by the grants from the National Natural Science Foundation of China (grant no. 81772443 and 81972145) and Natural Science Foundation of Shandong Province (grant no. ZR2020MH283).

REFERENCES

Attal, N. (2021). Spinal cord injury pain. *Rev. Neurol.* 177, 606–612. doi: 10.1016/j.neurol.2020.07.003

Bryce, T. N., Biering-Sørensen, F., Finnerup, N. B., Cardenas, D. D., Defrin, R., Lundeberg, T., et al. (2012). International spinal cord injury pain classification: part I. Background and description. *Spinal Cord* 50, 413–417. doi: 10.1038/sc.2011.156

Chaplan, S. R., Bach, F. W., Pogrel, J. W., Chung, J. M., and Yaksh, T. L. (1994). Quantitative assessment of tactile allodynia in the rat paw. *J. Neurosci. Methods* 53, 55–63. doi: 10.1016/0165-0270(94)90144-9

Chen, J., Wang, S., Fu, R., Zhou, M., Zhang, T., Pan, W., et al. (2018). RIP3 dependent NLRP3 inflammasome activation is implicated in acute lung injury in mice. *J. Transl. Med.* 16, 233. doi: 10.1186/s12967-018-1606-4

Chen, R., Yin, C., Fang, J., and Liu, B. (2021). The NLRP3 inflammasome: an emerging therapeutic target for chronic pain. *J. Neuroinflamm.* 18, 84. doi: 10.1186/s12974-021-02131-0

Chu, L. W., Cheng, K. I., Chen, J. Y., Cheng, Y. C., Chang, Y. C., Yeh, J. L., et al. (2020). Loganin prevents chronic constriction injury-provoked neuropathic pain by reducing TNF-α/IL-1β-mediated NF-κB activation and Schwann cell demyelination. *Phytomedicine* 67, 153166. doi: 10.1016/j.phymed.2019.153166

Detloff, M. R., Fisher, L. C., McGaughy, V., Longbrake, E. E., Popovich, P. G., and Basso, D. M. (2008). Remote activation of microglia and pro-inflammatory cytokines predict the onset and severity of below-level neuropathic pain after spinal cord injury in rats. *Exp. Neurol.* 212, 337–347. doi: 10.1016/j.expneurol.2008.04.009

Fakhri, S., Abbaszadeh, F., and Jorjani, M. (2021). On the therapeutic targets and pharmacological treatments for pain relief following spinal cord injury: a mechanistic review. *Biomed. Pharmacother.* 139, 111563. doi: 10.1016/j.biopha.2021.111563

Fang, P., Sun, G., and Wang, J. (2021). RIPK3-mediated necroptosis increases neuropathic pain via microglia activation: necrostatin-1 has therapeutic potential. *FEBS Open Bio* 11, 2858–2865. doi: 10.1002/2211-5463.13258

Finnerup, N. B., Norrbrink, C., Trok, K., Piehl, F., Johannesen, I. L., Sørensen, J. C., et al. (2014). Phenotypes and predictors of pain following traumatic spinal cord injury: a prospective study. *J. Pain*15, 40–48. doi: 10.1016/j.jpain.2013.09.008

Gwak, Y. S., and Hulsebosch, C. E. (2009). Remote astrocytic and microglial activation modulates neuronal hyperexcitability and below-level neuropathic pain after spinal injury in rat. *Neuroscience* 161, 895–903. doi: 10.1016/j.neuroscience.2009.03.055

Gwak, Y. S., Kang, J., Unabia, G. C., and Hulsebosch, C. E. (2012). Spatial and temporal activation of spinal glial cells: role of gliopathy in central neuropathic pain following spinal cord injury in rats. *Exp. Neurol.* 234, 362–372. doi: 10.1016/j.expneurol.2011.10.010

He, N., Qu, Y. J., Li, D. Y., and Yue, S. W. (2021). RIP3 Inhibition ameliorates chronic constriction injury-induced neuropathic pain by suppressing JNK signaling. *Aging* 13, 24417–24431. doi: 10.18632/aging.203691

Hongna, Y., Hongzhao, T., Quan, L., Delin, F., Guijun, L., Xiaolin, L., et al. (2021). Jia-Ji Electro-acupuncture improves locomotor function with spinal cord injury by regulation of autophagy flux and inhibition of necroptosis. *Front. Neurosci.* 14, 616864. doi: 10.3389/fnins.2020.616864

Hou, W., Zhou, Y., Li, C., Zhu, M., Huang, D., Luo, L., et al. (2018). Expression of receptor-interacting protein kinase 3 in an animal model of neuropathic pain. *Chin. J. Oncol. Prev. Treat.* 10, 105–109. doi: 10.3969/j.issn.1674-5671.2018.02.07

Kaczmarek, A., Vandenabeele, P., and Krysko, D. V. (2013). Necroptosis: the release of damage-associated molecular patterns and its physiological relevance. *Immunity* 38, 209–223. doi: 10.1016/j.immuni.2013.02.003

Kanno, H., Ozawa, H., Tateda, S., Yahata, K., and Itoi, E. (2015). Upregulation of the receptor-interacting protein 3 expression and involvement in neural tissue damage after spinal cord injury in mice. *BMC Neurosci.* 16, 62. doi: 10.1186/s12868-015-0204-0

Kasof, G. M., Prosser, J. C., Liu, D., Lorenzi, M. V., and Gomes, B. C. (2000). The RIP-like kinase, RIP3, induces apoptosis and NF-kappaB nuclear translocation and localizes to mitochondria. *FEBS Lett.* 473, 285–291. doi: 10.1016/S0014-5793(00)01473-3

Kawasaki, Y., Zhang, L., Cheng, J. K., and Ji, R. R. (2008). Cytokine mechanisms of central sensitization: distinct and overlapping role of interleukin-1beta, interleukin-6, and tumor necrosis factor-alpha in regulating synaptic and neuronal activity in the superficial spinal cord. *J. Neurosci.* 28:5189–5194. doi: 10.1523/JNEUROSCI.3338-07.2008

Kelley, N., Jeltema, D., Duan, Y., and He, Y. (2019). The NLRP3 inflammasome: an overview of mechanisms of activation and regulation. *Int. J. Mol. Sci.* 20, 3328. doi: 10.3390/ijms20133328

Khan, N., Lawlor, K. E., Murphy, J. M., and Vince, J. E. (2014). More to life than death: molecular determinants of necroptotic and non-necroptotic RIP3 kinase signaling. *Curr. Opin. Immunol.* 26:76–89. doi: 10.1016/j.coi.2013.10.017

Khan, T., Havey, R. M., Sayers, S. T., Patwardhan, A., and King, W. W. (1999). Animal models of spinal cord contusion injuries. *Lab. Anim. Sci.* 49, 161–172.

Kramer, J. L., Minhas, N. K., Jutzeler, C. R., Erskine, E. L., Liu, L. J., and Ramer, M. S. (2017). Neuropathic pain following traumatic spinal cord injury: models, measurement, and mechanisms. *J. Neurosci. Res.* 95, 1295–1306. doi: 10.1002/jnr.23881

Lawrence, T. (2009). The nuclear factor NF-kappaB pathway in inflammation. *Cold Spring Harb. Perspect. Biol.* 1, a001651. doi: 10.1101/cshperspect.a001651

Lee, S. H., Kwon, J. Y., Moon, J., Choi, J., Jhun, J., Jung, K., et al. (2020). Inhibition of RIPK3 pathway attenuates intestinal inflammation and cell death of inflammatory bowel disease and suppresses necroptosis in peripheral mononuclear cells of ulcerative colitis patients. *Immune Netw.* 20, e16. doi: 10.4110/in.2020.20.e16

Li, J., Zhao, P. P., Hao, T., Wang, D., Wang, Y., Zhu, Y. Z., et al. (2017). Urotensin II inhibitor eases neuropathic pain by suppressing the JNK/NF-κB pathway. *J. Endocrinol.* 232, 165–174. doi: 10.1530/JOE-16-0255

Li, Z., Zhu, J., and Wang, Y. (2021). ADAR3 alleviated inflammation and pyroptosis of neuropathic pain by targeting NLRP3 in chronic constriction injury mice. Gene, 805, 145909. doi: 10.1016/j.gene.2021.145909

Liang, S., Nian, Z., and Shi, K. (2020). Inhibition of RIPK1/RIPK3 ameliorates osteoclastogenesis through regulating NLRP3-dependent NF-κB and MAPKs signaling pathways. *Biochem. Biophys. Res. Commun.* 526, 1028–1035. doi: 10.1016/j.bbrc.2020.03.177

Liu, T., Zhang, L., Joo, D., and Sun, S. C. (2017). NF-κB signaling in inflammation. *Signal Transduct. Target Ther.* 2, 17023. doi: 10.1038/sigtrans.2017.23

Mangan, M. S. J., Olhava, E. J., Roush, W. R., Seidel, H. M., Glick, G. D., and Latz, E. (2018). Targeting the NLRP3 inflammasome in inflammatory diseases. *Nat. Rev. Drug Discov.* 17, 588–606. doi: 10.1038/nrd.2018.97

Meng, F. X., Hou, J. M., and Sun, T. S. (2017). *In vivo* evaluation of microglia activation by intracranial iron overload in central pain after spinal cord injury. *J. Orthop. Surg. Res.* 12, 75. doi: 10.1186/s13018-017-0578-z

Mestre, C., Pélissier, T., Fialip, J., Wilcox, G., and Eschalier, A. (1994). A method to perform direct transcutaneous intrathecal injection in rats. *J. Pharmacol. Toxicol. Methods* 32, 197–200. doi: 10.1016/1056-8719(94)90087-6

Mitchell, J. P., and Carmody, R. J. (2018). NF-κB and the transcriptional control of inflammation. *Int. Rev. Cell Mol. Biol.* 335, 41–84. doi: 10.1016/bs.ircmb.2017.07.007

Moriwaki, K., Balaji, S., McQuade, T., Malhotra, N., Kang, J., and Chan, F. K. (2014). The necroptosis adaptor RIPK3 promotes injury-induced cytokine expression and tissue repair. *Immunity* 41, 567–578. doi: 10.1016/j.immuni.2014.09.016

Moriwaki, K., and Chan, F. K. (2017). The inflammatory signal adaptor RIPK3: functions beyond necroptosis. *Int. Rev. Cell Mol. Biol.* 328, 253–275. doi: 10.1016/bs.ircmb.2016.08.007

Pilat, D., Piotrowska, A., Rojewska, E., Jurga, A., Slusarczyk, J., and Makuch, W., et al. (2016). Blockade of IL-18 signaling diminished neuropathic pain and enhanced the efficacy of morphine and buprenorphine. *Mol. Cell. Neurosci.* 71, 114–124. doi: 10.1016/j.mcn.2015.12.013

Pu, S., Li, S., Xu, Y., Wu, J., Lv, Y., and Du, D. (2018). Role of receptor-interacting protein 1/receptor-interacting protein 3 in inflammation and necrosis following chronic constriction injury of the sciatic nerve. *Neuroreport* 29, 1373–1378. doi: 10.1097/WNR.0000000000001120

Qian, J., Zhu, W., Lu, M., Ni, B., and Yang, J. (2017). D-β-hydroxybutyrate promotes functional recovery and relieves pain hypersensitivity in mice with spinal cord injury. *Br. J. Pharmacol.* 174, 1961–1971. doi: 10.1111/bph.13788

Sandhir, R., Gregory, E., He, Y. Y., and Berman, N. E. (2011). Upregulation of inflammatory mediators in a model of chronic pain after spinal cord injury. *Neurochem. Res.* 36, 856–862. doi: 10.1007/s11064-011-0414-5

Shi, Y., Huang, C., Zhao, Y., Cao, Q., Yi, H., Chen, X., et al. (2020). RIPK3 blockade attenuates tubulointerstitial fibrosis in a mouse model of diabetic nephropathy. *Sci. Rep.* 10, 10458. doi: 10.1038/s41598-020-67054-x

Shiao, R., and Lee-Kubli, C. A. (2018). Neuropathic pain after spinal cord injury: challenges and research perspectives. *Neurotherapeutics* 15, 635–653. doi: 10.1007/s13311-018-0633-4

Speir, M., and Lawlor, K. E. (2021). RIP-roaring inflammation: RIPK1 and RIPK3 driven NLRP3 inflammasome activation and autoinflammatory disease. *Semin. Cell Dev. Biol.* 109:114–124. doi: 10.1016/j.semcdb.2020.07.011

Sugaya, T., Kanno, H., Matsuda, M., Handa, K., Tateda, S., Murakami, T, et al. (2019). B-RAF^{V600E} inhibitor dabrafenib attenuates RIPK3-mediated necroptosis and promotes functional recovery after spinal cord injury. *Cells.* 8, 1582. doi: 10.3390/cells8121582

Sweis, R., and Biller, J. (2017). Systemic complications of spinal cord injury. *Curr. Neurol. Neurosci. Rep.* 17, 8. doi: 10.1007/s11910-017-0715-4

van Gorp, S., Deumens, R., Leerink, M., Nguyen, S., Joosten, E. A., and Marsala, M. (2014). Translation of the rat thoracic contusion model; part 1-supraspinally versus spinally mediated pain-like responses and spasticity. *Spinal Cord* 52, 524–528. doi: 10.1038/sc.2014.72

Vandenabeele, P., Declercq, W., Van Herreweghe, F., and Vanden Berghe, T. (2010). The role of the kinases RIP1 and RIP3 in TNF-induced necrosis. *Sci. Signal.* 3, re4. doi: 10.1126/scisignal.3115re4

Wang, Y., Jiao, J., Zhang, S., Zheng, C., and Wu, M. (2019). RIP3 inhibition protects locomotion function through ameliorating mitochondrial antioxidative capacity after spinal cord injury. *Biomed. Pharmacother.* 116, 109019. doi: 10.1016/j.biopha.2019.109019

Wang, Y. H., Li, Y., Wang, J. N., Zhao, Q. X., Wen, S., Wang, S. C., et al. (2020). A novel mechanism of specialized proresolving lipid mediators mitigating radicular pain: the negative interaction with NLRP3 inflammasome. *Neurochem. Res.* 45, 1860–1869. doi: 10.1007/s11064-020-03050-x

Yabal, M., Müller, N., Adler, H., Knies, N., Groß, C. J., Damgaard, R. B., et al. (2014). XIAP restricts TNF- and RIP3-dependent cell death and inflammasome activation. *Cell Rep.* 7, 1796–1808. doi: 10.1016/j.celrep.2014.05.008

Zhao, L., Tao, X., and Song, T. (2021). Astaxanthin alleviates neuropathic pain by inhibiting the MAPKs and NF-κB pathways. *Eur. J. Pharmacol.* 912, 174575. doi: 10.1016/j.ejphar.2021.174575

Zhou, K., Shi, L., Wang, Z., Zhou, J., Manaenko, A., Reis, C., et al. (2017). RIP1-RIP3-DRP1 pathway regulates NLRP3 inflammasome activation following subarachnoid hemorrhage. *Exp. Neurol.* 295, 116–124. doi: 10.1016/j.expneurol.2017.06.003

Conflict of Interest: The authors declare that the research was conducted in the absence of any commercial or financial relationships that could be construed as a potential conflict of interest.

Publisher's Note: All claims expressed in this article are solely those of the authors and do not necessarily represent those of their affiliated organizations, or those of the publisher, the editors and the reviewers. Any product that may be evaluated in this article, or claim that may be made by its manufacturer, is not guaranteed or endorsed by the publisher.

frontiers | Frontiers in Molecular Neuroscience

ORIGINAL RESEARCH
published: 27 April 2022
doi: 10.3389/fnmol.2022.874903

Acute Cerebral Ischemia Increases a Set of Brain-Specific miRNAs in Serum Small Extracellular Vesicles

Xin Zhou[1,2†], Chenxue Xu[3†], Dachong Chao[1], Zixin Chen[1], Shuyuan Li[1], Miaomiao Shi[3], Yuqiang Pei[3], Yujuan Dai[3], Juling Ji[4], Yuhua Ji[1,5] and Qiuhong Ji[3]**

[1] College of Life Science and Technology, Institute of Immunology, Jinan University, Guangzhou, China, [2] The First Affiliated Hospital, Jinan University, Guangzhou, China, [3] Department of Neurology, Affiliated Hospital of Nantong University, Nantong, China, [4] Department of Pathology, Medical School of Nantong University, Nantong, China, [5] Key Laboratory of Neuroregeneration of Jiangsu and Ministry of Education, Nantong University, Nantong, China

Small extracellular vesicles (sEVs) miRNAs are promising diagnosis and prognosis biomarkers for ischemic stroke (IS). This study aimed to determine the impact of IS on the serum sEVs miRNA profile of IS patients and a transient middle cerebral artery occlusion (tMCAO) mouse model. Small RNAseq was used to define the serum sEVs miRNA profile in IS patients and healthy controls (HC), and tMCAO mice and sham controls. Among the 1,444 and 1,373 miRNAs identified in human and mouse serum sEVs, the expression of 424 and 37 miRNAs was significantly altered in the IS patients and tMCAO mice, respectively ($|\text{Log}_2\text{FC}| \geq 1$, $p < 0.01$). Notably, five of the top 25 upregulated miRNAs in IS patients were brain-specific or enriched, including hsa-miR-9-3p, hsa-miR-124-3p, hsa-miR-143-3p, hsa-miR-98-5p, and hsa-miR-93-5p. Upregulation of these four miRNAs was further validated by qPCR. Nine of the 20 upregulated miRNAs in tMCAO mice were also brain-specific or enriched miRNAs. Temporal analysis indicated that the dynamics of mmu-miR-9-5p, mmu-miR-124-3p, mmu-miR-129-5p, and mmu-miR-433-3p were closely correlated with the evolution of ischemic brain injury, as their expression increased at 0.5 days after the onset of ischemia, peaked at day 1 or 3, and returned to normal levels at day 7 and 14. Notably, with the exceptions of mmu-miR-128-3p, the expression of the other eight miRNAs in the mouse serum sEVs was unaffected in the lipopolysaccharide (LPS)-induced neuroinflammation model. Together, in this study, we provided a comprehensive view of the influences of IS on the serum sEVs miRNA profile of IS patients and tMCAO mice and demonstrated the increment of a set of brain-specific miRNAs in serum sEVs after acute cerebral ischemia, which could be promising candidates directly reflecting the ischemic brain injury.

Keywords: ischemic stroke, serum sEVs, miRNAs, RNA-Seq, tMCAO

OPEN ACCESS

Edited by:
Juan Pablo de Rivero Vaccari, University of Miami, United States

Reviewed by:
Krishna Prahlad Maremanda, Texas A&M University, United States
Leda Torres, National Institute of Pediatrics, Mexico

***Correspondence:**
Qiuhong Ji
jiqiuhong@ntu.edu.cn
Yuhua Ji
tjyh@jnu.edu.cn

† These authors have contributed equally to this work

Specialty section:
This article was submitted to Brain Disease Mechanisms, a section of the journal Frontiers in Molecular Neuroscience

Received: *13 February 2022*
Accepted: *05 April 2022*
Published: *27 April 2022*

Citation:
Zhou X, Xu C, Chao D, Chen Z, Li S, Shi M, Pei Y, Dai Y, Ji J, Ji Y and Ji Q (2022) Acute Cerebral Ischemia Increases a Set of Brain-Specific miRNAs in Serum Small Extracellular Vesicles. Front. Mol. Neurosci. 15:874903. doi: 10.3389/fnmol.2022.874903

Abbreviations: sEVs, small extracellular vesicles; IS, ischemic stroke; tMCAO, transient middle cerebral artery occlusion; CT, Computed Tomography; MRI, Magnetic Resonance Imaging; HCs, healthy controls; HDL, high-density lipoprotein; LDL, low-density lipoprotein; n/a, not available; RBC, red blood cell; TIA, transient ischemic attack; WBC, white blood cell; TTC, 2,3,5-triphenyltetrazolium chloride; LPS, lipopolysaccharide; PBS, phosphate-buffered saline; NTA, nanoparticle-tracking analysis; TEM, transmission electron microscopy; qRT-PCR, quantitative reverse transcriptase real-time polymerase chain reaction; nt, nucleotides; FU, fluorescence intensity; BBB, blood-brain barrier; CNS, central nervous system; SDS-PAGE, sodium dodecyl sulfate polyacrylamide gel electrophoresis.

INTRODUCTION

Stroke is a leading cause of death and adult disability worldwide. Approximately 80% are ischemic stroke (IS) (Mortality and Causes of Death, 2016). Although CT (Computed Tomography) and MRI (Magnetic Resonance Imaging) are widely implemented in stroke diagnosis, biomarkers that could facilitate the IS diagnosis, prognosis prediction, and therapeutic evaluation are valuable for improving the clinical treatment of IS patients (Saenger and Christenson, 2010; Karakas and Zeller, 2017).

MiRNAs are a class of endogenous 22 nucleotides non-coding RNAs (Bartel, 2004). In addition to post-transcriptional regulation of gene expression by mediating targeted hydrolysis and translation inhibition, they are detectable in various biological fluids (Weber et al., 2010). Because of their stability and relative tissue specificity, circulating miRNAs are attractive candidates for biomarker research (Creemers et al., 2012; He et al., 2015). Small extracellular vesicles (sEVs), including exosomes, are nanoscale vesicles released by almost all cell types. sEVs are the dominant form of circulating RNA (Johnstone et al., 1989; Théry et al., 2002). Several groups, including us, have recently reported some serum exosomal miRNA candidates for IS diagnosis, including miR-9 and miR-124 (Ji et al., 2016), miR-223 (Chen et al., 2017), miR-422a and miR-125b-2-3p (Li D.B. et al., 2017), miR-21-5p and miR-30a-5p (Wang et al., 2018), and miR-17 family members (Van Kralingen et al., 2019). Serum sEVs contain hundreds of miRNAs (Li X. et al., 2017; Zhao et al., 2020). However, the effects of cerebral ischemia on miRNAs profile of serum sEVs is still unclear.

In this study, using an unbiased small RNAseq, we comprehensively examined the impact of acute cerebral ischemia on the profile of serum sEVs miRNAs in IS patients and a tMCAO mouse model. Besides the profound effects of cerebral ischemia on the serum sEVs miRNA profile, we noticed that the level of a set of brain-specific or enriched miRNAs significantly increased in both IS patients and tMCAO mouse models. Further animal experiments indicated that the temporal expression of these brain-specific miRNAs was closely correlated with the evolution of cerebral ischemia injury. It is worth noting that most of these altered brain-specific miRNAs were unaffected by the LPS-induced neuroinflammation.

MATERIALS AND METHODS

Subject Demographics and Clinical Characteristics

Ischemic stroke patients were recruited from those admitted to the Department of Neurology of the Affiliated Hospital of Nantong University between September 2016 and August 2018. Ischemic stroke was confirmed by either MRI or CT imaging. In addition, experienced neurologists determined the neurological deficits by using the NIHSS. We excluded patients with intracranial hemorrhage and infarction with unknown causes and those with malignant tumors or neurological and psychiatric diseases for all individuals involved in this study. Venous blood samples were collected on admission before any treatment. The average time of enrollment blood draw was 18.5 h. Non-stroke healthy controls (HCs) were recruited from those who underwent an annual medical examination. The demographics and clinical characteristics of the 40 IS patients and 33 HCs are provided in **Table 1**.

Transient Middle Cerebral Artery Occlusion Model

Male wild-type C57BL/6 mice (8–9 weeks) were purchased from Guangdong medical laboratory animal center and used in all experiments within 1 week of arrival. Anesthesia was induced with 4% isoflurane and maintained on 2% isoflurane in the air. Transient cerebral ischemia was conducted by occlusion of the left middle cerebral artery with a monofilament suture (602356, Doccol Corp., Redlands, CA, United States) for 60 min. Rectal body temperature was maintained at 37 ± 0.5°C during surgery. Sham-operated mice were subjected to all surgical procedures except suture advancement. One day after ischemia, the animals were euthanized with an overdose of isoflurane, and the left ventricular puncture drew blood.

2,3,5-Triphenyltetrazolium Chloride Staining and Measurement of Infarct Volume

For TTC staining, the brain was sectioned coronally at 1-mm thickness. The slices were immersed in 1% 2,3,5-triphenyltetrazolium chloride (TTC, Sigma Aldrich, St. Louis,

TABLE 1 | Baseline characteristics of study participants.

Parameter	HCs	IS (11–72 h)	*p* values*
Age and gender			
Total, *n*	33	40	
Male, *n* (%)	18 (55)	18 (45)	0.417
Age (y), mean (SD)	63.67 (8.9)	68.1 (11.9)	0.0813
Stroke risk factors, *n* (%)			
Hypertension	17 (51.5)	22 (55)	0.733
Diabetes mellitus	5 (15.2)	8 (20)	0.590
Hyerlipidaemia	6 (18.2)	9 (22.5)	0.594
Smoker	4 (12.1)	5 (12.5)	0.497
History of stroke/TIA	2 (6)	6 (15)	0.058
Laboratory parameters, mean ± SD			
Glucose, mmol/L	6.57 ± 1.73	7.14 ± 2.08	0.2133
Platelets, 10^9/L	210.9 ± 41.06	191.6 ± 55.7	0.1027
Triglycerides, mmol/L	1.19 ± 0.60	1.22 ± 0.88	0.8683
Total cholesterol, mmol/L	4.66 ± 0.82	4.35 ± 0.99	0.1551
HDL, mmol/L	1.33 ± 0.27	1.24 ± 0.37	0.2482
LDL, mmol/L	2.68 ± 0.54	2.46 ± 0.73	0.1553
WBC count, 10^9/L	5.85 ± 0.96	6.7 ± 2.69	0.0889
RBC count, 10^{12}/L	4.71 ± 0.43	4.52 ± 0.47	0.0784
NIHSS score			<0.01
Mean (25th–75th percentile)	0 (0)	10 (6.75-14)	
Infarct volume			
Mean (25th–75th percentile), mL	n/a	12.70 (3.04-25.87)	<0.01

**For Continuous variables, a Wilcoxon test was used to assess differences, while for categorical variables, a Fisher's exact test was used.*
HDL, high-density lipoprotein; LDL, low-density lipoprotein; n/a, not available, RBC, red blood cell; TIA, transient ischemic attack; WBC, white blood cell.

MO, United States) in saline for 30 min at 37°C and then fixed with 4% paraformaldehyde. Infarction volume was measured on six coronal sections using ImageJ.[1] The indirect infarct area, in which the intact area of the ipsilateral hemisphere was subtracted from the area of the contralateral hemisphere, was calculated. The ischemic volume was presented as the percentage of infarct volume of the contralateral hemisphere.

Lipopolysaccharide Challenge

Adult male C57BL/6 mice were randomized to receive intraperitoneal injections of either 1 mg/kg lipopolysaccharide (LPS) (*Escherichia coli* 0556:B5, Sigma Aldrich, St. Louis, MO, United States) or phosphate-buffered saline (PBS). The animals were euthanized at 8 h post-challenge with an overdose of isoflurane, and the left ventricular puncture drew blood.

Serum Preparation

Blood from both humans and mice was allowed to clot at room temperature for 30 min and stored at 4°C for 2 h. After centrifugation at 1,600 *g* for 10 min, serum was transferred to a new tube. Samples with visible hemolysis (reddish) were discarded at this step. Next, clear serum was centrifugated at 20,000 *g* for another 10 min at 4°C to remove cell debris and apoptotic bodies. Then, the supernatant was aliquoted and stored at −80° until analysis.

Serum Small Extracellular Vesicles Isolation

Before sEVs isolation, stored serum was thawed on ice and centrifuged at 21,000 *g* for 15 min at 4°C, and the supernatant was transferred to a new tube. According to the recommended protocol, 63 μL ExoQuick Solution (System Biosciences Inc., Mountain View, CA, United States) was added to every 250 μL serum and incubated at 4°C for 40 min after a brief up and down. After that, the ExoQuick/serum mixture was centrifuged at 1,500 *g* for 30 min, and the supernatant was removed by aspiration. Another 5 min centrifugation was performed to remove the residue liquid. Finally, the sEVs-containing pellet was resuspended in PBS.

Nanoparticle-Tracking Analysis

Size distribution and concentration of the isolated particles were measured by a Nanosight LM20 (NanoSight, Amesbury, United Kingdom), equipped with a 640-nm laser, and the software used for capturing and analyzing the data was Version 2.3 Build 0034. The instrument was routinely calibrated by 100 nm polystyrene latex standards and particle-free PBS. Before analysis, the isolated sEVs were homogenized. The measurement time was 60 s, and the Frames Per Second was 25. Three measurements were performed for each sample.

Transmission Electron Microscopy

Transmission electron microscopy (TEM) analysis on isolated particles was performed as described by Thery et al. (2006). Briefly, the pellets dissolved in PBS were mixed with an equal volume of 4% paraformaldehyde and were transferred onto Formvar/carbon-coated nickel grids. After staining with 4% w/v Uranyl Acetate, the morphology and size of sEVs were observed by a TEM (JEM-2100, JEOL, Tokyo, Japan).

SDS-PAGE and Western Blotting

Total proteins from dissolved pellets were extracted by RIPA lysis buffer (Pierce, Rockford, IL, United States). Protein concentrations were determined using a BCA protein assay kit (Pierce, Rockford, IL, United States). Proteins separated on 12% sodium dodecyl sulfate-polyacrylamide gel electrophoresis were stained by G250 or transferred onto PVDF membranes (Millipore, Bedford, MA, United States). After blocking for 1 h at room temperature with 5% bovine serum albumin, membranes were incubated overnight with antibodies against CD9, CD63, and CD81 (Abcam, Cambridge, MA, United States). After three times washing, the membrane was incubated with HRP-conjugated secondary antibodies and detected by enhanced chemiluminescence (Pierce, Rockford, IL, United States).

Exosomal RNA Extraction and Quantitation

The serum sEVs precipitated by Exoquick were resuspended in PBS. Then, total RNA was extracted using Trizol LS with the addition of 4 μg glycogen (Invitrogen, Life Technologies, CA, United States) as a carrier and overnight precipitation at −20°C. The RNA quantity was determined using NanoDrop (Thermo Fisher Scientific, Wilmington, DE, United States). The Agilent Bioanalyzer 2100 system assessed the RNA integrity with a small RNA chip (Agilent Technologies, Santa Clara, CA, United States).

Small RNA Library Construction and Deep Sequencing

The NEB Next® Small RNA Library Prep Set for Illumina® (NEB, Ipswich, MA, United States) was adopted to convert exosomal small RNA into cDNA libraries for next-generation sequencing. According to the manufacturer's recommendations, total exosomal RNA was ligated with 3′ and 5′ SR adaptors. Then small RNA molecules were reverse transcribed into cDNA, amplified using the adaptor primers for 14 cycles. The amplified libraries were resolved on a native 6% PAGE-gel. DNA fragments between 140 and 160 bp were recovered. Library quality was assessed on the Agilent 2100 Bioanalyzer system. Finally, the purified cDNA was used for cluster generation and sequenced using an Illumina HiSeq 2500 platform, and 50 bp single-end reads were generated. The sequence data were deposited in the National Center for Biotechnology Information (human[2]; mouse[3]).

Small RNA Sequencing Data Analysis

The small RNA sequencing data were processed as previously described with modification (Zhou et al., 2017). Briefly, clean reads were obtained by removing adapters, reads containing ploy-N, low-quality reads, and sequences smaller than 18 nt.

[1]http://imagej.nih.gov/ij/

[2]https://www.ncbi.nlm.nih.gov/bioproject/PRJNA607025

[3]https://www.ncbi.nlm.nih.gov/bioproject/PRJNA607346

Then, these clean reads were mapped to human and mouse reference genomes (hg38 and mm9) by hisat2 (Kim et al., 2015). The known miRNAs were identified based on miRBase 22.1. Next, DESeq2 software (Love et al., 2014) was used to normalize counts and calculate the differential expression of microRNAs. The differentially expressed miRNAs were selected as follows: $|\text{Log2Fold change}| \geq 1$ and p-value < 0.01.

Quantitative Reverse Transcriptase Real-Time Polymerase Chain Reaction for Serum Exosomal miRNA

The serum exosomal RNA for the qPCR assay was extracted from 500 μL human serum and 250 μL mouse serum. The procedures were the same as for RNA sequencing. The qRT-PCR was performed using MiDETECTA Track^{TM} miRNA qRT-PCR kits (Riobio Inc., Guangzhou, China) and a CFX 96 PCR system (Bio-Rad, Hercules, CA, United States) following the manufacturer's protocols. The *Ct* values were normalized by using the spiked 100 fmol synthetic cel-miR-39.

Data Analyses

Data are presented as the mean ± SEM. A comparison between means was assessed by unpaired Student's *t*-test or one-way analysis of variance using GraphPad Prism software (Version 5.01). $P < 0.05$ was considered statistically significant.

RESULTS

Isolation and Characterization of Small Extracellular Vesicles From Human and Mouse Serum

Considering the limited volume of human and mouse serum and the low yield of sEVs by ultracentrifugation, we chose ExoQuick, a method based on precipitation, to isolate serum sEVs as we did before (Ji et al., 2016; Zhou et al., 2017). TEM analysis showed the spherical vesicles with approximately 100 nm (**Figures 1A**, **2A**). NTA analysis indicated that the size of these isolated EVs ranged from 30 to 150 nm (**Figures 1B**, **2B**). The expression of exosomal markers of CD9, CD63, and CD81 was detected in both human and mouse serum precipitations (**Figures 1C,D**, **2C,D**). Notably, there were no or barely detectable bands in the sEVs-depleted serum, indicating the high serum sEVs recovery efficiency. Calnexin, a negative marker of exosomes, was not detected in sEVs from both human and mouse serum (**Supplementary Figure 1**). In short, particles obtained from human and C57BL/6 mouse serum by ExoQuick complied with the characteristics of sEVs (Lötvall et al., 2014).

Differential Serum Small Extracellular Vesicles miRNAs Between Ischemic Stroke Patients and Healthy Controls

The RNA content is very low in human serum exosomes (Zhao et al., 2020). To obtain enough exosomal RNA for small RNA sequencing, we extract sEVs from 2 mL of human serum. Therefore, in this study, 40 IS patients and 33 HCs were randomly divided into groups: group 1 included 20 IS patients and 17 HCs; group 2 included 20 IS patients and 16 HCs. 200 μL serum from each person was pooled. The remaining sample of each person was kept for subsequent PCR verification. Bioanalyzer analysis of the exosomal RNA revealed that ischemic stroke significantly increased the amount of serum exosomal RNA [29 ± 11 ng/mL (HCs) vs. 112 ± 26 ng/mL (IS), $p < 0.05$] (**Figures 3A,B**). The statistical summary of small RNA sequencing and categories of small RNA was provided in **Supplementary Tables 1**, **2**.

In this study, 1,084 and 990 known miRNAs were identified in the two HC groups, and 1,113 and 1,021 were identified in the two IS patient groups (**Supplementary Table 5**). These analyses identified 1,444 miRNAs, accounting for 54.2% of known human miRNAs (miRbase Release 22.1, 2,656 mature miRNAs, *Homo sapiens*). Differential expression analysis revealed that 208 and 216 miRNAs were up- and downregulated in IS patients, respectively (**Supplementary Tables 6**, **7**), accounting for 29.4% (424/1,440) of the total identified miRNAs. Notably, these differentials were low abundance miRNAs, as the sum read counts of these 424 differential miRNAs accounted for only less than 1% of the total identified. Considering the technical challenge of PCR analysis of these low abundance miRNAs, we focused on the top 25 overexpressed miRNAs, whose read counts accounted for over 85% of the upregulated in IS patients (**Table 2**). In the downregulated, miR-122-5p was the most abundant miRNA, whose read counts accounted for over 10% of those downregulated.

Differential Serum Small Extracellular Vesicles miRNAs Between Transient Middle Cerebral Artery Occlusion and Sham Mice

To determine the effects of acute ischemia on the miRNA profile of mouse serum sEVs, a 60 min tMCAO mouse model was established. The infarct volume in tMCAO mice was around 50% (**Figure 4**), consistent with the typical characteristics of this IS animal model. Moreover, serum from 7 to 9 tMCAO mice and the corresponding sham mice was pooled, and 500 μL serum was used for small RNA sequencing. Similar to the observation in IS patients, compared with sham controls, the RNA content increased in the serum sEVs from tMCAO mice (**Figures 3C,D**); however, there was no statistical difference (914.5 ± 3.1 vs. 1,539.0 ± 205.3 ng/mL, $p = 0.0932$).

The statistical summary of small RNA seq and categories of small RNA was provided in **Supplementary Tables 3**, **4**. In the two independent experiments, 739 and 864 known miRNAs were identified from the sham group, and 1,038 and 1,074 were identified from the tMCAO groups (**Supplementary Table 8**). Thus, 1,373 known miRNAs were identified in these analyses, which accounted for 71.7% of known miRNAs (miRbase Release 22.1, 1,978 mature miRNAs, *Mus musculus*). Compared with the sham group, 20 miRNAs were upregulated in the tMCAO group (**Table 3**), while 17 were downregulated (**Supplementary Tables 9**, **10**). In line with the

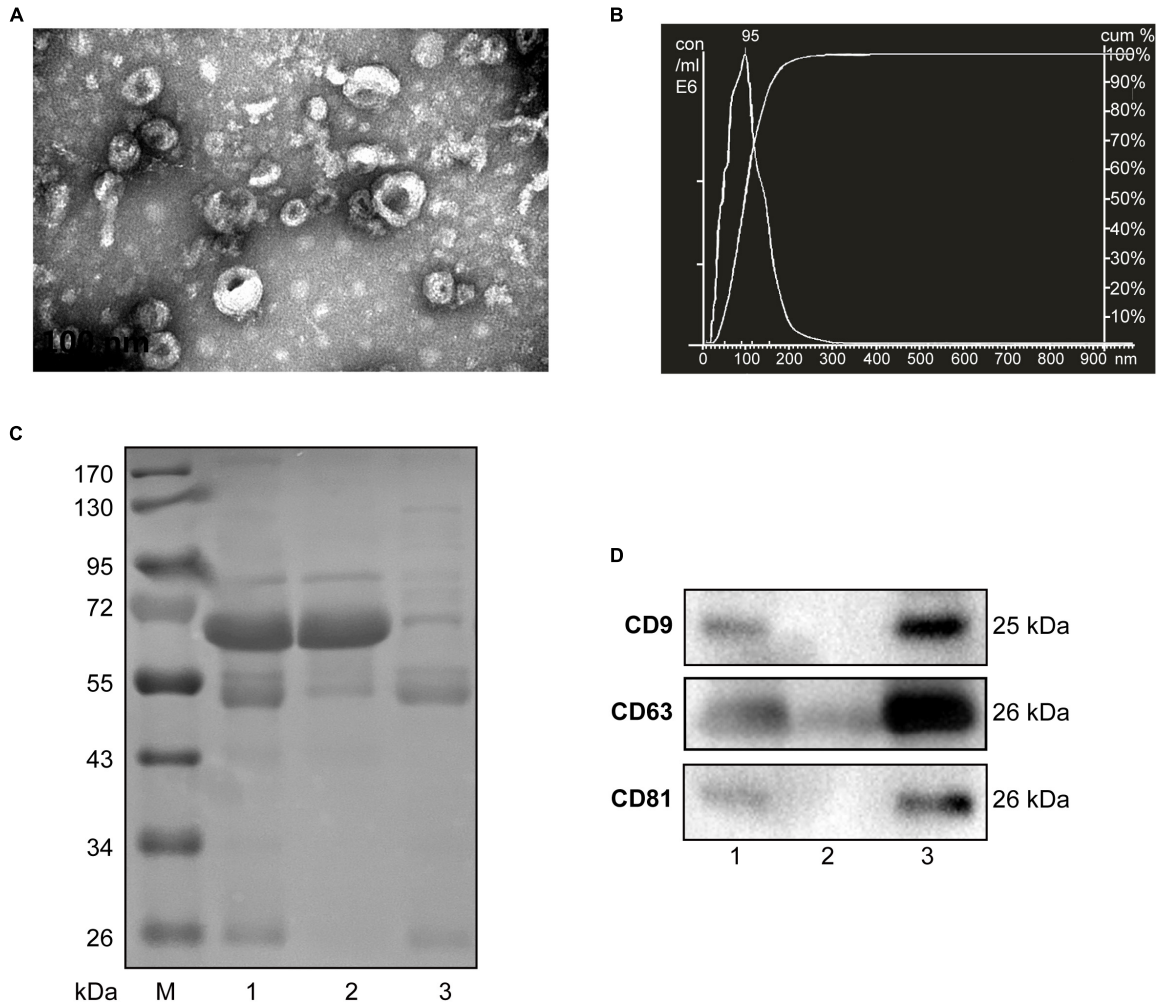

FIGURE 1 | Characterization of sEVs isolated from human serum. **(A)** The TEM image shows the spherical morphology of sEVs with a diameter of approximately 100 nm, bar = 100 nm. **(B)** NTA analysis plot illustrates the size distribution and concentration of the sEVs isolated human serum. **(C)** Proteins from serum, sEVs-depleted serum, and sEVs were separated by SDS-PAGE and stained by Coomassie blue. 40 μg proteins from serum and sEVs depleted serum were loaded. The amount of sEVs protein was adjusted by the serum volume corresponding to 40 μg serum protein. **(D)** The expression of CD9, CD81, and CD63, markers of exosomes, was detected by western blotting. Lane 1: total serum; lane 2: sEVs-depleted serum; lane 3: serum sEVs.

finding in IS patients, miR-122-5p was also the most abundant downregulated miRNA.

Acute Ischemia Increases a Panel of Brain-Specific miRNAs in Serum Small Extracellular Vesicles From Both Ischemic Stroke Patients and Transient Middle Cerebral Artery Occlusion Mice

In addition to stability, tissue specificity is another essential trait of circulating miRNAs as biomarkers. Based on the tissue-specific or enriched miRNAs information provided by these previous studies (Landgraf et al., 2007; Liang et al., 2007; Ludwig et al., 2016), we were excited to find that five brain-specific miRNAs were included in the top 25 upregulated miRNAs in IS patients: hsa-miR-9-3p, hsa-miR-124-3p, hsa-miR-143-3p, hsa-miR-98-5p, and hsa-miR-93-5p (**Table 2**). Likewise, 9 out of the 20 upregulated miRNAs in tMCAO mice are brain-specific or preferentially expressed in brain tissues, including mmu-miR-124-3p, mmu-miR-9-3p, mmu-miR-9-5p, mmu-miR-323-3p, mmu-miR-219b-5p, mmu-miR-129b-3p, mmu-miR-129-5p, mmu-miR-433-3p, and mmu-miR-128-3p (**Table 3**). The coordinate upregulation of a set of brain-specific miRNAs in serum sEVs from IS patients, and tMCAO mice suggested a conservative regulatory mechanism.

Validation of the Brain-Specific miRNAs Identified in Ischemic Stroke Patients

To validate the overexpressed brain-specific miRNAs identified by small RNAseq, the relative expression of 4 brain-specific miRNAs (hsa-miR-9-3p, hsa-miR-124-3p, hsa-miR-143-3p, and

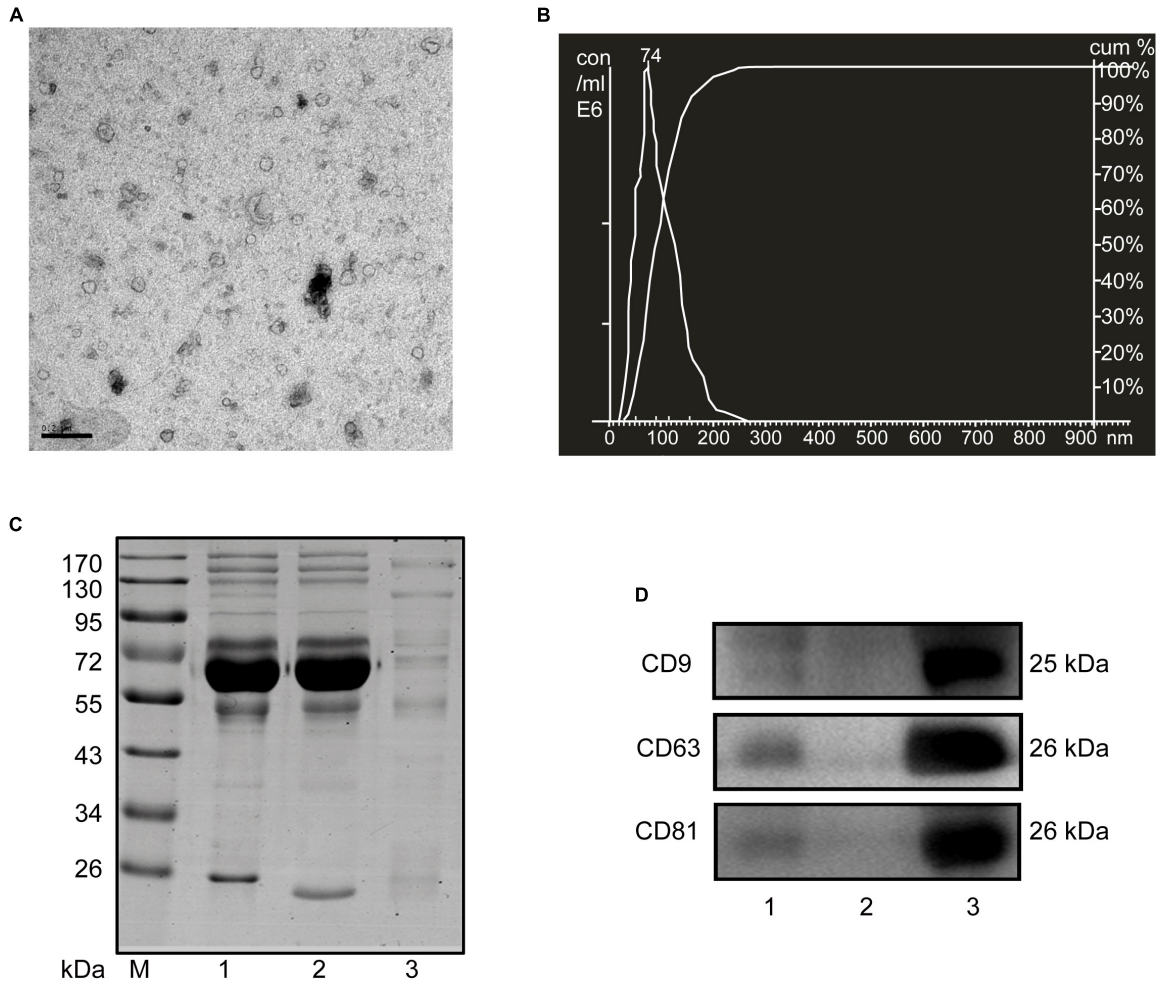

FIGURE 2 | Characterization of sEVs isolated from mouse serum. **(A)** The TEM image depicts the spherical morphology of the isolated sEVs, bar = 200 nm. **(B)** NTA analysis plot illustrates the size distribution and concentration of the sEVs isolated mouse serum. **(C)** Proteins from serum, sEVs-depleted serum, and sEVs were separated by SDS-PAGE and stained by Coomassie blue. 40 μg proteins from serum and sEVs depleted serum were loaded. The amount of sEVs protein was adjusted by the serum volume corresponding to 40 μg serum protein. **(D)** The expression of CD9, CD81, and CD63, markers of exosomes, was detected by western blotting. Lane 1: total serum; lane 2: sEVs-depleted serum; lane 3: serum sEVs.

hsa-miR-93-5p) was determined by using qRT-PCR in the individual serum samples for RNAseq analysis. Consistent with the tendency of the RNAseq results, the levels of all four miRNAs significantly increased in serum sEVs from IS patients, and miR-9-3p was the most significantly modulated (**Figure 5**).

Temporal Expression of Serum Small Extracellular Vesicles miR-124-3p, miR-9-5p, miR-129-5p, and miR-433-3p in Transient Middle Cerebral Artery Occlusion Mice

To explore the potential biological significance of the increament of these brain-specific miRNAs in the serum sEVs after cerebral ischemia, we examined the temporal dynamics of the mmu-miR-124-3p, mmu-miR-9-5p, mmu-miR-129-5p, and mmu-miR-433-3p in a tMCAO mouse model. As illustrated in **Figure 6**, these four miRNAs shared a similar expression pattern: their expression started to increase at 0.5 days after ischemia, peaked at day 1 or 3, and returned to normal levels at day 7 and 14 (**Figure 6**). This temporal expression pattern is coordinated with the evolution of ischemic injury in animal stroke models (Rewell et al., 2017).

Effects of Lipopolysaccharide Challenge on the Expression of Brain-Specific miRNAs in the Mouse Serum Small Extracellular Vesicles

To investigate whether these miRNAs could differentiate cerebral ischemia injury from other neurological and non-neurological diseases, we examined the levels of the nine miRNAs in the serum sEVs derived from LPS challenged mice, a widely used animal model of neuroinflammation. Three miRNAs involved in

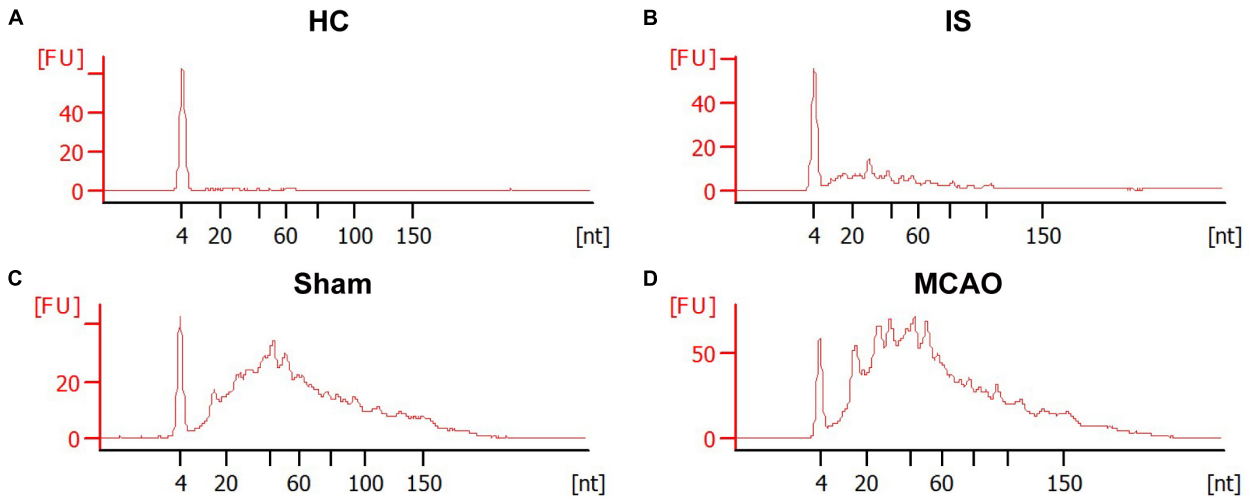

FIGURE 3 | The size distribution and relative abundance of sEVs RNA from IS patients and healthy controls, and tMCAO mice and sham controls. The electropherograms delineate the size distribution in nucleotides (nt) and fluorescence intensity (FU) of small RNA in serum sEVs. The representative electropherograms of HCs **(A)** and IS patients **(B)**; sham **(C)** and tMCAO mice **(D)**.

TABLE 2 | List of top 25 upregulated serum exosomal miRNAs in IS patients.

			HCs		IS		Tissue specificity	
miRNA species	**Log_2FC**	***P* value**	**1**	**2**	**1**	**2**	**Tissue**	**References**
hsa-miR-9-3p	7.15	4.41E-37	3.35	10.49	939.79	804.15	brain	Landgraf et al., 2007; Guo et al., 2014; Ludwig et al., 2016
hsa-miR-450b-5p	4.15	5.58E-91	82.04	77.91	1,473.48	1,377.38	n/a	
hsa-miR-124-3p	3.62	2.55E-118	430.27	422.51	5,631.87	4,819.10	brain	Landgraf et al., 2007; Guo et al., 2014; Ludwig et al., 2016
hsa-miR-143-3p	2.42	1.05E-05	13,541.80	15,502.34	37,232.75	117,740.19	brain	Landgraf et al., 2007; Guo et al., 2014
hsa-miR-30e-3p	2.18	3.04E-05	168.26	254.70	622.18	1,285.71	n/a	
hsa-miR-223-3p	2.15	1.92E-92	2,664.50	2,445.14	10,988.66	11,711.82	spleen	Guo et al., 2014
hsa-miR-340-5p	2.08	2.00E-07	190.86	305.64	862.27	1,235.82	n/a	
hsa-miR-4286	2.01	1.44E-27	358.28	361.08	1,564.71	1,337.93	n/a	
hsa-miR-450a-5p	2.00	1.17E-21	180.81	188.78	775.84	697.39	n/a	
hsa-miR-718	1.92	1.69E-28	226.85	233.73	862.96	878.42	n/a	
hsa-miR-223-5p	1.66	2.57E-28	439.48	480.94	1,417.91	1,479.50	spleen	Guo et al., 2014
hsa-miR-221-5p	1.58	7.62E-13	282.10	239.72	819.06	741.49	n/a	
hsa-miR-144-5p	1.54	1.89E-05	282.94	371.56	753.89	1,141.82	n/a	
hsa-let-7a-3p	1.36	5.32E-19	782.69	720.66	2,040.78	1,831.10	n/a	
hsa-miR-98-5p	1.30	1.67E-06	246.11	305.64	613.26	746.13	brain	Landgraf et al., 2007
hsa-miR-338-5p	1.29	1.32E-15	2,724.77	2,404.68	6,778.13	5,754.38	n/a	
hsa-miR-4448	1.25	9.67E-42	3,867.41	3,628.75	9,155.73	8,714.53	n/a	
hsa-miR-32-5p	1.25	3.39E-12	292.15	275.68	674.32	679.99	n/a	
hsa-miR-532-5p	1.20	2.17E-03	549.98	617.28	953.51	1,722.02	n/a	
hsa-miR-93-5p	1.15	7.22E-05	1,380.38	1,627.09	2,648.56	4,020.75	brain	Guo et al., 2014
hsa-miR-193a-5p	1.14	2.66E-09	909.93	807.55	2,062.05	1,720.86	muscle	
hsa-miR-425-3p	1.11	1.94E-08	615.27	575.33	1,402.14	1,162.71	n/a	
hsa-miR-24-3p	1.10	5.70E-13	1,405.49	1,276.50	3,067.69	2,688.62	n/a	
hsa-miR-374a-5p	1.06	8.23E-11	2,993.48	2,662.38	6,431.72	5,396.98	n/a	
hsa-miR-4443	1.01	2.09E-06	738.32	644.25	1,532.47	1,254.38	n/a	

n/a, not available.

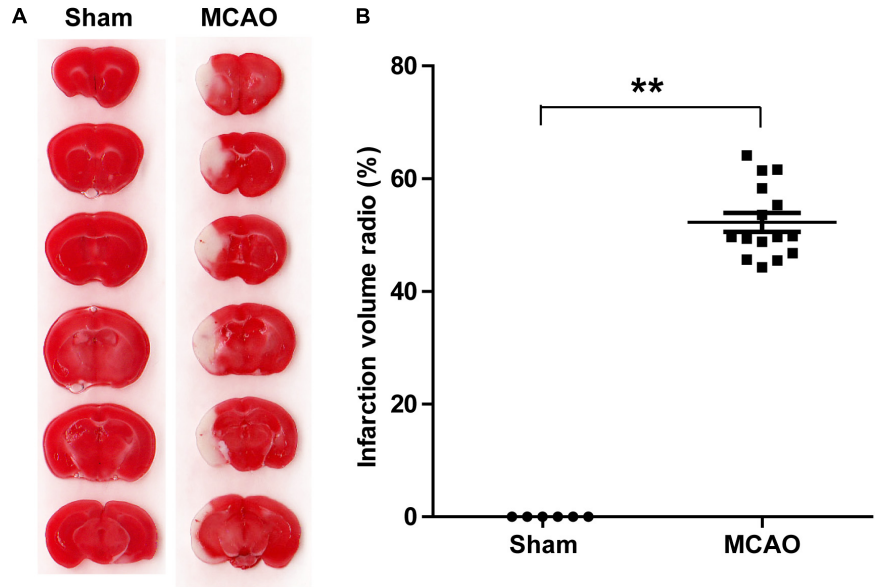

FIGURE 4 | A tMCAO mouse model. **(A)** A representative image of TTC staining, normal tissues were stained in red, while the infarction area was stained in white. The infarct volume was measured by TTC staining 24 h after the onset of ischemia. **(B)** The statistical analysis of infarct volume. The infarct volume was 51.24 ± 7.89% in the tMCAO group; sham group, $n = 6$, tMCAO group, $n = 15$, ** $P < 0.01$.

TABLE 3 | List of 20 upregulated serum exosomal miRNAs in tMCAO mice.

miRNA species	Fold change	*p*-value	Sham 1	Sham 2	tMCAO 1	tMCAO 2	Tissue	References
mmu-miR-124-3p	7.76	3.89E-06	0.00	0.00	78.19	59.71	brain	Lagos-Quintana et al., 2002; Landgraf et al., 2007; Guo et al., 2014; Ludwig et al., 2016
mmu-miR-9-3p	7.05	2.48E-09	1.79	1.66	261.41	194.77	brain	Lagos-Quintana et al., 2002; Landgraf et al., 2007; Guo et al., 2014; Ludwig et al., 2016
mmu-miR-668-3p	6.45	6.73E-04	0.00	0.00	31.46	24.17	n/a	
mmu-miR-770-3p	6.37	8.79E-04	0.00	0.00	29.15	23.46	n/a	
mmu-miR-9-5p	6.12	7.09E-14	12.56	1.66	547.34	427.93	brain	Lagos-Quintana et al., 2002; Guo et al., 2014
mmu-miR-323-3p	5.57	1.24E-03	0.00	1.66	43.95	37.67	brain	Guo et al., 2014; Ludwig et al., 2016
mmu-miR-219b-5p	5.39	2.03E-03	1.79	0.00	39.33	33.41	brain	Liang et al., 2007; Ludwig et al., 2016
mmu-miR-341-3p	4.98	6.87E-03	0.00	1.66	34.24	19.90	n/a	
mmu-miR-129b-3p	4.49	1.23E-08	8.97	4.99	158.69	152.83	brain	Liang et al., 2007; Guo et al., 2014; Ludwig et al., 2016
mmu-miR-129-5p	3.82	6.73E-08	8.97	21.64	189.23	244.53	brain	Guo et al., 2014; Ludwig et al., 2016
mmu-miR-433-3p	3.43	2.40E-06	8.97	16.64	151.29	125.11	brain	Ludwig et al., 2016
mmu-miR-598-3p	3.14	2.20E-03	5.38	4.99	54.13	36.96	n/a	
mmu-miR-300-3p	2.41	3.79E-03	17.94	8.32	78.65	60.42	n/a	
mmu-miR-434-3p	2.25	1.06E-04	35.88	34.95	184.60	152.12	n/a	
mmu-miR-107-3p	1.66	2.73E-03	145.30	83.22	397.89	321.30	n/a	
mmu-miR-382-5p	1.61	5.70E-03	48.43	51.60	177.66	127.95	n/a	
mmu-miR-128-3p	1.34	1.59E-03	6,709.11	9,163.98	20,672.90	19,481.50	brain	Lagos-Quintana et al., 2002; Guo et al., 2014; Ludwig et al., 2016
mmu-let-7d-5p	1.31	1.54E-03	726.52	675.73	1,889.07	1,580.93	n/a	
mmu-miR-423-5p	1.12	6.68E-03	1,462.01	1,266.58	2,693.65	3,234.36	n/a	
mmu-miR-328-3p	1.08	6.85E-03	832.36	888.77	1,905.73	1,738.02	n/a	

n/a, not available.

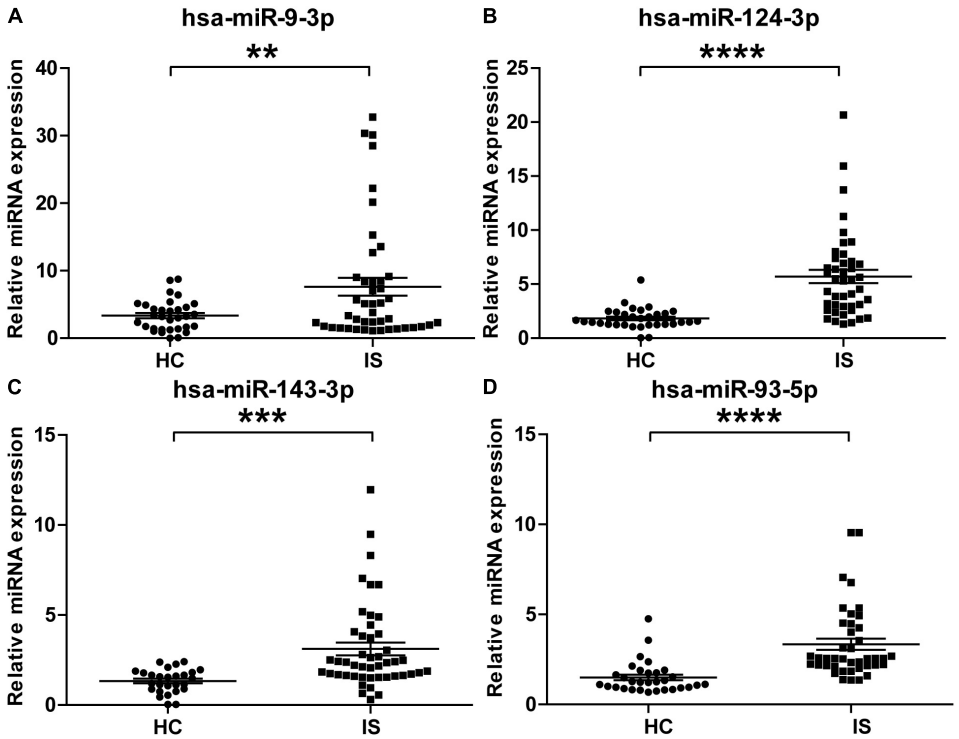

FIGURE 5 | Validation of the upregulation of the four brain-specific miRNAs in stroke patients. The expression of hsa-miR-9-3p **(A)**, hsa-miR-124-3p **(B)**, hsa-miR-143-3p **(C)**, and hsa-miR-93-5p **(D)** was assessed using qRT-PCR in the individual samples for small RNA sequencing. IS patients, $n = 40$, healthy controls (HCs), $n = 33$. The *Ct* value of target miRNAs was normalized against Cel-mir-39 and compared to the mean of healthy controls. Data are presented as Mean ± SEM. Unpaired Student's test vs. healthy control (**$P < 0.01$, ***$P < 0.001$, ****$P < 0.0001$).

inflammation, miRNA-181a-5p, miRNA-146a-5p, and miRNA-223-5p (Xie et al., 2013; Ferreira et al., 2015), were included as positive controls. Compared with the vehicle controls, the expression of these three inflammatory miRNAs significantly increased in the serum sEVs from LPS treated mice, especially miR-223-5p. However, except for miR-128-3p, LPS treatment did not significantly affect the levels of the other eight miRNAs (**Figure 7**).

DISCUSSION

By comprehensively analyzing the effects of acute cerebral ischemia on the serum sEVs miRNA profile of IS patients and tMCAO mice, this study revealed a significant increase in brain-specific miRNAs in the serum sEVs from both IS patients and tMCAO mice. Further animal studies indicated that the temporal expression of these brain-specific miRNAs in serum sEVs was closely correlated with the evolution of ischemic brain injury and recovery, and the expression of these miRNAs was unaffected by neuroinflammation.

A challenge in screening serum miRNAs for IS diagnosis is the poor reproducibility, as the candidate serum miRNAs identified in different studies can hardly be verified against each other (Eyileten et al., 2018). However, this situation has been greatly changed in the studies based on serum sEVs. The differential miRNAs identified in the present RNAseq study were well corroborated by these previous reports, such as the upregulation of hsa-miR-9 and hsa-miR-124 (Ji et al., 2016), hsa-miR-223 (Chen et al., 2017), and hsa-miR-450b-5p (Luo et al., 2019), as well as the downregulation of miR-422a and miR-125b-2-3 (Li D.B. et al., 2017). Our data also showed the overexpression of miRNA-21-3p and miRNA-30a-5p (Wang et al., 2018), but they did not reach the significance threshold. In a latest microarray study, four upregulated miRNAs (hsa-miR-17-5p, hsa-miR-20b-5p, hsa-miR-93-5p, hsa-miR-27b-3p) were identified in serum exosomes of IS patients (Van Kralingen et al., 2019), among which two (hsa-mir-20b-5p and hsa-mir-93-5p) were also included in our list (**Table 2** and **Supplementary Table 7**). The cross-validation of results from different studies highlights the advantages of using sEVs miRNAs for IS diagnosis and prognosis.

This advantage could be related to the features of sEVs miRNAs. Circulating miRNAs mainly exist in two forms, binding with protein/lipoprotein or packaged in membrane vesicles (Creemers et al., 2012). A recent study evidenced the different effects of cerebral ischemia on the different forms of circulating miRNA. In the three potential biomarkers for acute IS (miR-125a-5p, miR-125b-5p, and miR-143-3p), only a significant upregulation of miR-143-3p was observed in vesicles from IS patients (Tiedt et al., 2017). Our data consistently showed the overexpression of miR-143-3p in the serum sEVs of IS patients

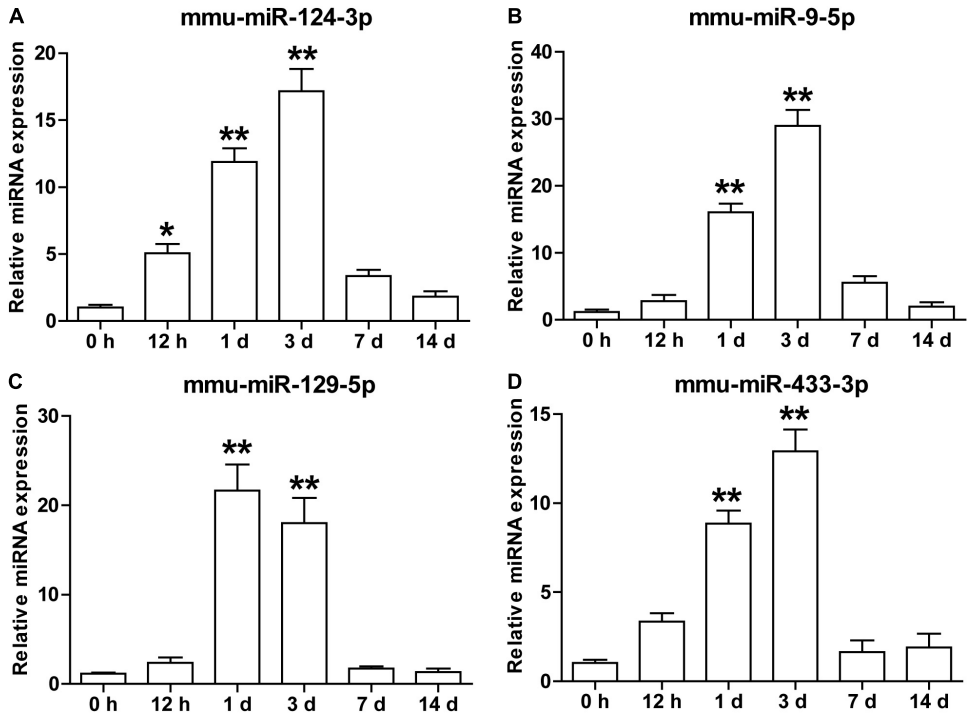

FIGURE 6 | The temporal expression of brain-specific miRNAs in the serum sEVs from the tMCAO mouse model. The levels of mmu-miR-124-3p **(A)**, mmu-miR-9-5p **(B)**, mmu-miR-129-5p **(C)**, and mmu-miR-433-3p **(D)** in mouse serum sEVs were detected by qRT-PCR at 0.5, 1, 3, 7, and 14 days after the onset of ischemia. The *Ct* value was normalized against mmu-miR-451. Each time point represents the mean of 3 pooled serum samples (4–6 animals per sample). Data were presented as Mean ± SEM. Statistical significance was determined by non-parametric one-way ANOVA followed by Dunn's post-test, $^{*}p < 0.05$, $^{**}p < 0.01$ vs. sham control (0 h).

(**Table 2** and **Figure 5**). The other two were not detected in this study, probably because of their low abundance in serum sEVs. Therefore, sEVs isolation could reduce the complexity of the samples by removing the protein/lipoprotein-binding RNA and produce a more stable result.

A survey on tumor biomarker studies emphasized the importance of tissue specificity of biomarkers. They argued that many potential miRNA biomarkers for cancer were those highly expressed in blood cells, which reflected a blood cell-based phenomenon rather than a cancer-specific origin. The most exciting finding of this study is the coordinate upregulation of a panel of brain-specific miRNAs in the serum sEVs from both IS patients (**Table 2**) and tMCAO mice (**Table 3**). miR-9 and miR-124 were the two significantly upregulated miRNAs shared by the IS patients and the tMCAO mice. Moreover, previous studies have proposed that these two miRNAs could be diagnosis and prognosis markers of IS (Ji et al., 2016; Rainer et al., 2016; He et al., 2019). The specificity and sensitivity of these brain-specific miRNAs in the diagnosis and prognosis of ischemic stroke need to be further evaluated in large-scale clinical studies.

An important issue for the translational application of circulating miRNAs in the IS diagnosis is the biological significance they reflect. Several recent biomarker studies on IS began to look at this issue. For instance, the elevated circulating miR-125a-5p, miR-125b-5p, and miR-143-3p may indicate the thrombotic processes (Tiedt et al., 2017), while the changes of miRNA-17 family members in sEVs could reflect the development of cerebrovascular disease (Van Kralingen et al., 2019).

The blood-brain barrier (BBB) is a strictly modulated interface between the peripheral circulation and the central nervous system (CNS) (Pardridge, 2003). Due to the nanoscale and the lack of specific markers, whether and when sEVs released by brain cells can cross the BBB remains uncertain (Shi et al., 2019). Our temporal analysis indicated that the dynamics of these brain-specific miRNAs were closely correlated with the progression of ischemic brain injury and recovery. These temporal dynamics implicated that sEVs in the brain could hardly cross the intact BBB, and the increament of these brain-specific miRNAs in serum sEVs could be closely associated with BBB disruption. Consistently, two recent studies also showed that sEVs could not cross intact BBB in normal conditions (Ridder et al., 2014; Chen et al., 2016).

However, in contrast to the reports that exosomes can cross BBB after LPS treatment (Ridder et al., 2014; Chen et al., 2016), our data suggested that sEVs harboring brain-specific miRNA could hardly cross the BBB under inflammatory circumstances because the expression of eight brain-specific miRNAs in the serum sEVs was not significantly affected by LPS treatment. This discrepancy may be due to the discrepancies in the tracking methods and experimental models. In a study, luciferase (Chen et al., 2016) was used to track sEVs in an *in vitro* BBB model

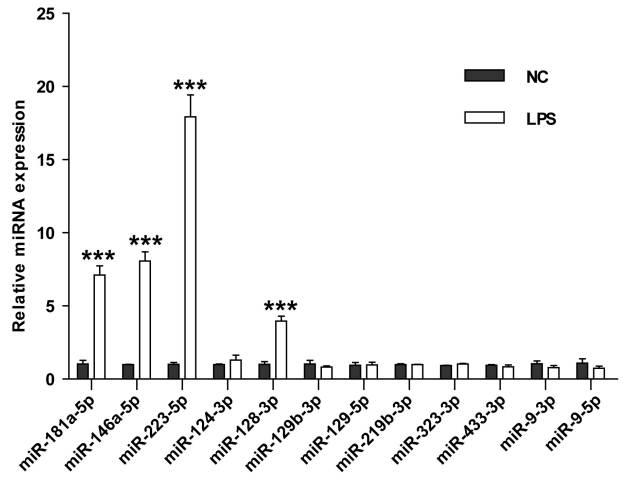

FIGURE 7 | The effects of LPS challenge on the expression of brain-specific miRNAs in the mouse serum sEVs. RT-PCR assessed the expression of nine brain-specific miRNAs and three inflammatory miRNAs in the mouse serum sEVs. Data were expressed as the fold change ± SEM (n = 3) compared to normal control (NC). Statistical significance was determined by student t-test. ***$p < 0.001$.

(Chen et al., 2016). In another study, a transgenic mouse expressing Cre recombinase specifically in the hematopoietic lineage was used to track blood sEVs (Ridder et al., 2014). More efforts and novel tracking methods are needed to provide direct evidence for the connections between the increased brain-specific miRNAs in serum sEVs and the compromise of BBB after cerebral ischemia.

CONCLUSION

In this study, we took a comprehensive view of the impact of acute ischemia on the serum sEVs miRNA profiles of ischemic stroke (IS) patients and MCAO mice for the first time. More importantly, this study demonstrated the increase of a set of brain-specific miRNAs in the serum sEVs after acute cerebral ischemia and suggested that these increased brain-specific miRNAs in serum sEVs could be promising biomarkers that directly reflect the ischemic brain injury.

DATA AVAILABILITY STATEMENT

The datasets presented in this study can be found in online repositories. The names of the repository/repositories and accession number(s) can be found below: https://www.ncbi.nlm.nih.gov/bioproject/PRJNA607025; mouse, https://www.ncbi.nlm.nih.gov/bioproject/PRJNA607346.

ETHICS STATEMENT

The studies involving human participants were reviewed and approved by the Ethics Committee of Affiliated Hospital of Nantong University. The patients/participants provided their written informed consent to participate in this study. The animal study was reviewed and approved by the Animal Experimental Committee of Jinan University.

AUTHOR CONTRIBUTIONS

YJ and QJ conceived and supervised the study. MS collected blood samples and clinical data. XZ, CX, SL, DC, YP, and YD performed experiments. ZC did the RNAseq data analysis. YJ, XZ, and QJ drafted the manuscript. JJ reviewed and revised the manuscript. All authors contributed to the article and approved the submitted version.

FUNDING

This study was funded by the National Natural Science Foundation of China (Nos. 82071553, 81761128018, 81572871,81201016, and 81272027), Natural Science Foundation of Jiangsu Province (No. BK20151277), Six Talents Peak Project of Jiangsu Province (No. 2017-WSN-094), and the Municipal Natural Science Foundation of Nantong (No. MS 32015026). The funders had no role in study design, data collection, analysis, decision to publish, and manuscript preparation.

SUPPLEMENTARY MATERIAL

The Supplementary Material for this article can be found online at: https://www.frontiersin.org/articles/10.3389/fnmol.2022.874903/full#supplementary-material

Supplementary Figure 1 | The expression of Calnexin, a negative marker of sEVs, was detected by western blotting. Calnexin was not detected in sEVs from both human and mouse serum (de-sEV: sEVs-depleted serum).

Supplementary Table 1 | Summary of small RNA-Seq analysis of human serum sEVs.

Supplementary Table 2 | Summary of small RNA classification in human serum sEVs.

Supplementary Table 3 | Summary of small RNA-Seq analysis of mouse sEVs.

Supplementary Table 4 | Summary of small RNA classification in mouse sEVs.

Supplementary Table 5 | List of miRNAs detected in the serum sEVs from IS patients and healthy controls.

Supplementary Table 6 | List of the normalized read counts of miRNAs detected in the serum sEVs from IS patients and healthy controls.

Supplementary Table 7 | List of differential serum sEVs miRNAs between IS patients and healthy controls.

Supplementary Table 8 | List of miRNAs detected in the serum sEVs from tMCAO and sham mice.

Supplementary Table 9 | List of the normalized read counts of miRNAs detected in the serum sEVs from tMCAO and sham mice.

Supplementary Table 10 | List of differential serum sEVs miRNAs between tMCAO and sham mice.

REFERENCES

Bartel, D. P. (2004). MicroRNAs: genomics, biogenesis, mechanism, and function. *Cell* 116, 281–297. doi: 10.1016/s0092-8674(04)00045-5

Chen, C. C., Liu, L., Ma, F., Wong, C. W., Guo, X. E., Chacko, J. V., et al. (2016). Elucidation of exosome migration across the blood-brain barrier model in vitro. *Cell Mol. Bioeng.* 9, 509–529. doi: 10.1007/s12195-016-0458-3

Chen, Y., Song, Y., Huang, J., Qu, M., Zhang, Y., Geng, J., et al. (2017). Increased circulating exosomal miRNA-223 is associated with acute ischemic stroke. *Front. Neurol.* 8:57. doi: 10.3389/fneur.2017.00057

Creemers, E. E., Tijsen, A. J., and Pinto, Y. M. (2012). Circulating microRNAs: novel biomarkers and extracellular communicators in cardiovascular disease? *Circ. Res.* 110, 483–495. doi: 10.1161/CIRCRESAHA.111.247452

Eyileten, C., Wicik, Z., De Rosa, S., Mirowska-Guzel, D., Soplinska, A., Indolfi, C., et al. (2018). MicroRNAs as diagnostic and prognostic biomarkers in ischemic stroke—a comprehensive review and bioinformatic analysis. *Cells* 7:249.

Ferreira, R. B., Ferreira, R., Albuquerque, D. M., Costa, F. F., and Franco-Penteado, C. F. (2015). miRNA-146a, miRNA-203a, and miRNA-223 modulate inflammatory response in LPS- acute lung injury in sickle cell transgenic mice. *Blood* 126, 3390–3390. doi: 10.1182/blood.V126.23.3390.3390

Guo, Z., Maki, M., Ding, R., Yang, Y., Zhang, B., and Xiong, L. (2014). Genome-wide survey of tissue-specific microRNA and transcription factor regulatory networks in 12 tissues. *Sci. Rep.* 4:5150. doi: 10.1038/srep05150

He, X. W., Shi, Y. H., Liu, Y. S., Li, G. F., Zhao, R., Hu, Y., et al. (2019). Increased plasma levels of miR-124-3p, miR-125b-5p and miR-192-5p are associated with outcomes in acute ischaemic stroke patients receiving thrombolysis. *Atherosclerosis* 289, 36–43. doi: 10.1016/j.atherosclerosis.2019.08.002

He, Y., Lin, J., Kong, D., Huang, M., Xu, C., Kim, T. K., et al. (2015). Current state of circulating MicroRNAs as cancer biomarkers. *Clin. Chem.* 61, 1138–1155.

Ji, Q., Ji, Y., Peng, J., Zhou, X., Chen, X., Zhao, H., et al. (2016). Increased brain-specific MiR-9 and MiR-124 in the serum exosomes of acute ischemic stroke patients. *PLoS One* 11:e0163645. doi: 10.1371/journal.pone.0163645

Johnstone, R. M., Bianchini, A., and Teng, K. (1989). Reticulocyte maturation and exosome release: transferrin receptor containing exosomes shows multiple plasma membrane functions. *Blood* 74, 1844–1851.

Karakas, M., and Zeller, T. (2017). A biomarker ocular: circulating MicroRNAs toward diagnostics for acute ischemic stroke. *Circ. Res.* 121, 905–907.

Kim, D., Langmead, B., and Salzberg, S. L. (2015). HISAT: a fast spliced aligner with low memory requirements. *Nat. Methods* 12, 357–360. doi: 10.1038/nmeth.3317

Lagos-Quintana, M., Rauhut, R., Yalcin, A., Meyer, J., Lendeckel, W., and Tuschl, T. (2002). Identification of tissue-specific microRNAs from mouse. *Curr. Biol.* 12, 735–739. doi: 10.1016/s0960-9822(02)00809-6

Landgraf, P., Rusu, M., Sheridan, R., Sewer, A., Iovino, N., Aravin, A., et al. (2007). A mammalian microRNA expression atlas based on small RNA library sequencing. *Cell* 129, 1401–1414. doi: 10.1016/j.cell.2007.04.040

Li, D. B., Liu, J. L., Wang, W., Li, R. Y., Yu, D. J., Lan, X. Y., et al. (2017). Plasma exosomal miR-422a and miR-125b-2-3p serve as biomarkers for ischemic stroke. *Curr. Neurovasc. Res.* 14, 330–337.

Li, X., Tsibouklis, J., Weng, T., Zhang, B., Yin, G., Feng, G., et al. (2017). Nano carriers for drug transport across the blood-brain barrier. *J. Drug Target* 25, 17–28. doi: 10.1080/1061186x.2016.1184272

Liang, Y., Ridzon, D., Wong, L., and Chen, C. (2007). Characterization of microRNA expression profiles in normal human tissues. *BMC Genomics* 8:166. doi: 10.1186/1471-2164-8-166

Lötvall, J., Hill, A. F., Hochberg, F., Buzás, E. I, Di Vizio, D., Gardiner, C., et al. (2014). Minimal experimental requirements for definition of extracellular vesicles and their functions: a position statement from the international society for extracellular vesicles. *J. Extracell. Vesicles* 3:26913. doi: 10.3402/jev.v3.26913

Love, M. I, Huber, W., and Anders, S. (2014). Moderated estimation of fold change and dispersion for RNA-seq data with DESeq2. *Genome Biol.* 15:550. doi: 10.1186/s13059-014-0550-8

Ludwig, N., Leidinger, P., Becker, K., Backes, C., Fehlmann, T., Pallasch, C., et al. (2016). Distribution of miRNA expression across human tissues. *Nucleic Acids Res.* 44, 3865–3877. doi: 10.1093/nar/gkw116

Luo, X., Wang, W., Li, D., Xu, C., Liao, B., Li, F., et al. (2019). Plasma exosomal miR-450b-5p as a possible biomarker and therapeutic target for transient ischaemic attacks in rats. *J. Mol. Neurosci* 69, 516–526. doi: 10.1007/s12031-019-01341-9

Mortality, G. B. D., and Causes of Death, C. (2016). Global, regional, and national life expectancy, all-cause mortality, and cause-specific mortality for 249 causes of death, 1980-2015: a systematic analysis for the global burden of disease study 2015. *Lancet* 388, 1459–1544. doi: 10.1016/S0140-6736(16)31012-1

Pardridge, W. M. (2003). Blood-brain barrier drug targeting: the future of brain drug development. *Mol. Interv.* 3, 90–105,51. doi: 10.1124/mi.3.2.90

Rainer, T. H., Leung, L. Y., Chan, C. P. Y., Leung, Y. K., Abrigo, J. M., Wang, D., et al. (2016). Plasma miR-124-3p and miR-16 concentrations as prognostic markers in acute stroke. *Clin. Biochem.* 49, 663–668.

Rewell, S. S. J., Churilov, L., Sidon, T. K., Aleksoska, E., Cox, S. F., Macleod, M. R., et al. (2017). Evolution of ischemic damage and behavioural deficit over 6 months after MCAo in the rat: selecting the optimal outcomes and statistical power for multi-centre preclinical trials. *PLoS One* 12:e0171688.

Ridder, K., Keller, S., Dams, M., Rupp, A. K., Schlaudraff, J., Del Turco, D., et al. (2014). Extracellular vesicle-mediated transfer of genetic information between the hematopoietic system and the brain in response to inflammation. *PLoS Biol.* 12:e1001874. doi: 10.1371/journal.pbio.1001874

Saenger, A. K., and Christenson, R. H. (2010). Stroke biomarkers: progress and challenges for diagnosis, prognosis, differentiation, and treatment. *Clin. Chem.* 56, 21–33. doi: 10.1373/clinchem.2009.133801

Shi, M., Sheng, L., Stewart, T., Zabetian, C. P., and Zhang, J. (2019). New windows into the brain: central nervous system-derived extracellular vesicles in blood. *Prog. Neurobiol.* 175, 96–106. doi: 10.1016/j.pneurobio.2019.01.005

Thery, C., Amigorena, S., Raposo, G., and Clayton, A. (2006). Isolation and characterization of exosomes from cell culture supernatants and biological fluids. *Curr. Protoc. Cell Biol.* Chapter 3, Unit322.

Théry, C., Zitvogel, L., and Amigorena, S. (2002). Exosomes: composition, biogenesis and function. *Nat. Rev. Immunol.* 2, 569–579. doi: 10.1038/nri855

Tiedt, S., Prestel, M., Malik, R., Schieferdecker, N., Duering, M., Kautzky, V., et al. (2017). RNA-Seq identifies circulating miR-125a-5p, miR-125b-5p, and miR-143-3p as potential biomarkers for acute ischemic stroke. *Circ. Res.* 121, 970–980. doi: 10.1161/CIRCRESAHA.117.311572

Van Kralingen, J. C., Mcfall, A., Ord, E. N. J., Coyle, T. F., Bissett, M., Mcclure, J. D., et al. (2019). Altered Extracellular Vesicle MicroRNA Expression in Ischemic Stroke and Small Vessel Disease. *Transl Stroke Res* 10, 495–508. doi: 10.1007/s12975-018-0682-3

Wang, W., Li, D. B., Li, R. Y., Zhou, X., Yu, D. J., Lan, X. Y., et al. (2018). Diagnosis of hyperacute and acute ischaemic stroke: The potential utility of exosomal MicroRNA-21-5p and MicroRNA-30a-5p. *Cerebrovasc. Dis.* 45, 204–212. doi: 10.1159/000488365

Weber, J. A., Baxter, D. H., Zhang, S., Huang, D. Y., Huang, K. H., Lee, M. J., et al. (2010). The microRNA spectrum in 12 body fluids. *Clin. Chem.* 56, 1733–1741. doi: 10.1373/clinchem.2010.147405

Xie, W., Li, Z., Li, M., Xu, N., and Zhang, Y. (2013). miR-181a and inflammation: miRNA homeostasis response to inflammatory stimuli in vivo. *Biochem. Biophy. Res. Commun.* 430, 647–652. doi: 10.1016/j.bbrc.2012.11.097

Zhao, F., Cheng, L., Shao, Q., Chen, Z., Lv, X., Li, J., et al. (2020). Characterization of serum small extracellular vesicles and their small RNA contents across humans, rats, and mice. *Sci. Rep.* 10:4197. doi: 10.1038/s41598-020-61098-9

Zhou, X., Jiao, Z., Ji, J., Li, S., Huang, X., Lu, X., et al. (2017). Characterization of mouse serum exosomal small RNA content: The origins and their roles in modulating inflammatory response. *Oncotarget* 8, 42712–42727. doi: 10.18632/oncotarget.17448

Conflict of Interest: The authors declare that the research was conducted in the absence of any commercial or financial relationships that could be construed as a potential conflict of interest.

Publisher's Note: All claims expressed in this article are solely those of the authors and do not necessarily represent those of their affiliated organizations, or those of the publisher, the editors and the reviewers. Any product that may be evaluated in this article, or claim that may be made by its manufacturer, is not guaranteed or endorsed by the publisher.

frontiers | Frontiers in Molecular Neuroscience

REVIEW
published: 25 May 2022
doi: 10.3389/fnmol.2022.894298

Focus on the Role of the NLRP3 Inflammasome in Multiple Sclerosis: Pathogenesis, Diagnosis, and Therapeutics

*Yueran Cui, Haiyang Yu, Zhongqi Bu, Lulu Wen, Lili Yan and Juan Feng**

Department of Neurology, Shengjing Hospital of China Medical University, Shenyang, China

Neuroinflammation is initiated with an aberrant innate immune response in the central nervous system (CNS) and is involved in many neurological diseases. Inflammasomes are intracellular multiprotein complexes that can be used as platforms to induce the maturation and secretion of proinflammatory cytokines and pyroptosis, thus playing a pivotal role in neuroinflammation. Among the inflammasomes, the nucleotide-binding oligomerization domain-, leucine-rich repeat- and pyrin domain-containing 3 (NLRP3) inflammasome is well-characterized and contributes to many neurological diseases, such as multiple sclerosis (MS), Alzheimer's disease (AD), and ischemic stroke. MS is a chronic autoimmune disease of the CNS, and its hallmarks include chronic inflammation, demyelination, and neurodegeneration. Studies have demonstrated a relationship between MS and the NLRP3 inflammasome. To date, the pathogenesis of MS is not fully understood, and clinical studies on novel therapies are still underway. Here, we review the activation mechanism of the NLRP3 inflammasome, its role in MS, and therapies targeting related molecules, which may be beneficial in MS.

Keywords: inflammation, NLRP3 inflammasome, multiple sclerosis, biomarker, treatment

OPEN ACCESS

Edited by:
Kiran Bhaskar,
University of New Mexico,
United States

Reviewed by:
Jong-Seok Moon,
Soonchunhyang University,
South Korea
Tianhao Hu,
The First Affiliated Hospital of China Medical University, China
Lyu Yi Qing,
King Saud University, Saudi Arabia

****Correspondence:***
Juan Feng
juanfeng@cmu.edu.cn

Specialty section:
This article was submitted to Brain Disease Mechanisms, a section of the journal Frontiers in Molecular Neuroscience

Received: *11 March 2022*
Accepted: *05 May 2022*
Published: *25 May 2022*

Citation:
Cui Y, Yu H, Bu Z, Wen L, Yan L and Feng J (2022) Focus on the Role of the NLRP3 Inflammasome in Multiple Sclerosis: Pathogenesis, Diagnosis, and Therapeutics. Front. Mol. Neurosci. 15:894298. doi: 10.3389/fnmol.2022.894298

INTRODUCTION

Neuroinflammation is caused by innate immune response; however, the dysregulation of innate immunity can be deleterious to the nervous system (Leite et al., 2022). It has been found that inflammasomes participate in innate immunity and link innate immunity with inflammation (Awad et al., 2018). Inflammasomes are cytosolic multiprotein platforms that exert their effects through pattern-recognition receptors (PRRs), thus inducing the maturation and secretion of proinflammatory cytokines interleukin-1β (IL-1β) and interleukin-18 (IL-18) (Kayagaki et al., 2015). PRRs form inflammasomes and act as sensors. To date, there are a few known PRRs, such as nucleotide-binding oligomerization domain-like receptor family members NLRP1, NLRP3, NLRC4, absent-in-melanoma 2 (AIM2), and pyrin, and they sense different kinds of stimuli (Broz and Dixit, 2016). Among inflammasomes, the nucleotide-binding oligomerization domain-, leucine-rich repeat-, and pyrin domain-containing 3 (NLRP3) inflammasome is reported to sense a wide range of stimuli and involve in a variety of diseases.

NLRP3 inflammasome was initially characterized in Muckle-Wells syndrome, which is an autoinflammatory disease (Martinon et al., 2002). As a common inflammasome, the NLRP3 inflammasome senses a wide range of danger- and pathogen-associated molecular patterns (DAMPs and PAMPs, respectively), and participates in a myriad of immune and inflammatory diseases (Peñin-Franch et al., 2022). There are three components of the NLRP3 inflammasome: NLRP3 protein (sensor), apoptosis-associated specklike protein containing a caspase-activation and recruitment domain (ASC) (adaptor), and pro-caspase-1 (effector) (Broz and Dixit, 2016) (**Figure 1**). NLRP3 protein itself comprises three domains: a C-terminal leucine-rich repeats (LRRs) domain, a central nucleotide binding and oligomerization domain (NACHT), and an N-terminal pyrin domain (PYD) (Kumar et al., 2011). Under normal conditions, LRRs and NACHT domains bind to each other, and NLRP3 protein is unable to bind ASC (Shao et al., 2015). Once stimulated, the two domains separate, and the NLRP3 protein binds to ASC *via* the PYD. ASC has two domains: a C-terminal caspase activation and recruitment domain (CARD) and an N-terminal PYD (Dick et al., 2016). When interacting with the NLRP3 protein, ASC can bind to pro-caspase-1 through the CARD, promoting the production of cleaved caspase-1, which in turn induces the maturation and release of IL-1β and IL-18 and the occurrence of pyroptosis (Shao et al., 2015; Liu et al., 2016). Pyroptosis, a form of programmed cell death that differs from apoptosis and necrosis, induces membrane rupture, leading to the release of inflammatory factors (Shi et al., 2017).

Multiple sclerosis (MS) is a common autoimmune, neurodegenerative disease of the central nervous system (CNS) (Calahorra et al., 2022). More than two million people around the world suffer from it, which brings a huge social and economic burden to patients (Browne et al., 2014; Kobelt et al., 2017). Clinically, MS is classified into four phenotypes: clinically isolated syndrome, primary progressive MS, secondary progressive MS, and progressive relapsing MS. There is no clear distinction among the different phenotypes. MS diagnosis requires a combination of clinical manifestations, imaging studies, and laboratory tests. Among the diagnostic techniques, MRI is very important (Brownlee et al., 2015). The clinical manifestations of MS patients are diverse and mainly include ataxia, cognitive dysfunction, and visual impairment (Pinke et al., 2020), which may be related to the complexity of its etiology. Currently, the exact etiology of MS is unclear and research has proposed several possibilities, which include genetic susceptibility and single nucleotide polymorphisms (SNP)

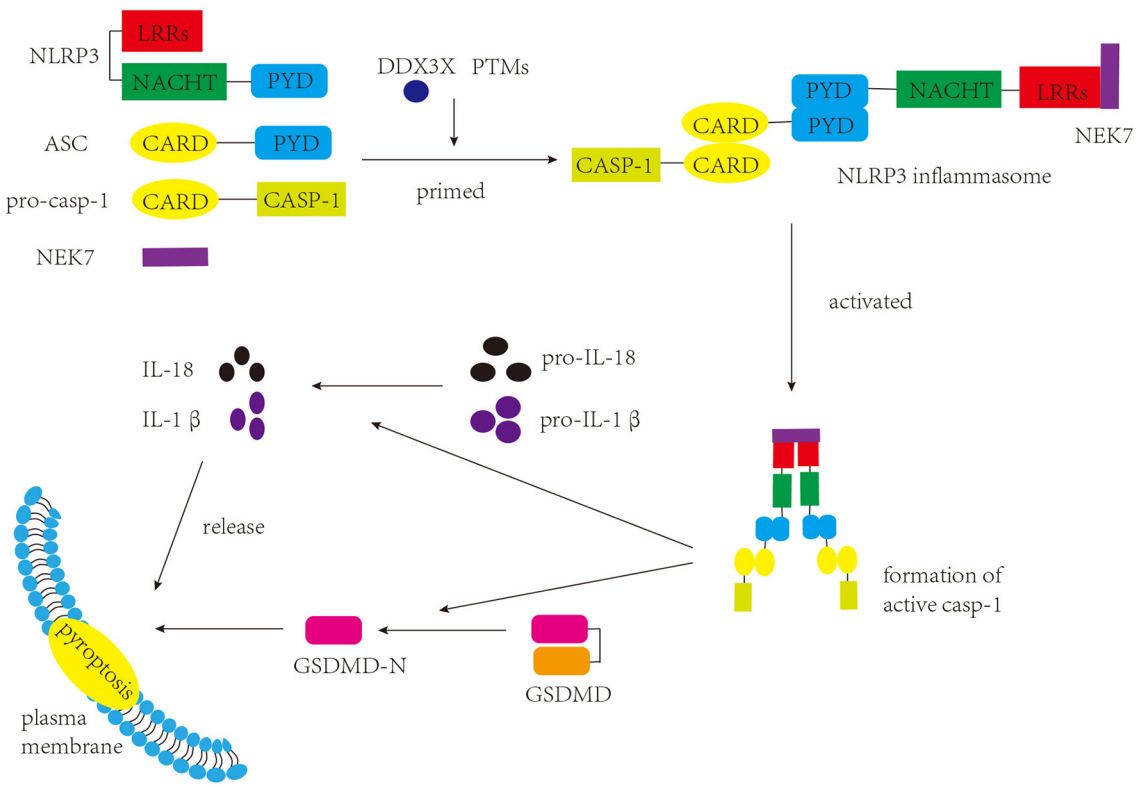

FIGURE 1 | Components and function of NLRP3 inflammasome. The NLRP3 inflammasome consists of three components: NLRP3, ASC, and pro-caspase-1. Once stimulated, the assembly and activation of the NLRP3 inflammasome lead to the production of active caspase-1. Caspase-1 cleaves GSDMD to produce GSDMD-N, which interacts with the plasma membrane and induces pyroptosis. Caspase-1 can also promote the maturation of pro-IL-1β and pro-IL-18 into IL-1β and IL-18, respectively, which are either secreted or released during pyroptosis.

of immune system-related genes, Epstein-Barr virus (EBV) infection, smoking, and reduced levels of Vitamin D (Hafler et al., 2007; Healy et al., 2009; Endriz et al., 2017; de Oliveira et al., 2020). In addition, dysfunction of the intestinal flora, a research hotspot in recent years, has also been reported to be related to MS (Pröbstel and Baranzini, 2018). According to studies, myelin-specific autoreactive CD4+ T cells may be activated in the periphery during early stages of MS. CD4+ T cells, B cells, and macrophages cross the blood-brain barrier and migrate into the CNS after destruction of the blood-brain barrier. Furthermore, antigen-presenting cells (APCs) induce differentiation of CD4+ T cells into the Th1 and Th17 cells, which exacerbate inflammatory response and contribute to the progression of MS (Shao et al., 2021). As the disease progresses, the infiltration of peripheral immune cells decreases, whereas neurodegenerative changes increase in the brain (Serafini et al., 2004; Rottlaender and Kuerten, 2015). Currently, clinical treatment for MS is not ideal. Disease-modifying therapies have been shown to be beneficial to MS patients and usually focus on recovery from relapses and slowing the progression. However, these therapies have serious side effects and do not inhibit the progressive increase in neurological disability. Therefore, more research is needed to develop effective treatment for MS patients.

MECHANISMS OF NLRP3 INFLAMMASOME ACTIVATION

NLRP3 inflammasome is the most widely studied inflammasome. However, the mechanism underlying its activation remains to be elucidated. The canonical activation pathway includes a priming step (signal 1) and an activating step (signal 2) (**Figure 2**) (Bauernfeind et al., 2009; Kelley et al., 2019). In the priming step, stimuli interact with the Toll-like receptor (TLR)-adaptor molecule myeloid differentiation primary response 88 (MyD88), interleukin-1 receptor (IL-1R) and/or cytokine receptors, such as the tumor necrosis factor receptor (TNFR), thus activating the nuclear factor kappa B (NF-kB) pathway, which increases the expression levels of NLRP3 protein and pro-IL-1β (Latz et al., 2013). Post-translational modifications (PTMs) of NLRP3 protein are crucial to NLRP3 inflammasome activation. Once the NLRP3 protein is stimulated by signal 2, it begins to undergo deubiquitination and phosphorylation, which allows it to oligomerize and form the NLRP3 inflammasome (He et al., 2016a; Jo et al., 2016). In the activating step, many DAMPs and PAMPs can promote the assembly and activation of the NLRP3 inflammasome, which causes the formation of cleaved caspase-1, inducing the release of IL-1β and IL-18 and pyroptosis (Kayagaki et al., 2015; Shi et al., 2015; Liu et al., 2016). Several regulatory mechanisms are involved in the canonical activation pathway. For example, VSIG4 is reported to mediate the inhibition of *Nlrp3* and *Il-1β* at the transcriptional level (Huang et al., 2019). In addition, NEK7 and DDX3X are thought to bind to the NLRP3 protein, which is crucial for NLRP3 inflammasome formation. DDX3X is an ATPase/RNA helicase of the DEAD-box family that directly binds to the NLRP3 protein. Research has reported that the knockdown of *Ddx3x* in peritoneal macrophages inhibits NLRP3 inflammasome activation and pyroptosis (Samir et al., 2019). Studies found that AKT could block the interaction between DDX3X and NLRP3 by phosphorylating DDX3X. Alternatively, AKT could also directly interact with NLRP3, thus inhibiting NLRP3 oligomerization (Zhao et al., 2020; Guo et al., 2021). NEK7 binds and bridges the NLRP3 protein, triggering NLRP3 inflammasome activation, which is affected by the status of NLRP3 S803, a site that is phosphorylated after priming and later dephosphorylated after activation (Sharif et al., 2019; Niu et al., 2021). A recent study showed that TRIM65, an E3 Ubiquitin Ligase, can interact with the NACHT domain of NLRP3 and promote ubiquitination of lys48 and lys63 of NLRP3, thus inhibiting the NEK7-NLRP3 interaction and suppressing the activation of NLRP3 inflammasome (Tang et al., 2021). In addition, misshapen (Msn)/NIK-related kinase 1 (MINK1) interacts with the NLRP3 LRR domain, inducing the phosphorylation of Ser725 and priming the activation of the NLRP3 inflammasome (Zhu et al., 2021). Moreover, research has demonstrated a negative feedback regulation between caspase-1 and MyD88, which may suggest self-regulation of the body (Avbelj et al., 2021). NLRP3 inflammasome activation can promote the formation of GSDMD-N, inducing pyroptosis. Gao et al. reported that TRIM21, a tripartite motif protein, binds to GSDMD *via* its PRY-SPRY domain, and positively regulates GSDMD-dependent pyroptosis. It maintains stable expression of GSDMD in resting cells, while inducing GSDMD-N aggregation during pyroptosis (Gao et al., 2022).

Several stimuli can activate the NLRP3 inflammasome, and it is impossible for NLRP3 inflammasome to directly bind to the stimulatory factors. These stimuli may generate major activation signals, triggering activation of the NLRP3 inflammasome. Many related studies have proposed some major activation signals, such as ion fluctuations, dysfunction of mitochondria, lysosomal disruption, and Golgi dispersal (Song et al., 2017; Shao et al., 2021). This is discussed in detail in the following sections.

The ion fluctuations involve K+, Ca2+, and Cl–. There is copious extracellular ATP due to tissue damage and immune cells activation during inflammation, and high concentrations of extracellular ATP activate P2X7R, which induces K+ efflux and then recruits Pannexin-1 to release intracellular ATP (Gombault et al., 2012; Bartlett et al., 2014; Di Virgilio et al., 2017). Moreover, two K+ channels, two-pore domain weak inwardly rectifying K+ channel 2 (TWIK2) and tandem pore domain halothane-inhibited K+ channel 1 (THIK1), have been reported to response to ATP, and regulate NLRP3 inflammasome activation (Di et al., 2018; Drinkall et al., 2022). Subsequently, the triggered K+ efflux can promote NEK7 to interact with NLRP3 *via* the catalytic domain of NEK7 and the LRR domain of NLRP3 (He et al., 2016b). Research has reported that a decrease in cytosolic K+ level triggers the activation of the NLRP3 inflammasome (Muñoz-Planillo et al., 2013). A type of K+ channel inhibitor has also been found to greatly inhibit NLRP3 inflammasome activation (Lamkanfi and Dixit, 2009). Ca2+ fluctuations have a crucial effect on the activation of NLRP3 inflammasome by triggering mitochondrial dysfunction. In detail, influent Ca2+ and the Ca2+ released from the stimulated endoplasmic reticulum can be transported

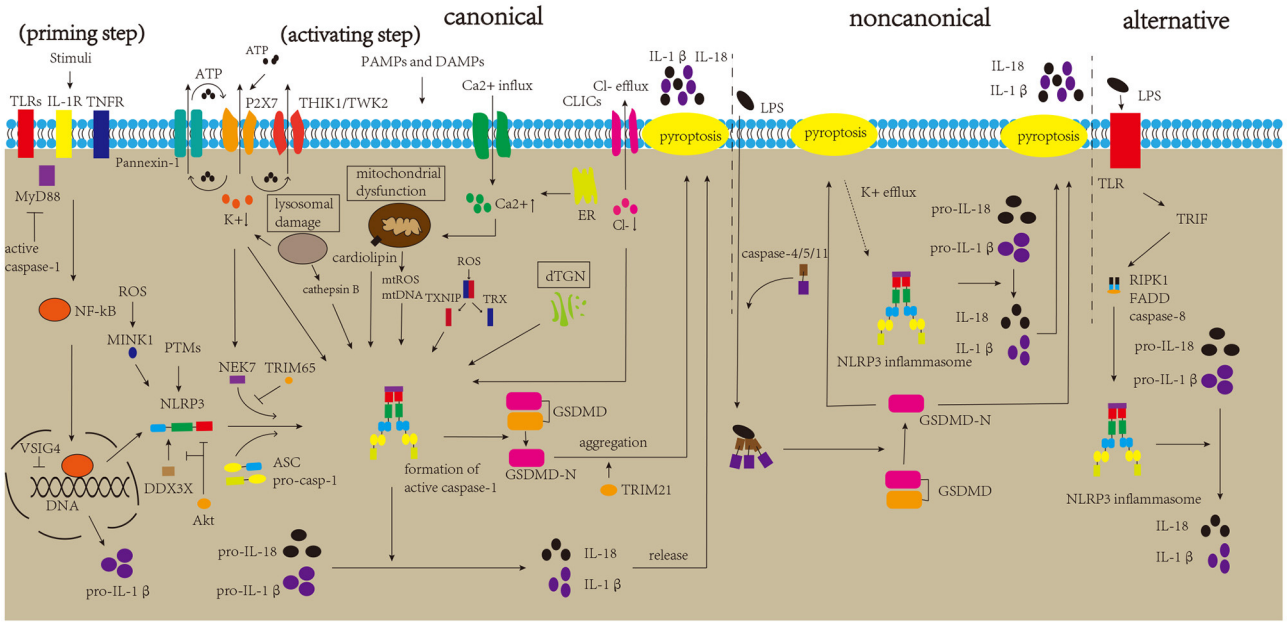

FIGURE 2 | Mechanisms of NLRP3 inflammasome activation. The canonical activation pathway of the NLRP3 inflammasome includes priming and activating step. In the priming step, stimulatory factors can bind to TLRs and other molecules, promoting the production of NLRP3 and pro-IL-1β. After priming, DAMPs and PAMPs can generate major activation signals, such as ion fluctuations, mitochondrial dysfunction, lysosomal damage, and dTGN, which affect the assembly and activation of the NLRP3 inflammasome. The activated NLRP3 inflammasome triggers the maturation of pro-caspase-1 into active caspase-1. Caspase-1 can induce the maturation and release of IL-1β and IL-18 and pyroptosis, thereby aggravating neuroinflammation. The non-canonical pathway is mediated by caspase-4/5/11, which directly sense cytosolic LPS, and K+ efflux due to pyroptosis can trigger NLRP3 inflammasome activation. The alternative pathway is mediated by the TLR4-TRIF-RIPK1-FADD-caspase-8 signaling pathway, triggering NLRP3 inflammasome activation.

into the mitochondria through uniporters to depolarize the mitochondrial membrane, activating voltage-gated channels of the mitochondria. Subsequent entry of many ions and metabolites trigger the production and release of reactive oxygen species (ROS) (Horng, 2014; Shenker et al., 2015). A recent study demonstrated that the transient receptor potential vanilloid type 1 (TRPV1) channel could regulate the activation of NLRP3 inflammasome by affecting Ca2+ influx. Moreover, its deletion suppressed NLRP3 inflammasome activation, thereby alleviating experimental autoimmune encephalomyelitis (EAE, a common animal model of MS) (Zhang et al., 2021). BAPTA-AM, a Ca2+ chelator, suppresses activation of the NLRP3 inflammasome (Wu et al., 2019). In addition, NLRP3 agonists have been found to induce Ca2+ signaling, triggering NLRP3 inflammasome activation (Murakami et al., 2012). A previous study suggested that the substitution of extracellular Cl- with gluconate increases the maturation and secretion of IL-1β (Verhoef et al., 2005). Levels of cytosolic Cl- were found to be reduced upon NLRP3 inflammasome activation, and inhibition of the Cl- channel could suppress NLRP3 inflammasome activation (Compan et al., 2012; Daniels et al., 2016). Mitochondrial dysfunction plays an important role in the activation of the NLRP3 inflammasome. Research has reported that stimulation of the NLRP3 inflammasome causes mitochondrial dysfunction, which leads to the production and release of mitochondrial ROS (mtROS) and the release of mitochondrial DNA (mtDNA) into the cytoplasm. Subsequently, mtROS can oxidize mtDNA, and mtDNA can be recognized by the NLRP3 inflammasome, leading to its activation (Shimada et al., 2012; Zhong et al., 2018; De Gaetano et al., 2021). Additionally, cardiolipin, which is located in the mitochondria, triggers NLRP3 inflammasome activation (Iyer et al., 2013). Under normal conditions, the thioredoxin interaction protein (TXNIP) and thioredoxin (TRX) bind to each other. Once the level of ROS increases, TRX oxidizes itself to remove ROS, along with the separation of TRX and TXNIP. The separated TXNIP can bind to NLRP3, triggering NLRP3 inflammasome activation. ROS have also been shown to promote the interaction between MINK1 and NLRP3 (Zhu et al., 2021). In addition, the ensuing inflammatory response recruits immune cells to increase ROS production, which suggests a feedback loop between ROS and the NLRP3 inflammasome (Franchi et al., 2009; Dominic et al., 2022). However, a few studies have reported that ROS are not necessary for this activation (Gabelloni et al., 2013; Gurung et al., 2015); therefore, the exact mechanism of mitochondrial dysfunction in the activation of the NLRP3 inflammasome requires further studies. Lysosomal rupture triggers the release of lysosomal contents, thereby triggering NLRP3 inflammasome activation (Halle et al., 2008; Hornung et al., 2008). Among lysosomal contents, cathepsin B is considered important for NLRP3 inflammasome activation. CA-074-Me suppresses NLRP3 inflammasome activation by inhibiting cathepsin B (Hornung et al., 2008). Besides that, it has

been reported that ruptured lysosomes could trigger K+ efflux, thus promoting NLRP3 inflammasome activation (Muñoz-Planillo et al., 2013). Moreover, research has demonstrated that stimuli can induce the disassembly of the trans-Golgi network (TGN), and dispersed TGN (dTGN) can recruit NLRP3 proteins *via* ionic bonding between phosphatidylinositol-4-phosphate (PtdIns4P, negatively charged, on the dTGN) and a polybasic region (on the NLRP3 protein), then inducing the assembly and activation of the NLRP3 inflammasome (Chen and Chen, 2018; Shao et al., 2021).

Apart from the canonical activation pathway, NLRP3 inflammasome is also activated *via* non-canonical and alternative pathways (**Figure 2**). Caspase-11 in mice was found to directly sense cytosolic lipopolysaccharide (LPS) and lead to the formation of pores in the plasma membrane, inducing pyroptosis and K+ efflux, thus triggering non-canonical NLRP3 inflammasome activation without the involvement of caspase-1 (Kayagaki et al., 2011; Hagar et al., 2013; Ramirez et al., 2018). Similarly, studies have demonstrated that caspase-4 and caspase-5 in humans promote non-canonical activation by directly binding to cytosolic LPS (Shi et al., 2014; Casson et al., 2015). Besides that, the involvement of caspase-8 in NLRP3 alternative activation also draws our attention, which is mediated by the TLR4-TRIF-RIPK1-FADD-caspase-8 signaling pathway (Gurung et al., 2014; Gurung and Kanneganti, 2015; Gaidt et al., 2016). Recently, Zhang et al. reported the important role of the caspase-8-dependent inflammasome in CNS inflammation (Zhang et al., 2018).

There is still a lot of unknown information about the mechanisms of NLRP3 inflammasome activation. For example, the temporal and spatial distribution of NLRP3 inflammasome after activation, the contradictory results of major activation signals in NLRP3 inflammasome activation, induction of activation after the generation of major activation signals, and the mechanistic details of non-canonical and alternative activation pathways.

NLRP3 INFLAMMASOME IN THE PATHOGENESIS/PATHOPHYSIOLOGY OF MS

Gene Polymorphisms of NLRP3 Signaling Pathway Molecules in MS

The NLRP3 inflammasome has been found to exert important effects in a myriad of diseases (Bonomini et al., 2019; Cheng et al., 2020; Yu et al., 2020). Occurrence of MS is closely related to the NLRP3 inflammasome (Gris et al., 2010; Olcum et al., 2020). Recent research has revealed that alterations in genes of NLRP3-related molecules are associated with susceptibility to MS. A study analyzed the association of SNPs of NLRP3 (rs-10754558, rs-35829419, rs-3806265, rs-4612666) with susceptibility to MS and revealed the pivotal role of NLRP3 polymorphisms in MS (Imani et al., 2018). Moreover, functional genetic variants in NLRP3 (Q705K) are associated with the severity of MS (Soares et al., 2019). In addition to NLRP3 genes, alterations in the gene expression of *PYCARD* and *CASP1* were reported in MS patients who initially presented with the clinically isolated syndrome, which showed an association between them and MS (Hagman et al., 2015). Mutations in the downstream cytokines have also been studied. Research has found that there is no relationship between the polymorphisms of IL-1β−511 (rs16944) and IL-1β +3,953 (rs1143634) and the risk of MS; however, further studies revealed that early-onset MS had a higher association with heterozygosity of rs16944 than with homozygosity of rs16944 in IL-1β (Huang et al., 2013; Isik et al., 2013). Soares et al. analyzed SNPs distribution in different clinical phenotypes of MS and found that variants of−511C>T could result in more frequent in MS (Soares et al., 2019). There are conflicting results regarding the role of IL-18 polymorphisms in MS. Research has revealed that polymorphisms in IL18−607 C/A are not significant, while polymorphisms at position−137 are related to MS risk. However, another study found that polymorphisms of the IL-18−137C/G gene were insignificant, while IL-18−607C/A gene polymorphisms were a potential genetic risk factor for susceptibility to MS (Karakas Celik et al., 2014; Orhan et al., 2016). A recent study analyzed gene polymorphisms of IL-18 and reported that the genotype of rs1946518 was markedly different between MS patients and the control group (Jahanbani-Ardakani et al., 2019).

NLRP3 Inflammasome-Related Molecules in MS

NLRP3 inflammasome-related molecules are involved in the pathogenesis of MS. Studies have reported increased expression levels of NLRP3 and IL-1β genes in MS plaques and elevated levels of ASC, caspase-1, and IL-18 in the sera of MS patients (Keane et al., 2018; Voet et al., 2018). In EAE, the expression levels of NLRP3 mRNA and protein were increased (Gris et al., 2010; Ke et al., 2017), and compared to the wild-type mice, *Nlrp3*$^{-/-}$ mice showed reduced numbers of Th1 and Th17 cells in the spinal cord and peripheral lymphoid tissues and markedly mild EAE (Gris et al., 2010; Inoue et al., 2012a). Recently, it was reported that thymic stromal lymphopoietin (TSLP) could directly induce NLRP3 expression through phosphorylation of Janus kinase (JAK) 2, and *Tslpr*$^{-/-}$ mice showed decreased NLRP3 expression and EAE scores (Yu et al., 2021). Zhang et al. (2018) reported that a deficiency of microglial ASC could attenuate the expansion of T cells and the infiltration of neutrophil, which suggests the important role of ASC in EAE. In addition, the expression of caspase-1 was found to increase at the mRNA and protein levels (Ke et al., 2017; Bai et al., 2018), and inhibition of caspase-1 could suppress inflammasomes activation, thus attenuating the severity of EAE (Ahmed et al., 2002; McKenzie et al., 2018). Furthermore, a previous study analyzed the severity of EAE in *Asc*$^{-/-}$ and *caspase-1*$^{-/-}$ models and demonstrated that *Asc*$^{-/-}$ mice showed a decreased number of MOG-specific T cells in the lymph nodes, delayed disease progression, and reduced clinical scores (Shaw et al., 2010). In addition, *Asc*$^{-/-}$ mice were more protected from EAE progression than *caspase-1*$^{-/-}$ mice.

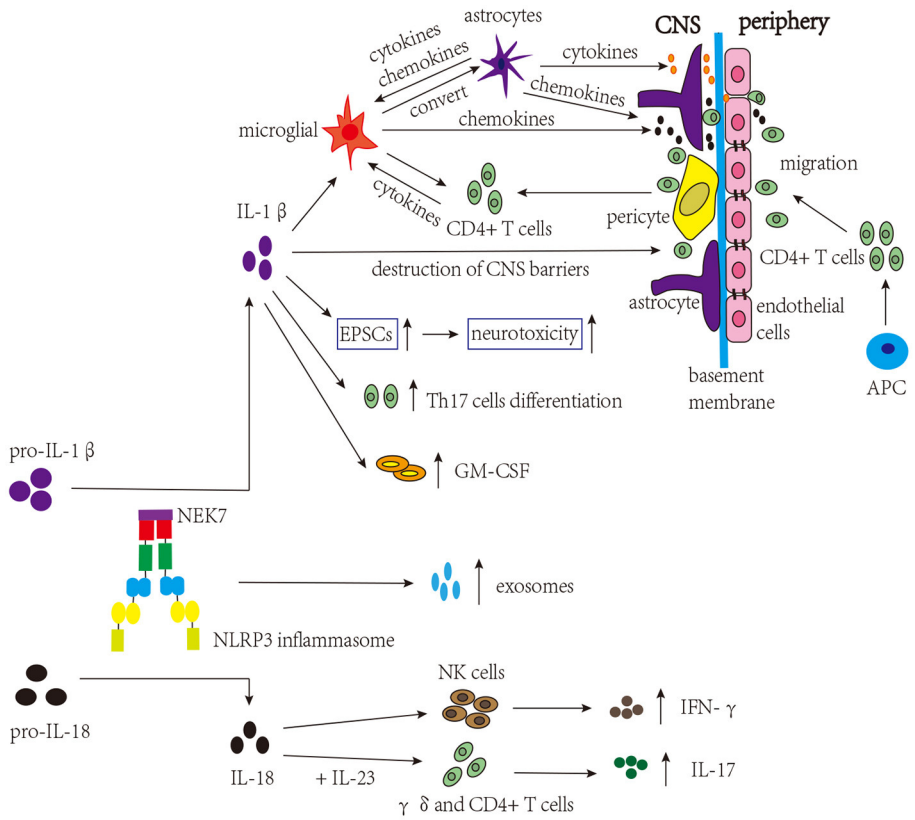

FIGURE 3 | NLRP3 inflammasome-related molecules are involved in the pathogenesis of MS. The NLRP3 inflammasome induces the migration of CD4+ T cells into the CNS and release of exosomes. IL-1β activates microglia, which present self-antigens to activate infiltrated CD4+ T cells, thereby amplifying neuroinflammation. Microglia can convert astrocytes to cytotoxic A1 phenotype and release chemokines to recruit CD4+ T cells. Activated astrocytes release proinflammatory cytokines and chemokines, affecting microglia, tight junctions of endothelial cells, and the infiltration of CD4+ T cells. IL-1β promotes the destruction of CNS barriers, facilitating the infiltration of CD4+ T cells. IL-1β can also increase the levels of EPSCs, contributing to the severity of MS. Moreover, IL-1β can increase the expression of GM-CSF and trigger the differentiation of Th17 cells, which are involved in the pathogenesis of MS. In addition, combined with IL-23, IL-18 can trigger γδ and CD4 + T cells to release innate IL-17, amplifying autoimmunity. IL-18 can also induce the production of IFN-γ by NK cells.

IL-1β and IL-18 in MS

Many studies have focused on the involvement of IL-1β and IL-18 in MS (**Figure 3**). As mentioned above, in the early stage of MS, the loss of integrity of CNS barriers can cause the infiltration of peripheral immune cells, and IL-1β promotes the destruction of CNS barriers (Kermode et al., 1990; Paul and Bolton, 1995; Paré et al., 2018). Briefly, immune mediators cause dysregulation of junctional components (tight junctions and adherens junctions) of CNS barriers, and the secretion of proinflammatory cytokines further triggers the infiltration of peripheral immune cells (Alvarez et al., 2011). Both CNS astrocytes and endothelial cells are involved in this process, and activated astrocytes can release proinflammatory cytokines that damage the tight junctions of endothelial cells. In addition, chemokines released by activated astrocytes can recruit leukocytes into the CNS, which is involved in the development of MS (Dong and Benveniste, 2001; Ching et al., 2007; Argaw et al., 2012). These proinflammatory cytokines and chemokines can also activate microglia (Correale and Farez, 2015). Microglia, which can be activated by IL-1β, are considered to be a kind of APCs that activate infiltrated CD4+ T cells, amplifying neuroinflammation. Besides that, microglia secrete chemokines that recruit immune cells. In turn, infiltrated CD4+ T cells secrete proinflammatory cytokines to activate microglia (Ferrari et al., 2004; Mallucci et al., 2015). According to existing research, microglia, astrocyte, and CD4+ T cells are the major cell types involved in NLRP3 inflammasome activation in MS. Studies have shown that the proportion of microglia expressing NLRP3 and IL-1β is positively associated with the degree of demyelination in MS patients (Malhotra et al., 2020). Furthermore, after activation, the NLRP3 inflammasome in activated microglia converts astrocytes to the neurotoxic A1 phenotype in MS, aggravating cognitive deficits (Hou B. et al., 2020). Tibolone and sinomenine were reported to alleviate astrocytic and microglial reactions and mobilization, respectively, decreasing NLRP3 inflammasome activation and EAE severity, which further supports the pathogenic role of the NLRP3 inflammasome in MS (Kiasalari et al., 2021; Mancino et al., 2022). Excitatory neurotransmitters can induce excitatory postsynaptic currents (EPSCs), which promote neurotoxicity and are involved in MS. IL-1β can increase the level of EPSCs in

corticostriatal slice cultures and cerebellum and contribute to the severity of EAE (Gentile et al., 2013; Mandolesi et al., 2013). In addition, it was found that IL-1β could promote the expression of granulocyte-macrophage colony-stimulating factor (GM-CSF) and the differentiation of Th17 cells, thus being involved in the pathogenesis of MS (Chung et al., 2009; Russi et al., 2018). However, a previous study found elevated levels of the IL-1β protein only in the spinal cord but not in the brain (McKenzie et al., 2018). In addition to IL-1β, the expression level of the IL-18 mRNA was increased in the CNS during EAE, and increased IL-18 levels could aggravate demyelination and neurodegeneration in EAE (Jander and Stoll, 1998; Shi et al., 2000; Jha et al., 2010). IL-18 triggers γδ and CD4+ T cells to release innate IL-17, thereby amplyfing autoimmunity (Lalor et al., 2011). Moreover, research has demonstrated that *Il-18*$^{-/-}$ mice are resistant to EAE, and the functions of natural killer (NK) cells and the production of autoreactive Th1 cells are impaired (Shi et al., 2000). Although studies on MS and EAE have shown the important role for IL-18 in the disease, the results are still conflicting. In one study, the symptoms of *Il-18*$^{-/-}$ mice were significantly alleviated, while in another study, the alleviation was not obvious, which may be related to the method of disease induction and generation of animal models (Gutcher et al., 2006; Gris et al., 2010). These studies indicate that IL-1β and IL-18 participate in the course of MS; however, further studies are needed to understand the exact mechanisms and target them for the treatment of MS.

NLRP3 Inflammasome and T Cells in MS

Research has demonstrated that the change in the population of T cells is perhaps not important in MS, whereas their migration into the CNS, induced by NLRP3 inflammasome, mediates the development of MS (Inoue et al., 2012a,b). As an important component of innate immunity, the NLRP3 inflammasome connects innate and adaptive immunity by promoting the production of IL-1β and IL-18, increasing the infiltration of peripheral immune cells into the CNS, and affecting the function of T and B cells. A previous study has proposed that Th cells need to be primed by APCs containing NLRP3 inflammasome before their migration into the CNS, and the study found several related results: (1). The number of immune cells migrating into the CNS was reduced in *Asc*$^{-/-}$ and *Nlrp3*$^{-/-}$ mice. (2). The expression levels of migration-related genes were increased by the NLRP3 inflammasome in Th cells and APCs. More specifically, increased levels of OPN, CCR2, and CXCR6 were found in Th cells, and the expression of α4β1 integrin, CCL2, CCL7, CCL8, and CXCL16 was increased in APCs. Interestingly, these components can bind with matched ligands or receptors (OPN-α4β1 integrin; CCR2-CCL2, CCL7, CCL8, and CXCL16; CXCR6-CXCL16) (Inoue et al., 2012a). Therefore, targeting immune cell migration is probably an effective treatment for MS. After migration, primed T cells play an important role in the course of the disease, and the NLRP3 inflammasome, in both T cells and microglia, has been reported to induce T cells to release proinflammatory cytokines involved in the pathogenesis of MS (Inoue et al., 2012a; Olcum et al., 2020).

NLRP3 Inflammasome and B Cells in MS

Although most studies suggest that MS is a kind of immune disease predominantly involving T cells, growing research has demonstrated that B cells are also crucial in the development of the disease (Li et al., 2018). The mechanism of action of B cells in MS includes four aspects: antigen presentation, cytokine production, antibody production, and ectopic lymphogenesis (Lazibat et al., 2018). B cells can present antigens to T cells, which is important for T cells activation, and the interaction between B and T cells is direct and two-way (Dalakas, 2008; Lazibat et al., 2018). Moreover, cytokines produced by B cells also exert effects on MS; for instance, B cells increase the expression of IL-6, activating Th17 responses in MS (Li et al., 2018). There are no antibodies in the CNS of healthy individuals; therefore, the presence of antibodies in the cerebrospinal fluid (CSF) of MS patients suggests that B cells are involved in the development of MS. Immunoglobulin G (IgG) and immunoglobulin M (IgM) oligoclonal bands could be used as biomarkers of MS and to predict the course of MS (Villar et al., 2005). Ectopic lymphogenesis refers to the formation of ectopic lymphoid structures, which are similar to follicles in MS patients and contain B cells; they are associated with EBV infection and may be involved in the development of MS (Serafini et al., 2004). Research has demonstrated a relationship between NLRP3 inflammasome and B cells. A recent study has reported that B cell-activating factor (BAFF) activates the NLRP3 inflammasome in B cells by triggering the binding of cIAP-TRAF2 to components of the NLRP3 inflammasome and by promoting K+ efflux and production of Src activity-dependent ROS (Lim et al., 2020). β-glucan and CpG, two major microbial antigens, have been reported to trigger NLRP3 inflammasome activation in circulating B cells. It was found that Dectin-1 activation *via* SYK and mammalian target of rapamycin (mTOR) participates in this process (Ali et al., 2017). Although there are many studies on the relationship between NLRP3 inflammasome and B cells, their relationship in MS is not clear, and further studies are needed to clarify the underlying mechanism.

NLRP3 Inflammasome and Exosomes in MS

In recent years, increasing attention has been paid to the role of exosomes, in tumors and autoimmune diseases, as important messengers in cell-to-cell communication (Prada et al., 2013; Paolicelli et al., 2019). It was revealed that exosomes could be selectively loaded with immunomodulatory proteins, which make them vital media for transmitting biological signals (Cypryk et al., 2018). Studies have found that damage to the CNS can induce inflammasomes activation, and exosome secretion is related to inflammasome activity. Therefore, exosomes induced by inflammasomes can promote the inflammatory response in recipient cells by transporting inflammasome-related components and other substances (de Rivero Vaccari et al., 2016; Hezel et al., 2017; Zhang et al., 2017). Zhang et al. (2017) found that inflammasome-derived exosomes could activate the NF-kB signaling pathway in recipient cells, thereby promoting an inflammatory response. Furthermore,

recent research has suggested that NLRP3 inflammasome activation in microglia could promote the secretion of exosomes and facilitate the transmission of α-synuclein in Parkinson's Disease (PD) (Si et al., 2021). However, a recent study found that exosomes loaded protective molecules can protect against cardiovascular damage (Pearce et al., 2021). The above studies indicate that exosomes may be protective or damaging, which is closely related to the environment and condition of the cells from which they originate. Besides that, the effects of exosomes on inflammasomes are also being studied. Research has demonstrated that exosomes/microvesicles from periodontal ligament stem cells of MS patients can inhibit NLRP3 inflammasome activation and attenuate the severity of EAE (Soundara Rajan et al., 2017). In detail, the effects of exosomes on NLRP3 inflammasome activation depend on the origin of exosomes, including inhibition (from plasma, mesenchymal stem cells, and macrophages) and promotion (from cancer cells) (Li et al., 2021). For example, Yan et al. (2020) reported that exosomes derived from human umbilical cord mesenchymal stem cells could inhibit NLRP3 inflammasome activation by releasing circular RNA homeodomain-interacting protein kinase 3 (circHIPK3). In addition, cancer-derived exosomes have been found to promote NLRP3 inflammasome activation in macropahges (Liang et al., 2020). However, the relationship between the NLRP3 inflammasome and exosomes in MS is not well-understood, and more studies are needed. Alteration of the components of these exosomes or inhibition of their transfer may be promising therapies for the treatment of MS.

NLRP3 Inflammasome and Intestinal Flora in MS

The intestinal flora has been a research hotspot in recent years. It develops from birth, is affected by a variety of internal and external factors, and reaches a relatively stable state of composition (Mueller et al., 2015). Recent studies have found that dyregulation of the intestinal flora affects the development of many diseases, including CNS disorders (Ochoa-Repáraz et al., 2009; Sommer and Bäckhed, 2013). This suggests the presence of communication between the intestine and CNS, which we refer to as gut-brain axis (GBA). GBA is a complicated bidirectional communication among the microbiota, gut and CNS, involving the microbiota and its metabolites, immune system, endocrine system, and nervous system (Rutsch et al., 2020). Gut microbiota can act on intestinal epithelial cells to regulate their growth and differentiation, expression of tight junction proteins, and permeability of mucous membranes, thereby maintaining the integrity of the intestinal epithelial barrier. Furthermore, the release of effector molecules following activation of the intestinal inflammasome by the intestinal flora can affect the CNS *via* the vagus nerve (Sharma et al., 2010; Rao et al., 2017). Many studies have suggested a relationship between intestinal flora and MS. The composition of intestinal flora in MS patients is different from that in healthy individuals. Studies have demonstrated that the abundance of Bacteroides decreased and that of Pseudomonas increased in the intestinal flora of MS patients, while the protein levels of NLRP3, ASC and cleaved caspase-1 increased in the CNS, and the mRNA levels of ASC and caspase-1 increased in the circulation (Pellegrini et al., 2020). It has been reported that overactivation of the NLRP3 inflammasome can promote the shift of intestinal flora to a proinflammatory phenotype, which in turn promotes neuroinflammation and neurodegeneration (Pellegrini et al., 2020). Mackay et al. reported that consumption of a high-fiber diet, which affects the host microbiota, increases the levels of IL-18 in the serum through GPR43 and GPR109A receptors, which are expressed on colonic epithelial cells, and trigger K+ efflux and Ca2+ mobilization in an NLRP3-dependent manner (Macia et al., 2015). Mechanistically, certain metabolites produced by the microbiota in the body can enter the bloodstream and directly affect peripheral immune cells. Alternatively, these metabolites can enter the brain through the bloodstream and affect immune cells in the CNS (Wikoff et al., 2009; Rothhammer et al., 2016), which is regulated by the NLRP3 inflammasome as an important component that bridges innate and adaptive immunity. However, the exact mechanism of interplay between the microbiota and NLRP3 inflammasome is currently unknown, as is the mechanism of the subsequent effects of this interaction on the CNS. A study proposed that the effect of the interaction between the microbiota and NLRP3 inflammasome on the CNS may be through regulation of the plasma level of the circHIPK2, which in turn affects astrocyte function (Zhang et al., 2019). Furthermore, the existence of GBA is further supported by a study showing improvement in severe constipation and other MS symptoms after fecal microbiota transplantation in three MS patients (Rutsch et al., 2020). Besides that, the use of probiotics or antibiotic cocktails could lead to attenuation of EAE (Colpitts et al., 2017; Camara-Lemarroy et al., 2018). Pertussis toxin is required for the induction of EAE and is a major virulence factor of *Bordetella pertussis*. A study demonstrated that pertussis toxin could trigger the activation of TLR4 and induce the formation of a pyrin-dependent inflammasome, which only leads to mild EAE in pyrin-, ASC-, or caspase-1-deficient models (Dumas et al., 2014). The above studies have shown a connection among intestinal flora, inflammasomes, and MS; however, the underlying mechanism is still unclear, and further research is needed to clarify the molecules, pathways, and organs involved. This will be an attractive research area for the development of MS treatment in the future.

NLRP3 INFLAMMASOME AS A BIOMARKER IN MS

Studies have shown that NLRP3 inflammasome-related components can be used as biomarkers for MS. For example, NLRP3 protein was found to be overexpressed in the monocytes of MS (Malhotra et al., 2020) and neuromyelitis optica spectrum disorders patients (Peng et al., 2019), compared to those of healthy individuals. In addition, elevated levels of ASC and caspase-1 were found in the sera of MS patients, and ASC was considered to be more sensitive and specific for the diagnosis of MS severity owing to its 90% specificity (Keane et al., 2018). A recent study showed that serum caspase-1 levels were elevated

during relapse in MS patients, suggesting that caspase-1 may act as a biomarker of MS disease activity (Beheshti et al., 2020).

As the downstream effectors of the NLRP3 inflammasome, IL-1β and IL-18 can be used as potential biomarkers for MS. The results of studies on the expression level of IL-1β in the sera and CSF of MS patients are contradictory, and the level of IL-1β was increased or not detected in different studies (Maimone et al., 1991; Peter et al., 1991; Dujmovic et al., 2009). However, the expression of IL-1β in the CSF is associated with cortical pathology in the early stage of MS and causes neurodegeneration, following neuroinflammation (Seppi et al., 2014). One study reported increased serum IL-18 levels in MS patients, and several other studies also reported increase in IL-18 levels in the sera and CSF of MS patients (Losy and Niezgoda, 2001; Chen et al., 2012; Jahanbani-Ardakani et al., 2019).

In recent years, the neurofilament protein has been considered a promising biomarker for MS. The neurofilament protein is a cytoskeletal protein expressed in neurons, and it can be released into the blood and CSF after the damage of neurons (Khalil et al., 2018; van Lieverloo et al., 2019). Serum neurofilament protein is a useful biomarker for progressive MS and pediatric MS, and its level is associated with the risk of disability in MS (Kapoor et al., 2020; Manouchehrinia et al., 2020; Reinert et al., 2020). It consists of three isotypes: a neurofilament light (NfL) chain, neurofilament intermediate (NfM) chain, and neurofilament heavy (NfH) chain. Elevated NfL levels in the CSF occur in all stages of MS, and their levels are correlated with the MS severity score (Salzer et al., 2010; Teunissen and Khalil, 2012). In addition, interleukin-1 receptor antagonist (IL-1RA) was considered a novel biomarker in MS patients and was associated with NfL in a separate cohort (Blandford et al., 2021). Neurofilament degradation is one of the main pathological damage caused by chronic exposure to *n*-hexane in humans (Huang, 2008; Wang et al., 2008). A recent study found that glibenclamide ameliorated 2,5-hexanedione (the toxic metabolite of *n*-hexane)-induced axon degeneration by inhibiting NLRP3 inflammasome activation, thus suppressing NfL reduction in rats (Hou L. et al., 2020). This suggests a relationship between the NLRP3 inflammasome and NfL; however, their exact relationship in MS is not fully understood, and further studies are needed.

TARGETING NLRP3 INFLAMMASOME-RELATED PATHWAYS FOR THE TREATMENT OF MS

In this section, we briefly summarize therapies targeting NLRP3 inflammasome-related pathways for the treatment of MS (**Table 1**).

Anti-IL-1 Therapies

IL-1β contributes to the progression of MS. Related therapies that have been studied to date include IL-1β-specific neutralizing antibody (canakinumab), IL-1 receptor antagonist (anakinra), and soluble decoy receptor for IL-1α and IL-1β (rilonacept), and the first two have been used in clinical practice (Chakraborty et al., 2012; Dinarello et al., 2012; Cavalli and Dinarello, 2018; Abbate et al., 2020). In addition, studies have demonstrated that cladribine can attenuate IL-1β-induced EPSCs and is beneficial for the treatment of MS (Musella et al., 2013). However, the use of anti-IL-1 therapies is costly, and their penetration across brain tissues is poor. Moreover, IL-1β is not the only downstream cytokine of the NLRP3 inflammasome; therefore, targeting upstream molecules of the NLRP3 inflammasome is perhaps more effective than anti-IL-1 therapies.

Targeting Upstream Major Activation Signals

It has been reported that β-hydroxybutyrate can attenuate K+ efflux and suppress oligomerization of NLRP3 and ASC, thus inhibiting NLRP3 inflammasome activation (Youm et al., 2015). Pannexin1 and P2X7R mediate K+ efflux. Probenecid, which blocks Pannexin1, attenuates NLRP3 inflammasome activation (Jian et al., 2016). Brilliant blue G is a P2X7R antagonist, and it suppresses neuroinflammation in subarachnoid hemorrhage animal models, which may be associated with the inhibition of K+ efflux (Chen et al., 2013). Therapies targeting Ca2+ and Cl- have also been studied, including U73122 and IAA-94 (Diaz et al., 2013; Potenzieri et al., 2020). However, therapies targeting ion fluctuations can produce unavoidable side effects caused by the dysregulation of ion-related reactions. Therefore, although therapies targeting ion fluctuations are effective in the experiment, their usage in clinical practice may be limited. ROS scavengers, including N-acetyl-L-cysteine (2R,4R)-4-aminopyrrolidine-2,4-dicarboxylate (APDC), and Mito-TEMPO, were found to inhibit ROS production and attenuate NLRP3 inflammasome activation (Dostert et al., 2008; Trnka et al., 2009). In addition, Yu et al. found that Bixin could scavenge ROS through the NRF2 signaling pathway and attenuate the severity of EAE (Yu et al., 2020). Studies have suggested that mtROS can damage NADPH oxidase, causing inflammasome activation (Dostert et al., 2008; Bordt and Polster, 2014). However, similar to ion fluctuations, mtROS are also involved in many biological reactions; thus, the inhibition of mtROS cause side effects, and therapies targeting mtROS require further study. It has been reported that cathepsin B released from lysosomes plays a role in NLRP3 inflammasome activation, and CA-074-Me attenuates NLRP3 inflammasome activation by inhibiting cathepsin B (Buttle et al., 1992; Hornung et al., 2008). In addition, gemcitabine and 5-fluorouracil have been shown to contribute to the activation of NLRP3 inflammasome, which is related to cathepsin B (Bruchard et al., 2013). Recently, research has demonstrated that curcumin can inhibit the release of ROS and cathepsin B, thereby inhibiting the progression of EAE (Hasanzadeh et al., 2020; Lu et al., 2020).

Targeting Upstream Regulatory Pathways

In addition to major activation signals, other regulatory mechanisms are involved in NLRP3 inflammasome activation. HU-308, a cannabinoid receptor 2 agonist, was reported to induce autophagy, thus attenuating NLRP3 inflammasome activation and severity of EAE (Shao et al., 2014). Moreover, a recent study found that caffeine can reduce NLRP3

TABLE 1 | Compounds targeting NLRP3 inflammasome-related pathways.

Classification	Target	Compound	Mechanism	References
Anti-IL-1 therapies	IL-1β	Canakinumab	IL-1β neutralizing antibody	Chakraborty et al., 2012; Dinarello et al., 2012
	IL-1β	Anakinra	IL-1 receptor antagonist	Dinarello et al., 2012; Cavalli and Dinarello, 2018
	IL-1β	Rilonacept	Soluble decoy receptor for IL-1	Dinarello et al., 2012; Abbate et al., 2020
	IL-1β	Cladribine	Decreases IL-1β-induced EPSCs	Musella et al., 2013
Upstream major activation signals	K+	β-hydroxybutyrate	Attenuates K+ efflux and oligomerization of NLRP3 and ASC	Youm et al., 2015
	K+	Probenecid	Blocks Pannexin1, which mediates K+ efflux	Jian et al., 2016
	K+	Brilliant blue G	A P2X7R antagonist, P2X7R is deemed to mediate K+ efflux	Chen et al., 2013
	Ca2+	U73122	A PLC inhibitor, can block oxaliplatin-induced intracellular Ca2+ influx	Potenzieri et al., 2020
	Cl-	IAA-94	blocks Cl- channels in cultured rabbit cardiomyocytes	Diaz et al., 2013
	Mitochondria	N-acetyl-L-cysteine, APDC	ROS inhibitors, decrease the production of IL-1β in THP1 cells	Dostert et al., 2008
	Mitochondria	MitoTEMPOL	An effective antioxidant, prevents lipid peroxidation and protects the mitochondria	Trnka et al., 2009
	Mitochondria	Bixin	Scavenges ROS through the NRF2 signaling pathway, inhibits EAE severity	Yu et al., 2020
	Lysosome	CA-074-Me	Causes selective inactivation of intracellular cathepsin B	Buttle et al., 1992; Hornung et al., 2008
	Lysosome	Gemcitabine, 5-fluorouracil	Induce the release of cathepsin B from lysosomes, thus triggering direct activation of the NLRP3 inflammasome	Bruchard et al., 2013
	Lysosome	Curcumin	Inhibits the release of ROS and cathepsin B, inhibits the progression of EAE	Hasanzadeh et al., 2020; Lu et al., 2020
Upstream regulatory pathways	Autophagy	HU-308	A cannabinoid receptor 2 agonist, induces autophagy	Shao et al., 2014
	Autophagy	Caffeine	Induces autophagy, inhibits NLRP3 inflammasome activation	Wang et al., 2022
	NO	CD47-Fc fusion protein	Increases the production of NO, thus reducing the level of IL-1β	Gao et al., 2016
	Post-translation modification	IFN-β	Induces the phosphorylation of STAT1, attenuating the severity of NLRP3 inflammasome-dependent EAE	Inoue et al., 2012b, 2016; Metwally et al., 2020
NLRP3 inflammasome-related components	NLRP3	MCC950	Binds to Walker B motif of the NACHT domain, inhibits ATPase activity of NLRP3, reduces the severity of EAE	Coll et al., 2019
	NLRP3	Bay11-7082	Binds to ATPase of NLRP3 NACHT domain, inhibits EAE severity	Lang et al., 2021
	NLRP3	Oridonin, RRx-001	Bind to cysteine 279 or 409 of NLRP3 in the NACHT domain, inhibit NEK7-NLRP3 interaction, attenuate EAE severity	He et al., 2018; Yang et al., 2020; Chen et al., 2021
	NLRP3	OLT1177	Inhibits NLRP3-ASC interaction by binding to ATPase of NLRP3 NACHT domain, ameliorates EAE severity	Sánchez-Fernández et al., 2019
	ASC	1,2,4-TTB	Inhibits oligomerization of ASC and NLRP3-ASC interaction, thus decreasing EAE scores	Pan et al., 2021
	ASC	IC100	Targets ASC and inhibits EAE progression	Desu et al., 2020
	Caspase-1	Ac-YVAD-CMK	A caspase-1 inhibitor, reduces the mRNA and protein levels of IL-1β	Mao et al., 2017
	Caspase-1	VX-765	A caspase-1 inhibitor, covalently modifies Cys285 of caspase-1	McKenzie et al., 2018
	GSDMD	Disulfiram	Covalently modifies Cys191/Cys192 in GSDMD, upregulates miR-30a expression in EAE	Zhao et al., 2016; Hu et al., 2020

inflammasome activation by inducing autophagy, thus attenuating the severity of EAE (Wang et al., 2022). It was found that the CD47-Fc fusion protein could reduce the production of NLRP3 inflammasome-induced IL-1β by promoting the production of NO, aiding to the treatment of EAE (Gao et al., 2016). In addition, as a first-line drug in the treatment of MS, IFN-β can induce the phosphorylation of STAT1, which mainly exerts therapeutic effects on NLRP3 inflammasome-dependent EAE (Inoue et al., 2012b, 2016; Metwally et al., 2020). However, the reactions involved in these regulatory mechanisms are more complicated, and side effects will inevitably occur, which means that therapies targeting molecules upstream of the NLRP3 inflammasome may not be as potent as directly targeting NLRP3 inflammasome-related components.

Targeting NLRP3 Inflammasome-Related Components

MCC950, a classic NLRP3 inhibitor, can bind to the Walker B motif of the NACHT domain of NLRP3 and inhibit ATPase activity, thereby reducing the severity of EAE (Coll et al., 2019). Furthermore, Bay11-7082 was found to interact with the ATPase of the NLRP3 NACHT domain and reduce EAE severity (Lang et al., 2021). The NEK7-NLRP3 interaction is important for activation of the NLRP3 inflammasome. Research has demonstrated that oridonin and RRx-001 can inhibit this interaction by binding to cysteine 279 of the NACHT domain of NLRP3 or covalently binding to cysteine 409 of NLRP3, thereby attenuating EAE severity (He et al., 2018; Yang et al., 2020; Chen et al., 2021). Besides that, it was reported that OLT1177 could interact with the ATPase of the NLRP3 NACHT domain, inhibiting NLRP3-ASC interaction and ameliorating EAE severity (Sánchez-Fernández et al., 2019). 1,2,4-TTB was found to inhibit the oligomerization of ASC and NLRP3-ASC interactions and reduce EAE scores (Pan et al., 2021). Recently, IC100 has been reported to target ASC and inhibit EAE progression (Desu et al., 2020). Caspase-1 is an effector of NLRP3 inflammasome activation, and several caspase-1 inhibitors have been reported. For example, Ac-YVAD-CMK, a caspase-1 inhibitors, decreases the mRNA and protein levels of IL-1β and improves the symptoms of PD models (Mao et al., 2017). Moreover, VX-765 can covalently modify Cys285 of caspase-1 for the treatment of inflammatory diseases (McKenzie et al., 2018). Research has reported that the level of GSDMD, which is crucial in pyroptosis, can be inhibited by disulfiram by upregulating miR-30a expression (Zhao et al., 2016). A recent study further showed that disulfiram covalently modified Cys191/Cys192 in GSDMD, thus blocking pore formation (Hu et al., 2020).

Taken together, there are many studies on therapies targeting NLRP3 inflammasome-related pathways. However, only a few drugs can be used clinically, and there are no drugs that can effectively cure MS. Therefore, further research is necessary, and studies on the NLRP3 inflammasome-related pathway can shed light on the treatment of MS patients.

THE INVOLVEMENT OF THE NLRP3 INFLAMMASOME IN NEURODEGENERATIVE DISEASES

In addition to MS, the NLRP3 inflammasome has important roles in neurodegenerative diseases such as Alzheimer's disease (AD), PD, and amyotrophic lateral sclerosis (ALS).

NLRP3 Inflammasome in AD

AD is a neurodegenerative disease with a very high prevalence, characterized by progressive loss of neurons and accumulation of extracellular amyloid beta (Aβ) (Piancone et al., 2021). The clinical manifestations of AD include dementia and cognitive dysfunction, which imposes a large burden on patients and their families (Swanton et al., 2018). Currently, the pathogenesis of AD is thought to be associated with the presence of amyloid plaques and neurofibrillary tangles, while neuroinflammation has also been found to be involved (DeTure and Dickson, 2019). Growing evidence suggests that the NLRP3 inflammasome is involved in the pathogenesis of AD. In 2008, a study reported that fibrillar Aβ could promote NLRP3 inflammasome activation, which was confirmed in subsequent studies (Halle et al., 2008). For example, amylin receptors participate in Aβ-induced NLRP3 inflammasome activation. Furthermore, Aβ can increase the level of ROS, which trigger NLRP3 inflammasome activation (Fu et al., 2017; Aminzadeh et al., 2018). Clinically, elevated expression levels of active caspase-1 and IL-1β can be found in AD patients (Blum-Degen et al., 1995; Heneka et al., 2013), which is related to the activation of the NLRP3 inflammasome. Further mechanistic studies were performed in the AD models. A study found that the levels of neuroinflammation and Aβ accumulation were reduced with concomitant improvement of neuronal function in NLRP3-deficient AD models (Heneka, 2017). Besides that, deletion of NLRP3 or caspase-1 in AD models was shown to decrease the levels of IL-1β and caspase-1 while promoting microglial differentiation to the M2 phenotype (Dempsey et al., 2017). The above studies have demonstrated the role of NLRP3 inflammasome activation in AD, but the underlying mechanisms still need to be explored.

NLRP3 Inflammasome in PD

PD is a common neurodegenerative disease characterized by a progressive loss of dopaminergic (DA) neurons in the substantia nigra and the formation of intracellular Lewy bodies by α-synuclein (Petrucci et al., 2014). The clinical manifestations of PD include typical motor symptoms and other non-motor symptoms; however, the underlying etiology is currently not clear. A previous study suggested the important role of the NLRP3 inflammasome in the pathogenesis of PD *in vitro* (Codolo et al., 2013), which is supported by a growing number of studies. In animal models, the levels of NLRP3 inflammasome-related molecules are increased, while deletion of NLRP3 could reduce the loss of DA neurons and improve motor dysfunction (Qiao et al., 2018; Lee et al., 2019). The involvement of the NLRP3 inflammasome in the pathogenesis of PD has also been reported in PD patients. A study reported increased expression levels of NLRP3 inflammasome-related molecules in PD patients;

however, in another study, it was found that although there was a difference in the expression level of NLRP3 in the sera of PD patients compared to those of controls, the levels of IL-1β and IL-18 were not significantly different (Zhang et al., 2016; Fan et al., 2020). Considering the important role of α-synuclein in the pathogenesis of PD, several studies have explored the relationship between α-synuclein and the NLRP3 inflammasome. Research has shown that α-synuclein can promote NLRP3 inflammasome activation in PD models, and further studies have revealed that α-synuclein increases the levels of cathepsin B and ROS, thus triggering NLRP3 inflammasome activation (Codolo et al., 2013; Chatterjee et al., 2020). Further studies are needed to explore the underlying mechanisms of the NLRP3 inflammasome in the pathogenesis of PD, which may shed light on the treatment of PD patients.

NLRP3 Inflammasome in ALS

ALS, a prevalent neurodegenerative disease, is characterized by the loss of motor neurons (Feng et al., 2021). ALS patients clinically present with a continuous aggravation of motor function loss until death. Mutations in Cu/Zn superoxide dismutase 1 (SOD1) have been found to be associated with ALS (Rosen et al., 1993). The etiology of ALS remains unclear, but the role of neuroinflammation and the NLRP3 inflammasome in ALS has received attention in recent years. Studies have found increased levels of NLRP3 and caspase-1 in astrocytes and the brains of ALS patients (Haidet-Phillips et al., 2011; Kadhim et al., 2016). Studies have used G93A-*SOD1* mutation models to simulate the pathogenesis of ALS. Research has revealed increased levels of NLRP3 inflammasome-related molecules and IL-1β in models, and genes knockout of caspase-1 and IL-1β can inhibit neuroinflammation (Johann et al., 2015; Lall and Baloh, 2017). Further studies are needed to explain these results and clarify the pathogenesis of ALS.

CONCLUSIONS

MS is an immune-mediated, demyelinating, neurodegenerative disease that occurs in the CNS. It predominantly affects young women and causes a huge social and economic burden. Nowadays, the underlying mechanism of MS is not fully understood, and there are still some limitations in the related diagnostics methods and therapies. In recent years, the role of inflammasomes in MS has received widespread attention. For the most widely studied NLRP3 inflammasome, we briefly introduced its composition, mechanisms of activation, and related research in MS, which may help us better understand its involvement in MS.

However, there are several unclear aspects of the NLRP3 inflammasome. For example, NLRP3 inflammasome activation is widely regulated, and it is necessary to clarify each step of the cascade of activation. Although there is a close relationship between the NLRP3 inflammasome and EAE, NLRP3 inflammasome-independent EAE also exists (Arnason, 1999). For example, 300 μg heat-killed mycobacteria was found to successfully induce EAE in $Asc^{-/-}$ or $Nlrp3^{-/-}$ animal models, while normal 200 μg Mtb mycobacteria could not (Inoue et al., 2012b). In addition, a previous study reported that aggressive immunization induces EAE in $caspase\text{-}1^{-/-}$ mice (Furlan et al., 1999). Therefore, the intensity of immunization has a great influence on the induction of EAE, which also suggests the important role of environmental factors in the heterogeneity of MS. A study proposed a possible mechanism for the development of NLRP3 inflammasome-independent EAE, which involves membrane-bound lymphotoxin-β receptor (LTβR) and CXC chemokine receptor 2 (CXCR2), but the exact mechanism is yet to be studied in depth (Inoue et al., 2016). Besides that, studies have shown that IFN-β, a long-used clinical first-line drug, is not therapeutically effective for some types of MS and EAE. Further mechanistic studies have identified IFN-β to have a therapeutic effect on NLRP3-dependent EAE models, which also reflects the heterogeneity of MS (Inoue et al., 2012b). Moreover, EAE mainly simulates MS through immune induction; however, there is no such artificial induction method of MS in patients which can fully simulate the heterogeneity and complexity of MS. Therefore, new and better animal models need to be developed. At present, relevant research on the role of the NLRP3 inflammasome in MS is mainly at the level of cells and animal models, and has not yet involved humans. Therefore, further in-depth studies are urgently required.

AUTHOR CONTRIBUTIONS

JF was responsible to conceive, design, and revise this review. YC wrote the original manuscript. HY and ZB completed the figures and tables. LW and LY searched and collected the related references. All authors contributed to the article and approved the submitted version.

FUNDING

This work was supported by the Outstanding Scientific Fund of Shengjing Hospital (to JF), Key Research and Development Program of Liaoning Province (No. 2020JH2/10300047 to JF), and National Natural Science Foundation of China (No. 81771271 to JF).

ACKNOWLEDGMENTS

We gratefully thank members of Feng's lab for their intellectual input.

REFERENCES

Abbate, A., Toldo, S., Marchetti, C., Kron, J., Van Tassell, B. W., and Dinarello, C. A. (2020). Interleukin-1 and the inflammasome as therapeutic targets in cardiovascular disease. *Circ. Res.* 126, 1260–1280. doi: 10.1161/CIRCRESAHA.120.315937

Ahmed, Z., Doward, A. I., Pryce, G., Taylor, D. L., Pocock, J. M., Leonard, J. P., et al. (2002). A role for caspase-1 and−3 in the pathology of experimental

allergic encephalomyelitis: inflammation versus degeneration. *Am. J. Pathol.* 161, 1577–1586. doi: 10.1016/S0002-9440(10)64436-7

Ali, M. F., Dasari, H., Van Keulen, V. P., and Carmona, E. M. (2017). Canonical stimulation of the NLRP3 inflammasome by fungal antigens links innate and adaptive B-lymphocyte responses by modulating IL-1beta and IgM production. *Front. Immunol.* 8, 1504. doi: 10.3389/fimmu.2017.01504

Alvarez, J. I., Cayrol, R., and Prat, A. (2011). Disruption of central nervous system barriers in multiple sclerosis. *Biochim. Biophys. Acta* 1812, 252–264. doi: 10.1016/j.bbadis.2010.06.017

Aminzadeh, M., Roghani, M., Sarfallah, A., and Riazi, G. H. (2018). TRPM2 dependence of ROS-induced NLRP3 activation in Alzheimer's disease. *Int. Immunopharmacol.* 54, 78–85. doi: 10.1016/j.intimp.2017.10.024

Argaw, A. T., Asp, L., Zhang, J., Navrazhina, K., Pham, T., Mariani, J. N., et al. (2012). Astrocyte-derived VEGF-A drives blood-brain barrier disruption in CNS inflammatory disease. *J. Clin. Invest.* 122, 2454–2468. doi: 10.1172/JCI60842

Arnason, B. G. (1999). Immunologic therapy of multiple sclerosis. *Annu. Rev. Med.* 50, 291–302. doi: 10.1146/annurev.med.50.1.291

Avbelj, M., Hafner-Bratkovič, I., Lainšček, D., Manček-Keber, M., Peternelj, T. T., Panter, G., et al. (2021). Cleavage-mediated regulation of Myd88 signaling by inflammasome-activated caspase-1. *Front. Immunol.* 12, 790258. doi: 10.3389/fimmu.2021.790258

Awad, F., Assrawi, E., Louvrier, C., Jumeau, C., Georgin-Lavialle, S., Grateau, G., et al. (2018). Inflammasome biology, molecular pathology and therapeutic implications. *Pharmacol. Ther.* 187, 133–149. doi: 10.1016/j.pharmthera.2018.02.011

Bai, X.-Y., Wang, X.-F., Zhang, L.-S., Du, P.-C., Cao, Z., and Hou, Y. (2018). Tetramethylpyrazine ameliorates experimental autoimmune encephalomyelitis by modulating the inflammatory response. *Biochem. Biophys. Res. Commun.* 503, 1968–1972. doi: 10.1016/j.bbrc.2018.07.143

Bartlett, R., Stokes, L., and Sluyter, R. (2014). The P2X7 receptor channel: recent developments and the use of P2X7 antagonists in models of disease. *Pharmacol. Rev.* 66, 638–675. doi: 10.1124/pr.113.008003

Bauernfeind, F. G., Horvath, G., Stutz, A., Alnemri, E. S., MacDonald, K., Speert, D., et al. (2009). Cutting edge: NF-kappaB activating pattern recognition and cytokine receptors license NLRP3 inflammasome activation by regulating NLRP3 expression. *J. Immunol.* 183, 787–791. doi: 10.4049/jimmunol.0901363

Beheshti, M., Salehi, Z., Abolfazli, R., Shirzad, H., and Izad, M. (2020). Increased level of caspase-1 in the serum of relapsing-remitting multiple sclerosis (RRMS) patients. *Iran. J. Allergy Asthma Immunol.* 19, 534–538. doi: 10.18502/ijaai.v19i5.4470

Blandford, S. N., Galloway, D. A., Williams, J. B., Arsenault, S., Brown, J., MacLean, G., et al. (2021). Interleukin-1 receptor antagonist: an exploratory plasma biomarker that correlates with disability and provides pathophysiological insights in relapsing-remitting multiple sclerosis. *Mult. Scler. Relat. Disord.* 52, 103006. doi: 10.1016/j.msard.2021.103006

Blum-Degen, D., Müller, T., Kuhn, W., Gerlach, M., Przuntek, H., and Riederer, P. (1995). Interleukin-1 beta and interleukin-6 are elevated in the cerebrospinal fluid of Alzheimer's and *de novo* Parkinson's disease patients. *Neurosci. Lett.* 202, 17–20. doi: 10.1016/0304-3940(95)12192-7

Bonomini, F., Dos Santos, M., Veronese, F., and Rezzani, R. (2019). NLRP3 inflammasome modulation by melatonin supplementation in chronic pristane-induced lupus nephritis. *Int. J. Mol. Sci.* 20, 3466. doi: 10.3390/ijms20143466

Bordt, E. A., and Polster, B. M. (2014). NADPH oxidase- and mitochondria-derived reactive oxygen species in proinflammatory microglial activation: a bipartisan affair? *Free Radic. Biol. Med.* 76, 34–46. doi: 10.1016/j.freeradbiomed.2014.07.033

Browne, P., Chandraratna, D., Angood, C., Tremlett, H., Baker, C., Taylor, B. V., et al. (2014). Atlas of multiple sclerosis 2013: a growing global problem with widespread inequity. *Neurology* 83, 1022–1024. doi: 10.1212/WNL.0000000000000768

Brownlee, W. J., Swanton, J. K., Altmann, D. R., Ciccarelli, O., and Miller, D. H. (2015). Earlier and more frequent diagnosis of multiple sclerosis using the McDonald criteria. *J. Neurol. Neurosurg. Psychiatry* 86, 584–585. doi: 10.1136/jnnp-2014-308675

Broz, P., and Dixit, V. M. (2016). Inflammasomes: mechanism of assembly, regulation and signalling. *Nat. Rev. Immunol.* 16, 407–420. doi: 10.1038/nri.2016.58

Bruchard, M., Mignot, G., Derangère, V., Chalmin, F., Chevriaux, A., Végran, F., et al. (2013). Chemotherapy-triggered cathepsin B release in myeloid-derived suppressor cells activates the Nlrp3 inflammasome and promotes tumor growth. *Nat. Med.* 19, 57–64. doi: 10.1038/nm.2999

Buttle, D. J., Murata, M., Knight, C. G., and Barrett, A. J. (1992). CA074 methyl ester: a proinhibitor for intracellular cathepsin B. *Arch. Biochem. Biophys.* 299, 377–380. doi: 10.1016/0003-9861(92)90290-d

Calahorra, L., Camacho-Toledano, C., Serrano-Regal, M. P., Ortega, M. C., and Clemente, D. (2022). Regulatory cells in multiple sclerosis: from blood to brain. *Biomedicines* 10, 335. doi: 10.3390/biomedicines10020335

Camara-Lemarroy, C., Metz, L., and Yong, V. (2018). Focus on the gut-brain axis: Multiple sclerosis, the intestinal barrier and the microbiome. *World J. Gastroenterol.* 24, 4217–4223. doi: 10.3748/wjg.v24.i37.4217

Casson, C. N., Yu, J., Reyes, V. M., Taschuk, F. O., Yadav, A., Copenhaver, A. M., et al. (2015). Human caspase-4 mediates noncanonical inflammasome activation against gram-negative bacterial pathogens. *Proc. Natl. Acad. Sci. U.S.A.* 112, 6688–6693. doi: 10.1073/pnas.1421699112

Cavalli, G., and Dinarello, C. A. (2018). Anakinra therapy for non-cancer inflammatory diseases. *Front. Pharmacol.* 9, 1157. doi: 10.3389/fphar.2018.01157

Chakraborty, A., Tannenbaum, S., Rordorf, C., Lowe, P. J., Floch, D., Gram, H., et al. (2012). Pharmacokinetic and pharmacodynamic properties of canakinumab, a human anti-interleukin-1β monoclonal antibody. *Clin. Pharmacokinet.* 51, e1–18. doi: 10.2165/11599820-000000000-00000

Chatterjee, K., Roy, A., Banerjee, R., Choudhury, S., Mondal, B., Halder, S., et al. (2020). Inflammasome and α-synuclein in Parkinson's disease: A cross-sectional study. *J. Neuroimmunol.* 338, 577089. doi: 10.1016/j.jneuroim.2019.577089

Chen, J., and Chen, Z. J. (2018). PtdIns4P on dispersed trans-Golgi network mediates NLRP3 inflammasome activation. *Nature* 564, 71–76. doi: 10.1038/s41586-018-0761-3

Chen, S., Ma, Q., Krafft, P. R., Hu, Q., Rolland, W., Sherchan, P., et al. (2013). P2X7R/cryopyrin inflammasome axis inhibition reduces neuroinflammation after SAH. *Neurobiol. Dis.* 58, 296–307. doi: 10.1016/j.nbd.2013.06.011

Chen, Y., He, H., Lin, B., Chen, Y., Deng, X., Jiang, W., et al. (2021). RRx-001 ameliorates inflammatory diseases by acting as a potent covalent NLRP3 inhibitor. *Cell. Mol. Immunol.* 18, 1425–1436. doi: 10.1038/s41423-021-00683-y

Chen, Y.-C., Chen, S.-D., Miao, L., Liu, Z.-G., Li, W., Zhao, Z.-X., et al. (2012). Serum levels of interleukin (IL)-18, IL-23 and IL-17 in Chinese patients with multiple sclerosis. *J. Neuroimmunol.* 243, 56–60. doi: 10.1016/j.jneuroim.2011.12.008

Cheng, Y., Pan, X., Wang, J., Li, X., Yang, S., Yin, R., et al. (2020). Fucoidan inhibits NLRP3 inflammasome activation by enhancing p62/SQSTM1-dependent selective autophagy to alleviate atherosclerosis. *Oxid. Med. Cell. Longev.* 2020, 3186306. doi: 10.1155/2020/3186306

Ching, S., Zhang, H., Belevych, N., He, L., Lai, W., Pu, X.-a., et al. (2007). Endothelial-specific knockdown of interleukin-1 (IL-1) type 1 receptor differentially alters CNS responses to IL-1 depending on its route of administration. *J. Neurosci.* 27, 10476–10486. doi: 10.1523/JNEUROSCI.3357-07.2007

Chung, Y., Chang, S. H., Martinez, G. J., Yang, X. O., Nurieva, R., Kang, H. S., et al. (2009). Critical regulation of early Th17 cell differentiation by interleukin-1 signaling. *Immunity* 30, 576–587. doi: 10.1016/j.immuni.2009.02.007

Codolo, G., Plotegher, N., Pozzobon, T., Brucale, M., Tessari, I., Bubacco, L., et al. (2013). Triggering of inflammasome by aggregated α-synuclein, an inflammatory response in synucleinopathies. *PLoS ONE* 8, e55375. doi: 10.1371/journal.pone.0055375

Coll, R. C., Hill, J. R., Day, C. J., Zamoshnikova, A., Boucher, D., Massey, N. L., et al. (2019). MCC950 directly targets the NLRP3 ATP-hydrolysis motif for inflammasome inhibition. *Nat. Chem. Biol.* 15, 556–559. doi: 10.1038/s41589-019-0277-7

Colpitts, S., Kasper, E., Keever, A., Liljenberg, C., Kirby, T., Magori, K., et al. (2017). A bidirectional association between the gut microbiota and CNS disease in a biphasic murine model of multiple sclerosis. *Gut Microbes* 8, 561–573. doi: 10.1080/19490976.2017.1353843

Compan, V., Baroja-Mazo, A., López-Castejón, G., Gomez, A. I., Martínez, C. M., Angosto, D., et al. (2012). Cell volume regulation

modulates NLRP3 inflammasome activation. *Immunity* 37, 487–500. doi: 10.1016/j.immuni.2012.06.013

Correale, J., and Farez, M. (2015). The role of astrocytes in multiple sclerosis progression. *Front. Neurol.* 6, 180. doi: 10.3389/fneur.2015.00180

Cypryk, W., Nyman, T. A., and Matikainen, S. (2018). From inflammasome to exosome-does extracellular vesicle secretion constitute an inflammasome-dependent immune response? *Front. Immunol.* 9, 2188. doi: 10.3389/fimmu.2018.02188

Dalakas, M. C. (2008). B cells as therapeutic targets in autoimmune neurological disorders. *Nat. Clin. Pract. Neurol.* 4, 557–567. doi: 10.1038/ncpneuro0901

Daniels, M. J. D., Rivers-Auty, J., Schilling, T., Spencer, N. G., Watremez, W., Fasolino, V., et al. (2016). Fenamate NSAIDs inhibit the NLRP3 inflammasome and protect against Alzheimer's disease in rodent models. *Nat. Commun.* 7, 12504. doi: 10.1038/ncomms12504

De Gaetano, A., Solodka, K., Zanini, G., Selleri, V., Mattioli, A. V., Nasi, M., et al. (2021). Molecular mechanisms of mtDNA-mediated inflammation. *Cells* 10, 2898. doi: 10.3390/cells10112898

de Oliveira, L. R. C., Mimura, L. A. N., Fraga-Silva, T. F. C., Ishikawa, L. L. W., Fernandes, A. A. H., Zorzella-Pezavento, S. F. G., et al. (2020). Calcitriol prevents neuroinflammation and reduces blood-brain barrier disruption and local macrophage/microglia activation. *Front. Pharmacol.* 11, 161. doi: 10.3389/fphar.2020.00161

de Rivero Vaccari, J. P., Brand, F., Adamczak, S., Lee, S. W., Perez-Barcena, J., Wang, M. Y., et al. (2016). Exosome-mediated inflammasome signaling after central nervous system injury. *J. Neurochem.* 136(Suppl. 1), 39–48. doi: 10.1111/jnc.13036

Dempsey, C., Rubio Araiz, A., Bryson, K. J., Finucane, O., Larkin, C., Mills, E. L., et al. (2017). Inhibiting the NLRP3 inflammasome with MCC950 promotes non-phlogistic clearance of amyloid-β and cognitive function in APP/PS1 mice. *Brain Behav. Immun.* 61, 306–316. doi: 10.1016/j.bbi.2016.12.014

Desu, H. L., Plastini, M., Illiano, P., Bramlett, H. M., Dietrich, W. D., de Rivero Vaccari, J. P., et al. (2020). IC100: a novel anti-ASC monoclonal antibody improves functional outcomes in an animal model of multiple sclerosis. *J. Neuroinflamm.* 17, 143. doi: 10.1186/s12974-020-01826-0

DeTure, M. A., and Dickson, D. W. (2019). The neuropathological diagnosis of Alzheimer's disease. *Mol. Neurodegener.* 14, 32. doi: 10.1186/s13024-019-0333-5

Di Virgilio, F., Dal Ben, D., Sarti, A. C., Giuliani, A. L., and Falzoni, S. (2017). The P2X7 receptor in infection and inflammation. *Immunity* 47, 15–31. doi: 10.1016/j.immuni.2017.06.020

Di, A., Xiong, S., Ye, Z., Malireddi, R. K. S., Kometani, S., Zhong, M., et al. (2018). The TWIK2 potassium efflux channel in macrophages mediates NLRP3 inflammasome-induced inflammation. *Immunity* 49, 56–65.e54. doi: 10.1016/j.immuni.2018.04.032

Diaz, R. J., Fernandes, K., Lytvyn, Y., Hawrylyshyn, K., Harvey, K., Hossain, T., et al. (2013). Enhanced cell-volume regulation in cyclosporin A cardioprotection. *Cardiovasc. Res.* 98, 411–419. doi: 10.1093/cvr/cvt056

Dick, M. S., Sborgi, L., Rühl, S., Hiller, S., and Broz, P. (2016). ASC filament formation serves as a signal amplification mechanism for inflammasomes. *Nat. Commun.* 7, 11929. doi: 10.1038/ncomms11929

Dinarello, C. A., Simon, A., and van der Meer, J. W. M. (2012). Treating inflammation by blocking interleukin-1 in a broad spectrum of diseases. *Nat. Rev. Drug Discov.* 11, 633–652. doi: 10.1038/nrd3800

Dominic, A., Le, N. T., and Takahashi, M. (2022). Loop between NLRP3 inflammasome and reactive oxygen species. *Antioxid. Redox Signal.* 36, 784–796. doi: 10.1089/ars.2020.8257

Dong, Y., and Benveniste, E. (2001). Immune function of astrocytes. *Glia* 36, 180–190. doi: 10.1002/glia.1107

Dostert, C., Pétrilli, V., Van Bruggen, R., Steele, C., Mossman, B. T., and Tschopp, J. (2008). Innate immune activation through Nalp3 inflammasome sensing of asbestos and silica. *Science* 320, 674–677. doi: 10.1126/science.1156995

Drinkall, S., Lawrence, C. B., Ossola, B., Russell, S., Bender, C., Brice, N. B., et al. (2022). The two pore potassium channel THIK-1 regulates NLRP3 inflammasome activation. *Glia.* 70, 1301–1316. doi: 10.1002/glia.24174

Dujmovic, I., Mangano, K., Pekmezovic, T., Quattrocchi, C., Mesaros, S., Stojsavljevic, N., et al. (2009). The analysis of IL-1 beta and its naturally occurring inhibitors in multiple sclerosis: the elevation of IL-1 receptor antagonist and IL-1 receptor type II after steroid therapy. *J. Neuroimmunol.* 207, 101–106. doi: 10.1016/j.jneuroim.2008.11.004

Dumas, A., Amiable, N., de Rivero Vaccari, J., Chae, J., Keane, R., Lacroix, S., et al. (2014). The inflammasome pyrin contributes to pertussis toxin-induced IL-1β synthesis, neutrophil intravascular crawling and autoimmune encephalomyelitis. *PLoS Pathog.* 10, e1004150. doi: 10.1371/journal.ppat.1004150

Endriz, J., Ho, P. P., and Steinman, L. (2017). Time correlation between mononucleosis and initial symptoms of MS. *Neurol. Neuroimmunol. Neuroinflamm.* 4, e308. doi: 10.1212/nxi.0000000000000308

Fan, Z., Pan, Y. T., Zhang, Z. Y., Yang, H., Yu, S. Y., Zheng, Y., et al. (2020). Systemic activation of NLRP3 inflammasome and plasma α-synuclein levels are correlated with motor severity and progression in Parkinson's disease. *J. Neuroinflammation* 17, 11. doi: 10.1186/s12974-019-1670-6

Feng, Y. S., Tan, Z. X., Wu, L. Y., Dong, F., and Zhang, F. (2021). The involvement of NLRP3 inflammasome in the treatment of neurodegenerative diseases. *Biomed. Pharmacother.* 138, 111428. doi: 10.1016/j.biopha.2021.111428

Ferrari, C. C., Depino, A. M., Prada, F., Muraro, N., Campbell, S., Podhajcer, O., et al. (2004). Reversible demyelination, blood-brain barrier breakdown, and pronounced neutrophil recruitment induced by chronic IL-1 expression in the brain. *Am. J. Pathol.* 165, 1827–1837. doi: 10.1016/S0002-9440(10)63438-4

Franchi, L., Eigenbrod, T., Muñoz-Planillo, R., and Nuñez, G. (2009). The inflammasome: a caspase-1-activation platform that regulates immune responses and disease pathogenesis. *Nat. Immunol.* 10, 241–247. doi: 10.1038/ni.1703

Fu, W., Vukojevic, V., Patel, A., Soudy, R., MacTavish, D., Westaway, D., et al. (2017). Role of microglial amylin receptors in mediating beta amyloid (Aβ)-induced inflammation. *J. Neuroinflamm.* 14, 199. doi: 10.1186/s12974-017-0972-9

Furlan, R., Martino, G., Galbiati, F., Poliani, P. L., Smiroldo, S., Bergami, A., et al. (1999). Caspase-1 regulates the inflammatory process leading to autoimmune demyelination. *J. Immunol.* 163, 2403–2409.

Gabelloni, M. L., Sabbione, F., Jancic, C., Fuxman Bass, J., Keitelman, I., Iula, L., et al. (2013). NADPH oxidase derived reactive oxygen species are involved in human neutrophil IL-1β secretion but not in inflammasome activation. *Eur. J. Immunol.* 43, 3324–3335. doi: 10.1002/eji.201243089

Gaidt, M., Ebert, T., Chauhan, D., Schmidt, T., Schmid-Burgk, J., Rapino, F., et al. (2016). Human monocytes engage an alternative inflammasome pathway. *Immunity* 44, 833–846. doi: 10.1016/j.immuni.2016.01.012

Gao, Q., Zhang, Y., Han, C., Hu, X., Zhang, H., Xu, X., et al. (2016). Blockade of CD47 ameliorates autoimmune inflammation in CNS by suppressing IL-1-triggered infiltration of pathogenic Th17 cells. *J. Autoimmun.* 69, 74–85. doi: 10.1016/j.jaut.2016.03.002

Gao, W., Li, Y., Liu, X., Wang, S., Mei, P., Chen, Z., et al. (2022). TRIM21 regulates pyroptotic cell death by promoting Gasdermin D oligomerization. *Cell Death Differ.* 29, 439–450. doi: 10.1038/s41418-021-00867-z

Gentile, A., Rossi, S., Studer, V., Motta, C., De Chiara, V., Musella, A., et al. (2013). Glatiramer acetate protects against inflammatory synaptopathy in experimental autoimmune encephalomyelitis. *J. Neuroimmune Pharmacol.* 8, 651–663. doi: 10.1007/s11481-013-9436-x

Gombault, A., Baron, L., and Couillin, I. (2012). ATP release and purinergic signaling in NLRP3 inflammasome activation. *Front. Immunol.* 3, 414. doi: 10.3389/fimmu.2012.00414

Gris, D., Ye, Z., Iocca, H. A., Wen, H., Craven, R. R., Gris, P., et al. (2010). NLRP3 plays a critical role in the development of experimental autoimmune encephalomyelitis by mediating Th1 and Th17 responses. *J. Immunol.* 185, 974–981. doi: 10.4049/jimmunol.0904145

Guo, X., Chen, S., Yu, W., Chi, Z., Wang, Z., Xu, T., et al. (2021). AKT controls NLRP3 inflammasome activation by inducing DDX3X phosphorylation. *FEBS Lett.* 595, 2447–2462. doi: 10.1002/1873-3468.14175

Gurung, P., Anand, P. K., Malireddi, R. K. S., Vande Walle, L., Van Opdenbosch, N., Dillon, C. P., et al. (2014). FADD and caspase-8 mediate priming and activation of the canonical and noncanonical Nlrp3 inflammasomes. *J. Immunol.* 192, 1835–1846. doi: 10.4049/jimmunol.1302839

Gurung, P., and Kanneganti, T.-D. (2015). Novel roles for caspase-8 in IL-1β and inflammasome regulation. *Am. J. Pathol.* 185, 17–25. doi: 10.1016/j.ajpath.2014.08.025

Gurung, P., Lukens, J. R., and Kanneganti, T.-D. (2015). Mitochondria: diversity in the regulation of the NLRP3 inflammasome. *Trends Mol. Med.* 21, 193–201. doi: 10.1016/j.molmed.2014.11.008

Gutcher, I., Urich, E., Wolter, K., Prinz, M., and Becher, B. (2006). Interleukin 18-independent engagement of interleukin 18 receptor-alpha is required for autoimmune inflammation. *Nat. Immunol.* 7, 946–953. doi: 10.1038/ni1377

Hafler, D. A., Compston, A., Sawcer, S., Lander, E. S., Daly, M. J., De Jager, P. L., et al. (2007). Risk alleles for multiple sclerosis identified by a genomewide study. *N. Engl. J. Med.* 357, 851–862. doi: 10.1056/NEJMoa073493

Hagar, J. A., Powell, D. A., Aachoui, Y., Ernst, R. K., and Miao, E. A. (2013). Cytoplasmic LPS activates caspase-11: implications in TLR4-independent endotoxic shock. *Science* 341, 1250–1253. doi: 10.1126/science.1240988

Hagman, S., Kolasa, M., Basnyat, P., Helminen, M., Kahonen, M., Dastidar, P., et al. (2015). Analysis of apoptosis-related genes in patients with clinically isolated syndrome and their association with conversion to multiple sclerosis. *J. Neuroimmunol.* 280, 43–48. doi: 10.1016/j.jneuroim.2015.02.006

Haidet-Phillips, A. M., Hester, M. E., Miranda, C. J., Meyer, K., Braun, L., Frakes, A., et al. (2011). Astrocytes from familial and sporadic ALS patients are toxic to motor neurons. *Nat. Biotechnol.* 29, 824–828. doi: 10.1038/nbt.1957

Halle, A., Hornung, V., Petzold, G. C., Stewart, C. R., Monks, B. G., Reinheckel, T., et al. (2008). The NALP3 inflammasome is involved in the innate immune response to amyloid-beta. *Nat. Immunol.* 9, 857–865. doi: 10.1038/ni.1636

Hasanzadeh, S., Read, M. I., Bland, A. R., Majeed, M., Jamialahmadi, T., and Sahebkar, A. (2020). Curcumin: an inflammasome silencer. *Pharmacol. Res.* 159, 104921. doi: 10.1016/j.phrs.2020.104921

He, H., Jiang, H., Chen, Y., Ye, J., Wang, A., Wang, C., et al. (2018). Oridonin is a covalent NLRP3 inhibitor with strong anti-inflammasome activity. *Nat. Commun.* 9, 2550. doi: 10.1038/s41467-018-04947-6

He, Y., Hara, H., and Núñez, G. (2016a). Mechanism and regulation of NLRP3 inflammasome activation. *Trends Biochem. Sci.* 41, 1012–1021. doi: 10.1016/j.tibs.2016.09.002

He, Y., Zeng, M. Y., Yang, D., Motro, B., and Núñez, G. (2016b). NEK7 is an essential mediator of NLRP3 activation downstream of potassium efflux. *Nature* 530, 354–357. doi: 10.1038/nature16959

Healy, B. C., Ali, E. N., Guttmann, C. R., Chitnis, T., Glanz, B. I., Buckle, G., et al. (2009). Smoking and disease progression in multiple sclerosis. *Arch. Neurol.* 66, 858–864. doi: 10.1001/archneurol.2009.122

Heneka, M. T. (2017). Inflammasome activation and innate immunity in Alzheimer's disease. *Brain Pathol.* 27, 220–222. doi: 10.1111/bpa.12483

Heneka, M. T., Kummer, M. P., Stutz, A., Delekate, A., Schwartz, S., Vieira-Saecker, A., et al. (2013). NLRP3 is activated in Alzheimer's disease and contributes to pathology in APP/PS1 mice. *Nature* 493, 674–678. doi: 10.1038/nature11729

Hezel, M. E. v., Nieuwland, R., Bruggen, R. v., and Juffermans, N. P. (2017). The ability of extracellular vesicles to induce a pro-inflammatory host response. *Int. J. Mol. Sci.* 18, 1285. doi: 10.3390/ijms18061285

Horng, T. (2014). Calcium signaling and mitochondrial destabilization in the triggering of the NLRP3 inflammasome. *Trends Immunol.* 35, 253–261. doi: 10.1016/j.it.2014.02.007

Hornung, V., Bauernfeind, F., Halle, A., Samstad, E. O., Kono, H., Rock, K. L., et al. (2008). Silica crystals and aluminum salts activate the NALP3 inflammasome through phagosomal destabilization. *Nat. Immunol.* 9, 847–856. doi: 10.1038/ni.1631

Hou, B., Zhang, Y., Liang, P., He, Y., Peng, B., Liu, W., et al. (2020). Inhibition of the NLRP3-inflammasome prevents cognitive deficits in experimental autoimmune encephalomyelitis mice via the alteration of astrocyte phenotype. *Cell Death Dis.* 11, 377. doi: 10.1038/s41419-020-2565-2

Hou, L., Yang, J., Li, S., Huang, R., Zhang, D., Zhao, J., et al. (2020). Glibenclamide attenuates 2,5-hexanedione-induced neurotoxicity in the spinal cord of rats through mitigation of NLRP3 inflammasome activation, neuroinflammation and oxidative stress. *Toxicol. Lett.* 331, 152–158. doi: 10.1016/j.toxlet.2020.06.002

Hu, J. J., Liu, X., Xia, S., Zhang, Z., Zhang, Y., Zhao, J., et al. (2020). FDA-approved disulfiram inhibits pyroptosis by blocking gasdermin D pore formation. *Nat. Immunol.* 21, 736–745. doi: 10.1038/s41590-020-0669-6

Huang, C. (2008). Polyneuropathy induced by n-hexane intoxication in Taiwan. *Acta Neurol. Taiwan* 17, 3–10.

Huang, J., Xie, Z.-K., Lu, R.-B., and Xie, Z.-F. (2013). Association of interleukin-1 gene polymorphisms with multiple sclerosis: a meta-analysis. *Inflamm. Res.* 62, 97–106. doi: 10.1007/s00011-012-0556-1

Huang, X., Feng, Z., Jiang, Y., Li, J., Xiang, Q., Guo, S., et al. (2019). VSIG4 mediates transcriptional inhibition of Nlrp3 and Il-1β in macrophages. *Sci. Adv.* 5, eaau7426. doi: 10.1126/sciadv.aau7426

Imani, D., Azimi, A., Salehi, Z., Rezaei, N., Emamnejad, R., Sadr, M., et al. (2018). Association of nod-like receptor protein-3 single nucleotide gene polymorphisms and expression with the susceptibility to relapsing-remitting multiple sclerosis. *Int. J. Immunogenet.* 45, 329–336. doi: 10.1111/iji.12401

Inoue, M., Chen, P.-H., Siecinski, S., Li, Q.-J., Liu, C., Steinman, L., et al. (2016). An interferon-β-resistant and NLRP3 inflammasome-independent subtype of EAE with neuronal damage. *Nat. Neurosci.* 19, 1599–1609. doi: 10.1038/nn.4421

Inoue, M., Williams, K. L., Gunn, M. D., and Shinohara, M. L. (2012a). NLRP3 inflammasome induces chemotactic immune cell migration to the CNS in experimental autoimmune encephalomyelitis. *Proc. Natl. Acad. Sci. U.S.A.* 109, 10480–10485. doi: 10.1073/pnas.1201836109

Inoue, M., Williams, K. L., Oliver, T., Vandenabeele, P., Rajan, J. V., Miao, E. A., et al. (2012b). Interferon-β therapy against EAE is effective only when development of the disease depends on the NLRP3 inflammasome. *Sci. Signal.* 5, ra38. doi: 10.1126/scisignal.2002767

Isik, N., Arman, A., Canturk, I. A., Gurkan, A. C., Candan, F., Aktan, S., et al. (2013). Multiple sclerosis: association with the interleukin-1 gene family polymorphisms in the Turkish population. *Int. J. Neurosci.* 123, 711–718. doi: 10.3109/00207454.2013.795563

Iyer, S. S., He, Q., Janczy, J. R., Elliott, E. I., Zhong, Z., Olivier, A. K., et al. (2013). Mitochondrial cardiolipin is required for Nlrp3 inflammasome activation. *Immunity* 39, 311–323. doi: 10.1016/j.immuni.2013.08.001

Jahanbani-Ardakani, H., Alsahebfosoul, F., Etemadifar, M., and Abtahi, S.-H. (2019). Interleukin 18 polymorphisms and its serum level in patients with multiple sclerosis. *Ann. Indian Acad. Neurol.* 22, 474–476. doi: 10.4103/aian.AIAN_515_18

Jander, S., and Stoll, G. (1998). Differential induction of interleukin-12, interleukin-18, and interleukin-1beta converting enzyme mRNA in experimental autoimmune encephalomyelitis of the Lewis rat. *J. Neuroimmunol.* 91, 93–99. doi: 10.1016/s0165-5728(98)00162-3

Jha, S., Srivastava, S. Y., Brickey, W. J., Iocca, H., Toews, A., Morrison, J. P., et al. (2010). The inflammasome sensor, NLRP3, regulates CNS inflammation and demyelination via caspase-1 and interleukin-18. *J. Neurosci.* 30, 15811–15820. doi: 10.1523/JNEUROSCI.4088-10.2010

Jian, Z., Ding, S., Deng, H., Wang, J., Yi, W., Wang, L., et al. (2016). Probenecid protects against oxygen-glucose deprivation injury in primary astrocytes by regulating inflammasome activity. *Brain Res.* 1643, 123–129. doi: 10.1016/j.brainres.2016.05.002

Jo, E. K., Kim, J. K., Shin, D. M., and Sasakawa, C. (2016). Molecular mechanisms regulating NLRP3 inflammasome activation. *Cell. Mol. Immunol.* 13, 148–159. doi: 10.1038/cmi.2015.95

Johann, S., Heitzer, M., Kanagaratnam, M., Goswami, A., Rizo, T., Weis, J., et al. (2015). NLRP3 inflammasome is expressed by astrocytes in the SOD1 mouse model of ALS and in human sporadic ALS patients. *Glia* 63, 2260–2273. doi: 10.1002/glia.22891

Kadhim, H., Deltenre, P., Martin, J. J., and Sébire, G. (2016). *In-situ* expression of Interleukin-18 and associated mediators in the human brain of sALS patients: hypothesis for a role for immune-inflammatory mechanisms. *Med. Hypotheses* 86, 14–17. doi: 10.1016/j.mehy.2015.11.022

Kapoor, R., Smith, K., Allegretta, M., Arnold, D., Carroll, W., Comabella, M., et al. (2020). Serum neurofilament light as a biomarker in progressive multiple sclerosis. *Neurology* 95, 436–444. doi: 10.1212/wnl.0000000000010346

Karakas Celik, S., Öz, Z. S., Dursun, A., Unal, A., Emre, U., Cicek, S., et al. (2014). Interleukin 18 gene polymorphism is a risk factor for multiple sclerosis. *Mol. Biol. Rep.* 41, 1653–1658. doi: 10.1007/s11033-013-3013-5

Kayagaki, N., Stowe, I. B., Lee, B. L., O'Rourke, K., Anderson, K., Warming, S., et al. (2015). Caspase-11 cleaves gasdermin D for non-canonical inflammasome signalling. *Nature* 526, 666–671. doi: 10.1038/nature15541

Kayagaki, N., Warming, S., Lamkanfi, M., Vande Walle, L., Louie, S., Dong, J., et al. (2011). Non-canonical inflammasome activation targets caspase-11. *Nature* 479, 117–121. doi: 10.1038/nature10558

Ke, P., Shao, B.-Z., Xu, Z.-Q., Chen, X.-W., Wei, W., and Liu, C. (2017). Activating α7 nicotinic acetylcholine receptor inhibits NLRP3 inflammasome through regulation of β-arrestin-1. *CNS Neurosci. Ther.* 23, 875–884. doi: 10.1111/cns.12758

Keane, R., Dietrich, W., and de Rivero Vaccari, J. (2018). Inflammasome proteins as biomarkers of multiple sclerosis. *Front. Neurol.* 9, 135. doi: 10.3389/fneur.2018.00135

Kelley, N., Jeltema, D., Duan, Y., and He, Y. (2019). The NLRP3 inflammasome: an overview of mechanisms of activation and regulation. *Int. J. Mol. Sci.* 20, 3328. doi: 10.3390/ijms20133328

Kermode, A. G., Thompson, A. J., Tofts, P., MacManus, D. G., Kendall, B. E., Kingsley, D. P., et al. (1990). Breakdown of the blood-brain barrier precedes symptoms and other MRI signs of new lesions in multiple sclerosis. Pathogenetic and clinical implications. *Brain* 113(Pt 5), 1477–1489. doi: 10.1093/brain/113.5.1477

Khalil, M., Teunissen, C., Otto, M., Piehl, F., Sormani, M., Gattringer, T., et al. (2018). Neurofilaments as biomarkers in neurological disorders. *Nat. Rev. Neurol.* 14, 577–589. doi: 10.1038/s41582-018-0058-z

Kiasalari, Z., Afshin-Majd, S., Baluchnejadmojarad, T., Azadi-Ahmadabadi, E., Fakour, M., Ghasemi-Tarie, R., et al. (2021). Sinomenine alleviates murine experimental autoimmune encephalomyelitis model of multiple sclerosis through inhibiting NLRP3 inflammasome. *J. Mol. Neurosci.* 71, 215–224. doi: 10.1007/s12031-020-01637-1

Kobelt, G., Thompson, A., Berg, J., Gannedahl, M., and Eriksson, J. (2017). New insights into the burden and costs of multiple sclerosis in Europe. *Multiple Scler.* 23, 1123–1136. doi: 10.1177/1352458517694432

Kumar, H., Kawai, T., and Akira, S. (2011). Pathogen recognition by the innate immune system. *Int. Rev. Immunol.* 30, 16–34. doi: 10.3109/08830185.2010.529976

Lall, D., and Baloh, R. H. (2017). Microglia and C9orf72 in neuroinflammation and ALS and frontotemporal dementia. *J. Clin. Invest.* 127, 3250–3258. doi: 10.1172/jci90607

Lalor, S. J., Dungan, L. S., Sutton, C. E., Basdeo, S. A., Fletcher, J. M., and Mills, K. H. G. (2011). Caspase-1-processed cytokines IL-1beta and IL-18 promote IL-17 production by gammadelta and CD4 T cells that mediate autoimmunity. *J. Immunol.* 186, 5738–5748. doi: 10.4049/jimmunol.1003597

Lamkanfi, M., and Dixit, V. M. (2009). Inflammasomes: guardians of cytosolic sanctity. *Immunol. Rev.* 227, 95–105. doi: 10.1111/j.1600-065X.2008.00730.x

Lang, Y., Chu, F., Liu, L., Zheng, C., Li, C., Shen, D., et al. (2021). Potential role of BAY11-7082, a NF-κB blocker inhibiting experimental autoimmune encephalomyelitis in C57BL/6J mice via declining NLRP3 inflammasomes. *Clin. Exp. Immunol.* doi: 10.1093/cei/uxab022

Latz, E., Xiao, T. S., and Stutz, A. (2013). Activation and regulation of the inflammasomes. *Nat. Rev. Immunol.* 13, 397–411. doi: 10.1038/nri3452

Lazibat, I., Rubinic Majdak, M., and Zupanic, S. (2018). Multiple sclerosis: new aspects of immunopathogenesis. *Acta Clin. Croat.* 57, 352–361. doi: 10.20471/acc.2018.57.02.17

Lee, E., Hwang, I., Park, S., Hong, S., Hwang, B., Cho, Y., et al. (2019). MPTP-driven NLRP3 inflammasome activation in microglia plays a central role in dopaminergic neurodegeneration. *Cell Death Differ.* 26, 213–228. doi: 10.1038/s41418-018-0124-5

Leite, J. A., Cavalcante-Silva, L. H. A., Ribeiro, M. R., de Morais Lima, G., Scavone, C., and Rodrigues-Mascarenhas, S. (2022). Neuroinflammation and neutrophils: modulation by ouabain. *Front. Pharmacol.* 13, 824907. doi: 10.3389/fphar.2022.824907

Li, R., Patterson, K. R., and Bar-Or, A. (2018). Reassessing B cell contributions in multiple sclerosis. *Nat. Immunol.* 19, 696–707. doi: 10.1038/s41590-018-0135-x

Li, Z., Chen, X., Tao, J., Shi, A., Zhang, J., and Yu, P. (2021). Exosomes regulate NLRP3 inflammasome in diseases. *Front Cell Dev Biol* 9, 802509. doi: 10.3389/fcell.2021.802509

Liang, M., Chen, X., Wang, L., Qin, L., Wang, H., Sun, Z., et al. (2020). Cancer-derived exosomal TRIM59 regulates macrophage NLRP3 inflammasome activation to promote lung cancer progression. *J. Exp. Clin. Cancer Res.* 39, 176. doi: 10.1186/s13046-020-01688-7

Lim, K. H., Chen, L. C., Hsu, K., Chang, C. C., Chang, C. Y., Kao, C. W., et al. (2020). BAFF-driven NLRP3 inflammasome activation in B cells. *Cell Death Dis.* 11, 820. doi: 10.1038/s41419-020-03035-2

Liu, X., Zhang, Z., Ruan, J., Pan, Y., Magupalli, V. G., Wu, H., et al. (2016). Inflammasome-activated gasdermin D causes pyroptosis by forming membrane pores. *Nature* 535, 153–158. doi: 10.1038/nature18629

Losy, J., and Niezgoda, A. (2001). IL-18 in patients with multiple sclerosis. *Acta Neurol. Scand.* 104, 171–173. doi: 10.1034/j.1600-0404.2001.00356.x

Lu, L., Qi, S., Chen, Y., Luo, H., Huang, S., Yu, X., et al. (2020). Targeted immunomodulation of inflammatory monocytes across the blood-brain barrier by curcumin-loaded nanoparticles delays the progression of experimental autoimmune encephalomyelitis. *Biomaterials* 245, 119987. doi: 10.1016/j.biomaterials.2020.119987

Macia, L., Tan, J., Vieira, A. T., Leach, K., Stanley, D., Luong, S., et al. (2015). Metabolite-sensing receptors GPR43 and GPR109A facilitate dietary fibre-induced gut homeostasis through regulation of the inflammasome. *Nat. Commun.* 6, 6734. doi: 10.1038/ncomms7734

Maimone, D., Gregory, S., Arnason, B. G., and Reder, A. T. (1991). Cytokine levels in the cerebrospinal fluid and serum of patients with multiple sclerosis. *J. Neuroimmunol.* 32, 67–74. doi: 10.1016/0165-5728(91)90073-g

Malhotra, S., Costa, C., Eixarch, H., Keller, C. W., Amman, L., Martínez-Banaclocha, H., et al. (2020). NLRP3 inflammasome as prognostic factor and therapeutic target in primary progressive multiple sclerosis patients. *Brain* 143, 1414–1430. doi: 10.1093/brain/awaa084

Mallucci, G., Peruzzotti-Jametti, L., Bernstock, J., and Pluchino, S. (2015). The role of immune cells, glia and neurons in white and gray matter pathology in multiple sclerosis. *Prog. Neurobio* 127, 1–22. doi: 10.1016/j.pneurobio.2015.02.003

Mancino, D. N. J., Lima, A., Roig, P., García Segura, L. M., De Nicola, A. F., and Garay, L. I. (2022). Tibolone restrains neuroinflammation in mouse experimental autoimmune encephalomyelitis. *J. Neuroendocrinol.* 34, e13078. doi: 10.1111/jne.13078

Mandolesi, G., Musella, A., Gentile, A., Grasselli, G., Haji, N., Sepman, H., et al. (2013). Interleukin-1β alters glutamate transmission at purkinje cell synapses in a mouse model of multiple sclerosis. *J. Neurosc.* 33, 12105–12121. doi: 10.1523/JNEUROSCI.5369-12.2013

Manouchehrinia, A., Stridh, P., Khademi, M., Leppert, D., Barro, C., Michalak, Z., et al. (2020). Plasma neurofilament light levels are associated with risk of disability in multiple sclerosis. *Neurology* 94, e2457–e2467. doi: 10.1212/wnl.0000000000009571

Mao, Z., Liu, C., Ji, S., Yang, Q., Ye, H., Han, H., et al. (2017). The NLRP3 inflammasome is involved in the pathogenesis of Parkinson's disease in rats. *Neurochem. Res.* 42, 1104–1115. doi: 10.1007/s11064-017-2185-0

Martinon, F., Burns, K., and Tschopp, J. (2002). The inflammasome: a molecular platform triggering activation of inflammatory caspases and processing of proIL-beta. *Mol. Cell* 10, 417–426. doi: 10.1016/s1097-2765(02)00599-3

McKenzie, B. A., Mamik, M. K., Saito, L. B., Boghozian, R., Monaco, M. C., Major, E. O., et al. (2018). Caspase-1 inhibition prevents glial inflammasome activation and pyroptosis in models of multiple sclerosis. *Proc. Natl. Acad. Sci. U.S.A.* 115, E6065–E6074. doi: 10.1073/pnas.1722041115

Metwally, H., Tanaka, T., Li, S., Parajuli, G., Kang, S., Hanieh, H., et al. (2020). Noncanonical STAT1 phosphorylation expands its transcriptional activity into promoting LPS-induced IL-6 and IL-12p40 production. *Sci. Signal.* 13, eaay0574. doi: 10.1126/scisignal.aay0574

Mueller, N., Bakacs, E., Combellick, J., Grigoryan, Z., and Dominguez-Bello, M. (2015). The infant microbiome development: mom matters. *Trends Mol. Med.* 21, 109–117. doi: 10.1016/j.molmed.2014.12.002

Muñoz-Planillo, R., Kuffa, P., Martínez-Colón, G., Smith, B. L., Rajendiran, T. M., and Núñez, G. (2013). K? efflux is the common trigger of NLRP3 inflammasome activation by bacterial toxins and particulate matter. *Immunity* 38, 1142–1153. doi: 10.1016/j.immuni.2013.05.016

Murakami, T., Ockinger, J., Yu, J., Byles, V., McColl, A., Hofer, A. M., et al. (2012). Critical role for calcium mobilization in activation of the NLRP3 inflammasome. *Proc. Natl. Acad. Sci. U.S.A.* 109, 11282–11287. doi: 10.1073/pnas.1117765109

Musella, A., Mandolesi, G., Gentile, A., Rossi, S., Studer, V., Motta, C., et al. (2013). Cladribine interferes with IL-1β synaptic effects in experimental multiple sclerosis. *J. Neuroimmunol.* 264. doi: 10.1016/j.jneuroim.2013.08.009

Niu, T., De Rosny, C., Chautard, S., Rey, A., Patoli, D., Groslambert, M., et al. (2021). NLRP3 phosphorylation in its LRR domain

critically regulates inflammasome assembly. *Nat. Commun.* 12, 5862. doi: 10.1038/s41467-021-26142-w

Ochoa-Repáraz, J., Mielcarz, D., Ditrio, L., Burroughs, A., Foureau, D., Haque-Begum, S., et al. (2009). Role of gut commensal microflora in the development of experimental autoimmune encephalomyelitis. *J. Immunol.* 183, 6041–6050. doi: 10.4049/jimmunol.0900747

Olcum, M., Tastan, B., Kiser, C., Genc, S., and Genc, K. (2020). Microglial NLRP3 inflammasome activation in multiple sclerosis. *Adv. Protein Chem. Struct. Biol.* 119, 247–308. doi: 10.1016/bs.apcsb.2019.08.007

Orhan, G., Eruyar, E., Mungan, S. Ö., Ak, F., and Karahalil, B. (2016). The association of IL-18 gene promoter polymorphisms and the levels of serum IL-18 on the risk of multiple sclerosis. *Clin. Neurol. Neurosurg.* 146, 96–101. doi: 10.1016/j.clineuro.2016.04.027

Pan, R. Y., Kong, X. X., Cheng, Y., Du, L., Wang, Z. C., Yuan, C., et al. (2021). 1,2,4-Trimethoxybenzene selectively inhibits NLRP3 inflammasome activation and attenuates experimental autoimmune encephalomyelitis. *Acta Pharmacol. Sin.* 42, 1769–1779. doi: 10.1038/s41401-021-00613-8

Paolicelli, R. C., Bergamini, G., and Rajendran, L. (2019). Cell-to-cell communication by extracellular vesicles: focus on microglia. *Neuroscience* 405, 148–157. doi: 10.1016/j.neuroscience.2018.04.003

Paré, A., Mailhot, B., Lévesque, S. A., Juzwik, C., Ignatius Arokia Doss, P. M., Lécuyer, M.-A., et al. (2018). IL-1β enables CNS access to CCR2 monocytes and the generation of pathogenic cells through GM-CSF released by CNS endothelial cells. *Proc. Natl. Acad. Sci. U.S.A.* 115, E1194–E1203. doi: 10.1073/pnas.1714948115

Paul, C., and Bolton, C. (1995). Inhibition of blood-brain barrier disruption in experimental allergic encephalomyelitis by short-term therapy with dexamethasone or cyclosporin A. *Int. J. Immunopharmacol.* 17, 497–503. doi: 10.1016/0192-0561(95)00034-y

Pearce, L., Davidson, S. M., and Yellon, D. M. (2021). Does remote ischaemic conditioning reduce inflammation? A focus on innate immunity and cytokine response. *Basic Res. Cardiol.* 116, 12. doi: 10.1007/s00395-021-00852-0

Pellegrini, C., Antonioli, L., Calderone, V., Colucci, R., Fornai, M., and Blandizzi, C. (2020). Microbiota-gut-brain axis in health and disease: is NLRP3 inflammasome at the crossroads of microbiota-gut-brain communications? *Prog. Neurobiol.* 191, 101806. doi: 10.1016/j.pneurobio.2020.101806

Peng, Y., Chen, J., Dai, Y., Jiang, Y., Qiu, W., Gu, Y., et al. (2019). NLRP3 level in cerebrospinal fluid of patients with neuromyelitis optica spectrum disorders: Increased levels and association with disease severity. *Mult. Scler. Relat. Disord.* 39, 101888. doi: 10.1016/j.msard.2019.101888

Peñin-Franch, A., García-Vidal, J. A., Martínez, C. M., Escolar-Reina, P., Martínez-Ojeda, R. M., Gómez, A. I., et al. (2022). Galvanic current activates the NLRP3 inflammasome to promote type I collagen production in tendon. *Elife* 11, e73675. doi: 10.7554/eLife.73675

Peter, J. B., Boctor, F. N., and Tourtellotte, W. W. (1991). Serum and CSF levels of IL-2, sIL-2R, TNF-alpha, and IL-1 beta in chronic progressive multiple sclerosis: expected lack of clinical utility. *Neurology* 41, 121–123. doi: 10.1212/wnl.41.1.121

Petrucci, S., Consoli, F., and Valente, E. M. (2014). Parkinson Disease Genetics: A "Continuum" from Mendelian to Multifactorial Inheritance. *Curr. Mol. Med.* 14, 1079–1088. doi: 10.2174/1566524014666141010155509

Piancone, F., La Rosa, F., Marventano, I., Saresella, M., and Clerici, M. (2021). The Role of the Inflammasome in Neurodegenerative Diseases. *Molecules* 26(4). doi: 10.3390/molecules26040953

Pinke, K. H., Zorzella-Pezavento, S. F. G., de Campos Fraga-Silva, T. F., Mimura, L. A. N., de Oliveira, L. R. C., Ishikawa, L. L. W., et al. (2020). Calming down mast cells with ketotifen: a potential strategy for multiple sclerosis therapy? *Neurotherapeutics* 17, 218–234. doi: 10.1007/s13311-019-00775-8

Potenzieri, A., Riva, B., and Genazzani, A. A. (2020). Unexpected Ca-mobilization of oxaliplatin via H1 histamine receptors. *Cell Calcium* 86, 102128. doi: 10.1016/j.ceca.2019.102128

Prada, I., Furlan, R., Matteoli, M., and Verderio, C. (2013). Classical and unconventional pathways of vesicular release in microglia. *Glia* 61, 1003–1017. doi: 10.1002/glia.22497

Pröbstel, A.-K., and Baranzini, S. E. (2018). The role of the gut microbiome in multiple sclerosis risk and progression: towards characterization of the "MS microbiome". *Neurotherapeutics* 15, 126–134. doi: 10.1007/s13311-017-0587-y

Qiao, C., Zhang, Q., Jiang, Q., Zhang, T., Chen, M., Fan, Y., et al. (2018). Inhibition of the hepatic Nlrp3 protects dopaminergic neurons via attenuating systemic inflammation in a MPTP/p mouse model of Parkinson's disease. *J. Neuroinflammation* 15, 193. doi: 10.1186/s12974-018-1236-z

Ramirez, M., Poreba, M., Snipas, S., Groborz, K., Drag, M., and Salvesen, G. (2018). Extensive peptide and natural protein substrate screens reveal that mouse caspase-11 has much narrower substrate specificity than caspase-1. *J. Biol. Chem.* 293, 7058–7067. doi: 10.1074/jbc.RA117.001329

Rao, S., Schieber, A. M. P., O'Connor, C. P., Leblanc, M., Michel, D., and Ayres, J. S. (2017). Pathogen-mediated inhibition of anorexia promotes host survival and transmission. *Cell* 168, 503–516.e512. doi: 10.1016/j.cell.2017.01.006

Reinert, M., Benkert, P., Wuerfel, J., Michalak, Z., Ruberte, E., Barro, C., et al. (2020). Serum neurofilament light chain is a useful biomarker in pediatric multiple sclerosis. *Neurol Neuroimmunol. Neuroinflamm.* 7, e749. doi: 10.1212/nxi.0000000000000749

Rosen, D. R., Siddique, T., Patterson, D., Figlewicz, D. A., Sapp, P., Hentati, A., et al. (1993). Mutations in Cu/Zn superoxide dismutase gene are associated with familial amyotrophic lateral sclerosis. *Nature* 362, 59–62. doi: 10.1038/362059a0

Rothhammer, V., Mascanfroni, I. D., Bunse, L., Takenaka, M. C., Kenison, J. E., Mayo, L., et al. (2016). Type I interferons and microbial metabolites of tryptophan modulate astrocyte activity and central nervous system inflammation via the aryl hydrocarbon receptor. *Nat. Med.* 22, 586–597. doi: 10.1038/nm.4106

Rottlaender, A., and Kuerten, S. (2015). Stepchild or prodigy? Neuroprotection in multiple sclerosis (MS) research. *Int. J. Mol. Sci.* 16, 14850–14865. doi: 10.3390/ijms160714850

Russi, A. E., Walker-Caulfield, M. E., and Brown, M. A. (2018). Mast cell inflammasome activity in the meninges regulates EAE disease severity. *Clin. Immunol.* 189, 14–22. doi: 10.1016/j.clim.2016.04.009

Rutsch, A., Kantsjo, J. B., and Ronchi, F. (2020). The gut-brain axis: how microbiota and host inflammasome influence brain physiology and pathology. *Front. Immunol.* 11, 604179. doi: 10.3389/fimmu.2020.604179

Salzer, J., Svenningsson, A., and Sundström, P. (2010). Neurofilament light as a prognostic marker in multiple sclerosis. *Mult. Scler.* 16, 287–292. doi: 10.1177/1352458509359725

Samir, P., Kesavardhana, S., Patmore, D. M., Gingras, S., Malireddi, R. K. S., Karki, R., et al. (2019). DDX3X acts as a live-or-die checkpoint in stressed cells by regulating NLRP3 inflammasome. *Nature* 573, 590–594. doi: 10.1038/s41586-019-1551-2

Sánchez-Fernández, A., Skouras, D. B., Dinarello, C. A., and López-Vales, R. (2019). OLT1177 (Dapansutrile), a selective NLRP3 inflammasome inhibitor, ameliorates experimental autoimmune encephalomyelitis pathogenesis. *Front. Immunol.* 10, 2578. doi: 10.3389/fimmu.2019.02578

Seppi, D., Puthenparampil, M., Federle, L., Ruggero, S., Toffanin, E., Rinaldi, F., et al. (2014). Cerebrospinal fluid IL-1β correlates with cortical pathology load in multiple sclerosis at clinical onset. *J. Neuroimmunol.* 270, 56–60. doi: 10.1016/j.jneuroim.2014.02.014

Serafini, B., Rosicarelli, B., Magliozzi, R., Stigliano, E., and Aloisi, F. (2004). Detection of ectopic B-cell follicles with germinal centers in the meninges of patients with secondary progressive multiple sclerosis. *Brain Pathol.* 14, 164–174. doi: 10.1111/j.1750-3639.2004.tb00049.x

Shao, B.-Z., Wei, W., Ke, P., Xu, Z.-Q., Zhou, J.-X., and Liu, C. (2014). Activating cannabinoid receptor 2 alleviates pathogenesis of experimental autoimmune encephalomyelitis via activation of autophagy and inhibiting NLRP3 inflammasome. *CNS Neurosci. Ther.* 20, 1021–1028. doi: 10.1111/cns.12349

Shao, B.-Z., Xu, Z.-Q., Han, B.-Z., Su, D.-F., and Liu, C. (2015). NLRP3 inflammasome and its inhibitors: a review. *Front. Pharmacol.* 6, 262. doi: 10.3389/fphar.2015.00262

Shao, S., Chen, C., Shi, G., Zhou, Y., Wei, Y., Fan, N., et al. (2021). Therapeutic potential of the target on NLRP3 inflammasome in multiple sclerosis. *Pharmacol. Ther.* 227, 107880. doi: 10.1016/j.pharmthera.2021.107880

Sharif, H., Wang, L., Wang, W. L., Magupalli, V. G., Andreeva, L., Qiao, Q., et al. (2019). Structural mechanism for NEK7-licensed activation of NLRP3 inflammasome. *Nature* 570, 338–343. doi: 10.1038/s41586-019-1295-z

Sharma, R., Young, C., and Neu, J. (2010). Molecular modulation of intestinal epithelial barrier: contribution of microbiota. *J. Biomed. Biotechnol.* 2010, 305879. doi: 10.1155/2010/305879

Shaw, P. J., Lukens, J. R., Burns, S., Chi, H., McGargill, M. A., and Kanneganti, T. D. (2010). Cutting edge: critical role for PYCARD/ASC in the development of experimental autoimmune encephalomyelitis. *J. Immunol.* 184, 4610–4614. doi: 10.4049/jimmunol.1000217

Shenker, B. J., Ojcius, D. M., Walker, L. P., Zekavat, A., Scuron, M. D., and Boesze-Battaglia, K. (2015). Aggregatibacter actinomycetemcomitans cytolethal distending toxin activates the NLRP3 inflammasome in human macrophages, leading to the release of proinflammatory cytokines. *Infect. Immun.* 83, 1487–1496. doi: 10.1128/iai.03132-14

Shi, F. D., Takeda, K., Akira, S., Sarvetnick, N., and Ljunggren, H. G. (2000). IL-18 directs autoreactive T cells and promotes autodestruction in the central nervous system via induction of IFN-gamma by NK cells. *J. Immunol.* 165, 3099–3104. doi: 10.4049/jimmunol.165.6.3099

Shi, J., Gao, W., and Shao, F. (2017). Pyroptosis: gasdermin-mediated programmed necrotic cell death. *Trends Biochem. Sci.* 42, 245–254. doi: 10.1016/j.tibs.2016.10.004

Shi, J., Zhao, Y., Wang, K., Shi, X., Wang, Y., Huang, H., et al. (2015). Cleavage of GSDMD by inflammatory caspases determines pyroptotic cell death. *Nature* 526, 660–665. doi: 10.1038/nature15514

Shi, J., Zhao, Y., Wang, Y., Gao, W., Ding, J., Li, P., et al. (2014). Inflammatory caspases are innate immune receptors for intracellular LPS. *Nature* 514, 187–192. doi: 10.1038/nature13683

Shimada, K., Crother, T. R., Karlin, J., Dagvadorj, J., Chiba, N., Chen, S., et al. (2012). Oxidized mitochondrial DNA activates the NLRP3 inflammasome during apoptosis. *Immunity* 36, 401–414. doi: 10.1016/j.immuni.2012.01.009

Si, X., Fang, Y., Li, L., Gu, L., Yin, X., Yan, Y., et al. (2021). From inflammasome to Parkinson's disease: does the NLRP3 inflammasome facilitate exosome secretion and exosomal alpha-synuclein transmission in Parkinson's disease? *Exp. Neurol.* 336, 113525. doi: 10.1016/j.expneurol.2020.113525

Soares, J. L., Oliveira, E. M., and Pontillo, A. (2019). Variants in NLRP3 and NLRC4 inflammasome associate with susceptibility and severity of multiple sclerosis. *Mult. Scler. Relat. Disord.* 29, 26–34. doi: 10.1016/j.msard.2019.01.023

Sommer, F., and Bäckhed, F. (2013). The gut microbiota–masters of host development and physiology. *Nat. Rev. Microbiol.* 11, 227–238. doi: 10.1038/nrmicro2974

Song, L., Pei, L., Yao, S., Wu, Y., and Shang, Y. (2017). NLRP3 inflammasome in neurological diseases, from functions to therapies. *Front. Cell. Neurosci.* 11, 63. doi: 10.3389/fncel.2017.00063

Soundara Rajan, T., Giacoppo, S., Diomede, F., Bramanti, P., Trubiani, O., and Mazzon, E. (2017). Human periodontal ligament stem cells secretome from multiple sclerosis patients suppresses NALP3 inflammasome activation in experimental autoimmune encephalomyelitis. *Int. J. Immunopathol. Pharmacol.* 30, 238–252. doi: 10.1177/0394632017722332

Swanton, T., Cook, J., Beswick, J. A., Freeman, S., Lawrence, C. B., and Brough, D. (2018). Is targeting the inflammasome a way forward for neuroscience drug discovery? *SLAS Discov.* 23, 991–1017. doi: 10.1177/2472555218786210

Tang, T., Li, P., Zhou, X., Wang, R., Fan, X., Yang, M., et al. (2021). The E3 ubiquitin ligase TRIM65 negatively regulates inflammasome activation through promoting ubiquitination of NLRP3. *Front. Immunol.* 12, 741839. doi: 10.3389/fimmu.2021.741839

Teunissen, C., and Khalil, M. (2012). Neurofilaments as biomarkers in multiple sclerosis. *Mult. Scler.* 18, 552–556. doi: 10.1177/1352458512443092

Trnka, J., Blaikie, F. H., Logan, A., Smith, R. A. J., and Murphy, M. P. (2009). Antioxidant properties of MitoTEMPOL and its hydroxylamine. *Free Radic. Res.* 43, 4–12. doi: 10.1080/10715760802582183

van Lieverloo, G., Wieske, L., Verhamme, C., Vrancken, A., van Doorn, P., Michalak, Z., et al. (2019). Serum neurofilament light chain in chronic inflammatory demyelinating polyneuropathy. *J. Peripher. Nerv. Syst.* 24, 187–194. doi: 10.1111/jns.12319

Verhoef, P. A., Kertesy, S. B., Lundberg, K., Kahlenberg, J. M., and Dubyak, G. R. (2005). Inhibitory effects of chloride on the activation of caspase-1, IL-1beta secretion, and cytolysis by the P2X7 receptor. *J. Immunol.* 175, 7623–7634. doi: 10.4049/jimmunol.175.11.7623

Villar, L. M., Sádaba, M. C., Roldán, E., Masjuan, J., González-Porqué, P., Villarrubia, N., et al. (2005). Intrathecal synthesis of oligoclonal IgM against myelin lipids predicts an aggressive disease course in MS. *J. Clin. Investig.* 115, 187–194. doi: 10.1172/jci200522833

Voet, S., Mc Guire, C., Hagemeyer, N., Martens, A., Schroeder, A., Wieghofer, P., et al. (2018). A20 critically controls microglia activation and inhibits inflammasome-dependent neuroinflammation. *Nat. Commun.* 9, 2036. doi: 10.1038/s41467-018-04376-5

Wang, H. Q., Song, K. Y., Feng, J. Z., Huang, S. Y., Guo, X. M., Zhang, L., et al. (2022). Caffeine inhibits activation of the NLRP3 inflammasome via autophagy to attenuate microglia-mediated neuroinflammation in experimental autoimmune encephalomyelitis. *J. Mol. Neurosci.* 72, 97–112. doi: 10.1007/s12031-021-01894-8

Wang, Q., Hou, L., Zhang, C., Song, F., and Xie, K. (2008). Changes of cytoskeletal proteins in nerve tissues and serum of rats treated with 2,5-hexanedione. *Toxicology* 244, 166–178. doi: 10.1016/j.tox.2007.11.009

Wikoff, W. R., Anfora, A. T., Liu, J., Schultz, P. G., Lesley, S. A., Peters, E. C., et al. (2009). Metabolomics analysis reveals large effects of gut microflora on mammalian blood metabolites. *Proc. Natl. Acad. Sci. U.S.A.* 106, 3698–3703. doi: 10.1073/pnas.0812874106

Wu, X., Ren, G., Zhou, R., Ge, J., and Chen, F. H. (2019). The role of Ca(2+) in acid-sensing ion channel 1a-mediated chondrocyte pyroptosis in rat adjuvant arthritis. *Lab. Invest.* 99, 499–513. doi: 10.1038/s41374-018-0135-3

Yan, B., Zhang, Y., Liang, C., Liu, B., Ding, F., Wang, Y., et al. (2020). Stem cell-derived exosomes prevent pyroptosis and repair ischemic muscle injury through a novel exosome/circHIPK3/ FOXO3a pathway. *Theranostics* 10, 6728–6742. doi: 10.7150/thno.42259

Yang, X., Cao, X., Wei, X., and Zheng, P. (2020). Oridonin ameliorates experimental autoimmune encephalomyelitis by inhibiting NF-κB signaling in T lymphocytes. *Xi Bao Yu Fen Zi Mian Yi Xue Za Zhi* 36, 492–498.

Youm, Y.-H., Nguyen, K. Y., Grant, R. W., Goldberg, E. L., Bodogai, M., Kim, D., et al. (2015). The ketone metabolite β-hydroxybutyrate blocks NLRP3 inflammasome-mediated inflammatory disease. *Nat. Med.* 21, 263–269. doi: 10.1038/nm.3804

Yu, X., Lv, J., Wu, J., Chen, Y., Chen, F., and Wang, L. (2021). The autoimmune encephalitis-related cytokine TSLP in the brain primes neuroinflammation by activating the JAK2-NLRP3 axis. *Clin. Exp. Immunol.* 207, 113–122. doi: 10.1093/cei/uxab023

Yu, Y., Wu, D., Li, J., Deng, S., Liu, T., Zhang, T., et al. (2020). Bixin attenuates experimental autoimmune encephalomyelitis by suppressing TXNIP/NLRP3 inflammasome activity and activating NRF2 signaling. *Front. Immunol.* 11, 593368. doi: 10.3389/fimmu.2020.593368

Zhang, C. J., Jiang, M., Zhou, H., Liu, W., Wang, C., Kang, Z., et al. (2018). TLR-stimulated IRAKM activates caspase-8 inflammasome in microglia and promotes neuroinflammation. *J. Clin. Invest.* 128, 5399–5412. doi: 10.1172/jci121901

Zhang, P., Shao, X. Y., Qi, G. J., Chen, Q., Bu, L. L., Chen, L. J., et al. (2016). Cdk5-dependent activation of neuronal inflammasomes in Parkinson's disease. *Mov. Disord.* 31, 366–376. doi: 10.1002/mds.26488

Zhang, Y., Hou, B., Liang, P., Lu, X., Wu, Y., Zhang, X., et al. (2021). TRPV1 channel mediates NLRP3 inflammasome-dependent neuroinflammation in microglia. *Cell Death Dis.* 12, 1159. doi: 10.1038/s41419-021-04450-9

Zhang, Y., Huang, R., Cheng, M., Wang, L., Chao, J., Li, J., et al. (2019). Gut microbiota from NLRP3-deficient mice ameliorates depressive-like behaviors by regulating astrocyte dysfunction via circHIPK2. *Microbiome* 7, 116. doi: 10.1186/s40168-019-0733-3

Zhang, Y., Liu, F., Yuan, Y., Jin, C., Chang, C., Zhu, Y., et al. (2017). Inflammasome-Derived Exosomes Activate NF-κB Signaling in Macrophages. *J. Proteome Res.* 16, 170–178. doi: 10.1021/acs.jproteome.6b00599

Zhao, M., Sun, D., Guan, Y., Wang, Z., Sang, D., Liu, M., et al. (2016). Disulfiram and diphenhydramine hydrochloride upregulate miR-30a to suppress IL-17-associated autoimmune inflammation. *J. Neurosci.* 36, 9253–9266. doi: 10.1523/jneurosci.4587-15.2016

Zhao, W., Shi, C. S., Harrison, K., Hwang, I. Y., Nabar, N. R., Wang, M., et al. (2020). AKT regulates NLRP3 inflammasome activation by phosphorylating NLRP3 serine 5. *J. Immunol.* 205, 2255–2264. doi: 10.4049/jimmunol.2000649

Zhong, Z., Liang, S., Sanchez-Lopez, E., He, F., Shalapour, S., Lin, X.-J., et al. (2018). New mitochondrial DNA synthesis enables NLRP3 inflammasome activation. *Nature* 560, 198–203. doi: 10.1038/s41586-018-0372-z

Zhu, K., Jin, X., Chi, Z., Chen, S., Wu, S., Sloan, R. D., et al. (2021). Priming of NLRP3 inflammasome activation by Msn kinase MINK1 in macrophages. *Cell. Mol. Immunol.* 18, 2372–2382. doi: 10.1038/s41423-021-00761-1

Conflict of Interest: The authors declare that the research was conducted in the absence of any commercial or financial relationships that could be construed as a potential conflict of interest.

The reviewer TH declared a shared parent affiliation with the authors to the handling editor at the time of review.

Publisher's Note: All claims expressed in this article are solely those of the authors and do not necessarily represent those of their affiliated organizations, or those of the publisher, the editors and the reviewers. Any product that may be evaluated in this article, or claim that may be made by its manufacturer, is not guaranteed or endorsed by the publisher.

frontiers | Frontiers in Molecular Neuroscience

TYPE Mini Review
PUBLISHED 09 September 2022
DOI 10.3389/fnmol.2022.910298

OPEN ACCESS

EDITED BY
Miguel Diaz-Hernandez,
Complutense University of Madrid,
Spain

REVIEWED BY
Alberto Camacho-Morales,
Autonomous University of Nuevo
León, Mexico

*CORRESPONDENCE
Gyongyi Szabo
gszabo1@bidmc.harvard.edu

†These authors have contributed
equally to this work

SPECIALTY SECTION
This article was submitted to
Brain Disease Mechanisms,
a section of the journal
Frontiers in Molecular Neuroscience

RECEIVED 08 April 2022
ACCEPTED 18 July 2022
PUBLISHED 09 September 2022

CITATION
Ramos A, Joshi RS and Szabo G (2022)
Innate immune activation: Parallels
in alcohol use disorder and Alzheimer's
disease.
Front. Mol. Neurosci. 15:910298.
doi: 10.3389/fnmol.2022.910298

Innate immune activation: Parallels in alcohol use disorder and Alzheimer's disease

Adriana Ramos[1†], Radhika S. Joshi[1†] and Gyongyi Szabo[1,2*]

[1]Beth Israel Deaconess Medical Center, Harvard Medical School, Boston, MA, United States, [2]Broad Institute of MIT and Harvard, Cambridge, MA, United States

Alcohol use disorder is associated with systemic inflammation and organ dysfunction especially in the liver and the brain. For more than a decade, studies have highlighted alcohol abuse-mediated impairment of brain function and acceleration of neurodegeneration through inflammatory mechanisms that directly involve innate immune cells. Furthermore, recent studies indicate overlapping genetic risk factors between alcohol use and neurodegenerative disorders, specifically regarding the role of innate immunity in the pathomechanisms of both areas. Considering the pressing need for a better understanding of the relevance of alcohol abuse in dementia progression, here we summarize the molecular mechanisms of neuroinflammation observed in alcohol abuse and Alzheimer's disease, the most common cause of dementia. In addition, we highlight mechanisms that are already established in the field of Alzheimer's disease that may be relevant to explore in alcoholism to better understand alcohol mediated neurodegeneration and dementia, including the relevance of the liver-brain axis.

KEYWORDS

alcohol, microglia, Alzheimer's disease, innate immunity, liver-brain axis, neuroinflammation

Introduction

Alcohol use disorder (AUD), characterized by uncontrolled alcohol drinking, is one of the leading causes of preventable deaths in the United States with a significant socio-economic burden on society (Spillane et al., 2020). Alcoholism is associated with dysfunction of multiple organs leading to cirrhosis, cardiovascular complications, and neuronal dysfunction. Along with the acute sedative effect of ethanol, chronic alcohol abuse is associated with cognitive dysfunction, dementia, neurodegeneration and gray and white matter shrinkage (Crews, 2008; Wilcox et al., 2014; Zahr, 2014; Yang et al., 2016; Schwarzinger et al., 2018; Rehm et al., 2019).

Over the past few decades, we and others have shown that alcohol consumption leads to excessive inflammation in vital organs including liver, intestines, and brain (Crews, 2012; Szabo et al., 2012; Szabo and Lippai, 2014; Bishehsari et al., 2017). Ethanol-induced innate immune activation in the liver plays a central role in alcoholic liver disease and several strategies of intervention that involve targeting the peripheral innate immune system have been proposed (Xu et al., 2017; Tornai and Szabo, 2020). Moreover, alcohol-induced innate immune activation in the central nervous system (CNS) has been shown to mediate neurotoxicity and ethanol-induced behaviors including alcohol addiction and cognitive decline in preclinical and clinical settings (Crews, 2008; Henriques et al., 2018; Erickson et al., 2019b) (see also **Tables 1**, **2**). Indeed, antagonism of IL-1 receptor signaling and the NLRP3 inflammasome reduces inflammation and alcohol consumption (Marshall et al., 2016; Erickson et al., 2019b; Lowe et al., 2020a). In addition, genetic studies demonstrated involvement of the innate immune system in the pathogenesis of AUD. These studies reported polymorphisms associated with AUD in immune-related genes such as NFκB or IL-10 (Crews, 2012; Kapoor et al., 2021). Furthermore, the integration of GWAS and eQTL data helped identify causal variants for AUD involved in the regulation of PU.1, an important transcription factor for myeloid cells and a demonstrated master regulator of the inflammatory response in microglia (Kapoor et al., 2021; Pimenova et al., 2021).

Risk alleles for Alzheimer's disease (AD) are also enriched in myeloid cells and overlapping variants for AUD and AD exist in enhancer regions of the *SPI1* gene (gene that encodes for PU.1 protein) (Bertram et al., 2008; Guerreiro et al., 2013). In addition to genetics, AUD and AD share common pathophysiological mechanisms involving important neuroinflammation and neurodegeneration hallmarks (see section "Alcohol abuse and progression of AD") (Bertram et al., 2008; Crews, 2008; Guerreiro et al., 2013; Heneka et al., 2013; Hong et al., 2016; Hammond et al., 2019; Kapoor et al., 2021). Over the years, several features of microglia (including morphology, motility, proliferation, and secretion) have been studied in detail in various models of AD and AUD independently and are reviewed elsewhere. In this review, we discuss the common pathways that lead to reactive microglia in AD and AUD, and introduce mechanisms explored in AD that may be relevant in the context of AUD. Furthermore, we discuss the implication of these common inflammatory mechanisms on the potentially detrimental effect of alcohol abuse on the progression of AD.

With these components in mind, this review focuses on the role of innate immunity in ethanol-induced neuroinflammation. Since microglia are the primary mediators of innate immunity in the central nervous system, we describe features of microglia activation and their mechanism in AUD.

We also discuss the contribution of the peripheral innate immune system in regulating brain function, especially in the context of AUD. Since the liver is the primary site of alcohol metabolism and a major regulator of innate-immune activation, we hypothesize that, in addition to the direct effect of alcohol or its metabolites on the brain, liver-derived peripheral cytokines, hepatotoxins and circulating immune populations can communicate to the CNS to induce inflammation in AUD. Finally, since these pathways may provide novel insight into the role of alcohol abuse on features of AD, we discuss myeloid cell infiltration and the role of liver-brain axis in AD.

Hence, this review is divided into three broad sections that describe (a) innate immunity in AUD, (b) innate immunity in AD, and (c) studies where effects of alcohol abuse on features of AD have been investigated. This comparison between the features of innate immune activation in AUD and AD will provide new opportunities for future investigations, especially in the context of the dual insult models of AUD and AD. A list of abbreviations and gene symbols is included (see **Table 3**).

Brain innate immunity in alcohol use disorder

Neuroinflammatory mechanisms mediated by microglia

Microglia proliferation and morphology in alcohol use disorder

Effects of alcohol are wide spread in the brain and include cytokine and chemokine release, immune cell infiltration, synapse loss and neuronal death (**Figure 1** and **Table 1**). Microglia, the resident immune cells of the brain, are the key mediators in these processes. Under physiological conditions, microglia survey the brain parenchyma (Nimmerjahn et al., 2005) and take care of many critical CNS functions, enabled by their capacity to release soluble factors, engulf extracellular material and dead cells or migrate to the sites of infection (Butovsky et al., 2014; Paolicelli et al., 2022). Transcriptomic studies demonstrate that the pattern of microglia states varies with the etiology of the disease and severity though commonalities have been found and highlighted across diseases including AUD (Masuda et al., 2020; Chen and Colonna, 2021). Microglia can respond to inflammation through changes in cell morphology, motility, cytokine release, transcriptomic and epigenetic changes. These responses and thus the reactive state of microglia varies with the stimulus and its intensity (Paolicelli et al., 2022). Traditionally, studies have tried to classify microglia as homeostatic Vs activated or M1 (pro-inflammatory) Vs M2 (alternatively activated, anti-inflammatory) based on (1) Morphological features (2) Surface antigen markers (3) Phagocytic ability (4) Cytokine release (Beynon and Walker, 2012; Marshall et al., 2013; Crews and Vetreno, 2016; Paolicelli et al., 2022). In this regard,

TABLE 1 Features of innate immune activation in rodent models of alcohol use disorder.

	Outcome compared to control	Technique	Model	Ethanol paradigm	Brain region	References
Microglia proliferation	↑ proliferation	Cx3cr1-EYFP positive cells/IF	Mouse	10d binge	Prefrontal cortex	Socodato et al., 2020
		Iba1 positive cells/IF		5m chronic treatment	Motor cortex	Alfonso-Loeches et al., 2016
		Iba1 positive cells/IF		10d binge	Cortex	Qin and Crews, 2012a
		$Cd11b^{+}$ $CD45^{low}$ counts/FC	Rat	4d binge	Hippocampus, Entorhinal cortex	Peng et al., 2017
		Iba1 positive cells/IF		4d binge	Hippocampus	Marshall et al., 2013
Microglia morphology	Hyper-ramified	Iba1 positive cells/IF	Mouse	10d binge	Prefrontal cortex	Socodato et al., 2020
	Bushy	Iba1 positive cells/IF		6weeks LDC	Hippocampus	Lowe et al., 2020b
		Iba1 positive cells/DAB		NIAAA	Hippocampus, Cortex	Lowe et al., 2018
		Iba1 positive cells/DAB		5m chronic treatment	Motor cortex	Alfonso-Loeches et al., 2016
		Cd11b (OX-42) positive cells/IHC	Rat	4d binge	Hippocampus	Marshall et al., 2013
Microglia lysosomal expression and phagocytosis	↑ phagocytosis ↑ CD68 expression	Iba1, CD68, PSD-95/IF	Mouse	10d binge	Cortex	Socodato et al., 2020
	↑ phagocytosis of beads	IF	Mouse primary microglia	70 mM Ethanol, 90 min	Cortex	
	↑ CD68	qRT- PCR	Mouse	Single binge	Total brain	Walter and Crews, 2017
		qRT- PCR, WB		5m chronic treatment	Cortex	Alfonso-Loeches et al., 2016
	= CD68	CD68/IHC	Rat	4d binge	Hippocampus, entorhinal cortex	Marshall et al., 2013
	↓ CD68	CD68/FC, qRT-PCR	Mouse	6week LDC	Hippocampus	Lowe et al., 2020b
	↓ phagocytosis of Aβ	FC	Rat primary microglia	75 mM Ethanol, 24 h	Frontal cortex	Kalinin et al., 2018
Cytokine and chemokine expression	↑ TNFα, IL-1β	ELISA	Mouse	6wk LDC	Hippocampus	Lowe et al., 2020b
	↑ TNFα, ↓ IL-6, CCL2	qRT-PCR		10d binge	Cortex	Socodato et al., 2020
	↑ TNFα, IL-18, MCP-1, IL-17, IL-23	qRT-PCR		NIAAA	Cortex	Lowe et al., 2018
	↑ TNFα, IL-6, MCP-1	ELISA		10d binge	Total brain	Qin et al., 2008; Qin and Crews, 2012a
	↑ IFN-γ, IL-33, Cx3CL1, CXCL2, ↓CCL4	ELISA, qRT-PCR		5m chronic treatment	Cortex	Alfonso-Loeches et al., 2016
	↑TNFα, IL-1β, IL-17, IFN-γ, MCP-1, MIP-1, CX3CL1	ELISA		5m chronic treatment	Striatum	Pascual et al., 2015
	↑ TNFα, IL-1β, IL-6, CCL2, 1L-10, 1L-4	qRT-PCR		Single binge	Total brain	Walter and Crews, 2017

(Continued)

TABLE 1 (Continued)

	Outcome compared to control	Technique	Model	Ethanol paradigm	Brain region	References
	↑ TNFα, CCL2	qRT-PCR	BV2 cell line	85 mM Ethanol, 24 h	N/A	
	↑ TNFα, IL-1β	ELISA, qRT-PCR	Mouse and Rat primary microglia	10–100 mM Ethanol, 3-24 h	Cortex	Fernandez-Lizarbe et al., 2009
	↑ TNFα, IL-1β	qRT-PCR	Rat organotypic slice cultures	100 mM Ethanol, 24–96 h	Hippocampal-Entorhinal cortex	Crews et al., 2021
	= TNFα, IL-6 (Trend toward ↓)	ELISA	Rat	4d binge	Hippocampus, Entorhinal cortex	Marshall et al., 2013
Expression of immune mediators	↑ Acetylated HMGB1	WB	Mouse	6wk LDC	Cerebellum	Lippai et al., 2013b
	↑ HMGB1	qRT-PCR		NIAAA	Cortex	Lowe et al., 2018
	↑ iNOS, COX-2	qRT-PCR		Single binge	Total brain	Walter and Crews, 2017
	↑ HMGB1 in EVs	ELISA	Rat organotypic slice cultures	25–100 mM Ethanol, 48 h	Hippocampus-Entorhinal cortex	Coleman et al., 2017
	↑ iNOS, COX-2	WB	Mouse and Rat primary microglia	50 mM Ethanol up to 24 h	Cortex	Fernandez-Lizarbe et al., 2009

4d binge: 4 day alcohol binge model, ∼ 9 g/kg/day in rats.
10d binge: 10 daily alcohol binges- 1.5 g/kg or 5 g/kg in mice.
5m chronic treatment: 5 month chronic alcohol administration through drinking water at 10% v/v in mice.
6wk LDC- 6 weeks of Lieber-DeCarli liquid diet with 5% v/v ethanol, in mice.
NIAAA: 10 days of Lieber-DeCarli liquid diet with 5% v/v ethanol + 5g/kg alcohol binge 9h before sacrifice in mice.
Primary cultures: Primary microglia cultures derived from either rat or mouse.
Single binge: 6g/kg alcohol binge.
DAB- 3,3'Diaminobenzidine.
IF- Immunofluorescence.
IHC-Immunohistochemistry.
FC- Flow Cytometry.

homeostatic microglia have a ramified branched appearance. In response to mild inflammatory stimuli, microglia can show increased branching and a hyper-ramified appearance, also may express anti-inflammatory markers (also referred as M2 markers). During a more severe inflammatory condition, microglia may appear bushy with fewer, thicker branches and bigger soma and secrete pro-inflammatory cytokines, resembling M1 state. Finally, under extreme inflammatory conditions microglia appear amoeboid (Frautschy et al., 1998; Beynon and Walker, 2012). However, recent advances challenge the direct correlation between microglia morphology and their reactiveness and phagocytic ability (Paolicelli et al., 2022). Thus this simplistic classification is now considered out of date (Paolicelli et al., 2022). Therefore, throughout this review, we will refrain from classifying microglia in either of these categories and instead describe various features as reported in literature.

In response to alcohol, microglia can undergo proliferation and also exhibit a spectrum of morphological and molecular transformations, changing their overall function. Indeed, increased microglia proliferation has been reported in the cortex and hippocampus of chronic ethanol-treated mice (McClain et al., 2011; Qin and Crews, 2012a; Marshall et al., 2013; Alfonso-Loeches et al., 2016; Peng et al., 2017; Socodato et al., 2020) and post-mortem brain samples of AUD patients (Qin et al., 2008; Rubio-Araiz et al., 2017).

Several preclinical models of AUD report a moderate change in microglia morphology toward more bushy appearance (**Figure 1** and **Table 1**) (Fernandez-Lizarbe et al., 2009; Lowe et al., 2020b; Socodato et al., 2020).

Microglia phagocytosis in alcohol use disorder

Microglia are the resident phagocytes of the brain and are involved in the clearance of non-functional synapses, pathogenic peptides, myelin debris, and dying neurons (Wyss-Coray et al., 2001; Takahashi et al., 2005; Schafer et al., 2012; Lampron et al., 2015). Microglia exhibit increased phagocytosis during development and in response to inflammatory stimuli (Paolicelli et al., 2011; Kettenmann et al., 2013). The effect of ethanol on microglia phagocytosis appears to be very dynamic and context dependent (**Table 1**). Walter and Crews observed that the levels of lysosomal marker CD68 changes over the withdrawal period of 24 h

TABLE 2 Mechanisms that lead to ethanol-reactive microglia in alcohol use disorder.

	Brief description	Model	Ethanol paradigm	Brain region	References
TLR4 activation					
Features of pathway activation	↑ TLR4, Localization of TLR4 in lipid rafts	Mouse & Rat primary microglia	50 mM Ethanol up to 24 h	Cortex	Fernandez-Lizarbe et al., 2013
	↑ MAPK, JNK signaling	Mouse and Rat primary microglia	10–100 mM Ethanol, 3–24 h	Cortex	Fernandez-Lizarbe et al., 2009
	↑ Release of TNFα				
Phenotype in TLR4 KO	**Protection against ethanol-induced:**	Mouse	5m chronic treatment	Cortex	Alfonso-Loeches et al., 2016
	Alterations in microglia morphology, proliferation				
	Peripheral macrophage infiltration				
	Increased ROS and BBB damage				
	Increase in NLRP3				
	Cytokine, chemokine expression (IL-1β, TLR4, IL-33, CXCL2, CX3CL1, IFN-γ)				
	Cytokine, chemokine expression (TNFα, IL-1β, IFN-γ, IL-17, MCP-1, MIP-1)			Striatum	Pascual et al., 2015
	Anxiety				
Inflammasome activation					
Features of pathway activation	↑ Cleaved IL-1β, Caspase-1	Mouse	6wk LDC	Cerebellum	Lippai et al., 2013b
	↑ NLRP3, Cleaved Caspase-1, ASC dimerization, IL-1β release	Mouse Primary cultures	10–50 mM Ethanol	Cortex	Alfonso-Loeches et al., 2016
	↑Caspase-1 immunoreactivity	Mouse	5m chronic treatment	Cortex	Alfonso-Loeches et al., 2016
Phenotypes on inflammasome inhibition	Protection against cytokine, chemokine expression (TNFα, IL-1β, MCP-1)		6wk LDC	Cerebellum	Lippai et al., 2013b
	Reduction in alcohol consumption and ethanol preference		Two-bottle choice test	N/A	Lowe et al., 2020a
Activation of Complement system					
Features of pathway activation	↑ *C1q*	Slice cultures	100 mM Ethanol, 24–96 h	Hippocampal-Entorhinal cultures	Crews et al., 2021
	↑ *C1q*	Mouse	6wk LDC	Hippocampus, Cerebellum	Lowe et al., 2020b
	↑ *C1q*, *C3*, *C3ar1*	Rat primary cultures	75 mM Ethanol, 24 h	Frontal cortex	Kalinin et al., 2018
	↓ *C1q*	Mouse	10d binge	Cortex	Socodato et al., 2020

after acute alcohol binge, with an initial decline followed by a significant increase that peaks 18 h post binge (Walter and Crews, 2017). Chronic alcohol treatment also appears to increase CD68 levels in the cortex and cerebellum (Lippai et al., 2013a; Alfonso-Loeches et al., 2016; Socodato et al., 2020), although Lowe et al. reported a reduction in CD68 levels in the hippocampi (Lowe et al., 2020b). Furthermore, ethanol pre-treatment reduces phagocytosis of Aβ in primary microglia cultures (Kalinin et al., 2018), consistent with the effect of alcohol on peripheral macrophages (Bukong et al., 2018). Thus, duration of ethanol withdrawal, brain region of interest and phagocytic substrate are

TABLE 3 Abbreviations and gene symbols.

AD- Alzheimer's Disease	LPS-Lipopolysaccharides	CCR-C-C Motif Chemokine Receptor	C3- Complement Component 3	BACE1- Beta-Secretase 1
AUD- Alcohol Use Disorder	TNFα- Tumor Necrosis Factor α	CCL-2- C-C Motif Chemokine Ligand 2	TGFβ-Transforming Growth Factor β	GWAS – Genome-Wide Association Study
EAE-Experimental Autoimmune Encephalomyelitis	DAMPs-Damage-Associated Molecular Patterns	CX3CR1- C-X3-C Motif Chemokine Receptor 1	APP-Amyloid β Precursor Protein	PU.1-Purine rich transcription factor, encoded by *SPI-1* (Spi-1 Proto-Oncogene)
TBI-Traumatic Brain Injury	HMGB1- High-Mobility Group protein 1	CXCL-1- Chemokine (C-X-C motif) ligand 1	BBB- Blood Brain Barrier	TREM2-Triggering Receptor Expressed On Myeloid Cells 2
PRRs- Pattern Recognition Receptors	iNOS- Nitric Oxide Synthases, inducible isoform	MIP-1- Macrophage Inflammatory Proteins	ALS- Amyotrophic Lateral Sclerosis	mir-155- MicroRNA 155
TLRs- Toll Like Receptors	COX-2-Cyclooxygenase-2	MCP-1- Monocyte Chemoattractant Protein-1	FTD- Frontotemporal Dementia	MAPT-Microtubule Associated Protein Tau
NLRP3- NLR Family Pyrin Domain Containing 3	IL- Interleukin family	IFN-Interferon	KO- Knockout Out (mice)	ROS- Reactive Oxygen Species
ASC-Apoptosis-associated Speck-like protein containing a CARD	IL-1Ra- Interleukin-1 Receptor Antagonist	Let-7b – *Lethal-7b*	LRP-1- LDL Receptor Related Protein 1	CNS- Central Nervous System
ASH- Alcoholic Steatohepatitis	NASH- Non-Alcoholic Steatohepatitis	NF-kB – Nuclear Factor kappa B	eQTL – Expression Quantitative Trait Loci	

important in the assessment of ethanol's effect on microglia phagocytosis (**Table 1**).

Release of cytokines and DAMPs by microglia in alcohol use disorder

As mentioned above, alcohol-reactive microglia secrete inflammatory cytokines and chemokines, which are detected at the tissue level in the brain parenchyma or cell culture supernatants (**Figure 1** and **Table 1**). Numerous studies have reported ethanol-induced increases in cytokines and chemokines (TNFα, IL-1β, IL-6, IL-17, IL-23, CCL2, CXCL1, MIP-1α) in various brain regions (Qin et al., 2008; Alfonso-Loeches et al., 2010; Qin and Crews, 2012a; Lippai et al., 2013a,b; Pascual et al., 2015; Walter and Crews, 2017; Lowe et al., 2018, 2020b; Xu et al., 2020). Furthermore, *in vitro* experiments show that direct stimulation of microglia with ethanol produces TNFα, IL-1β and immune mediators such as iNOS, COX-2, among other cytokines (Fernandez-Lizarbe et al., 2009; Walter and Crews, 2017; Lee et al., 2021). Microglia depletion experiments (see also- Section "Insights from microglia depletion experiments in AUD") highlight microglia as the major source of cytokine secretion in AUD. In addition some studies have reported increase in anti-inflammatory IL-4 and IL-10 in brain during ethanol withdrawal, though direct contribution of microglia was demonstrated to be minimal (Marshall et al., 2013; Walter and Crews, 2017). Interestingly, ethanol increased both pro-inflammatory (CD86, CD32) and anti-inflammatory surface markers (CD206) on microglia (Peng and Nixon, 2021). Thus, M1-M2 classification, abundantly used in the alcohol field to describe the dichotomy of pro-inflammatory Vs anti-inflammatory states of microglia are insufficient to bring out nuances of reactive states in AUD (see also- Alzheimer's disease-related mechanisms unexplored in alcoholism: disease associated microglia).

In addition, chronic ethanol treatment up-regulates expression of DAMPs such as HMGB1 in pre-clinical models and post-mortem alcoholic patient samples (Crews et al., 2013; Lippai et al., 2013b; Coleman et al., 2017, 2018). Interestingly, HMGB-1 and micro-RNA let-7b complexes are released in micro-vesicles upon ethanol stimulation and mediate neuronal cell death through TLR-7 (Coleman et al., 2017). Moreover, HMGB1 forms complexes with IL-1β in hippocampal tissue of alcoholic patients and these complexes are shown to have enhanced inflammatory properties (Coleman et al., 2018).

Release of extracellular vesicles by microglia in alcohol use disorder

Extracellular vesicles (EVs) are membrane bound vesicles released by the endocytic machinery into the extracellular space by a variety of cell types including microglia. EVs carry biomolecules such as nucleic acids, peptides, and lipids depending on the cell type of origin and stimulus (Thery et al., 2002; Gupta and Pulliam, 2014; Yang et al., 2018). Circulating EVs can be stable and cross the blood brain barrier, forming a potential route of liver-brain communication and therapeutic intervention (Gupta and Pulliam, 2014) (**Figure 2**). Microglia have been shown to release EVs in response to ATP (Bianco et al., 2005) and inflammatory stimuli such as LPS

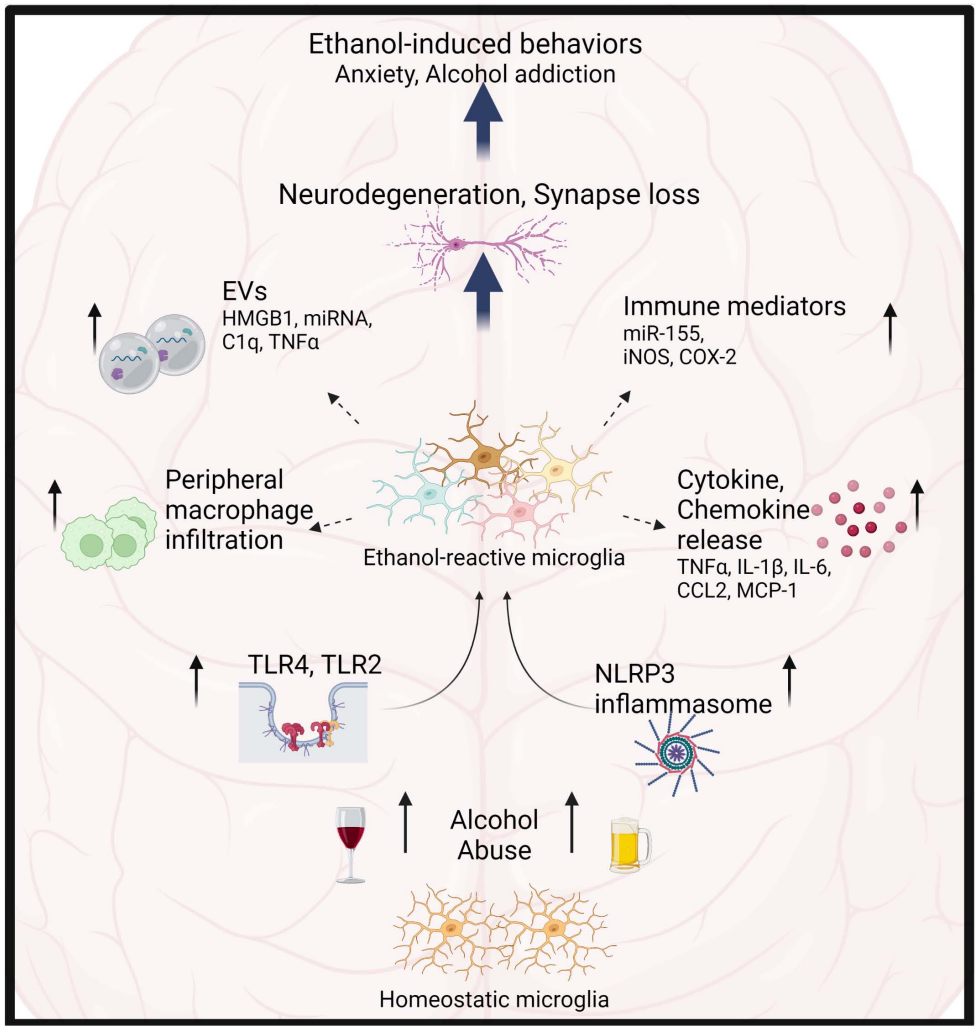

FIGURE 1
Microglia play critical role in alcohol-induced neuroinflammation. Alcohol abuse leads to microglia activation primarily through TLR4, 2, and NLRP3 inflammasomes. Consequently, microglia show increased proliferation, morphological transformation, release of cytokines, chemokines, EVs and immune mediators. This results in infiltration of peripheral macrophages, neurotoxicity, synapse loss and modulation of ethanol-induced behaviors.

(Verderio et al., 2012; Yang et al., 2018). In addition, microglia-derived EVs are thought to propagate inflammation in mouse models of EAE and TBI (Verderio et al., 2012; Kumar et al., 2017). Importantly, microglia-derived EVs contribute toward processing, clearance and spread of Aβ and tau pathology (Rajendran et al., 2006; Tamboli et al., 2010; Asai et al., 2015; Polanco et al., 2016). We and others have shown that ethanol stimulates release of exosomes in plasma that contribute to the pathogenesis of alcoholic hepatitis (Momen-Heravi et al., 2015; Saha et al., 2016; Ibanez et al., 2020; Babuta and Szabo, 2022). In addition, ethanol treatment increases pro-inflammatory cargo of microglia derived EVs including micro-RNA let-7b, C1q, *Tnfa* mRNA, and HMGB1 (Coleman et al., 2017; Mukherjee et al., 2020; Crews et al., 2021) (**Figure 1**). Indeed, Crews et al. showed that ethanol-induced EVs alone are able to propagate pro-inflammatory changes in naïve organotypic slice cultures (Crews et al., 2021). Moreover, they showed that depletion of microglia abrogates pro-inflammatory cargo of ethanol-induced EVs, suggesting that microglia-derived EVs may be a potential route of ethanol-induced neuroinflammation.

Main microglial pathways involved in alcohol use disorder: TLR4, NLRP3 inflammasome and complement system

At the mechanistic level, ethanol is thought to mediate its immune activation primarily via the PRRs-TLR4 and NLRP3, both of which are expressed predominantly in microglia in CNS (Zhang et al., 2014). TLR4, a member of the toll-like receptor family, is a transmembrane protein. Its activation leads to inflammatory cytokine production primarily through

the NF-kB pathway (Kawasaki and Kawai, 2014). Increased TLR2, 3, 4 immunoreactivity has been reported in alcoholic brain tissue (Crews et al., 2013). Ethanol increases the expression of TLR2, 4 in microglia and astrocytes as well as increases their clustering in Caveolin positive lipid rafts (Blanco et al., 2008; Fernandez-Lizarbe et al., 2008, 2013). Deficiency in TLR4 or TLR2 provides protection against a broad range of pro-inflammatory changes mediated by alcohol (**Table 2**). Indeed, TLR4 or TLR2 deficiency attenuates ethanol-induced cytokine and chemokine release, activation of immune mediators (iNOS, COX-2), increased ROS, neuronal death, and anxiety like behavior (Fernandez-Lizarbe et al., 2009, 2013; Alfonso-Loeches et al., 2010; Pascual et al., 2015). In addition, TLR4 KO models provide protection against ethanol-induced microglia proliferation, infiltration of peripheral macrophages, activated microglia morphology and NLRP3 activation (Alfonso-Loeches et al., 2010, 2016). Ethanol treatment also induces TNFα responses in the cerebellum through induction of miR-155, in a TLR4-dependent manner (Lippai et al., 2013a).

Beyond TLR4, NLRP3 inflammasome is also responsible for ethanol-induced immune activation in the CNS (**Table 2**). Inflammasomes are cytosolic multiprotein complexes that regulate the release of cytokines (Broz and Dixit, 2016). Increased NLRP3 immunoreactivity and inflammasome activation was reported in post-mortem AUD brain samples, preclinical models of AUD and cultured microglia (Zou and Crews, 2012; Lippai et al., 2013b; Alfonso-Loeches et al., 2016). We have shown that genetic deficiency of NLRP3, the adaptor protein ASC, or inhibition of inflammasome signaling using IL-1Ra (anakinra) provides partial protection against ethanol mediated increases in TNFα, MCP-1, IL-1β (Lippai et al., 2013b). Moreover, inflammasome inhibition (NLRP3 inhibitor -MCC950 and Caspase-1 inhibitor- VX765) results in decreased alcohol preference in two-bottle choice test in mice (Lowe et al., 2020a). In hippocampal slice cultures, inhibition of inflammasome signaling by an IL-1β neutralizing antibody protects against ethanol-induced loss of neurogenesis (Zou and Crews, 2012).

The complement system mediates the recognition and elimination of pathogens and cellular debris by innate immune cells by guiding their phagocytic function. Seminal work by Stevens et al. and Paolicelli et al. shaped our understanding of the role of the complement system in microglia activity and synaptic pruning under homeostatic and disease conditions (Stevens et al., 2007; Paolicelli et al., 2011; Furman et al., 2012; Hong et al., 2016). In the CNS, complement proteins are mainly expressed in microglia and astrocytes (Zhang et al., 2014; Dalakas et al., 2020). Excessive alcohol consumption has been linked to increased expression of complement components *in vivo* in Raphe nucleus, cerebellum and hippocampus (Lowe et al., 2020b; Lee et al., 2021). Alcohol treatment of microglia cultures or organotypic slice cultures also shows increased expression of complement components, which can have neurotoxic effects (Kalinin et al., 2018; Mukherjee et al., 2020; Crews et al., 2021). However, there are contrasting reports of a reduction in *C1q* levels in frontal cortex of mice treated with ethanol (Socodato et al., 2020). Thus, further investigation using deficiency of complement components can help delineate the role of complement system in ethanol-induced neurotoxicity and behaviors.

Insights from microglia depletion experiments in alcohol use disorder

In addition to microglia, other immune cell types in the brain (astrocytes, oligodendrocyte precursor cells, and endothelial cells) also express PRRs and contribute to ethanol-induced neuroinflammation (see section "Main microglial pathways involved in AUD: TLR4, NLRP3 inflammasome and complement system"). Specific contribution of microglia in ethanol-induced inflammation has been highlighted in studies where microglia were depleted in AUD models. Depletion of microglia by CSF1R inhibitor PLX6522 reduces ethanol-induced inflammatory signatures (such as TNFα, CCL2), increases anti-inflammatory markers (IL-10 and IL-4), and reduces alcohol consumption (Crews et al., 2017; Warden et al., 2020). Moreover, inhibition of microglia activation protects against ethanol-induced aberrant synapse loss, anxiety and depressive behavior (Socodato et al., 2020; Warden et al., 2020; Lee et al., 2021). Microglia-specific transcriptomic changes upon alcohol exposure identified several genes involved in interferon, TGFβ, TLR signaling, and genes associated with alcohol consumption (McCarthy et al., 2018; Erickson et al., 2019a), providing further insights into microglia specific regulation in AUD. Detailed reviews on the role of microglia ablation in ethanol-induced behaviors have been previously published (Erickson et al., 2019b).

Mechanisms of innate immune cell infiltration and communication into the brain parenchyma in alcohol use disorder

The peripheral innate immune system communicates with the CNS to elicit an inflammatory response (Dantzer et al., 2008; Bettcher et al., 2021). The communication between these two systems is established through trans-vascular mechanisms that involve passive or active transport of molecules and cells across the BBB (Varatharaj and Galea, 2017). In addition, the communication between the peripheral immune system and the brain may also involve the circumventricular organs, which are fenestrated and highly permeable regions of the brain (Profaci et al., 2020), that are in close contact with the big reservoir of immune cells located in the pia layer of the brain meninges (Alves de Lima et al., 2020).

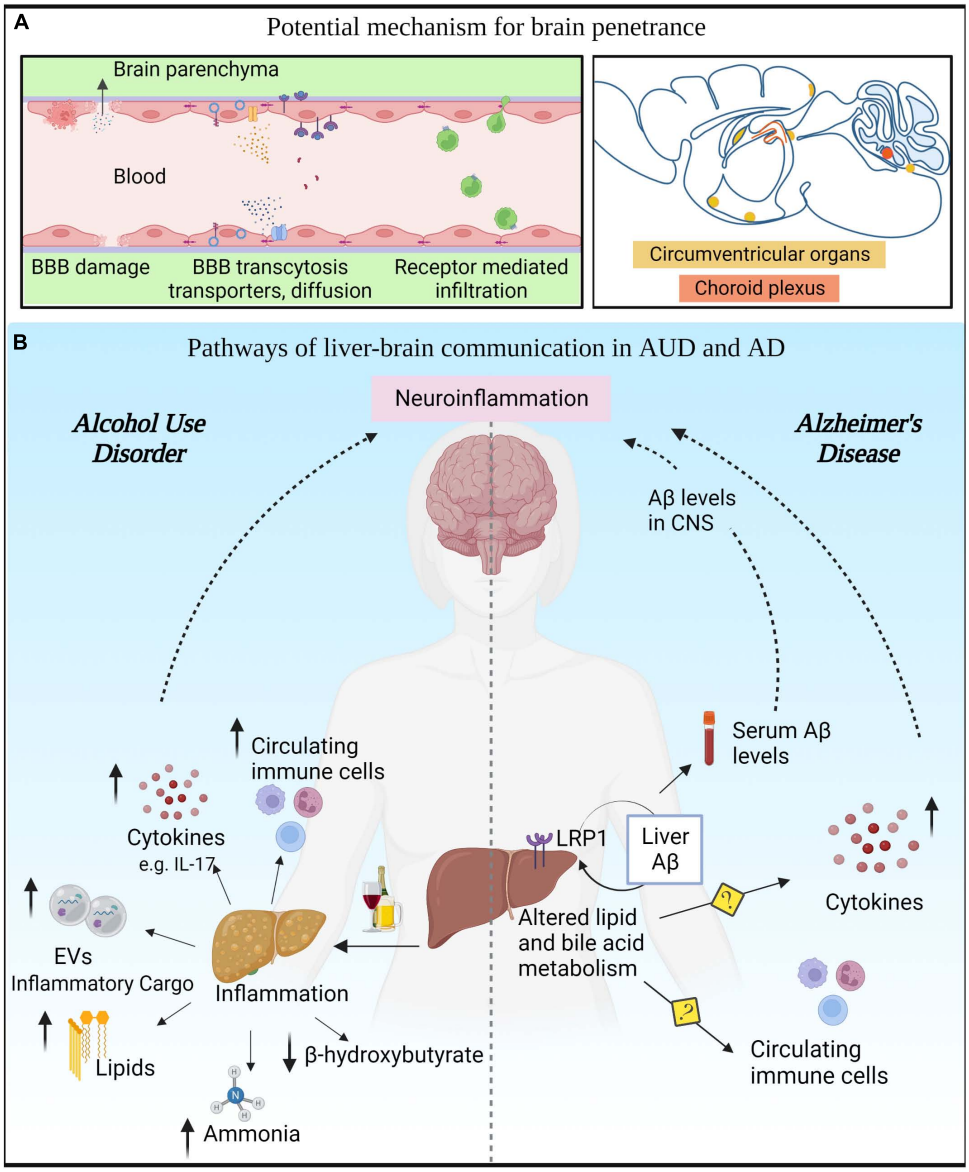

FIGURE 2
Liver-brain axis in alcohol use disorder (AUD) and Alzheimer's disease (AD). **(A)** Various modes of communication between the peripheral circulation and the brain. **(B)** AUD leads to innate immune activation in liver that results in secretion of cytokines, chemokines, toxic lipids, EVs, and hepatotoxins in the circulation that can reach the CNS. In AD, altered liver metabolism of lipids and bile acids can modulate Aβ levels in the periphery and consequently in the CNS.

Peripheral myeloid cells, including monocytes and neutrophils, have been reported to invade the CNS in pathological conditions (Ajami et al., 2018; Jordao et al., 2019; Cugurra et al., 2021) such as TBI and stroke (Herisson et al., 2018; Alam et al., 2020). Although it is likely that same mechanism of infiltration can occur in alcohol use disorders (AUD), clinical evidence that confirms this hypothesis is lacking. However, preclinical studies suggest that immune cell infiltration into the brain parenchyma is a driver of neuroinflammation and a relevant pathomechanism in AUD. Several studies have reported the presence of infiltrating monocytes in the brain parenchyma of rodents exposed to alcohol (Alfonso-Loeches et al., 2016; Hanslik and Ulland, 2020). Some of these studies linked this invasion to an alcohol-mediated disruption of the BBB (Haorah et al., 2005; Xu et al., 2019), although we have demonstrated that the recruitment of peripheral monocytes relies on a chemotactic mechanism involving the CCR2/CCR5 axis (Lowe et al., 2020b).

Hence, the pharmacological blockage of this pathway reverts monocyte infiltration together with microglia activation and other neuroinflammatory outcomes (Haorah et al., 2005). Since the pharmacological intervention referenced specifically targets infiltration of myeloid cells in the brain, monocyte infiltration could be considered a driver of CNS inflammation in this model.

In addition, chronic alcohol abuse causes an increase of systemic inflammation directly affecting the stability of the BBB and increasing the influx of pro-inflammatory mediators into the brain parenchyma (Singh et al., 2007; Alikunju et al., 2011). The BBB consists of specialized endothelial cells lining the cerebral blood vessels, surrounded by pericytes and astrocytes which can sense peripheral inflammation and subsequently drive neuroinflammation in the brain parenchyma (Profaci et al., 2020). Hence, endothelial cells and pericytes appear to mediate the neuroinflammatory mechanisms induced by alcohol (Haorah et al., 2007; Singh et al., 2007; Floreani et al., 2010; Drieu et al., 2020). Similarly, the glymphatic system, whose function specifically depends on the BBB-associated astrocytes, is also impaired by high doses of alcohol (Lundgaard et al., 2018).

Liver-brain axis in alcohol use disorder

Chronic alcohol abuse has a detrimental effect on the brain and the liver. The liver is the major organ involved in the metabolization of alcohol, although alcohol can also be metabolized by certain brain cell types (Jin et al., 2021). Thus, the function of the liver and the brain are very tightly regulated in situations of alcohol abuse, and patients with AUD often develop alcoholic liver disease (ALD), which can progress from steatosis to cirrhosis (Addolorato et al., 2016). During these processes, the liver loses its capacity to detoxify alcohol, subsequently increasing the production and release of hepatotoxins, toxic lipids, and cytokines into circulation with the development of systemic inflammation (Gao et al., 2011). The increase of unmetabolized alcohol, alcohol metabolites, interleukins, microRNAs and other liver-derived byproducts in the blood stream might induce neuroinflammation and brain damage (Szabo and Lippai, 2014). Indeed, preclinical evidence has highlighted the role of liver IL-17A in the induction of glia activation and brain damage. Specifically the pharmacological and genetic intervention to block peripheral IL-17A restored brain function and reduced voluntary alcohol consumption in an alcoholic liver disease model (Ma et al., 2016). In addition, preclinical and clinical studies demonstrate that lower hepatic synthesis of beta-hydroxybutyrate is linked to depression and white matter alterations in AUD (Leclercq et al., 2020).

Epidemiological data indicate that a diverse array of liver pathologies such as ASH, NASH, and viral steatohepatitis, are associated with cognitive and neuropsychiatric decline (Perry et al., 2008; de la Monte et al., 2009; Colognesi et al., 2020). In addition, recent studies have connected liver and brain abnormalities in AUD, suggesting that liver dysfunction predicts severity of executive impairment in AUD patients (Crespi et al., 2019; Lanquetin et al., 2021). Beyond epidemiological studies, preclinical evidence indicates that neuroinflammation (in particular, microglia activation) is implicated in cognitive decline during liver failure (Butterworth, 2011; Zemtsova et al., 2011; McMillin et al., 2016; Sun et al., 2019; Balzano et al., 2020; Hsu et al., 2021). Among all liver disorders, hepatic encephalopathy clearly exemplifies the influence of liver on brain homeostasis (Felipo, 2013). In this pathology, ammonia is believed to be the main liver byproduct that contributes to brain dysfunction. Indeed, several studies have demonstrated that hyperammonemia leads to glia activation (Zemtsova et al., 2011), brain swelling, and cognitive decline (Balzano et al., 2020). Additionally, we propose how other liver byproducts are likely to modulate neuroinflammation (**Figure 2**):

1. *Liver derived cytokines*. Considering the liver is one of the main sources of cytokines in the body (Robinson et al., 2016), it is plausible that liver cytokines reach the blood stream and have the capacity to affect other organs including the brain. Since cytokines are large hydrophilic molecules, they might penetrate the BBB encapsulated in exosomes or exert their effects through endothelial cells without crossing the BBB (Salvador et al., 2021).
2. *Liver derived micro-RNAs*. miRNAs are a class of non-coding RNAs with the capacity to regulate a broad array of biological functions from transcription to translation. These molecules can be transported in the blood stream via EVs (Mori et al., 2019) that can cross the BBB and protect miRNA from degradation (Alvarez-Erviti et al., 2011). Several studies demonstrated that alcohol alters the miRNA profile in the liver and the brain (Lim et al., 2021). In particular, miRNA-155 is upregulated in alcohol abuse and acts as a master regulator of inflammation in both organs. We previously reported that miR-155 mediates alcohol induced neuroinflammation and brain injury (Lippai et al., 2013a). Consequently, mice deficient in miR-155 were protected from pro-inflammatory cytokines and brain injury following ethanol exposure. Since the mice used in this study were constitutive knockouts (KO), the extent of contribution of liver miR-155 in the effects observed in the brain remains unknown.
3. *Liver exosomes and lipids*. As previously mentioned (see section "Release of extracellular vesicles by microglia"), exosomes produced in the liver and secreted into circulation can cross the BBB to reach the brain parenchyma, acting as a direct communicator between the liver and brain. In addition, bioactive lipid- ceramides are upregulated in alcoholic steatohepitits (Longato et al., 2012; Ramirez et al., 2013). Ceramides are important in exosome biogenesis and can cross BBB to exert neuroinflammatory effect (de la Monte et al., 2009).

Brain innate immunity in Alzheimer's disease

Alzheimer's disease (AD) is a neurodegenerative disorder that manifests as memory loss and cognitive decline, and is characterized by accumulation of Aβ and the formation of intracellular neurofibrillary tangles (Heneka et al., 2015; Ennerfelt and Lukens, 2020). Recent genome wide association studies demonstrated the relevance of innate immunity in the pathogenesis of AD. These genetic findings are supported by preclinical and clinical research that explains the role of innate immunity in AD (Heneka et al., 2015; Ennerfelt and Lukens, 2020). In this section, we highlight mechanisms linked to AUD that are also involved in the progression of AD, and discuss AD targets that could be relevant to explore in AUD. We believe that convergent mechanisms may explain the plausible involvement of alcohol abuse in the progression of AD.

Main microglial pathways involved in Alzheimer's disease

Common players described in alcohol use disorder and Alzheimer's disease: TLR4, NLRP3 inflammasome, and complement mediated mechanisms in microglia

In the CNS, TLR4 expression is enriched in microglia, and its activation is involved in the progression of AD and cognitive decline (Walter et al., 2007; Balducci et al., 2017; Zhou et al., 2020). Multiple lines of evidence highlight the involvement of TLR4 in the progression of AD and activation of these receptors was observed in microglia surrounding Aβ plaques (Walter et al., 2007), suggesting that Aβ peptides can be sensed through TLR4 (Walter et al., 2007). In addition, stimulation of TLR4 in microglia modulates the cell's capacity to engulf Aβ plaques and subsequently affect disease progression (Wendeln et al., 2018).

While several inflammasomes are implicated in AD, the NLRP3 inflammasome in particular has been linked to the progression of AD (Dempsey et al., 2017; Heneka, 2017; Ising et al., 2019). Pharmacological intervention or genetic deletion of NLRP3 in preclinical models of familial AD, reduced Aβ plaques (Heneka et al., 2013), tau pathology (Ising et al., 2019), synaptic dysfunction and cognitive decline (Heneka et al., 2013). Furthermore, different studies have demonstrated that Aβ or tau aggregates activate the NLRP3 inflammasome, causing the subsequent release of IL-1β, Caspase-1 and ASC specs that perpetuate the aggregation of Aβ via a positive feedback loop (Venegas et al., 2017; Luciunaite et al., 2020).

As mentioned earlier (see section "Main microglial pathways involved in AUD: TLR4, NLRP3 inflammasome and complement system") complement system plays essential role in microglia mediated phagocytosis during development and disease. This cascade is involved in AD, where Aβ mediated activation of C1q and C3 complexes guide microglia toward synapse pruning and elimination (Schafer et al., 2016; Wu et al., 2019). In the context of Aβ elimination, findings are controversial, and inhibition of this cascade has been linked with increased (Maier et al., 2008) and decreased amyloid load (Schafer et al., 2016; Wu et al., 2019).

Alzheimer's disease-related mechanisms unexplored in alcoholism: disease associated microglia

Depending on their pattern of cytokine expression, microglia may be classified as M1 (inflammatory) or M2 (anti-inflammatory). This classification, although still used and useful for some approaches, is too simplistic to describe the complex physiology and phenotypes of these cells. The development of single cell approaches has allowed researchers to define cell populations of microglia associated with disease. Initially, disease associated microglia (DAM) was an example of a unique microglia population that evolves during the progression of Alzheimer's pathology. This population is characterized by the loss of homeostatic function, with a pattern of expression that does not occur under the classical M1 or M2 phenotypes, and is conserved in mouse and humans (Butovsky et al., 2014; Keren-Shaul et al., 2017; Deczkowska et al., 2018). A similar microglia subset was found in ALS, FTD and aging, and DAM became a common feature among neurodegenerative diseases. This population is characterized by the expression of markers such as TREM2 or APOE, genes that were previously associated with genetic risk factors for AD and other neurodegenerative disorders, although the functional role of this cell subset is still unclear (Butovsky et al., 2014; Keren-Shaul et al., 2017; Deczkowska et al., 2018). In AD, DAM has been linked to the presence of amyloid plaques, but its association to neural cell death or synapse loss remains unknown. Since Aβ plaques are absent in other neurodegenerative pathologies in which DAM is present, common signaling patterns across neurodegenerative diseases that trigger the appearance of this subset is possible. Therefore, an open question remains whether similar populations exist in models of alcohol abuse, or whether alcohol influences the progression of DAM in neurodegenerative models. One feature that seems to be clear is that DAM appears in conditions in which there is accumulation of apoptotic neurons and myelin debris, and such features are present in the brain pathology associated with AUD (Vargas et al., 2014; Guo et al., 2021; Liu et al., 2021; Qin et al., 2021). Furthermore, multiple transcriptional studies reported that alcohol consumption modulates the expression of TREM2 in microglia cells (Erickson et al., 2019a), and TREM2 is required for DAM activation (Krasemann et al., 2017).

Systemic inflammation and immune cell infiltration in Alzheimer's disease

Multiple lines of evidence highlight the role of systemic inflammation in the progression of AD. Epidemiological studies consistently report that patients with AD have higher levels of proinflammatory cytokines (such as TNF and IL-6) (Kim et al., 2017; Bettcher et al., 2021) in their blood. In addition, genetic studies have provided evidence on the etiological role of innate immunity in AD (Lambert et al., 2013; Jansen et al., 2019; Wightman et al., 2021). These studies suggest that the potential causative genes for AD are strongly expressed in immune-related tissues (including liver and spleen) and in immune cell types (such as microglia cells within the CNS). Since then, microglia has been well studied, but the importance of peripheral innate immune cells inducing brain pathology cannot be ruled out. In support of this idea, recent studies highlighted the relevance of peripheral interventions that target innate immune cells as a strategy to revert neurodegeneration and cognitive decline (Bettcher et al., 2021).

Finally, monocytes and neutrophils are recruited to the AD brain, a process that happens as a result of a leaky BBB due to vascular injury (Sweeney et al., 2018), or following chemoattractant mechanisms such as the CCR2/CCL2 or CX3CR1/CX3CL1 axis in the case of monocytes (Naert and Rivest, 2011). Infiltration due to damage in the BBB is linked with neuroinflammation, microglia activation, and reduced synaptic plasticity (Fiala et al., 2002; Sweeney et al., 2018); infiltration that follows chemoattractant mechanisms is linked with neuroprotection. Hence, CCL2 positively recruited monocytes are better phagocytes than microglial cells with a higher capacity to engulf Aβ decreasing amyloid pathology and disease progression (Naert and Rivest, 2011; Guedes et al., 2018).

Liver-brain axis in Alzheimer's disease

The main lines of evidence linking the liver to AD involve the metabolism of lipids (Sutphen et al., 2015; Kim et al., 2016; Nho et al., 2019; Khodabakhsh et al., 2021) and bile acids (Sutphen et al., 2015; Nho et al., 2019), and the role of the liver in the clearance of circulating Aβ (Estrada et al., 2019). As previously mentioned, the liver is in charge of the metabolic detoxification and clearance of the bloodstream to avoid multi-organ failure. In the context of AD, the process of metabolic clearance involves the degradation of systemic Aβ loading. Bile acids and hepatocytes mediate the degradation and uptake of circulatory Aβ, respectively. Specifically, LRP-1 expressed in hepatocytes, binds to Aβ and mediates its uptake from the circulation. The expression of LRP-1 is drastically reduced in conditions of alcohol abuse, obesity or diabetes (Sutphen et al., 2015; Xiang et al., 2015; Estrada et al., 2019), which might subsequently affect the clearance of Aβ .

Furthermore, brain features of AD including accumulation of aberrant lipids and increased abundance of Aβ were observed in a transgenic mouse model in which the synthesis of human amyloid was restricted to the liver (Lam et al., 2021). These mice presented clear signs of neuroinflammation and neurodegeneration together with cognitive decline. This study demonstrates the importance of the liver in maintaining brain homeostasis in the context of AD, and serves as proof that the toxicity of the periphery, specially coming from the liver, can affect the CNS.

In addition, liver deterioration induced by high sugar and high cholesterol diets accelerates AD pathology and cognitive decline (Kim et al., 2016), providing further evidence of the involvement of liver failure in the deterioration of brain function.

Beyond Aβ clearance, the liver is involved in the production and metabolism of lipids. Lipid metabolism, together with neuroinflammation, is one of the main pathomechanisms involved in the pathology of AD (Jansen et al., 2019; Chew et al., 2020), although it has been primarily studied in the context of the CNS. Clinical and preclinical studies have recently highlighted that the metabolism of lipids is impaired at systemic level and not just in the CNS of AD patients, and even peripheral lipid metabolites were proposed as candidate biomarkers to predict cognitive decline in AD (Beal, 2011). Although it is still not clear how the metabolism of lipids in the periphery affect the CNS, we cannot exclude the hypothesis that these lipids could communicate across the BBB (Andreone et al., 2017; Pifferi et al., 2021) or even wrongly influence the reprogramming of innate immune cells (Batista-Gonzalez et al., 2019) (**Figure 2**).

Alcohol abuse and progression of Alzheimer's disease

Clinical studies

Many studies have evaluated the effect of alcohol abuse on brain function, dementia and cognitive decline. However, the field lacks epidemiological data investigating the effect of alcohol in AD. Thus, as far as we know, the available data do not support a strong association between alcohol consumption and AD (Tyas, 2001), although some studies suggest a positive association (Schwarzinger et al., 2018).

Despite inconclusive responses from epidemiological analyses, genetic studies indicate that light or moderate consumption of alcohol later in life is associated with learning and memory deficits in AD patients that carried an *APOE 4* mutation, as APOE was highly enriched in astrocytes and microglia cells in the CNS (Koch et al., 2019). In addition, a

recent study showed overlapping genetic risk factors (such as *SPI1* or *MAPT*) in AD and AUD (Kapoor et al., 2021). This study combined genetic, transcriptomic and epigenetic data to support molecular commonalities among these disorders, highlighting the role of the innate immunity.

Beyond AD, the association of alcohol abuse with other forms of dementia such as alcohol related dementia, Korsakoff Syndrome, or vascular associated dementia is more clear (Schwarzinger et al., 2018), and the role of alcohol in the brain pathology of these syndromes has been previously reviewed (Wiegmann et al., 2020; Parial et al., 2021; Visontay et al., 2021).

Preclinical studies

Dementia and neurodegeneration, the hallmarks of AD, are also observed in AUD patients and preclinical models (Obernier et al., 2002; Alfonso-Loeches et al., 2010; Qin and Crews, 2012b; Coleman et al., 2017; Lundgaard et al., 2018; Mira et al., 2019). However, studies evaluating the direct effect of alcohol on Aβ plaques or neurofibrillary tangles are limited. Chronic alcohol administration exacerbated memory deficits and sensorimotor processing in the 3X-Tg mouse model of AD (Hoffman et al., 2019). In this model alcohol caused up-regulation of Aβ and hyperphosphorylated tau in a region-specific manner (Ibanez et al., 2019). Similarly, four weeks drinking in the dark paradigm exacerbated memory deficits and Aβ plaques in APP23/PS45 mice. The authors observed that ethanol treatment increased APP and BACE1 levels *in vitro* neuronal cell line and in the AD mouse model. Interestingly, a model of moderate alcohol consumption, was found to improve memory performance of 3X-Tg mice, possibly through the effect of alcohol on Aβ aggregation (Belmadani et al., 2004). Although these studies suggest that heavy alcohol consumption may exacerbate AD symptoms, the causative role of innate immune activation in the CNS and periphery in this process remains unknown. Primary microglia cultures treated with ethanol show reduced engulfment of Aβ, suggesting a possible link between increased Aβ burden and alcohol abuse (Kalinin et al., 2018). Considering the commonalities in the innate immune activation in AD and AUD, it is tempting to speculate that alcohol induced-innate immune reactions in the CNS and periphery will exacerbate AD pathology, although a direct relationship remains to be established (Crews, 2008). Moreover, a detailed investigation into the dose of alcohol and the stage of progression of AD needs to be considered while evaluating the effect of alcohol-induced inflammation in AD.

Conclusion

As reviewed here, compelling evidence suggests that AD and AUD share common pathological mechanisms that involve the activation of the innate immune system. In both disorders there is clear evidence for the role of microglia, and both disorders can be viewed as systemic diseases in which the peripheral compartments and liver can regulate and influence the response of the CNS. Despite initial preclinical and clinical evidence of these shared pathomechanisms, the specific role of alcohol abuse in AD progression has not been disentangled and larger longitudinal epidemiological studies and preclinical research in AD models in the context of alcohol abuse is awaited.

Author contributions

AR, RJ, and GS wrote and edited the manuscript. All authors contributed to the article and approved the submitted version.

Funding

This study was supported by NIH grant-R01AG072899 and NIAAA grant-5R01AA017729.

Acknowledgments

We would like to thank Dr. Olivia Potvin, Dr. Mrigya Babuta for their help with manuscript preparation and editing. We also thank NIH and NIAAA grants for funding and support. Figures created using BioRender.com.

Conflict of interest

GS was the editor-in-Chief of Hepatology Communication., consults for Cyta Therapeutics, Durect, Evive, Merck, Novartis, Pandion Therapeutics, Pfizer, Surrozen and Terra Firma, received royalties from UptoDate and Springer and also holds equity in Glympse Bio, Zomagen and Satellite Bio.

The remaining authors declare that the research was conducted in the absence of any commercial or financial relationships that could be construed as a potential conflict of interest.

Publisher's note

References

Addolorato, G., Mirijello, A., Barrio, P., and Gual, A. (2016). Treatment of alcohol use disorders in patients with alcoholic liver disease. *J. Hepatol.* 65, 618–630.

Ajami, B., Samusik, N., Wieghofer, P., Ho, P. P., Crotti, A., Bjornson, Z., et al. (2018). Single-cell mass cytometry reveals distinct populations of brain myeloid cells in mouse neuroinflammation and neurodegeneration models. *Nat. Neurosci.* 21, 541–551. doi: 10.1038/s41593-018-0100-x

Alam, A., Thelin, E. P., Tajsic, T., Khan, D. Z., Khellaf, A., Patani, R., et al. (2020). Cellular infiltration in traumatic brain injury. *J. Neuroinflamm.* 17:328.

Alfonso-Loeches, S., Pascual-Lucas, M., Blanco, A. M., Sanchez-Vera, I., and Guerri, C. (2010). Pivotal role of TLR4 receptors in alcohol-induced neuroinflammation and brain damage. *J. Neurosci.* 30, 8285–8295.

Alfonso-Loeches, S., Urena-Peralta, J., Morillo-Bargues, M. J., Gomez-Pinedo, U., and Guerri, C. (2016). Ethanol-induced TLR4/NLRP3 neuroinflammatory response in microglial cells promotes leukocyte infiltration across the BBB. *Neurochem. Res.* 41, 193–209. doi: 10.1007/s11064-015-1760-5

Alikunju, S., Abdul Muneer, P. M., Zhang, Y., Szlachetka, A. M., and Haorah, J. (2011). The inflammatory footprints of alcohol-induced oxidative damage in neurovascular components. *Brain Behav. Immun.* 25(Suppl. 1), S129–S136. doi: 10.1016/j.bbi.2011.01.007

Alvarez-Erviti, L., Seow, Y., Yin, H., Betts, C., Lakhal, S., and Wood, M. J. (2011). Delivery of siRNA to the mouse brain by systemic injection of targeted exosomes. *Nat. Biotechnol.* 29, 341–345. doi: 10.1038/nbt.1807

Alves de Lima, K., Rustenhoven, J., and Kipnis, J. (2020). Meningeal immunity and its function in maintenance of the central nervous system in health and disease. *Annu. Rev. Immunol.* 38, 597–620. doi: 10.1146/annurev-immunol-102319-103410

Andreone, B. J., Chow, B. W., Tata, A., Lacoste, B., Ben-Zvi, A., Bullock, K., et al. (2017). Blood-brain barrier permeability is regulated by lipid transport-dependent suppression of caveolae-mediated transcytosis. *Neuron* 94, 581–594e5. doi: 10.1016/j.neuron.2017.03.043

Asai, H., Ikezu, S., Tsunoda, S., Medalla, M., Luebke, J., Haydar, T., et al. (2015). Depletion of microglia and inhibition of exosome synthesis halt tau propagation. *Nat. Neurosci.* 18, 1584–1593. doi: 10.1038/nn.4132

Babuta, M., and Szabo, G. (2022). Extracellular vesicles in inflammation: Focus on the microRNA cargo of EVs in modulation of liver diseases. *J. Leukoc. Biol.* 111, 75–92. doi: 10.1002/JLB.3MIR0321-156R

Balducci, C., Frasca, A., Zotti, M., La Vitola, P., Mhillaj, E., Grigoli, E., et al. (2017). Toll-like receptor 4-dependent glial cell activation mediates the impairment in memory establishment induced by beta-amyloid oligomers in an acute mouse model of Alzheimer's disease. *Brain Behav. Immun.* 60, 188–197. doi: 10.1016/j.bbi.2016.10.012

Balzano, T., Dadsetan, S., Forteza, J., Cabrera-Pastor, A., Taoro-Gonzalez, L., Malaguarnera, M., et al. (2020). Chronic hyperammonemia induces peripheral inflammation that leads to cognitive impairment in rats: Reversed by anti-TNF-alpha treatment. *J. Hepatol.* 73, 582–592. doi: 10.1016/j.jhep.2019.01.008

Batista-Gonzalez, A., Vidal, R., Criollo, A., and Carreno, L. J. (2019). New insights on the role of lipid metabolism in the metabolic reprogramming of macrophages. *Front. Immunol.* 10:2993. doi: 10.3389/fimmu.2019.02993

Beal, E. (2011). Lipid biomarkers for early-stage Alzheimer disease. *Nat. Rev. Neurol.* 7:474.

Belmadani, A., Kumar, S., Schipma, M., Collins, M. A., and Neafsey, E. J. (2004). Inhibition of amyloid-beta-induced neurotoxicity and apoptosis by moderate ethanol preconditioning. *Neuroreport* 15, 2093–2096. doi: 10.1097/00001756-200409150-00019

Bertram, L., Lange, C., Mullin, K., Parkinson, M., Hsiao, M., Hogan, M. F., et al. (2008). Genome-wide association analysis reveals putative Alzheimer's disease susceptibility loci in addition to APOE. *Am. J. Hum. Genet.* 83, 623–632. doi: 10.1016/j.ajhg.2008.10.008

Bettcher, B. M., Tansey, M. G., Dorothee, G., and Heneka, M. T. (2021). Peripheral and central immune system crosstalk in Alzheimer disease - a research prospectus. *Nat. Rev. Neurol.* 17, 689–701.

Beynon, S. B., and Walker, F. R. (2012). Microglial activation in the injured and healthy brain: What are we really talking about? Practical and theoretical issues associated with the measurement of changes in microglial morphology. *Neuroscience* 225, 162–171. doi: 10.1016/j.neuroscience.2012.07.029

Bianco, F., Pravettoni, E., Colombo, A., Schenk, U., Moller, T., Matteoli, M., et al. (2005). Astrocyte-derived ATP induces vesicle shedding and IL-1 beta release from microglia. *J. Immunol.* 174, 7268–7277. doi: 10.4049/jimmunol.174.11.7268

Bishehsari, F., Magno, E., Swanson, G., Desai, V., Voigt, R. M., Forsyth, C. B., et al. (2017). Alcohol and gut-derived inflammation. *Alcohol. Res.* 38, 163–171.

Blanco, A. M., Perez-Arago, A., Fernandez-Lizarbe, S., and Guerri, C. (2008). Ethanol mimics ligand-mediated activation and endocytosis of IL-1RI/TLR4 receptors via lipid rafts caveolae in astroglial cells. *J. Neurochem.* 106, 625–639. doi: 10.1111/j.1471-4159.2008.05425.x

Broz, P., and Dixit, V. M. (2016). Inflammasomes: Mechanism of assembly, regulation and signalling. *Nat. Rev. Immunol.* 16, 407–420.

Bukong, T. N., Cho, Y., Iracheta-Vellve, A., Saha, B., Lowe, P., Adejumo, A., et al. (2018). Abnormal neutrophil traps and impaired efferocytosis contribute to liver injury and sepsis severity after binge alcohol use. *J. Hepatol.* 69, 1145–1154. doi: 10.1016/j.jhep.2018.07.005

Butovsky, O., Jedrychowski, M. P., Moore, C. S., Cialic, R., Lanser, A. J., Gabriely, G., et al. (2014). Identification of a unique TGF-beta-dependent molecular and functional signature in microglia. *Nat. Neurosci.* 17, 131–143. doi: 10.1038/nn.3599

Butterworth, R. F. (2011). Hepatic encephalopathy: A central neuroinflammatory disorder? *Hepatology* 53, 1372–1376.

Chen, Y., and Colonna, M. (2021). Microglia in Alzheimer's disease at single-cell level. Are there common patterns in humans and mice? *J. Exp. Med.* 218:e20202717. doi: 10.1084/jem.20202717

Chew, H., Solomon, V. A., and Fonteh, A. N. (2020). Involvement of lipids in Alzheimer's Disease pathology and potential therapies. *Front. Physiol.* 11:598. doi: 10.3389/fphys.2020.00598

Coleman, L. G., Zou, J., and Crews, F. T. (2017). Microglial-derived miRNA let-7 and HMGB1 contribute to ethanol-induced neurotoxicity via TLR7. *J. Neuroinflamm.* 14:22. doi: 10.1186/s12974-017-0799-4

Coleman, L. G., Zou, J., Qin, L., and Crews, F. T. (2018). HMGB1/IL-1beta complexes regulate neuroimmune responses in alcoholism. *Brain Behav. Immun.* 72, 61–77. doi: 10.1016/j.bbi.2017.10.027

Colognesi, M., Gabbia, D., and De Martin, S. (2020). Depression and cognitive impairment-extrahepatic manifestations of NAFLD and NASH. *Biomedicines* 8:229. doi: 10.3390/biomedicines8070229

Crespi, C., Galandra, C., Manera, M., Basso, G., Poggi, P., and Canessa, N. (2019). Executive impairment in alcohol use disorder reflects structural changes in large-scale brain networks: A joint independent component analysis on gray-matter and white-matter features. *Front. Psychol.* 10:2479. doi: 10.3389/fpsyg.2019.02479

Crews, F. T. (2008). Alcohol-related neurodegeneration and recovery: Mechanisms from animal models. *Alcohol Res. Health* 31, 377–388.

Crews, F. T. (2012). Immune function genes, genetics, and the neurobiology of addiction. *Alcohol Res.* 34, 355–361.

Crews, F. T., and Vetreno, R. P. (2016). Mechanisms of neuroimmune gene induction in alcoholism. *Psychopharmacology* 233, 1543–1557.

Crews, F. T., Lawrimore, C. J., Walter, T. J., and Coleman, L. G. JR. (2017). The role of neuroimmune signaling in alcoholism. *Neuropharmacology* 122, 56–73.

Crews, F. T., Qin, L., Sheedy, D., Vetreno, R. P., and Zou, J. (2013). High mobility group box 1/Toll-like receptor danger signaling increases brain neuroimmune activation in alcohol dependence. *Biol. Psychiatry* 73, 602–612. doi: 10.1016/j.biopsych.2012.09.030

Crews, F. T., Zou, J., and Coleman, L. G. JR. (2021). Extracellular microvesicles promote microglia-mediated pro-inflammatory responses to ethanol. *J. Neurosci. Res.* 99, 1940–1956. doi: 10.1002/jnr.24813

Cugurra, A., Mamuladze, T., Rustenhoven, J., Dykstra, T., Beroshvili, G., Greenberg, Z. J., et al. (2021). Skull and vertebral bone marrow are myeloid cell reservoirs for the meninges and CNS parenchyma. *Science* 373:eabf7844. doi: 10.1126/science.abf7844

Dalakas, M. C., Alexopoulos, H., and Spaeth, P. J. (2020). Complement in neurological disorders and emerging complement-targeted therapeutics. *Nat. Rev. Neurol.* 16, 601–617. doi: 10.1038/s41582-020-0400-0

Dantzer, R., O'Connor, J. C., Freund, G. G., Johnson, R. W., and Kelley, K. W. (2008). From inflammation to sickness and depression: When the immune system subjugates the brain. *Nat. Rev. Neurosci.* 9, 46–56. doi: 10.1038/nrn2297

de la Monte, S. M., Longato, L., Tong, M., Denucci, S., and Wands, J. R. (2009). The liver-brain axis of alcohol-mediated neurodegeneration: Role of toxic lipids. *Int. J. Environ. Res. Public Health* 6, 2055–2075. doi: 10.3390/ijerph6072055

Deczkowska, A., Keren-Shaul, H., Weiner, A., Colonna, M., Schwartz, M., and Amit, I. (2018). Disease-associated microglia: A universal immune sensor of neurodegeneration. *Cell* 173, 1073–1081. doi: 10.1016/j.cell.2018.05.003

Dempsey, C., Rubio Araiz, A., Bryson, K. J., Finucane, O., Larkin, C., Mills, E. L., et al. (2017). Inhibiting the NLRP3 inflammasome with MCC950 promotes non-phlogistic clearance of amyloid-beta and cognitive function in APP/PS1 mice. *Brain Behav. Immun.* 61, 306–316. doi: 10.1016/j.bbi.2016.12.014

Drieu, A., Lanquetin, A., Levard, D., Glavan, M., Campos, F., Quenault, A., et al. (2020). Alcohol exposure–induced neurovascular inflammatory priming impacts ischemic stroke and is linked with brain perivascular macrophages. *JCI Insight* 5:e129226. doi: 10.1172/jci.insight.129226

Ennerfelt, H. E., and Lukens, J. R. (2020). The role of innate immunity in Alzheimer's disease. *Immunol. Rev.* 297, 225–246.

Erickson, E. K., Blednov, Y. A., Harris, R. A., and Mayfield, R. D. (2019a). Glial gene networks associated with alcohol dependence. *Sci. Rep.* 9:10949.

Erickson, E. K., Grantham, E. K., Warden, A. S., and Harris, R. A. (2019b). Neuroimmune signaling in alcohol use disorder. *Pharmacol. Biochem. Behav.* 177, 34–60.

Estrada, L. D., Ahumada, P., Cabrera, D., and Arab, J. P. (2019). Liver dysfunction as a novel player in Alzheimer's progression: Looking outside the brain. *Front. Aging Neurosci.* 11:174. doi: 10.3389/fnagi.2019.00174

Felipo, V. (2013). Hepatic encephalopathy: Effects of liver failure on brain function. *Nat. Rev. Neurosci.* 14, 851–858.

Fernandez-Lizarbe, S., Montesinos, J., and Guerri, C. (2013). Ethanol induces TLR4/TLR2 association, triggering an inflammatory response in microglial cells. *J. Neurochem.* 126, 261–273. doi: 10.1111/jnc.12276

Fernandez-Lizarbe, S., Pascual, M., and Guerri, C. (2009). Critical role of TLR4 response in the activation of microglia induced by ethanol. *J. Immunol.* 183, 4733–4744.

Fernandez-Lizarbe, S., Pascual, M., Gascon, M. S., Blanco, A., and Guerri, C. (2008). Lipid rafts regulate ethanol-induced activation of TLR4 signaling in murine macrophages. *Mol. Immunol.* 45, 2007–2016. doi: 10.1016/j.molimm.2007.10.025

Fiala, M., Liu, Q. N., Sayre, J., Pop, V., Brahmandam, V., Graves, M. C., et al. (2002). Cyclooxygenase-2-positive macrophages infiltrate the Alzheimer's disease brain and damage the blood-brain barrier. *Eur. J. Clin. Invest.* 32, 360–371. doi: 10.1046/j.1365-2362.2002.00994.x

Floreani, N. A., Rump, T. J., Abdul Muneer, P. M., Alikunju, S., Morsey, B. M., Brodie, M. R., et al. (2010). Alcohol-induced interactive phosphorylation of Src and toll-like receptor regulates the secretion of inflammatory mediators by human astrocytes. *J. Neuroimmune Pharmacol.* 5, 533–545. doi: 10.1007/s11481-010-9213-z

Frautschy, S. A., Yang, F., Irrizarry, M., Hyman, B., Saido, T. C., Hsiao, K., et al. (1998). Microglial response to amyloid plaques in APPsw transgenic mice. *Am. J. Pathol.* 152, 307–317.

Furman, J. L., Sama, D. M., Gant, J. C., Beckett, T. L., Murphy, M. P., Bachstetter, A. D., et al. (2012). Targeting astrocytes ameliorates neurologic changes in a mouse model of Alzheimer's disease. *J. Neurosci.* 32, 16129–16140. doi: 10.1523/JNEUROSCI.2323-12.2012

Gao, B., Seki, E., Brenner, D. A., Friedman, S., Cohen, J. I., Nagy, L., et al. (2011). Innate immunity in alcoholic liver disease. *Am. J. Physiol. Gastrointest. Liver Physiol.* 300, G516–G525.

Guedes, J. R., Lao, T., Cardoso, A. L., and El Khoury, J. (2018). Roles of microglial and monocyte chemokines and their receptors in regulating Alzheimer's disease-associated amyloid-beta and tau pathologies. *Front. Neurol.* 9:549. doi: 10.3389/fneur.2018.00549

Guerreiro, R., Wojtas, A., Bras, J., Carrasquillo, M., Rogaeva, E., Majounie, E., et al. (2013). TREM2 variants in Alzheimer's disease. *N. Engl. J. Med.* 368, 117–127.

Guo, F., Zhang, Y. F., Liu, K., Huang, X., Li, R. X., Wang, S. Y., et al. (2021). Chronic exposure to alcohol inhibits new myelin generation in adult mouse brain. *Front. Cell Neurosci.* 15:732602. doi: 10.3389/fncel.2021.732602

Gupta, A., and Pulliam, L. (2014). Exosomes as mediators of neuroinflammation. *J. Neuroinflamm.* 11:68.

Hammond, T. R., Marsh, S. E., and Stevens, B. (2019). Immune signaling in neurodegeneration. *Immunity* 50, 955–974.

Hanslik, K. L., and Ulland, T. K. (2020). The role of microglia and the Nlrp3 inflammasome in Alzheimer's disease. *Front. Neurol.* 11:570711. doi: 10.3389/fneur.2020.570711

Haorah, J., Knipe, B., Gorantla, S., Zheng, J., and Persidsky, Y. (2007). Alcohol-induced blood–brain barrier dysfunction is mediated via inositol 1, 4, 5-triphosphate receptor (IP3R)-gated intracellular calcium release. *J. Neurochem.* 100, 324–336. doi: 10.1111/j.1471-4159.2006.04245.x

Haorah, J., Knipe, B., Leibhart, J., Ghorpade, A., and Persidsky, Y. (2005). Alcohol-induced oxidative stress in brain endothelial cells causes blood-brain barrier dysfunction. *J. Leukoc. Biol.* 78, 1223–1232.

Heneka, M. T. (2017). Inflammasome activation and innate immunity in Alzheimer's disease. *Brain Pathol.* 27, 220–222.

Heneka, M. T., Golenbock, D. T., and Latz, E. (2015). Innate immunity in Alzheimer's disease. *Nat. Immunol.* 16, 229–236.

Heneka, M. T., Kummer, M. P., Stutz, A., Delekate, A., Schwartz, S., Vieira-Saecker, A., et al. (2013). NLRP3 is activated in Alzheimer's disease and contributes to pathology in APP/PS1 mice. *Nature* 493, 674–678.

Henriques, J. F., Portugal, C. C., Canedo, T., Relvas, J. B., Summavielle, T., and Socodato, R. (2018). Microglia and alcohol meet at the crossroads: Microglia as critical modulators of alcohol neurotoxicity. *Toxicol. Lett.* 283, 21–31. doi: 10.1016/j.toxlet.2017.11.002

Herisson, F., Frodermann, V., Courties, G., Rohde, D., Sun, Y., Vandoorne, K., et al. (2018). Direct vascular channels connect skull bone marrow and the brain surface enabling myeloid cell migration. *Nat. Neurosci.* 21, 1209–1217. doi: 10.1038/s41593-018-0213-2

Hoffman, J. L., Faccidomo, S., Kim, M., Taylor, S. M., Agoglia, A. E., May, A. M., et al. (2019). Alcohol drinking exacerbates neural and behavioral pathology in the 3xTg-AD mouse model of Alzheimer's disease. *Int. Rev. Neurobiol.* 148, 169–230. doi: 10.1016/bs.irn.2019.10.017

Hong, S., Beja-Glasser, V. F., Nfonoyim, B. M., Frouin, A., Li, S., Ramakrishnan, S., et al. (2016). Complement and microglia mediate early synapse loss in Alzheimer mouse models. *Science* 352, 712–716.

Hsu, S. J., Zhang, C., Jeong, J., Lee, S. I., McConnell, M., Utsumi, T., et al. (2021). Enhanced meningeal lymphatic drainage ameliorates neuroinflammation and hepatic encephalopathy in cirrhotic rats. *Gastroenterology* 160, 1315–1329e13. doi: 10.1053/j.gastro.2020.11.036

Ibanez, F., Montesinos, J., Urena-Peralta, J. R., Guerri, C., and Pascual, M. (2019). TLR4 participates in the transmission of ethanol-induced neuroinflammation via astrocyte-derived extracellular vesicles. *J. Neuroinflamm.* 16:136. doi: 10.1186/s12974-019-1529-x

Ibanez, F., Urena-Peralta, J. R., Costa-Alba, P., Torres, J. L., Laso, F. J., Marcos, M., et al. (2020). Circulating MicroRNAs in extracellular vesicles as potential biomarkers of alcohol-induced neuroinflammation in adolescence: Gender differences. *Int. J. Mol. Sci.* 21:6730. doi: 10.3390/ijms21186730

Ising, C., Venegas, C., Zhang, S., Scheiblich, H., Schmidt, S. V., Vieira-Saecker, A., et al. (2019). NLRP3 inflammasome activation drives tau pathology. *Nature* 575, 669–673. doi: 10.1038/s41586-019-1769-z

Jansen, I. E., Savage, J. E., Watanabe, K., Bryois, J., Williams, D. M., Steinberg, S., et al. (2019). Genome-wide meta-analysis identifies new loci and functional pathways influencing Alzheimer's disease risk. *Nat. Genet.* 51, 404–413.

Jin, S., Cao, Q., Yang, F., Zhu, H., Xu, S., Chen, Q., et al. (2021). Brain ethanol metabolism by astrocytic ALDH2 drives the behavioural effects of ethanol intoxication. *Nat. Metab.* 3, 337–351. doi: 10.1038/s42255-021-00357-z

Jordao, M. J. C., Sankowski, R., Brendecke, S. M., Sagar, Locatelli, G., Tai, Y. H., et al. (2019). Single-cell profiling identifies myeloid cell subsets with distinct fates during neuroinflammation. *Science* 363:eaat7554. doi: 10.1126/science.aat7554

Kalinin, S., Gonzalez-Prieto, M., Scheiblich, H., Lisi, L., Kusumo, H., Heneka, M. T., et al. (2018). Transcriptome analysis of alcohol-treated microglia reveals downregulation of beta amyloid phagocytosis. *J. Neuroinflamm.* 15:141. doi: 10.1186/s12974-018-1184-7

Kapoor, M., Chao, M. J., Johnson, E. C., Novikova, G., Lai, D., Meyers, J. L., et al. (2021). Multi-omics integration analysis identifies novel genes for alcoholism with potential overlap with neurodegenerative diseases. *Nat. Commun.* 12:5071. doi: 10.1038/s41467-021-25392-y

Kawasaki, T., and Kawai, T. (2014). Toll-like receptor signaling pathways. *Front. Immunol.* 5:461. doi: 10.3389/fimmu.2014.00461

Keren-Shaul, H., Spinrad, A., Weiner, A., Matcovitch-Natan, O., Dvir-Szternfeld, R., Ulland, T. K., et al. (2017). A unique microglia type associated with restricting development of Alzheimer's disease. *Cell* 169, 1276–1290.e17. doi: 10.1016/j.cell.2017.05.018

Kettenmann, H., Kirchhoff, F., and Verkhratsky, A. (2013). Microglia: New roles for the synaptic stripper. *Neuron* 77, 10–18. doi: 10.1016/j.neuron.2012.12.023

Khodabakhsh, P., Bazrgar, M., Dargahi, L., Mohagheghi, F., Asgari Taei, A., Parvardeh, S., et al. (2021). Does Alzheimer's disease stem in the gastrointestinal system? *Life Sci.* 287:120088.

Kim, D. G., Krenz, A., Toussaint, L. E., Maurer, K. J., Robinson, S. A., Yan, A., et al. (2016). Non-alcoholic fatty liver disease induces signs of Alzheimer's disease (AD) in wild-type mice and accelerates pathological signs of AD in an AD model. *J. Neuroinflamm.* 13:1. doi: 10.1186/s12974-015-0467-5

Kim, Y. S., Lee, K. J., and Kim, H. (2017). Serum tumour necrosis factor-alpha and interleukin-6 levels in Alzheimer's disease and mild cognitive impairment. *Psychogeriatrics* 17, 224–230.

Koch, M., Fitzpatrick, A. L., Rapp, S. R., Nahin, R. L., Williamson, J. D., Lopez, O. L., et al. (2019). Alcohol consumption and risk of dementia and cognitive decline among older adults with or without mild cognitive impairment. *JAMA Netw. Open* 2:e1910319.

Krasemann, S., Madore, C., Cialic, R., Baufeld, C., Calcagno, N., El Fatimy, R., et al. (2017). The TREM2-APOE pathway drives the transcriptional phenotype of dysfunctional microglia in neurodegenerative diseases. *Immunity* 47, 566–581.e9. doi: 10.1016/j.immuni.2017.08.008

Kumar, A., Stoica, B. A., Loane, D. J., Yang, M., Abulwerdi, G., Khan, N., et al. (2017). Microglial-derived microparticles mediate neuroinflammation after traumatic brain injury. *J. Neuroinflamm.* 14:47. doi: 10.1186/s12974-017-0819-4

Lam, V., Takechi, R., Hackett, M. J., Francis, R., Bynevelt, M., Celliers, L. M., et al. (2021). Synthesis of human amyloid restricted to liver results in an Alzheimer disease-like neurodegenerative phenotype. *PLoS Biol.* 19:e3001358. doi: 10.1371/journal.pbio.3001358

Lambert, J. C., Ibrahim-Verbaas, C. A., Harold, D., Naj, A. C., Sims, R., Bellenguez, C., et al. (2013). Meta-analysis of 74,046 individuals identifies 11 new susceptibility loci for Alzheimer's disease. *Nat. Genet.* 45, 1452–1458. doi: 10.1038/ng.2802

Lampron, A., Larochelle, A., Laflamme, N., Prefontaine, P., Plante, M. M., Sanchez, M. G., et al. (2015). Inefficient clearance of myelin debris by microglia impairs remyelinating processes. *J. Exp. Med.* 212, 481–495. doi: 10.1084/jem.20141656

Lanquetin, A., Leclercq, S., De Timary, P., Segobin, S., Naveau, M., Coulbault, L., et al. (2021). Role of inflammation in alcohol-related brain abnormalities: A translational study. *Brain Commun.* 3:fcab154. doi: 10.1093/braincomms/fcab154

Leclercq, S., Le Roy, T., Furgiuele, S., Coste, V., Bindels, L. B., Leyrolle, Q., et al. (2020). Gut microbiota-induced changes in β-hydroxybutyrate metabolism are linked to altered sociability and depression in alcohol use disorder. *Cell Rep.* 33:108238. doi: 10.1016/j.celrep.2020.108238

Lee, J. S., Lee, S. B., Kim, D. W., Shin, N., Jeong, S. J., Yang, C. H., et al. (2021). Social isolation-related depression accelerates ethanol intake via microglia-derived neuroinflammation. *Sci. Adv.* 7:eabj3400. doi: 10.1126/sciadv.abj3400

Lim, Y., Beane-Ebel, J. E., Tanaka, Y., Ning, B., Husted, C. R., Henderson, D. C., et al. (2021). Exploration of alcohol use disorder-associated brain miRNA-mRNA regulatory networks. *Transl. Psychiatry* 11:504. doi: 10.1038/s41398-021-01635-w

Lippai, D., Bala, S., Csak, T., Kurt-Jones, E. A., and Szabo, G. (2013a). Chronic alcohol-induced microRNA-155 contributes to neuroinflammation in a TLR4-dependent manner in mice. *PLoS One* 8:e70945. doi: 10.1371/journal.pone.0070945

Lippai, D., Bala, S., Petrasek, J., Csak, T., Levin, I., Kurt-Jones, E. A., et al. (2013b). Alcohol-induced IL-1beta in the brain is mediated by NLRP3/ASC inflammasome activation that amplifies neuroinflammation. *J. Leukoc. Biol.* 94, 171–182. doi: 10.1189/jlb.1212659

Liu, W., Vetreno, R. P., and Crews, F. T. (2021). Hippocampal TNF-death receptors, caspase cell death cascades, and IL-8 in alcohol use disorder. *Mol. Psychiatry* 26, 2254–2262. doi: 10.1038/s41380-020-0698-4

Longato, L., Ripp, K., Setshedi, M., Dostalek, M., Akhlaghi, F., Branda, M., et al. (2012). Insulin resistance, ceramide accumulation, and endoplasmic reticulum stress in human chronic alcohol-related liver disease. *Oxid. Med. Cell Longev.* 2012:479348.

Lowe, P. P., Cho, Y., Tornai, D., Coban, S., Catalano, D., and Szabo, G. (2020a). Inhibition of the inflammasome signaling cascade reduces alcohol consumption in female but not male mice. *Alcohol Clin. Exp. Res.* 44, 567–578. doi: 10.1111/acer.14272

Lowe, P. P., Gyongyosi, B., Satishchandran, A., Iracheta-Vellve, A., Cho, Y., Ambade, A., et al. (2018). Reduced gut microbiome protects from alcohol-induced neuroinflammation and alters intestinal and brain inflammasome expression. *J. Neuroinflamm.* 15:298. doi: 10.1186/s12974-018-1328-9

Lowe, P. P., Morel, C., Ambade, A., Iracheta-Vellve, A., Kwiatkowski, E., Satishchandran, A., et al. (2020b). Chronic alcohol-induced neuroinflammation involves CCR2/5-dependent peripheral macrophage infiltration and microglia alterations. *J. Neuroinflamm.* 17:296. doi: 10.1186/s12974-020-01972-5

Luciunaite, A., Mcmanus, R. M., Jankunec, M., Racz, I., Dansokho, C., Dalgediene, I., et al. (2020). Soluble Abeta oligomers and protofibrils induce NLRP3 inflammasome activation in microglia. *J. Neurochem.* 155, 650–661. doi: 10.1111/jnc.14945

Lundgaard, I., Wang, W., Eberhardt, A., Vinitsky, H. S., Reeves, B. C., Peng, S., et al. (2018). Beneficial effects of low alcohol exposure, but adverse effects of high alcohol intake on glymphatic function. *Sci. Rep.* 8:2246. doi: 10.1038/s41598-018-20424-y

Ma, H. Y., Xu, J., Liu, X., Zhu, Y., Gao, B., Karin, M., et al. (2016). The role of IL-17 signaling in regulation of the liver-brain axis and intestinal permeability in Alcoholic Liver Disease. *Curr. Pathobiol. Rep.* 4, 27–35. doi: 10.1007/s40139-016-0097-3

Maier, M., Peng, Y., Jiang, L., Seabrook, T. J., Carroll, M. C., and Lemere, C. A. (2008). Complement C3 deficiency leads to accelerated amyloid beta plaque deposition and neurodegeneration and modulation of the microglia/macrophage phenotype in amyloid precursor protein transgenic mice. *J. Neurosci.* 28, 6333–6341. doi: 10.1523/JNEUROSCI.0829-08.2008

Marshall, S. A., Casachahua, J. D., Rinker, J. A., Blose, A. K., Lysle, D. T., and Thiele, T. E. (2016). IL-1 receptor signaling in the basolateral amygdala modulates binge-like ethanol consumption in male C57BL/6J mice. *Brain Behav. Immun.* 51, 258–267. doi: 10.1016/j.bbi.2015.09.006

Marshall, S. A., Mcclain, J. A., Kelso, M. L., Hopkins, D. M., Pauly, J. R., and Nixon, K. (2013). Microglial activation is not equivalent to neuroinflammation in alcohol-induced neurodegeneration: The importance of microglia phenotype. *Neurobiol. Dis.* 54, 239–251.

Masuda, T., Sankowski, R., Staszewski, O., and Prinz, M. (2020). Microglia heterogeneity in the single-cell era. *Cell Rep.* 30, 1271–1281.

McCarthy, G. M., Farris, S. P., Blednov, Y. A., Harris, R. A., and Mayfield, R. D. (2018). Microglial-specific transcriptome changes following chronic alcohol consumption. *Neuropharmacology* 128, 416–424. doi: 10.1016/j.neuropharm.2017.10.035

McClain, J. A., Morris, S. A., Deeny, M. A., Marshall, S. A., Hayes, D. M., Kiser, Z. M., et al. (2011). Adolescent binge alcohol exposure induces long-lasting partial activation of microglia. *Brain Behav. Immun.* 25(Suppl. 1), S120–S128. doi: 10.1016/j.bbi.2011.01.006

McMillin, M., Grant, S., Frampton, G., Andry, S., Brown, A., and Demorrow, S. (2016). Fractalkine suppression during hepatic encephalopathy promotes neuroinflammation in mice. *J. Neuroinflamm.* 13:198. doi: 10.1186/s12974-016-0674-8

Mira, R. G., Lira, M., Tapia-Rojas, C., Rebolledo, D. L., Quintanilla, R. A., and Cerpa, W. (2019). Effect of alcohol on hippocampal-dependent plasticity and behavior: Role of glutamatergic synaptic transmission. *Front. Behav. Neurosci.* 13:288. doi: 10.3389/fnbeh.2019.00288

Momen-Heravi, F., Saha, B., Kodys, K., Catalano, D., Satishchandran, A., and Szabo, G. (2015). Increased number of circulating exosomes and their microRNA cargos are potential novel biomarkers in alcoholic hepatitis. *J. Transl. Med.* 13:261. doi: 10.1186/s12967-015-0623-9

Mori, M. A., Ludwig, R. G., Garcia-Martin, R., Brandao, B. B., and Kahn, C. R. (2019). Extracellular miRNAs: From biomarkers to mediators of physiology and disease. *Cell Metab.* 30, 656–673.

Mukherjee, S., Cabrera, M. A., Boyadjieva, N. I., Berger, G., Rousseau, B., and Sarkar, D. K. (2020). Alcohol increases exosome release from microglia to promote complement C1q-induced cellular death of proopiomelanocortin neurons in the hypothalamus in a rat model of fetal alcohol spectrum disorders. *J. Neurosci.* 40, 7965–7979. doi: 10.1523/JNEUROSCI.0284-20.2020

Naert, G., and Rivest, S. (2011). CC chemokine receptor 2 deficiency aggravates cognitive impairments and amyloid pathology in a transgenic mouse model of Alzheimer's disease. *J. Neurosci.* 31, 6208–6220. doi: 10.1523/JNEUROSCI.0299-11.2011

Nho, K., Kueider-Paisley, A., Ahmad, S., Mahmoudiandehkordi, S., Arnold, M., Risacher, S. L., et al. (2019). Association of altered liver enzymes with Alzheimer disease diagnosis, cognition, neuroimaging measures, and cerebrospinal fluid biomarkers. *JAMA Netw. Open* 2:e197978. doi: 10.1001/jamanetworkopen.2019.7978

Nimmerjahn, A., Kirchhoff, F., and Helmchen, F. (2005). Resting microglial cells are highly dynamic surveillants of brain parenchyma in vivo. *Science* 308, 1314–1318.

Obernier, J. A., White, A. M., Swartzwelder, H. S., and Crews, F. T. (2002). Cognitive deficits and CNS damage after a 4-day binge ethanol exposure in rats. *Pharmacol. Biochem. Behav.* 72, 521–532.

Paolicelli, R. C., Bolasco, G., Pagani, F., Maggi, L., Scianni, M., Panzanelli, P., et al. (2011). Synaptic pruning by microglia is necessary for normal brain development. *Science* 333, 1456–1458.

Paolicelli, R., Sierra, A., Stevens, B., Tremblay, M. E., Aguzzi, A., Ajami, B., et al. (2022). *Defining microglial states and nomenclature: A roadmap to 2030. SSRN Electron. J.* [Preprint]. doi: 10.2139/ssrn.4065080

Parial, L. L., Lam, S. C., Ho, J. Y. S., Suen, L. K. P., and Leung, A. Y. M. (2021). Public knowledge of the influence of modifiable cardiovascular risk factors on dementia: A systematic literature review and meta-analysis. *Aging Ment. Health* 25, 1395–1409. doi: 10.1080/13607863.2020.1786801

Pascual, M., Balino, P., Aragon, C. M., and Guerri, C. (2015). Cytokines and chemokines as biomarkers of ethanol-induced neuroinflammation and anxiety-related behavior: Role of TLR4 and TLR2. *Neuropharmacology* 89, 352–359. doi: 10.1016/j.neuropharm.2014.10.014

Peng, H., and Nixon, K. (2021). Microglia phenotypes following the induction of alcohol dependence in adolescent rats. *Alcohol Clin. Exp. Res.* 45, 105–116. doi: 10.1111/acer.14504

Peng, H., Geil Nickell, C. R., Chen, K. Y., Mcclain, J. A., and Nixon, K. (2017). Increased expression of M1 and M2 phenotypic markers in isolated microglia after four-day binge alcohol exposure in male rats. *Alcohol* 62, 29–40. doi: 10.1016/j.alcohol.2017.02.175

Perry, W., Hilsabeck, R. C., and Hassanein, T. I. (2008). Cognitive dysfunction in chronic hepatitis C: A review. *Dig. Dis. Sci.* 53, 307–321.

Pifferi, F., Laurent, B., and Plourde, M. (2021). Lipid transport and metabolism at the blood-brain interface: Implications in health and disease. *Front. Physiol.* 12:645646. doi: 10.3389/fphys.2021.645646

Pimenova, A. A., Herbinet, M., Gupta, I., Machlovi, S. I., Bowles, K. R., Marcora, E., et al. (2021). Alzheimer's-associated PU.1 expression levels regulate microglial inflammatory response. *Neurobiol. Dis.* 148:105217. doi: 10.1016/j.nbd.2020.105217

Polanco, J. C., Scicluna, B. J., Hill, A. F., and Gotz, J. (2016). Extracellular vesicles isolated from the brains of rTg4510 mice seed tau protein aggregation in a threshold-dependent manner. *J. Biol. Chem.* 291, 12445–12466. doi: 10.1074/jbc.M115.709485

Profaci, C. P., Munji, R. N., Pulido, R. S., and Daneman, R. (2020). The blood-brain barrier in health and disease: Important unanswered questions. *J. Exp. Med.* 217:e20190062. doi: 10.1084/jem.20190062

Qin, L., and Crews, F. T. (2012a). Chronic ethanol increases systemic TLR3 agonist-induced neuroinflammation and neurodegeneration. *J. Neuroinflamm.* 9:130. doi: 10.1186/1742-2094-9-130

Qin, L., and Crews, F. T. (2012b). NADPH oxidase and reactive oxygen species contribute to alcohol-induced microglial activation and neurodegeneration. *J Neuroinflamm.* 9:5. doi: 10.1186/1742-2094-9-5

Qin, L., He, J., Hanes, R. N., Pluzarev, O., Hong, J. S., and Crews, F. T. (2008). Increased systemic and brain cytokine production and neuroinflammation by endotoxin following ethanol treatment. *J. Neuroinflamm.* 5:10. doi: 10.1186/1742-2094-5-10

Qin, L., Zou, J., Barnett, A., Vetreno, R. P., Crews, F. T., and Coleman, L. G. JR. (2021). TRAIL mediates neuronal death in AUD: A link between neuroinflammation and neurodegeneration. *Int. J. Mol. Sci.* 22:2547. doi: 10.3390/ijms22052547

Rajendran, L., Honsho, M., Zahn, T. R., Keller, P., Geiger, K. D., Verkade, P., et al. (2006). Alzheimer's disease beta-amyloid peptides are released in association with exosomes. *Proc. Natl. Acad. Sci. U.S.A.* 103, 11172–11177.

Ramirez, T., Longato, L., Dostalek, M., Tong, M., Wands, J. R., and De La Monte, S. M. (2013). Insulin resistance, ceramide accumulation and endoplasmic reticulum stress in experimental chronic alcohol-induced steatohepatitis. *Alcohol Alcohol.* 48, 39–52.

Rehm, J., Hasan, O. S. M., Black, S. E., Shield, K. D., and Schwarzinger, M. (2019). Alcohol use and dementia: A systematic scoping review. *Alzheimers Res. Ther.* 11:1.

Robinson, M. W., Harmon, C., and O'Farrelly, C. (2016). Liver immunology and its role in inflammation and homeostasis. *Cell Mol. Immunol.* 13, 267–276.

Rubio-Araiz, A., Porcu, F., Perez-Hernandez, M., Garcia-Gutierrez, M. S., Aracil-Fernandez, M. A., Gutierrez-Lopez, M. D., et al. (2017). Disruption of blood-brain barrier integrity in postmortem alcoholic brain: Preclinical evidence of TLR4 involvement from a binge-like drinking model. *Addict Biol* 22, 1103–1116. doi: 10.1111/adb.12376

Saha, B., Momen-Heravi, F., Kodys, K., and Szabo, G. (2016). MicroRNA cargo of extracellular vesicles from alcohol-exposed monocytes signals naive monocytes to differentiate into M2 macrophages. *J. Biol. Chem.* 291, 149–159. doi: 10.1074/jbc.M115.694133

Salvador, A. F., De Lima, K. A., and Kipnis, J. (2021). Neuromodulation by the immune system: A focus on cytokines. *Nat. Rev. Immunol.* 21, 526–541.

Schafer, D. P., Heller, C. T., Gunner, G., Heller, M., Gordon, C., Hammond, T., et al. (2016). Microglia contribute to circuit defects in Mecp2 null mice independent of microglia-specific loss of Mecp2 expression. *Elife* 5:e15224. doi: 10.7554/eLife.15224

Schafer, D. P., Lehrman, E. K., Kautzman, A. G., Koyama, R., Mardinly, A. R., Yamasaki, R., et al. (2012). Microglia sculpt postnatal neural circuits in an activity and complement-dependent manner. *Neuron* 74, 691–705. doi: 10.1016/j.neuron.2012.03.026

Schwarzinger, M., Pollock, B. G., Hasan, O. S. M., Dufouil, C., Rehm, J., and Qalydays Study Group (2018). Contribution of alcohol use disorders to the burden of dementia in France 2008-13: A nationwide retrospective cohort study. *Lancet Public Health* 3, e124–e132. doi: 10.1016/S2468-2667(18)30022-7

Singh, A. K., Jiang, Y., Gupta, S., and Benlhabib, E. (2007). Effects of chronic ethanol drinking on the blood brain barrier and ensuing neuronal toxicity in alcohol-preferring rats subjected to intraperitoneal LPS injection. *Alcohol Alcohol.* 42, 385–399. doi: 10.1093/alcalc/agl120

Socodato, R., Henriques, J. F., Portugal, C. C., Almeida, T. O., Tedim-Moreira, J., Alves, R. L., et al. (2020). Daily alcohol intake triggers aberrant synaptic pruning leading to synapse loss and anxiety-like behavior. *Sci. Signal.* 13:eaba5754. doi: 10.1126/scisignal.aba5754

Spillane, S., Shiels, M. S., Best, A. F., Haozous, E. A., Withrow, D. R., Chen, Y., et al. (2020). Trends in alcohol-induced deaths in the United States, 2000-2016. *JAMA Netw. Open* 3:e1921451. doi: 10.1001/jamanetworkopen.2019.21451

Stevens, B., Allen, N. J., Vazquez, L. E., Howell, G. R., Christopherson, K. S., Nouri, N., et al. (2007). The classical complement cascade mediates CNS synapse elimination. *Cell* 131, 1164–1178.

Sun, X., Han, R., Cheng, T., Zheng, Y., Xiao, J., So, K. F., et al. (2019). Corticosterone-mediated microglia activation affects dendritic spine plasticity and motor learning functions in minimal hepatic encephalopathy. *Brain Behav. Immun.* 82, 178–187. doi: 10.1016/j.bbi.2019.08.184

Sutphen, C. L., Jasielec, M. S., Shah, A. R., Macy, E. M., Xiong, C., Vlassenko, A. G., et al. (2015). Longitudinal cerebrospinal fluid biomarker changes in preclinical Alzheimer disease during middle age. *JAMA Neurol.* 72, 1029–1042.

Sweeney, M. D., Sagare, A. P., and Zlokovic, B. V. (2018). Blood-brain barrier breakdown in Alzheimer disease and other neurodegenerative disorders. *Nat. Rev. Neurol.* 14, 133–150.

Szabo, G., and Lippai, D. (2014). Converging actions of alcohol on liver and brain immune signaling. *Int. Rev. Neurobiol.* 118, 359–380. doi: 10.1016/B978-0-12-801284-0.00011-7

Szabo, G., Petrasek, J., and Bala, S. (2012). Innate immunity and alcoholic liver disease. *Dig. Dis.* 30(Suppl. 1), 55–60.

Takahashi, K., Rochford, C. D., and Neumann, H. (2005). Clearance of apoptotic neurons without inflammation by microglial triggering receptor expressed on myeloid cells-2. *J. Exp. Med.* 201, 647–657.

Tamboli, I. Y., Barth, E., Christian, L., Siepmann, M., Kumar, S., Singh, S., et al. (2010). Statins promote the degradation of extracellular amyloid {beta}-peptide by microglia via stimulation of exosome-associated insulin-degrading enzyme (IDE) secretion. *J. Biol. Chem.* 285, 37405–37414. doi: 10.1074/jbc.M110.149468

Thery, C., Zitvogel, L., and Amigorena, S. (2002). Exosomes: Composition, biogenesis and function. *Nat. Rev. Immunol.* 2, 569–579.

Tornai, D., and Szabo, G. (2020). Emerging medical therapies for severe alcoholic hepatitis. *Clin. Mol. Hepatol.* 26, 686–696.

Tyas, S. L. (2001). Alcohol use and the risk of developing Alzheimer's disease. *Alcohol Res. Health* 25, 299–306.

Varatharaj, A., and Galea, I. (2017). The blood-brain barrier in systemic inflammation. *Brain Behav. Immun.* 60, 1–12.

Vargas, W. M., Bengston, L., Gilpin, N. W., Whitcomb, B. W., and Richardson, H. N. (2014). Alcohol binge drinking during adolescence or dependence during adulthood reduces prefrontal myelin in male rats. *J. Neurosci.* 34, 14777–14782.

Venegas, C., Kumar, S., Franklin, B. S., Dierkes, T., Brinkschulte, R., Tejera, D., et al. (2017). Microglia-derived ASC specks cross-seed amyloid-beta in Alzheimer's disease. *Nature* 552, 355–361. doi: 10.1038/nature25158

Verderio, C., Muzio, L., Turola, E., Bergami, A., Novellino, L., Ruffini, F., et al. (2012). Myeloid microvesicles are a marker and therapeutic target for neuroinflammation. *Ann. Neurol.* 72, 610–624. doi: 10.1002/ana.23627

Visontay, R., Rao, R. T., and Mewton, L. (2021). Alcohol use and dementia: New research directions. *Curr. Opin. Psychiatry* 34, 165–170.

Walter, S., Letiembre, M., Liu, Y., Heine, H., Penke, B., Hao, W., et al. (2007). Role of the toll-like receptor 4 in neuroinflammation in Alzheimer's disease. *Cell Physiol. Biochem.* 20, 947–956.

Walter, T. J., and Crews, F. T. (2017). Microglial depletion alters the brain neuroimmune response to acute binge ethanol withdrawal. *J. Neuroinflamm.* 14:86. doi: 10.1186/s12974-017-0856-z

Warden, A. S., Wolfe, S. A., Khom, S., Varodayan, F. P., Patel, R. R., Steinman, M. Q., et al. (2020). Microglia control escalation of drinking in alcohol-dependent mice: Genomic and synaptic drivers. *Biol. Psychiatry* 88, 910–921. doi: 10.1016/j.biopsych.2020.05.011

Wendeln, A. C., Degenhardt, K., Kaurani, L., Gertig, M., Ulas, T., Jain, G., et al. (2018). Innate immune memory in the brain shapes neurological disease hallmarks. *Nature* 556, 332–338. doi: 10.1038/s41586-018-0023-4

Wiegmann, C., Mick, I., Brandl, E. J., Heinz, A., and Gutwinski, S. (2020). Alcohol and dementia - what is the link? A systematic review. *Neuropsychiatr. Dis. Treat.* 16, 87–99. doi: 10.2147/NDT.S198772

Wightman, D. P., Jansen, I. E., Savage, J. E., Shadrin, A. A., Bahrami, S., Holland, D., et al. (2021). A genome-wide association study with 1,126,563 individuals identifies new risk loci for Alzheimer's disease. *Nat. Genet.* 53, 1276–1282.

Wilcox, C. E., Dekonenko, C. J., Mayer, A. R., Bogenschutz, M. P., and Turner, J. A. (2014). Cognitive control in alcohol use disorder: Deficits and clinical relevance. *Rev. Neurosci.* 25, 1–24.

Wu, T., Dejanovic, B., Gandham, V. D., Gogineni, A., Edmonds, R., Schauer, S., et al. (2019). Complement C3 is activated in human AD brain and is required for neurodegeneration in mouse models of amyloidosis and tauopathy. *Cell Rep.* 28, 2111–2123.e6. doi: 10.1016/j.celrep.2019.07.060

Wyss-Coray, T., Lin, C., Yan, F., Yu, G. Q., Rohde, M., Mcconlogue, L., et al. (2001). TGF-beta1 promotes microglial amyloid-beta clearance and reduces plaque burden in transgenic mice. *Nat. Med.* 7, 612–618. doi: 10.1038/87945

Xiang, Y., Bu, X. L., Liu, Y. H., Zhu, C., Shen, L. L., Jiao, S. S., et al. (2015). Physiological amyloid-beta clearance in the periphery and its therapeutic potential for Alzheimer's disease. *Acta Neuropathol.* 130, 487–499.

Xu, G., Li, C., Parsiola, A. L., Li, J., Mccarter, K. D., Shi, R., et al. (2019). Dose-dependent influences of ethanol on ischemic stroke: Role of inflammation. *Front. Cell Neurosci.* 13:6. doi: 10.3389/fncel.2019.00006

Xu, J., Ma, H. Y., Liu, X., Rosenthal, S., Baglieri, J., Mccubbin, R., et al. (2020). Blockade of IL-17 signaling reverses alcohol-induced liver injury and excessive alcohol drinking in mice. *JCI Insight* 5:e131277. doi: 10.1172/jci.insight.131277

Xu, M. J., Zhou, Z., Parker, R., and Gao, B. (2017). Targeting inflammation for the treatment of alcoholic liver disease. *Pharmacol. Ther.* 180, 77–89.

Yang, X., Tian, F., Zhang, H., Zeng, J., Chen, T., Wang, S., et al. (2016). Cortical and subcortical gray matter shrinkage in alcohol-use disorders: A voxel-based meta-analysis. *Neurosci. Biobehav. Rev.* 66, 92–103. doi: 10.1016/j.neubiorev.2016.03.034

Yang, Y., Boza-Serrano, A., Dunning, C. J. R., Clausen, B. H., Lambertsen, K. L., and Deierborg, T. (2018). Inflammation leads to distinct populations of extracellular vesicles from microglia. *J. Neuroinflamm.* 15:168. doi: 10.1186/s12974-018-1204-7

Zahr, N. M. (2014). Structural and microstructral imaging of the brain in alcohol use disorders. *Handb. Clin. Neurol.* 125, 275–290. doi: 10.1016/B978-0-444-62619-6.00017-3

Zemtsova, I., Gorg, B., Keitel, V., Bidmon, H. J., Schror, K., and Haussinger, D. (2011). Microglia activation in hepatic encephalopathy in rats and humans. *Hepatology* 54, 204–215.

Zhang, Y., Chen, K., Sloan, S. A., Bennett, M. L., Scholze, A. R., O'Keeffe, S., et al. (2014). An RNA-sequencing transcriptome and splicing database of glia, neurons, and vascular cells of the cerebral cortex. *J. Neurosci.* 34, 11929–11947. doi: 10.1523/JNEUROSCI.1860-14.2014

Zhou, Y., Chen, Y., Xu, C., Zhang, H., and Lin, C. (2020). TLR4 targeting as a promising therapeutic strategy for Alzheimer disease treatment. *Front Neurosci* 14:602508. doi: 10.3389/fnins.2020.602508

Zou, J., and Crews, F. T. (2012). Inflammasome-IL-1beta signaling mediates ethanol inhibition of hippocampal neurogenesis. *Front. Neurosci.* 6:77. doi: 10.3389/fnins.2012.00077

frontiers | Frontiers in Molecular Neuroscience

TYPE Original Research
PUBLISHED 14 September 2022
DOI 10.3389/fnmol.2022.926791

OPEN ACCESS

EDITED BY
Rochelle Marie Hines,
University of Nevada, Las Vegas,
United States

REVIEWED BY
Divine C. Nwafor,
West Virginia University, United States
Hongquan Wang,
Tianjin Medical University Cancer Institute and Hospital, China
Liang Huo,
ShengJing Hospital of China Medical University, China

*CORRESPONDENCE
Bing Li
libingbm@163.com

†These authors have contributed equally to this work

SPECIALTY SECTION
This article was submitted to Brain Disease Mechanisms, a section of the journal Frontiers in Molecular Neuroscience

RECEIVED 23 April 2022
ACCEPTED 18 August 2022
PUBLISHED 14 September 2022

CITATION
Wang X-K, Gao C, Zhong H-Q, Kong X-Y, Qiao R, Zhang H-C, Chen B-Y, Gao Y and Li B (2022) TNAP—a potential cytokine in the cerebral inflammation in spastic cerebral palsy.
Front. Mol. Neurosci. 15:926791.
doi: 10.3389/fnmol.2022.926791

TNAP—a potential cytokine in the cerebral inflammation in spastic cerebral palsy

Xiao-Kun Wang[1†], Chao Gao[2,3†], He-Quan Zhong[1], Xiang-Yu Kong[1], Rui Qiao[4], Hui-Chun Zhang[2], Bai-Yun Chen[2], Yang Gao[2] and Bing Li[1*]

[1]Research Center for Clinical Medicine, JinShan Hospital, Fudan University, Shanghai, China, [2]Department of Rehabilitation, Children's Hospital Affiliated to Zhengzhou University, Henan Children's Hospital, Zhengzhou Children's Hospital, Zhengzhou, China, [3]Henan Key Laboratory of Children's Genetics and Metabolic Diseases, Zhengzhou, China, [4]College of Acupuncture-Massage and Rehabilitation, Yunnan University of Traditional Chinese Medicine, Yunnan, China

Objective: Several studies have shown the significance of neuroinflammation in the pathological progress of cerebral palsy (CP). However, the etiology of CP remains poorly understood. Spastic CP is the most common form of CP, comprising 80% of all cases. Therefore, identifying the specific factors may serve to understand the etiology of spastic CP. Our research aimed to find some relevant factors through protein profiling, screening, and validation to help understand the pathogenesis of cerebral palsy.

Materials and methods: In the current study, related clinical parameters were assessed in 18 children with spastic CP along with 20 healthy individuals of the same age. Blood samples of the spastic CP children and controls were analyzed with proteomics profiling to detect differentially expressed proteins. On the other hand, after hypoxic-ischemic encephalopathy (HIE) was induced in the postnatal day 7 rat pups, behavioral tests were performed followed by detection of the differentially expressed markers and inflammatory cytokines in the peripheral blood and cerebral cortex of the CP model rats by Elisa and Western blot. Independent sample *t*-tests, one-way analysis of variance, and the Pearson correlation were used for statistical analysis.

Abbreviations: CP, cerebral palsy; CNS, central nervous system; ST, spastic typecerebral palsy; Ctrl, control; ALPL, Theliver/bone/kidneyalkaline phosphatase gene; TNAP, tissue-nonspecific alkaline phosphatase; HIE, hypoxic-ischemic encephalopathy; IL-6/17, interleukin-6/17; CRP, C-reactive protein; IL-10, interleukin-10; NF-κB, nuclear factor kappa-B; GMFCS-ER, The Gross Motor Function Classification System for cerebral palsy-Extended and Revised; MRI, Magnetic Resonance Imaging; T1W, T1-weighted; T2W, T2-weighted; PVL, periventricular leukomalacia; PWMI, periventricular white matter injury; LYM, percentage of lymphocytes; 25 (OH)D, 25 hydroxyvitamin D; Cr, creatinine; P6 (P7,P11,P39,P42), postnatal day 6; TTC, triphenyl tetrazolium chloride; OPN, osteopontin; FC, fold change; FDR, false discovery rate; PPI, protein-protein interaction; MAPK, mitogen-activated protein kinase; PPi, inorganic pyrophosphate; PLP, pyridoxal-5-phosphate; PEA, phosphor-ethanolamine; GPI, glycosyl-inositol-phosphate; BBB, blood-brain barrier; MMI, moderate motor dysfunction; SMI, severe motor dysfunction.

Results: Through proteomic analysis, differentially expressed proteins were identified. Among them, tissue-nonspecific alkaline phosphatase (TNAP), the gene expression product of alkaline phosphatase *(ALPL)*, was downregulated in spastic CP. In addition, significantly lower TNAP levels were found in the children with CP and model rats. In contrast, compared with the sham rats, the model rats demonstrated a significant increase in osteopontin and proinflammatory biomarkers in both the plasma and cerebral cortex on the ischemic side whereas serum 25 hydroxyvitamin D and IL-10 were significantly decreased. Moreover, serum TNAP level was positively correlated with serum CRP and IL-10 in model rats.

Conclusion: These results suggest that TNAP is the potential molecule playing a specific and critical role in the neuroinflammation in spastic CP, which may provide a promising target for the diagnosis and treatment of spastic CP.

KEYWORDS

spastic cerebral palsy, hypoxic ischemic encephalopathy, TNAP, ALPL, proteomics

Introduction

Cerebral palsy (CP) is the most common neurological dysfunction in children, frequently accompanied by cognitive, language, and behavioral defects, and can be secondary to epilepsy and musculoskeletal problems (Chambers et al., 2017). CP may be brought about by brain injuries in the majority of children. The pathological changes in CP may be characterized by liquefaction necrosis and astrogliosis in the cerebral cortex, white matter, basal ganglia, and the cerebellum (Sanches et al., 2021).

Clinically, depending on the type and distribution of motor abnormalities and the location of the brain injuries (Johnson, 2002), CP can be classified as spastic, dyskinetic, or ataxic. Spastic CP is the most common form of CP, comprising 80% of all cases (Vitrikas et al., 2020). At present, the etiology of CP still remains unclear, making its clinical diagnosis difficult (Skoutelis et al., 2020). It has been revealed by several research that spastic CP is closely related to inflammation, cellular energy depletion, excitotoxicity, and oxidative stress which are caused by premature delivery, hypoxia, and intrauterine infections (Novak et al., 2017; Galea et al., 2019). There is also evidence that CP may be associated with the persistence of chronic inflammatory processes in the central nervous system (CNS; Yoshida et al., 2019). Multiple factors involved in chronic inflammation, such as cytokines, angiogenic factors, chemokines, and oxidative stress markers, have been implicated in the pathogenesis of CP. Several molecules, including interleukin (IL)-1β, IL-6, and tumor necrosis factor (TNF), have been observed more frequently in the case of CP (Cordeiro et al., 2016; Magalhaes et al., 2018). In recent years, modern mass spectrometry-based proteomic methodologies have high sensitivity capable of identifying low abundant proteins over wide dynamic ranges, consequently identifying novel disease-specific biomarkers and providing biological annotations for disease stages (Di Falco, 2018). Therefore, we hypothesize that critical neuroinflammatory signals play a specific and critical role and mediate the pathological progression in the neuroinflammation in spastic CP, providing a promising target for diagnosis and treatment of spastic CP.

Materials and methods

Study participants

A total of 18 children with CP aged 8–26 months were enrolled in this study from January 2019 to September 2021. According to the European Cerebral Palsy Monitoring Group's classification system (Sik et al., 2021), the participants were diagnosed with spastic type CP (ST group; 18 participants). The diagnoses and classifications of the children were determined by two independent clinicians. Meanwhile, 20 children aged 8–26 months, with no confirmed neurodevelopmental disorders after careful physical examinations, were included into the study as healthy controls (**Table 1**). The subjects involved were free from genetic disorders, brain disorders, and metabolic disorders. The research protocol of this clinical study was approved by the ethics committee of Henan Province Children's Hospital. Informed consent was obtained from the parents or the legal guardians of the child prior to the onset of the study.

TABLE 1 Clinical characteristics of our cohort.

		ST (n = 18)	Control (n = 20)
Sex	Male	9	10
	Female	9	10
Age in months		8–26	8–25
Weight, kg		9.03 ± 1.62	11.26 ± 1.31
Enhanced muscle tension		+	-
Decreased muscle tension		-	-
Hyperreflexia		+	-
Stereotypical movements		-	-

Proteomic analyses

The sample we tested was plasma. Four spastic CP samples and four control samples were used for proteomic analysis. A 100 μg protein sample was taken from each sample and digested overnight at 37°C. Each sample was processed and labeled with the instruction of iTRAQ Reagent-8 Multiplexing Kit (AB Sciex, UK). The labeled sample was mixed in equal volumes, desalted, and lyophilized. High-performance liquid chromatography was performed with a Rigol L3000 system and a C18 chromatographic column (Waters BEH C18, 5 mm). A Diane NCS3500 system (Thermo Science FicTM) equipped with a trap and an analytical column was used to fractionate the labeled samples, and the precursor ions decomposed by the higher-energy C-trap dissociation (HCD) method were sent to a tandem mass spectrometry Q Exactive HF-X MS (Thermo Fisher, Waltham, MA) for data acquisition and analysis.

Clinical parameters of cerebral palsy participants

Gross motor function classification

The Gross Motor Function Classification System for cerebral palsy-Extended and Revised (GMFCS-ER; Piscitelli et al., 2021) was used for gross motor function classification. The subjects involved in this motor function assessment covered two different age groups (0 < 2 and 2–4 years old). The motor indicators required by this system included maintaining erecting head, turning over, sitting alone, crawling, standing, and walking. According to motor function performance, the motor dysfunction was divided into five grades, grade I indicating the slightest gross motor dysfunction, and grade V indicating the worst. In sum, GMFCS grades I to III were classified as mild to moderate motor dysfunction, and GMFCS grades IV to V were classified as severe motor dysfunction.

Neuroimaging examination

All brain MRI scans were acquired on a 3.0T MR scanner (Discovery MR750, GE Medical Systems, USA). Imaging sequences included transverse T1-weighted (T1W), T2-weighted (T2W), T2-fluid attenuated inversion-recovery (FLAIR), and sagittal T1W imaging, with a section of 4–5 mm thick. No enhanced scanning was performed in all cases. The obtained brain MRI images were evaluated by the pediatric neuroradiologists and CP specialists participating in our study. The findings were divided into periventricular white matter injury (PWMI): periventricular leukomalacia (PVL), ventriculomegaly; diffuse brain injuries: subcortical softening foci, myelin dysplasia, cerebral atrophy, basal ganglia/thalamic lesions; focal lesions: focal cerebral ischemia, porencephalia; cerebral dysplasia: dysplasia of the corpus callosum, cerebellar dysplasia; and normal brain MRI imaging.

Additional blood sample examinations

Three-milliliter venous blood was taken from all subjects on an empty stomach in the morning. An ADVIA2400 automatic biochemical analysis instrument produced by German Siemens was used to assess the percentage of lymphocytes (LYM) in the blood. An i-CHROMA Reader immunofluorescence analyzer from Boditech MED Inc., South Korea, was used to determine the C-reactive protein (CRP) level. A Roche Cobas e602 analyzer (Roche Diagnostics, Switzerland), was used to detect 25 hydroxyvitamin D [25 (OH)D], and creatinine (Cr).

Animal models

Forty-six 3-day-old Sprague Dawley pup rats were acquired from Shanghai Jihui Experimental Animal Breeding Co. Ltd. The pups were fed by their mothers until weaning. All rats were reared in an animal room with sufficient water and food under a 12-h light-dark cycle. The animal experiments were conducted in accordance with the National Institutes of Health Guide for the Care and Use of Laboratory Animals and the 3R principle.

Forty pups were randomly divided into Sham and Model groups (n = 20). On postnatal day 7 (P7), the Model group was subjected to an operation to construct the hypoxic-ischemic encephalopathy (HIE) model, while the operation without occlusion of the artery was performed on the Sham group on the same day (P7); 10 pups from each group were sacrificed on the 7th day post-operationally, and the remaining 10 pups were sacrificed on the 35th day post-operationally. Another eight pups were sacrificed 48 h after the operation for triphenyl tetrazolium chloride (TTC) staining and Nissl staining. The pups of each group were weighed every other day. The righting reflex test was performed from P6 to P11, and the balance beam experiment was performed from P39 to P42 (**Figure 1A**). Behavioral testing and collection of animal samples were all conducted between 8:00 am and 3:00 pm.

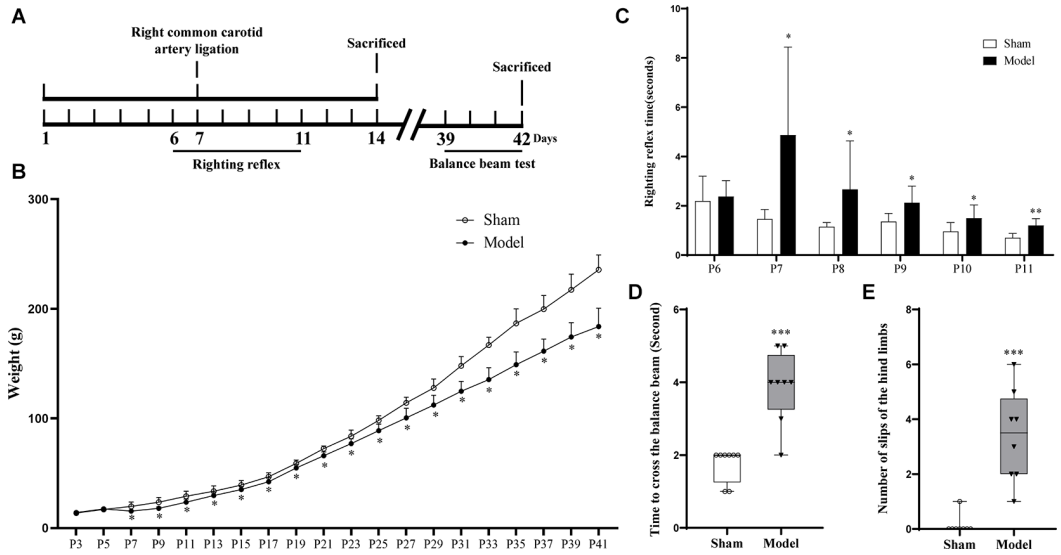

FIGURE 1
(A) Flow chart of the HIE animal model experiments. **(B)** After the operation, the Model group showed continuously significantly less weight than the Sham group ($p < 0.05$, $n = 10$). **(C)** The Model group showed significantly longer righting reflex time from P7 to P11 than the Sham group ($p < 0.05$, $n = 8$). **(D)** Compared with the Sham group, the model group showed a longer time to pass the balance beam and **(E)** higher frequency of leg-slips ($p < 0.001$, $n = 8$). *Denotes statistical significance. *$p < 0.05$ vs. Sham. **$p < 0.01$ vs. Sham; ***$p < 0.001$ vs. Sham.

HIE model construction

The HIE model CP has been widely accepted and recognized as an animal model of CP (Rice et al., 1981). And the operation processes were as follows: on P7, the Model group pups were anesthetized with isoflurane, and the right common carotid artery was ligated. After waking, the pups were placed in a cabin with 8% oxygen and 92% nitrogen for 2.5 h. Finally, the pups were sent back to their mother. As for the Sham group, the common carotid artery was isolated without ligation.

Behavioral test

Righting reflex test: The pups were placed on their back on a platform and the time for successful righting was recorded. Balance beam test: After three consecutive days of training, the pups successfully passed a crossbar placed 50 cm above the ground, which was 2 cm broad and 120 cm long. On the 4th test day, the time to pass the crossbar and the number of slips of the hind limbs while passing the crossbar were recorded.

TTC and Nissl staining

TTC staining: The sham and model pups were euthanized 48 h post-HIE model creation. After the heart was perfused with normal saline, the pup brains were dissected to make 2 mm thick sections for TTC (Sigma Aldrich, USA) staining.

Nissl staining: At 35 days post-HIE model creation, the pups were perfused and fixed after being sacrificed, and the brains were removed for sectioning. After rehydration, the brain slices stained with 0.5% tar violet (Macklin, China), were observed under an OLYMPUS-BX51microscope (OLYMPUS, Japan) and photographed with the cell Sens Standard 1.12 (OLYMPUS, Japan).

ELISA

Fresh plasma was collected from children and centrifuged at 3,000 rpm, 10 min. On the other hand, after the rats were anesthetized, arterial blood was collected from the abdominal aorta into an EDTA anticoagulation blood collection tube, and plasma was obtained *via* centrifugation at 3,000 rpm/min for 10 min. Human tissue nonspecific alkaline phosphatase (TNAP; ml906210V), rat tissue nonspecific alkaline phosphatase (TNAP; ml497021V), Rat 25 (OH)D (ml038318V), Rat osteopontin (OPN; ml003147V), Rat C-reactive protein (CRP; ml038253V), Rat interleukin (IL)-6 (ml102828V), Rat IL-10 (ml002813V), and Rat IL-17 (ml003003V) were detected according to the Elisa kit (Enzyme-linked Biotechnology Co., Ltd, Shanghai) manufacturer's recommended procedure.

Western blot

The expression levels of TNAP, NF-κB, IL-10, and IL-6 in the right cortex of the pups on the 7th and 35th days post-HIE modeling were measured by Western blot. The primary antibodies used were rabbit anti-TNAP (DF6225, Affinity), mouse anti-IL-6 (ab9324, Abcam), rabbit anti-NF-κB (#8242, Cell Signaling Technology), and rabbit anti-IL-10 (ab9969, Abcam). The internal control was rabbit anti-β-Actin (ab8227, Abcam). The gray values were quantified and analyzed by Image J software (NIH).

Data analysis and functional annotations

LIMMA (PMID25605792), R software package (version 3.5.2) were used to screen differentially expressed proteins ($|\text{Log2Fc}| > 0.5$ and FDR ≤ 0.05).

The results were shown as the mean ± standard deviation. SPSS 23.0 statistical software was used for comparative analysis, the independent sample *t*-test was used for the analysis of differences between the two groups, and one-way analysis of variance (ANOVA) was used to evaluate the differences between multiple groups. The Pearson correlation coefficient was used to measure the correlation between two types of data. A p-value < 0.05 was considered to indicate statistical significance.

Results

Proteomics profiling analysis and validation of candidates by ELISA

Four blood samples from each group from the same batch of the ST group and Ctrl group were used for protein profile detection, which identified 10 upregulated proteins and 27 downregulated proteins (**Figures 2A,B**; **Supplementary Table S1**). Then, the Search Tool for the Retrieval of Interacting Genes/Proteins (STRING) database was used to construct a protein-protein interaction (PPI) network of differential proteins (**Figure 2C**), and the top 10 important proteins were identified by the MNC algorithm, including *ALPL*/TNAP, *FN1*, *SERPINA1*, and *PF4* (**Figure 2D**).

To select candidates for validation, proteins were first chosen from our analysis described above. Meanwhile, blood samples from another group of 12 ST patients and 15 Ctrl children in the study cohort were collected which were not subjected to mass spectrometry analysis above. Compared with the Ctrl group, TNAP was significantly decreased in the ST group ($p < 0.001$, **Figure 2E**; **Supplementary Table S2**).

GMFCS levels, blood count, and biochemical tests, MRI results of children with spastic CP

The severity of motor impairment in the ST group ($n = 18$) was categorized by GMFCS grading. According to the GMFCS grading, there was no patient in grade I; four patients (22.2%) were in grade II, five (27.8%) were in grade III, six (33.3%) were in grade IV, and three (16.7%) were in grade V. Therefore, the participants at GMFCS Grade II and III which were classified as moderate motor dysfunction comprised 50% ($n = 9$) and those at Grade IV and V which were classified ($n = 9$) as severe motor dysfunction accounts for the other 50% (**Table 2**). Additionally, the percentage of peripheral blood lymphocytes and the contents of serum CRP, 25 (OH)D, and Cr were measured in both the ST group (18 participants) and the Ctrl group (20 participants). Compared with those in the Ctrl group, the percentage of lymphocytes and CRP levels in the ST group was significantly increased ($p < 0.001$, **Figures 3A,B**), while the 25 (OH)D and Cr levels were significantly reduced ($p < 0.001$, **Figures 3C,D**). Moreover, a direct association was also identified between the serum TNAP content and CRP, 25 (OH)D levels in the ST group (**Figure 3E**; **Supplementary Table S3**).

The cranial MRI findings of the 18 patients in the spastic group were as follows (**Table 3**): PVL was observed in 10 patients (55.6%), including three with ventriculomegaly and/or irregular shape of the lateral ventricles, four with abnormal signal foci in the ventricular white matter, and three with dysplasia of the corpus callosum. Cerebral atrophy was observed in two patients, supratentorial hydrocephalus in two patients, basal ganglia/thalamus lesions in two patients, porencephalia in one patient, and periventricular hemorrhagic infarction in one patient (**Figure 4**, **Table 3**).

Changes in TNAP and inflammation-related cytokines in the peripheral blood of rats with CP

After HIE modeling, infarction foci and liquefication or atrophy of the injured brain tissue (**Supplementary Figures S1A, S1B**) were observed in the Model group, and the amount of Nissl bodies was reduced relative to the Sham group (**Supplementary Figure S2**). From the day of modeling (P7), the weight of the pups in the Model group was significantly lower than that in the Sham group ($p < 0.05$; **Figure 1B**; **Supplementary Table S4**), and the righting reflex time of the Model group after modeling (P7–11) was significantly longer than that of the Sham group ($p < 0.05$; **Figure 1C**; **Supplementary Table S5**). On the 35th day post-HIE-modeling, the time for the Model group to pass the balance beam and the

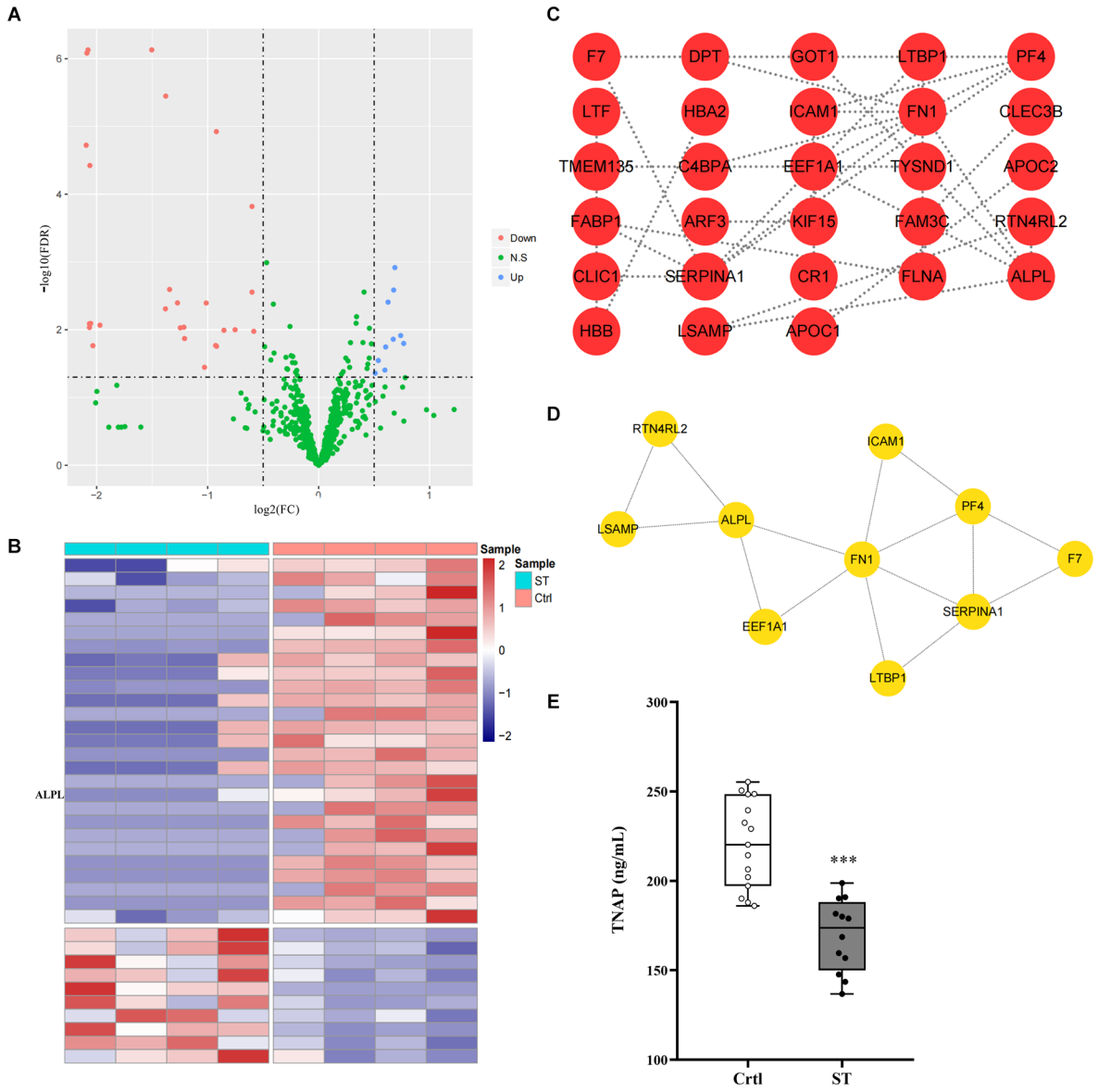

FIGURE 2
(A,B) Volcano map and heatmap showing 37 differentially expressed proteins between the ST group and the Ctrl group. The red and blue dots represented upregulated and downregulated proteins, respectively, and green represented proteins with no significant difference. The co-differential genes *RP1*, *ALPL*, and *FABP1* identified by expression profile chip detection and mass spectrometry detection were marked in panel **(B)**. **(C)** |Log2Fc| > 0.5 and FDR < 0.05 were used as the criteria for screening differentially expressed proteins. The PPI network diagram showed the differentially expressed proteins in the plasma of children in the ST group and the Ctrl group. Each dot in the network represented a protein, and the connection between the dots represented the relationship between them. The more connected lines there were, the more important the protein may be in the PPI network (minimum required interaction score > 0.4). **(D)** The top 10 genes in terms of degree in the PPI network screened by the MNC algorithm according to the test results of the plasma protein profiles of the children in the ST group and Ctrl group; the lines between the dots represented the relationship between them. **(E)** The content of TNAP in the plasma of children in the ST group and Ctrl group. Compared with that in the control group, the expression level of TNAP in the plasma of children in the spastic type CP group was significantly lower ($p < 0.001$, $n = 12$ for ST; $n = 15$ for Ctrl). ***$p < 0.001$ vs. Ctrl.

number of leg slips were significantly more than those of the Sham group ($p < 0.001$; Figures 1D,E; Supplementary Table S6). In sum, these results suggested that the HIE model rats mimicked the clinical and pathological changes in children with spastic CP and therefore modeling was successful.

On the 7th day and 35th day post-HIE modeling, the levels of serum TNAP ($p < 0.01$, Figure 5A) and IL-10 ($p < 0.001$, $p < 0.01$, Figure 5I) in the Model group were significantly lower than those in the Sham group, while the levels of IL-6 ($p < 0.001$, $p < 0.01$, Figure 5D) and CRP ($p < 0.001$, Figure 5E) were

TABLE 2 Classification of the gross motor function in children with spastic CP.

Characteristics	ST (n = 18)	Control (n = 20)
GMFCS level		
MMI	9 (50%)	\
Level II	4 (22.2%)	\
Level III	5 (27.8%)	\
SMI	9 (50%)	\
Level IV	6 (33.3%)	\
Level V	3 (16.7%)	\

MMI, moderate motor dysfunction; SMI, severe motor dysfunction.

significantly higher. Furthermore, the levels of OPN ($p < 0.001$, Figure 5C) and IL-17 ($p < 0.001$, Figure 5H) in pups in the Model group were significantly higher than those in pups in the Sham group while the serum 25 (OH)D content was significantly reduced on day 7 post-HIE ($p < 0.001$, Figure 5B). In addition, 7 days and 35 days after HIE modeling, the level of serum TNAP was correlated with those of serum CRP and IL-10 (Figures 5F,G,J,K; Supplementary Table S7).

Changes in TNAP and inflammation-related cytokines in the brain tissue of rats with cerebral palsy

It was observed that the Model group displayed significantly lower expression levels of TNAP and IL-10 in the cortex on the injured side than the Sham group ($p < 0.01$; Figures 6A,D,E)

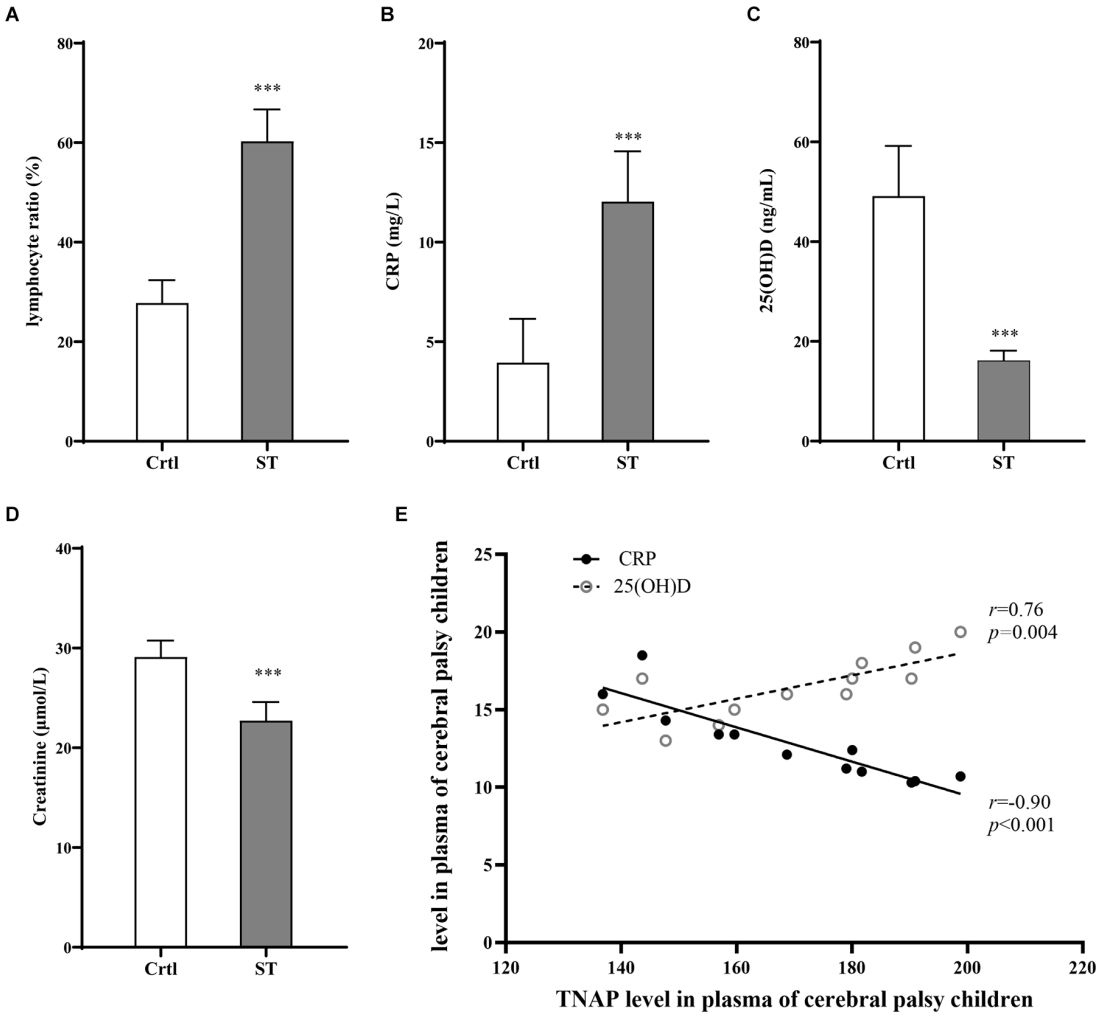

FIGURE 3
Results of blood tests for the Ctrl group (n = 20) and ST group (n = 18). **(A)** Compared with that of the Ctrl group, the percentage of lymphocytes in the ST group was significantly increased ($p < 0.001$). **(B)** The level of CRP in the ST group was significantly higher than that in the Ctrl group ($p < 0.001$). **(C)** Compared with those in the Ctrl group, the levels of 25 (OH)D in the ST group were significantly lower ($p < 0.001$). **(D)** The plasma Cr of the ST group was significantly lower than that in the Ctrl group ($p < 0.001$). **(E)** In the ST group, the level of TNAP was positively correlated with CRP ($p < 0.001$, $r = -0.90$) and 25 (OH)D ($p = 0.004$, $r = 0.76$). ***$p < 0.001$ vs. Ctrl.

TABLE 3 The appearance of brain MRI in children with spastic CP.

Cranial MRI findings	ST (n = 18)	Control (n = 20)
PVL	10 (55.6%)	\
ventriculomegaly	3	
abnormal signal foci	4	
dysplasia of corpus callosum	3	
Diffuse brain injury	6 (33.3%)	\
cerebral atrophy	2	
supratentorial hydrocephalus	2	
basal ganglia/thalamus lesions	2	
Focal lesion	2 (11.1%)	\
porencephalia	1	
periventricular hemorrhagic infarction	1	
Normal	\	20 (100%)

while the IL-6 ($p < 0.05$, $p < 0.01$; **Figure 6F**) and NF-κB ($p < 0.001$, $p < 0.01$; **Figure 6G**) levels were significantly higher in Model group on day 7 and 35 post-HIE. Moreover, there was a strong positive correlation in TNAP levels between serum and brain tissue in HIE model rats both on the 7th and 35th days post HIE modeling (**Figures 6B,C**; **Supplementary Table S8**).

Discussion

CP is not a disease in the traditional sense, but rather a clinical description of a series of signs and symptoms acquired during the antenatal, perinatal, or early postnatal period of life, due to a non-progressive brain injury, which may be shared by children or some adults (Kesar et al., 2012). Among several subtypes of CP, spastic CP is the most common one with the highest incidence. Whereas the molecular mechanism of the pathological changes in spastic CP is still unclear. In our study, proteomics profiling analysis was applied to analyze expressive levels of the genes involved in spastic CP. Ultimately, TNAP was screened out as the drastically down-regulated protein, which was in line with the findings in several spastic CP patients.

To confirm whether TNAP and CP were directly correlated, TNAP in the plasma and cerebral cortex of HIE model rats was evaluated. HIE model, the stable and widely used CP model demonstrates long-term ischemia and hypoxia which is consistent with the characteristics of spastic CP. Through Nissl staining and other methods, brain injury was observed in the model rats with CP, which was indicated by impaired motor function and muscle coordination in the righting reflex and balance beam tests. Together, these findings showed that the HIE model rats displayed clinical manifestations of CP successfully. Moreover, the results of our research were in line with the changes in the plasma of the children with CP, and there was a strong correlation between plasma TNAP and the cerebral TNAP in the injured cortex, which suggests that the changes in TNAP are related to CP occurrence.

The main biological function of TNAP is to hydrolyze the extracellular substrates inorganic pyrophosphate (PPi), pyridoxal-5-phosphate (PLP), and phosphor-ethanolamine (PEA; Mao et al., 2019). PLP is the main active form of vitamin B6 that exerts biological functions in the body (Zhang et al., 2021). TNAP is an ectoenzyme that is anchored to the outer cell membrane and to extracellular vesicles *via* its glycosyl-inositol-phosphate (GPI)-anchor. TNAP, not only has a high expression in the liver, kidney, and bone tissues but also plays an important role in the proliferation and differentiation of neurons during the development of the brain (Nwafor et al., 2021).

As to the role of TNAP in the pathological changes of spastic CP, a multitude of literature provided some leads. Graser et al. (2021) reported that TNAP contributes to the balance between proinflammatory ATP effects and the anti-inflammatory effects of its breakdown product adenosine, which has received attention. Different research teams have explored the mechanism of TNAP involvement in inflammation. As a start, Beck et al found that insufficient TNAP phosphatase activity leads to the accumulation of PPi and osteopathy, which can initiate the accumulation of calcium crystals in the joints and consequently initiate inflammatory processes (Beck et al., 2009). Subsequently, Akpinar (2018) showed that neuromuscular conditions such as CP may lead to vitamin D deficiency and under-nutrition in general. The major circulating metabolite of vitamin D, 25 (OH)D, is widely used as a biomarker of vitamin D status (Cashman et al., 2022); it can regulate the level of immune-inflammatory factors and plays an important role in the growth and development of the body. In addition, Huang et al. (2015) observed that 25 (OH)D can inhibit the production of inflammatory molecules in neuroglial cells by inhibiting the MAPK pathway and the production of downstream inflammatory molecules. In our study, the plasma levels of TNAP, 25 (OH)D, OPN, and Cr in children with spastic CP were significantly lower than those in the control group, which is consistent with the results of related studies.

Recently, some studies reported that OPN is a physiological substrate of TNAP and identified at least two preferred sites of dephosphorylation by TNAP. Yadav et al. (2014) found that low expression of TNAP led to elevated OPN, which can activate inflammatory factors such as IL-6 and IL-17 in bone cells, thus triggering inflammation. It has been reported (Albertsson et al., 2014) that OPN also promotes the secretion of proinflammatory cytokines and inhibits the production of anti-inflammatory factors such as IL-10. In this study, we also observed that a decrease of TNAP in children with spastic CP and in model rats triggered an increase in OPN expression, resulting in upregulation of IL-6, IL-17, and other proinflammatory factors in peripheral blood.

For the present, cranial MRI findings play an important role in evaluating the extension and severity of brain injury, detecting ischemia and/or diffuse axonal injury, and complementing the neurological evaluation (Pagnozzi et al., 2017). The European Cerebral Palsy Study reported (Ashwal et al., 2004) abnormal cranial MRI findings in 88.3% of patients, of which PVL was

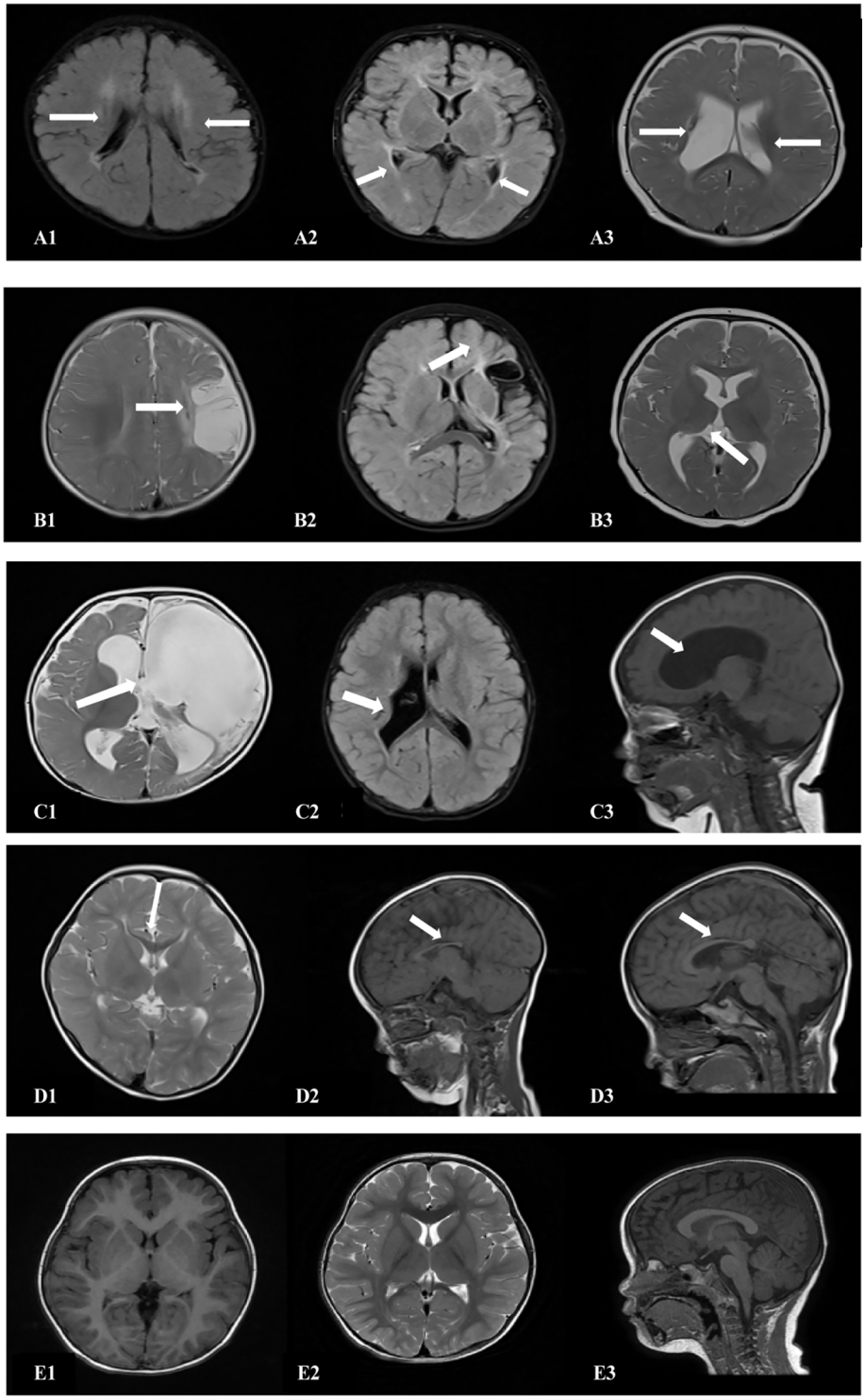

FIGURE 4
Cranial MRI findings of the 18 patients in the ST group. **(A1,2)** (transverse): Irregularly shaped bilateral ventricles with nearby, irregular, patchy T1 and T2 hypersignals. **(A3)** (transverse section): Enlarged bilateral ventricles with nearby, patchy T2 signals. **(B1)** (transverse section): Left frontotemporal parietal atrophy with subcortical softening foci. **(B2)** (transverse section): Reduced volume of the left basal ganglia. **(B3)** (transverse section): Decreased volume of the left thalamus. **(C1)** (transverse): Left partial cerebral perforation malformation with supratentorial hydrocephalus. **(C2)** (transverse section): Right ventricular para-body brain penetration malformation with surrounding gliosis. **(C3)** (sagittal section): Supratentorial hydrocephalus. **(D1)** (transverse section): Thinning of the corpus callosum. **(D2)** (sagittal): Noticeably thinner and shorter corpus callosum. **(D3)** (sagittal section): Significantly shorter corpus callosum. **(E1–3)** (TI/T2 transverse/sagittal): Normal brain MRI.

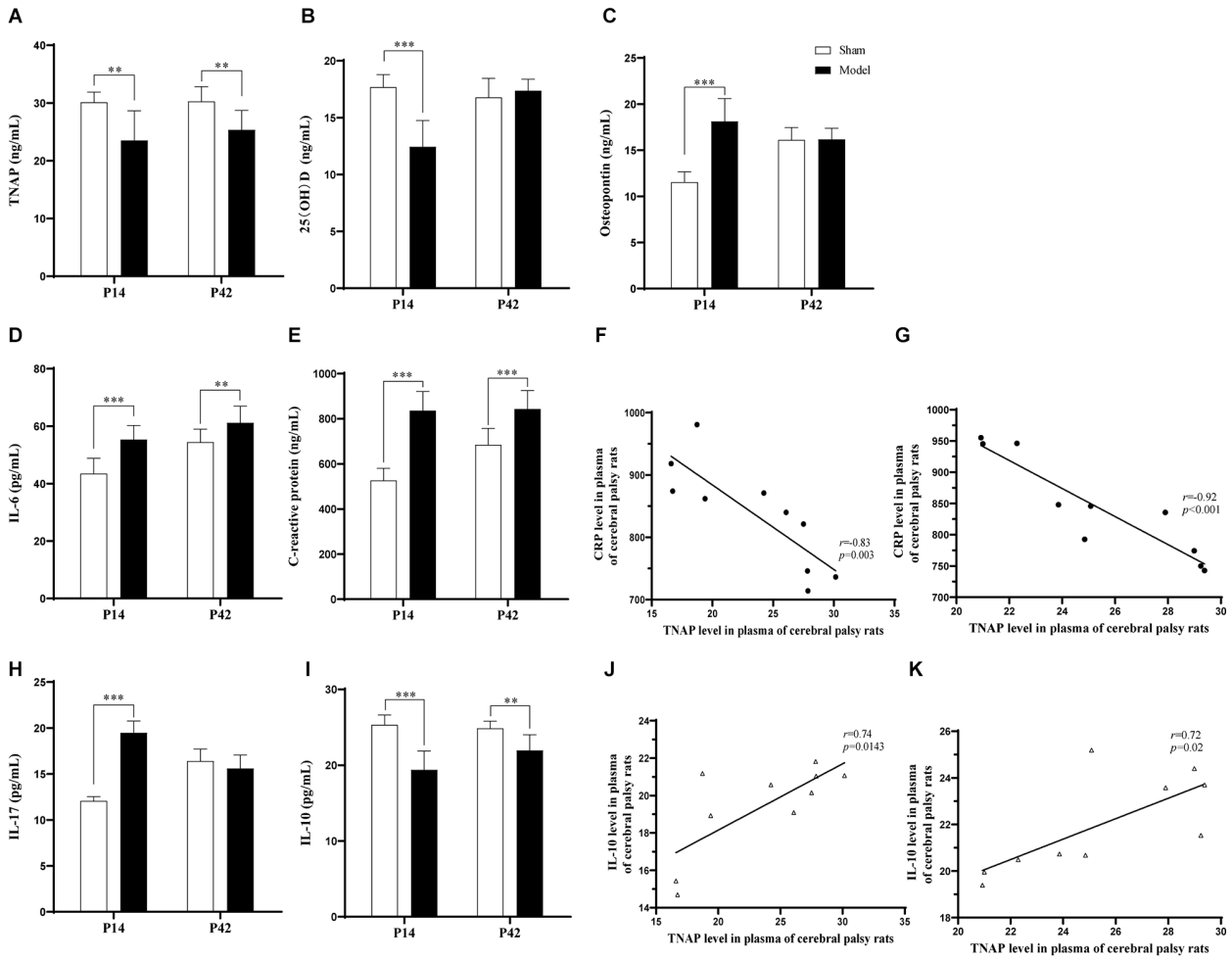

FIGURE 5
(A,B,I) Seven days after HIE modeling, compared with those in the Sham group, the levels of TNAP (p = 0.001, n = 10), 25 (OH)D ($p < 0.001$, n = 10), and IL-10 ($p < 0.001$, n = 10) were significantly reduced in the Model group. **(C–E,H)** The levels of OPN, IL-6, CRP, and IL-17 were significantly greater in the Model group than in the Sham group ($p < 0.001$, n = 10). **(F,J)** Seven days after HIE modeling, the plasma levels of TNAP were positively correlated with those of CRP (p = 0.003, $r = -0.83$, n = 10) and IL-10 (p = 0.0143, r = 0.74, n = 10). **(A,D,E)** Thirty-five days after HIE modeling, compared with the Sham group, the Model group had significantly lower levels of TNAP (p = 0.002, n = 10), IL-6 (p = 0.009, n = 10), and CRP ($p < 0.001$, n = 10), while the level of IL-10 was significantly decreased (p = 0.001, n = 10). **(G,K)** Thirty-five days after HIE-modeling, the plasma TNAP were correlated with CRP ($p < 0.001$, $r = -0.92$, n = 10) and IL-10 (p = 0.02, r = 0.72, n = 10). $^{**}p < 0.01$ vs. Sham; $^{***}p < 0.001$ vs. Sham.

the most common, accounting for approximately 42.5%. The main manifestations of brain damage in spastic CP are PVL, and the main imaging findings are an irregular expansion of the lateral ventricles; paraventricular tissue softening; decreased white matter volume; and dysplasia of the corpus callosum. In our study, 10 (55.6%) of 18 children with spastic CP showed PVL on cranial MRI, and the lesion location was consistent with the literature mentioned above. The pathogenesis of PVL is multifaceted (Lawrence and Wynn, 2018; Cerisola et al., 2019; Magalhaes et al., 2019; Zhou et al., 2019), including maternal infection, cerebral ischemia, and vulnerability of brain white matter (Bax et al., 2006), among which the response of fetuses and newborns to inflammatory damage is the key. Hence, neuroinflammation, such as infiltration of leukocytes in the brain parenchyma along with activation of astrocytes and microglia can be observed in the brain of CP patients, which may cause further impairment of white matter. In recent years, Nwafor et al. speculated that TNAP's regulatory phosphatase activity on a number of BBB endothelial proteins may play an important role in maintaining blood-brain barrier (BBB) integrity. Therefore, the decrease in TNAP expression levels in children with spastic CP may be one of the reasons for the pathological changes, such as BBB dysfunction and neuroinflammation (Nwafor et al., 2020).

Apart from neuroinflammation, there are also abnormal changes in the pro-inflammatory factors in the peripheral blood

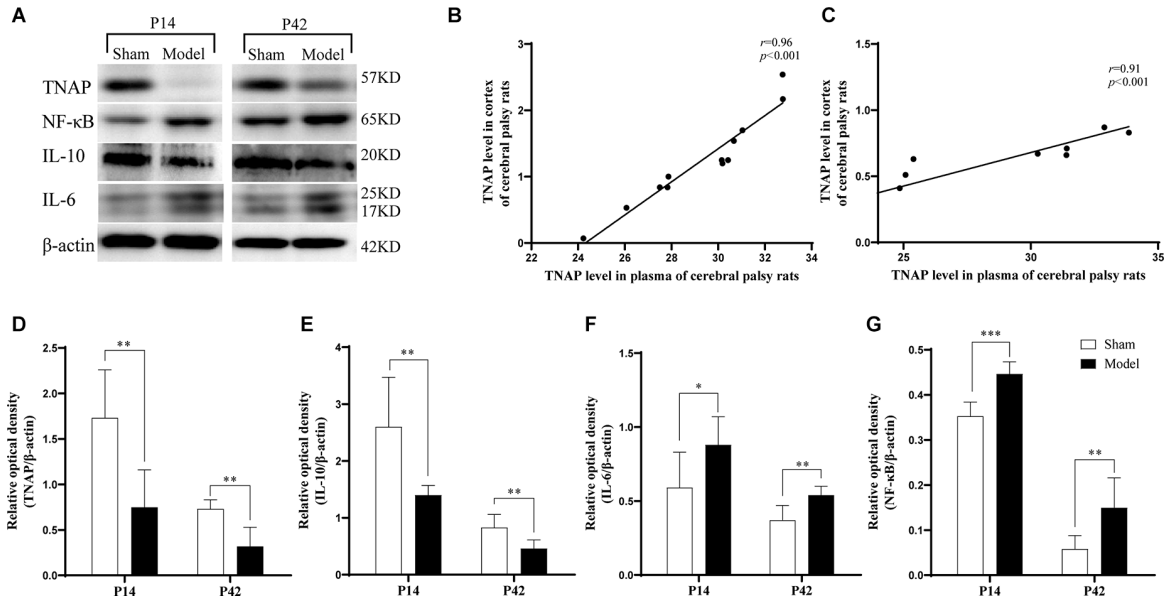

FIGURE 6
(A) Representative Western blot images of TNAP, IL-10, IL-6, and NF-κB in the injured cerebral cortex. **(D–G)** Compared with those in the Sham group, the cortex expression levels of TNAP and IL-10 were significantly reduced in the Model group ($p < 0.01$, $n = 6$). Compared with those in the Sham group, the levels of IL-6 ($p < 0.05$, $p < 0.01$, $n = 6$) and NF-κB ($p < 0.001$, $p < 0.05$, $n = 6$) were significantly increased in the Model group. **(B,C)** On day 7 ($p < 0.001$, $r = 0.96$, $n = 12$) and day 35 post-HIE-modeling ($p < 0.001$, $r = 0.91$, $n = 12$), there was a positive correlation in the levels of TNAP between the peripheral plasma and the brain. *Denotes statistical significance. *$p < 0.05$ vs. Sham. **$p < 0.01$ vs. Sham; ***$p < 0.001$ vs. Sham.

(Kaukola et al., 2004; Carlo et al., 2011; Patra et al., 2017). Some clinical studies suggested that anti-inflammatory therapy can improve the clinical manifestations of cerebral palsy (Chernykh et al., 2014; Allan, 2020). In this study, it was revealed that the levels of CRP and lymphocytes in the peripheral blood of children with spastic CP were significantly higher than those of the control group, indicating the occurrence of inflammatory reactions in the subject group. Similarly, the expression of CRP, IL-6, and IL-17 was significantly increased in the peripheral blood of model rats, while the level of the anti-inflammatory factor IL-10 was significantly decreased. We observed signs of brain damage, such as edema, atrophy, and liquefaction, in brain tissue slices of the injured cerebral hemisphere of model rats. Likewise, upregulation of IL-6 expression and downregulation of IL-10 expression were also detected in the cerebral cortex of model rats, confirming that inflammation is also involved in the brain injury process of spastic CP.

More importantly, downregulation of TNAP expression in the children with spastic CP along with low expression of TNAP and high expression of NF-κB in the cerebral cortex of HIE model rats were observed. In addition, the expression level of TNAP correlated well with CRP in both children with CP and HIE model rats. It was held by the previous study that TNAP is an inhibitor of NF-κB activity, and low expression of TNAP can induce NF-κB pathway activation (Hu et al., 2004). Meanwhile, it has been confirmed that the NF-κB pathway is a key transcriptional pathway in neuroinflammation caused by cerebral ischemia and hypoxia, which may promote the abnormal expression of inflammatory factors (Peng et al., 2022). Previous studies have suggested that cerebral ischemia and hypoxia can occur through the NF-κB/IL-6 pathway, resulting in rapid IL-6 release (Borsini et al., 2020). Moreover, IL-17 can activate downstream signaling pathways such as NF-κB, leading to the expression of proinflammatory chemokines and cytokines (Wang et al., 2021). Furthermore, McDonald et al. (2018) have reported that umbilical cord blood (UCB) cells therapy has well-documented neuroprotective effects on HIE model *via* anti-inflammatory effects.

Our research on the pathogenesis of TNAP in CP still requires to be further deepened and improved. For example, the effect of regulating the expression level of TNAP on the symptoms in CP model animals could be carried out in our follow-up research. Furthermore, a weakness of the present study is that TNAP is a relatively small protein with no known regulatory domains, and we could not obtain ALPL knockdown mice to use as animal models. Therefore, it is urgent to evaluate the inflammatory reactions and molecular mechanisms in *ALPL* knockdown mice.

In all, based on the analysis of the correlation between TNAP in peripheral blood and inflammatory factors and the high correlation between brain and peripheral blood TNAP, we suggest that the downregulation of TNAP expression in

spastic CP might weaken the inhibition of NF-κB, leading to an abnormally high expression of NF-κB, the upregulation of the proinflammatory cytokines IL-6 and IL-17, and the downregulation of the anti-inflammatory factor IL-10, which contributes to the neuroinflammation in the progression of spastic CP. Our study was designed to pinpoint the chief molecule playing a specific and critical role in the neuroinflammation in spastic CP, which may provide a promising target for the diagnosis and treatment of spastic CP. To further our exploration, our future study will focus on the molecular mechanism of how TNAP regulates the pro-inflammatory factors related to CP neuroinflammation.

Data availability statement

The data presented in the study are deposited in the ProteomeXchange Consortium repository, accession number PXD034911.

Ethics statement

The studies involving human participants were reviewed and approved by the ethics committee of Henan Province Children's Hospital. Written informed consent to participate in this study was provided by the participants' legal guardian/next of kin. The animal study was reviewed and approved by the National Institutes of Health Guide for the Care and Use of Laboratory Animals.

Author contributions

BL designed the study and revised the manuscript. X-KW performed experiments, analyzed the data and was a major contributor in writing the manuscript. CG acquired the clinical data. H-QZ, X-YK, and RQ performed the experiments and recorded the results. H-CZ, B-YC, and YG participated in data analysis. All authors contributed to the article and approved the submitted version.

Funding

This work was supported by the National Natural Science Foundation of China (grant numbers: 81774444 and 82174522), Key special project of Traditional Chinese medicine research of Henan Province (20-21ZY1072), and international cooperation project of the Ministry of Science and Technology of China (G2021026025L).

Conflict of interest

The authors declare that the research was conducted in the absence of any commercial or financial relationships that could be construed as a potential conflict of interest.

Publisher's note

All claims expressed in this article are solely those of the authors and do not necessarily represent those of their affiliated organizations, or those of the publisher, the editors and the reviewers. Any product that may be evaluated in this article, or claim that may be made by its manufacturer, is not guaranteed or endorsed by the publisher.

Supplementary material

The Supplementary Material for this article can be found online at: https://www.frontiersin.org/articles/10.3389/fnmol.2022.926791/full#supplementary-material.

SUPPLEMENTARY FIGURE 1
(A) When compared with sham group, the HIE rat's cerebral infarct area was increased and the center of the infarction was uniformly pale after 48 h-HIE. **(B)** The brain tissue of the injured side of the cerebral palsy group was significantly liquefied and atrophy post 35 days-HIE.

SUPPLEMENTARY FIGURE 2
Representative images of the Nissl staining of pups. **(A–C)** The Nissl staining results in the Sham group (**B**: cortex; **C**: striatum). **(D–F)** The neuronal degeneration in the cortex and striatum after HIE in rat pups.

References

Akpinar, P. (2018). Vitamin D status of children with cerebral palsy: should vitamin D levels be checked in children with cerebral palsy? *North Clin Istanb* 5, 341–347. doi: 10.14744/nci.2017.09581

Albertsson, A. M., Zhang, X., Leavenworth, J., Bi, D., Nair, S., Qiao, L., et al. (2014). The effect of osteopontin and osteopontin-derived peptides on preterm brain injury. *J. Neuroinflammation* 11:197. doi: 10.1186/s12974-014-0197-0

Allan, D. S. (2020). Using umbilical cord blood for regenerative therapy: proof or promise? *Stem Cells* 38, 590–595. doi: 10.1002/stem.3150

Ashwal, S., Russman, B. S., Blasco, P. A., Miller, G., Sandler, A., Shevell, M., et al. (2004). Practice parameter: diagnostic assessment of the child with cerebral palsy: report of the Quality Standards Subcommittee of the American Academy of Neurology and the Practice Committee of the Child Neurology Society. *Neurology* 62, 851–863. doi: 10.1212/01.wnl.0000117981.35364.1b

Bax, M., Tydeman, C., and Flodmark, O. (2006). Clinical and MRI correlates of cerebral palsy: the European Cerebral Palsy Study. *JAMA* 296, 1602–1608. doi: 10.1001/jama.296.13.1602

Beck, C., Morbach, H., Richl, P., Stenzel, M., and Girschick, H. J. (2009). How can calcium pyrophosphate crystals induce inflammation in hypophosphatasia or chronic inflammatory joint diseases? *Rheumatol. Int.* 29, 229–238. doi: 10.1007/s00296-008-0710-9

Borsini, A., Di Benedetto, M. G., Giacobbe, J., and Pariante, C. M. (2020). Pro- and anti-inflammatory properties of interleukin (IL6) *in vitro*: relevance for major depression and for human hippocampal neurogenesis. *Int. J. Neuropsychopharmacol.* 23, 738–750. doi: 10.1093/ijnp/pyaa055

Carlo, W. A., McDonald, S. A., Tyson, J. E., Stoll, B. J., Ehrenkranz, R. A., Shankaran, S., et al. (2011). Cytokines and neurodevelopmental outcomes in extremely low birth weight infants. *J. Pediatr.* 159, 919–925.e3. doi: 10.1016/j.jpeds.2011.05.042

Cashman, K. D., Ritz, C., Carlin, A., and Kennedy, M. (2022). Vitamin D biomarkers for Dietary Reference Intake development in children: a systematic review and meta-analysis. *Am. J. Clin. Nutr.* 115, 544–558. doi: 10.1093/ajcn/nqab357

Cerisola, A., Baltar, F., Ferran, C., and Turcatti, E. (2019). [Mechanisms of brain injury of the premature baby]. *Medicina (B Aires)* 79, 10–14. Available online at: https://www.medicinabuenosaires.com/PMID/31603836.pdf.

Chambers, C., Sokhey, T., Gaebler-Spira, D., and Kording, K. P. (2017). The integration of probabilistic information during sensorimotor estimation is unimpaired in children with Cerebral Palsy. *PLoS One* 12:e0188741. doi: 10.1371/journal.pone.0188741

Chernykh, E. R., Kafanova, M. Y., Shevela, E. Y., Sirota, S. I., Adonina, E. I., Sakhno, L. V., et al. (2014). Clinical experience with autologous M2 macrophages in children with severe cerebral palsy. *Cell Transplant.* 23, S97–S104. doi: 10.3727/096368914X684925

Cordeiro, C. N., Savva, Y., Vaidya, D., Argani, C. H., Hong, X., Wang, X., et al. (2016). Mathematical modeling of the biomarker milieu to characterize preterm birth and predict adverse neonatal outcomes. *Am. J. Reprod. Immunol.* 75, 594–601. doi: 10.1111/aji.12502

Di Falco, M. R. (2018). Mass spectrometry-based proteomics. *Methods Mol. Biol.* 1775, 93–106. doi: 10.1007/978-1-4939-7804-5_9

Galea, C., McIntyre, S., Smithers-Sheedy, H., Reid, S. M., Gibson, C., Delacy, M., et al. (2019). Cerebral palsy trends in Australia (1995–2009): a population-based observational study. *Dev. Med. Child Neurol.* 61, 186–193. doi: 10.1111/dmcn.14011

Graser, S., Liedtke, D., and Jakob, F. (2021). TNAP as a new player in chronic inflammatory conditions and metabolism. *Int. J. Mol. Sci.* 22:919. doi: 10.3390/ijms22020919

Hu, W. H., Mo, X. M., Walters, W. M., Brambilla, R., and Bethea, J. R. (2004). TNAP, a novel repressor of NF-κB-inducing kinase, suppresses NF-κB activation. *J. Biol. Chem.* 279, 35975–35983. doi: 10.1074/jbc.M405699200

Huang, Y. N., Ho, Y. J., Lai, C. C., Chiu, C. T., and Wang, J. Y. (2015). 1,25-Dihydroxyvitamin D3 attenuates endotoxin-induced production of inflammatory mediators by inhibiting MAPK activation in primary cortical neuron-glia cultures. *J. Neuroinflammation* 12:147. doi: 10.1186/s12974-015-0370-0

Johnson, A. (2002). Prevalence and characteristics of children with cerebral palsy in Europe. *Dev. Med. Child Neurol.* 44, 633–640. doi: 10.1111/j.1469-8749.2002.tb00848.x

Kaukola, T., Satyaraj, E., Patel, D. D., Tchernev, V. T., Grimwade, B. G., Kingsmore, S. F., et al. (2004). Cerebral palsy is characterized by protein mediators in cord serum. *Ann. Neurol.* 55, 186–194. doi: 10.1002/ana.10809

Kesar, T. M., Sawaki, L., Burdette, J. H., Cabrera, M. N., Kolaski, K., Smith, B. P., et al. (2012). Motor cortical functional geometry in cerebral palsy and its relationship to disability. *Clin. Neurophysiol.* 123, 1383–1390. doi: 10.1016/j.clinph.2011.11.005

Lawrence, S. M., and Wynn, J. L. (2018). Chorioamnionitis, IL-17A and fetal origins of neurologic disease. *Am. J. Reprod. Immunol.* 79:e12803. doi: 10.1111/aji.12803

Magalhaes, R. C., Moreira, J. M., Lauar, A. O., da Silva, A. A. S., Teixeira, A. L., and Silva, A. C. S. E. (2019). Inflammatory biomarkers in children with cerebral palsy: a systematic review. *Res. Dev. Disabil.* 95:103508. doi: 10.1016/j.ridd.2019.103508

Magalhaes, R. C., Pimenta, L. P., Barbosa, I. G., Moreira, J. M., de Barros, J., Teixeira, A. L., et al. (2018). Inflammatory molecules and neurotrophic factors as biomarkers of neuropsychomotor development in preterm neonates: a systematic review. *Int. J. Dev. Neurosci.* 65, 29–37. doi: 10.1016/j.ijdevneu.2017.10.006

Mao, X., Liu, S., Lin, Y., Chen, Z., Shao, Y., Yu, Q., et al. (2019). Two novel mutations in the ALPL gene of unrelated Chinese children with Hypophosphatasia: case reports and literature review. *BMC Pediatr.* 19:456. doi: 10.1186/s12887-019-1800-4

McDonald, C. A., Penny, T. R., Paton, M. C. B., Sutherland, A. E., Nekkanti, L., Yawno, T., et al. (2018). Effects of umbilical cord blood cells and subtypes, to reduce neuroinflammation following perinatal hypoxic-ischemic brain injury. *J. Neuroinflammation* 15:47. doi: 10.1186/s12974-018-1089-5

Novak, I., Morgan, C., Adde, L., Blackman, J., Boyd, R. N., Brunstrom-Hernandez, J., et al. (2017). Early, accurate diagnosis and early intervention in cerebral palsy: advances in diagnosis and treatment. *JAMA Pediatr.* 171, 897–907. doi: 10.1001/jamapediatrics.2017.1689

Nwafor, D. C., Brichacek, A. L., Ali, A., and Brown, C. M. (2021). Tissue-nonspecific alkaline phosphatase in central nervous system health and disease: a focus on brain microvascular endothelial cells. *Int. J. Mol. Sci.* 22:5257. doi: 10.3390/ijms22105257

Nwafor, D. C., Chakraborty, S., Brichacek, A. L., Jun, S., Gambill, C. A., Wang, W., et al. (2020). Loss of tissue-nonspecific alkaline phosphatase (TNAP) enzyme activity in cerebral microvessels is coupled to persistent neuroinflammation and behavioral deficits in late sepsis. *Brain Behav. Immun.* 84, 115–131. doi: 10.1016/j.bbi.2019.11.016

Pagnozzi, A. M., Dowson, N., Doecke, J., Fiori, S., Bradley, A. P., Boyd, R. N., et al. (2017). Identifying relevant biomarkers of brain injury from structural MRI: validation using automated approaches in children with unilateral cerebral palsy. *PLoS One* 12:e0181605. doi: 10.1371/journal.pone.0181605

Patra, A., Huang, H., Bauer, J. A., and Giannone, P. J. (2017). Neurological consequences of systemic inflammation in the premature neonate. *Neural Regen. Res.* 12, 890–896. doi: 10.4103/1673-5374.208547

Peng, X., Wang, J., Peng, J., Jiang, H., and Le, K. (2022). Resveratrol improves synaptic plasticity in hypoxic-ischemic brain injury in neonatal mice via alleviating SIRT1/NF-κB signaling-mediated neuroinflammation. *J. Mol. Neurosci.* 72, 113–125. doi: 10.1007/s12031-021-01908-5

Piscitelli, D., Ferrarello, F., Ugolini, A., Verola, S., and Pellicciari, L. (2021). Measurement properties of the Gross Motor Function Classification System, Gross Motor Function Classification System-Expanded & Revised, Manual Ability Classification System and Communication Function Classification System in cerebral palsy: a systematic review with meta-analysis. *Dev. Med. Child Neurol.* 63, 1251–1261. doi: 10.1111/dmcn.14910

Rice, J. E., 3rd, Vannucci, R. C., and Brierley, J. B. (1981). The influence of immaturity on hypoxic-ischemic brain damage in the rat. *Ann. Neurol.* 9, 131–141. doi: 10.1002/ana.410090206

Sanches, E. F., Carvalho, A. S., van de Looij, Y., Toulotte, A., Wyse, A. T., Netto, C. A., et al. (2021). Experimental cerebral palsy causes microstructural brain damage in areas associated to motor deficits but no spatial memory impairments in the developing rat. *Brain Res.* 1761:147389. doi: 10.1016/j.brainres.2021.147389

Sik, N., Sarioglu, F. C., Oztekin, O., and Sarioglu, B. (2021). Evaluation of the relationship between cranial magnetic resonance imaging findings and clinical status in children with cerebral palsy. *Turk. J. Med. Sci.* 51, 1296–1301. doi: 10.3906/sag-2010-187

Skoutelis, V. C., Kanellopoulos, A. D., Kontogeorgakos, V. A., Dinopoulos, A., and Papagelopoulos, P. J. (2020). The orthopaedic aspect of spastic cerebral palsy. *J. Orthop.* 22, 553–558. doi: 10.1016/j.jor.2020.11.002

Vitrikas, K., Dalton, H., and Breish, D. (2020). Cerebral palsy: an overview. *Am. Fam. Physician* 101, 213–220. Available online at: https://www.aafp.org/dam/brand/aafp/pubs/afp/issues/2020/0215/p213.pdf.

Wang, W., Wang, Y., Zou, J., Jia, Y., Wang, Y., Li, J., et al. (2021). The mechanism action of german chamomile (Matricaria recutita L.) in the treatment of eczema: based on dose-effect weight coefficient network pharmacology. *Front. Pharmacol.* 12:706836. doi: 10.3389/fphar.2021.706836

Yadav, M. C., Huesa, C., Narisawa, S., Hoylaerts, M. F., Moreau, A., Farquharson, C., et al. (2014). Ablation of osteopontin improves the skeletal phenotype of phospho1$^{-/-}$ mice. *J. Bone Miner. Res.* 29, 2369–2381. doi: 10.1002/jbmr.2281

Yoshida, R. A., Gorjao, R., Mayer, M. P. A., Corazza, P. F. L., Guare, R. O., Ferreira, A., et al. (2019). Inflammatory markers in the saliva of cerebral palsy individuals with gingivitis after periodontal treatment. *Braz. Oral Res.* 33:e033. doi: 10.1590/1807-3107bor-2019.vol33.0033

Zhang, L., Zhao, J., Dong, J., Liu, Y., Xuan, K., and Liu, W. (2021). GSK3β rephosphorylation rescues ALPL deficiency-induced impairment of odontoblastic differentiation of DPSCs. *Stem Cell Res. Ther.* 12:225. doi: 10.1186/s13287-021-02235-7

Zhou, K. Q., Green, C. R., Bennet, L., Gunn, A. J., and Davidson, J. O. (2019). The role of connexin and pannexin channels in perinatal brain injury and inflammation. *Front. Physiol.* 10:141. doi: 10.3389/fphys.2019.00141

frontiers | Frontiers in Molecular Neuroscience

TYPE Systematic Review
PUBLISHED 26 September 2022
DOI 10.3389/fnmol.2022.981442

OPEN ACCESS

EDITED BY
Rochelle Marie Hines,
University of Nevada, Las Vegas,
United States

REVIEWED BY
David James Brooks,
Newcastle University, United Kingdom
Jens P. Bankstahl,
Hannover Medical School, Germany

*CORRESPONDENCE
Rupert Lanzenberger
rupert.lanzenberger@meduniwien.ac.at

†PRESENT ADDRESS
Gregor Gryglewski,
Child Study Center, Yale University,
New Haven, CT, United States

SPECIALTY SECTION
This article was submitted to
Brain Disease Mechanisms,
a section of the journal
Frontiers in Molecular Neuroscience

RECEIVED 29 June 2022
ACCEPTED 01 September 2022
PUBLISHED 26 September 2022

CITATION
Eggerstorfer B, Kim J-H, Cumming P,
Lanzenberger R and Gryglewski G
(2022) Meta-analysis of molecular
imaging of translocator protein
in major depression.
Front. Mol. Neurosci. 15:981442.
doi: 10.3389/fnmol.2022.981442

Meta-analysis of molecular imaging of translocator protein in major depression

Benjamin Eggerstorfer [1], Jong-Hoon Kim [2], Paul Cumming [3,4], Rupert Lanzenberger [1*] and Gregor Gryglewski [1†]

[1]Department of Psychiatry and Psychotherapy, Comprehensive Center for Clinical Neurosciences and Mental Health (C3NMH), Medical University of Vienna, Vienna, Austria, [2]Department of Psychiatry, Gachon University College of Medicine, Gil Medical Center, Neuroscience Research Institute, GAIHST, Gachon University, Incheon, South Korea, [3]Department of Nuclear Medicine, Inselspital, Bern University, Bern, Switzerland, [4]School of Psychology and Counselling, Queensland University of Technology, Brisbane, QLD, Australia

Molecular neuroimaging studies provide mounting evidence that neuroinflammation plays a contributory role in the pathogenesis of major depressive disorder (MDD). This has been the focus of a number of positron emission tomography (PET) studies of the 17-kDa translocator protein (TSPO), which is expressed by microglia and serves as a marker of neuroinflammation. In this meta-analysis, we compiled and analyzed all available molecular imaging studies comparing cerebral TSPO binding in MDD patients with healthy controls. Our systematic literature search yielded eight PET studies encompassing 238 MDD patients and 164 healthy subjects. The meta-analysis revealed relatively increased TSPO binding in several cortical regions (anterior cingulate cortex: Hedges' g = 0.6, 95% CI: 0.36, 0.84; hippocampus: g = 0.54, 95% CI: 0.26, 0.81; insula: g = 0.43, 95% CI: 0.17, 0.69; prefrontal cortex: g = 0.36, 95% CI: 0.14, 0.59; temporal cortex: g = 0.39, 95% CI: −0.04, 0.81). While the high range of effect size in the temporal cortex might reflect group-differences in body mass index (BMI), exploratory analyses failed to reveal any relationship between elevated TSPO availability in the other four brain regions and depression severity, age, BMI, radioligand, or the binding endpoint used, or with treatment status at the time of scanning. Taken together, this meta-analysis indicates a widespread ∼18% increase of TSPO availability in the brain of MDD patients, with effect sizes comparable to those in earlier molecular imaging studies of serotonin transporter availability and monoamine oxidase A binding.

KEYWORDS

depression, meta-analysis, molecular imaging, neuroinflammation, positron emission tomography, translocator protein

Introduction

A constellation of molecular, inflammatory, and metabolic alterations is widely held to be relevant in the pathophysiology of major depressive disorder (MDD) (Otte et al., 2016), an often-devastating psychiatric condition with a worldwide prevalence of about 5% (Ferrari et al., 2013). The composite of these alterations may manifest in perturbation of normal neurotransmission and neuroplasticity, associated with morphological and functional changes in multiple structures and functional networks of the brain, as shown by neuroimaging studies (Schmaal et al., 2020). Compelling evidence derived from genome-wide association studies, epidemiological studies, and randomized controlled trials suggests involvement of the immune system in a variety of psychiatric disorders, including psychotic disorders and mood disorders such as MDD (The Network, and Pathway Analysis Subgroup of the Psychiatric Genomics Consortium, 2015; Hughes and Ashwood, 2020). An involvement of the immune system is implied by the broad similarity between core symptoms of MDD and so-called "sickness behavior" that occurs during an acute inflammatory state (Dantzer et al., 2008). Furthermore, a comprehensive review of laboratory findings in patients with MDD showed elevated peripheral proinflammatory markers such as C-reactive protein (CRP), certain interleukins, and tumor necrosis factor alpha (TNF-α), all of which is consistent with the occurrence of a pro-inflammatory state (Osimo et al., 2020). Support for a neuroinflammatory component of MDD is also provided by *post-mortem* studies showing elevated immune cytokine levels in various brain regions, and likewise by findings of raised inflammatory markers in the cerebrospinal fluid of MDD patients (Enache et al., 2019).

Peripheral inflammation might trigger a central neuroinflammatory reaction via several mechanisms. One candidate mechanism entails a humoral pathway whereby a leaky blood-brain barrier is permissive to the entry of cytokines from the circulation into the central nervous system (CNS) (Huang et al., 2021). Other propose a neural pathway whereby afferent nerves convey peripheral cytokine signals to the CNS (Miller et al., 2009), or communication along the gut-brain axis (Li et al., 2022a). In addition, a central inflammatory process could arise via immunologically active cells in the CNS (Miller and Raison, 2016).

Microglia are the resident macrophages of the brain, accounting for 5–10% of all cells in the central nervous system (Pelvig et al., 2008; Mondelli et al., 2017). In the healthy CNS, microglia are habitually present in a dormant state with ramified morphology, but nonetheless release neurotrophic factors that contribute to the regulation of synaptic homeostasis, especially in the contexts of neurotoxic or traumatic brain injury (Rodríguez-Gómez et al., 2020; Bravo et al., 2022). Indeed, a diverse range of factors can provoke microglial activation and changes in morphological phenotype (Wolf et al., 2017), for example in response to a high dietary intake of sucrose (Patkar et al., 2021), which is a characteristic of modern western diets. Activated microglia promote an inflammatory cascade involving the release of cytokines, chemokines, and other inflammatory mediators such as nitric oxide and reactive oxygen species, which together trigger reciprocal activation of astroglia, thus amplifying CNS inflammatory responses after an initial insult (Miller et al., 2009).

The expression of the 18-kDA translocator protein (TSPO) in the mitochondrial membrane of resting microglia increases as part of neuroinflammatory reactions. Numerous radiotracers have been characterized for single-photon emission computed tomography (SPECT) and positron emission tomography (PET) studies of TSPO, including [^{11}C]PK11195, [^{18}F]FEPPA and [^{11}C]PBR28 (Cumming et al., 2018). Although inferences related to inflammatory states and TSPO should consider that TSPO expression is not unique to microglia and that elevated TSPO binding in humans could also be attributable to local proliferation of myeloid cells or increased recruitment of monocytes (Narayan et al., 2017; Owen et al., 2017), TSPO remains the most widely used marker of inflammation in the living brain in diverse studies of neuropsychiatric disorders, including MDD (Mondelli et al., 2017; Enache et al., 2019).

A first systematic review on this topic appearing in 2021 revealed a relatively small number of TSPO PET studies investigating microglial reactions in patients with MDD (Gritti et al., 2021). Furthermore, published findings were not entirely consistent, and have not hitherto included all relevant TSPO PET studies (Enache et al., 2019; Schubert et al., 2021a). Hence, we aimed in this meta-analysis to analyze all available TSPO PET studies comparing TSPO binding in MDD vs. healthy control groups. We also undertook an exploratory search for possible associations of TSPO PET results with depression severity, body mass index (BMI), and other factors.

Materials and methods

Data collection

The bibliographic databases PubMed, Scopus, PsycInfo, and Web of Science were searched systematically using the terms ("mood disorders" or "affective disorders" or "depression" or "major depressive disorder" or "bipolar disorder" or "major depressive episode") and ("neuroinflammation" or "inflammation" or "microglia" or "TSPO" or "translocator protein") and ("positron emission tomography" or "PET" or "molecular imaging") in December 2021. The literature search was conducted in accordance with the guidelines of the PRISMA statement (Moher et al., 2009), and the selection of included studies was performed using the Rayyan software (Ouzzani et al., 2016). Studies were included if they fulfilled the following inclusion criteria: peer-reviewed English or German language original articles, *in vivo* TSPO studies, and studies that reported means and standard deviation (SD) values or effect sizes of

molecular imaging outcome measures reflecting cerebral TSPO binding in groups of patients with unipolar depression and healthy controls for several different brain regions. Exclusion criteria were case studies, reviews and meta-analyses, pre-clinical studies, *post-mortem* studies, and studies in patients with a diagnosis of comorbid psychiatric, somatic, or neurological disorders. The systematic search as well included SPECT studies, although no such studies emerged. **Figure 1** shows the detailed selection of publications in a flow chart based on the PRISMA statement (Moher et al., 2009). In case of overlapping samples, the study with largest sample size was selected. The corresponding author of one eligible publication shared data for additional regions based on the Hammers atlas (Hammers et al., 2003; Su et al., 2016). Results of a study that reported results separately for both hemispheres were averaged across hemispheres (Joo et al., 2021). Results from a study that separately reported results for medically treated and untreated MDD patients in groups of equal size were averaged to a single patient group (Setiawan et al., 2018). For one study that reported results in graphical format only (Hannestad et al., 2013), mean and SD values were estimated using WebPlotDigitizer, version 4.5 (Rohatgi, 2021). Demographic variables (age, sex, BMI), depression severity, type of tracer, type of outcome measure, and psychiatric medication history (medication-free interval, number of medication-free subjects) were extracted from the studies included in our analyses. For studies that reported Montgomery–Åsberg Depression Rating Scale (MADRS) score only (Hannestad et al., 2013; Su et al., 2016; Richards et al., 2018), the equivalent Hamilton Depression Rating Scale (HDRS) score, as provided by the conversion of Leucht et al. (2018), was used for further calculations.

Statistics

The statistical analysis was conducted using R 4.1.2 and the metafor package, version 3.0-2 (Viechtbauer, 2010).

TSPO PET studies can report several outcome measures, including the binding potential (BP_{ND}), which describes the specific binding relative to a reference tissue. In cases where the arterial input function has been measured, the preferred endpoint is the equilibrium distribution volume of the tracer in brain (V_T; ml/g), which is sometimes corrected for the plasma-free fraction (V_T/f_P). The diversity of outcome measures makes it compulsory to calculate standardized effect size estimates to allow their combination in a meta-analysis. Consequently, we calculated Hedges' g (Hedges, 1981), the standardized mean difference between MDD and control groups for each dataset and selected brain region. Another factor is the polymorphism of TSPO in certain populations, which imparts low specific binding of most second-generation PET TSPO tracers to carriers of the rs6971 allele (Owen et al., 2012). Therefore, in this study we used endpoints that had been corrected for group composition with respect to the high and low binding alleles. To gauge the overall relative increase in TSPO in depressed individuals, the percentage increase in mean TSPO binding was calculated for each study, weighted for sample size and averaged across all reported brain regions.

Meta-analyses were performed separately for each of five brain regions that were reported in at least three published studies, namely anterior cingulate cortex, prefrontal cortex, insula, hippocampus, and temporal cortex. We applied a random effects model with restricted maximum likelihood estimation of variance. In a random-effects model, the weighting of the individual study estimates are inversely proportional to the sum of their sample variance (f_i) and the between-study variance (f^2). To gauge variation of study results caused by between-study heterogeneity, we calculated Higgins' I^2 (Higgins and Thompson, 2002). Sensitivity analyses were performed using leave-one-out analysis.

We investigated the influence of variables on estimated effects, including depression severity, proportion of untreated patients, type of tracer used, outcome measure, BMI, sex ratio, mean age, and age differences between groups through the use of scatter plots and exploratory mixed-effects models.

Results

The systematic literature search yielded 11 eligible studies, three of which reported data from other studies (Setiawan et al., 2015; Li et al., 2018b; Turkheimer et al., 2021), resulting in final inclusion of eight studies with 238 MDD patients and 164 healthy controls (**Table 1**).

Anterior cingulate cortex

Six studies with a total of 178 MDD patients and 124 healthy controls reported on TSPO binding in anterior cingulate cortex (**Figure 2A**). Effects were clearly homogeneous (I^2 = 0%), and the results disclosed an exclusion of zero in the confidence intervals [0.60; 95%CI: (0.36, 0.84)] strongly supporting an elevation of TSPO binding in the anterior cingulate cortex in MDD patients. This result was robust to leave-one-out analysis. The funnel plot for anterior cingulate cortex showed symmetry. Exploratory mixed-effects models on investigated variables revealed no significant influences of age, gender, etc. Furthermore, investigation of scatterplots did not indicate any association between explored variables and estimated effects.

Prefrontal cortex

Seven studies comprising 188 patients and 134 controls reported on TSPO in regions with the frontal cortex,

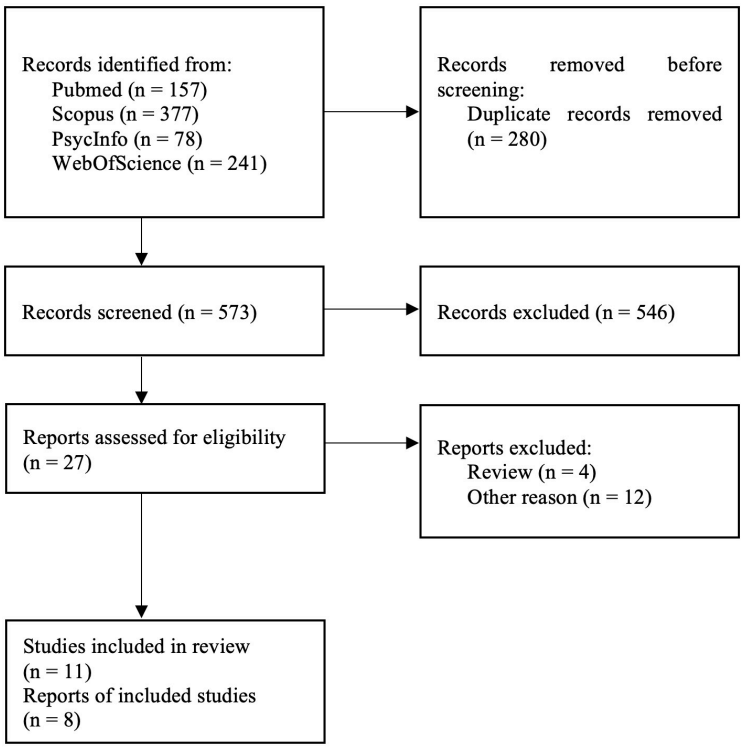

FIGURE 1
PRISMA flowchart showing the inclusion of studies for the meta-analysis (Moher et al., 2009).

predominantly the prefrontal cortex (Figure 2B). One study reported on the subgenual prefrontal cortex as a subregion and one reported the entire frontal cortex (Hannestad et al., 2013; Richards et al., 2018); both were compiled into a single frontal brain region. Despite this lumping, there was a distinct homogeneity of effects (I^2 = 0%), and the confidence intervals excluded zero [0.36; 95%CI: (0.14, 0.59)], indicating significantly increased TSPO binding sites in the prefrontal cortex in patients. The result remained steady in a leave-one-out analysis. The funnel plot for the frontal cortex was slightly asymmetrical, indicating potential publication bias favoring decreases. Exploratory mixed-effects models on tested/recorded variables did not indicate any significant influences. The scatterplot analysis also indicated no relationship between variables and effect sizes on TSPO binding.

Insula

Five studies covering 150 patients and 104 controls reported on insular cortex TSPO binding (Figure 2C). Homogeneity of effects was evident (I^2 = 0%), and confidence intervals again excluded zero [0.43; 95%CI: (0.17, 0.69)], exposing a clearly upregulated TSPO expression in the insula of patients with MDD. Visual inspection of funnel plot indicated missing studies on the right lower side. The result was robust to leave-one-out analysis and the exploratory mixed-effects models carried out to search for possible confounding variables did not reveal any significant interactions. No relationships were observed in the visual inspection of scatterplots.

Hippocampus

Four studies counting 135 patients and 96 healthy controls report on hippocampal TSPO (Figure 3A). A homogeneity of effects was apparent (I^2 = 0%), and there was exclusion of zero in the confidence intervals [0.54; 95%CI: (0.26, 0.81)], indicating elevated TSPO binding in the hippocampus of MDD patients. The funnel plot showed a marginal asymmetry favoring negative results. The hippocampal result was robust to leave-one-out analysis and further exploratory analyses of variables showed no significant influence on estimated effects.

Temporal cortex

Five studies including 145 patients and 106 healthy controls reported on TSPO binding in the temporal cortex (Figure 3B). An increase of temporal cortex TSPO binding was found,

TABLE 1 Key data of selected studies.

Study		Tracer	Outcome measure	Pharmakokinetic model	Healthy controls				MDD Patients						Medication
Author(s)	Year				*n*	F	Age	BMI	*n*	F	Age	BMI	HDRS	% untreated	
Hannestad et al. (2013)	2013	[^{11}C]PBR28	V_T	MA1	10	6	39	26.7	10	5	37	25.4	20*	**	2 patients on stable medication dose or suspended medication (> 4 weeks)
Su et al. (2016)	2016	[^{11}C]PK11195	BP_{ND}	SRTM (SVCA)	13	8	68	Missing	5	3	73.2	Missing	8*	**	Not specified
Richards et al. (2018)	2018	[^{11}C]PBR28	V_T/f_P	2TCM	20	10	31.6	26.01	28	11	39.2	27.8	24*	42.86	16 patients on stable medication, 12 patients medication free (> 2 weeks)
Holmes et al. (2018)	2018	[^{11}C]PK11195	BP_{ND}	SRTM (cerebellar GM)	13	6	33	23	14	7	30	23	20	100	Medication free > 8 months
Setiawan et al. (2018)	2018	[^{18}F]FEPPA	V_T	2TCM	30	14	33.2	24.9	50	31	34.45	24.6	21.05	38	19 patients medication free (> 6 weeks)
Li et al. (2018a)	2018	[^{18}F]FEPPA	V_T	2TCM	30	15	27.4	24.3	50	25	28.7	24.5	20.6	**	Medication free
Schubert et al. (2021a)	2021	[^{11}C]PK11195	BP_{ND}	SRTM (SVCA)	25	14	37.3	24.2	51	46	36.2	27.2	18.5	17.5	9 patients medication free,
Joo et al. (2021)	2021	[^{11}C]PK11195	BP_{ND}	SRTM (SVCA)	23	10	24.5	23.6	30	17	24.6	23.6	24.3	100	Medication free / treatment naive
Sum: 8					164				238						

MDD, major depressive disorder; F, number of female participants; HDRS, Hamilton Depression Rating Scale (17-item); BMI, body mass index; V_T, distribution volume of the tracer; V_T/f_P, V_T corrected for plasma-free fraction; BP_{ND}, binding potential; MA1, multilinear analysis; SRTM, simplified reference tissue modeling; SVCA, supervised cluster analysis; 2TCM, two tissue compartment model; GM, gray matter; *equivalent to reported Montgomery Åsberg Rating scale (Leucht et al., 2018); **not reported.

but confidence intervals included zero [0.39; 95%CI: (−0.04, 0.81)]. There was moderate heterogeneity of effect estimates in temporal cortex (I^2 = 57%). Leave-one-out analysis revealed that excluding data of Hannestad et al. (2013) resulted in a significant decrease of heterogeneity and a shift of confidence intervals excluding zero [0.57; 95%CI: (0.25, 0.88), I^2 = 21%]. We note that, relative to controls, the MDD group of Hannestad et al. (2013) study had the lowest mean BMI, and the largest mean BMI difference between groups, and that the study excluded patients with elevated peripheral inflammatory markers, which may together have biased the results. Visual inspection of the funnel plot suggested a negative publication bias and revealed that smaller studies reported lower effect sizes in the temporal cortex.

Discussion

The results of this meta-analysis strongly indicate elevated binding of TSPO in all investigated regions in MDD patients vs. healthy controls, which suggests neuroinflammation extending across a range of cortical brain regions previously implicated in executive function (prefrontal cortex), mood (anterior cingulate, hippocampus), sensory processing and homeostatic state (insula), and affective processing (temporal lobe). We note a considerable overlap with brain regions showing reduced perfusion in a meta-analysis of spin-labeling fMRI studies in MDD (Wang and Yang, 2022), and partial concurrence with regions of decreased metabolism to FDG-PET (Su et al., 2014). The present meta-analysis indicates an approximately 29% elevation in the expression of TSPO in the anterior cingulate cortex in a group of more than one hundred MDD patients. The anterior cingulate cortex exhibited the most robust results among investigated regions, with a medium to large effect size, and with five of six studies reporting increased TSPO binding. That *in vivo* TSPO PET finding concurs with *post-mortem* data showing regional microglial activation in the dorsal anterior cingulate cortex of suicide victims with MDD (Torres-Platas et al., 2014; Snijders et al., 2021). The anterior cingulate cortex is considered to be a key structure in circuit models of mood processing and in mediating attention and executive function, and its disruption is thought to impair the ability to process affective information or emotions (Price and Drevets, 2010; Rolls, 2019), which are deficits commonly reported in MDD patients (Naranjo et al., 2011). Furthermore, Li et al. (2018a) identified an association between attentional deficits and increased TSPO expression in the frontal cortex, potentially underpinning the regionally pronounced increase of TSPO availability in patients.

As a key part of the limbic system, the hippocampus is among the brain regions most often studied in mood disorders (Belleau et al., 2019). Our finding of higher TSPO binding in the hippocampus of MDD patients may have some bearing

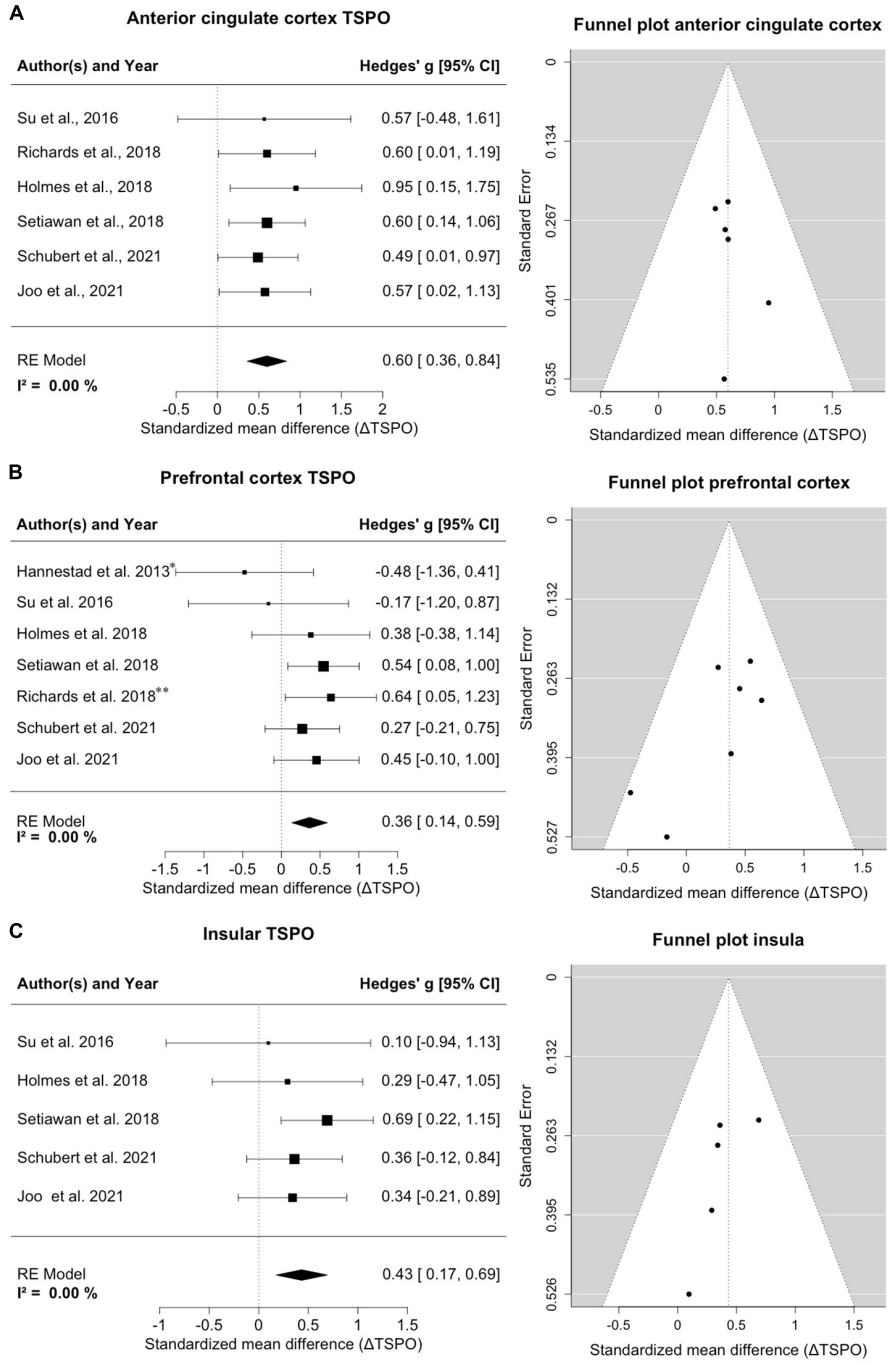

FIGURE 2
Significant increase of TSPO binding in anterior cingulate cortex (ACC), prefrontal cortex (PFC) and insula in MDD patients. **(A)** A forest plot of TSPO binding in the ACC clearly shows an effect size of 0.60, 95%CI: (0.36, 0.84). The corresponding funnel plot is displayed on the right. **(B)** The forest plot of TSPO in PFC displays an effect size of 0.36, 95%CI: (0.14, 0.59). *Data of frontal cortex; **data of subgenual prefrontal cortex. On the right is the funnel plot of estimates of prefrontal cortex. **(C)** A forest plot for TSPO binding in the insula shows an effect size of 0.43, 95%CI: (0.17, 0.69). Alongside the corresponding funnel plot is displayed.

on reports of impaired hippocampal neurogenesis and reduced volume as an anatomic correlate of depressive behavior and cognitive changes (Cole et al., 2011; Chesnokova et al., 2016; Roddy et al., 2019). Similarly, we saw pronounced increases in TSPO-PET signals in the prefrontal cortex, which is also known as a region showing functional and structural changes in depressions (Pizzagalli and Roberts, 2022). Furthermore, a recent review identified the anterior cingulate cortex, prefrontal

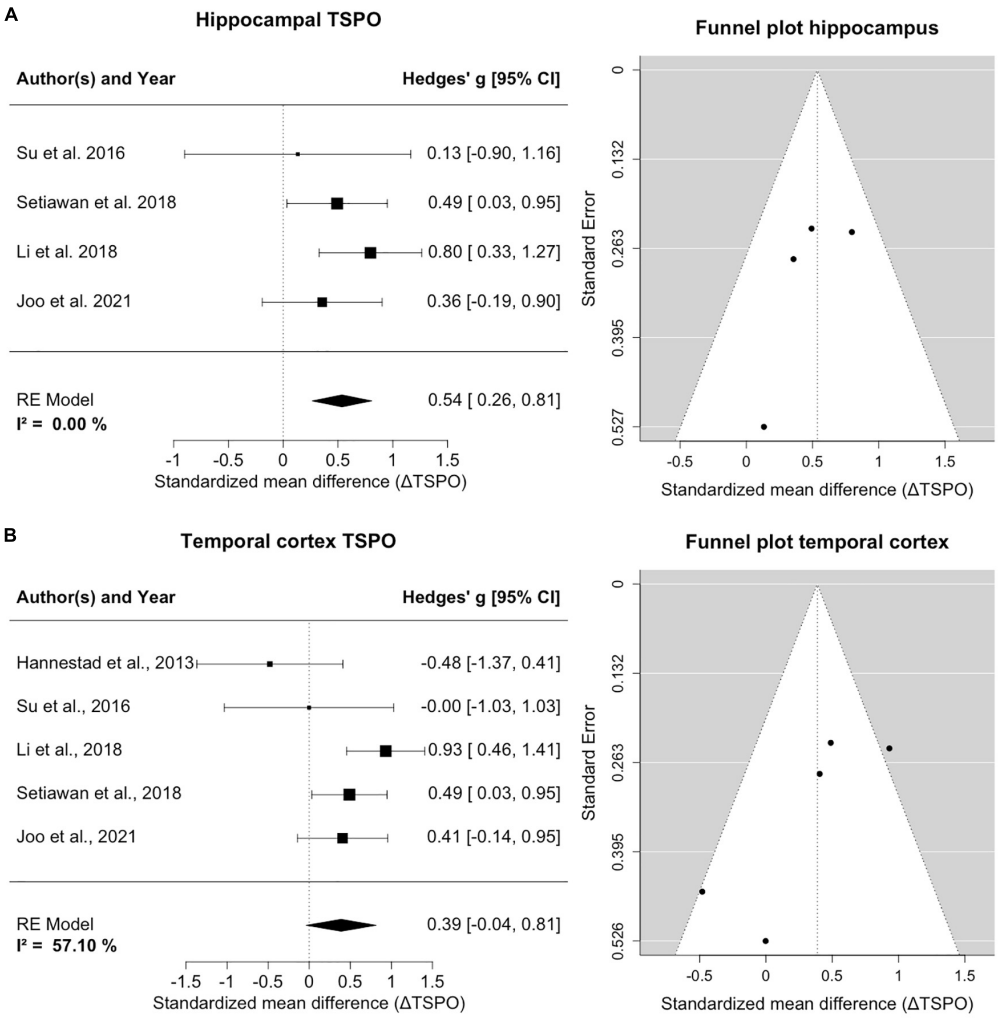

FIGURE 3
TSPO binding is increased in hippocampus and temporal cortex of MDD patients compared to controls. **(A)** The forest plot for TSPO binding in the hippocampus shows an effect size of 0.54, 95%CI: (0.26, 0.81). The funnel plot of hippocampal estimates is shown on the right side. **(B)** The forest plot of TSPO binding in the temporal cortex indicates an effect size of 0.39, 95%CI: (−0.04, 0.95). The corresponding funnel plot is displayed alongside.

cortex, temporal cortex, and the insula as the main cerebral regions with disrupted functional connectivity in association with the impaired emotional processing of MDD patients, thus broadly overlapping with regions of increased TSPO PET signal (Li et al., 2022b).

We focused on TSPO PET results in the five brain regions most frequently reported in the eight studies included in our meta-analysis, with a consistent finding of increased TSPO expression in key cortical regions associated with the pathophysiology of depression. A small number of the included studies reported modest differences between groups or even increased TSPO availability in healthy individuals compared to patients, which may contribute to the low effect size estimates in the temporal cortex (Hannestad et al., 2013; Su et al., 2016). Whereby Su et al. (2016) scanned patients with very low MADRS scores and Hannestad et al. (2013) reported relatively higher TSPO expression in healthy individuals in all regions, although that finding was non-significant, with very low sample size, and large inter-subject variability. A few published reports including additional regions likewise indicated a trend toward elevated TSPO expression (Li et al., 2018a; Setiawan et al., 2018), which needs however to be confirmed by studies in large and homogeneous patient samples.

A few exploratory studies have investigated possible factors influencing the effect size in TSPO-PET studies. A [^{11}C]PBR28 PET study by Tuisku et al. (2019) found an inverse relationship between tracer V_T with BMI in healthy subjects. The same report also showed that women exhibited higher V_T than men, and that increasing age was a factor predicting higher V_T in the frontal and temporal cortices of MDD patients;

we did not recapitulate those findings in our meta-analysis of TSPO-PET studies. In our regional analyses, there were no discernible effects of depression score, age, BMI, percentage of untreated patients, sex distribution, choice of tracer, and the choice of TSPO PET outcome measure. Visual inspection of scatterplots indicated a trend toward higher effect sizes in studies of MDD patients with higher depression scores, which was however not supported by mixed-effects model analysis. We concede that the number of studies in our regional analyses was limited, and propose that a more comprehensive meta-analysis using individual subject data would be necessary to provide a reliable assessment of confounding factors on the availability of TSPO (Plavén-Sigray et al., 2018, 2021). A key finding of Setiawan et al. was that duration of untreated MDD significantly correlated with TSPO V_T in three of the examined regions (prefrontal cortex, anterior cingulate cortex, and insula), and that disease duration was a predictor for greater TSPO expression in MDD patients (Setiawan et al., 2018). Available data on disease duration, current episode, and duration of non-treatment in included studies were sparse; only two studies reported current episode duration, and three studies included disease duration as potential confounding variables. An additional factor of interest might be disease-related alterations in regional brain volume, which could lead to artifactual findings of altered TSPO availability. However, one study reporting volumetric brain data found no group differences in regional tissue volumes, despite elevated TSPO availability in patients compared to healthy subjects (Holmes et al., 2018). Furthermore, large multi-center trials reported only small effects of MDD on brain volumetric outcomes (Thompson et al., 2020), which is thus unlikely to account for the differences in TSPO binding in MDD patients compared with healthy controls.

The results of this meta-analysis support the clinical implications of findings from a recent systematic review and meta-analysis (Köhler-Forsberg et al., 2019), which reported that adjunctive anti-inflammatory therapy can alleviate certain MDD symptoms. Moreover, the discipline of clinical psychiatry has long been searching for unambiguous objective diagnostic measures in what may well be heterogeneous disorders. Certainly, the elevation of cortical TSPO binding in MDD patients has an effect size comparable to that seen in our previous meta-analysis showing slightly reduced availability of serotonin transporters in MDD (Gryglewski et al., 2014). However, the present effect size is lower than that reported in a [^{11}C]harmine PET study showing increased availability of binding sites for monoamine oxidase A (MAO-A), the enzyme metabolizing serotonin (Meyer et al., 2006). At present, no PET molecular biomarker is pathognomonic of depression, but the composite of results with various tracers might eventually serve to identify molecular sub-types of the disorder, and further investigation might test the hypothesis that there is spatial overlap between increased TSPO binding and altered markers of serotonin innervation and metabolism, or other established molecular imaging results.

TSPO may not only serve as a diagnostic marker in combination with other neuroimaging modalities, but it might also exert as a direct target for putative therapeutic effects in stress-related diseases such as MDD (Rupprecht et al., 2022). While the present results may present microglia as a therapeutic target, a treatment trial with minocycline failed to rectify the elevated TSPO-PET binding in a cohort of patients with treatment-resistant depression (Attwells et al., 2021). On the other hand, findings of a recently published randomized clinical trial suggest that the easily available serum CRP levels could serve as a predictive biomarker to screen for MDD patients who might benefit from add-on minocycline to antidepressant treatment (Nettis et al., 2021). Furthermore, another recent study suggests that specific inflammatory biomarkers that are known to be produced by activated microglia and which correlate with TSPO V_T, might serve for selection of MDD patients most apt to benefit from augmentative anti-inflammatory therapy (Attwells et al., 2020). Similarly, we recently showed complex relationships between individual plasma levels of the cytokine adiponectin with TSPO-PET results in healthy control and MDD patient groups (Joo et al., 2021).

We note some limitations of this meta-analysis. First, our analysis was limited to the regions that were most frequently reported in molecular imaging studies investigating TSPO in MDD. Some of the included studies involved additional brain regions such as the parietal cortex, the occipital cortex, or non-cortical regions such as the thalamus, amygdala, and putamen (Hannestad et al., 2013; Su et al., 2016; Holmes et al., 2018; Richards et al., 2018; Setiawan et al., 2018). Corresponding data on other brain areas, including the motor cortex and the visual cortex are not yet reported in the literature. Due to the use of different radiotracers and quantification methods, TSPO PET studies can be inherently difficult to compare. By calculating standardized mean differences, we attempted to avoid distortions due to the different measurement scales. Furthermore, we used random-effect models to accommodate the anticipated heterogeneity. However, this approach does not completely eliminate bias from variation between study populations (Lin and Aloe, 2021). As is well known, current TSPO PET tracers indicate only the overall level of microglial activation, but do not differentiate between the anti-inflammatory and pro-inflammatory microglial phenotypes. In addition, TSPO ligands are not entirely specific for microglia, but can indicate other neuroinflammatory changes, including activation of astroglia cells and monocyte-derived macrophages (Cosenza-Nashat et al., 2009). However, the preponderance of the TSPO-PET signal in brain tissue is likely indicative of microglial activation (Setiawan et al., 2018). PET imaging studies using newer radioligands for biomarkers of inflammation other than TSPO, such as monoamine oxidase B,

cyclooxygenase, colony stimulating factor 1 receptor, and the purinergic $P2X_7$ receptor may eventually confirm the state of neuroinflammation in MDD (Narayanaswami et al., 2018; Zhou et al., 2021). We concede that some regional analyses in this meta-analysis involve a small number of studies, which limits their statistical power and may have impeded detection of a publication bias. A further limitation is that most studies included in this meta-analysis used the first-generation radioligand [^{11}C]PK11195, which has a relatively low specific binding signal and brain uptake (Kreisl et al., 2010; Cumming et al., 2018; Kobayashi et al., 2018), albeit not having the TSPO allelic dependence of second-generation tracers. In this context a meta-analysis on TSPO-PET in schizophrenia reported that differences between patients and healthy subjects were only apparent from studies using [^{11}C]PK11195, without any such difference evident in the studies using second-generation TSPO radioligands like [^{11}C]PBR28 and [^{18}F]FEPPA, noting that these findings were driven by small studies with low variability in outcomes (Marques et al., 2019). Of interest, a recent study revealed that the Korean population seems to lack the polymorphism of the rs6971 allele, thereby suggesting a lower impact on second-generation TSPO PET tracer binding in this patient group (Lee et al., 2022). Analytic procedures also affect the signal-to-noise ratio of TSPO PET measurement, in the absence of a valid reference region for calculating the binding potential (BP_{ND}) (Cumming et al., 2018). In an effort to select the most appropriate reference region, most of the included studies reported BP_{ND} as the outcome measure, as calculated by the simplified reference tissue model using a supervised clustering approach to segment the reference region (Turkheimer et al., 2007; Boellaard et al., 2008; Yaqub et al., 2012; Schubert et al., 2021b). Holmes et al. relied on cerebellar gray matter as a pseudoreference region due to the lower variance in BP_{ND} results compared to the data-driven approach (Kropholler et al., 2007; Holmes et al., 2018). The gold standard endpoint is therefore total distribution volume (V_T), which calls for serial arterial sampling with correction for tracer metabolism (Wimberley et al., 2021). The most common pharmacokinetic model to calculate V_T in the included studies was a two-tissue compartment model, which appears to be the most feasible for second-generation TSPO ligands (Fujita et al., 2008; Rusjan et al., 2011). Ichise et al. (2002) and Hannestad et al. (2013). relied on a multilinear analysis to calculate V_T because of lower standard errors in estimates compared to the two-tissue compartment model. Notwithstanding, mixed-effects models did not indicate any effects of radioligand type or outcome measures on the finding of increased TSPO expression in MDD patients.

In summary, this systematic meta-analysis clearly highlights prior findings of increased TSPO binding in MDD patients compared to healthy controls in the broadest sample of TSPO PET data yet assembled. In MDD patients, we saw an ∼18% relative increase in TSPO expression, which was present in all investigated brain regions, and with effect sizes of comparable magnitude to those in previous PET studies of availability of serotonin transporters and monoamine oxidase A binding in MDD (Meyer et al., 2006; Gryglewski et al., 2014). The findings were robust to depression severity, BMI, medication status, and other explored variables, and statistical analysis indicates that the effect was driven by significant increases of TSPO in one third of the MDD patients. Hence, TSPO elevation is indeed a feature of MDD, and future *in-vivo* studies with novel radioligands targeting neuroinflammation may prove to support the occurrence of a central inflammatory component in MDD.

Data availability statement

Processed data is available from the authors upon reasonable request. Please contact the corresponding author for any questions or requests.

Author contributions

BE and GG performed data collection and analysis. PC and J-HK proposed the study. All authors contributed to the interpretation of results and drafting of the manuscript and approved the final version of the manuscript.

Funding

This research was funded in part by the Austrian Science Fund (FWF) (KLI 1006, PI: RL). This work was also supported in part by the National Research Foundation of Korea (NRF) grant funded by the Korea Government (MSIT) (2020R1A4A1019623) to J-HK.

Conflict of interest

RL received travel grants and/or conference speaker honoraria within the last 3 years from Bruker BioSpin MR, Heel, and support from Siemens Healthcare regarding clinical research using PET/MR. He has been a shareholder of the start-up company BM Health GmbH since 2019.

The remaining authors declare that the research was conducted in the absence of any commercial or financial relationships that could be construed as a potential conflict of interest.

Publisher's note

References

Attwells, S., Setiawan, E., Rusjan, P. M., Xu, C., Kish, S. J., Vasdev, N., et al. (2021). A double-blind placebo-controlled trial of minocycline on translocator protein distribution volume in treatment-resistant major depressive disorder. *Transl. Psychiatry* 11:334. doi: 10.1038/s41398-021-01450-1453

Attwells, S., Setiawan, E., Wilson, A. A., Rusjan, P. M., Miler, L., Xu, C., et al. (2020). Replicating predictive serum correlates of greater translocator protein distribution volume in brain. *Neuropsychopharmacology* 45, 925–931. doi: 10.1038/s41386-019-0561-y

Belleau, E. L., Treadway, M. T., and Pizzagalli, D. A. (2019). The impact of stress and major depressive disorder on hippocampal and medial prefrontal cortex morphology. *Biol. Psychiatry* 85, 443–453. doi: 10.1016/j.biopsych.2018.09.031

Boellaard, R., Turkheimer, F. E., Hinz, R., Schuitemaker, A., Scheltens, P., van Berckel, B. N. M., et al. (2008). "Performance of a modified supervised cluster algorithm for extracting reference region input functions from (R)-[11C]PK11195 brain PET studies," in *Proceedings of the 2008 IEEE Nuclear Science Symposium Conference Record (IEEE)*, (Piscataway, NJ).

Bravo, J., Ribeiro, I., Terceiro, A. F., Andrade, E. B., Portugal, C. C., Lopes, I. M., et al. (2022). Neuron-Microglia contact-dependent mechanisms attenuate methamphetamine-induced microglia reactivity and enhance neuronal plasticity. *Cells* 11:355. doi: 10.3390/CELLS11030355

Chesnokova, V., Pechnick, R. N., and Wawrowsky, K. (2016). Chronic peripheral inflammation, hippocampal neurogenesis, and behavior. *Brain Behav. Immun.* 58, 1–8. doi: 10.1016/j.bbi.2016.01.017

Cole, J., Costafreda, S. G., McGuffin, P., and Fu, C. H. Y. (2011). Hippocampal atrophy in first episode depression: a meta-analysis of magnetic resonance imaging studies. *J. Affect. Disord.* 134, 483–487. doi: 10.1016/j.jad.2011.05.057

Cosenza-Nashat, M., Zhao, M. L., Suh, H. S., Morgan, J., Natividad, R., Morgello, S., et al. (2009). Expression of the translocator protein of 18 kDa by microglia, macrophages and astrocytes based on immunohistochemical localization in abnormal human brain. *Neuropathol. Appl. Neurobiol.* 35, 306–328. doi: 10.1111/j.1365-2990.2008.01006.x

Cumming, P., Burgher, B., Patkar, O., Breakspear, M., Vasdev, N., Thomas, P., et al. (2018). Sifting through the surfeit of neuroinflammation tracers. *J. Cereb. Blood Flow Metab.* 38, 204–224. doi: 10.1177/0271678X17748786

Dantzer, R., O'Connor, J. C., Freund, G. G., Johnson, R. W., and Kelley, K. W. (2008). From inflammation to sickness and depression: when the immune system subjugates the brain. *Nat. Rev. Neurosci.* 9, 46–56. doi: 10.1038/nrn2297

Enache, D., Pariante, C. M., and Mondelli, V. (2019). Markers of central inflammation in major depressive disorder: a systematic review and meta-analysis of studies examining cerebrospinal fluid, positron emission tomography and post-mortem brain tissue. *Brain Behav. Immun.* 81, 24–40. doi: 10.1016/j.bbi.2019.06.015

Ferrari, A. J., Somerville, A. J., Baxter, A. J., Norman, R., Patten, S. B., Vos, T., et al. (2013). Global variation in the prevalence and incidence of major depressive disorder: a systematic review of the epidemiological literature. *Psychol. Med.* 43, 471–481. doi: 10.1017/S0033291712001511

Fujita, M., Imaizumi, M., Zoghbi, S. S., Fujimura, Y., Farris, A. G., Suhara, T., et al. (2008). Kinetic analysis in healthy humans of a novel positron emission tomography radioligand to image the peripheral benzodiazepine receptor, a potential biomarker for inflammation. *Neuroimage* 40, 43–52. doi: 10.1016/j.neuroimage.2007.11.011

Gritti, D., Delvecchio, G., Ferro, A., Bressi, C., and Brambilla, P. (2021). Neuroinflammation in major depressive disorder: a review of pet imaging studies examining the 18-kDa translocator protein. *J. Affect. Disord.* 292, 642–651. doi: 10.1016/j.jad.2021.06.001

Gryglewski, G., Lanzenberger, R., Kranz, G. S., and Cumming, P. (2014). Meta-analysis of molecular imaging of serotonin transporters in major depression. *J. Cereb. Blood Flow Metab.* 34, 1096–1103. doi: 10.1038/jcbfm.2014.82

Hammers, A., Allom, R., Koepp, M. J., Free, S. L., Myers, R., Lemieux, L., et al. (2003). Three-dimensional maximum probability atlas of the human brain, with particular reference to the temporal lobe. *Hum. Brain Mapp.* 19, 224–247. doi: 10.1002/hbm.10123

Hannestad, J., DellaGioia, N., Gallezot, J. D., Lim, K., Nabulsi, N., Esterlis, I., et al. (2013). The neuroinflammation marker translocator protein is not elevated in individuals with mild-to-moderate depression: a [11C]PBR28 PET study. *Brain Behav. Immun.* 33, 131–138. doi: 10.1016/j.bbi.2013.06.010

Hedges, L. V. (1981). Distribution theory for Glass's estimator of effect size and related estimators. *J. Educ. Behav. Statistics* 6, 107–128.

Higgins, J. P. T., and Thompson, S. G. (2002). Quantifying heterogeneity in a meta-analysis. *Stat. Med.* 21, 1539–1558. doi: 10.1002/sim.1186

Holmes, S. E., Hinz, R., Conen, S., Gregory, C. J., Matthews, J. C., Anton-Rodriguez, J. M., et al. (2018). Elevated translocator protein in anterior cingulate in major depression and a role for inflammation in suicidal thinking: a positron emission tomography study. *Biol. Psychiatry* 83, 61–69. doi: 10.1016/j.biopsych.2017.08.005

Huang, X., Hussain, B., and Chang, J. (2021). Peripheral inflammation and blood-brain barrier disruption: effects and mechanisms. *CNS Neurosci. Ther.* 27, 36–47. doi: 10.1111/cns.13569

Hughes, H. K., and Ashwood, P. (2020). Overlapping evidence of innate immune dysfunction in psychotic and affective disorders. *Brain Behav. Immun. Health* 2:100038. doi: 10.1016/j.bbih.2020.100038

Ichise, M., Toyama, H., Innis, R. B., and Carson, E. (2002). Strategies to improve neuroreceptor parameter estimation by linear regression analysis. *J. Cereb. Blood Flow Metab.* 22:1271–1281.

Joo, Y.-H., Lee, M.-W., Son, Y.-D., Chang, K.-A., Yaqub, M., Kim, H.-K., et al. (2021). In Vivo Cerebral Translocator Protein (TSPO) binding and its relationship with blood adiponectin levels in treatment-naïve young adults with major depression: a [11C]PK11195 PET study. *Biomedicines* 10:34. doi: 10.3390/biomedicines10010034

Kobayashi, M., Jiang, T., Telu, S., Zoghbi, S. S., Gunn, R. N., Rabiner, E. A., et al. (2018). 11 C-DPA-713 has much greater specific binding to translocator protein 18 kDa (TSPO) in human brain than 11 C-(R)-PK11195. *J. Cereb. Blood Flow Metab.* 38, 393–403. doi: 10.1177/0271678X17699223

Köhler-Forsberg, O., N. Lydholm, C., Hjorthøj, C., Nordentoft, M., Mors, O., and Benros, M. E. (2019). Efficacy of anti-inflammatory treatment on major depressive disorder or depressive symptoms: meta-analysis of clinical trials. *Acta Psychiatr. Scand.* 139, 404–419. doi: 10.1111/acps.13016

Kreisl, W. C., Fujita, M., Fujimura, Y., Kimura, N., Jenko, K. J., Kannan, P., et al. (2010). Comparison of [11C]-(R)-PK 11195 and [11C]PBR28, two radioligands for translocator protein (18 kDa) in human and monkey: implications for positron emission tomographic imaging of this inflammation biomarker. *Neuroimage* 49, 2924–2932. doi: 10.1016/j.neuroimage.2009.11.056

Kropholler, M. A., Boellaard, R., Nm Van Berckel, B., Schuitemaker, A., Kloet, R. W., Lubberink, M. J., et al. (2007). Evaluation of reference regions for (R)-[11 C]PK11195 studies in Alzheimer's disease and Mild Cognitive Impairment. *J. Cereb. Blood Flow Metab.* 27, 1965–1974. doi: 10.1038/sj.jcbfm.9600488

Lee, H., Noh, Y., Kim, W. R., Seo, H. -E., and Park, H. -M. (2022). Translocator Protein (18 kDa) Polymorphism (rs6971) in the Korean Population. *Dement Neurocogn. Disord* 21:71. doi: 10.12779/dnd.2022.21.2.71

Leucht, S., Fennema, H., Engel, R. R., Kaspers-Janssen, M., and Szegedi, A. (2018). Translating the HAM-D into the MADRS and vice versa with equipercentile linking. *J. Affect. Disord.* 226, 326–331. doi: 10.1016/j.jad.2017.09.042

Li, H., Sagar, A. P., and Kéri, S. (2018a). Microglial markers in the frontal cortex are related to cognitive dysfunctions in major depressive disorder. *J. Affect. Disord.* 241, 305–310. doi: 10.1016/j.jad.2018.08.021

Li, H., Sagar, A. P., and Kéri, S. (2018b). Translocator protein (18 kDa TSPO) binding, a marker of microglia, is reduced in major depression during cognitive-behavioral therapy. *Prog. Neuropsychopharmacol. Biol. Psychiatry* 83, 1–7. doi: 10.1016/j.pnpbp.2017.12.011

Li, B., Yang, W., Ge, T., Wang, Y., and Cui, R. (2022a). Stress induced microglial activation contributes to depression. *Pharmacol. Res.* 179:106145. doi: 10.1016/J.PHRS.2022.106145

Li, J., Chen, J., Kong, W., Li, X., and Hu, B. (2022b). Abnormal core functional connectivity on the pathology of MDD and antidepressant treatment: a systematic review. *J. Affect. Disord.* 296, 622–634. doi: 10.1016/j.jad.2021.09.074

Lin, L., and Aloe, A. M. (2021). Evaluation of various estimators for standardized mean difference in meta-analysis. *Stat. Med.* 40, 403–426. doi: 10.1002/sim.8781

Marques, T. R., Ashok, A. H., Pillinger, T., Veronese, M., Turkheimer, F. E., Dazzan, P., et al. (2019). Neuroinflammation in schizophrenia: meta-analysis of in vivo microglial imaging studies. *Psychol. Med.* 49, 2186–2196. doi: 10.1017/S0033291718003057

Meyer, J. H., Ginovart, N., Boovariwala, A., Sagrati, S., Hussey, D., Garcia, A., et al. (2006). Elevated monoamine oxidase a levels in the brain an explanation for the monoamine imbalance of major depression. *Arch. Gen. Psychiatry* 63:1209–1216 doi: 10.1001/archpsyc.63.11.1209

Miller, A. H., and Raison, C. L. (2016). The role of inflammation in depression: from evolutionary imperative to modern treatment target. *Nat. Rev. Immunol.* 16, 22–34. doi: 10.1038/nri.2015.5

Miller, A. H., Maletic, V., and Raison, C. L. (2009). Inflammation and its discontents: the role of cytokines in the pathophysiology of major depression. *Biol. Psychiatry* 65, 732–741. doi: 10.1016/j.biopsych.2008.11.029

Moher, D., Liberati, A., Tetzlaff, J., and Altman, D. G. (2009). Preferred reporting items for systematic reviews and meta-analyses: the PRISMA statement. *BMJ* 339, 332–336. doi: 10.1136/bmj.b2535

Mondelli, V., Vernon, A. C., Turkheimer, F., Dazzan, P., and Pariante, C. M. (2017). Brain microglia in psychiatric disorders. *Lancet Psychiatry* 4, 563–572. doi: 10.1016/S2215-036630101-30103

Naranjo, C., Kornreich, C., Campanella, S., Noël, X., Vandriette, Y., Gillain, B., et al. (2011). Major depression is associated with impaired processing of emotion in music as well as in facial and vocal stimuli. *J. Affect. Disord.* 128, 243–251. doi: 10.1016/j.jad.2010.06.039

Narayan, N., Mandhair, H., Smyth, E., Dakin, S. G., Kiriakidis, S., Wells, L., et al. (2017). The macrophage marker translocator protein (TSPO) is down-regulated on pro-inflammatory 'M1' human macrophages. *PLoS One* 12: e0185767. doi: 10.1371/journal.pone.0185767

Narayanaswami, V., Dahl, K., Bernard-Gauthier, V., Josephson, L., Cumming, P., and Vasdev, N. (2018). Emerging PET radiotracers and targets for imaging of neuroinflammation in neurodegenerative diseases: outlook beyond TSPO. *Mol. Imaging* 17:1536012118792317. doi: 10.1177/1536012118792317

Nettis, M. A., Lombardo, G., Hastings, C., Zajkowska, Z., Mariani, N., Nikkheslat, N., et al. (2021). Augmentation therapy with minocycline in treatment-resistant depression patients with low-grade peripheral inflammation: results from a double-blind randomised clinical trial. *Neuropsychopharmacology* 46, 939–948. doi: 10.1038/s41386-020-00948-946

Osimo, E. F., Pillinger, T., Rodriguez, I. M., Khandaker, G. M., Pariante, C. M., and Howes, O. D. (2020). Inflammatory markers in depression: a meta-analysis of mean differences and variability in 5,166 patients and 5,083 controls. *Brain Behav. Immun.* 87, 901–909. doi: 10.1016/j.bbi.2020.02.010

Otte, C., Gold, S. M., Penninx, B. W., Pariante, C. M., Etkin, A., Fava, M., et al. (2016). Major depressive disorder. *Nat. Rev. Dis. Primers* 2:16065. doi: 10.1038/nrdp.2016.65

Ouzzani, M., Hammady, H., Fedorowicz, Z., and Elmagarmid, A. (2016). Rayyan-a web and mobile app for systematic reviews. *Syst. Rev.* 5:210. doi: 10.1186/s13643-016-0384-384

Owen, D. R., Narayan, N., Wells, L., Healy, L., Smyth, E., Rabiner, E. A., et al. (2017). Pro-inflammatory activation of primary microglia and macrophages increases 18 kDa translocator protein expression in rodents but not humans. *J. Cereb. Blood Flow Metab.* 37, 2679–2690. doi: 10.1177/0271678X17710182

Owen, D. R., Yeo, A. J., Gunn, R. N., Song, K., Wadsworth, G., Lewis, A., et al. (2012). An 18-kDa Translocator Protein (TSPO) polymorphism explains differences in binding affinity of the PET radioligand PBR28. *J. Cereb. Blood Flow Metab.* 32, 1–5. doi: 10.1038/jcbfm.2011.147

Patkar, O. L., Mohamed, A. Z., Narayanan, A., Mardon, K., Cowin, G., Bhalla, R., et al. (2021). A binge high sucrose diet provokes systemic and cerebral inflammation in rats without inducing obesity. *Sci. Rep.* 11:11252. doi: 10.1038/s41598-021-90817-z

Pelvig, D. P., Pakkenberg, H., Stark, A. K., and Pakkenberg, B. (2008). Neocortical glial cell numbers in human brains. *Neurobiol. Aging* 29, 1754–1762. doi: 10.1016/j.neurobiolaging.2007.04.013

Pizzagalli, D. A., and Roberts, A. C. (2022). Prefrontal cortex and depression. *Neuropsychopharmacology* 47, 225–246. doi: 10.1038/s41386-021-01101-1107

Plavén-Sigray, P., Matheson, G. J., Collste, K., Ashok, A. H., Coughlin, J. M., Howes, O. D., et al. (2018). Positron emission tomography studies of the glial cell marker translocator protein in patients with psychosis: a meta-analysis using individual participant data. *Biol. Psychiatry* 84, 433–442. doi: 10.1016/j.biopsych.2018.02.1171

Plavén-Sigray, P., Matheson, G. J., Coughlin, J. M., Hafizi, S., Laurikainen, H., Ottoy, J., et al. (2021). Meta-analysis of the glial marker TSPO in psychosis revisited: reconciling inconclusive findings of patient-control differences. *Biol. Psychiatry* 89, e5–e8. doi: 10.1016/j.biopsych.2020.05.028

Price, J. L., and Drevets, W. C. (2010). Neurocircuitry of mood disorders. *Neuropsychopharmacology* 35, 192–216. doi: 10.1038/npp.2009.104

Richards, E. M., Zanotti-Fregonara, P., Fujita, M., Newman, L., Farmer, C., Ballard, E. D., et al. (2018). PET radioligand binding to translocator protein (TSPO) is increased in unmedicated depressed subjects. *EJNMMI Res.* 8:57. doi: 10.1186/s13550-018-0401-409

Roddy, D. W., Farrell, C., Doolin, K., Roman, E., Tozzi, L., Frodl, T., et al. (2019). The hippocampus in depression: more than the sum of its parts? advanced hippocampal substructure segmentation in depression. *Biol. Psychiatry* 85, 487–497. doi: 10.1016/j.biopsych.2018.08.021

Rodríguez-Gómez, J. A., Kavanagh, E., Engskog-Vlachos, P., Engskog, M. K. R., Herrera, A. J., Espinosa-Oliva, A. M., et al. (2020). Microglia: agents of the CNS pro-inflammatory response. *Cells* 9:1717. doi: 10.3390/cells9071717

Rohatgi, A. (2021). *WebPlotDigitizer: Version 4.5*. Available online at: https://automeris.io/WebPlotDigitizer (accessed November 1, 2021).

Rolls, E. T. (2019). The cingulate cortex and limbic systems for emotion, action, and memory. *Brain Struct. Funct.* 224, 3001–3018. doi: 10.1007/s00429-019-01945-1942

Rupprecht, R., Wetzel, C. H., Dorostkar, M., Herms, J., Albert, N. L., Schwarzbach, J., et al. (2022). Translocator protein (18kDa) TSPO: a new diagnostic or therapeutic target for stress-related disorders? *Mol. Psychiatry* 27, 1–9

Rusjan, P. M., Wilson, A. A., Bloomfield, P. M., Vitcu, I., Meyer, J. H., Houle, S., et al. (2011). Quantitation of translocator protein binding in human brain with the novel radioligand [18 F]-FEPPA and positron emission tomography. *J. Cereb. Blood Flow Metab.* 31, 1807–1816. doi: 10.1038/jcbfm.2011.55

Schmaal, L., Pozzi, E., C. Ho, T., van Velzen, L. S., Veer, I. M., Opel, et al. (2020). ENIGMA MDD: seven years of global neuroimaging studies of major depression through worldwide data sharing. *Transl. Psychiatry* 10:172. doi: 10.1038/s41398-020-0842-846

Schubert, J. J., Veronese, M., Fryer, T. D., Manavaki, R., Kitzbichler, M. G., Nettis, M. A., et al. (2021a). A modest increase in 11C-PK11195-Positron emission tomography TSPO binding in depression is not associated with serum C-Reactive protein or body mass index. *Biol. Psychiatry Cogn. Neurosci. Neuroimaging* 6, 716–724. doi: 10.1016/j.bpsc.2020.12.017

Schubert, J., Tonietto, M., Turkheimer, F., Zanotti-Fregonara, P., and Veronese, M. (2021b). Supervised clustering for TSPO PET imaging. *Eur. J. Nucl. Med. Mol. Imaging* 49, 257–268. doi: 10.1007/s00259-021-05309-z

Setiawan, E., Attwells, S., Wilson, A. A., Mizrahi, R., Rusjan, P. M., Miler, L., et al. (2018). Association of translocator protein total distribution volume with duration of untreated major depressive disorder: a cross-sectional study. *Lancet Psychiatry* 5, 339–347. doi: 10.1016/S2215-036630048-30048

Setiawan, E., Wilson, A. A., Mizrahi, R., Rusjan, P. M., Miler, L., Rajkowska, G., et al. (2015). Role of translocator protein density, a marker of neuroinflammation, in the brain during major depressive episodes. *JAMA Psychiatry* 72, 268–275. doi: 10.1001/jamapsychiatry.2014.2427

Snijders, G. J. L. J., Sneeboer, M. A. M., Fernández-Andreu, A., Udine, E., Boks, M. P., Ormel, P. R., et al. (2021). Distinct non-inflammatory signature of microglia in post-mortem brain tissue of patients with major depressive disorder. *Mol. Psychiatry* 26, 3336–3349. doi: 10.1038/s41380-020-00896-z

Su, L., Cai, Y., Xu, Y., Dutt, A., Shi, S., and Bramon, E. (2014). Cerebral metabolism in major depressive disorder: a voxel-based meta-analysis of positron emission tomography studies. *BMC Psychiatry* 14:321. doi: 10.1186/s12888-014-0321-329

Su, L., Faluyi, Y. O., Hong, Y. T., Fryer, T. D., Mak, E., Gabel, S., et al. (2016). Neuroinflammatory and morphological changes in late-life depression: the NIMROD study. *Br. J. Psychiatry* 209, 525–526. doi: 10.1192/bjp.bp.116.190165

The Network, and Pathway Analysis Subgroup of the Psychiatric Genomics Consortium (2015). Psychiatric genome-wide association study analyses implicate neuronal, immune and histone pathways. *Nat. Neurosci.* 18, 199–209. doi: 10.1038/nn.3922

Thompson, P. M., Jahanshad, N., Ching, C. R. K., Salminen, L. E., Thomopoulos, S. I., Bright, J., et al. (2020). ENIGMA and global neuroscience: a decade of large-scale studies of the brain in health and disease across more than 40 countries. *Transl. Psychiatry* 10:100. doi: 10.1038/s41398-020-0705-701

Torres-Platas, S. G., Cruceanu, C., Chen, G. G., Turecki, G., and Mechawar, N. (2014). Evidence for increased microglial priming and macrophage recruitment in the dorsal anterior cingulate white matter of depressed suicides. *Brain Behav. Immun.* 42, 50–59. doi: 10.1016/j.bbi.2014.05.007

Tuisku, J., Plavén-Sigray, P., Gaiser, E. C., Airas, L., Al-Abdulrasul, H., Brück, A., et al. (2019). Effects of age, BMI and sex on the glial cell marker TSPO — a multicentre [11C]PBR28 HRRT PET study. *Eur. J. Nucl. Med. Mol. Imaging* 46, 2329–2338. doi: 10.1007/s00259-019-04403-4407

Turkheimer, F. E., Althubaity, N., Schubert, J., Nettis, M. A., Cousins, O., Dima, D., et al. (2021). Increased serum peripheral C-reactive protein is associated with reduced brain barriers permeability of TSPO radioligands in healthy volunteers and depressed patients: implications for inflammation and depression. *Brain Behav. Immun.* 91, 487–497. doi: 10.1016/j.bbi.2020.10.025

Turkheimer, F. E., Edison, P., Pavese, N., Roncaroli, F., Anderson, A. N., Hammers, A., et al. (2007). Reference and target region modeling of [11C]-(R)-PK11195 brain studies. *J. Nucl. Med.* 48, 158–167.

Viechtbauer, W. (2010). Conducting meta-analyses in R with the metafor package. *JSS J. Statistical Software* 36, 1–48.

Wang, Y. M., and Yang, Z. Y. (2022). Aberrant pattern of cerebral blood flow in patients with major depressive disorder: a meta-analysis of arterial spin labelling studies. *Psychiatry Res. Neuroimaging* 321:111458.

Wimberley, C., Lavisse, S., Hillmer, A., Hinz, R., Turkheimer, F., and Zanotti-Fregonara, P. (2021). Kinetic modeling and parameter estimation of TSPO PET imaging in the human brain. *Eur. J. Nucl. Med. Mol. Imaging* 49, 246–256. doi: 10.1007/s00259-021-05248-5249

Wolf, S. A., Boddeke, H. W. G. M., and Kettenmann, H. (2017). Microglia in physiology and disease. *Annu. Rev. Physiol.* 79, 619–643.

Yaqub, M., Nm Van Berckel, B., Schuitemaker, A., Hinz, R., Turkheimer, F. E., Tomasi, G., et al. (2012). Optimization of supervised cluster analysis for extracting reference tissue input curves in (R)-[11 C]PK11195 brain PET studies. *J. Cereb. Blood Flow Metab.* 32, 1600–1608. doi: 10.1038/jcbfm.2012.59

Zhou, X., Ji, B., Seki, C., Nagai, Y., Minamimoto, T., Fujinaga, M., et al. (2021). PET imaging of colony-stimulating factor 1 receptor: a head-to-head comparison of a novel radioligand, 11C-GW2580, and 11C-CPPC, in mouse models of acute and chronic neuroinflammation and a rhesus monkey. *J. Cereb. Blood Flow Metab.* 41, 2410–2422. doi: 10.1177/0271678X211004146

frontiers | Frontiers in Molecular Neuroscience

TYPE Review
PUBLISHED 11 October 2022
DOI 10.3389/fnmol.2022.1013706

OPEN ACCESS

EDITED BY
Michael P. McDonald,
University of Tennessee Health Science Center (UTHSC), United States

REVIEWED BY
Ruiyi Zhang,
University of Calgary, Canada
Ningbo Xu,
Southern Medical University, China

*CORRESPONDENCE
Li Wang
wangli120@swmu.edu.cn
Nathupakorn Dechsupa
nathupakorn.d@cmu.ac.th

†These authors have contributed equally to this work and share first authorship

SPECIALTY SECTION
This article was submitted to Brain Disease Mechanisms, a section of the journal Frontiers in Molecular Neuroscience

RECEIVED 07 August 2022
ACCEPTED 22 September 2022
PUBLISHED 11 October 2022

CITATION
Yang G, Fan X, Mazhar M, Guo W, Zou Y, Dechsupa N and Wang L (2022) Neuroinflammation of microglia polarization in intracerebral hemorrhage and its potential targets for intervention.
Front. Mol. Neurosci. 15:1013706.
doi: 10.3389/fnmol.2022.1013706

Neuroinflammation of microglia polarization in intracerebral hemorrhage and its potential targets for intervention

Guoqiang Yang[1,2,3†], Xuehui Fan[4,5†], Maryam Mazhar[6,7], Wubin Guo[8], Yuanxia Zou[1,2], Nathupakorn Dechsupa[2]* and Li Wang[1,7]*

[1]Research Center for Integrated Chinese and Western Medicine, The Affiliated Traditional Chinese Medicine Hospital of Southwest Medical University, Luzhou, China, [2]Molecular Imaging and Therapy Research Unit, Department of Radiologic Technology, Faculty of Associated Medical Sciences, Chiang Mai University, Chiang Mai, Thailand, [3]Acupuncture and Rehabilitation Department, The Affiliated Traditional Chinese Medicine Hospital of Southwest Medical University, Luzhou, China, [4]Key Laboratory of Medical Electrophysiology, Ministry of Education and Medical Electrophysiological Key Laboratory of Sichuan Province, Collaborative Innovation Center for Prevention of Cardiovascular Diseases, Institute of Cardiovascular Research, Southwest Medical University, Luzhou, China, [5]First Department of Medicine, Medical Faculty Mannheim, University Medical Centre Mannheim (UMM), University of Heidelberg, Mannheim, Germany, [6]National Traditional Chinese Medicine Clinical Research Base and Drug Research Center of the Affiliated Traditional Chinese Medicine Hospital of Southwest Medical University, Luzhou, China, [7]Institute of Integrated Chinese and Western Medicine, Southwest Medical University, Luzhou, China, [8]Department of General Surgery, The Affiliated Traditional Chinese Medicine Hospital of Southwest Medical University, Luzhou, China

Microglia are the resident immune cells of the central nervous system (CNS) and play a key role in neurological diseases, including intracerebral hemorrhage (ICH). Microglia are activated to acquire either pro-inflammatory or anti-inflammatory phenotypes. After the onset of ICH, pro-inflammatory mediators produced by microglia at the early stages serve as a crucial character in neuroinflammation. Conversely, switching the microglial shift to an anti-inflammatory phenotype could alleviate inflammatory response and incite recovery. This review will elucidate the dynamic profiles of microglia phenotypes and their available shift following ICH. This study can facilitate an understanding of the self-regulatory functions of the immune system involving the shift of microglia phenotypes in ICH. Moreover, suggestions for future preclinical and clinical research and potential intervention strategies are discussed.

KEYWORDS

intracerebral hemorrhage, microglia, phenotype shift, neuroimmunology, neuroinflammation

Introduction

Intracerebral hemorrhage (ICH) is a destructive disease because of its increased mortality and morbidity rates, accounting for nearly 10%–20% of stroke cases worldwide (Dasari et al., 2021; Liu et al., 2022; Yang et al., 2022). After ICH, vessel rupture of brain parenchyma contributes to the aggregation of red blood cells (RBCs) and the formation of hematoma to oppress brain tissue structure forming primary brain injury (PBI). Erythrocyte hemolysis in hematoma results in secondary brain injury (SBI) and non-reversing neurological deficits duet o the toxic hemolytic products (Ziai, 2013). Surgical treatment is not conducive to a hematoma in the majority of hemorrhage strokes due to doubtful clinical effectiveness and side effects of surgery (Hemphill et al., 2015). Evidence suggests that inflammatory responses firmly participate in and contribute to the SBI pathophysiological processes following ICH (Chen S. et al., 2015). During this pathological process, the CNS resident microglia and monocytes derived macrophages infiltrate from the circulation at the hemorrhagic site. These microglia/macrophages act as primary modulator for the hematoma resolution and alleviation of neuroinflammation in SBI (Bai et al., 2020; Liu et al., 2022).

Microglia, as the primary immune cells, account for 5% to 10% of brain cells in the central nervous system (CNS) and are referred to as the brain's macrophage (Eldahshan et al., 2019; Bian et al., 2020). Following physiological conditions, microglia interact with other cells, including neurons, astrocytes, and oligodendrocytes, displaying their function in the brain following ICH (Prinz et al., 2019). It is essential in sustaining brain homeostasis. When different neuropathologic changes disrupt normal function in the brain, activated microglia exert their regulatory effects (Wan et al., 2016). The highly diverse property of microglia and their phenotypes depend on the kinds of stressors or neuropathology (Wolf et al., 2017). Specifically, microglia polarization produces pro-inflammatory (IL-1β, IL-6, TNF-α, CXCL8, CCL2, and CCL5) or anti-inflammatory (IL-4, IL-10, IL-13, IL-1Ra, and TGFβ) mediators during the different pathological phases, participating in ICH progression (Friedman et al., 2018; Bai et al., 2020).

Pathological analyses following ICH have uncovered that microglia mediated neuroinflammation can be recognized as a major contributor to inflammatory injury following ICH (Yang et al., 2014a; Zhang Z. et al., 2017). The severe microglial neuroinflammation caused by the hematoma and hemolysis after ICH contributes to brain injury (Vinukonda et al., 2019; Wang et al., 2019a). Chang et al. (2017) have proven that microglia quickly responded to hemorrhagic damage after 1–1.5 h of ICH onset and showed a microglial protective phenotype. In this study, IL-10 mediated microglia phagocytosis and hematoma resolution (Chang et al., 2017).

Different microglial phenotypes play a primary and complex function in the SBI-induced inflammatory damage and brain rehabilitation following ICH. Therefore, the neuroprotective effect of microglia can be regarded as a hopeful target in the inflammatory response following ICH therapy. Jing et al. (2019) have reported that after blocking the erythrocyte CD47, activated microglia can be enhanced to phagocytose the hematoma and reduce neurological deficits, brain edema, and neuronal reduction (Chang et al., 2018). Microglial depletion contributes to intense brain tissue damage, including brain swelling, neuronal loss, and neurological defects following ICH (Jin et al., 2017; Sekerdag et al., 2018; Yang X. et al., 2018). The reactive microglia show a biphasic influence on responding to inflammation processes following ICH, which acts as a double-edged sword displaying offensive and defensive effects in brain injury. This study focuses on current empirical investigations on reactive microglia in the ICH-induced SBI pathological process to elucidate how the pivotal elements affect this process, providing an optimistic viewpoint for improving novel medicinal strategies.

Microglial function following ICH

ICH-induced hematoma is a significant factor resulting in brain damage following ICH. The compression and dissection of mechanical impairment obstruct adjacent brain parenchyma structures. Simultaneously, within hours to days, extravasated erythrocytes release blood products with neurotoxicity, including cytotoxic hemoglobin, heme, and iron in the hematoma, which initiate SBI inducing sustained cerebral edema and brain tissue damage following ICH (Zhao et al., 2009; Wang G. et al., 2018). This process can be regulated through the activation of peroxisome proliferator-activated receptor γ (PPAR-γ) and modulation of the CCR4/ERK/Nrf2 signaling pathway to promote phagocytosis and shift microglia for conferring immune balance (Deng et al., 2020; Tschoe et al., 2020; Zhuang et al., 2021).

The collapse of the blood-brain barrier (BBB) and its resulting brain swelling is a notable life-threatening event in the pathophysiology of hemorrhagic stroke (Su et al., 2017; Fang et al., 2020). Ample evidence has shown that it is essential that microglial activation displays a significant role in SBI after ICH (Carson et al., 2006). It has been reported that M1 polarization of microglia provokes the production of pro-inflammatory factors, such as TNF-α, and IL-6, which aggravate the inflammatory response (Wang, 2010; Zhou et al., 2014). Chen A. Q. et al. (2019) have shown that M1-type microglia-induced TNF-α mediates endothelial necroptosis leading to BBB disruption. After being given the anti-TNF-α treatment, pathologic changes, including endothelial necroptosis and BBB destruction, and stroke outcomes were significantly alleviated following ischemic stroke (Chen A. Q. et al., 2019). Besides, some

medicines displaying neuroprotective function attenuated the LPS-induced NO release, TNF-α secretion, and NFκB expression of microglia to mediate BBB protection and neural repairation by promoting the production of anti-inflammatory cytokines (Zlokovic, 2008; Liu et al., 2017; Chen J. et al., 2019). Similarly, IL-4 and IL-10 induced an alternative microglia phenotype with anti-inflammatory function, which can be recognized as therapeutic targets to modulate the BBB physiology in ICH (Ronaldson and Davis, 2020).

Microglia phenotypes and their polarization after ICH

Previously, microglia polarization associated with M1 and M2 phenotypes was widely used in previous research work. Due to the development of omics technology in experiments, recently, a novel class of microglia polarization bridges the standard M1/M2 contradiction, resulting in an intense controversy to further study microglia polarization (Ransohoff, 2016).

First, Chiu et al. (2013) utilized flow cytometry and deep RNA sequencing to indicate that microglia isolated from the SOD1 (G93A) mutant mouse model of amyotrophic lateral sclerosis (ALS) differed from SOD1 (WT), LPS-induced microglia, and M1/M2 macrophages. This study freshly provided a new definition for ALS-specific microglia' functional phenotypes in isolated spinal cord microglia of ALS mice model (Chiu et al., 2013). Besides, single-cell RNA-sequence (scRNA-seq) analyses have suggested assembled expression of M1 and M2 markers and complex microglia-state changes in the total mouse lifespan and the damaged brain (Ajami et al., 2018; Hammond et al., 2019; Masuda et al., 2019). Furthermore, accurate classification of different microglia subpopulations is founded upon species-related differences and different pathological environments. Different subtypes of microglia are associated with a core pattern of activation, in which the pro-inflammatory-activation state shifts toward an anti-inflammatory situation in maintaining tissue homeostasis or resulting in CNS pathology (Voet et al., 2019; Lassmann, 2020). However, due to the complicated existence of microglial phenotypes found by novel technologies in diseases, the established meaningful program of microglial polarization of M1 and M2 phenotypes hindered research progress and should need to be debated (Ransohoff, 2016). Overall, an elusive definition of microglial polarization exists, and it is oversimple to describe M1 or M2 phenotypes for the complex biology of microglia.

Recently, a study performed by Keren-Shaul et al. (2017) specified a subtype of microglia named disease-associated microglia (DAM), which develops in two steps in Alzheimer's disease (AD)-transgenic (Tg-AD) and triggering receptor expressed on myeloid cells 2 $(TREM2)^{-/-}$ Tg-AD mouse brains by transcriptional single-cell analysis (Da Mesquita and Kipnis, 2017; Ozaki et al., 2022). Microglial activation to DAM is instigated in an independent program away from TREM2, followed by activation in a TREM2-dependent manner. Such a special microglial type has the prospect of confining neurodegeneration, which may have meaningful implications for future therapy of AD and other neurodegenerative illnesses (Keren-Shaul et al., 2017; Deczkowska et al., 2018). Subsequently, genome-wide transcriptomic analyses (GWTAs) indicated DAM's existence under various pathological disorders, including aging and ALS pathology (Keren-Shaul et al., 2017). Although the microglia DAM and M1 phenotype gene profiles are partially overlaid, the apparent differences in their molecular signatures exist (Garcia-Revilla et al., 2019). Interestingly, a transcriptomic framework of microglial activation uncovered that DAM demonstrates double anti-inflammatory and pro-inflammatory sub-profiles in (AD and aging models; Rangaraju et al., 2018; Gao et al., 2019). The progressive transition from homeostatic microglia to reactive DAM relies on TREM2, which is mainly located on the microglia surface in brain tissue (Arcuri et al., 2017; Mecca et al., 2018; Xu et al., 2022). The activated TREM2 alleviated microglia neuroinflammation, neurological deficits, and neuronal loss by activating the PI3K/Akt signaling pathway in perihematomal areas following ICH (Chen et al., 2020).

Moreover, in 2019, Gao et al. (2019) reported that the regulators, including CEBPα, IRF1, and LXRβ, modulate pro- and anti-inflammatory DAM genes *via* Erk signaling. However, some researchers reported that DAM represents a switch depending on TREM2, a risk gene, and such a switch substantially alters microglial function (Brown and St George-Hyslop, 2017). Therefore, it is pretty clear that microglia is exquisitely sensitive to brain tissue pathological changes.

Multiple investigations have explored microglial spatiotemporal fixed subclasses during evolution and illness, determining the precise molecular hallmarks and various cellular kinetics utilizing single-cell analyses (Prinz et al., 2017; Masuda et al., 2019). Olah et al. (2020) have suggested the existence of four microglial subclasses and clarified the importance of these subclasses according to the scRNA-seq from the human cerebral cortex samples associated with AD. Lately, a study by Ochocka and his colleagues has demonstrated microglia cellular and functional heterogeneity utilizing scRNA-seq and flow cytometry. Their investigation obtained numerous microglial groups and gene expression profiles underlying a distinct group image with different roles. Reactive microglia displayed the distinct spatial distribution in naïve and GL261 glioma-bearing mice through performing the scRNA-seq of $CD11b^{+}$ myeloid cells (Ochocka et al., 2021). Furthermore, the technologies of transcriptomes and epigenetic landscapes have been utilized by Gosselin et al. (2017) to examine separated human microglia derived from surgically resected brain tissue, uncovering an environment-

dependent transcriptional network that can sufficiently specify microglia-specific schedules of gene expression. These results can identify significant microglia-subclasses associated with neurodegenerative diseases and behavioral disorders and can be used to understand microglia's roles in human brain diseases (Gosselin et al., 2017).

Diverse pathologic occurrences or changes in the brain activate microglia, whose intricate functions facilitate the presence of individual pro- and anti-inflammatory effects in ICH. The meaning of defining microglial subclasses through single-cell analysis is to confirm precise microglia function and identify microglia-subclasses molecules mediating astrocyte-microglial communication. In addition, the importance of clustering negotiate its potentially coordinated functions with astrocytes and discover new ways to address the complexity of biology in inflammatory conditions and different pathologies (Vainchtein and Molofsky, 2020). During the ICH progress, microglial activation and polarization modulators have clinical and translational implications, including critical signaling pathways, transcription factors (TFs), and particularly microglia M1- and M2-subclasses markers, providing evidence for coordinating microglial function to alleviate ICH-induced brain damage (Lan et al., 2017). The pro-inflammatory microglia-induced damage-enhancing mediators, such as inflammatory cytokines, chemokines, matrix metalloproteinases, and reactive oxygen species, overwhelmed the anti-inflammatory microglia with potential reparative roles after the onset of ICH (Bai et al., 2020). Therefore, confirming the modulators and these influencing factors makes it attractive to induce the microglia polarization to a neuroprotective subclass, which provides novel insight into alleviating the microglia pathologic changes after ICH. According to the above analyses of microglia polarization in ICH and studies about surface markers of microglial subtypes (Klebe et al., 2015; Keren-Shaul et al., 2017; Rangaraju et al., 2018; Bai et al., 2020), it is critical to shift the microglia pro-inflammatory to the anti-inflammatory subclass to improve the outcomes following SBI (**Figure 1**).

Potential therapeutic targets and strategies of microglia-induced neuroinflammation after ICH

Many studies have emphasized the autogenous regulation of microglia during ICH progress. Wu et al. (2017) have shown that the expression of soluble epoxide hydrolase increased in microglia following ICH, resulting in neuroinflammatory responses, and inhibiting its expression can suppress microglia-mediated neuroinflammation. The deficiency of TWIK-related K^+ channel 1 (TREK-1) can induce increased recruitment of microglia and neutrophils and the production of pro-inflammatory factors following ICH-induced SBI; the TREK-1 can be harnessed into a promising therapeutical target in BBB dysfunction and microglia neuroinflammation for the treatment of ICH (Fang et al., 2019). Besides, the integrin Mac-1 expressed by microglia acting together with the endocytic receptor LRP1 in the neurovascular unit promoted thrombolytic tissue plasminogen activator (tPA)-induced platelet-derived growth factor-cc (PDGF-cc) activation, which increased the permeability of BBB following ischemic stroke (Su et al., 2017).

On the contrary, microglia are implicated in anti-inflammatory and phagocytic effects to improve neurologic deficits following ICH. The relationship between regulatory T lymphocytes (Tregs) and microglia neuroinflammatory reaction has been verified. A study by Zhou et al. (2017) demonstrated that Tregs alleviated ICH-mediated neuroinflammation because of the shift of the M2 anti-inflammatory from the M1 pro-inflammatory subclass *via* the regulation of the IL-10/GSK3β/PTEN axis after ICH (Wang et al., 2015; Taylor et al., 2017).

Regulatory mechanisms in microglia-induced neuroinflammation in ICH

After ICH, the functions of anti-inflammatory microglia are performed through diverse signal axes that constitute a complicated network implicated in numerous biological procedures. Investigating the related biological signaling pathways and their molecular foundation is beneficial to illustrating attractive methods to moderate targets, thus improving the neuropathological deficits in ICH-induced brain damage.

Some studies have verified that adenosine monophosphate-activated protein kinase (AMPK) regulated the balance for the switch between a pro- and an anti-inflammatory subclass, which serves as a primary sensor of brain injuries and diseases, and is considered a candidate molecule (Ohnishi et al., 2007; Saito et al., 2019). Adiponectin receptor 1 (AdipoR1) is always expressed by microglia, and the expression level of endogenous C1q/TNF-related protein 9 (CTRP9), activating AdipoR1 to regulate the AMPK signaling pathway, plays an increasing trend during the first 24 h after ICH (Zhao et al., 2018). Administration of CTRP9 treatment improved AdipoR1 and p-AMPK protein expression levels and decreased the protein expression levels of inflammatory cytokines and phosphorylated NFκB (P-NFκB), attenuating neuroinflammation *via* AdipoR1/AMPK/NFκB signaling pathway (Zhao et al., 2018). Activated AdipoR1 by CTRP9 treatment attenuated neuropathological deficits and improved BBB dysfunction by activating the APPL1/AMPK/Nrf2 signal axis in a collagenase-induced ICH mouse model (Xu et al., 2018; Zhao et al., 2021). This evidence suggested that CTRP9 could be recognized as an encouraging therapy to ameliorate BBB dysfunction in ICH

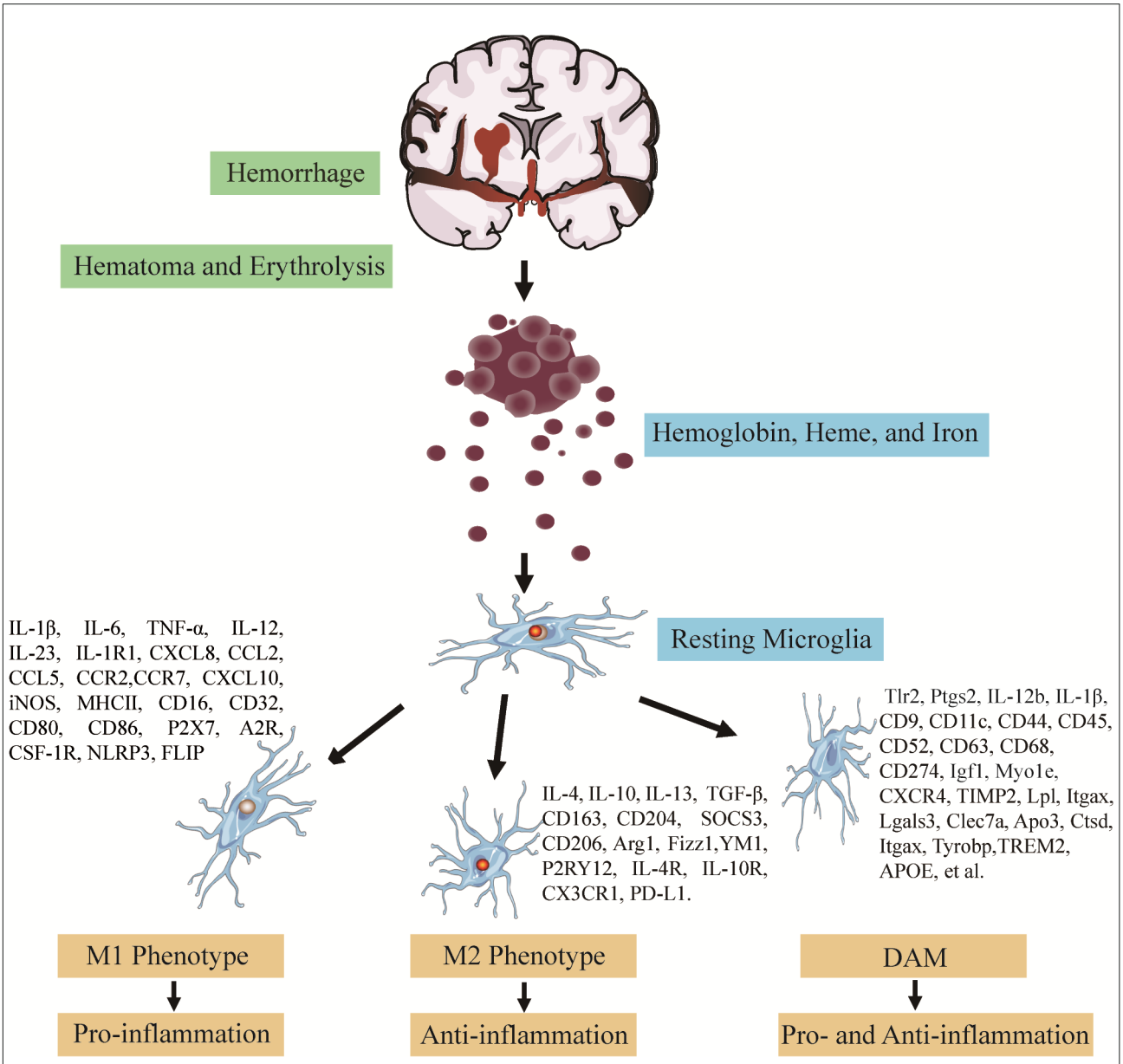

FIGURE 1
Polarization of activated microglia following intracerebral hemorrhage (ICH). The polarization of activated microglia in response to stimulation with erythrocyte lysates after ICH can be broadly classified into three categories. Each category has its related cytokines, chemokines, and surface markers: (1) pro-inflammatory microglia elevate the pro-inflammatory factors and destruc tive effects on the brain; (2) anti-inflammatory microglia mainly exert neuroprotective effects; (3) disease-associated microglia (DAM). Recent, an increasing number of studies by single-cell RNA-sequence and Various other omics methods have revealed that microglia can also be polarized into neuroprotective and neurodestructive phenotypes, remaining to be further investigated.

patients. Likewise, the activation of melanocortin receptor 4 (MC4R) improves neuropathological function *via* the AMPK signal, and intervening MC4R can be effective in animal experiments and utilized as a potential therapeutic approach for ICH management (Chen et al., 2018).

As mentioned above, Treg cells restrain microglia-mediated neuroinflammation from improving neurological function by activating NFκB through the JNK/ERK pathway (Yang et al., 2014b; Lan et al., 2017; Zhou et al., 2017). The treatment of hyperbaric oxygen preconditioning (HBOP) has attenuated the production of pro-inflammatory cytokine levels and p-JNK, suggesting potential relevance between JNK phosphorylation and downregulation of immunoactivity and protein levels of M1 markers (Yang L. et al., 2015; Wang et al., 2019b). As many limitations, including hesitations concerning effectiveness, surgical damages, complications, and drug side effects, exist

in current clinical practice, there are few standardized clinical interventions for ICH treatment. Therefore, hyperbaric oxygen therapy provides a potential alternative medicine to treat ICH, and the mechanisms of HBOP for intervening in ICH need additional investigation and confirmation.

Toll-like receptor 4 (TLR4) confer an essential function in the innate immune response, known as a pattern recognition receptor (Fang et al., 2013). The deficiency of TLR4 attenuated perihematomal inflammatory response associated with a decrease in the recruitment of pro-inflammatory microglia in a striatal blood injection-induced ICH mice model (Sansing et al., 2011; Wang et al., 2013). Moreover, TLR4 also inhibits the microglial phagocytic capacity for RBCs, contributing to the deceleration of CD36-mediated hematoma absorption and severe neurological deficits in ICH (Fang et al., 2014; Li Q. et al., 2021). Autophagy mediated by TLR4 activated microglia-induced neuroinflammation in mice with ICH (Yang Z. et al., 2015). The function of TLR4 has been elaborated in detail following ICH in many studies. Therefore, therapeutic strategies targeting TLR4 are relatively promising interventions and may represent future candidates for ICH therapy.

DNA damage motivates the body's innate immune response. As a DNA sensor, cGMP-AMP synthase (cGAS) can detect the disease-damaged DNA and triggers its downstream stimulator of interferon gene (STING), subsequently phosphorylating interferon regulatory factor 3 (IRF3) to upregulate the production of type I interferon (IFN; Lei et al., 2022). cGAS is a critical regulator of inflammatory and autophagy responses, and Sharma et al. (2020) found that cGAS is upregulated to mediate inflammation through increasing inflammatory genes (Ccl5 and Cxcl10) and autophagy responses *via* activating the two major autophagy initiators, LC3A and LC3B, in striatal damage of brain. It has been reported that tPA administration augments neutrophil extracellular traps (NETs) markers in the ischemic mice brain cortex and their plasma. DNase I and deficiency of peptidyl arginine deiminase 4 (PAD4), which can inhibit NETs, reversed tPA-mediated upregulation of cGAS.However, cGAMP application suppressed DNase I-mediated antihemorrhagic effects by downregulating the STING and INF in tPA-treated mice following ischemic stroke (Wang et al., 2021). Moreover, Jiang et al. (2021) have elucidated that cGAS knockdown improved M2 phenotype polarization of microglia to attenuate microglial inflammatory response by hindering the cGAS-STING signal axis in mice with stroke, highlighting that such signal axis can be used as a potential therapeutic target. Subsequently, the experiment performed by Shi et al. (2022) also demonstrated that inhibiting the cGAS-STING pathway through a cGAS inhibitor integrated versatile immunosuppressive nanoparticle in microglia contributed to improving an anti-inflammatory phenotype polarization in rats following stroke.

It is well known that c-type lectin-like receptors (CLRs) are mainly expressed in myeloid cells as a family of transmembrane pattern recognition receptors (Drouin et al., 2020). CLRs' dysregulation results in the production of inflammatory mediators and the development of inflammatory diseases following excessive injury. Microglial macrophage-inducible C-type lectin (Mincle), a critical member in CLRs, widely expressed on antigen-presenting cells (APCs), including macrophages, binds nuclear spliceosome-Associated Protein 130 (SAP130) from necrotic cells to enhance neuroinflammation (Del Fresno et al., 2020; He et al., 2022). After the injury, Mincle and its activated downstream spleen tyrosine kinase (Syk) boost inflammatory gene expression levels in alcohol-induced liver injury mice (Kim et al., 2018). Besides, activated Mincle/Syk signal worsened intestinal mucosal inflammation by enhancing macrophage pyroptosis, and inhibition of the Mincle/Syk signaling pathway displayed a potential therapeutic function to attenuate inflammatory response in Crohn's Disease (Gong et al., 2020). Furthermore, many investigations have suggested that inhibiting the Mincle/Syk signal axis exerts a neuroprotective role associated with various brain diseases in preclinical research. Different intervention treatments, including Syk inhibitor BAY61-3606, acupuncture, and MSCs engraftment, have been used to attenuate microglia-mediated neuroinflammation by impeding Mincle/Syk signaling pathway in microglia following hemorrhage stroke, ischemic stroke, and traumatic brain injury (TBI; He et al., 2015, 2022; de Rivero Vaccari et al., 2015; Liu X. Y. et al., 2018; Li Y. et al., 2021). According to the above analysis, the Mincle/Syk signaling pathway can be utilized as a promising therapeutical target in ICH.

Although much pre-clinical research has proved the mechanisms against microglial neuroinflammation, there is still a need for further investigation of promising interventions to promote its use in clinical research (**Figure 2**).

Therapeutic targets and strategies for microglia-induced neuroinflammation in ICH

Increasing genetic and epigenetic evidence has demonstrated that miRNAs confer crucial functions in regulating gene expression and microglia polarization after ICH (Yang Z. et al., 2018). Yang Z. et al. (2018) found that let-7a regulates microglia M2 polarization at 3 days after ICH in mice by intervening in a target gene named Casein Kinase 2 Interacting Protein 1 (CKIP-1). In this study, overexpressing let-7a lessened the protein expression level of CKIP-1, enhancing microglia M2 polarization (IL-10 and Arg-1) and alleviating the inflammatory response, while inhibiting let-7a augmented the protein expression level of CKIP-1, contributing to microglia M1 polarization (IL-1β and TNF-α). Overexpression of miRNA-7 can restrain TLR4 protein expression level from alleviating the microglia inflammatory response in ICH rats and

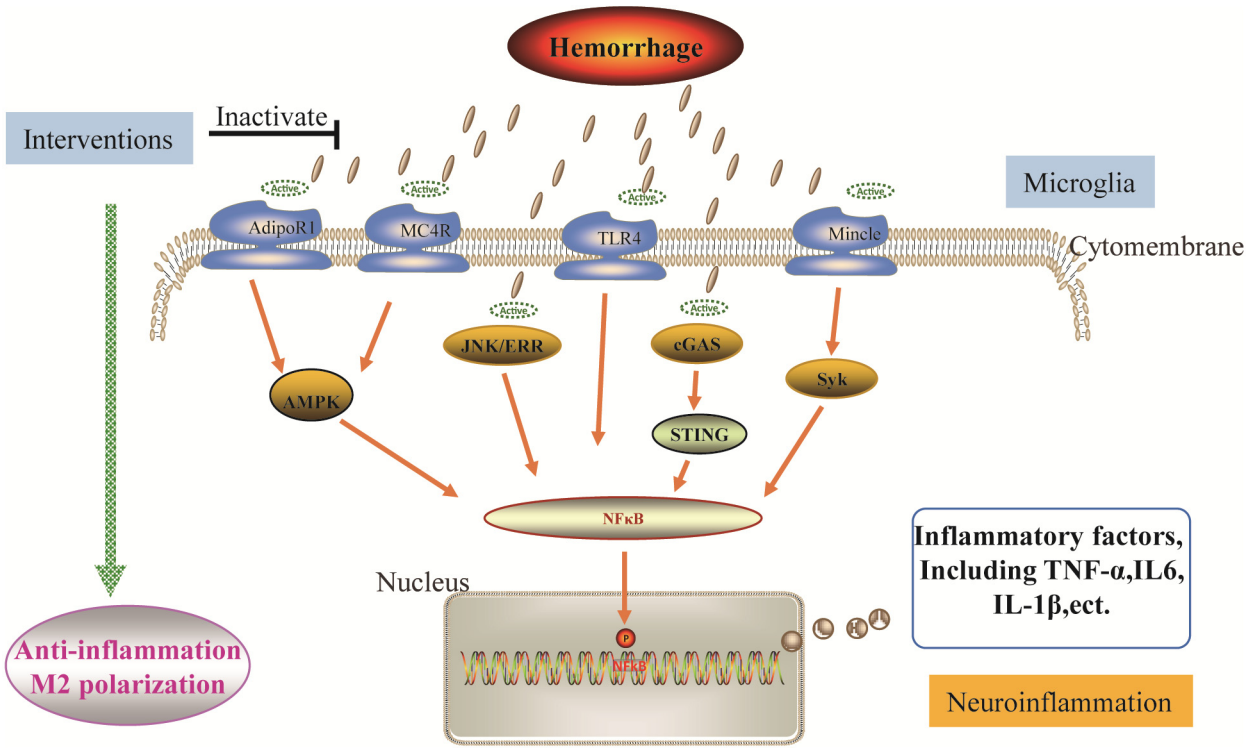

FIGURE 2
Potential interventions for the neuroinflammation following ICH. Interventions induce the polarization of pro-inflammatory microglia towards the anti inflammatory phenotype through different mechanisms, exerting beneficial effects. The mechanisms associated with ICH include the AdipoR1/MC4R-AMPK pathway, JNK-ERR pathway, TLR4 pathway, cGAS-STING pathway, and Mincle-Syk pathway, activation of which enhances the microglial neuroinflammation. After the corresponding intervention inhibits these pathways, the Ml phenotype shifts to the M2 phenotype of microglia.

a lipoprotein-induced microglial inflammation model (Zhang et al., 2018). Further studies have suggested that targeting TLR4 exerted a neuroprotective role in resisting ICH-induced brain injury by impeding the Prx1/TLR4/NFκB signaling axis at 3 days after ICH, providing a promising anti-neuroinflammatory approach for hemorrhagic stroke (Liu et al., 2016). Meanwhile, studies have reported that miRNA-182-5p and miRNA-27a modulate the inflammatory response by targeting TLR4 in a middle cerebral artery occlusion (MCAO) rat model and lipopolysaccharide (LPS)-stimulated microglia respectively (Lv et al., 2017; Wang J. et al., 2018). In their studies, overexpression of miRNA-182-5p and miRNA-27a downregulated the protein expression level of TLR4 resulting in the increase of released inflammatory factors.

Recent evidence has clarified that blockage of miRNA-222 attenuated inflammation in erythrocyte lysate-induced microglia and improved brain water content (BWC), neuropathologic deficits, and inflammatory response in ICH mice. In this study, integrin subunit β8 (ITGB8) was specified as a direct target modulated in the negative by miRNA-222, alleviating inflammation and apoptosis in microglia (Bai and Niu, 2020). Previously, the choline of inflammatory response was inhibited by miRNA-132 by intervening in acetylcholinesterase (AChE). A study by Zhang Y. et al. (2017) found that overexpressing miRNA-132 with an injection of lentiviruses encoding miR-132 into the right caudate nuclei before 14 days inhibited the activation of pro-inflammatory microglia, improved BBB dysfunction, and decreased neuronal loss at day 3 in autologous blood-induced ICH. Additionally, miRNAs, the pivotal mediators in autophagic activation-induced inflammation of microglia, can posttranscriptionally and negatively modulate gene expression and function (Wang et al., 2017). Wang et al. (2017) and Yu et al. (2017a) found that miRNA-144 can enhance hemoglobin-mediated activation of the microglial autophagic inflammatory response by directly targeting mTOR' 3' untranslated regions (UTRs) to downregulate the gene and protein expression level of mTOR in a hemoglobin-mediated primary hippocampal microglial cell inflammatory model or autologous blood-induced ICH mice after 24 h. Similarly, miR-124 improved microglia M2 phenotype polarization to alleviate inflammatory injury by targeting the 3'-UTR of C/EBP-α *in vitro* and *in vivo* experiments (Yu et al., 2017b). The administration of miR-124 mimics significantly alleviated BWC, neurological deficits,

C/EBP-α gene, and protein expression levels compared with those in the injection of miR-124 inhibitor in mice with ICH at 3 days. Furthermore, a similar negative regulation of miR-124 to C/EBP-α in gene and protein expression levels was also observed in transduced microglia with miR-124 mimics or miR-124 inhibitors, which were stimulated with erythrocyte lysates.

Up to now, autophagy is a dualistic function, and it is difficult to assess whether it has harmful or beneficial effects after ICH. Excessive autophagy has been reported to worsen endoplasmic reticulum stress (ERS)-mediated brain impairment at 6 h following ICH. However, autophagy strengthened the protective function of ERS by removing the cell debris at 7 days following ICH-induced SBI in rats (Duan et al., 2017). Tan et al. (2020) have elucidated that enhancing autophagy attenuated oxidative stress damage after ICH *via* increasing the expression levels of antioxidant proteins; on the contrary, the autophagy inhibitor reversed the neuroprotection after ICH. Recently, some studies showed that autophagy positively modulates inflammation in ICH (Shi et al., 2018; Xiao et al., 2020).

The interleukins (ILs) levels regarding the ICH advancement are modulated through the intervention of microglial functions. Xu et al. (2020) have found that the treatment of intranasal delivery of IL-4 nanoparticles activating the IL-4/STAT6 axis improved extended functional recuperation and hematoma resolution in collagenase- and blood-induced ICH mice models. On the contrary, IL-15, as a pro-inflammatory cytokine, coordinates the homeostasis and microglia immunoreactive intensity after CNS inflammatory occurrences, and upregulation of the expression level of IL-15 in astrocytes exacerbates brain edema, neurological deficits, and microglia inflammatory factors' expression by mediating the crosstalk between astrocytes and microglia in patients and mice with ICH (Shi et al., 2020). Besides, Yu et al. (2016) have found that an IL-17A-neutralizing antibody in opposition to IL-17A can attenuate microglial activation and block ICH-induced cytokine expression levels, including TNF-α, IL-1β, and IL-6. The study by Shi et al. (2018) further illustrated that microglial autophagy and neuroinflammation could be boosted by IL-17A; utilization of an IL-17A-neutralizing antibody remarkably diminished brain edema and enhanced neurological deficits in mice with ICH; suppressing ATG5 and ATG7, the essential autophagy genes of autophagy, decreased microglial autophagy and inflammation (Yuan et al., 2017). Another study also found that intraventricular injection of IL-33 ameliorated neuronal and white matter damage-induced neurological dysfunction following ICH by promoting the microglia M2 polarization (Chen Z. et al., 2019).

Considerable evidence suggests that NFκB translocates to the nucleus after ICH, which produced pro-inflammatory factors, including TNF-α and IL-6, which respond to the series of pathological changes. It indicates that inhibiting the NFκB signaling pathway through different interventions, such as miRNAs, GATA-binding protein 4, and some Chinese medicines, provides a more available anti-neuroinflammatory strategy and therapy for ICH treatment (Dong et al., 2011; Hu et al., 2011; Liu et al., 2016; Shang et al., 2019; Xu et al., 2019). Therefore, regulation of NFκB activity confers hopeful clinical usefulness in ICH.

Many studies have proved that the inhibition of glycogen synthase kinase-3β (GSK-3β) exerts a neuroprotective function in animal experiments after ICH (Zhao et al., 2017, 2019; Zheng et al., 2017). The inhibition of GSK-3β significantly improved the hematoma resolution and cognitive deficits through the enhancement of microglia phagocytosis and differentiation of M2-phenotype microglia in rats with ICH (Liu Z. et al., 2018; Li R. et al., 2019). The study by Zhao et al. (2019) demonstrated that 6-bromoindirubin-3'-oxime (BIO), utilized as a typical inhibitor of GSK-3β blocking GSK-3βTyr216 phosphorylation, exerted a protective effect against microglia activation-induced neuroinflammation by increasing the number of anti-inflammatory microglia. Besides, it has been shown that LiCl treatment downregulated GSK-3β to decrease the death of mature oligodendrocytes (OLGs) and enhance the expression of brain-derived neurotrophic factor (BDNF; Li et al., 2020).

It has been shown that activation of PPAR-γ by rosiglitazone protected against BBB damage and ameliorated hemorrhage transformation maybe favor microglial polarization toward anti-inflammatory phenotype (Luo et al., 2006; Li Y. et al., 2019). Phagocytosis is necessary to improve the hematoma resolution, which attenuates hemorrhage-induced toxic effects on surrounding brain parenchyma and may be essential for healing following ICH. Zhao et al. (2007) found that PPAR-γ activators remarkably improved PPAR-γ-regulated gene expression, including CD36 and catalase, whereas diminishing pro-inflammatory gene expression, including TNF-α, IL-1β, MMP-9, and iNOS, and neuronal impairment by activating phagocytosis of microglia. Conversely, such phagocytosis function was particularly impeded through PPAR-γ gene knockdown or anti-CD36 antibody following ICH (Zhao et al., 2007). Besides, PPAR-γ activation is also essential for improving the phagocytic capability of the microglia anti-inflammatory phenotype by CD36 (Zhao et al., 2009). Similarly, an exogenous PPAR-γ activator named 15 (S)-hydroxyeicosatetraenoic acid facilitated functional healing and neuroprotection after ICH (Xu et al., 2017). Founded on a thorough fundamental investigation, PPAR-γ activators have been broadly utilized in clinical therapy. Activated PPAR-γ by simvastatin, improving microglia-mediated erythrocyte phagocytosis, and displaying neuroprotective function, has been verified in ICH patients (Chen et al., 2017; Wang Y. et al., 2018).

Matrix metalloproteinases (MMPs) upregulated following ICH symbolize a universal superfamily of structurally associated

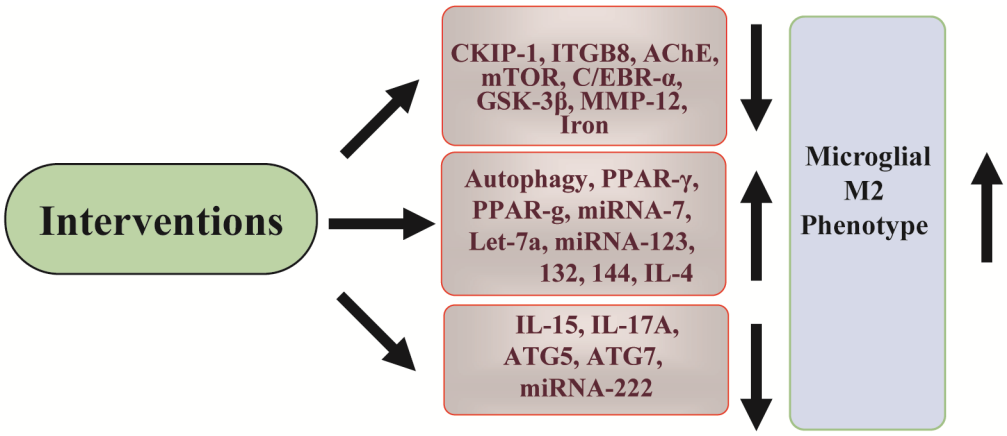

FIGURE 3
Summary of targets for ICH microglial polarization. Different available interventions can be used to inhibit microglial neuroinflammation. The targets cover signaling pathway proteins, single proteins, genes, and miRNAs. Through modulating these targets, the M1 phenotype of microglia can be switched to the M2 phenotype.

zinc-dependent endopeptidases and can lessen the extracellular matrix (EM). Activated microglia are involved in MMPs' synthesis and secretion (Lattanzi et al., 2020). The influence of MMPs on EM collapse initiated through inflammation is a basis of stroke, which has been reported in many studies (Florczak-Rzepka et al., 2012). Wells et al. (2005) studied the function of MMPs in mice with ICH and found that MMP-12 levels were the most elevated. The following experiments showed that MMP-12 null mice demonstrated substantial neurological recuperation of forelimb and decreased reliance on the ipsilateral forelimb relative to WT mice, and more Iba1 immunostaining positive cells conferred with macrophage morphology were conscripted to the injured site in WT mice. This evidence suggests that MMP-12 is harmful and results in the development of SBI following ICH (Wells et al., 2005). Subsequent studies found that MMP-12 expression in the peri-hematoma decreased when given stem cell therapy and minocycline after ICH. Simultaneously, microglia infiltration-induced inflammatory response decreased (Wasserman and Schlichter, 2007; Liang et al., 2014). Therefore, MMP-induced microglial activation has evolved an underlying intervening target for ICH. Minocycline induces activated M1 microglia into the M2 microglia phenotype (Miao et al., 2018). However, Wasserman et al. (2007) found that although minocycline therapy virtually ameliorates the increase of MMP-12 and TNF-α early, its effectiveness is yielded at 1 week. These results suggested that we should be cautious in inferring ICH from the encouraging effects of minocycline therapy in other brain injury decreases (Wasserman et al., 2007). Other studies also found that stem cell therapy significantly reduced microglial infiltration and MMP-12 expression in surrounding hemorrhage sites following ICH (Liang et al., 2014; Chen M. et al., 2015).

Increasing evidence reveals that the released ferrous iron from erythrolysis is a primary pathogenic factor in hematoma after ICH (Li et al., 2022). The iron toxicity-mediated microglial activation pro-inflammatory response is a substantial reason for brain impairment in ICH. Deferoxamine (DFA) is an iron chelator that can penetrate the BBB and binds to iron. Decreasing iron accumulation through intraperitoneal administration of DFA can moderately promote the outcomes and reduce microglial activation after ICH (Wu et al., 2011; Hatakeyama et al., 2013; Hu et al., 2019). As an inhibitor of microglial activation, minocycline can decrease injured brain iron to prevent neuronal death in ICH (Zhao et al., 2011; Cao et al., 2018). Similarly, as an iron chelator having brain permeability, VK-28 can polarize microglia to a microglial M2 phenotype, reduce BWC, decrease white matter injury, and improve neurobehavioral deficits following ICH (Li et al., 2017; Dai et al., 2019). Observational research proved that it is evident that the complicated regulatory system modulated microglia function, comprehending it critically to clarify phenotypic and genotypic deviations and acquire promising therapies following ICH.

More therapeutic targets have now participated in regulating microglial neuroinflammation; however, further pre-clinical investigation is still needed to promote their use in clinical research (**Figure 3**).

Conclusion

This review objectively discusses and assesses the function of microglia activation in modulating ICH-induced brain damage. Increasing evidence suggests that pro- or anti-inflammatory microglia phenotypes have dissimilative functions and

meanings, which help us fully comprehend microglia function by regulating related intracellular and extracellular signaling pathways. Moreover, we provide an overall comprehension of cellular and molecular mechanisms responsible for regulating microglia activation after ICH. Although the number of trustworthy clinical trials is reasonably limited and the molecular genetic investigations regarding microglia phenotypic shifts are lacking, our work confers optimistic discernment on a practical intervening approach targeting microglia function in ICH-induced brain injury. Additional studies on therapeutic strategies related to microglia activation-induced neuroinflammation are critical for estimating the possibility of the encouraging treatment noted above.

Author contributions

ND and LW: conceptualization, project administration, Science and Technology Project of Sichuan Province, National Natural Science Foundation of China, and funding acquisition. GY and XF: writing—original draft preparation. MM: writing—review and editing. GY, WG, and YZ: visualization. All authors contributed to the article and approved the submitted version.

Funding

This research was funded by National Traditional Chinese Medicine Inheritance and Innovation Team (No.: ZYYCXTD-C-202207), the Science and Technology Project of Sichuan Province (No.: 2019YFS0543), the Luzhou-Southwest Medical University Science and Technology Strategic Cooperation Project (2021LZXNYD-P04), National Natural Science Foundation of China (No.: 2021XJYJS02), Brain Disease Innovation Team of the Affiliated Traditional Chinese Medicine Hospital of Southwest Medical University (2022-CXTD-05), Luzhou Science and Technology Project (2020, 124), Sichuan Traditional Chinese Medicine Project (2021) No. 13, Southwestern Medical University Hospital (2020) No. 33, and the Project of Southwest Medical University (2021ZKQN125).

Acknowledgments

We thank the Chinese Scholarship Council (CSC) for the financial support for XF.

Conflict of interest

The authors declare that the research was conducted in the absence of any commercial or financial relationships that could be construed as a potential conflict of interest.

Publisher's note

References

Ajami, B., Samusik, N., Wieghofer, P., Ho, P. P., Crotti, A., Bjornson, Z., et al. (2018). Single-cell mass cytometry reveals distinct populations of brain myeloid cells in mouse neuroinflammation and neurodegeneration models. *Nat. Neurosci.* 21, 541–551. doi: 10.1038/s41593-018-0100-x

Arcuri, C., Mecca, C., Bianchi, R., Giambanco, I., and Donato, R. (2017). The pathophysiological role of microglia in dynamic surveillance, phagocytosis and structural remodeling of the developing CNS. *Front. Mol. Neurosci.* 10:191. doi: 10.3389/fnmol.2017.00191

Bai, Y. Y., and Niu, J. Z. (2020). miR222 regulates brain injury and inflammation following intracerebral hemorrhage by targeting ITGB8. *Mol. Med. Rep.* 21, 1145–1153. doi: 10.3892/mmr.2019.10903

Bai, Q., Xue, M., and Yong, V. W. (2020). Microglia and macrophage phenotypes in intracerebral haemorrhage injury: therapeutic opportunities. *Brain* 143, 1297–1314. doi: 10.1093/brain/awz393

Bian, Z., Gong, Y., Huang, T., Lee, C. Z. W., Bian, L., Bai, Z., et al. (2020). Deciphering human macrophage development at single-cell resolution. *Nature* 582, 571–576. doi: 10.1038/s41586-020-2316-7

Brown, G. C., and St George-Hyslop, P. H. (2017). Deciphering microglial diversity in Alzheimer's disease. *Science* 356, 1123–1124. doi: 10.1126/science.aan7893

Cao, S., Hua, Y., Keep, R. F., Chaudhary, N., and Xi, G. (2018). Minocycline effects on intracerebral hemorrhage-induced iron overload in aged rats: brain iron quantification with magnetic resonance imaging. *Stroke* 49, 995–1002. doi: 10.1161/STROKEAHA.117.019860

Carson, M. J., Doose, J. M., Melchior, B., Schmid, C. D., and Ploix, C. C. (2006). CNS immune privilege: hiding in plain sight. *Immunol. Rev.* 213, 48–65. doi: 10.1111/j.1600-065X.2006.00441.x

Chang, C. F., Goods, B. A., Askenase, M. H., Hammond, M. D., Renfroe, S. C., Steinschneider, A. F., et al. (2018). Erythrocyte efferocytosis modulates macrophages towards recovery after intracerebral hemorrhage. *J. Clin. Invest.* 128, 607–624. doi: 10.1172/JCI95612

Chang, C. F., Wan, J., Li, Q., Renfroe, S. C., Heller, N. M., Wang, J., et al. (2017). Alternative activation-skewed microglia/macrophages promote hematoma resolution in experimental intracerebral hemorrhage. *Neurobiol. Dis.* 103, 54–69. doi: 10.1016/j.nbd.2017.03.016

Chen, A. Q., Fang, Z., Chen, X. L., Yang, S., Zhou, Y. F., Mao, L., et al. (2019). Microglia-derived TNF-α mediates endothelial necroptosis aggravating blood brain-barrier disruption after ischemic stroke. *Cell Death Dis.* 10:487. doi: 10.1038/s41419-019-1716-9

Chen, J., Jin, H., Xu, H., Peng, Y., Jie, L., Xu, D., et al. (2019). the neuroprotective effects of Necrostatin-1 on subarachnoid hemorrhage in rats are possibly mediated

by preventing blood-brain barrier disruption and RIP3-mediated necroptosis. *Cell Transplant.* 28, 1358–1372. doi: 10.1177/0963689719867285

Chen, M., Li, X., Zhang, X., He, X., Lai, L., Liu, Y., et al. (2015). The inhibitory effect of mesenchymal stem cell on blood-brain barrier disruption following intracerebral hemorrhage in rats: contribution of TSG-6. *J. Neuroinflammation* 12:61. doi: 10.1186/s12974-015-0284-x

Chen, S., Peng, J., Sherchan, P., Ma, Y., Xiang, S., Yan, F., et al. (2020). TREM2 activation attenuates neuroinflammation and neuronal apoptosis via PI3K/Akt pathway after intracerebral hemorrhage in mice. *J. Neuroinflammation* 17:168. doi: 10.1186/s12974-020-01853-x

Chen, Q., Shi, X., Tan, Q., Feng, Z., Wang, Y., Yuan, Q., et al. (2017). Simvastatin promotes hematoma absorption and reduces hydrocephalus following intraventricular hemorrhage in part by upregulating CD36. *Transl. Stroke Res.* 8, 362–373. doi: 10.1007/s12975-017-0521-y

Chen, S., Yang, Q., Chen, G., and Zhang, J. H. (2015). An update on inflammation in the acute phase of intracerebral hemorrhage. *Transl. Stroke Res.* 6, 4–8. doi: 10.1007/s12975-014-0384-4

Chen, Z., Xu, N., Dai, X., Zhao, C., Wu, X., Shankar, S., et al. (2019). Interleukin-33 reduces neuronal damage and white matter injury via selective microglia M2 polarization after intracerebral hemorrhage in rats. *Brain Res. Bull.* 150, 127–135. doi: 10.1016/j.brainresbull.2019.05.016

Chen, S., Zhao, L., Sherchan, P., Ding, Y., Yu, J., Nowrangi, D., et al. (2018). Activation of melanocortin receptor 4 with RO27–3225 attenuates neuroinflammation through AMPK/JNK/p38 MAPK pathway after intracerebral hemorrhage in mice. *J. Neuroinflammation* 15:106. doi: 10.1186/s12974-018-1140-6

Chiu, I. M., Morimoto, E. T., Goodarzi, H., Liao, J. T., O'Keeffe, S., Phatnani, H. P., et al. (2013). A neurodegeneration-specific gene-expression signature of acutely isolated microglia from an amyotrophic lateral sclerosis mouse model. *Cell Rep.* 4, 385–401. doi: 10.1016/j.celrep.2013.06.018

Da Mesquita, S., and Kipnis, J. (2017). DAMed in (Trem) 2 Steps. *Cell* 169, 1172–1174. doi: 10.1016/j.cell.2017.05.039

Dai, S., Hua, Y., Keep, R. F., Novakovic, N., Fei, Z., and Xi, G. (2019). Minocycline attenuates brain injury and iron overload after intracerebral hemorrhage in aged female rats. *Neurobiol. Dis.* 126, 76–84. doi: 10.1016/j.nbd.2018.06.001

Dasari, R., Bonsack, F., and Sukumari-Ramesh, S. (2021). Brain injury and repair after intracerebral hemorrhage: the role of microglia and brain-infiltrating macrophages. *Neurochem. Int.* 142:104923. doi: 10.1016/j.neuint.2020.104923

de Rivero Vaccari, J. C., Brand, F. J., 3rd, Berti, A. F., Alonso, O. F., Bullock, M. R., and de Rivero Vaccari, J. P. (2015). Mincle signaling in the innate immune response after traumatic brain injury. *J. Neurotrauma* 32, 228–236. doi: 10.1089/neu.2014.3436

Deczkowska, A., Keren-Shaul, H., Weiner, A., Colonna, M., Schwartz, M., and Amit, I. (2018). Disease-associated microglia: a universal immune sensor of neurodegeneration. *Cell* 173, 1073–1081. doi: 10.1016/j.cell.2018.05.003

Del Fresno, C., Cueto, F. J., and Sancho, D. (2020). Sensing tissue damage by myeloid C-Type lectin receptors. *Curr. Top. Microbiol. Immunol.* 429, 117–145. doi: 10.1007/82_2019_194

Deng, S., Sherchan, P., Jin, P., Huang, L., Travis, Z., Zhang, J. H., et al. (2020). Recombinant CCL17 enhances hematoma resolution and activation of CCR4/ERK/Nrf2/CD163 signaling pathway after intracerebral hemorrhage in mice. *Neurotherapeutics* 17, 1940–1953. doi: 10.1007/s13311-020-00908-4

Dong, X. Q., Yu, W. H., Hu, Y. Y., Zhang, Z. Y., and Huang, M. (2011). Oxymatrine reduces neuronal cell apoptosis by inhibiting Toll-like receptor 4/nuclear factor kappa-B-dependent inflammatory responses in traumatic rat brain injury. *Inflamm. Res.* 60, 533–539. doi: 10.1007/s00011-010-0300-7

Drouin, M., Saenz, J., and Chiffoleau, E. (2020). C-Type lectin-like receptors: head or tail in cell death immunity. *Front. Immunol.* 11:251. doi: 10.3389/fimmu.2020.00251

Duan, X. C., Wang, W., Feng, D. X., Yin, J., Zuo, G., Chen, D. D., et al. (2017). Roles of autophagy and endoplasmic reticulum stress in intracerebral hemorrhage-induced secondary brain injury in rats. *CNS Neurosci. Ther.* 23, 554–566. doi: 10.1111/cns.12703

Eldahshan, W., Fagan, S. C., and Ergul, A. (2019). Inflammation within the neurovascular unit: focus on microglia for stroke injury and recovery. *Pharmacol. Res.* 147:104349. doi: 10.1016/j.phrs.2019.104349

Fang, H., Chen, J., Lin, S., Wang, P., Wang, Y., Xiong, X., et al. (2014). CD36-mediated hematoma absorption following intracerebral hemorrhage: negative regulation by TLR4 signaling. *J. Immunol.* 192, 5984–5992. doi: 10.4049/jimmunol.1400054

Fang, Y., Gao, S., Wang, X., Cao, Y., Lu, J., Chen, S., et al. (2020). Programmed cell deaths and potential crosstalk with blood-brain barrier dysfunction after hemorrhagic stroke. *Front. Cell Neurosci.* 14:68. doi: 10.3389/fncel.2020.00068

Fang, Y., Tian, Y., Huang, Q., Wan, Y., Xu, L., Wang, W., et al. (2019). Deficiency of TREK-1 potassium channel exacerbates blood-brain barrier damage and neuroinflammation after intracerebral hemorrhage in mice. *J. Neuroinflammation* 16:96. doi: 10.1186/s12974-019-1485-5

Fang, H., Wang, P. F., Zhou, Y., Wang, Y. C., and Yang, Q. W. (2013). Toll-like receptor 4 signaling in intracerebral hemorrhage-induced inflammation and injury. *J. Neuroinflammation* 10:27. doi: 10.1186/1742-2094-10-27

Florczak-Rzepka, M., Grond-Ginsbach, C., Montaner, J., and Steiner, T. (2012). Matrix metalloproteinases in human spontaneous intracerebral hemorrhage: an update. *Cerebrovasc. Dis.* 34, 249–262. doi: 10.1159/000341686

Friedman, B. A., Srinivasan, K., Ayalon, G., Meilandt, W. J., Lin, H., Huntley, M. A., et al. (2018). Diverse brain myeloid expression profiles reveal distinct microglial activation states and aspects of Alzheimer's disease not evident in mouse models. *Cell Rep.* 22, 832–847. doi: 10.1016/j.celrep.2017.12.066

Gao, T., Jernigan, J., Raza, S. A., Dammer, E. B., Xiao, H., Seyfried, N. T., et al. (2019). Transcriptional regulation of homeostatic and disease-associated-microglial genes by IRF1, LXRβ and CEBPα. *Glia* 67, 1958–1975. doi: 10.1002/glia.23678

Garcia-Revilla, J., Alonso-Bellido, I. M., Burguillos, M. A., Herrera, A. J., Espinosa-Oliva, A. M., Ruiz, R., et al. (2019). Reformulating pro-oxidant microglia in neurodegeneration. *J. Clin. Med.* 8:1719. doi: 10.3390/jcm8101719

Gong, W., Zheng, T., Guo, K., Fang, M., Xie, H., Li, W., et al. (2020). Mincle/Syk signalling promotes intestinal mucosal inflammation through induction of macrophage pyroptosis in Crohn's disease. *J. Crohn's and Colitis* 14, 1734–1747. doi: 10.1093/ecco-jcc/jjaa088

Gosselin, D., Skola, D., Coufal, N. G., Holtman, I. R., Schlachetzki, J. C. M., Sajti, E., et al. (2017). An environment-dependent transcriptional network specifies human microglia identity. *Science* 356:eaal3222. doi: 10.1126/science.aal3222

Hammond, T. R., Dufort, C., Dissing-Olesen, L., Giera, S., Young, A., Wysoker, A., et al. (2019). Single-cell RNA sequencing of microglia throughout the mouse lifespan and in the injured brain reveals complex cell-state changes. *Immunity* 50, 253–271.e6. doi: 10.1016/j.immuni.2018.11.004

Hatakeyama, T., Okauchi, M., Hua, Y., Keep, R. F., and Xi, G. (2013). Deferoxamine reduces neuronal death and hematoma lysis after intracerebral hemorrhage in aged rats. *Transl. Stroke Res.* 4, 546–553. doi: 10.1007/s12975-013-0270-5

He, X., Huang, Y., Liu, Y., Zhang, X., Yue, P., Ma, X., et al. (2022). BAY613606 attenuates neuroinflammation and neurofunctional damage by inhibiting microglial Mincle/Syk signaling response after traumatic brain injury. *Int. J. Mol. Med.* 49:5. doi: 10.3892/ijmm.2021.5060

He, Y., Xu, L., Li, B., Guo, Z. N., Hu, Q., Guo, Z., et al. (2015). Macrophage-inducible C-Type lectin/spleen tyrosine kinase signaling pathway contributes to neuroinflammation after subarachnoid hemorrhage in rats. *Stroke* 46, 2277–2286. doi: 10.1161/STROKEAHA.115.010088

Hemphill, J. C., 3rd, Greenberg, S. M., Anderson, C. S., Becker, K., Bendok, B. R., Cushman, M., et al. (2015). Guidelines for the management of spontaneous intracerebral hemorrhage: a guideline for healthcare professionals from the american heart association/american stroke association. *Stroke* 46, 2032–2060. doi: 10.1161/STR.0000000000000069

Hu, Y. Y., Huang, M., Dong, X. Q., Xu, Q. P., Yu, W. H., and Zhang, Z. Y. (2011). Ginkgolide B reduces neuronal cell apoptosis in the hemorrhagic rat brain: possible involvement of Toll-like receptor 4/nuclear factor-kappa B pathway. *J. Ethnopharmacol.* 137, 1462–1468. doi: 10.1016/j.jep.2011.08.034

Hu, S., Hua, Y., Keep, R. F., Feng, H., and Xi, G. (2019). Deferoxamine therapy reduces brain hemin accumulation after intracerebral hemorrhage in piglets. *Exp. Neurol.* 318, 244–250. doi: 10.1016/j.expneurol.2019.05.003

Jiang, G. L., Yang, X. L., Zhou, H. J., Long, J., Liu, B., Zhang, L. M., et al. (2021). cGAS knockdown promotes microglial M2 polarization to alleviate neuroinflammation by inhibiting cGAS-STING signaling pathway in cerebral ischemic stroke. *Brain Res. Bull.* 171, 183–195. doi: 10.1016/j.brainresbull.2021.03.010

Jin, W. N., Shi, S. X., Li, Z., Li, M., Wood, K., Gonzales, R. J., et al. (2017). Depletion of microglia exacerbates postischemic inflammation and brain injury. *J. Cereb. Blood Flow. Metab.* 37, 2224–2236. doi: 10.1177/0271678X17694185

Jing, C., Bian, L., Wang, M., Keep, R. F., Xi, G., Hua, Y., et al. (2019). Enhancement of hematoma clearance with CD47 blocking antibody in experimental intracerebral hemorrhage. *Stroke* 50, 1539–1547. doi: 10.1161/STROKEAHA.118.024578

Keren-Shaul, H., Spinrad, A., Weiner, A., Matcovitch-Natan, O., Dvir-Szternfeld, R., Ulland, T. K., et al. (2017). A unique microglia type associated

with restricting development of Alzheimer's disease. *Cell* 169, 1276–1290.e17. doi: 10.1016/j.cell.2017.05.018

Kim, J. W., Roh, Y. S., Jeong, H., Yi, H. K., Lee, M. H., Lim, C. W., et al. (2018). Spliceosome-associated protein 130 exacerbates alcohol-induced liver injury by inducing NLRP3 inflammasome-mediated IL-1β in mice. *Am. J. Pathol.* 188, 967–980. doi: 10.1016/j.ajpath.2017.12.010

Klebe, D., McBride, D., Flores, J. J., Zhang, J. H., and Tang, J. (2015). Modulating the immune response towards a neuroregenerative peri-injury milieu after cerebral hemorrhage. *J. Neuroimmune Pharmacol.* 10, 576–586. doi: 10.1007/s11481-015-9613-1

Lan, X., Han, X., Li, Q., Yang, Q. W., and Wang, J. (2017). Modulators of microglial activation and polarization after intracerebral haemorrhage. *Nat. Rev. Neurol.* 13, 420–433. doi: 10.1038/nrneurol.2017.69

Lassmann, H. (2020). Pathology of inflammatory diseases of the nervous system: human disease versus animal models. *Glia* 68, 830–844. doi: 10.1002/glia.23726

Lattanzi, S., Di Napoli, M., Ricci, S., and Divani, A. A. (2020). Matrix metalloproteinases in acute intracerebral hemorrhage. *Neurotherapeutics* 17, 484–496. doi: 10.1007/s13311-020-00839-0

Lei, C., Tan, Y., Ni, D., Peng, J., and Yi, G. (2022). cGAS-STING signaling in ischemic diseases. *Clin. Chim. Acta* 531, 177–182. doi: 10.1016/j.cca.2022.04.003

Li, Y., Dong, Y., Ran, Y., Zhang, Y., Wu, B., Xie, J., et al. (2021). Three-dimensional cultured mesenchymal stem cells enhance repair of ischemic stroke through inhibition of microglia. *Stem Cell Res. Ther.* 12:358. doi: 10.1186/s13287-021-02416-4

Li, Q., Lan, X., Han, X., Durham, F., Wan, J., Weiland, A., et al. (2021). Microglia-derived interleukin-10 accelerates post-intracerebral hemorrhage hematoma clearance by regulating CD36. *Brain Behav. Immun.* 94, 437–457. doi: 10.1016/j.bbi.2021.02.001

Li, Z., Liu, Y., Wei, R., Khan, S., Zhang, R., Zhang, Y., et al. (2022). Iron neurotoxicity and protection by deferoxamine in intracerebral hemorrhage. *Front. Mol. Neurosci.* 15:927334. doi: 10.3389/fnmol.2022.927334

Li, R., Liu, Z., Wu, X., Yu, Z., Zhao, S., and Tang, X. (2019). Lithium chloride promoted hematoma resolution after intracerebral hemorrhage through GSK-3β-mediated pathways-dependent microglia phagocytosis and M2-phenotype differentiation, angiogenesis and neurogenesis in a rat model. *Brain Res. Bull.* 152, 117–127. doi: 10.1016/j.brainresbull.2019.07.019

Li, Q., Wan, J., Lan, X., Han, X., Wang, Z., and Wang, J. (2017). Neuroprotection of brain-permeable iron chelator VK-28 against intracerebral hemorrhage in mice. *J. Cereb. Blood Flow. Metab.* 37, 3110–3123. doi: 10.1177/0271678X17709186

Li, M., Xia, M., Chen, W., Wang, J., Yin, Y., Guo, C., et al. (2020). Lithium treatment mitigates white matter injury after intracerebral hemorrhage through brain-derived neurotrophic factor signaling in mice. *Transl. Res.* 217, 61–74. doi: 10.1016/j.trsl.2019.12.006

Li, Y., Zhu, Z. Y., Lu, B. W., Huang, T. T., Zhang, Y. M., Zhou, N. Y., et al. (2019). Rosiglitazone ameliorates tissue plasminogen activator-induced brain hemorrhage after stroke. *CNS Neurosci. Ther.* 25, 1343–1352. doi: 10.1111/cns.13260

Liang, H., Guan, D., Gao, A., Yin, Y., Jing, M., Yang, L., et al. (2014). Human amniotic epithelial stem cells inhibit microglia activation through downregulation of tumor necrosis factor-α, interleukin-1β and matrix metalloproteinase-12 *in vitro* and in a rat model of intracerebral hemorrhage. *Cytotherapy* 16, 523–534. doi: 10.1016/j.jcyt.2013.11.007

Liu, X., Chen, X., Zhu, Y., Wang, K., and Wang, Y. (2017). Effect of magnolol on cerebral injury and blood brain barrier dysfunction induced by ischemia-reperfusion *in vivo* and *in vitro*. *Metab. Brain Dis.* 32, 1109–1118. doi: 10.1007/s11011-017-0004-6

Liu, X. Y., Dai, X. H., Zou, W., Yu, X. P., Teng, W., Wang, Y., et al. (2018). Acupuncture through Baihui (DU20) to Qubin (GB7) mitigates neurological impairment after intracerebral hemorrhage. *Neural Regen. Res.* 13, 1425–1432. doi: 10.4103/1673-5374.235298

Liu, Z., Li, R., Jiang, C., Zhao, S., Li, W., and Tang, X. (2018). The neuroprotective effect of lithium chloride on cognitive impairment through glycogen synthase kinase-3β inhibition in intracerebral hemorrhage rats. *Eur. J. Pharmacol.* 840, 50–59. doi: 10.1016/j.ejphar.2018.10.019

Liu, D. L., Zhao, L. X., Zhang, S., and Du, J. R. (2016). Peroxiredoxin 1-mediated activation of TLR4/NF-kappaB pathway contributes to neuroinflammatory injury in intracerebral hemorrhage. *Int. Immunopharmacol.* 41, 82–89. doi: 10.1016/j.intimp.2016.10.025

Liu, J., Zhu, Z., and Leung, G. K. (2022). Erythrophagocytosis by Microglia/Macrophage in intracerebral hemorrhage: from mechanisms to translation. *Front. Cell Neurosci.* 16:818602. doi: 10.3389/fncel.2022.818602

Luo, Y., Yin, W., Signore, A. P., Zhang, F., Hong, Z., Wang, S., et al. (2006). Neuroprotection against focal ischemic brain injury by the peroxisome proliferator-activated receptor-γ agonist rosiglitazone. *J. Neurochem.* 97, 435–448. doi: 10.1111/j.1471-4159.2006.03758.x

Lv, Y. N., Ou-Yang, A. J., and Fu, L. S. (2017). MicroRNA-27a negatively modulates the inflammatory response in lipopolysaccharide-stimulated microglia by targeting TLR4 and IRAK4. *Cell Mol. Neurobiol.* 37, 195–210. doi: 10.1007/s10571-016-0361-4

Masuda, T., Sankowski, R., Staszewski, O., Bottcher, C., Amann, L., and Sagar, et al. (2019). Spatial and temporal heterogeneity of mouse and human microglia at single-cell resolution. *Nature* 566, 388–392. doi: 10.1038/s41586-019-0924-x

Mecca, C., Giambanco, I., Donato, R., and Arcuri, C. (2018). Microglia and aging: the role of the TREM2-DAP12 and CX3CL1-CX3CR1 axes. *Int. J. Mol. Sci.* 19:318. doi: 10.3390/ijms19010318

Miao, H., Li, R., Han, C., Lu, X., and Zhang, H. (2018). Minocycline promotes posthemorrhagic neurogenesis via M2 microglia polarization via upregulation of the TrkB/BDNF pathway in rats. *J. Neurophysiol.* 120, 1307–1317. doi: 10.1152/jn.00234.2018

Ochocka, N., Segit, P., Walentynowicz, K. A., Wojnicki, K., Cyranowski, S., Swatler, J., et al. (2021). Single-cell RNA sequencing reveals functional heterogeneity of glioma-associated brain macrophages. *Nat. Commun.* 12:1151. doi: 10.1038/s41467-021-21407-w

Ohnishi, M., Katsuki, H., Fujimoto, S., Takagi, M., Kume, T., and Akaike, A. (2007). Involvement of thrombin and mitogen-activated protein kinase pathways in hemorrhagic brain injury. *Exp. Neurol.* 206, 43–52. doi: 10.1016/j.expneurol.2007.03.030

Olah, M., Menon, V., Habib, N., Taga, M. F., Ma, Y., Yung, C. J., et al. (2020). Single cell RNA sequencing of human microglia uncovers a subset associated with Alzheimer's disease. *Nat. Commun.* 11:6129. doi: 10.1038/s41467-020-19737-2

Ozaki, E., Delaney, C., Campbell, M., and Doyle, S. L. (2022). Minocycline suppresses disease-associated microglia (DAM) in a model of photoreceptor cell degeneration. *Exp. Eye Res.* 217:108953. doi: 10.1016/j.exer.2022.108953

Prinz, M., Erny, D., and Hagemeyer, N. (2017). Ontogeny and homeostasis of CNS myeloid cells. *Nat. Immunol.* 18, 385–392. doi: 10.1038/ni.3703

Prinz, M., Jung, S., and Priller, J. (2019). Microglia biology: one century of evolving concepts. *Cell* 179, 292–311. doi: 10.1016/j.cell.2019.08.053

Rangaraju, S., Dammer, E. B., Raza, S. A., Rathakrishnan, P., Xiao, H., Gao, T., et al. (2018). Identification and therapeutic modulation of a pro-inflammatory subset of disease-associated-microglia in Alzheimer's disease. *Mol. Neurodegener.* 13:24. doi: 10.1186/s13024-018-0254-8

Ransohoff, R. M. (2016). A polarizing question: do M1 and M2 microglia exist? *Nat. Neurosci.* 19, 987–991. doi: 10.1038/nn.4338

Ronaldson, P. T., and Davis, T. P. (2020). Regulation of blood-brain barrier integrity by microglia in health and disease: a therapeutic opportunity. *J. Cereb. Blood Flow Metab.* 40, S6–S24. doi: 10.1177/0271678X20951995

Saito, M., Saito, M., and Das, B. C. (2019). Involvement of AMP-activated protein kinase in neuroinflammation and neurodegeneration in the adult and developing brain. *Int. J. Dev. Neurosci.* 77, 48–59. doi: 10.1016/j.ijdevneu.2019.01.007

Sansing, L. H., Harris, T. H., Welsh, F. A., Kasner, S. E., Hunter, C. A., and Kariko, K. (2011). Toll-like receptor 4 contributes to poor outcome after intracerebral hemorrhage. *Ann. Neurol.* 70, 646–656. doi: 10.1002/ana.22528

Sekerdag, E., Solaroglu, I., and Gursoy-Ozdemir, Y. (2018). Cell death mechanisms in stroke and novel molecular and cellular treatment options. *Curr. Neuropharmacol.* 16, 1396–1415. doi: 10.2174/1570159X16666180302115544

Shang, Y., Dai, S., Chen, X., Wen, W., and Liu, X. (2019). MicroRNA-93 regulates the neurological function, cerebral edema and neuronal apoptosis of rats with intracerebral hemorrhage through TLR4/NF-κB signaling pathway. *Cell Cycle* 18, 3160–3176. doi: 10.1080/15384101.2019.1670509

Sharma, M., Rajendrarao, S., Shahani, N., Ramirez-Jarquin, U. N., and Subramaniam, S. (2020). Cyclic GMP-AMP synthase promotes the inflammatory and autophagy responses in Huntington disease. *Proc. Natl. Acad. Sci. U S A* 117, 15989–15999. doi: 10.1073/pnas.2002144117

Shi, S. X., Li, Y. J., Shi, K., Wood, K., Ducruet, A. F., and Liu, Q. (2020). IL (Interleukin)-15 bridges astrocyte-microglia crosstalk and exacerbates brain injury following intracerebral hemorrhage. *Stroke* 51, 967–974. doi: 10.1161/STROKEAHA.119.028638

Shi, H., Wang, J., Wang, J., Huang, Z., and Yang, Z. (2018). IL-17A induces autophagy and promotes microglial neuroinflammation through ATG5 and ATG7 in intracerebral hemorrhage. *J. Neuroimmunol.* 323, 143–151. doi: 10.1016/j.jneuroim.2017.07.015

Shi, J., Yang, Y., Yin, N., Liu, C., Zhao, Y., Cheng, H., et al. (2022). Engineering CXCL12 biomimetic decoy-integrated versatile immunosuppressive nanoparticle

for ischemic stroke therapy with management of overactivated brain immune microenvironment. *Small Methods* 6:e2101158. doi: 10.1002/smtd.202101158

Su, E. J., Cao, C., Fredriksson, L., Nilsson, I., Stefanitsch, C., Stevenson, T. K., et al. (2017). Microglial-mediated PDGF-CC activation increases cerebrovascular permeability during ischemic stroke. *Acta Neuropathol.* 134, 585–604. doi: 10.1007/s00401-017-1749-z

Tan, X., Yang, Y., Xu, J., Zhang, P., Deng, R., Mao, Y., et al. (2020). Luteolin exerts neuroprotection via modulation of the p62/Keap1/Nrf2 pathway in intracerebral hemorrhage. *Front. Pharmacol.* 10:1551. doi: 10.3389/fphar.2019.01551

Taylor, R. A., Chang, C. F., Goods, B. A., Hammond, M. D., Mac Grory, B., Ai, Y., et al. (2017). TGF-β1 modulates microglial phenotype and promotes recovery after intracerebral hemorrhage. *J. Clin. Invest.* 127, 280–292. doi: 10.1172/JCI88647

Tschoe, C., Bushnell, C. D., Duncan, P. W., Alexander-Miller, M. A., and Wolfe, S. Q. (2020). Neuroinflammation after intracerebral hemorrhage and potential therapeutic targets. *J. Stroke* 22, 29–46. doi: 10.5853/jos.2019.02236

Vainchtein, I. D., and Molofsky, A. V. (2020). Astrocytes and microglia: in sickness and in health. *Trends Neurosci.* 43, 144–154. doi: 10.1016/j.tins.2020.01.003

Vinukonda, G., Liao, Y., Hu, F., Ivanova, L., Purohit, D., Finkel, D. A., et al. (2019). Human cord blood-derived unrestricted somatic stem cell infusion improves neurobehavioral outcome in a rabbit model of intraventricular hemorrhage. *Stem Cells Transl. Med.* 8, 1157–1169. doi: 10.1002/sctm.19-0082

Voet, S., Prinz, M., and van Loo, G. (2019). Microglia in central nervous system inflammation and multiple sclerosis pathology. *Trends Mol. Med.* 25, 112–123. doi: 10.1016/j.molmed.2018.11.005

Wan, S., Cheng, Y., Jin, H., Guo, D., Hua, Y., Keep, R. F., et al. (2016). Microglia activation and polarization after intracerebral hemorrhage in mice: the role of protease-activated receptor-1. *Transl. Stroke Res.* 7, 478–487. doi: 10.1007/s12975-016-0472-8

Wang, J. (2010). Preclinical and clinical research on inflammation after intracerebral hemorrhage. *Prog. Neurobiol.* 92, 463–477. doi: 10.1016/j.pneurobio.2010.08.001

Wang, Y., Chen, Q., Tan, Q., Feng, Z., He, Z., Tang, J., et al. (2018). Simvastatin accelerates hematoma resolution after intracerebral hemorrhage in a PPARγ-dependent manner. *Neuropharmacology* 128, 244–254. doi: 10.1016/j.neuropharm.2017.10.021

Wang, M., Hua, Y., Keep, R. F., Wan, S., Novakovic, N., Xi, G., et al. (2019a). Complement inhibition attenuates early erythrolysis in the hematoma and brain injury in aged rats. *Stroke* 50, 1859–1868. doi: 10.1161/STROKEAHA.119.025170

Wang, M., Cheng, L., Chen, Z. L., Mungur, R., Xu, S. H., Wu, J., et al. (2019b). Hyperbaric oxygen preconditioning attenuates brain injury after intracerebral hemorrhage by regulating microglia polarization in rats. *CNS Neurosci. Ther.* 25, 1126–1133. doi: 10.1111/cns.13208

Wang, G., Shi, Y., Jiang, X., Leak, R. K., Hu, X., Wu, Y., et al. (2015). HDAC inhibition prevents white matter injury by modulating microglia/macrophage polarization through the GSK3β/PTEN/Akt axis. *Proc. Natl. Acad. Sci. U S A* 112, 2853–2858. doi: 10.1073/pnas.1501441112

Wang, Y. C., Wang, P. F., Fang, H., Chen, J., Xiong, X. Y., and Yang, Q. W. (2013). Toll-like receptor 4 antagonist attenuates intracerebral hemorrhage-induced brain injury. *Stroke* 44, 2545–2552. doi: 10.1161/STROKEAHA.113.001038

Wang, G., Wang, L., Sun, X. G., and Tang, J. (2018). Haematoma scavenging in intracerebral haemorrhage: from mechanisms to the clinic. *J. Cell. Mol. Med.* 22, 768–777. doi: 10.1111/jcmm.13441

Wang, J., Xu, Z., Chen, X., Li, Y., Chen, C., Wang, C., et al. (2018). MicroRNA-182-5p attenuates cerebral ischemia-reperfusion injury by targeting Toll-like receptor 4. *Biochem. Biophys. Res. Commun.* 505, 677–684. doi: 10.1016/j.bbrc.2018.09.165

Wang, Z., Yuan, B., Fu, F., Huang, S., and Yang, Z. (2017). Hemoglobin enhances miRNA-144 expression and autophagic activation mediated inflammation of microglia via mTOR pathway. *Sci. Rep.* 7:11861. doi: 10.1038/s41598-017-12067-2

Wang, R., Zhu, Y., Liu, Z., Chang, L., Bai, X., Kang, L., et al. (2021). Neutrophil extracellular traps promote tPA-induced brain hemorrhage via cGAS in mice with stroke. *Blood* 138, 91–103. doi: 10.1182/blood.2020008913

Wasserman, J. K., and Schlichter, L. C. (2007). Minocycline protects the blood-brain barrier and reduces edema following intracerebral hemorrhage in the rat. *Exp. Neurol.* 207, 227–237. doi: 10.1016/j.expneurol.2007.06.025

Wasserman, J. K., Zhu, X., and Schlichter, L. C. (2007). Evolution of the inflammatory response in the brain following intracerebral hemorrhage and effects of delayed minocycline treatment. *Brain Res.* 1180, 140–154. doi: 10.1016/j.brainres.2007.08.058

Wells, J. E., Biernaskie, J., Szymanska, A., Larsen, P. H., Yong, V. W., and Corbett, D. (2005). Matrix metalloproteinase (MMP)-12 expression has a negative impact on sensorimotor function following intracerebral haemorrhage in mice. *Eur. J. Neurosci.* 21, 187–196. doi: 10.1111/j.1460-9568.2004.03829.x

Wolf, S. A., Boddeke, H. W., and Kettenmann, H. (2017). Microglia in physiology and disease. *Annu. Rev. Physiol.* 79, 619–643. doi: 10.1146/annurev-physiol-022516-034406

Wu, C. H., Shyue, S. K., Hung, T. H., Wen, S., Lin, C. C., Chang, C. F., et al. (2017). Genetic deletion or pharmacological inhibition of soluble epoxide hydrolase reduces brain damage and attenuates neuroinflammation after intracerebral hemorrhage. *J. Neuroinflammation* 14:230. doi: 10.1186/s12974-017-1005-4

Wu, H., Wu, T., Xu, X., Wang, J., and Wang, J. (2011). Iron toxicity in mice with collagenase-induced intracerebral hemorrhage. *J. Cereb. Blood Flow Metab.* 31, 1243–1250. doi: 10.1038/jcbfm.2010.209

Xiao, H., Chen, H., Jiang, R., Zhang, L., Wang, L., Gan, H., et al. (2020). NLRP6 contributes to inflammation and brain injury following intracerebral haemorrhage by activating autophagy. *J. Mol. Med. (Berl)* 98, 1319–1331. doi: 10.1007/s00109-020-01962-3

Xu, Y. J., Au, N. P. B., and Ma, C. H. E. (2022). Functional and phenotypic diversity of microglia: implication for microglia-based therapies for Alzheimer's disease. *Front. Aging Neurosci.* 14:896852. doi: 10.3389/fnagi.2022.896852

Xu, H., Cao, J., Xu, J., Li, H., Shen, H., Li, X., et al. (2019). GATA-4 regulates neuronal apoptosis after intracerebral hemorrhage via the NF-κB/Bax/Caspase-3 pathway both *in vivo* and *in vitro*. *Exp. Neurol.* 315, 21–31. doi: 10.1016/j.expneurol.2019.01.018

Xu, J., Chen, Z., Yu, F., Liu, H., Ma, C., Xie, D., et al. (2020). IL-4/STAT6 signaling facilitates innate hematoma resolution and neurological recovery after hemorrhagic stroke in mice. *Proc. Natl. Acad. Sci. U S A* 117, 32679–32690. doi: 10.1073/pnas.2018497117

Xu, R., Wang, S., Li, W., Liu, Z., Tang, J., and Tang, X. (2017). Activation of peroxisome proliferator-activated receptor-γ by a 12/15-lipoxygenase product of arachidonic acid: a possible neuroprotective effect in the brain after experimental intracerebral hemorrhage. *J. Neurosurg.* 127, 522–531. doi: 10.3171/2016.7.JNS1668

Xu, N., Zhang, Y., Doycheva, D. M., Ding, Y., Zhang, Y., Tang, J., et al. (2018). Adiponectin attenuates neuronal apoptosis induced by hypoxia-ischemia via the activation of AdipoR1/APPL1/LKB1/AMPK pathway in neonatal rats. *Neuropharmacology* 133, 415–428. doi: 10.1016/j.neuropharm.2018.02.024

Yang, G., Fan, X., Mazhar, M., Yang, S., Xu, H., Dechsupa, N., et al. (2022). Mesenchymal stem cell application and its therapeutic mechanisms in intracerebral hemorrhage. *Front. Cell Neurosci.* 16:898497. doi: 10.3389/fncel.2022.898497

Yang, Z., Jiang, X., Zhang, J., Huang, X., Zhang, X., Wang, J., et al. (2018). Let-7a promotes microglia M2 polarization by targeting CKIP-1 following ICH. *Immunol. Lett.* 202, 1–7. doi: 10.1016/j.imlet.2018.07.007

Yang, Z., Liu, B., Zhong, L., Shen, H., Lin, C., Lin, L., et al. (2015). Toll-like receptor-4-mediated autophagy contributes to microglial activation and inflammatory injury in mouse models of intracerebral haemorrhage. *Neuropathol. Appl. Neurobiol.* 41, e95–e106. doi: 10.1111/nan.12177

Yang, X., Ren, H., Wood, K., Li, M., Qiu, S., Shi, F. D., et al. (2018). Depletion of microglia augments the dopaminergic neurotoxicity of MPTP. *FASEB J.* 32, 3336–3345. doi: 10.1096/fj.201700833RR

Yang, L., Tang, J., Chen, Q., Jiang, B., Zhang, B., Tao, Y., et al. (2015). Hyperbaric oxygen preconditioning attenuates neuroinflammation after intracerebral hemorrhage in rats by regulating microglia characteristics. *Brain Res.* 1627, 21–30. doi: 10.1016/j.brainres.2015.08.011

Yang, Z., Zhao, T., Zou, Y., Zhang, J. H., and Feng, H. (2014a). Curcumin inhibits microglia inflammation and confers neuroprotection in intracerebral hemorrhage. *Immunol. Lett.* 160, 89–95. doi: 10.1016/j.imlet.2014.03.005

Yang, Z., Yu, A., Liu, Y., Shen, H., Lin, C., Lin, L., et al. (2014b). Regulatory T cells inhibit microglia activation and protect against inflammatory injury in intracerebral hemorrhage. *Int. Immunopharmacol.* 22, 522–525. doi: 10.1016/j.intimp.2014.06.037

Yu, A., Duan, H., Zhang, T., Pan, Y., Kou, Z., Zhang, X., et al. (2016). IL-17A promotes microglial activation and neuroinflammation in mouse models of intracerebral haemorrhage. *Mol. Immunol.* 73, 151–157. doi: 10.1016/j.molimm.2016.04.003

Yu, A., Zhang, T., Zhong, W., Duan, H., Wang, S., Ye, P., et al. (2017a). miRNA-144 induces microglial autophagy and inflammation following intracerebral hemorrhage. *Immunol. Lett.* 182, 18–23. doi: 10.1016/j.imlet.2017.01.002

Yu, A., Zhang, T., Duan, H., Pan, Y., Zhang, X., Yang, G., et al. (2017b). MiR-124 contributes to M2 polarization of microglia and confers brain inflammatory protection via the C/EBP-α pathway in intracerebral hemorrhage. *Immunol. Lett.* 182, 1–11. doi: 10.1016/j.imlet.2016.12.003

Yuan, B., Shen, H., Lin, L., Su, T., Zhong, L., and Yang, Z. (2017). Autophagy promotes microglia activation through beclin-1-atg5 pathway in intracerebral hemorrhage. *Mol. Neurobiol.* 54, 115–124. doi: 10.1007/s12035-015-9642-z

Zhang, X. D., Fan, Q. Y., Qiu, Z., and Chen, S. (2018). MiR-7 alleviates secondary inflammatory response of microglia caused by cerebral hemorrhage through inhibiting TLR4 expression. *Eur. Rev. Med. Pharmacol. Sci.* 22, 5597–5604. doi: 10.26355/eurrev_201809_15824

Zhang, Y., Han, B., He, Y., Li, D., Ma, X., Liu, Q., et al. (2017). MicroRNA-132 attenuates neurobehavioral and neuropathological changes associated with intracerebral hemorrhage in mice. *Neurochem. Int.* 107, 182–190. doi: 10.1016/j.neuint.2016.11.011

Zhang, Z., Zhang, Z., Lu, H., Yang, Q., Wu, H., Wang, J., et al. (2017). Microglial polarization and inflammatory mediators after intracerebral hemorrhage. *Mol. Neurobiol.* 54, 1874–1886. doi: 10.1007/s12035-016-9785-6

Zhao, L., Chen, S., Sherchan, P., Ding, Y., Zhao, W., Guo, Z., et al. (2018). Recombinant CTRP9 administration attenuates neuroinflammation via activating adiponectin receptor 1 after intracerebral hemorrhage in mice. *J. Neuroinflammation* 15:215. doi: 10.1186/s12974-018-1256-8

Zhao, X., Grotta, J., Gonzales, N., and Aronowski, J. (2009). Hematoma resolution as a therapeutic target: the role of microglia/macrophages. *Stroke* 40, S92–S94. doi: 10.1161/STROKEAHA.108.533158

Zhao, F., Hua, Y., He, Y., Keep, R. F., and Xi, G. (2011). Minocycline-induced attenuation of iron overload and brain injury after experimental intracerebral hemorrhage. *Stroke* 42, 3587–3593. doi: 10.1161/STROKEAHA.111.623926

Zhao, W., Kong, F., Gong, X., Guo, Z., Zhao, L., and Wang, S. (2021). Activation of AdipoR1 with rCTRP9 preserves BBB integrity through the APPL1/AMPK/Nrf2 signaling pathway in ICH mice. *Oxid. Med. Cell. Longev.* 2021:2801263. doi: 10.1155/2021/2801263

Zhao, S., Liu, Z., Yu, Z., Wu, X., Li, R., and Tang, X. (2019). BIO alleviates inflammation through inhibition of GSK-3β in a rat model of intracerebral hemorrhage. *J. Neurosurg.* 1–9. doi: 10.3171/2019.4.JNS183501. [Online ahead of print].

Zhao, X., Sun, G., Zhang, J., Strong, R., Song, W., Gonzales, N., et al. (2007). Hematoma resolution as a target for intracerebral hemorrhage treatment: role for peroxisome proliferator-activated receptor γ in microglia/macrophages. *Ann. Neurol.* 61, 352–362. doi: 10.1002/ana.21097

Zhao, Y., Wei, Z. Z., Zhang, J. Y., Zhang, Y., Won, S., Sun, J., et al. (2017). GSK-3β inhibition induced neuroprotection, regeneration and functional recovery after intracerebral hemorrhagic stroke. *Cell Transplant.* 26, 395–407. doi: 10.3727/096368916X694364

Zheng, J., Liu, Z., Li, W., Tang, J., Zhang, D., and Tang, X. (2017). Lithium posttreatment confers neuroprotection through glycogen synthase kinase-3β inhibition in intracerebral hemorrhage rats. *J. Neurosurg.* 127, 716–724. doi: 10.3171/2016.7.JNS152995

Zhou, Y., Wang, Y., Wang, J., Anne Stetler, R., and Yang, Q. W. (2014). Inflammation in intracerebral hemorrhage: from mechanisms to clinical translation. *Prog. Neurobiol.* 115, 25–44. doi: 10.1016/j.pneurobio.2013.11.003

Zhou, K., Zhong, Q., Wang, Y. C., Xiong, X. Y., Meng, Z. Y., Zhao, T., et al. (2017). Regulatory T cells ameliorate intracerebral hemorrhage-induced inflammatory injury by modulating microglia/macrophage polarization through the IL-10/GSK3β/PTEN axis. *J. Cereb. Blood Flow Metab.* 37, 967–979. doi: 10.1177/0271678X16648712

Zhuang, J., Peng, Y., Gu, C., Chen, H., Lin, Z., Zhou, H., et al. (2021). Wogonin accelerates hematoma clearance and improves neurological outcome via the PPAR-γ pathway after intracerebral hemorrhage. *Transl. Stroke Res.* 12, 660–675. doi: 10.1007/s12975-020-00842-9

Ziai, W. C. (2013). Hematology and inflammatory signaling of intracerebral hemorrhage. *Stroke* 44, S74–S78. doi: 10.1161/STROKEAHA.111.000662

Zlokovic, B. V. (2008). The blood-brain barrier in health and chronic neurodegenerative disorders. *Neuron* 57, 178–201. doi: 10.1016/j.neuron.2008.01.003

frontiers | Frontiers in Molecular Neuroscience

TYPE Original Research
PUBLISHED 11 October 2022
DOI 10.3389/fnmol.2022.976108

OPEN ACCESS

EDITED BY
Walter Gulisano,
University of Catania, Italy

REVIEWED BY
Roberto Piacentini,
Catholic University of the Sacred Heart, Italy
Michael R. Nichols,
University of Missouri–St. Louis, United States

*CORRESPONDENCE
Gary A. Rosenberg
grosenberg@salud.unm.edu

SPECIALTY SECTION
This article was submitted to Brain Disease Mechanisms, a section of the journal Frontiers in Molecular Neuroscience

RECEIVED 23 June 2022
ACCEPTED 05 September 2022
PUBLISHED 11 October 2022

CITATION
Sánchez KE, Bhaskar K and Rosenberg GA (2022) Apoptosis-associated speck-like protein containing a CARD-mediated release of matrix metalloproteinase 10 stimulates a change in microglia phenotype.
Front. Mol. Neurosci. 15:976108.
doi: 10.3389/fnmol.2022.976108

Apoptosis-associated speck-like protein containing a CARD-mediated release of matrix metalloproteinase 10 stimulates a change in microglia phenotype

Kathryn E. Sánchez[1], Kiran Bhaskar[2,3] and Gary A. Rosenberg[1,3]*

[1]Center for Memory and Aging, University of New Mexico, Albuquerque, NM, United States, [2]Department of Molecular Genetics and Microbiology, University of New Mexico, Albuquerque, NM, United States, [3]Department of Neurology, University of New Mexico, Albuquerque, NM, United States

Inflammation contributes to amyloid-β and tau pathology in Alzheimer's disease (AD). Microglia facilitate an altered immune response that includes microgliosis, upregulation of inflammasome proteins, and elevation of matrix-metalloproteinases (MMPs). Studies of cerebrospinal fluid (CSF) and blood in dementia patients show upregulation of two potential biomarkers of inflammation at the cellular level, MMP10 and apoptosis-associated speck-like protein containing a CARD (ASC). However, little is known about their relationship in the context of brain inflammation. Therefore, we stimulated microglia cultures with purified insoluble ASC speck aggregates and MMP10 to elucidate their role. We found that ASC specks altered microglia shape and stimulated the release of MMP3 and MMP10. Furthermore, MMP10 stimulated microglia released additional MMP10 along with the inflammatory cytokines, tumor-necrosis factor-α (TNFα), Interleukin 6 (IL-6), and CXCL1 CXC motif chemokine ligand 1 (CXCL1). A broad-spectrum MMP inhibitor, GM6001, prevented TNFα release. With these results, we conclude that MMP10 and ASC specks act on microglial cells to propagate inflammation.

KEYWORDS

inflammasome, apoptosis-associated speck like protein containing a CARD (ASC), matrix-metalloproteinase 10 (MMP10), microglia, cytokine

Introduction

Fifty-five million people in the world are currently affected by dementia, and this number is predicted to double every 20 years according to the World Health Organization. It will eventually reach 78 million by 2030 and 139 million by 2050 due to a rapidly aging population (Prince et al., 2013). The expected rise in dementia is concerning since patient quality of life is greatly diminished by symptoms, which include agitation, apathy, aggression, psychosis, hallucinations, and delusions. Though the presence of amyloid-β and tau neurofibrillary tangles in the brain are canonical pathological hallmarks of Alzheimer's disease, these two pathological proteins are often associated with central nervous system inflammation. More specifically, patient samples demonstrate evidence of altered microglial activity and elevated cytokine levels. Such microglial activity includes microgliosis, the upregulation of inflammasome adaptor proteins, and elevated MMP levels (Ueno et al., 2009; Kerkhofs et al., 2020; Scott et al., 2020; Erhardt et al., 2021; Jiang et al., 2021).

The NLRP3 inflammasome is a multiprotein complex that is comprised of the following proteins: NACHT, LRR, and PYD domain-containing protein 3 (NLRP3); the adaptor protein apoptosis-associated speck-like protein containing a CARD (ASC); and inflammatory caspase 1 (cysteine-dependent aspartate-directed protease 1) (Latz et al., 2013; Rathinam and Fitzgerald, 2016; Reis et al., 2020; Zheng et al., 2020). The ASC and pro-caspase 1 components of the complex lead to caspase 1 activation that results in the processing of cytoplasmic targets, including IL-1β and IL-18 (Sutterwala et al., 2006; Franklin et al., 2014; Facci et al., 2018; Ribeiro et al., 2020; Scott et al., 2020). The NLRP3 inflammasome complex is predicted to contribute to AD, as it promotes neuroinflammation in response to amyloid-β. Assembled ASC (called ASC speck or pyroptosome) has prion-like activity, and is capable of propagating inflammation between immune cells (Franklin et al., 2014). One important inflammasome adaptor protein, ASC, is elevated in the immune cells of AD patients and is associated with the inflammasome complex (Franklin et al., 2014; Scott et al., 2020). ASC specks recruit and activate caspase-1, which results in 1β (IL-1β) cleavage and pyroptotic cell death (Franklin et al., 2014; White et al., 2017; Scott et al., 2020). Immune cells then release ASC specks into the extracellular space, which can further propagate inflammation by maturing IL-1β and IL-18 (Venegas et al., 2017). Finally, our previous research showed elevated ASC specks in the CSF of patients with tauopathies compared to healthy subjects (Jiang et al., 2021).

While it is still unclear how inflammasome-based maturation of IL-1β is related to another important mediator of inflammation, matrix metalloproteinase (MMPs), previous research suggests that IL-1β stimulates the release of MMP1, MMP9, and MMP13 in chondrocytes (Zhang et al., 2018). Furthermore, MMP1 is also upregulated in fibroblasts in response to IL-1β (Lew et al., 2018). These studies emphasize a likely relationship between inflammasome activation and MMP release. However, how the prion-like ASC speck, an inflammatory protein that is a prerequisite for IL-1β activation, can affect MMP expression is still unknown.

Matrix-metalloproteinases are endopeptidases that are elevated in Alzheimer's disease (Lorenzl et al., 2003; Rosenberg, 2009; Erhardt et al., 2021). For example, MMP9 and MMP10 are elevated in the CSF of patients with dementia (Lorenzl et al., 2003; Erhardt et al., 2021; Jiang et al., 2021). The elevation of MMPs is notable since they cleave numerous targets including extracellular matrix proteins, G-protein coupled receptors, and tight junction proteins (Yang et al., 2007; Ueno et al., 2009; Yang and Rosenberg, 2011; Allen et al., 2016). The innate immune cells of the central nervous system, microglia, respond to fluctuations in MMP activity. For example, MMP13 and MMP3 both alter the inflammatory profile of microglia (Connolly et al., 2016; Sánchez and Maguire-Zeiss, 2020; Brelstaff et al., 2021). MMP13 exposure changes microglia morphology and proinflammatory protein expression (Sánchez and Maguire-Zeiss, 2020). MMP3 is a stromelysin like MMP10, and can stimulate the upregulation and release of the proinflammatory cytokine TNFα in microglia cell lines (Kim et al., 2005; Connolly et al., 2016). While MMP3 is investigated in this work, it is notably not as novel as MMP10 due to these previous studies.

Though it is well established that both inflammasome adaptor proteins and MMPs contribute to the inflammation documented in Alzheimer's disease, the relationship between assembled ASC specks and MMP10 has not been investigated in microglia. To that end, we have evaluated the consequences of ASC speck stimulation on primary microglia. After confirming that MMP10 is released in response to ASC specks, we also assessed how MMP10 further perpetuates microglia-mediated inflammation. Here, we report that MMP10 stimulates a pro-inflammatory response in microglia. Overall, our findings have identified the inflammasome as a future therapeutic target to combat MMP mediated inflammation.

Materials and methods

Animals

The use of C57Bl/6j pups for primary microglia culture and all other animal work was performed at the University of New Mexico Health Sciences Center where the protocol for such experiments were approved by the Institutional Animal Care and Use Committee (IACUC).

Culture of ASC-mCerulean macrophages

Inflammasome reporter macrophages stably transduced with constructs for the expression of ASC-mCerulean have been previously described (Heneka et al., 2013; Stutz et al., 2013; Franklin et al., 2014; Jiang et al., 2021). The immortalized macrophages were grown in DMEM (Thermo Fisher) supplemented with 10% v/v Fetal Bovine Serum (FBS; Thermo Fisher Fisher). When cells reached 60% confluence (P8-P12), they were seeded on petri dishes (100 mm; Thermo Fisher Scientific) in preparation for ASC-speck purification.

Purification of ASC specks

ASC-mCerulean expressing macrophages were grown in a 10-mm petri dish and stimulated with lipopolysaccharide (LPS) (250 ng/mL; InvivoGen) for 3 h. Without removing the cell-culture media, macrophages were then activated 1 h with nigericin (20 μM; InvivoGen) as previously described (Fernandes-Alnemri and Alnemri, 2008; Stutz et al., 2013; Franklin et al., 2014). Macrophages were subsequently harvested and lysed in 0.5 mL lysis buffer (20 mM Hepes-KOH, pH 7.5, 10 mM KCl, 1.5 mM $MgCl_2$, 1 mM EDTA, 1 mM EGTA, 320 mM sucrose) and kept on ice for 30 min. The lysate was subsequently centrifuged for 10 min to remove the bulk nuclei (1500 rpm; Eppendorf Centrifuge 5415 R). The resulting supernatant was transferred to a new tube and diluted with 0.5 mL lysis buffer and 1 mL CHAPS buffer (20 mM Hepes-KOH, pH 7.5, 5 mM $MgCl_2$, 0.5 mM EGTA, 0.1 mM PMSF, 0.1% CHAPS). After dilution, samples were centrifuged for 10 min to pellet the ASC pyroptosomes (5,000 rpm). For further purification, the crude pellet was resuspended in 1 mL CHAPS buffer and subsequently transferred to a new tube when layered over a 40% Percoll cushion (1 mL; 40% v/v Percoll in 2.5 M sucrose) and centrifuged at 14,000 rpm for 10 min as previously established (Stutz et al., 2013). Lastly, the ASC-specks were resuspended in CHAPS buffer for further use in cell culture experiments.

Primary microglia culture

A minimum of five C57BL/6j pups were used for all dissections and experiments, and postnatal (P0-3) mouse pup cortices were used to generate primary microglia cultures (Daniele et al., 2014, 2015; Sánchez and Maguire-Zeiss, 2020). Cortices were dissected, subsequently homogenized, and grown in a T75 flask for 16-21 days in Microglia Culture Media (MCM; 1× Minimal Essential Medium Earle's (MEM) supplemented with: 1 mM L-glutamine, 1 mM sodium pyruvate, 0.6% v/v D-(+)-glucose, 100 μg/ml Penicillin/Streptomycin (P/S), 4% v/v Fetal Bovine Serum (FBS), 6% v/v Horse Serum). To enrich for microglia, flasks were shaken for 3 h, and the cells of all pups were mixed immediately before plating. Cells were then plated in microglia growth media (MGM) containing 5% v/v Fetal Bovine Serum (MGM; Minimum Essential Medium Earle's (MEM), supplemented with 1 mM sodium pyruvate, 0.6% (v/v) D-(+)-glucose, 1 mM L-glutamine, 100 μg/mL penicillin/streptomycin, and 5% v/v Fetal Bovine Serum) (Béraud et al., 2011, 2013; Daniele et al., 2014, 2015; Sánchez and Maguire-Zeiss, 2020). For all experiments, microglia were plated in a 24-well format at a minimum density of 5.0×10^4 on sterile glass coverslips (12 mm; Deckglaser).

Stimulation of primary microglia

Primary mouse microglia were exposed to 20 or 40 nM catalytic MMP10 (cMMP10; Enzo), PBS (VEH), 25 μM GM6001 (pan-MMP inhibitor; Tocris) + cMMP10, or the positive control LPS (100 ng/mL; Invivogen) in MGM containing 1% FBS (Thermo Fisher) for 24 h in a volume 0.5 mL MGM (24-well). For experiments with treatment of ASC-specks, cells were untreated or stimulated with macrophage derived ASC speck (43.6 μg/mL) in MGM containing 5% FBS in 0.2 mL MGM (24-well) for 12 h as ASC-specks have been investigated previously at this dose and time-point in microglia (Franklin et al., 2014; Friker et al., 2020). The concentration of the ASC specks was estimated with a Pierce BCA Protein Assay Kit (Thermo Fisher) that was read with the Biotek Synergy H1 microplate reader.

Enzyme-linked immunosorbent assays

The protein levels of mouse TNFα, total MMP-3, and IL-1β were determined with enzyme-linked immunosorbent assays (ELISAs) according to the manufacturer's instructions (R&D Systems). Briefly, 50 μL of undiluted cell culture media was placed into each well, which were pre-coated with capture antibody. After a 2 h incubation, washes were performed followed by the addition of an enzyme-linked polyclonal antibody specific for the mouse antigen. After a 2 h incubation, washes were conducted again. Wells were incubated with substrate solution for 30 min and immediately read after the addition of stop solution with the Biotek Synergy H1 microplate reader.

Mesoscale discovery

Levels of numerous pro-inflammatory cytokines were quantified with the V-Plex Mouse Proinflammatory Panel 1 Mouse Kit according to instructions provided by the manufacturer with minor modifications (MesoScale Discovery). Briefly, 50 μL of undiluted cell culture media was placed into each well, which were pre-coated with capture antibody. After a 2 h incubation, two washes were performed followed by the addition of a detection antibody for 2 h. Washes were repeated, and plates were subsequently developed and read using the Mesoscale Discovery MESO QuickPlex SQ 120 system.

MMP10 protein levels were measured in murine microglia with the human MMP10 R-plex MesoScale Discovery kit according to instructions provided by the manufacturer (MesoScale Discovery) since tools to detect MMP10 are limited and MMPs are well conserved in mammals (Zhang et al., 2006; Page-McCaw et al., 2007; Page-McCaw, 2008). Minor modifications were made to optimize the kit for cell culture. Briefly, 25 μL of undiluted cell culture media was placed into each well, which were pre-coated with capture antibody. After a 1 h incubation, two washes were performed followed by the addition of a detection antibody for 1 h. Washes were repeated, and plates were subsequently developed and read using the Mesoscale Discovery MESO QuickPlex SQ 120 system. To determine that MMP10 levels were not elevated due to the cMMP10 that was added externally to the media, a sample of alone was spiked with 40 nM cMMP10. The sample was subsequently added to the MSD plate and measured in the exact same way as the conditioned media (without any cells). The amount of exogenous cMMP10 that was detected by the kit was considered background from treatment and negligible compared to the MMP10 measured in the cMMP10 treated cells.

All MSD data was analyzed with Discovery Workbench 4.0. All measurements were performed in three independent experiments. Each experiment had three technical replicates per treatment.

Iba1 immunocytochemistry

Cells were subjected to a 5 min wash with 1× phosphate buffered saline (PBS) and fixed for 20 min with PBS containing 4% (w/v) paraformaldehyde and 4% (w/v) sucrose, pH 7.4 at room temperature. Incubation for 5 min with PBS containing 0.1% (v/v) Triton X-100 was done to permeabilize cells. Microglia were subsequently blocked for 1 h with PBS containing 10% (v/v) goat serum and incubated overnight at 4°C with rabbit Iba-1 (1:750; Wako) in blocking buffer containing 10% goat serum. After incubation with Alexa Fluor 546 goat IgG secondary antibody (1:1000) in PBS containing 0.1% (v/v) triton X-100 and 1% goat serum, cells were counterstained with 4′,6-diamidino-2-phenylindole (DAPI; 13.0 ng/μL) in PBS, followed by two 5 min PBS washes (Daniele et al., 2015; Sánchez and Maguire-Zeiss, 2020). Coverslips were subsequently mounted with Hydromount (Electron Microscopy Services) in preparation for imaging with the Nikon Eclipse Ti-S inverted fluorescent microscope.

Quantification of microglia morphology

Iba1 positive microglia were imaged and analyzed as previously established (Sánchez and Maguire-Zeiss, 2020). Five unique regions from each coverslip were captured at random by a blinded observer. To ensure that all areas of the coverslip were accurately shown, each coverslip was imaged in a snake-like pattern. To quantify cell morphology, Image J software (National Institute of Health) was used. Briefly, image type was transformed to 8-bit, followed by the adjustment of each image to a uniform threshold. Note that threshold was optimized so that the entire area of the whole cell was included. Each cell was then manually selected with the wand tool to collect its measurements. These Image J measurements included whole cell body area, Feret ratio (minimum Feret/maximum Feret), roundness ($4 \times \text{area}/\pi \times \text{major axis}^2$ or inverse of aspect ratio), and circularity ($4\pi \times \text{area/perimeter}^2$). Note that according to ImageJ, maximum Feret is the greatest distance between any two points of a selected object while minimum Feret is the shortest distance. Cells were not included in the analysis if they were Iba1 negative, lacked a nucleus, or had more than one nucleus. A minimum of 3–4 technical replicates (wells) per treatment were used in one independent experiment to evaluate microglia morphology. Values from individual cells is reported here instead since cells are not homogenous in primary mouse cultures. Values from individual cells are represented on the graphs and were used to conduct the statistical tests as described below.

Quantification of microglia phenotype

A blinded observer manually classified microglia phenotype based on the number of processes on each Iba1 positive cell using the images obtained to evaluate morphology. The cells were organized into three categories; rod-like (2–3 processes small cell body), ameboid (large cell body no processes), and complex (4 or more processes) since these categories are based on previously established literature (Ayoub and Salm, 2003; Fernández-Arjona et al., 2017; Martini et al., 2020). This data was used to calculate the number of cells that were not rod-like in each frame or image.

Statistical analysis

All experiments were performed a minimum of three times independently unless otherwise noted. Each experiment contained at least three technical replicates for each treatment group. GraphPad Prism, Version 8 was used to analyze all data. Either a Student's *t*-test or one-way analysis of variance (ANOVA) was used to analyze data for all experiments excluding the LPS group, which was used as a positive control. The appropriate statistical test was selected based on the number of groups of interest analyzed. For the comparison of two groups a Student's *t*-test was utilized while a one-way ANOVA was employed to compare three experimental groups. Since cells in primary murine cultures lack uniformity, data points shown represent individual cells for morphology as established in previous literature. More specifically, the average value for each well was not used due to this lack of homogeneity (Allen et al., 2016; Hoenen et al., 2016; De Biase et al., 2017; Winland et al., 2017; Abdolhoseini et al., 2019; Svoboda et al., 2019). For every analysis, significance threshold was set at $P \leq 0.05$. Data are represented as mean ± SEMS.

Results

Exposure to the inflammasome adaptor protein ASC can induce morphological changes in microglia

Since it is well established that microglia respond to their environment by adopting an ameboid shape in the presence of inflammatory stimuli such as LPS, we wanted to evaluate the impact of enriched ASC aggregates (ASC-specks) on microglia morphology (Torres-Platas et al., 2014; De Biase et al., 2017; Winland et al., 2017). To that end we examined the consequences of ASC-specks treatment on microglial shape 12 h post-treatment. Insoluble ASC-specks cause microglia display a more complex or ameboid shape compared to VEH (**Figure 1A**). When quantified, ASC-specks

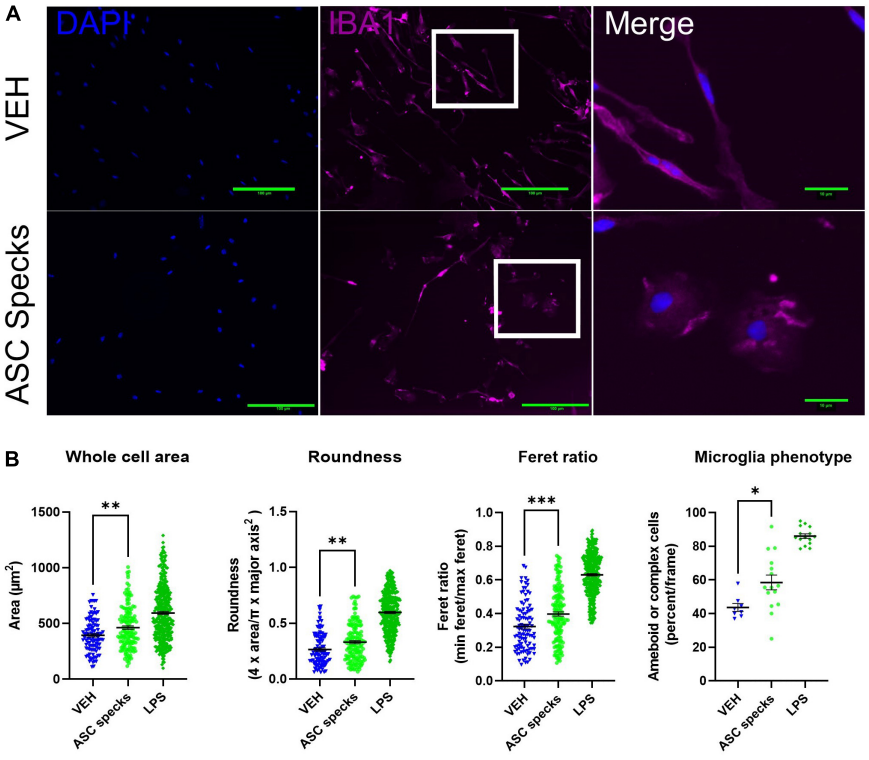

FIGURE 1
Aggregated ASC specks alter microglia shape. Iba1 immunocytochemistry was conducted to quantify cell morphology. **(A)** Microglia were stimulated with ASC specks (43.6 µg/mL) or vehicle (VEH) for 12 h. Microglia structure was visualized with Iba1 (magenta) while the nucleus was stained with DAPI (blue). Microglia that are enlarged are indicated by the white box and shown in the far-right column of each row. **(B)** Consistent with a modification in shape, ASC speck treatment resulted in a morphological shift in microglia. The experiment was conducted one time with three technical replicates (wells) and the values reported are the measurement from each individual cell; VEH n = 103 cells, ASC speck n = 147 cells, and LPS = 360 cells. The percentage of proinflammatory microglia per frame is also altered by treatment; VEH n = 8 images, ASC speck n = 15 images, and LPS = 15 images). Values are reported as mean ± SEM; Unpaired Student's *t*-test compared to VEH; $^{*}P \leq 0.05$, $^{**}P \leq 0.01$, and $^{***}P \leq 0.001$.

display a significantly elevated cell body area, roundness, and Feret ratio. This finding was corroborated since ASC-speck stimulated microglia also display a higher percentage of ameboid or complex cells (Figure 1B).

Microglial exposure to ASC-specks stimulates matrix-metalloproteinases release

Since ASC-specks are elevated in patients with AD and can alter microglial morphology, further studies were warranted. Given that the IL-1β regulates MMP release (Lew et al., 2018), the impact of ASC-specks was evaluated 12 h post-exposure in microglia (Franklin et al., 2014). MMP3 and MMP10 release by primary microglia was measured with ELISA and MSD respectively (Figure 2). Stimulation with ASC-specks (43.6 μg/mL) resulted in the statistically significant release of MMP3 compared to VEH (Figure 2A). LPS served as a positive control for MMP3 release. MMP10 was also elevated upon stimulation of microglia with purified ASC-specks and was significantly higher compared to VEH treated cells based on MSD analyses (Figure 2B). One human plasma sample served as a positive control for the MMP10 measured with MSD. Overall, the elevation in MMPs demonstrated that ASC-specks treatment can stimulate MMP release and that microglia are a source of MMP10.

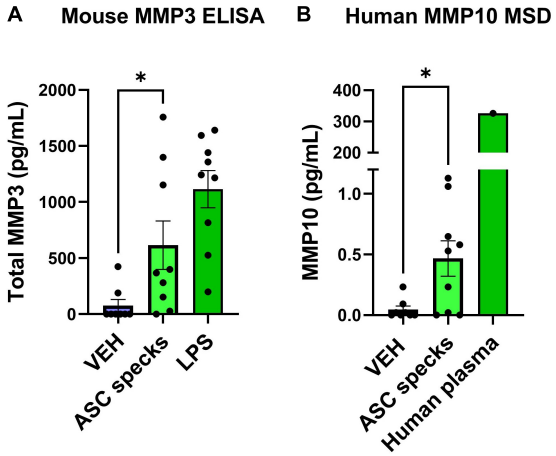

FIGURE 2
Purified ASC speck aggregates stimulate the release of MMPs. ELISA and MSD were performed on supernatants derived from microglia after ASC speck or VEH stimulation. **(A)** Microglia treated with purified ASC specks (43.6 μg/mL) for 12 h increased the release of MMP3 (n = 9 wells/treatment). LPS treated microglia are shown and served as a positive control. **(B)** MMP10 is also released by these cells as determined by MSD (n = 9–8 wells/treatment). One human plasma sample served as a positive control. The values shown are derived from three independent experiments in which there were three technical replicates, or wells, per treatment. Each independent experiment is shown in the graph and was statistically analyzed together. Values are reported as mean ± SEM; Unpaired Student's t-test; $^*P \leq 0.05$.

Microglial stimulation with cMMP10 results in morphological alterations that can be reversed with a pan-matrix-metalloproteinases inhibitor

Since MMP10 is elevated in the central nervous system of dementia patients (Erhardt et al., 2021), the next step was to evaluate the consequences of ASC-specks mediated release of cMMP10 on microglia. To that end, the impact of cMMP10 (40 nM) was assessed by evaluating the shape of murine cortical microglia 24 h post-stimulation (Figure 3). To determine the impact of MMP-inhibition, microglia were also stimulated for 24 h with recombinant catalytic MMP10 (cMMP10; 40 nM) alone or catalytic MMP10 with the pan-MMP inhibitor GM6001. Iba1 immunocytochemistry and ImageJ analyses was used to determine microglia shape as previously described (Sánchez and Maguire-Zeiss, 2020; Figure 3A). cMMP10 induced a statistically significant change in all morphometric measurements, and those alterations were reversed after GM6001 stimulation (Figure 3B). LPS served as a positive control. Whole cell body area, roundness and Feret ratio were higher in vehicle-treated cells compared to cMMP10-stimulated microglia indicative of a rounder appearance (Figure 3B). Lastly, cMMP10 increases the percentage of ameboid or complex microglial compared to VEH. Taken together, changes in these morphological indicate that cells no longer resemble a rod and now have an ameboid shape. These morphological changes were reversed with the pan-MMP inhibitor GM6001, as whole cell area, roundness, and Feret ratio of cells treated with cMMP10 + GM6001 were not significantly different from VEH. GM6001 is not significantly different from VEH (not shown). Overall, these morphological changes indicate a shift in cMMP10-stimulated microglia to a phagocytic shape which likely indicate functional changes in the microglia.

Microglial exposure to cMMP10 stimulates the release of proinflammatory cytokines

After establishing that microglial morphology is altered by cMMP10 treatment, we sought to better comprehend the functional implications of cMMP10 on cytokine release. To that end, we evaluated the release of proinflammatory proteins

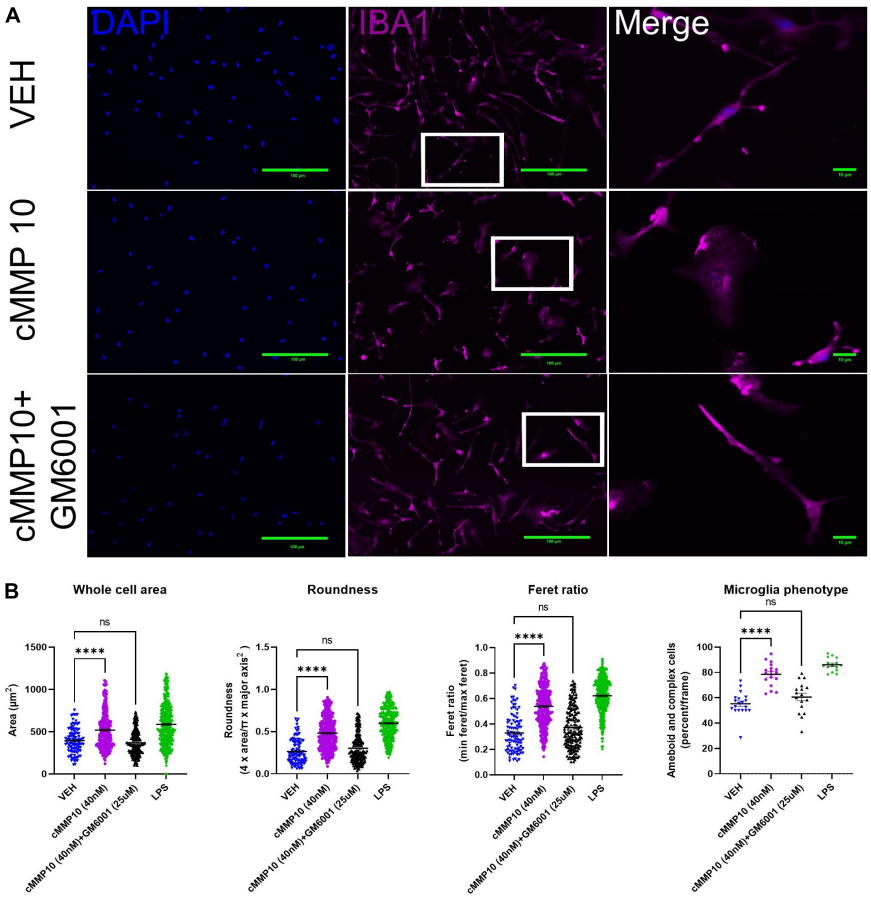

FIGURE 3
cMMP10 induced morphology changes are reversed in microglia with the pan-MMP inhibitor GM6001. **(A)** Iba1 immunocytochemistry (magenta) was conducted on microglia to analyze cell morphology after exposure to 40 nM cMMP10 or vehicle (VEH) for 24 h. Microglia that are enlarged are indicated by the white box and are shown in the far-right column of each row. **(B)** Consistent with a visual change, cMMP10 exposure led to a change in morphological parameters such as whole cell area, roundness, and Feret ratio compared to vehicle treatment; VEH n = 103 cells, cMMP10 n = 340 cells, cMMP10 + GM6001 = 184 cells, and LPS = 360 cells. cMMP10 exposure also increased the percentage of proinflammatory microglia (ameboid or complex); VEH n = 19 images, cMMP10 n = 18 images, cMMP10 + GM6001 = 17 images, and LPS n = 15 images. Notably these changes are reversed by the pan-MMP10 inhibitor GM6001 (no significance compared to VEH). LPS was used as a positive control. Through the experiment was conducted with three technical replicates per treatment, values reported are the measurement from individual cells. When the average of each well is used to perform statistical analysis instead, the trend observed still holds. Values are reported as mean ± SEM; One-way ANOVA compared to VEH; Dunnett's *post-hoc* test; $^{****}P \leq 0.0001$.

twenty-four hours after exposure to cMMP10. A statistically significant increase in the levels of the proinflammatory cytokine IL-6 and chemokine CXCL1 was detected in microglia treated with 40 nM of MMP10, with CXCL1 being released in a dose responsive manner (Figure 4A). TNFα was also observed in microglia upon stimulation with both 20 and 40 nM cMMP10 compared to vehicle-control cells (Figure 4B). Moreover, the release of TNFα was reversed when cMMP10 was incubated with GM6001, as TNFα levels in this group were not significantly compared to VEH (Figure 4B). Note that TNFα release in cells treated with GM6001 alone was undetectable (not shown). In contrast, unlike LPS-induced IL-1β and IL-4 release, stimulation of microglia with either dose of cMMP10 did not result in the secretion of IL-1β or IL-4 secretion (Figure 4C). LPS served as a positive control for the release of all proinflammatory factors shown.

cMMP10 mediated changes on microglia lead to the continued release of MMP10, but not other stromelysins

Since MMP10 activates the release of other MMPs in certain cell types, we wanted to determine if MMP10 stimulates microglial release of stromelysins. More specifically, we wanted to evaluate if cMMP10 could lead to the release of MMP3 or even the autocrine release of MMP10 itself in microglia

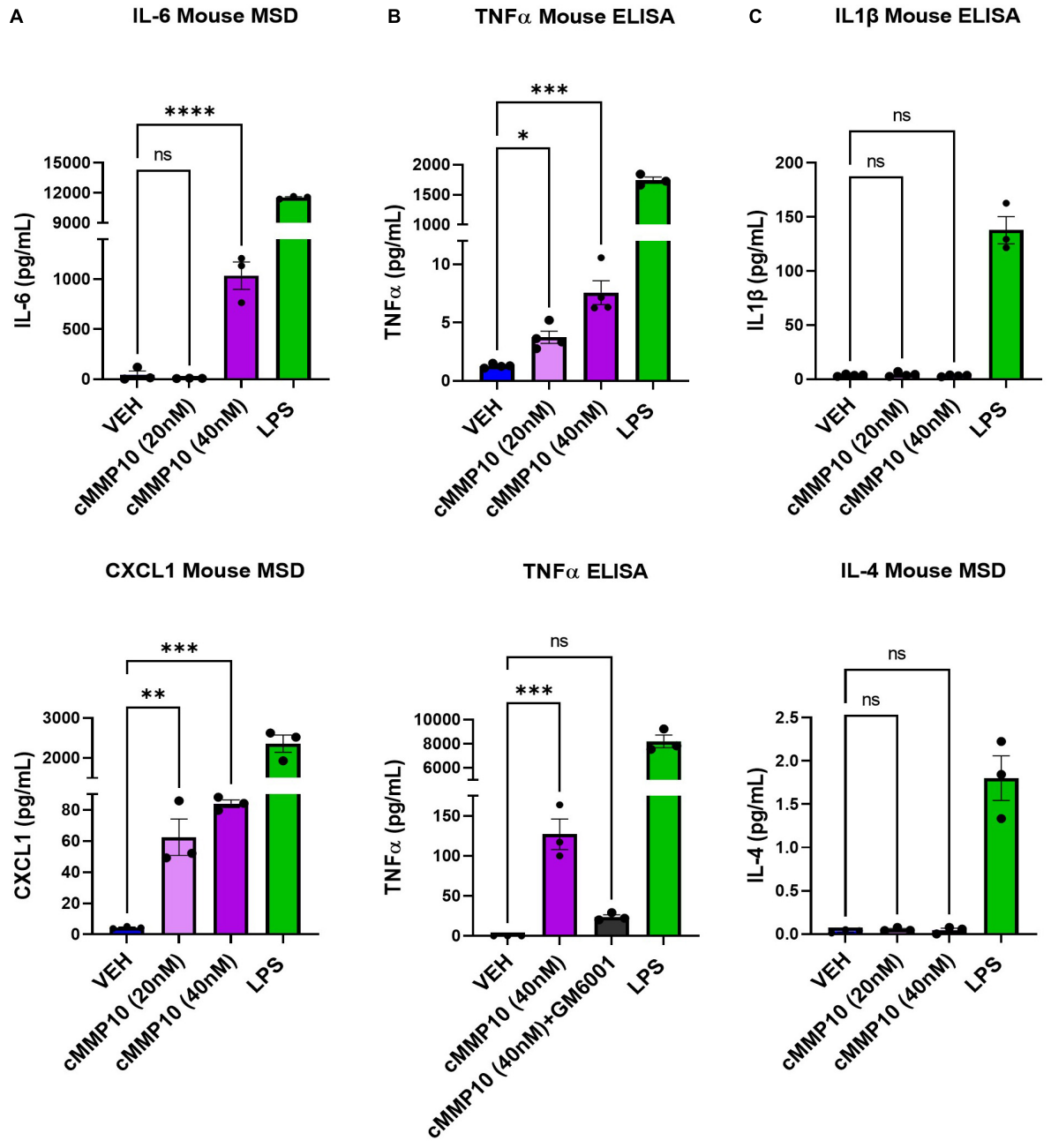

FIGURE 4
The release of classical proinflammatory cytokines is increased in cMMP10-stimulated microglia. Microglia were exposed to cMMP10 (20 or 40 nM) or vehicle (VEH) for 24 h. **(A)** Cells stimulated with 40 nM cMMP10, but not 20 nM cMMP10, significantly increase IL-6. These cells also release CXCL1 release in a dose responsive manner to cMMP10. **(B)** cMMP10-exposed microglia demonstrate higher levels of TNFα in a dose responsive manner compared to VEH treated cells (ELISA; n = 4 wells/treatment). **(B)** The increase of TNFα following cMMP10 exposure was reversed when cMMP10 was incubated with the pan-MMP10 inhibitor GM6001 (ELISA; n = 3 wells/treatment). **(C)** cMMP10 is not sufficient to stimulate the release of IL-1β or IL-4. Values reported are representative of one experiment performed with three technical replicates, or wells, per treatment. The experiment was conducted independently two additional times. Values are reported as mean ± SEM; One-way ANOVA compared to VEH; Dunnett's *post-hoc* test; $^{****}P \leq 0.0001$, $^{***}P \leq 0.001$, $^{**}P \leq 0.01$, and $^{*}P \leq 0.05$.

(Knäuper et al., 1997; Lausch et al., 2009). To that end, first we noted that autocrine-effect and release of MMP10, with an overall increase in the release of MMP10 compared to VEH (Figure 5A). One human plasma sample served as a positive control for MMP10 detection with MSD. In contrast, MMP3 production was not affected when quantified 24 h post-cMMP10 treatment compared to vehicle-treated microglia (Figure 5A). These microglia were capable of

releasing MMP3, as LPS-stimulation induced MMP3 release (**Figure 5B**).

Discussion

Matrix-metalloproteinases are elevated in dementia, and downstream consequences of their activity are relevant to consider. Recently, we found that both MMP10 and the assembled inflammasome complex ASC-specks are elevated in the CSF of dementia patients (Erhardt et al., 2021; Jiang et al., 2021). Microglial cell cultures were utilized to characterize the inflammatory consequences of ASC-speck mediated release of MMP10. Importantly, a novel role of the inflammasome-adaptor protein, ASC, and its assembled form (ASC-specks or pyroptosomes), was identified. Here, we show for the first time that assembled ASC-specks can increase the release of MMPs in primary microglia. We found an increase in MMP3 and MMP10 levels of microglia after ASC-specks exposure. We also ascertained the consequences of ASC/inflammasome-mediated MMP10 release on microglia. More specifically, we found that MMP10 stimulation altered microglial phenotype, suggesting that MMP10 sustains inflammation (**Figure 6**). Its ability to perpetuate continual inflammation is critical to the chronic activation state of microglia observed in disease since it alters their ability to harness autoimmunity (McGeer et al., 1988; Schwartz et al., 2003; McGeer and McGeer, 2008; Perry et al., 2010; Perry and Teeling, 2013).

Our findings indicate that ASC-speck exposure induces morphological changes and stimulates the release of both MMP10 and MMP3 in microglia. The ability of ASC-specks to influence microglia phenotype corroborates previous work. For example, ASC-specks can be released extracellularly and propagate from cell to cell like a prion in the presence of Danger Associated Molecular Patterns (DAMPs) such as amyloid-β and phosphorylated tau (Franklin et al., 2014; Venegas et al., 2017; Jiang et al., 2021). As a consequence, ASC-specks are taken up by adjacent immune cells and trigger a phagocytic phenotype that culminates in the release of IL-1β (Baroja-Mazo et al., 2014; Franklin et al., 2014; Venegas et al., 2017). Taken together, both our findings and previous work suggests that ASC-specks are capable of inducing morphofunctional changes in microglia. Previous literature has also linked the inflammasome to MMP release. IL-1β transcriptionally regulates MMPs, for example MMP13 and MMP9, in multiple cell types (Cheng et al., 2010; Hashimoto et al., 2013; Zhang et al., 2018; Sánchez and Maguire-Zeiss, 2020). IL-1β leads to the release of MMP-1,9,13 in chondrocytes. Furthermore, MMP1 is upregulated by fibroblasts in response to IL-1β.

We also establish that MMP10 stimulation of microglia results in morphological and functional changes through a classical inflammatory pathways regulated by NF-κB such as IL-6, CXCL1, and TNFα (Libermann and Baltimore, 1990; Brasier, 2010; Burke et al., 2014; Daniele et al., 2015). This finding supports previous work that indicate MMPs can stimulate phenotypic changes in microglia. For example, MMP13-stimulation of primary mouse microglia leads to altered shape and the release of TNFα (Sánchez and Maguire-Zeiss, 2020). More relevant to this work, MMP3 is a second example more closely related to MMP10 since it is another stromelysin that is capable of impacting microglia (Connolly et al., 2016; Hu et al., 2016; Brelstaff et al., 2021). Due to the previously established literature related to MMP3, MMP10 was investigated further in our work instead. MMP3 exposure stimulates IL-6 release in AC128 microglial cells and TNFα in BV2 cells (Kim et al., 2005; Connolly et al., 2016). More recently, MMP3 expression has been shown to be a marker of senescent microglia (Brelstaff et al., 2021).

There were other inflammatory factors notably absent after MMP10 stimulation. Often, it has been reported that MMPs can stimulate the release of other MMPs in immune cells (Knäuper et al., 1997; Lausch et al., 2009; Sánchez and Maguire-Zeiss, 2020). For example, in a similar study conducted, microglia released MMP9 in response to MMP13 stimulation (Sánchez and Maguire-Zeiss, 2020). Here we report that MMP10 does not have the capability to release MMP3 in microglia. More specifically, MMP3 was not released by cells though MMP10 was continually released. This finding supports the idea that

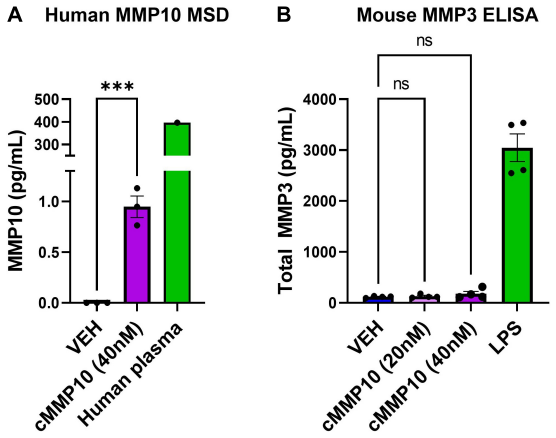

FIGURE 5
Microglia release more MMP10 in response to cMMP10 treatment. ELISAs and MSD were conducted with supernatants collected after exposure to cMMP10 or VEH. **(A)** Microglia treated with cMMP10 (40 nM) for 24 h increased the release of MMP10 as measured by the MMP10 MSD R-plex (n = 3–4 wells/treatment). One human plasma served as a positive control. **(B)** Microglial MMP3 release did not occur in response to MMP10 at any dose (n = 4 wells/treatment; no significance). LPS served as a positive control. Values reported are representative of one experiment that had a minimum of three biological replicates, or wells, per treatment. This experiment was performed independently at least two additional times. Values are reported as mean ± SEM; Unpaired Student's t-test (MSD) or one-way ANOVA compared to VEH (ELISA) Dunnett's $post$-hoc test; $^{***}P \leq 0.001$.

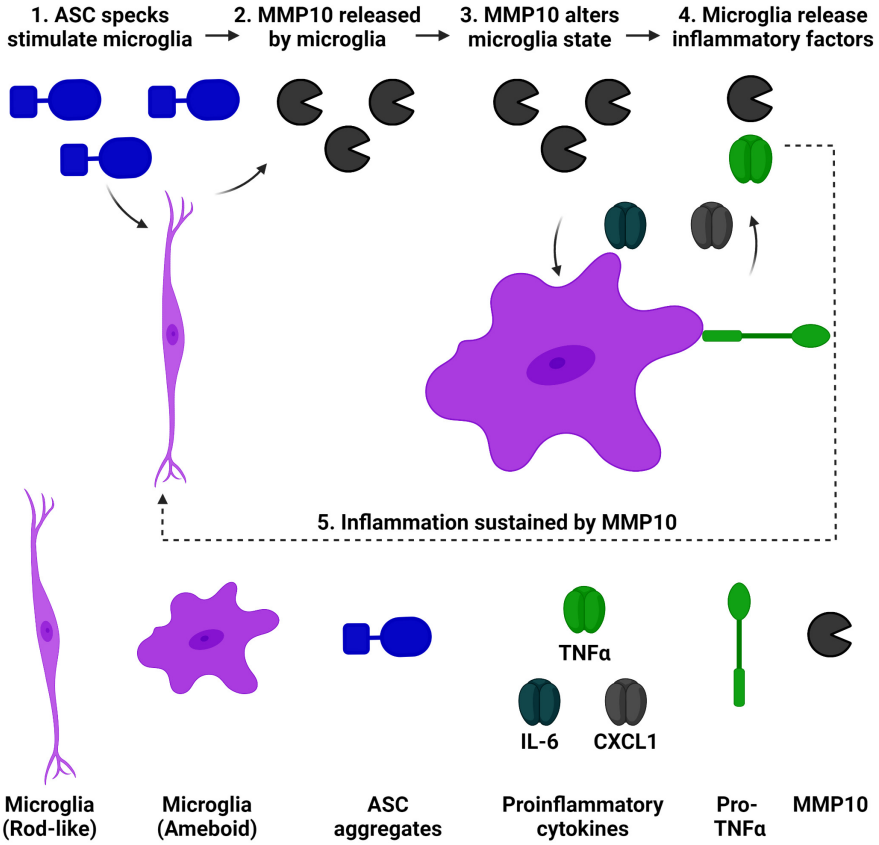

FIGURE 6
ASC speck-mediated of release of MMP10 may perpetuate inflammation of microglia. We have established that ASC-speck aggregates can stimulate the release of MMP10 in primary microglia. As a result of exposure to MMP10, adjacent microglia will take on a pro-inflammatory state. This phenotype includes altered morphology and the release of inflammatory factors TNFα, IL-6, and CXCL1. In addition to classical proinflammatory cytokines, even more MMP10 is released so that it can act on adjacent microglia to continue the cycle of inflammation since IL-4 is not present. Taken together, these findings suggest that MMP10 perpetuates a chronic inflammatory state. Image created with BioRender.

MMP10 and MMP3 are functionally redundant since they are both stromelysins. Perhaps functional redundancy is why only one stromelysin was released upon MMP stimulation. Furthermore, while microglial activation has been previously viewed to be polarized that view is no longer held. In fact, microglia transcriptomics has established how they can express both proinflammatory and anti-inflammatory molecules at the same time (Chen and Trapp, 2016; De Biase et al., 2017; Li et al., 2021), which is a topic for further investigation given the context of current findings.

IL-1β and IL-4 were also not released by microglia upon cMMP10 stimulation. This finding is consistent with previous work related to MMP-induced inflammation of microglia. MMPs do not necessarily stimulate IL-1β release in microglia, as previously demonstrated with MMP13 (Sánchez and Maguire-Zeiss, 2020). Our finding further supports the possibility that MMP-mediated inflammation is inflammasome independent. However, future investigations can better determine that hypothesis. Furthermore, the absence of IL-4 indicates that the microglia are unable to stimulate a repair response to counteract cMMP10 mediated inflammation. In fact, it shifts microglia to a neuroprotective phenotype by influencing functions such as phagocytosis (Yi et al., 2020; Zhang et al., 2021).

Though inflammatory biomarkers have recently emerged as possible contributors to central nervous system damage, many studies have yet to understand the molecular relationship between proteins elevated in patient samples (Lorenzl et al., 2002, 2003; Annese et al., 2015; Connolly et al., 2016; Sánchez and Maguire-Zeiss, 2020; Erhardt et al., 2021). For example, both inflammasome adaptor proteins and MMPs are elevated in AD (Lorenzl et al., 2002, 2003; Antonell et al., 2020; Erhardt et al., 2021). Overall, the results presented here demonstrate that dementia outcomes may be improved through the pharmaceutical targeting of both MMPs and inflammasome related proteins (Caplan and Maguire-Zeiss, 2018). Though the development of MMP inhibitors has well documented obstacles, it is interesting that we were successful at inhibiting the detrimental effects

of this proinflammatory activity with the drug GM6001 (**Figures 4**, **5**). In fact, microglia no longer released TNFα or transformed their morphological phenotype. Both clinically relevant MMP and inflammasome inhibitors warrant further investigation (Allen et al., 2016; Bozzelli et al., 2019; Giriwono et al., 2019). Though this work has described the autocrine effects of MMP10 on microglia, MMP10 target(s) in microglia is yet to be identified. In fact, the TNFα is known to be one of the potential targets of MMP10 cleavage. This is possible given that MMPs are capable of cleaving TNF and that MMP10 stimulation led to the release of TNFα (Könnecke and Bechmann, 2013). One other possible MMP10 target we may study in the future is TREM2 (Guerreiro et al., 2013; Jonsson et al., 2013; Sims et al., 2017; Ulland and Colonna, 2018). *TREM2* variants increase the risk of late onset AD by 2–4-fold, and TREM2 is essential to the metabolic shift related to mTOR signaling in inflammatory microglia (Guerreiro et al., 2013; Sims et al., 2017; Ulland and Colonna, 2018). More pertinent to this study, TREM2 protein levels correlate with MMP10 levels in patients with dementia (Whelan et al., 2019). After identification of a target, potential pathways downstream of the target would also be interesting to examine given the molecular mechanisms linked to altered MMP activity in immune cells. More specifically, tau-mediated release of MMP3 results in decreased phagocytic activity in microglia. This occurs through, both the NF-κB and senescence pathways of microglia, providing evidence that MMP10 should be evaluated in a similar context in the future given the findings of this study (Brelstaff et al., 2021). More specifically, pathways of interest would include those related to TLR signaling (MyD88, NF-κB, etc.) phagocytosis (CD68, TREM2, CX3CR1, etc.), and senescence (P19ARF). Given the limitations of *in vitro* models used in this paper, fully understanding the contribution of specific MMP10 to disease in humans necessitates the use of specific inhibitors and animal models in future studies. For example, MMP10 knockout mice will be used to further corroborate the MMP inhibitor studies. Due to the well-established relationship between IL-1β and MMPs, it is also important to consider that MMP-mediated damage could be prevented by inhibiting inflammasome adaptor proteins. Based on this, future studies will investigate the pathways related to ASC-mediated MMP release. By conducting the proposed investigations, pharmaceutical interventions may be developed in AD.

Data availability statement

The raw data supporting the conclusions of this article will be made available by the authors, without undue reservation.

Ethics statement

The animal study was reviewed and approved by University of New Mexico IACUC.

Author contributions

KS wrote the initial draft and performed all experiments. KB provided feedback on scientific interpretation and edited drafts. GR and KS planned and interpreted experiments. All authors contributed to the article and approved the submitted version.

Funding

The National Institute of Neurological Disorders and Stroke (NINDS) and National Institute on Aging (NIA), and BrightFocus Foundation grant numbers UH3 NS100598 (MARK VCID I) and UF1 NS100598 to GR (MARK VCID II) were the sources of funding for this work as part of the MARKVCID Consortium. This work was also funded by the National Institute of Aging grant number P20 AG068077 to GR as part of the Alzheimer's Disease Research Center Program.

Acknowledgments

We would like to thank our colleagues in the Rosenberg and Bhaskar labs for their assistance with this project. We also thank Shanya Jiang for her training and expertise in inflammasome related experiments. We would also like to thank Sasha Hobson for her assistance with MSD.

Conflict of interest

The authors declare that the research was conducted in the absence of any commercial or financial relationships that could be construed as a potential conflict of interest.

Publisher's note

References

Abdolhoseini, M., Kluge, M. G., Walker, F. R., and Johnson, S. J. (2019). Segmentation, tracing, and quantification of microglial cells from 3D image stacks. *Sci. Rep.* 9:8557. doi: 10.1038/s41598-019-44917-6

Allen, M., Ghosh, S., Ahern, G. P., Villapol, S., Maguire-Zeiss, K. A., and Conant, K. (2016). Protease induced plasticity: Matrix metalloproteinase-1 promotes neurostructural changes through activation of protease activated receptor 1. *Sci. Rep.* 6:35497. doi: 10.1038/srep35497

Annese, V., Herrero, M. T., Di Pentima, M., Gomez, A., Lombardi, L., Ros, C. M., et al. (2015). Metalloproteinase-9 contributes to inflammatory glia activation and nigro-striatal pathway degeneration in both mouse and monkey models of 1-methyl-4-phenyl-1,2,3,6-tetrahydropyridine (MPTP)-induced Parkinsonism. *Brain Struct. Funct.* 220, 703–727. doi: 10.1007/s00429-014-0718-8

Antonell, A., Tort-Merino, A., Ríos, J., Balasa, M., Borrego-Écija, S., Auge, J. M., et al. (2020). Synaptic, axonal damage and inflammatory cerebrospinal fluid biomarkers in neurodegenerative dementias. *Alzheimers Dement.* 16, 262–272. doi: 10.1016/J.JALZ.2019.09.001

Ayoub, A. E., and Salm, A. K. (2003). Increased morphological diversity of microglia in the activated hypothalamic supraoptic nucleus. *J. Neurosci.* 23, 7759–7766. doi: 10.1523/JNEUROSCI.23-21-07759.2003

Baroja-Mazo, A., Martín-Sánchez, F., Gomez, A. I., Martínez, C. M., Amores-Iniesta, J., Compan, V., et al. (2014). The NLRP3 inflammasome is released as a particulate danger signal that amplifies the inflammatory response. *Nat. Immunol.* 15, 738–748. doi: 10.1038/NI.2919

Béraud, D., Hathaway, H. A., Trecki, J., Chasovskikh, S., Johnson, D. A., Johnson, J. A., et al. (2013). Microglial activation and antioxidant responses induced by the Parkinson's disease protein α-synuclein. *J. Neuroimmune Pharmacol.* 8, 94–117. doi: 10.1007/s11481-012-9401-0

Béraud, D., Twomey, M., Bloom, B., Mittereder, A., Ton, V., Neitzke, K., et al. (2011). α-synuclein alters toll-like receptor expression. *Front. Neurosci.* 5:80. doi: 10.3389/fnins.2011.00080

Bozzelli, P. L., Yin, T., Avdoshina, V., Mocchetti, I., Conant, K. E., and Maguire-Zeiss, K. A. (2019). HIV-1 Tat promotes astrocytic release of CCL2 through MMP/PAR-1 signaling. *Glia* 67, 1719–1729. doi: 10.1002/glia.23642

Brasier, A. R. (2010). The nuclear factor-κB–interleukin-6 signalling pathway mediating vascular inflammation. *Cardiovasc. Res.* 86:211. doi: 10.1093/CVR/CVQ076

Brelstaff, J. H., Mason, M., Katsinelos, T., McEwan, W. A., Ghetti, B., Tolkovsky, A. M., et al. (2021). Microglia become hypofunctional and release metalloproteases and tau seeds when phagocytosing live neurons with P301S tau aggregates. *Sci. Adv.* 7:eabg4980.

Burke, S. J., Lu, D., Sparer, T. E., Masi, T., Goff, M. R., Karlstad, M. D., et al. (2014). NF-κB and STAT1 control CXCL1 and CXCL2 gene transcription. *Am. J. Physiol. Endocrinol. Metab.* 306, E131–E149. doi: 10.1152/AJPENDO.00347.2013

Caplan, I. F., and Maguire-Zeiss, K. A. (2018). Toll-like receptor 2 signaling and current approaches for therapeutic modulation in synucleinopathies. *Front. Pharmacol.* 9:417. doi: 10.3389/fphar.2018.00417

Chen, Z., and Trapp, B. D. (2016). Microglia and neuroprotection. *J. Neurochem.* 136, 10–17. doi: 10.1111/jnc.13062

Cheng, C. Y., Kuo, C. T., Lin, C. C., Hsieh, H. L., and Yang, C. M. (2010). IL-1beta induces expression of matrix metalloproteinase-9 and cell migration via a c-Src-dependent, growth factor receptor transactivation in A549 cells. *Br. J. Pharmacol.* 160, 1595–1610. doi: 10.1111/J.1476-5381.2010.00858.X

Connolly, C., Magnusson-Lind, A., Lu, G., Wagner, P. K., Southwell, A. L., Hayden, M. R., et al. (2016). Enhanced immune response to MMP3 stimulation in microglia expressing mutant huntingtin. *Neuroscience* 325, 74–88. doi: 10.1016/j.neuroscience.2016.03.031

Daniele, S. G., Beraud, D., Davenport, C., Cheng, K., Yin, H., and Maguire-Zeiss, K. A. (2015). Activation of MyD88-dependent TLR1/2 signaling by misfolded -synuclein, a protein linked to neurodegenerative disorders. *Sci. Signal.* 8:ra45. doi: 10.1126/scisignal.2005965

Daniele, S. G., Edwards, A. A., and Maguire-Zeiss, K. A. (2014). Isolation of cortical microglia with preserved immunophenotype and functionality from murine neonates. *J. Vis. Exp.* 83:e51005. doi: 10.3791/51005

De Biase, L. M., Schuebel, K. E., Fusfeld, Z. H., Jair, K., Hawes, I. A., Cimbro, R., et al. (2017). Local cues establish and maintain region-specific phenotypes of basal ganglia microglia. *Neuron* 95, 341–356.e6. doi: 10.1016/j.neuron.2017.06.020

Erhardt, E. B., Adair, J. C., Knoefel, J. E., Caprihan, A., Prestopnik, J., Thompson, J., et al. (2021). Inflammatory biomarkers aid in diagnosis of dementia. *Front. Aging Neurosci.* 13:717344. doi: 10.3389/FNAGI.2021.717344

Facci, L., Barbierato, M., Zusso, M., Skaper, S. D., and Giusti, P. (2018). Serum amyloid A primes microglia for ATP-dependent interleukin-1β release. *J. Neuroinflammation* 15:164. doi: 10.1186/s12974-018-1205-6

Fernandes-Alnemri, T., and Alnemri, E. S. (2008). Chapter thirteen assembly, purification, and assay of the activity of the ASC pyroptosome. *Methods Enzymol.* 442, 251–270. doi: 10.1016/S0076-6879(08)01413-4

Fernández-Arjona, M., del, M., Grondona, J. M., Granados-Durán, P., Fernández-Llebrez, P., and López-Ávalos, M. D. (2017). Microglia morphological categorization in a rat model of neuroinflammation by hierarchical cluster and principal components analysis. *Front. Cell. Neurosci.* 11:235. doi: 10.3389/fncel.2017.00235

Franklin, B. S., Bossaller, L., De Nardo, D., Ratter, J. M., Stutz, A., Engels, G., et al. (2014). The adaptor ASC has extracellular and "prionoid" activities that propagate inflammation. *Nat. Immunol.* 15, 727–737. doi: 10.1038/ni.2913

Friker, L. L., Scheiblich, H., Hochheiser, I. V., Brinkschulte, R., Riedel, D., Latz, E., et al. (2020). β-amyloid clustering around ASC fibrils boosts its toxicity in microglia. *Cell Rep.* 30, 3743–3754.e6. doi: 10.1016/J.CELREP.2020.02.025

Giriwono, P. E., Shirakawa, H., Ohsaki, Y., Sato, S., Aoyama, Y., Ho, H. J., et al. (2019). Geranylgeraniol suppresses the expression of IRAK1 and TRAF6 to inhibit NFκB activation in lipopolysaccharide-induced inflammatory responses in human macrophage-like cells. *Int. J. Mol. Sci.* 20:2320. doi: 10.3390/ijms20092320

Guerreiro, R., Wojtas, A., Bras, J., Carrasquillo, M., Rogaeva, E., Majounie, E., et al. (2013). TREM2 variants in Alzheimer's disease. *N. Engl. J. Med.* 368, 117–127. doi: 10.1056/NEJMOA1211851

Hashimoto, K., Otero, M., Imagawa, K., De Andrés, M. C., Coico, J. M., Roach, H. I., et al. (2013). Regulated transcription of human matrix metalloproteinase 13 (MMP13) and interleukin-1β (IL1B) genes in chondrocytes depends on methylation of specific proximal promoter CpG sites. *J. Biol. Chem.* 288, 10061–10072. doi: 10.1074/jbc.M112.421156

Heneka, M. T., Kummer, M. P., Stutz, A., Delekate, A., Schwartz, S., Vieira-Saecker, A., et al. (2013). NLRP3 is activated in Alzheimer's disease and contributes to pathology in APP/PS1 mice. *Nature* 493, 674–678. doi: 10.1038/NATURE11729

Hoenen, C., Gustin, A., Birck, C., Kirchmeyer, M., Beaume, N., Felten, P., et al. (2016). Alpha-synuclein proteins promote pro-inflammatory cascades in microglia: Stronger effects of the a53t mutant. *PLoS One* 11:e0162717. doi: 10.1371/journal.pone.0162717

Hu, T., You, Q., Chen, D., Tong, J., Shang, L., Luo, J., et al. (2016). Inhibiting matrix metalloproteinase 3 ameliorates neuronal loss in the ganglion cell layer of rats in retinal ischemia/reperfusion. *Neurochem. Res.* 41, 1107–1118. doi: 10.1007/s11064-015-1800-1

Jiang, S., Maphis, N. M., Binder, J., Chisholm, D., Weston, L., Duran, W., et al. (2021). Proteopathic tau primes and activates interleukin-1β via myeloid-cell-specific MyD88- and NLRP3-ASC-inflammasome pathway. *Cell Rep.* 36:109720. doi: 10.1016/J.CELREP.2021.109720

Jonsson, T., Stefansson, H., Steinberg, S., Jonsdottir, I., Jonsson, P. V., Snaedal, J., et al. (2013). Variant of TREM2 associated with the risk of Alzheimer's disease. *N. Engl. J. Med.* 368:107. doi: 10.1056/NEJMOA1211103

Kerkhofs, D., Van Hagen, B. T., Milanova, I. V., Schell, K. J., Van Essen, H., Wijnands, E., et al. (2020). Pharmacological depletion of microglia and perivascular macrophages prevents vascular cognitive impairment in Ang II-induced hypertension. *Theranostics* 10:9512. doi: 10.7150/THNO.44394

Kim, Y. S., Kim, S. S., Cho, J. J., Choi, D. H., Hwang, O., Shin, D. H., et al. (2005). Matrix metalloproteinase-3: A novel signaling proteinase from apoptotic neuronal cells that activates microglia. *J. Neurosci.* 25, 3701–3711. doi: 10.1523/JNEUROSCI.4346-04.2005

Knäuper, V., Smith, B., López-Otin, C., and Murphy, G. (1997). Activation of progelatinase B (proMMP-9) by active collagenase-3 (MMP-13). *Eur. J. Biochem.* 248, 369–373. doi: 10.1111/j.1432-1033.1997.00369.x

Könnecke, H., and Bechmann, I. (2013). The role of microglia and matrix metalloproteinases involvement in neuroinflammation and gliomas. *Clin. Dev. Immunol.* 2013:914104. doi: 10.1155/2013/914104

Latz, E., Xiao, T. S., and Stutz, A. (2013). Activation and regulation of the inflammasomes. *Nat. Rev. Immunol.* 13, 397–411. doi: 10.1038/nri3452

Lausch, E., Keppler, R., Hilbert, K., Cormier-Daire, V., Nikkel, S., Nishimura, G., et al. (2009). Mutations in MMP9 and MMP13 determine the mode of inheritance

and the clinical spectrum of metaphyseal anadysplasia. *Am. J. Hum. Genet.* 85, 168–178. doi: 10.1016/j.ajhg.2009.06.014

Lew, J. H., Naruishi, K., Kajiura, Y., Nishikawa, Y., Ikuta, T., Kido, J. I., et al. (2018). High glucose-mediated cytokine regulation in gingival fibroblasts and THP-1 macrophage: A possible mechanism of severe periodontitis with diabetes. *Cell. Physiol. Biochem.* 50, 987–1004. doi: 10.1159/000494481

Li, J., Shui, X., Sun, R., Wan, L., Zhang, B., Xiao, B., et al. (2021). Microglial Phenotypic Transition: Signaling Pathways and Influencing Modulators Involved in Regulation in Central Nervous System Diseases. *Front. Cell. Neurosci.* 15:359. doi: 10.3389/FNCEL.2021.736310/BIBTEX

Libermann, T. A., and Baltimore, D. (1990). Activation of interleukin-6 gene expression through the NF-kappa B transcription factor. *Mol. Cell. Biol.* 10:2327. doi: 10.1128/MCB.10.5.2327

Lorenzl, S., Albers, D. S., LeWitt, P. A., Chirichigno, J. W., Hilgenberg, S. L., Cudkowicz, M. E., et al. (2003). Tissue inhibitors of matrix metalloproteinases are elevated in cerebrospinal fluid of neurodegenerative diseases. *J. Neurol. Sci.* 207, 71–76. doi: 10.1016/S0022-510X(02)00398-2

Lorenzl, S., Albers, D. S., Narr, S., Chirichigno, J., and Beal, M. F. (2002). Expression of MMP-2, MMP-9, and MMP-1 and their endogenous counterregulators TIMP-1 and TIMP-2 in postmortem brain tissue of Parkinson's disease. *Exp. Neurol.* 178, 13–20. doi: 10.1006/exnr.2002.8019

Martini, A. C., Helman, A. M., McCarty, K. L., Lott, I. T., Doran, E., Schmitt, F. A., et al. (2020). Distribution of microglial phenotypes as a function of age and Alzheimer's disease neuropathology in the brains of people with Down syndrome. *Alzheimers Dement.* 12:e12113. doi: 10.1002/DAD2.12113

McGeer, P. L., Itagaki, S., Boyes, B. E., and McGeer, E. G. (1988). Reactive microglia are positive for HLA-DR in the substantia nigra of Parkinson's and Alzheimer's disease brains. *Neurology* 38, 1285–1291. doi: 10.1212/WNL.38.8.1285

McGeer, P. L., and McGeer, E. G. (2008). Glial reactions in Parkinson's disease. *Mov. Disord.* 23, 474–483. doi: 10.1002/mds.21751

Page-McCaw, A. (2008). Remodeling the model organism: Matrix metalloproteinase functions in invertebrates. *Semin. Cell Dev. Biol.* 19, 14–23. doi: 10.1016/j.semcdb.2007.06.004

Page-McCaw, A., Ewald, A. J., and Werb, Z. (2007). Matrix metalloproteinases and the regulation of tissue remodelling. *Nat. Rev. Mol. Cell Biol.* 83, 221–233. doi: 10.1038/nrm2125

Perry, V. H., Nicoll, J. A. R., and Holmes, C. (2010). Microglia in neurodegenerative disease. *Nat. Rev. Neurol.* 6, 193–201. doi: 10.1038/NRNEUROL.2010.17

Perry, V. H., and Teeling, J. (2013). Microglia and macrophages of the central nervous system: The contribution of microglia priming and systemic inflammation to chronic neurodegeneration. *Semin. Immunopathol.* 35:601. doi: 10.1007/S00281-013-0382-8

Prince, M., Bryce, R., Albanese, E., Wimo, A., Ribeiro, W., and Ferri, C. P. (2013). The global prevalence of dementia: A systematic review and metaanalysis. *Alzheimers Dement.* 9, 63–75.e2. doi: 10.1016/J.JALZ.2012.11.007

Rathinam, V. A. K., and Fitzgerald, K. A. (2016). Inflammasome complexes: Emerging mechanisms and effector functions. *Cell* 165, 792–800. doi: 10.1016/j.cell.2016.03.046

Reis, A. S., Barboza, R., Murillo, O., Barateiro, A., Peixoto, E. P. M., Lima, F. A., et al. (2020). Inflammasome activation and IL-1 signaling during placental malaria induce poor pregnancy outcomes. *Sci. Adv.* 6:eaax6346. doi: 10.1126/sciadv.aax6346

Ribeiro, D. E., Oliveira-Giacomelli, Á, Glaser, T., Arnaud-Sampaio, V. F., Andrejew, R., Dieckmann, L., et al. (2020). Hyperactivation of P2X7 receptors as a culprit of COVID-19 neuropathology. *Mol. Psychiatry* 26, 1044–1059. doi: 10.1038/s41380-020-00965-3

Rosenberg, G. A. (2009). Matrix metalloproteinases and their multiple roles in neurodegenerative diseases. *Lancet Neurol.* 8, 205–216. doi: 10.1016/S1474-4422(09)70016-X

Sánchez, K., and Maguire-Zeiss, K. (2020). MMP13 expression is increased following mutant α-synuclein exposure and promotes inflammatory responses in microglia. *Front. Neurosci.* 14:585544. doi: 10.3389/fnins.2020.585544

Schwartz, M., Shaked, I., Fisher, J., Mizrahi, T., and Schori, H. (2003). Protective autoimmunity against the enemy within: Fighting glutamate toxicity. *Trends Neurosci.* 26, 297–302. doi: 10.1016/S0166-2236(03)00126-7

Scott, X. O., Stephens, M. E., Desir, M. C., Dietrich, W. D., Keane, R. W., Vaccari, J. P., et al. (2020). The inflammasome adaptor protein ASC in mild cognitive impairment and Alzheimer's disease. *Int. J. Mol. Sci.* 21:4674. doi: 10.3390/IJMS21134674

Sims, R., Van Der Lee, S. J., Naj, A. C., Bellenguez, C., Badarinarayan, N., Jakobsdottir, J., et al. (2017). Rare coding variants in PLCG2, ABI3 and TREM2 implicate microglial-mediated innate immunity in Alzheimer's disease. *Nat. Genet.* 49:1373. doi: 10.1038/NG.3916

Stutz, A., Horvath, G. L., Monks, B. G., and Latz, E. (2013). ASC speck formation as a readout for inflammasome activation. *Methods Mol. Biol.* 1040, 91–101. doi: 10.1007/978-1-62703-523-1_8

Sutterwala, F. S., Ogura, Y., Szczepanik, M., Lara-Tejero, M., Lichtenberger, G. S., Grant, E. P., et al. (2006). Critical role for NALP3/CIAS1/cryopyrin in innate and adaptive immunity through its regulation of caspase-1. *Immunity* 24, 317–327. doi: 10.1016/j.immuni.2006.02.004

Svoboda, D. S., Barrasa, M. I., Shu, J., Rietjens, R., Zhang, S., Mitalipova, M., et al. (2019). Human iPSC-derived microglia assume a primary microglia-like state after transplantation into the neonatal mouse brain. *Proc. Natl. Acad. Sci. U. S. A.* 116, 25293–25303. doi: 10.1073/pnas.1913541116

Torres-Platas, S. G., Comeau, S., Rachalski, A., Bo, G. D., Cruceanu, C., Turecki, G., et al. (2014). Morphometric characterization of microglial phenotypes in human cerebral cortex. *J. Neuroinflammation* 11:12. doi: 10.1186/1742-2094-11-12

Ueno, M., Wu, B., Nishiyama, A., Huang, C. L., Hosomi, N., Kusaka, T., et al. (2009). The expression of matrix metalloproteinase-13 is increased in vessels with blood-brain barrier impairment in a stroke-prone hypertensive model. *Hypertens. Res.* 32, 332–338. doi: 10.1038/hr.2009.26

Ulland, T. K., and Colonna, M. (2018). TREM2 — a key player in microglial biology and Alzheimer disease. *Nat. Rev. Neurol.* 1411, 667–675. doi: 10.1038/s41582-018-0072-1

Venegas, C., Kumar, S., Franklin, B. S., Dierkes, T., Brinkschulte, R., Tejera, D., et al. (2017). Microglia-derived ASC specks cross-seed amyloid-β in Alzheimer's disease. *Nature* 552, 355–361. doi: 10.1038/NATURE25158

Whelan, C. D., Mattsson, N., Nagle, M. W., Vijayaraghavan, S., Hyde, C., Janelidze, S., et al. (2019). Multiplex proteomics identifies novel CSF and plasma biomarkers of early Alzheimer's disease. *Acta Neuropathol. Commun.* 7:169. doi: 10.1186/S40478-019-0795-2/FIGURES/3

White, C. S., Lawrence, C. B., Brough, D., and Rivers-Auty, J. (2017). Inflammasomes as therapeutic targets for Alzheimer's disease. *Brain Pathol.* 27, 223–234. doi: 10.1111/bpa.12478

Winland, C. D., Welsh, N., Sepulveda-Rodriguez, A., Vicini, S., and Maguire-Zeiss, K. A. (2017). Inflammation alters AMPA-stimulated calcium responses in dorsal striatal D2 but not D1 spiny projection neurons. *Eur. J. Neurosci.* 46, 2519–2533. doi: 10.1111/ejn.13711

Yang, Y., Estrada, E. Y., Thompson, J. F., Liu, W., and Rosenberg, G. A. (2007). Matrix metalloproteinase-mediated disruption of tight junction proteins in cerebral vessels is reversed by synthetic matrix metalloproteinase inhibitor in focal ischemia in rat. *J. Cereb. Blood Flow Metab.* 27, 697–709. doi: 10.1038/sj.jcbfm.9600375

Yang, Y., and Rosenberg, G. A. (2011). MMP-mediated disruption of claudin-5 in the blood-brain barrier of rat brain after cerebral ischemia. *Methods Mol. Biol.* 762, 333–345. doi: 10.1007/978-1-61779-185-7_24

Yi, S., Jiang, X., Tang, X., Li, Y., Xiao, C., Zhang, J., et al. (2020). IL-4 and IL-10 promotes phagocytic activity of microglia by up-regulation of TREM2. *Cytotechnology* 72:589. doi: 10.1007/S10616-020-00409-4

Zhang, J., Rong, P., Zhang, L., He, H., Zhou, T., Fan, Y., et al. (2021). IL4-driven microglia modulate stress resilience through BDNF-dependent neurogenesis. *Sci. Adv.* 7, 9888–9905. doi: 10.1126/SCIADV.ABB9888/SUPPL_FILE/ABB9888_SM.PDF

Zhang, L., Ma, S., Su, H., and Cheng, J. (2018). Isoliquiritigenin inhibits IL-1&-induced production of matrix metalloproteinase in articular chondrocytes. *Mol. Ther. Methods Clin. Dev.* 9, 153–159. doi: 10.1016/j.omtm.2018.02.006

Zhang, S., Dailey, G. M., Kwan, E., Glasheen, B. M., Sroga, G. E., and Page-McCaw, A. (2006). An MMP liberates the Ninjurin A ectodomain to signal a lossof cell adhesion. *Genes Dev.* 20:1899. doi: 10.1101/GAD.1426906

Zheng, D., Liwinski, T., and Elinav, E. (2020). Inflammasome activation and regulation: Toward a better understanding of complex mechanisms. *Cell Discov.* 6:36. doi: 10.1038/s41421-020-0167-x

frontiers | Frontiers in Molecular Neuroscience

TYPE Original Research
PUBLISHED 19 October 2022
DOI 10.3389/fnmol.2022.931859

OPEN ACCESS

EDITED BY
Andreas Vlachos,
University of Freiburg, Germany

REVIEWED BY
Peter Jedlicka,
Goethe University Frankfurt, Germany
Miquel Bosch,
International University of Catalonia, Spain

*CORRESPONDENCE
Kristin Michaelsen-Preusse
k.michaelsen@tu-braunschweig.de

†These authors have contributed equally to this work and share first authorship

SPECIALTY SECTION
This article was submitted to Neuroplasticity and Development, a section of the journal Frontiers in Molecular Neuroscience

RECEIVED 29 April 2022
ACCEPTED 21 September 2022
PUBLISHED 19 October 2022

CITATION
Hosseini S, van Ham M, Erck C, Korte M and Michaelsen-Preusse K (2022) The role of α-tubulin tyrosination in controlling the structure and function of hippocampal neurons. *Front. Mol. Neurosci.* 15:931859. doi: 10.3389/fnmol.2022.931859

The role of α-tubulin tyrosination in controlling the structure and function of hippocampal neurons

Shirin Hosseini[1,2†], Marco van Ham[3†], Christian Erck[3], Martin Korte[1,2] and Kristin Michaelsen-Preusse[1*]

[1]Department of Cellular Neurobiology, Zoological Institute, Technische Universität Braunschweig, Braunschweig, Germany, [2]Research Group Neuroinflammation and Neurodegeneration, Helmholtz Centre for Infection Research, Braunschweig, Germany, [3]Research Group Cellular Proteome Research, Helmholtz Centre for Infection Research, Braunschweig, Germany

Microtubules (MTs) are central components of the neuronal cytoskeleton and play a critical role in CNS integrity, function, and plasticity. Neuronal MTs are diverse due to extensive post-translational modifications (PTMs), particularly detyrosination/tyrosination, in which the C-terminal tyrosine of α-tubulin is cyclically removed by a carboxypeptidase and reattached by a tubulin-tyrosine ligase (TTL). The detyrosination/tyrosination cycle of MTs has been shown to be an important regulator of MT dynamics in neurons. TTL-null mice exhibit impaired neuronal organization and die immediately after birth, indicating TTL function is vital to the CNS. However, the detailed cellular role of TTL during development and in the adult brain remains elusive. Here, we demonstrate that conditional deletion of TTL in the neocortex and hippocampus during network development results in a pathophysiological phenotype defined by incomplete development of the corpus callosum and anterior commissures due to axonal growth arrest. TTL loss was also associated with a deficit in spatial learning, impaired synaptic plasticity, and reduced number of spines in hippocampal neurons, suggesting that TTL also plays a critical role in hippocampal network development. TTL deletion after postnatal development, specifically in the hippocampus and in cultured hippocampal neurons, led to a loss of spines and impaired spine structural plasticity. This indicates a novel and important function of TTL for synaptic plasticity in the adult brain. In conclusion, this study reveals the importance of α-tubulin tyrosination, which defines the dynamics of MTs, in controlling proper network formation and suggests TTL-mediated tyrosination as a new key determinant of synaptic plasticity in the adult brain.

KEYWORDS

microtubules, tubulin-tyrosine ligase, dendritic spine, synaptic plasticity, memory

Introduction

Microtubules (MTs) are part of the cytoskeleton involved in a variety of cellular functions, including cell division, intracellular transport, and cell shape. They form bundles that are particularly prominent in neurons. Since neurons are differentiated cells, the organization of MTs is critically important for the elaborate architecture of axons and dendrites (Dent and Baas, 2014). They play, for instance, critical roles in the formation and maintenance of axonal growth cones during development and in regeneration after injury (Bradke et al., 2012). In neurons, MTs consist of both highly dynamic and stable subpopulations that correlate with neuronal subcompartments. In the axon, a higher percentage of the total microtubule mass is stable compared to the situation in the dendrite (Baas et al., 2016). Beyond this general role in supporting neurite integrity and organelle transport, MTs may be even more actively involved in signal transduction (Dent and Baas, 2014). At the plus-ends of highly dynamic MTs, end-binding proteins (+TIPs) are associated with signaling cascades important for neuronal structure and plasticity (Baas et al., 2016).

Dynamic MTs substantially contribute to modulating synaptic structure and function. In the presynaptic compartment, dynamic MTs control neurotransmission by promoting the transport of synaptic vesicles for neurotransmitter release (Qu et al., 2019). At the postsynapse, which is predominantly localized at dendritic spines in cortical brain regions, the major cytoskeletal element is F-actin (Hotulainen and Hoogenraad, 2010), yet a structural and functional interplay between dendritic MTs and the actin cytoskeleton within spines has been described (Jaworski et al., 2009). Dynamic MTs frequently invade dendritic spines and are important for spinogenesis, synaptic targeting of NMDA receptors, and even synaptic plasticity (Gu et al., 2008; Kapitein et al., 2011; Martel et al., 2016). This is supported by the fact that blocking dynamic MTs by low doses of nocodazole impairs long-term potentiation (LTP) (Jaworski et al., 2009). Consistent with these findings, the transient accumulation of dynamic MTs in hippocampal dendritic spines is necessary for learning and memory processes in contextual fear conditioning, NMDA-dependent memory tasks, and memory discrimination tasks (Uchida et al., 2014; Martel et al., 2016). Although the general importance of dynamic MTs for synaptic function and plasticity has been demonstrated, the detailed molecular mechanisms by which dynamic MTs are regulated in neurons remain mostly elusive.

Post-translational modifications (PTMs) of tubulin subunits increase their diversity and provide potential mechanisms for the functional specialization of MTs (Wloga and Gaertig, 2010). Conserved tubulin PTMs include detyrosination/tyrosination, acetylation, glycylation, and glutamylation (Janke and Bulinski, 2011). Post-translational detyrosination/tyrosination has been described mainly in the nervous tissue. In this process, tubulin at the carboxyl-terminus of the alpha-tubulin subunit can be modified by the cyclic release and re-addition of the tyrosine residue. Two enzymes are involved in these reactions: tubulin tyrosine carboxypeptidase (Aillaud et al., 2017; Nieuwenhuis et al., 2017) and tubulin tyrosine ligase (TTL) (Barra et al., 1988), respectively.

We have previously shown that conventional deletion of TTL blocks neurite extension *in vivo* and arrests neuronal development, leading to perinatal death (Erck et al., 2005). TTL null embryos showed a disrupted cortico-thalamic loop and impaired layering of the neocortex (Erck et al., 2005). In contrast, *in vitro* cultured TTL null hippocampal neurons showed accelerated neurite and axonal growth compared with wild-type neurons (Erck et al., 2005). These results were confirmed by TTL knockdown experiments in cultured rat hippocampal neurons, showing a 40% increase in neurite growth and, in contrast, a 35% decrease in neurite growth after TTL overexpression (Prota et al., 2013). Apparently, suppression of TTL *in vivo* disrupted mechanisms important for the control of neurite outgrowth, but not neurite outgrowth *per se* (Erck et al., 2005). Thus, the evolutionarily highly conserved tubulin tyrosination cycle in neurons most likely plays a crucial role in neurite formation and microtubule stabilization. Whereas, detyrosinated MTs tend to be rather stable, tyrosination renders them more dynamic (Webster et al., 1987), suggesting that post-translational detyrosination/tyrosination of tubulin might represent a mechanism for modulating MT dynamics not only during neurite growth and stabilization but, beyond this, also in synaptic plasticity. Consistent with this, recent evidence has suggested that modulation of MT dynamics in the adult brain may also be involved in learning processes and memory formation and may be impaired in neurodegenerative diseases, such as Alzheimer's disease (Dent, 2017).

We, therefore, aimed to investigate how MT dynamics can modulate brain development and control neuronal function in adult mice using conditional deletion of TTL in different mouse lines. Our results suggest that tyrosination of α-tubulin plays a critical role not only during brain development, particularly in cortical regions, but also in functional processes and structural plasticity in mature hippocampal neurons. Knowledge about the detailed role of the tubulin tyrosination cycle controlling MT dynamics during neuronal plasticity could be used in the future to develop new treatment strategies for neurodegenerative diseases.

Materials and methods

Mice

Mice were housed under specific pathogen-free conditions in the animal facility of the Helmholtz Center for Infection

Research (Braunschweig, Germany). Animal care and all procedures were performed in accordance with institutional, state, and federal guidelines. The targeting construct was generated using the Gene Bridges' Red/ET recombination technique and standard protocols (Gene Bridges GmbH, Heidelberg, Germany). Briefly, a loxP site was inserted 494bp upstream of exon 4 using a PGK-neo-loxP template and two primers with a 50-bp homolog for this region. Subsequently, the PCR product was inserted into a 7,130-bp genomic fragment by Red/ET recombination. Subsequently, the selection marker was removed by transformation in 294-Cre *Escherichia coli*. The second loxP site was then inserted 416 bp downstream of exon 5 using PGK-neo-FRT. After Red/ET recombination, the targeting vector was sequenced and electroporated into embryonic stem (ES) cells. Selected positive ES cell clones were transiently transfected with FLP recombinase to delete the selection marker. One ES cell clone was injected into C57BL/6 blastocysts, resulting in four chimeric males that were used for breeding with C57BL/6 females to allow germline transmission. Heterozygous progenies were backcrossed to C57BL/6 and finally crossed to NexCre (Goebbels et al., 2006) and CaMKIIα-Cre line T29-1 mice (Tsien et al., 1996).

The following primers were selected for genotyping the mice.

TTL-loxed allele:	Forward	CCAGAGGCCCGGTTTCCCAGG
	Reverse	CTCTTCTAAGATGATGCCCTATGG
TTL-wt allele:	Forward	CCAGAGGCCCGGTTTCCCAGG
	Reverse	GAACTGATGGCGAGCTCAGACC
TTL-deleted allele:	Forward	CCAGAGGCCCGGTTTCCCAGG
	Reverse	GAGCTAGCTGCCCTGCTAGAGC
Cre-recombinase:	Forward	ACGACCAGGTGACAGCAATG
	Reverse	CTCGACCAGTTTAGTTACCC

Genotyping of conventional TTL knockout mice was performed as previously described (Erck et al., 2003, 2005).

The experiments performed with mice were approved according to animal welfare law in Germany. All protocols used in this project have been reviewed and approved by the local committees at TU Braunschweig and the authorities (LAVES, Oldenburg, Germany 33.19-42502-04-20/3498) according to the national guidelines of the animal welfare law in Germany ["Tierschutzgesetz in der Fassung der Bekanntmachung vom 18. Mai 2006 (BGBl. I S. 1206, 1313), das zuletzt durch Artikel 20 des Gesetzes vom 9. Dezember 2010 (BGBl. I S. 1934) geändert worden ist."].

Western blotting

To quantify the expression of tyrosinated tubulin in the cortical part and the PSD-95 level as a marker of the excitatory postsynaptic compartment in the cortex and hippocampus of 10-week-old $TTL^{lox/lox/NexCre+}$ mice and control littermates, Western immunoblotting was performed.

In brief, the mice were deeply anesthetized with CO_2 and decapitated. Tissue was isolated and lysed in a buffer containing 25-mM Tris pH 7.5, 1-mM EDTA, 1-mM EGTA, and 1% SDS. Ten-microgram total lysates were analyzed according to standard protocols as previously described (Hosseini et al., 2020). Membranes were incubated overnight at 4°C with an anti-Tyr-alpha-tubulin antibody (1:500, Synaptic Systems Cat# 302 117, RRID:AB_2620047), an anti-alpha-tubulin antibody (1:2,000, Synaptic Systems Cat# 302 411, RRID:AB_2631215), or an anti-PSD-95 antibody (1:1,000, Synaptic Systems Cat# 124 011, RRID:AB_10804286). After washing, the membranes were incubated for 1 h at room temperature with the appropriate secondary peroxidase-conjugated antibodies from Jackson ImmunoResearch. Immunoblots were analyzed by luminometry using a cooled charge-coupled camera (Fuji, Japan) and AIDA software (Raytest, Straubenhault, Germany).

Immunohistochemistry and DiI staining

Ten-week-old $TTL^{lox/lox/NexCre+}$ mice and control littermates were perfused first with physiological saline containing heparin and then with phosphate-buffered 4% paraformaldehyde (PFA). The brains were carefully dissected and postfixed overnight with the same fixative at 4°C. Fifty-μm-thick coronal and sagittal sections were cut using an HM650V Vibratome (Thermo Scientific, USA). Sections were collected in 0.1-M Tris-buffered saline pH 7.4 (TBS), containing sodium azide and stored at 4°C until further use. For immunohistochemistry, free-floating sections were washed with TBS and blocked with TBS containing 5% normal donkey serum and 0.3% Triton X-100 for 1 h at room temperature. Sections were then incubated overnight at room temperature with primary antibodies diluted in a blocking buffer, including an anti-Tyr-alpha-tubulin antibody (1:500, Synaptic Systems Cat# 302 117, RRID:AB_2620047), an anti-Cre recombinase antibody (1:500, Synaptic Systems Cat# 257 003, RRID:AB_2619968), an anti-MAP-2 antibody (1:500, Synaptic Systems Cat# 188 011, RRID:AB_2147096), and an anti-parvalbumin antibody (1:500, Synaptic Systems Cat# 195 011, RRID:AB_2619882). After washing with TBS, sections were incubated with appropriate fluorophore- or peroxidase-conjugated secondary antibodies (Dianova or Molecular Probes) diluted in TBS containing 2% bovine serum albumin (BSA) for 1 h. Peroxidase-conjugated secondary antibodies were detected by DAB staining (Sigma Aldrich, USA). Cell nuclei were counterstained with DAPI (Sigma Aldrich, USA). Finally, the sections were washed extensively with TBS, rinsed briefly with distilled water, air dried, and mounted on glass slides with Entellan™ in toluene (Merck Millipore, Germany). Images were acquired using a 510 Meta confocal laser scanning microscope (Zeiss, Germany) or

an ECLIPSE Ti-E-inverted microscope (Nikon, Japan) with a DS2-MBWc camera (Nikon, Japan). Bright-field images for a brain wave analysis were acquired with an SZX12 microscope (Olympus, Japan) and a DP26 camera (Olympus, Japan). Data acquisition and analysis were performed using LSM software (Zeiss, Germany), NIS elements (Nikon, Japan), or Photoshop.

For DiI staining, brains from the 10-week-old mice were isolated and fixed as described above. After fixation, the brains were washed with PBS. Brain sections (50 μm) were prepared using an HM650V Vibratome (Fisher Scientific^{TM}, USA). A series of sections was stained with DiI (1,1'-dioctadecyl 3,3,3'-tetramethylindocarbocyanine perchlorate, Molecular Probes) using the SWITCH (system-wide control of interaction time and kinetics of chemicals) technique (Murray et al., 2015). The sections were imaged using an ECLIPSE Ti-E-inverted microscope (Nikon, Japan) with a DS2-MBWc camera (Nikon, Japan). Image analysis was performed using Fiji software (BioVoxxel). To quantify the area density of the cortico-thalamic neuronal projections, the corrected total fluorescence intensity was measured in each region of interest (ROI), as shown in the representative images (**Figure 1G**). To quantify the size of the corpus callosum, the area of the medial corpus callosum and lateral corpus callosum (as shown in the representative images, **Figure 1H**), defined using polygon selection, was measured. Data were normalized to the control group. All slides were coded, and analysis was performed blindly.

Golgi-Cox staining

To investigate the density of dendritic spines, Golgi-Cox staining was performed. For this purpose, the left hemispheres of 4–5-month-old $TTL^{lox/lox/NexCre+}$ and $TTL^{lox/lox/CaMKII\alpha-Cre+}$ mice and control littermates were incubated with the FD rapid Golgi stain kit (FD NeuroTechnologies, Inc., Columbia, SC, USA) according to the manufacturer's protocol. Hemispheres were then blocked in 2% agar, and 200-μm-thick coronal sections were cut using a vibratome (Leica VT 1,000 S, Germany) and mounted on gelatin-coated glass slides. The sections were then processed for signal development before dehydration through graded alcohols and mounting with Permount (Fisher Scientific, USA). To examine the morphology of hippocampal neurons in Golgi-Cox-stained sections, second- or third-order branching of apical dendrites in CA1 and CA3 and dendrites in the superior and inferior dentate gyrus subregions of the hippocampus (10 cells per animal) was analyzed three-dimensionally (Z-stack thickness of 0.5 μm) using an Axioplan 2 imaging microscope (Zeiss, Germany) equipped with a 63X (N.A. 1) oil objective and a digital camera (AxioCamMRm, Zeiss, Germany). For all selected neurons, spine density per micrometer of dendrites was calculated using the Fiji software (BioVoxxel) on the segments of dendritic branches longer than 60–70 μm that were at least 50 μm from the soma. The total number of spines along the segments of dendritic branches was manually counted by an investigator who was blinded to all experimental groups.

Behavioral experiments

For behavioral assessment, 4–5-month-old $TTL^{lox/lox/NexCre+}$, $TTL^{lox/lox/CaMKII\alpha-Cre+}$ mice, and control littermates were used. All behavioral experiments were performed at the same time of the day during the light period in dim light between 9:00 a.m. and 4:00 p.m. by a blinded experimenter for all groups.

Open-field test

In this study, spontaneous locomotor activity, readiness to explore, and initial screening of anxiety-like behavior were examined with the open-field test, as described previously (Walsh and Cummins, 1976). Briefly, the mice were placed on one side of a white PVC arena (50 cm × 50 cm × 50 cm) for 5 min. The central (30 cm × 30 cm × 30 cm) and core (10 cm × 10 cm × 10 cm) zones of the arena were defined as the middle section. Between each experimental run, the apparatus was completely cleaned with ethanol 70% to reduce odor perception. Movement data, including total distance traveled, average speed, frequency of core visits, and percentage of time the mice spent in the periphery and center zones of the arena, were collected using Video Mot 2 (TSE Systems GmbH, Bad Homburg, Germany) or ANY-maze (Stoelting, USA) behavioral tracking software.

Morris water maze test

To investigate the cognitive behavior of the mice, spatial learning and memory formation were examined using the Morris water maze paradigm. Spatial learning in the Morris water maze is a hippocampus-dependent task that requires animals to find a hidden platform based on visual cues around the pool (Morris, 1984). The maze consisted of a circular pool with a diameter of 160 cm filled with 19–20°C opaque water (titanium dioxide, Euro OTC Pharma). The transparent platform was 10 cm in diameter and hidden 1 cm below the water surface. Before training, a visible platform task was performed as pre-training to ensure that swimming ability and visual acuity were intact in both experimental groups. In addition, this phase was important to allow the animals to become accustomed to the test situation. During this phase, the animals had two trials (maximum 60 s each) per day for three consecutive days to reach the visible platform, changing position during the trials (data not shown). Training was then conducted for 8 days in the Morris water maze, with the invisible platform located in the northwest (NW) quadrant. Each day, the animals were placed in the water for four trials, with different starting points (SW, S, E, and NE) randomly assigned to a 5-min interval between trials. The animals were allowed to swim

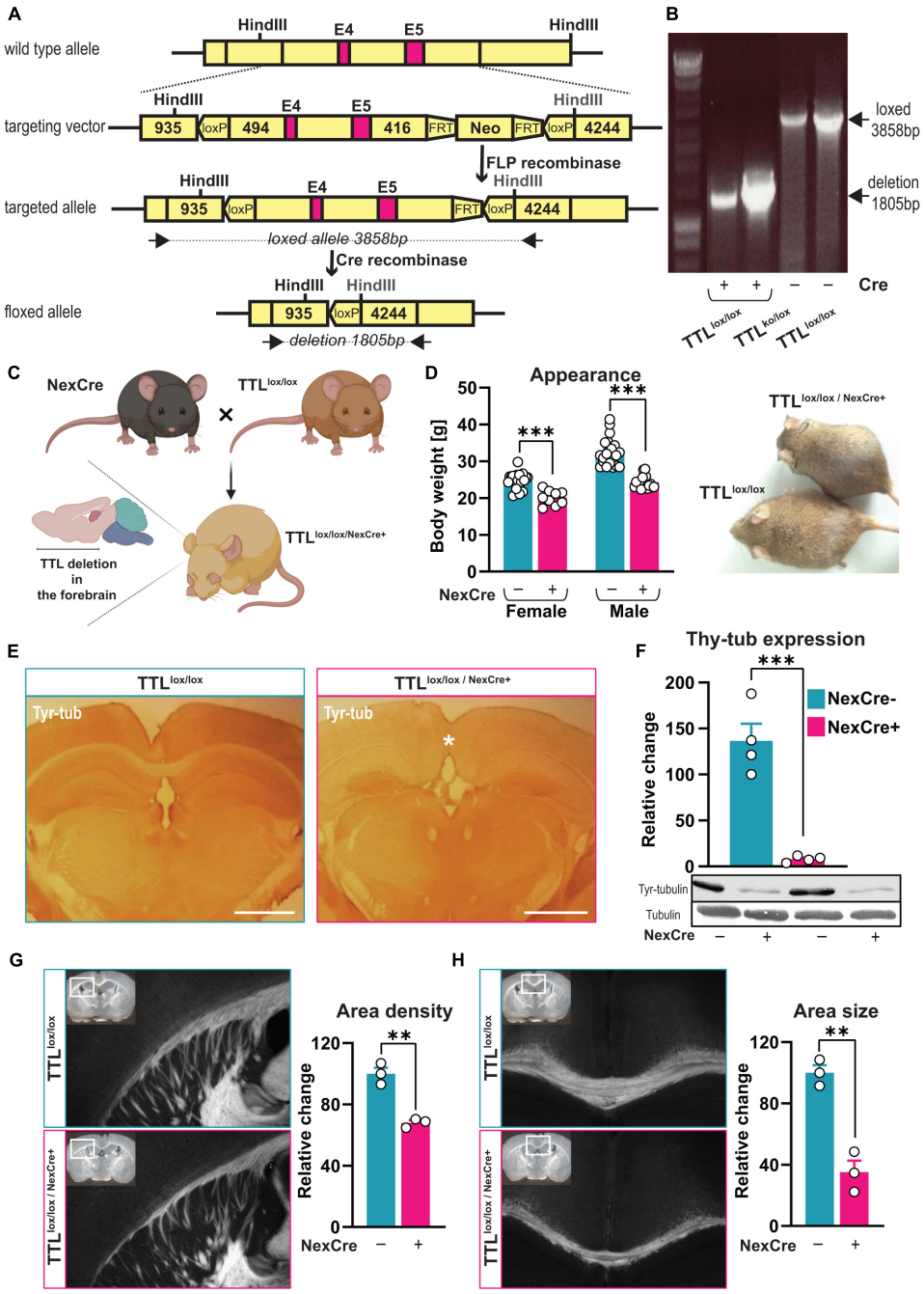

FIGURE 1

Generation of a TTL conditional knock-out mouse line. **(A)** A schematic overview of the targeted allele and the resulting floxed allele. Exons 4 and 5 (E4 and E5) are flanked with loxP sites, and the neomycin cassette (Neo) was removed by FLP recombinase. The floxed allele shows the resulting genomic DNA structure after Cre-recombinase deletion of Exons 4 and 5, leaving one loxP site. Black arrows indicate the oligos used [see panel **(B)**]. The indicated *Hind*III sites were used to determine the genomic structures. FRT: FLP-recognition target. **(B)** Representative image showing the genomic deletion of the target allele. Genomic DNA was isolated from mouse embryonic fibroblasts (MEFs) transduced to express different amounts of Cre-recombinase/EGFP fusion protein (Cre+). PCR was used to detect the deleted floxed allele [1,805 base pairs (bp)]. The 3,858-bp band corresponds to the PCR product of the non-targeted loxP/loxP allele in non-transduced control cells (Cre-). **(C)** Schematic representation of $TTL^{lox/lox/NexCre+}$ mouse generation (the figure was created using BioRender.com). **(D)** 10-week-old female and male $TTL^{lox/lox/NexCre+}$ mice displayed lower body weight compared to their control littermates (n = 9–21, unpaired t-test, $p < 0.001$). **(E)** An overview of the decreased levels of tyrosinated α-tubulin in the neocortex and hippocampus of $TTL^{lox/lox/NexCre+}$ mice. Brain sections were immunostained with an antibody against tyrosinated α-tubulin (scale bar = 1 mm). **(F)** Western blot analysis of cortical extracts from the

(Continued)

FIGURE 1 (Continued)
10-week-old mice showed an approximately 95% reduction in tyrosinated α-tubulin in the $TTL^{lox/lox/NexCre+}$ mice compared with the control mice. The relative intensities of the signals were measured by densitometry and normalized to total α-tubulin (n = 4). Representative immunoblots using antibodies against tyrosinated α-tubulin and total α-tubulin are shown. **(G,H)** Reduced development of cortico-thalamic neuron projections **(G)** and corpus callosum **(H)** in brains of $TTL^{lox/lox/NexCre+}$ mice. Brain sections from the 10-week-old $TTL^{lox/lox/NexCre+}$ mice and the control littermates were stained using the DiI/SWITCH method. Representative images are shown (overviews are shown as insets, and white boxes indicate a higher magnification area). Measurements of the relative area density of cortico-thalamic neuronal projections and the area size of the corpus callosum (with Fiji) revealed a 32% reduction in the density of cortico-thalamic neuronal projections **(G)** and a 65% reduction in the size of the corpus callosum in the NexCre + mice compared with the control [**(H)**, see also the asterisk in panel **(E)**, the right panel, n = 3]. Data are presented as mean ± SEM, $^{**}p < 0.01$ and $^{***}p < 0.001$.

freely for 60 s or until they reached the platform. Otherwise, they were led to the platform and allowed to sit on it for 20 s. For the qualitative aspects of spatial memory formation during the 8-day acquisition training, the trace map for finding the platform was analyzed as a search strategy. Over time, the mice switched from egocentric strategies independent of the hippocampus, such as scanning, characterized by >75% surface coverage; chaining, characterized by >75% time in a donut-shaped annulus zone; and random swimming characterized by >80% surface coverage, to an allocentric-directed swimming search strategy characterized by >50% time in Whishaw's corridors (a 40° target corridor) that depends on the hippocampus (Garthe et al., 2009; Garthe and Kempermann, 2013). To assess memory retrieval, three probe trial tests were conducted on the 3rd and 6th days of the acquisition training before the four trials of the training began that day. Another test of reference memory was conducted 24 h after the last day of the acquisition training (Day 9). During the probe trials, the platform was removed and the animals were allowed to swim freely for 45 s.

All data, including escape latency (time to reach the platform), percentage of time spent in the four quadrants of the pool, percentage of time spent in the peripheral (thigmotaxis), donut-shaped annulus (chaining), central circle (scanning), and Whishaw's corridors (direct search) of the pool, were recorded using Video Mot 2 (TSE Systems GmbH, Bad Homburg, Germany) or ANY-maze (Stoelting, USA) behavioral tracking software.

Electrophysiological experiments

Hippocampi of 4–5-month-old mice were dissected, and 400-μm-thick transverse acute hippocampal slices were cut using a manual tissue chopper. The slices were then immediately incubated in an interface chamber (Scientific System Design) at 32°C for 2 h and continuously perfused with oxygen-enriched artificial cerebrospinal fluid (aCSF, pH 7.2) at a flow rate of 0.5 ml/min. The aCSF contained the following chemicals (in mM): 124 NaCl, 4.9 KCl, 1.2 KH_2PO_4, 2. $MgSO_4$, 2. $CaCl_2$, 24.6 $NaHCO_3$, 10 D-glucose equilibrated with 95% O_2-5% CO_2 (32 L/h).

For stimulation, a monopolar, lacquer-coated stainless steel electrode (5 MΩ; AM Systems) was placed in the stratum radiatum of the CA1 region to generate field excitatory postsynaptic potentials (fEPSP) from Schaffer collateral/commissural CA1 synapses. For recording the fEPSP (measured as its initial slope function), an electrode (5 MΩ; AM Systems, USA) was placed in the apical dendritic layer of the CA1 region, and signals were amplified with a differential amplifier (Model 1700, AM Systems). Signals were digitized using a CED 1401 analog-to-digital converter (Cambridge Electronic Design). The slopes of the fEPSPs were monitored during recording.

An input-output curve (afferent stimulation vs. a fEPSP slope) measuring basal synaptic transmission was obtained 2 h after pre-incubation. The intensity of the test stimulation was adjusted so that the slope of the fEPSP was 40% of the maximum fEPSP response. In the $TTL^{lox/lox/NexCre+}$ and the corresponding control group, long-term potentiation (LTP) was induced by a "strong" tetanization protocol (STET), consisting of three stimulus trains of 100 pulses at 100 Hz (stimulus duration of 0.2 ms/polarity, an intertrain interval of 10 min, total of 300 pulses). Four biphasic 0.2-Hz constant current pulses (0.1 ms/polarity) were used for baseline recording. In $TTL^{lox/lox/CaMKII\alpha-Cre+}$ mice and littermate controls, 20 min after baseline recording, LTP was induced by θ-burst stimulation (TBS) with four bursts at 100 Hz repeated 10 times at an interval of 200 ms. This stimulation was repeated three times at an interval of 10 s. In all electrophysiological experiments, only healthy sections with a stable baseline were included in the data analysis. The slope of fEPSPs was measured over time and normalized to the baseline. Data acquisition and offline analysis were performed with the IntraCell software (version 1.5, LIN, Magdeburg, 2000, Germany).

Live-cell imaging

To investigate activity-dependent structural plasticity, organotypic hippocampal slice cultures (OHCs) from the $TTL^{lox/lox}$ mice were prepared on postnatal Day 5 and maintained in an Eagle basal medium (Thermo Fisher Scientific, USA), containing 25% horse serum, 1-mM L-glutamine (Sigma Aldrich, USA), 0.5% glucose, and 25% HBSS (Invitrogen, USA), as previously described (Michaelsen-Preusse et al., 2014). After 72 h of incubation, the antimitotic agent was added for 24 h and removed by a 100% media change, followed by weekly media changes of 50%. At DIV 14, OHCs were transfected

with pmApple-N1 (for dendritic spine structural analysis) and pCAG-Cre:GFP plasmids (for TTL deletion) by electroporation of single cells as previously described (Michaelsen-Preusse et al., 2014). DNA constructs were electroporated in HBSS (Invitrogen) at RT with 5 V, 1 mA, and a 220-Hz train.

After 4 days, OHCs were incubated in aCSF (as described above) saturated with 95% O_2 and 5% CO_2 at 32°C for 20 min in an imaging chamber of the Olympus Fluoview 1000 laser scanning microscope equipped with a UPLFLN 60x water (NA = 1) immersion objective and Olympus Fluoview Ver. 4.0, a software at a constant percentage of laser exposure, with a pixel size of 0.069 μm. The apical dendritic segment of the pyramidal neuron was imaged 20 min before chemical LTP induction (cLTP). Then, cLTP was induced by incubating OHCs in 10-mM glycine (AppliChem, Germany) and 3-μM strychnine (an inhibitory ionotropic glycine receptor blocker) (Sigma Aldrich, USA) in aCSF for 10 min. Then, the cLTP solution was exchanged for aCSF, and the same dendritic segment was imaged again every 20 min for 1 h after stimulation. The density of dendritic spines was analyzed as described above in the Golgi-Cox staining section. In addition, 15 spines along each dendrite were randomly selected for further morphological assessment, and the diameter of the spine head was measured using Fiji software (BioVoxxel) by an investigator who was blinded to all experimental groups.

Statistical analysis

Data were analyzed and plotted using GraphPad Prism 8 (GraphPad Software, Inc., USA) and presented as mean ± SEM. Differences in body weight, dendritic spine density, spine head diameter, relative changes in intensity and size, total distance traveled, average velocity, and number of core visits were examined with a Student's *T*-test, whereas a two-way ANOVA test was used for the behavioral and electrophysiological experiments. The Bonferroni multiple comparison correction was used as a *post hoc* test. The minimum significance value was considered as $p < 0.05$. The minimum number of animals in all experiments was calculated *a priori* using G*Power 3.1.9.4 software (Heinrich Heine College, Düsseldorf, Germany). All statistical analyses and *n* of the different experimental groups were reported in the respective results or figure legends.

Results

Generation of a tubulin-tyrosine ligase conditional knock-out mouse line

Previous findings have shown that full ablation of TTL leads to perinatal death (Erck et al., 2005). Thus, to investigate the role of α-tubulin tyrosination, specifically in adult brain structure and function, a mouse line was generated that allows tissue- and time-specific deletion of TTL. To this end, a targeting vector was created in which the inserted LoxP sites flanked Exons 4 and 5 (**Figure 1A**; Erck et al., 2003). Deletion of both exons, which contain parts of the active domain as well as the ATP-binding domain (Szyk et al., 2011), therefore, should result in a truncated and inactive TTL product consisting of 157 amino acid residues. The targeting vector was electroporated into embryonic stem cells (ES), and, as confirmed by PCR and Southern blot analysis, two ES cell clones with the correctly integrated targeting construct were obtained. One clone was injected into C57BL/6 blastocysts, resulting in four chimeric males that were used for breeding to enable germline transmission. Heterozygous progenies were backcrossed with C57BL/6 and finally interbred to obtain homozygous $TTL^{lox/lox}$ mice. The mice were born with a normal Mendelian ratio, were fertile, and had no obvious abnormalities or impaired TTL activity. In addition, the $TTL^{lox/lox}$ mice were crossed with conventional heterozygous $TTL^{\pm}$ mice (Erck et al., 2005) to obtain $TTL^{ko/lox}$ mice that support efficient deletion of only one loxed allele.

To demonstrate efficient deletion of the *ttl* gene, mouse embryonic fibroblasts (MEFs) were isolated from $TTL^{lox/lox}$ cultivars and transduced to induce expression of a Cre recombinase/EGFP fusion protein. Using deletion-specific PCR on transduced MEFs, a unique PCR product was detected only in Cre recombinase-expressing cells (**Figure 1B**). Western blot analysis failed to reveal a truncated TTL protein product indicative of unstable mRNA and/or protein products (data not shown). Remarkably, a first attempt to generate a conditional TTL knockout mouse line—with an inserted loxP site 109 base pairs upstream of the ATG codon—showed the same lethal phenotype as observed in conventional TTL knockout mice, even before Cre recombinase-dependent excision (data not shown). This suggests that an intact 5′-flanking region within the *ttl* gene is required for proper TTL expression.

Mice lacking tubulin-tyrosine ligase in the neocortex and hippocampus are viable, albeit with obvious impairments in brain development

Previously, it has been shown that, in conventional $TTL^{-/-}$ embryos, TTL activity is absent in both cortical and thalamic parts of the developing brain, resulting in severe blockade of ascending and descending neuronal projections (Erck et al., 2005). To study cognitive function in the absence of TTL, a mouse strain expressing Cre recombinase under the control of the *nex* promoter was used to drive TTL deletion only in the forebrain (**Figure 1C**; Goebbels et al., 2006). In a previous study, the NexCre expression pattern was analyzed using different lacZ reporter mice. The strongest Cre activity was observed in the neocortex and hippocampus, starting

around embryonic Day 11.5. Cre-mediated recombination marked pyramidal neurons and mossy fibers of the dentate gyrus but was absent in proliferating neural precursors of the ventricular zone, interneurons, oligodendrocytes, and astrocytes (Goebbels et al., 2006).

In contrast to the conventional TTL knockout mice, the $TTL^{lox/lox/NexCre+}$ mice were born in a normal Mendelian ratio, and were healthy and fertile. Yet, compared with control littermates (males: 32.45 ± 0.82 g, females: 24.81 ± 0.52 g), adult mice were smaller and had significantly lower body weights [males: 24.28 ± 0.39 g (unpaired *t*-test: $t = 8.48$, df = 37, $p < 0.001$), females: 20.08 ± 0.65 g (unpaired *t*-test: $t = 5.40$, df = 25, $p < 0.001$), **Figure 1D**].

The efficiency of TTL deletion in Cre recombinase-expressing cells was assessed by immunostaining of tyrosinated α-tubulin. Ten-week-old control mice ($TTL^{lox/lox/NexCre-}$) showed the expected general immunoreactivity throughout the brain (**Figure 1E**, the left panel). In contrast, age-matched $TTL^{lox/lox/NexCre+}$ mice exhibited approximately 95% reduced levels of tyrosinated α-tubulin in the neocortex and pyramidal neurons of the hippocampus (**Figure 1E**, the right panel). This was also confirmed by Western blotting of cortical extracts from the $TTL^{lox/lox/NexCre+}$ mice (NexCre-: 136.5 ± 18.70%, NexCre+: 7.97 ± 1.67%, unpaired *t*-test: $t = 6.84$, df = 6, $p < 0.001$, **Figure 1F**).

In addition, double immunostaining with antibodies directed against Cre recombinase and tyrosinated tubulin (**Supplementary Figures 1A,B**) revealed the expected Cre recombinase expression pattern in the pyramidal cell layer of the hippocampus but not in granule cells in the dentate gyrus, as well as general immunostaining with tyrosinated α-tubulin in 10-week-old control mice ($TTL^{wt/lox/NexCre+}$). The same Cre expression pattern was found in the $TTL^{lox/lox/NexCre+}$ mice, but tyrosinated tubulin immunostaining was largely absent. Only a few cells, most likely NexCre-negative interneurons and astrocytes, were immunopositive for tyrosinated α-tubulin. High levels of tyrosinated α-tubulin were observed in the thalamus, where there are actually no Cre recombinase-expressing cells (**Supplementary Figure 1A**, the asterisk). Normal levels of tyrosinated α-tubulin were detected in the granule cells of the dentate gyrus (**Supplementary Figure 1A**, the arrow), most likely due to transient expression of Cre recombinase over time in this area (Goebbels et al., 2006). The described absence of Cre recombinase expression in interneurons of $TTL^{lox/lox/NexCre+}$ mice was supported by the presence of parvalbumin-positive neurons with strong immunoreactivity for tyrosinated α-tubulin (**Supplementary Figure 1C**).

To test whether projecting neurons from the cortex in $TTL^{lox/lox/NexCre+}$ mice were able to find their targets in other brain regions and make contacts, brain slices were labeled with DiI, a fluorescent lipophilic cationic indocarbocyanine dye, using the SWITCH technique (Murray et al., 2015) to visualize neuronal trajectories. In contrast to conventional TTL-deficient embryos, high numbers of projecting axons exiting the cortex were observed in the 10-week-old $TTL^{lox/lox/NexCre+}$ mice, albeit with an approximately 32% reduction in fiber area density (67.99 ± 1.68%) compared with control littermates (100 ± 3.94%, unpaired *t*-test: t = 7.48, df = 4, $p = 0.0017$, **Figure 1G**).

The development of the corpus callosum begins with the growth of pioneer axons located in the cingulate cortex and crossing the midline at E15.5, followed by neocortical axons crossing at E16.5. The vast majority of axons forming the corpus callosum originate from the neocortical layers II, III, and V (Richards et al., 2004). To examine the integrity of the fiber tracts, coronal sections from the 10-week-old mice were analyzed using the DiI/SWITCH technique as described above. In the $TTL^{lox/lox/NexCre+}$ mice, the corpus callosum exhibited hypoplasia, a 65% reduction in the area size of the fiber tracts (NexCre-: 100 ± 4.91%, NexCre+: 35.15 ± 7.55%, unpaired *t*-test: $t = 7.19$, df = 4, $p = 0.002$, **Figure 1H**). In addition, rostro-caudal reduction of the corpus callosum was evident from the absence of midline-crossing fibers at the splenium (see asterisks in **Figure 1E** and **Supplementary Figure 2A**). This indicates a developmental arrest of the corpus callosum at Day E16-17 in $TTL^{lox/lox/NexCre+}$ mice.

In addition, analysis of serial slices revealed a reduction in hippocampal commissure (HC) size leading to midline gap formation in the $TTL^{lox/lox/NexCre+}$ mice (**Supplementary Figures 2B,C**).

To reveal details about the late onset of developmental differences between control mice and $TTL^{lox/lox/NexCre+}$ mice, we analyzed newborn pups to follow the time course of downregulation of tyrosinated α-tubulin. Western blot analysis of cortex lysates from P3 and P5-aged pups showed no apparent reduction in tyrosinated α-tubulin in the $TTL^{lox/lox/NexCre+}$ mice. Starting at P7 (**Supplementary Figure 2D**) and even more markedly in the adult mice (**Figure 1F**), the amount of tyrosinated α-tubulin decreased. Although Cre recombinase expression began at E11.5, resulting in deletion of the TTL gene, a complete loss of tyrosinated α-tubulin was observed much later potentially, indicating a long half-life of the TTL protein. Although the developmental arrest of projecting neurons was already observed at E16/E17, a reduced amount of tyrosinated α-tubulin could not be confirmed by Western blotting at this time point. These results underline the importance of TTL as even a small reduction in tyrosinated α-tubulin, which could not be detected by Western blotting, led to a strong phenotype. In a previous study, hippocampal neurons from conventional TTL knock-out embryos were shown to exhibit accelerated growth of neuronal processes in the first hours after plating (Erck et al., 2005). To investigate this *in vivo*, dendrite formation was determined in the neocortex of adult $TTL^{lox/lox/NexCre+}$ mice. In control mice ($TTL^{lox/lox}$), the peripheral cortex (Layers II and III) was filled with parallel-aligned bundles of microtubules

decorated with microtubule-associated protein 2 (MAP-2), a marker for dendrites (**Supplementary Figure 2E**, the left panel). At the edge of the marginal zone, also called Exner's plexus, MAP-2 distribution appeared more diffuse. In contrast, the $TTL^{lox/lox/NexCre+}$ mice showed only a diffuse meshwork of MAP-2-positive structures/microtubules. Neither were oriented dendrites clearly visible, nor was the boundary between the marginal zone and the inner mass of the cortex distinct (**Supplementary Figure 2E**, the right panel). Thus, neurons from the $TTL^{lox/lox/NexCre+}$ mice showed altered maturation, and dendrites failed to develop properly *in vivo* in the absence of TTL.

Increased anxiety and impaired spatial learning in mice lacking tubulin-tyrosine ligase in the neocortex and hippocampus

Recent evidence has shown that microtubules are highly dynamic and play an important role in memory formation. In particular, learning is associated with changes in microtubule turnover and stability, as pharmacological manipulations of microtubule dynamics alter learning and memory processes (Uchida and Shumyatsky, 2015). To investigate the importance of α-tubulin tyrosination for hippocampal function, general locomotor activity and anxiety-related behavior as well as spatial learning were examined in conditional TTL KO mice (**Figure 2**).

The $TTL^{lox/lox/NexCre+}$ mice traveled a significantly longer distance (96.42 ± 13.38 m) with a higher average speed (16.07 ± 2.22 cm/s) compared to the control mice in the open field test (distance: 52.95 ± 1.70 m, speed: 8.82 ± 0.28 cm/s) (unpaired *t*-test: $t = 3.75$, df = 12, $p = 0.002$, **Figures 2A,B**). The $TTL^{lox/lox/NexCre+}$ mice showed less visits to the core area of the open-field arena (NexCre-: 19 ± 3 times, NexCre + : 9 ± 2 times, unpaired *t*-test: $t = 3.03$, df = 12, $p = 0.01$, **Figure 2C**) and spent less time in the center and more time in the periphery [two-way ANOVA: $F_{interaction}$ (1, 24) = 21.64, $p = 0.001$, **Figure 2D**]. These results indicate hyperactivity and increased anxiety-related behavior in the $TTL^{lox/lox/NexCre+}$ mice compared with the littermate controls.

To investigate spatial learning, the mice were trained in the Morris water maze for 8 days. Here, the latency to reach a hidden platform was analyzed to assess spatial learning on consecutive days. As shown in **Figure 2E**, the swimming time to reach the platform decreased over the course of the 8-day acquisition training in control animals [one-way RM ANOVA $F_{(7,49)} = 16.24$, $p < 0.0001$], but not in the $TTL^{lox/lox/NexCre+}$ mice [one-way RM ANOVA $F_{(7,35)} = 1.80$, $p = 0.12$], indicating an impairment in learning. A daily comparison between the two groups showed that the escape latency was significantly higher in the $TTL^{lox/lox/NexCre+}$ animals than in the control mice during the different training days [two-way RM ANOVA $F_{Genotype}$ (1, 12) = 23, $p = 0.0004$]. To assess spatial reference memory, the animals were subjected to probe trials without the platform on Days 3 and 6 before the training and 24 h after the last training session on Day 9. The $TTL^{lox/lox/NexCre+}$ mice spent less time in the target quadrant (TQ) compared to the control animals [two-way RM ANOVA $F_{Genotype}$ (1, 12) = 10.32, $p = 0.0075$], which was significant at Day 6 ($p = 0.026$, **Figure 2F**). Learning impairment can be further revealed by analyzing search strategies during the training (**Figures 2G–K**). Based on the time spent in the different zones of the pool, including Wishaw's corridor (direct swimming), a donut-shaped zone (chaining), a central zone (scanning), and the entire area of the pool (random search), the search strategies used by the animals can be divided into (i) a hippocampus-dependent, allocentric strategy (direct swimming, suggesting the formation of a spatial memory) and (ii) hippocampus-independent, egocentric strategies (lack of spatial memory formation), including chaining, scanning, and random search (**Figure 2G**). Over time, mice learn to use the more efficient allocentric strategy to navigate to the hidden platform (Garthe et al., 2009; Garthe and Kempermann, 2013). The results showed that the $TTL^{lox/lox/NexCre+}$ mice failed to switch from the hippocampus-independent strategies to the hippocampus-dependent strategy during the training period (**Figures 2H,I**). Further quantification showed that the $TTL^{lox/lox/NexCre+}$ mice were significantly less likely to use the hippocampus-dependent strategy (**Figure 2J**) and more likely to use the hippocampus-independent strategies (**Figure 2K**) on Days 3, 6, 7, and 8 of the training compared to the control mice [two-way RM ANOVA $F_{Genotype}$ (1, 12) = 18.41, $p = 0.001$]. Overall, these results show a severe impairment in learning in $TTL^{lox/lox/NexCre+}$ mice.

Impaired hippocampal long-term synaptic plasticity and reduced spine density in forebrain-specific tubulin-tyrosine ligase knockout mice

To further investigate the cellular basis for the observed memory impairment in the $TTL^{lox/lox/NexCre+}$ mice we analyzed long-term potentiation (LTP). For this purpose, acute hippocampal slices from 4- to 5-month-old control mice and $TTL^{lox/lox/NexCre+}$ mice were prepared. LTP was triggered by three stimulus trains (HFS) at the Schaffer collateral/commissural CA3-CA1 pathway, and field excitatory postsynaptic potentials (fEPSP) were recorded in the stratum radiatum of the CA1 hippocampal region (**Figure 3A**). Before LTP assessment, to evaluate changes in basal synaptic transmission, the dependence of the slope of fEPSPs on stimulation intensity was analyzed in input/output curves (**Figure 3B**). No differences were found between experimental groups [two-way

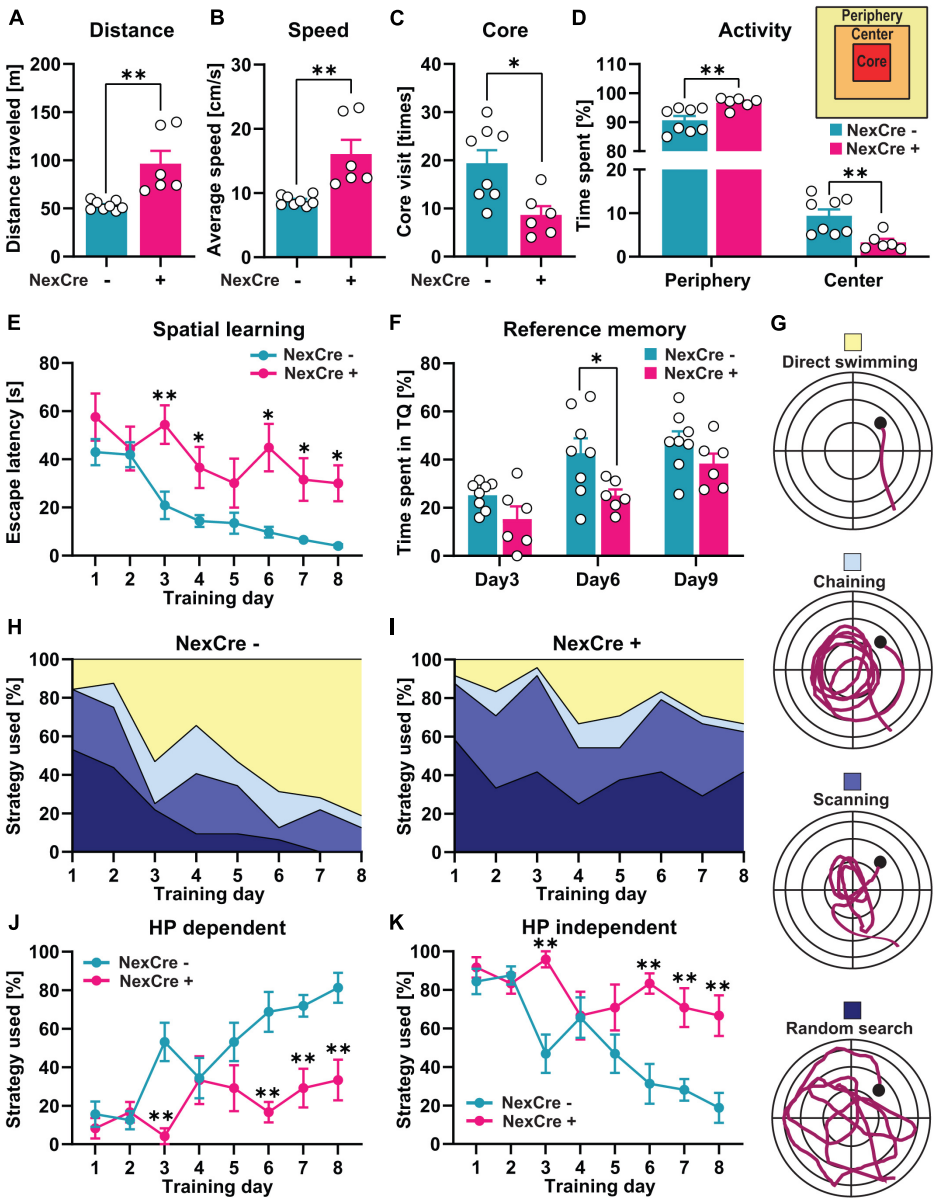

FIGURE 2
Absence of TTL in the neocortex and hippocampus results in impaired cognitive function. **(A–D)** 4–5-month-old $TTL^{lox/lox/NexCre+}$ mice compared with control mice traveled a longer distance **(A)**, had a higher average speed **(B)**, a lower number of core visits **(C)**, and spent more time in the periphery and less time in the center zones of the open-field arena **(D)**. **(E,F)** In the Morris water test, increased escape latency **(E)** and lower percent time spent in the target quadrant **(F)** indicate impaired spatial learning and memory formation in the $TTL^{lox/lox/NexCre+}$ mice compared with the control mice. **(G–K)** Analysis of learning strategies used during water maze training **(G)** showed that the $TTL^{lox/lox/NexCre+}$ mice used a less hippocampus-dependent search strategy and more hippocampus-independent search strategies to find the hidden platform compared with the control mice during 8 days of learning **(H–K)**. Data are presented as mean ± SEM, $^{*}p < 0.05$ and $^{**}p < 0.01$, $N = 6–8$ in each group.

RM ANOVA $F_{(1,15)} = 0.09$, $p = 0.76$, Figure 3B]. This result suggests that basal synaptic transmission was not affected by the deletion of TTL during development. After baseline recording, LTP was induced and strong potentiation was observed in the hippocampus of the control mice. However, in the $TTL^{lox/lox/NexCre+}$ mice, LTP was severely impaired (Figure 3C), indicating perturbed hippocampal networks.

As a next step, spine density was analyzed by the Golgi-Cox method in the $TTL^{lox/lox/NexCre+}$ and control mice. Changes in dendritic spine density and morphology, indeed, have been shown to correlate with defects in synaptic plasticity and

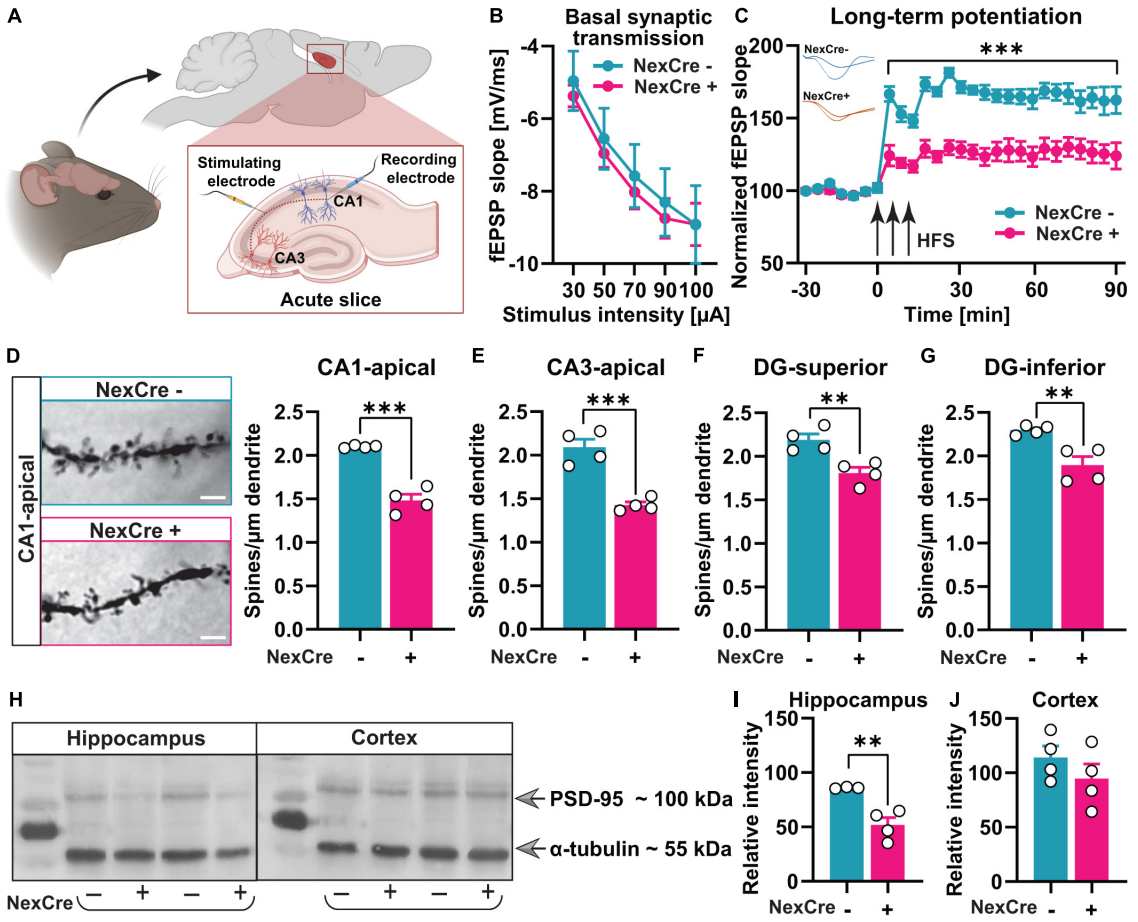

FIGURE 3
Absence of TTL in neocortex and hippocampus results in impaired synaptic plasticity and reduced density of dendritic spines. **(A)** A schematic overview of the location of stimulating and recording electrodes in acute hippocampal slices (the figure was created using BioRender.com). **(B)** Input-output curves of field excitatory postsynaptic potential (fEPSP) slopes in 7–10 hippocampal slices obtained from both tested groups did not show any significant differences. **(C)** LTP measurements in acute hippocampal slices from 4 to 5-month-old $TTL^{lox/lox/NexCre+}$ and control mice showed severe LTP impairment. FEPSPs (normalized to baseline values) from 7 to 10 slices each of the $TTL^{lox/lox/NexCre+}$ and control mice before and after high-frequency stimulation (HFS) are shown. **(D–G)** Brains of the 4–5-month-old $TTL^{lox/lox/NexCre+}$ and control mice were subjected to Golgi-Cox staining, and dendritic spines in hippocampal neurons were counted. Representative examples of dendritic spines in CA1 hippocampal neurons are shown for each group (63×); a scale bar = 2 µm **(D)**. The density of dendritic spines in $TTL^{lox/lox/NexCre+}$ was lower in the apical dendrites of CA1 **(D)** and CA3 neurons **(E)**, and in granule cells in the superior **(F)** and inferior **(G)** blades of the dentate gyrus compared with the control mice. In each group, 4 mice and 10 dendrites per mouse were analyzed and averaged. **(H)** Western blot analysis of hippocampus and cortex lysates from the 10-week-old mice showed that **(I)** PSD-95 levels were reduced in hippocampi of the $TTL^{lox/lox/NexCre+}$ mice compared with the control mice **(J)**, and this was not the case in the cortex. The relative intensities of the signals were measured by densitometry and normalized to total α-tubulin (n = 3–4). Data are presented as mean ± SEM, $^{**}p < 0.01$ and $^{***}p < 0.001$.

cognitive function in general (Moser et al., 1994). After deletion of TTL, dendritic spine density was reduced in CA1 (Δ29.5%, unpaired t-test: t = 8.65, df = 6, p = 0.0001, Figure 3D) and CA3 (Δ31.8%, unpaired t-test: t = 6.50, df = 6, p = 0.0006, Figure 3E), consistent with the loss of tyrosinated α-tubulin, particularly in hippocampal pyramidal cells (Supplementary Figures 1A,B). Further analysis revealed significantly decreased dendritic spine density in granule cells, which was evident in both suprapyramidal (Δ17.4%, unpaired t-test: t = 4.05, df = 6, p = 0.006, Figure 3F) and infrapyramidal (Δ17.5%, unpaired t-test: t = 3.97, df = 6, p = 0.007, Figure 3G) blades of the dentate gyrus in the $TTL^{lox/lox/NexCre+}$ mice compared to the controls. Normal levels of tyrosinated α-tubulin were observed in the dentate gyrus, likely due to transient expression of Cre recombinase over time in this area (Goebbels et al., 2006; Supplementary Figure 1A, the arrow). Hence, impaired network formation in cortical input areas of the hippocampus as well as in hippocampal pyramidal cells might negatively affect the entire hippocampal network and, consequently, the granule cells in the dentate gyrus region.

In the dentate gyrus, synaptic contacts are predominantly formed by different systems of afferents, the entorhinal

and commissural-associational fibers. It is suggested that a reduction in these afferent fibers leads to a reduction in postsynaptic compartments on dentate gyrus neurons (Geinisman et al., 1992).

The reduced spine density in the absence of TTL suggests a role of TTL in synaptogenesis. Therefore, postsynaptic density protein 95 (PSD-95), a marker of excitatory postsynaptic boutons, was analyzed as well and found to be less abundant in hippocampal lysates from the $TTL^{lox/lox/NexCre+}$ mice (NexCre-: 85.97 ± 0.43%, NexCre+: 51.80 ± 6.74%, unpaired *t*-test: $t = 4.28$, df = 5, $p = 0.008$, **Figures 3H,I**). This was not the case in the neocortex (NexCre-: 114.1 ± 10.47%, NexCre+: 94.5 ± 13.63%, unpaired *t*-test: $t = 1.14$, df = 6, $p = 0.29$, **Figures 3H,J**), indicating a role of TTL more for axonal outgrowth in this region. In summary, deletion of TTL in the hippocampus leads to impaired synapse formation as well as defects in synaptic plasticity and spatial learning.

CA1 pyramidal cell-specific tubulin-tyrosine ligase deletion in the hippocampus reveals an acute role for synaptic plasticity

The results presented so far showed that tyrosination of α-tubulin in the neocortex and hippocampus during development is important for network formation and that forebrain-specific deletion of TTL, therefore, leads to cognitive deficits and impaired synaptic plasticity. In a next step, we were, therefore, interested in whether TTL is also acutely involved in synaptic plasticity processes underlying learning and memory formation in mature neurons. For this purpose, we crossed the $TTL^{lox/lox}$ mice with a specific calcium-calmodulin kinase II (CaMKII)α-Cre reporter mouse line [Tg(Camk2a-cre)T29-1Stl, **Figure 4A**]. Cre-dependent lacZ reporter expression in this line predominantly showed labeling of the CA1 pyramidal cell layer in the hippocampus, starting during the 3rd to 4th postnatal weeks (Tsien et al., 1996). By this means, developmental defects can be prevented. The $TTL^{lox/lox/CaMKII\alpha-Cre+}$ mice were born with a normal Mendelian ratio, were healthy, and fertile. A previous study has shown that target gene deletion was nearly complete at 3 months of age in the hippocampus of CaMKIIα-Cre + mice (Chen et al., 2017). To ensure that the TTL deletion was complete in mature CA1 pyramidal neurons, adult animals at 4–5 months of age were used in this study.

Prior to the assessment of long-term plasticity, the input/output curves were analyzed to reveal potential deficits in basal synaptic transmission (**Figure 4B**). The results showed no significant differences between the two groups, indicating that basal synaptic transmission was not affected in the absence of TTL, specifically in CA1 pyramidal neurons [two-way RM ANOVA $F_{(1,40)} = 1.03$, $p = 0.31$, **Figure 4B**]. In a next step, to assess synaptic plasticity, LTP was examined in the $TTL^{lox/lox/CaMKII\alpha-Cre+}$ and control mice (**Figures 4C,D**). For this purpose, after a 20-min baseline recording, θ-burst stimulation (TBS) was used to induce LTP at the Schaffer collateral/commissural CA3-CA1 pathway in acute slices from the $TTL^{lox/lox/CaMKII\alpha-Cre+}$ and control mice. Control slices showed robust induction of LTP and a sustained maintenance phase (**Figure 4C**). In contrast, the $TTL^{lox/lox/CaMKII\alpha-Cre+}$ slices showed a significant reduction [two-way RM ANOVA $F_{Genotype}$ (1, 42) = 5.50, $p = 0.02$, **Figure 4C**], especially in the maintenance phase of LTP, as shown by the mean value of LTP in the last 5 min of recording (163.2 ± 8.7% in the control slices vs. 138.1 ± 6.3% in the mutant sections, unpaired *t*-test: $t = 2.36$, df = 42, $p = 0.02$, **Figure 4D**). The impairment in LTP observed in the $TTL^{lox/lox/CaMKII\alpha-Cre+}$ mice suggests that postsynaptic plasticity in the mature hippocampus is acutely compromised by loss of TTL.

To investigate the possible cellular mechanism underlying the observed LTP deficit in the $TTL^{lox/lox/CaMKII\alpha-Cre+}$ mice, the morphology of neurons in the hippocampus was analyzed by Golgi-Cox staining (**Figures 4E–H**). As mentioned above, changes in the density of dendritic spines have been shown to correlate with defects in LTP (Moser et al., 1994). Consistent with the predominantly CA1-specific deletion of TTL, only the number of dendritic spines on CA1 pyramidal neurons in the hippocampus of the $TTL^{lox/lox/CaMKII\alpha-Cre+}$ mice showed a significant reduction compared with the control mice (Δ25%, unpaired *t*-test: $t = 7.60$, df = 5, $p = 0.0006$, **Figure 4E**). Dendritic spines in the other hippocampal subregions, including CA3 and dentate gyrus, did not show significant differences compared to the control mice (CA3: Δ0.65%, unpaired *t*-test: $t = 0.15$, df = 5, $p = 0.88$, **Figure 4F**; DG-superior: Δ2.20%, unpaired *t*-test: $t = 0.39$, df = 5, $p = 0.70$, **Figure 4G**; DG-inferior: Δ5.60, unpaired *t*-test: $t = 0.81$, df = 5, $p = 0.45$, **Figure 4H**).

The TTL knockout mice ($TTL^{lox/lox/CaMKII\alpha-Cre+}$) were also behaviorally characterized. This was first done in the open-field arena to examine general locomotor activity and assess anxiety-related behavior (**Figures 5A–D**). Analysis of total distance traveled (**Figure 5A**), average speed (**Figure 5B**), number of visits to the core area (**Figure 5C**), and overall activity and time spent in the peripheral and central zones of the arena (**Figure 5D**) revealed no significant differences between the $TTL^{lox/lox/CaMKII\alpha-Cre+}$ mice and the control littermates [distance, Cre-: 15.45 ± 1.21 m, Cre + : 19.17 ± 1.54 m; unpaired *t*-test: $t = 1.92$, df = 10, $p = 0.08$, **Figure 5A**; speed, Cre-: 5.38 ± 0.5 cm/s, Cre + : 6.42 ± 0.5 cm/s; unpaired *t*-test: $t = 1.41$, df = 10, $p = 0.19$, **Figure 5B**; core visit: Cre-: 9 ± 2 times, Cre + : 9 ± 2 times; unpaired *t*-test: $t = 0.018$, df = 10, $p = 0.98$, **Figure 5C**; activity in the periphery and the center: two-way ANOVA $F_{Genotype}$ (1, 20) = 0.0001, $p > 0.99$, **Figure 5D**]. These results show that deletion of TTL in mature CA1 pyramidal neurons alone ($TTL^{lox/lox/CaMKII\alpha-Cre+}$) does not alter general behavior as it was observed for the forebrain-specific deletion ($TTL^{lox/lox/NexCre+}$).

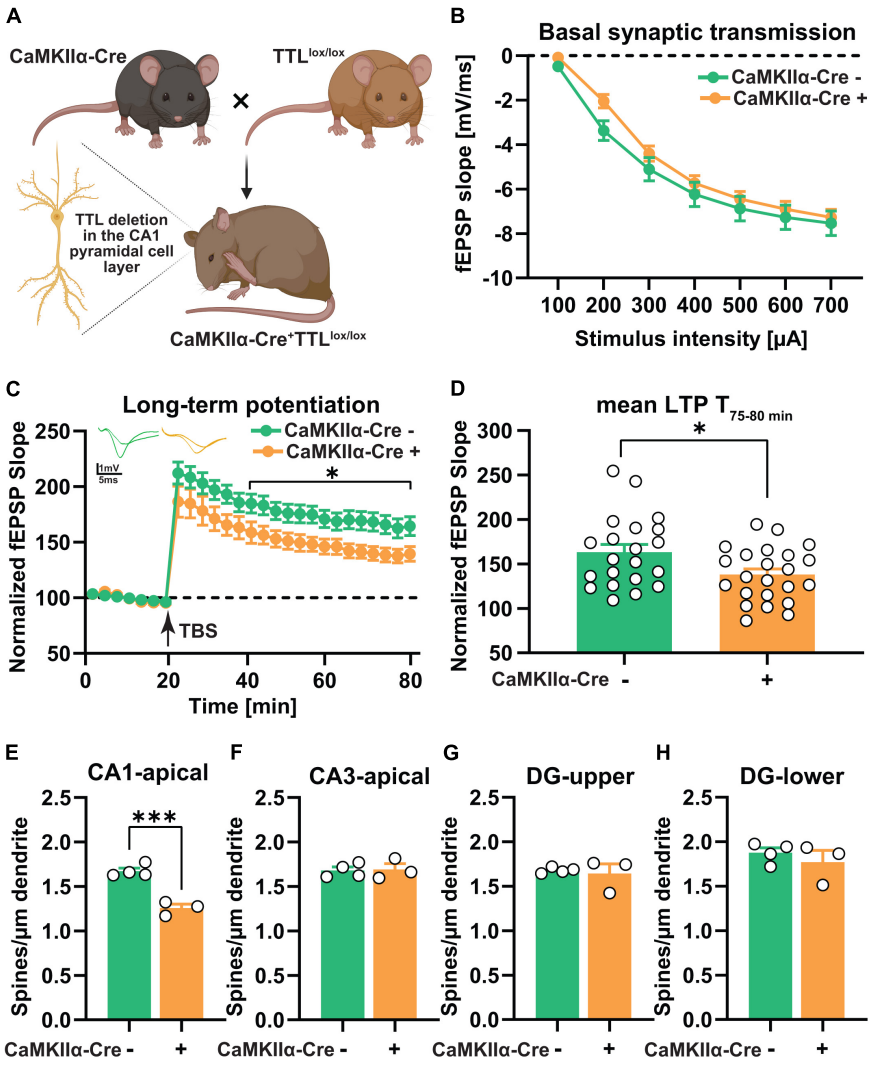

FIGURE 4
CA1-specific TTL deletion in the hippocampus results in impaired long-term synaptic plasticity. **(A)** Schematic representation of $TTL^{lox/lox/CaMKII\alpha-Cre+}$ mouse generation (the figure was created using BioRender.com). **(B)** Input-output curves of field excitatory postsynaptic potential (fEPSP) slopes in hippocampal slices obtained from both tested groups did not show any significant differences. **(C)** Acute hippocampal slices from the $TTL^{lox/lox/CaMKII\alpha-Cre+}$ mice showed significantly lower LTP compared with the control mice. FEPSPs (normalized to baseline values) of 21–23 slices each from the $TTL^{lox/lox/CaMKII\alpha-Cre+}$ and control mice before and after θ-burst stimulation (TBS) are shown **(C)**. The $TTL^{lox/lox/CaMKII\alpha-Cre+}$ mice showed significantly reduced maintenance (T, 75–80 min) of LTP compared with the control mice **(D)**. **(E–H)** Dendritic spine density in CA1 pyramidal neurons was lower in the $TTL^{lox/lox/CaMKII\alpha-Cre+}$ mice compared with the control mice **(E)**, whereas, dendritic spine density in CA3 neurons **(F)** and granule cells located in the superior **(G)**, and inferior **(H)** blades of the dentate gyrus showed no significant differences. In each group, 3–4 mice and 10 dendrites per mouse were analyzed and averaged. Data are presented as mean ± SEM, $^{*}p < 0.05$ and $^{***}p < 0.001$.

Previous findings on the involvement of the hippocampus in learning and memory have suggested that different cortical regions and hippocampal CA fields subserve important roles (Suthana et al., 2009). Therefore, the $TTL^{lox/lox/CaMKII\alpha-Cre+}$ mice were trained in the Morris water maze (Figures 5E–K). In contrast to the $TTL^{lox/lox/NexCre+}$ mice, swimming time to reach the hidden platform significantly decreased in both the $TTL^{lox/lox/CaMKII\alpha-Cre+}$ [one-way RM ANOVA $F_{(7,28)} = 4.34$, $p = 0.002$] and control mice [one-way RM ANOVA $F_{(7,42)} = 4.66$, $p = 0.0006$] during the 8-day acquisition training. The learning performance of the $TTL^{lox/lox/CaMKII\alpha-Cre+}$ mice did not differ from the control animals [two-way RM ANOVA $F_{Genotype}$ (1, 10) = 4.58, $p = 0.057$, Figure 5E]. The reference memory tests on Days 3, 6, and 9 showed also no significant differences in time spent in the target quadrant between the $TTL^{lox/lox/CaMKII\alpha-Cre+}$ and control mice [two-way RM ANOVA $F_{Genotype}$ (1, 10) = 0.042, $p = 0.84$, Figure 5F]. Evaluation of the respective search

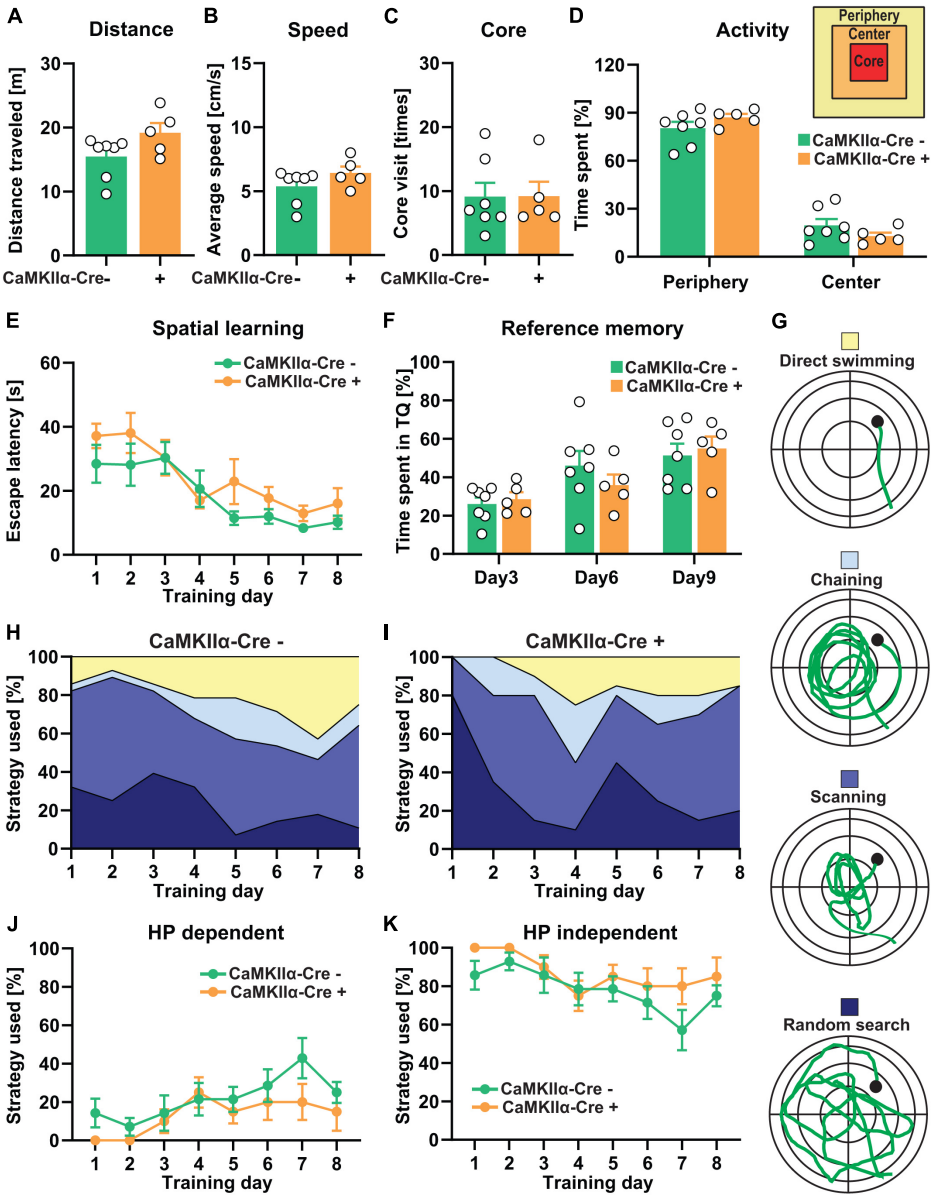

FIGURE 5
CA1-specific TTL deletion in the hippocampus does not lead to severe impairment of cognitive functions. **(A–D)** Total distance traveled **(A)**, average speed **(B)**, number of core visits **(C)**, and percentage of activity of mice in the periphery and the center of the open-field arena **(D)** showed no significant differences between the $TTL^{lox/lox/CaMKII\alpha-Cre+}$ and control mice. **(E–K)** In the Morris water maze test, during the 8-day acquisition training, escape latency significantly decreased in both the $TTL^{lox/lox/CaMKII\alpha-Cre+}$ and control groups, indicating spatial learning, but it was not significantly changed between the groups **(E)**. **(F)** The percentage of time the $TTL^{lox/lox/CaMKII\alpha-Cre+}$ and control mice spent in the target quadrant did not show significant differences. **(G)** Different search strategies, including hippocampus-dependent (direct swimming) and hippocampus-independent (random search, scanning, and chaining), were presented and color-coded **(H,I)**. The $TTL^{lox/lox/CaMKII\alpha-Cre+}$ mice used slightly less hippocampus-dependent **(J)** and more hippocampus-independent **(K)** search strategies compared with the control mice. Data are presented as mean ± SEM, N = 5–7 in each group.

strategies showed that the hippocampus-dependent search strategy increased over time, whereas, the hippocampus-independent search strategies decreased in both the control and $TTL^{lox/lox/CaMKII\alpha-Cre+}$ mice (Figures 5G–I). However, the $TTL^{lox/lox/CaMKII\alpha-Cre+}$ mice showed a slight reduction in the usage of hippocampus-dependent strategies (Figure 5J) and, instead, used more the hippocampus-independent strategies (Figure 5K) compared with the control animals; however, this was not significant [two-way RM ANOVA $F_{Genotype}$ (1, 10) = 3.05, p = 0.11]. These results suggest that the specific deletion of α-tubulin tyrosination in mature CA1 pyramidal neurons does not lead to severe impairments in spatial learning,

in contrast to observations in the $TTL^{lox/lox/NexCre+}$ mice, in which abnormalities of the entire brain network, including incomplete development of the corpus callosum and anterior commissures due to axonal growth arrest, can be observed.

Deletion of tubulin-tyrosine ligase in single cells in hippocampal slice cultures shows a crucial role for activity-dependent spine structural plasticity

To even further characterize the acute role of TTL for synaptic plasticity at the single-cell level, we used TTL deletion in organotypic hippocampal slice cultures. Slice cultures (OHCs) were obtained from the $TTL^{lox/lox}$ mice at postnatal Day 5 and then transfected with pmApple-N1 and pCAG-Cre:GFP plasmids at days *in vitro* (DIV) 14 using single-cell electroporation as described previously (Michaelsen-Preusse et al., 2014). By this means, we were able to avoid defects resulting from improper synapse development (**Figure 6A**). Electroporation of single cells with the pCAG-Cre:GFP plasmid resulted in expression of Cre recombinase fused to GFP in $TTL^{lox/lox}$ cells in OHCs. Further transfection of the cells with the pmApple-N1 plasmid allowed detailed visualization of neuronal structure. The cells expressing only mApple were used as controls (Cre-) (**Figure 6A**). To elucidate the role of α-tubulin tyrosination in activity-dependent structural plasticity of dendritic spines, NMDAR-dependent LTP was induced by administration of 10-mM glycine for 10 min and 4 days after transfection (chemical LTP, cLTP). Glycine-induced cLTP is reported to result in a significant increase in synaptic efficacy that is comparable in many aspects to the long-term potentiation induced by θ-burst stimulation (Fortin et al., 2010; Michaelsen-Preusse et al., 2016). Spines located at the proximal apical dendrites of pyramidal neurons were imaged before and 60 min after cLTP induction. Assessment of dendritic spine density showed that, in line with our *in vivo* data, also, acute depletion of TTL in Cre + cells resulted in a significant reduction in the number of dendritic spines compared with control Cre- cells [two-way ANOVA $F_{Genotype}$ (1, 12) = 7.61, p = 0.01, **Figure 6B**]. In both control and TTL-depleted single neurons, cLTP induction did not trigger new spine formation, as the number of dendritic spines before and 60 min after cLTP was comparable in each group [two-way ANOVA $F_{TimeaftercLTP}$ (1, 12) = 0.15, p = 0.70, **Figure 6B**]. In line with the results described above, indicating a role for TTL in plasticity processes, we found that spine structural plasticity was disrupted in TTL-deficient neurons (**Figure 6C**). Sixty min after cLTP induction, Cre- control neurons showed a significant increase in a spine head diameter (unpaired t-test: t = 2.48, df = 6, p = 0.04, **Figures 6C,D**). In contrast, positive spine structural plasticity was not detectable in the absence of TTL (unpaired t-test: t = 0.70, df = 6, p = 0.50, **Figure 6C**). These experiments demonstrate that tyrosination of α-tubulin at the postsynapse is important for structural plasticity processes.

Discussion

Microtubules have pleiotropic roles in various cellular processes, and posttranslational modification (PTMs) of tubulin is one of the main factors modulating their diverse function as it results in a specific microtubule surface pattern known as the "tubulin code." Yet, the detailed physiological role of this code remains poorly understood (Janke and Bulinski, 2011; Janke and Magiera, 2020). The first tubulin PTM was described as an RNA-independent enzymatic incorporation of tyrosine observed mainly in neuronal cells (Song et al., 2015). In neurons, both detyrosinated and tyrosinated tubulins have been shown to be distributed in patches along axonal MTs, with detyrosinated tubulins enriched in proximal segments of axon shafts and tyrosinated ones in growth cones (Brown et al., 1993). Detyrosinated MTs are resistant to degradation, whereas tyrosination of α-tubulin has been defined as a marker for dynamic MTs. Indeed, the distal regions of neurites are predominantly tyrosinated (Moutin et al., 2021). In this study, we were interested whether this modification might be important for development but, moreover, also, for neuronal plasticity processes. A crucial role during early development was suggested by our previous results in TTL-null mice that died within 24 h of birth with respiratory problems, ataxia, and severely altered neuronal morphologies (Erck et al., 2005). It was later determined that the severe perinatal mortality in the TTL-null mice may be related to alterations in neurite formation, axon guidance, and increased Rac1 signaling (Marcos et al., 2009). We now aimed to investigate the detailed role of detyrosination/tyrosination PTM both during forebrain development and in mature neurons using conditional deletion of TTL at different time points and in different brain regions.

Tubulin-tyrosine ligase deletion in post mitotic glutamatergic projection neurons in the neocortex and hippocampus exploiting the Nex promoter resulted in pronounced effects on network formation. The development of the cortico-thalamic loop appeared to be reduced, but correct synaptic connections were formed between the TTL-deficient cortical neurons and the TTL-positive-projecting thalamic neurons. This suggests that, although deletion of the TTL gene by NexCre begins at E11.5 (Goebbels et al., 2006), the effects on growth of cortical or thalamic axons, which begins at E13 (López-Bendito and Molnár, 2003), are limited. On the other hand, we defined a developmental arrest at E16/E17, manifested by reduced formation of projecting axons in the developing corpus callosum and ventral commissures. Remarkably, using Western blot analyses, we observed a reduction in α-tubulin

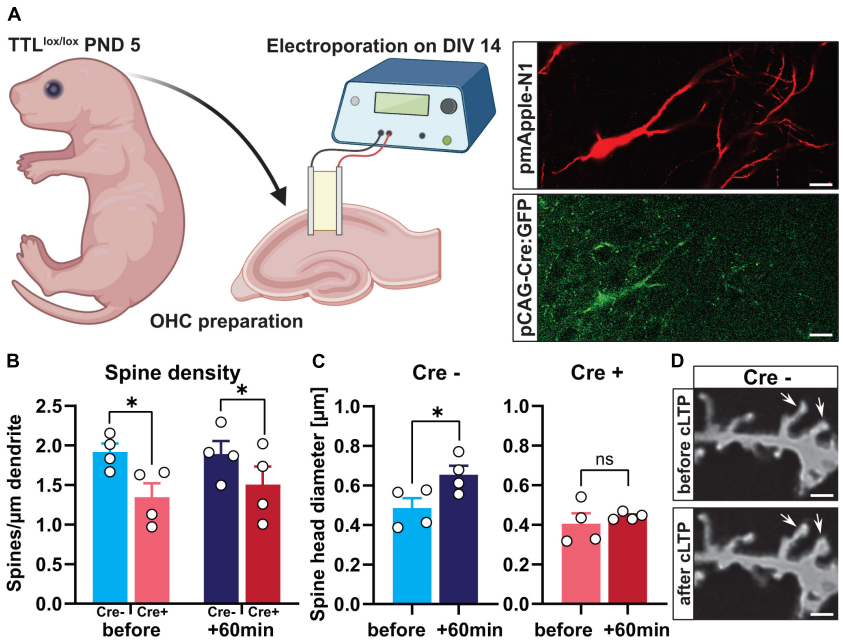

FIGURE 6
Single-cell deletion of TTL in hippocampal slice cultures impairs activity-dependent structural plasticity. **(A)** Schematic representation of single-cell deletion of TTL in hippocampal slice cultures derived from $TTL^{lox/lox}$ mice at postnatal Day 5. Cells were transfected with pmApple-N1 and pCAG-Cre:GFP plasmids by single-cell electroporation (a scale bar = 20 µm) (the figure was generated using BioRender.com). **(B)** Assessment of dendritic spine density showed that acute depletion of TTL in Cre + cells resulted in a significant reduction in the number of dendritic spines compared with control Cre- cells, but cLTP induction did not trigger new spine formation ($N = 4$ in each group). **(C,D)** Sixty minutes after cLTP induction, Cre- control neurons showed a significant increase in a spine-head diameter, which was not the case in Cre + cells lacking TTL **(C)**. Representative examples of dendritic spines in Cre- control cells before and after cLTP induction are shown (60×); scale = 2 µm **(D)**. $N = 4$ cells in each group and 15 spines along each dendrite were randomly selected, measured, and averaged for head diameter assessment. Data are presented as mean ± SEM, $^*p < 0.05$.

tyrosination only from postnatal Day 7. Thus, we conclude that cortical neurons forming the cortico-thalamic loop or callosal projections, such as the corpus callosum, begin projecting before TTL protein is completely absent and that cortical neurons forming the ventral commissures later in development do not project because of the complete loss of TTL at this time point. Previously, it has been shown that *in vitro* isolated TTL-deficient hippocampal neurons initially grow faster, develop multiple axons, and are more branched (Erck et al., 2005). This is in marked contrast to the *in vivo* data, where normal axon formation, e.g., by the corpus callosum in both hemispheres in the $TTL^{lox/lox/NexCre+}$ mice, was drastically reduced. Apparently, suppression of TTL disrupted mechanisms essential for controlling neurite outgrowth, but not neurite outgrowth *per se* (Erck et al., 2005). Furthermore, previous findings showed that initiation of neurite outgrowth *in vitro* is generally not dependent on microtubule assembly. In neuronal cultures treated with taxol, processes formed despite inhibition of the microtubule assembly, maintenance of stable acetylated alpha-tubulin, and the absence of dynamic tyrosinated alpha-tubulin. These results suggest that the initial steps of neurite formation do not depend on the microtubule assembly and suggest that microtubules assembled in the cell body may be translocated to developing neurites as they form (Smith, 1994). However, further experiments are needed to fully uncover the underlying mechanism.

Behavioral analysis showed that the $TTL^{lox/lox/NexCre+}$ mice exhibited hyperactivity and anxiety-related behaviors. Indeed, healthy neuronal function and proper network formation are crucial events based on normal cytoskeletal organization and dendritic branching. Immunoreactivity of microtubule-associated protein 2 (MAP-2) has been shown to be reduced in the hippocampus and prefrontal cortex of postmortem tissue from patients with schizophrenia (Shelton et al., 2015). Moreover, several features of mouse models associated with schizophrenia, such as anxiety, cognitive deficits, hyperactivity, social impairments, and glutamatergic transmission, are due to genetic deletion of MAPs (Bonini et al., 2017). Additionally, a knock-out model for MAP1B resembles the phenotype of the conventional TTL knock-out mouse in terms of impaired formation of the corpus callosum, thalamo-cortical loop, and hippocampal and anterior commissures (Del RíO et al., 2004). These observations support the idea that tyrosinated α-tubulin is a downstream target for phosphorylated MAPs. Our results also demonstrate the diffuse and reduced immunoreactivity of MAP-2 in the neocortex of $TTL^{lox/lox/NexCre+}$ mice. This underscores

previous findings that attention deficits and hyperactivity disorders may be due to delayed establishment of corticolimbic circuitry or impaired dopamine neurotransmission (Drerup et al., 2010).

Moreover, stathmin has been shown to affect microtubule dynamics by promoting microtubule depolymerization or preventing polymerization of tubulin heterodimers, potentially regulating anxiety, fear, and learning (Uchida et al., 2014; Uchida and Shumyatsky, 2015). STMN1 KO mice exhibited anxious hyperactivity, impaired object recognition, and lower levels of neutral and social exploratory behavior at the baseline compared with wild-type mice (Nguyen et al., 2019). This suggests that changes in microtubule dynamics due to inhibition of the post-translational modifications may trigger a hyperactivity phenotype.

In addition to hyperactivity, the $TTL^{lox/lox/NexCre+}$ mice showed severe impairment in spatial learning and decreased use of hippocampus-dependent search strategies in the water maze test. It has been shown that the synaptic events required for the consolidation of memory traces in cortical networks require time-dependent, coordinated, and correct hippocampal-cortical interactions, but the underlying mechanisms remain unclear (Frankland et al., 2001; Lesburguères et al., 2011). Furthermore, decreased expression of MAP-2 and resulting dystrophic neurites can be found associated with impaired learning and memory formation in Alzheimer's disease models (Ma et al., 2014). Apart from the maldevelopment of hippocampal and cortical circuits in $TTL^{lox/lox/NexCre+}$ mice, which are most likely responsible for the observed deficits in spatial memory formation, the proper transport of organelles and synaptic components, including vesicles containing glutamate receptor subunits and other cargoes, to postsynaptic sites along MTs crucial for learning and memory formation (Setou et al., 2000) might be impaired in these mice.

In line with the severe deficits in spatial learning in forebrain-specific TTL knock-out mice, our results showed that long-term synaptic plasticity was also severely impaired as indicated by decreased LTP and reduced dendritic spine density after deletion of TTL in $TTL^{lox/lox/NexCre+}$ mice. Basal synaptic transmission was not affected, which might point toward potentially compensatory mechanisms due to chronic loss of TTL, leading to a normal steady-state level of synaptic ligand-gated ion channel expression.

Furthermore, our results showed that PSD-95 levels were decreased in the neocortex and hippocampus of these mice. In general, three groups of proteins have been described that can discriminate between microtubules enriched in either tyrosinated or detyrosinated α-tubulin: (i) microtubule + TIP-binding proteins (Steinmetz and Akhmanova, 2008), (ii) microtubule-destabilizing proteins (Peris et al., 2009), and (iii) molecular motor proteins (Konishi and Setou, 2009). Of these, the microtubule + end-binding protein EB3 regulates dendritic morphology by directly interacting with PSD-95, and local accumulation of PSD-95 in spine heads directs dynamic microtubules into these spines (Hu et al., 2011). It can be hypothesized that a large pool of stable detyrosinated microtubules is present in the dendrites of TTL-deficient neurons and that highly motile microtubules, which can enter spines during the induction of synaptic plasticity, for instance, are sparse or completely absent. This may explain the observed reduction in PSD-95 protein levels in $TTL^{lox/lox/NexCre+}$ mice and the resulting lower density of dendritic spines, as well as the impaired LTP after deletion of TTL.

The results obtained from the $TTL^{lox/lox/NexCre+}$ mice revealed the importance of α-tubulin tyrosination for the proper formation of the cortical-hippocampal network. To also understand the acute role of this PTM in synaptic plasticity, we used the T29-1 CaMKIIα-Cre mouse line to specifically remove TTL from the CA1 pyramidal cell layer of the hippocampus in the third to fourth postnatal weeks, and, therefore, after networks are already established (Tsien et al., 1996). Intriguingly, CA1-specific deletion of TTL in the $TTL^{lox/lox/CaMKII\alpha-Cre+}$ mice also resulted in impaired Schaffer-collateral LTP and decreased spine density in hippocampal CA1 neurons, indicating a role also for synaptic integrity and synaptic plasticity in the adult brain. It can be concluded that the tyrosination status of α-tubulin is not only important for brain development but also plays an essential role in basal brain function as well as plasticity processes in the adult CNS.

In contrast to $TTL^{lox/lox/NexCre+}$ mice, in $TTL^{lox/lox/CaMKII\alpha-Cre+}$ mice, mainly, the maintenance phase of LTP is impaired. The specific role of tyrosination/detyrosination posttranslational modification of the microtubule for the induction and maintenance phases of LTP yet needs to be elucidated. It has been shown that stathmin is dephosphorylated in the early phase, which enhances its microtubule-destabilizing activity by promoting stathmin-tubulin binding, whereas, these processes are reversed in the late phase, leading to an increase in microtubule/KIF5-mediated localization of the GluA2 subunit of AMPA receptors to synaptic sites (Uchida and Shumyatsky, 2015). In the first 8 h after learning, changes in phosphorylation of stathmin undergo two phases that lead to biphasic shifts in microtubule stability/instability. These shifts, in turn, regulate memory formation by controlling synaptic transport of the GluA2 subunit of AMPA receptors in the second phase (Uchida and Shumyatsky, 2015). Therefore, altered microtubule stabilization in CA1 neurons could, indeed, affect the localization of the GluA2 subunit of AMPA receptors to synaptic sites, which, in turn, could affect the late phase of LTP.

For further confirmation of the importance of the tubulin codes, we additionally investigated the role of TTL in activity-dependent spine structural plasticity in hippocampal slice cultures. Indeed, loss of TTL in cultured hippocampal neurons led to an impairment of spine structural plasticity after cLTP induction. Overall, these results confirm the fact that dynamic

MTs targeting spines are important for activity-dependent changes in synapse structure and function. The dynamics of MTs are necessary for the transport of cargoes required for signal transduction by kinesin and dynein along MTs to the dendrite spine head (Dent, 2017). Spine entry of dynamic microtubules is triggered by *N*-methyl-*D*-aspartic acid (NMDA) receptor activation and calcium influx and requires dynamic actin remodeling (Schätzle et al., 2018). Therefore, these results may also highlight the direct importance of α-tubulin tyrosination for actin microtubule crosstalk in orchestrating synaptic function and plasticity. Despite the impairments in functional plasticity in $TTL^{lox/lox/CaMKII\alpha-Cre+}$ animals, they did not show behavioral or cognitive impairments. This might be, indeed, expected as the knock out was confined to the CA1 region only and did not alter hippocampal function in total. However, the trend toward a reduction in hippocampus-dependent search strategies that we observed in the $TTL^{lox/lox/CaMKII\alpha-Cre+}$ mice is consistent with the fact that the CA1 region is strongly involved especially in the allocentric encoding of spatial information (Suthana et al., 2009).

In summary, TTL activity is a prerequisite for proper cortical development and function. Loss of TTL has been shown to be associated with an imbalance of tyrosinated and detyrosinated pools of α-tubulin resulting in reduced MT dynamics and subsequent dyslocalization of microtubule-binding proteins and arrest of neuronal growth (Erck et al., 2005; Gu et al., 2008). Our data support the finding that mutations in tubulins lead to brain malformations and can be associated with various brain disorders and diseases (Moutin et al., 2021). In fact, in neurodegenerative processes, the content of detyrosinated/tyrosinated tubulins has been shown to be altered in neurons and may be an early marker of disease development (Zhang et al., 2015). The tubulin code as generated by post-translational modifications of tubulins is thus an important intrinsic cue for proper neuronal integrity and function. We found that the α-tubulin tyrosination cycle provides the molecular and structural basis for fine-tuning neuronal connectivity and is a novel key component of synaptic plasticity and memory formation.

Data availability statement

The raw data supporting the conclusions of this article will be made available by the authors, without undue reservation.

Ethics statement

This animal study was reviewed and approved by Nds. Landesamt für Verbraucherschutz und Lebensmittelsicherheit, LAVES.

Author contributions

KM-P, MH, CE, and MK conceived and designed the research. SH, MH, and CE performed the experiments. All authors analyzed the data, wrote the manuscript, and approved the submitted version.

Funding

This work was supported by the Deutsche Forschungsgemeinschaft (FOR629). MK was funded by the Helmholtz-Gemeinschaft, Zukunftsthema "Immunology and Inflammation" (ZT-0027) and by the DFG (SFB854, TP25). We acknowledge support by the Open Access Publication Funds of Technische Universität Braunschweig.

Acknowledgments

We thank the late Dr. Jürgen Wehland for his long-standing enthusiasm for tubulin-modifying enzymes and initiating this project. We are thankful to Dr. Klaus-Armin Nave (Max Planck Institute, Göttingen, Germany) for kindly providing Cre-expressing mouse lines. We also thank a lot Diane Mundil for her excellent technical assistance. The schematic illustrations were created using BioRender.com.

Conflict of interest

The authors declare that the research was conducted in the absence of any commercial or financial relationships that could be construed as a potential conflict of interest.

Publisher's note

Supplementary material

The Supplementary Material for this article can be found online at: https://www.frontiersin.org/articles/10.3389/fnmol.2022.931859/full#supplementary-material

References

Aillaud, C., Bosc, C., Peris, L., Bosson, A., Heemeryck, P., Van Dijk, J., et al. (2017). Vasohibins/SVBP are tubulin carboxypeptidases (TCPs) that regulate neuron differentiation. *Science* 358, 1448–1453. doi: 10.1126/science.aao4165

Baas, P. W., Rao, A. N., Matamoros, A. J., and Leo, L. (2016). Stability properties of neuronal microtubules. *Cytoskeleton* 73, 442–460. doi: 10.1002/cm.21286

Barra, H. S., Arce, C. A., and Argaraña, C. E. (1988). Posttranslational tyrosination/detyrosination of tubulin. *Mol. Neurobiol.* 2, 133–153. doi: 10.1007/BF02935343

Bonini, S. A., Mastinu, A., Ferrari-Toninelli, G., and Memo, M. (2017). Potential Role of Microtubule Stabilizing Agents in Neurodevelopmental Disorders. *Int. J. Mol. Sci.* 18:1627. doi: 10.3390/ijms18081627

Bradke, F., Fawcett, J. W., and Spira, M. E. (2012). Assembly of a new growth cone after axotomy: The precursor to axon regeneration. *Nat. Rev. Neurosci.* 13, 183–193. doi: 10.1038/nrn3176

Brown, A., Li, Y., Slaughter, T., and Black, M. M. (1993). Composite microtubules of the axon: Quantitative analysis of tyrosinated and acetylated tubulin along individual axonal microtubules. *J. Cell Sci.* 104, 339–352. doi: 10.1242/jcs.104.2.339

Chen, C. M., Orefice, L. L., Chiu, S. L., Legates, T. A., Hattar, S., Huganir, R. L., et al. (2017). Wnt5a is essential for hippocampal dendritic maintenance and spatial learning and memory in adult mice. *Proc. Natl. Acad. Sci. U S A.* 114, E619–E628. doi: 10.1073/pnas.1615792114

Del RíO, J. A., González-Billault, C., Ureña, J. M., Jiménez, E. M., Barallobre, M. A. J., and Pascual, M. (2004). MAP1B is required for Netrin 1 signaling in neuronal migration and axonal guidance. *Curr. Biol.* 14, 840–850. doi: 10.1016/j.cub.2004.04.046

Dent, E. W. (2017). Of microtubules and memory: Implications for microtubule dynamics in dendrites and spines. *Mol. Biol. Cell* 28, 1–8. doi: 10.1091/mbc.e15-11-0769

Dent, E. W., and Baas, P. W. (2014). Microtubules in neurons as information carriers. *J. Neurochem.* 129, 235–239. doi: 10.1111/jnc.12621

Drerup, J. M., Hayashi, K., Cui, H., Mettlach, G. L., Long, M. A., Marvin, M., et al. (2010). Attention-deficit/hyperactivity phenotype in mice lacking the cyclin-dependent kinase 5 cofactor p35. *Biol. Psychiatry* 68, 1163–1171. doi: 10.1016/j.biopsych.2010.07.016

Erck, C., Macleod, R. A., and Wehland, J. (2003). Cloning and genomic organization of the TTL gene on mouse chromosome 2 and human chromosome 2q13. *Cytogenet. Genome Res.* 101, 47–53. doi: 10.1159/000073418

Erck, C., Peris, L., Andrieux, A., Meissirel, C., Gruber, A. D., Vernet, M., et al. (2005). A vital role of tubulin-tyrosine-ligase for neuronal organization. *Proc. Natl. Acad. Sci. U S A.* 102, 7853–7858.

Fortin, D. A., Davare, M. A., Srivastava, T., Brady, J. D., Nygaard, S., Derkach, V. A., et al. (2010). Long-Term Potentiation-Dependent Spine Enlargement Requires Synaptic Ca^{2+}-Permeable AMPA Receptors Recruited by CaM-Kinase I. *J. Neurosci.* 30, 11565–11575. doi: 10.1523/JNEUROSCI.1746-10.2010

Frankland, P. W., O'brien, C., Ohno, M., Kirkwood, A., and Silva, A. J. (2001). α-CaMKII-dependent plasticity in the cortex is required for permanent memory. *Nature* 411, 309–313. doi: 10.1038/35077089

Garthe, A., Behr, J., and Kempermann, G. (2009). Adult-generated hippocampal neurons allow the flexible use of spatially precise learning strategies. *PLoS One* 4:e5464. doi: 10.1371/journal.pone.0005464

Garthe, A., and Kempermann, G. (2013). An old test for new neurons: Refining the Morris water maze to study the functional relevance of adult hippocampal neurogenesis. *Front. Neurosci.* 7:63. doi: 10.3389/fnins.2013.00063

Geinisman, Y., Detoledo-Morrell, L., Morrell, F., Persina, I. S., and Rossi, M. (1992). Age-related loss of axospinous synapses formed by two afferent systems in the rat dentate gyrus as revealed by the unbiased stereological dissector technique. *Hippocampus* 2, 437–444. doi: 10.1002/hipo.450020411

Goebbels, S., Bormuth, I., Bode, U., Hermanson, O., Schwab, M. H., and Nave, K. A. (2006). Genetic targeting of principal neurons in neocortex and hippocampus of NEX-Cre mice. *Genesis* 44, 611–621. doi: 10.1002/dvg.20256

Gu, J., Firestein, B. L., and Zheng, J. Q. (2008). Microtubules in dendritic spine development. *J. Neurosci.* 28, 12120–12124.

Hosseini, S., Michaelsen-Preusse, K., Grigoryan, G., Chhatbar, C., Kalinke, U., and Korte, M. (2020). Type I Interferon Receptor Signaling in Astrocytes Regulates Hippocampal Synaptic Plasticity and Cognitive Function of the Healthy CNS. *Cell Rep.* 31:107666. doi: 10.1016/j.celrep.2020.107666

Hotulainen, P., and Hoogenraad, C. C. (2010). Actin in dendritic spines: Connecting dynamics to function. *J. Cell Biol.* 189, 619–629.

Hu, X., Ballo, L., Pietila, L., Viesselmann, C., Ballweg, J., Lumbard, D., et al. (2011). BDNF-induced increase of PSD-95 in dendritic spines requires dynamic microtubule invasions. *J. Neurosci.* 31, 15597–15603. doi: 10.1523/JNEUROSCI.2445-11.2011

Janke, C., and Bulinski, J. C. (2011). Post-translational regulation of the microtubule cytoskeleton: Mechanisms and functions. *Nat. Rev. Mol. Cell Biol.* 12, 773–786.

Janke, C., and Magiera, M. M. (2020). The tubulin code and its role in controlling microtubule properties and functions. *Nat. Rev. Mol. Cell Biol.* 21, 307–326.

Jaworski, J., Kapitein, L. C., Gouveia, S. M., Dortland, B. R., Wulf, P. S., Grigoriev, I., et al. (2009). Dynamic microtubules regulate dendritic spine morphology and synaptic plasticity. *Neuron* 61, 85–100.

Kapitein, L. C., Yau, K. W., Gouveia, S. M., Van Der Zwan, W. A., Wulf, P. S., Keijzer, N., et al. (2011). NMDA receptor activation suppresses microtubule growth and spine entry. *J. Neurosci.* 31, 8194–8209. doi: 10.1523/JNEUROSCI.6215-10.2011

Konishi, Y., and Setou, M. (2009). Tubulin tyrosination navigates the kinesin-1 motor domain to axons. *Nat. Neurosci.* 12, 559–567. doi: 10.1038/nn.2314

Lesburguères, E., Gobbo, O. L., Alaux-Cantin, S., Hambucken, A., Trifilieff, P., and Bontempi, B. (2011). Early tagging of cortical networks is required for the formation of enduring associative memory. *Science* 331, 924–928. doi: 10.1126/science.1196164

López-Bendito, G., and Molnár, Z. (2003). Thalamocortical development: How are we going to get there? *Nat. Rev. Neurosci.* 4, 276–289. doi: 10.1038/nrn1075

Ma, Q.-L., Zuo, X., Yang, F., Ubeda, O. J., Gant, D. J., Alaverdyan, M., et al. (2014). Loss of MAP function leads to hippocampal synapse loss and deficits in the Morris Water Maze with aging. *J. Neurosci.* 34, 7124–7136. doi: 10.1523/JNEUROSCI.3439-13.2014

Marcos, S., Moreau, J., Backer, S., Job, D., Andrieux, A., and Bloch-Gallego, E. (2009). Tubulin tyrosination is required for the proper organization and pathfinding of the growth cone. *PLoS One* 4:e5405. doi: 10.1371/journal.pone.0005405

Martel, G., Uchida, S., Hevi, C., Chévere-Torres, I., Fuentes, I., Park, Y. J., et al. (2016). Genetic Demonstration of a Role for Stathmin in Adult Hippocampal Neurogenesis, Spinogenesis, and NMDA Receptor-Dependent Memory. *J. Neurosci.* 36, 1185–1202. doi: 10.1523/JNEUROSCI.4541-14.2016

Michaelsen-Preusse, K., Kellner, Y., Korte, M., and Zagrebelsky, M. (2014). "Analysis of actin turnover and spine dynamics in hippocampal slice cultures," in *Laser Scanning Microscopy and Quantitative Image Analysis of Neuronal Tissue*, eds L. Bakota and R. Brandt (New York, NY: Springer), 189–217. doi: 10.1093/jmicro/dfaa001

Michaelsen-Preusse, K., Zessin, S., Grigoryan, G., Scharkowski, F., Feuge, J., Remus, A., et al. (2016). Neuronal profilins in health and disease: Relevance for spine plasticity and Fragile X syndrome. *Proc. Natl. Acad. Sci. U S A.* 113, 3365–3370. doi: 10.1073/pnas.1516697113

Morris, R. (1984). Developments of a water-maze procedure for studying spatial learning in the rat. *J. Neurosci. Methods* 11, 47–60.

Moser, M.-B., Trommald, M., and Andersen, P. (1994). An increase in dendritic spine density on hippocampal CA1 pyramidal cells following spatial learning in adult rats suggests the formation of new synapses. *Proc. Natl. Acad. Sci. U S A.* 91, 12673–12675. doi: 10.1073/pnas.91.26.12673

Moutin, M. J., Bosc, C., Peris, L., and Andrieux, A. (2021). Tubulin post-translational modifications control neuronal development and functions. *Dev. Neurobiol.* 81, 253–272.

Murray, E., Cho, J. H., Goodwin, D., Ku, T., Swaney, J., Kim, S. Y., et al. (2015). Simple, Scalable Proteomic Imaging for High-Dimensional Profiling of Intact Systems. *Cell* 163, 1500–1514. doi: 10.1016/j.cell.2015.11.025

Nguyen, T. B., Prabhu, V. V., Piao, Y. H., Oh, Y. E., Zahra, R. F., and Chung, Y. C. (2019). Effects of Stathmin 1 Gene Knockout on Behaviors and Dopaminergic Markers in Mice Exposed to Social Defeat Stress. *Brain Sci.* 9:215. doi: 10.3390/brainsci9090215

Nieuwenhuis, J., Adamopoulos, A., Bleijerveld, O. B., Mazouzi, A., Stickel, E., Celie, P., et al. (2017). Vasohibins encode tubulin detyrosinating activity. *Science* 358, 1453–1456.

Peris, L., Wagenbach, M., Lafanechère, L., Brocard, J., Moore, A. T., Kozielski, F., et al. (2009). Motor-dependent microtubule disassembly driven by tubulin tyrosination. *J. Cell Biol.* 185, 1159–1166. doi: 10.1083/jcb.200902142

Prota, A. E., Magiera, M. M., Kuijpers, M., Bargsten, K., Frey, D., Wieser, M., et al. (2013). Structural basis of tubulin tyrosination by tubulin tyrosine ligase. *J. Cell Biol.* 200, 259–270.

Qu, X., Kumar, A., Blockus, H., Waites, C., and Bartolini, F. (2019). Activity-Dependent Nucleation of Dynamic Microtubules at Presynaptic Boutons Controls Neurotransmission. *Curr. Biol.* 29, 4231.–4240.e5. doi: 10.1016/j.cub.2019.10.049

Richards, L. J., Plachez, C., and Ren, T. (2004). Mechanisms regulating the development of the corpus callosum and its agenesis in mouse and human. *Clin. Genet.* 66, 276–289.

Schätzle, P., Esteves Da Silva, M., Tas, R. P., Katrukha, E. A., Hu, H. Y., Wierenga, C. J., et al. (2018). Activity-Dependent Actin Remodeling at the Base of Dendritic Spines Promotes Microtubule Entry. *Curr. Biol.* 28, 2081–2093.e6. doi: 10.1016/j.cub.2018.05.004

Setou, M., Nakagawa, T., Seog, D.-H., and Hirokawa, N. (2000). Kinesin superfamily motor protein KIF17 and mLin-10 in NMDA receptor-containing vesicle transport. *Science* 288, 1796–1802. doi: 10.1126/science.288.5472.1796

Shelton, M. A., Newman, J. T., Gu, H., Sampson, A. R., Fish, K. N., Macdonald, M. L., et al. (2015). Loss of Microtubule-Associated Protein 2 Immunoreactivity Linked to Dendritic Spine Loss in Schizophrenia. *Biol. Psychiatry* 78, 374–385. doi: 10.1016/j.biopsych.2014.12.029

Smith, C. L. (1994). The initiation of neurite outgrowth by sympathetic neurons grown in vitro does not depend on assembly of microtubules. *J. Cell Biol.* 127, 1407–1418.

Song, W., Cho, Y., Watt, D., and Cavalli, V. (2015). Tubulin-tyrosine Ligase (TTL)-mediated Increase in Tyrosinated α-Tubulin in Injured Axons Is Required for Retrograde Injury Signaling and Axon Regeneration. *J. Biol. Chem.* 290, 14765–14775. doi: 10.1074/jbc.M114.622753

Steinmetz, M. O., and Akhmanova, A. (2008). Capturing protein tails by CAP-Gly domains. *Trends Biochem. Sci.* 33, 535–545.

Suthana, N. A., Ekstrom, A. D., Moshirvaziri, S., Knowlton, B., and Bookheimer, S. Y. (2009). Human hippocampal CA1 involvement during allocentric encoding of spatial information. *J. Neurosci.* 29, 10512–10519. doi: 10.1523/JNEUROSCI.0621-09.2009

Szyk, A., Deaconescu, A. M., Piszczek, G., and Roll-Mecak, A. (2011). Tubulin tyrosine ligase structure reveals adaptation of an ancient fold to bind and modify tubulin. *Nat. Struct. Mol. Biol.* 18, 1250–1258. doi: 10.1038/nsmb.2148

Tsien, J. Z., Chen, D. F., Gerber, D., Tom, C., Mercer, E. H., Anderson, D. J., et al. (1996). Subregion- and cell type-restricted gene knockout in mouse brain. *Cell* 87, 1317–1326.

Uchida, S., Martel, G., Pavlowsky, A., Takizawa, S., Hevi, C., Watanabe, Y., et al. (2014). Learning-induced and stathmin-dependent changes in microtubule stability are critical for memory and disrupted in ageing. *Nat. Commun.* 5:4389. doi: 10.1038/ncomms5389

Uchida, S., and Shumyatsky, G. P. (2015). Deceivingly dynamic: Learning-dependent changes in stathmin and microtubules. *Neurobiol. Learn. Mem.* 124, 52–61. doi: 10.1016/j.nlm.2015.07.011

Walsh, R. N., and Cummins, R. A. (1976). The Open-Field Test: A critical review. *Psychol. Bull.* 83, 482–504. doi: 10.1037/0033-2909.83.3.482

Webster, D. R., Gundersen, G. G., Bulinski, J. C., and Borisy, G. G. (1987). Differential turnover of tyrosinated and detyrosinated microtubules. *Proc. Natl. Acad. Sci. U S A.* 84, 9040–9044. doi: 10.1073/pnas.84.24.9040

Wloga, D., and Gaertig, J. (2010). Post-translational modifications of microtubules. *J. Cell Sci.* 123, 3447–3455. doi: 10.1242/jcs.063727

Zhang, F., Su, B., Wang, C., Siedlak, S. L., Mondragon-Rodriguez, S., Lee, H. G., et al. (2015). Posttranslational modifications of α-tubulin in alzheimer disease. *Transl. Neurodegener.* 4:9. doi: 10.1186/s40035-015-0030-4

frontiers | Frontiers in Molecular Neuroscience

TYPE Review
PUBLISHED 24 October 2022
DOI 10.3389/fnmol.2022.1013933

OPEN ACCESS

EDITED BY
Juan Pablo de Rivero Vaccari,
University of Miami, United States

REVIEWED BY
Fumitaka Shimizu,
Yamaguchi University, Japan
Nadine Ahmed Kerr,
University of Miami, United States

*CORRESPONDENCE
Siming Yang
ysm0117@126.com
Xiaobing Fu
fuxiaobing@vip.sina.com

†These authors have contributed equally to this work

SPECIALTY SECTION
This article was submitted to Brain Disease Mechanisms, a section of the journal Frontiers in Molecular Neuroscience

RECEIVED 08 August 2022
ACCEPTED 20 September 2022
PUBLISHED 24 October 2022

CITATION
Yang J, Ran M, Li H, Lin Y, Ma K, Yang Y, Fu X and Yang S (2022) New insight into neurological degeneration: Inflammatory cytokines and blood–brain barrier. *Front. Mol. Neurosci.* 15:1013933. doi: 10.3389/fnmol.2022.1013933

New insight into neurological degeneration: Inflammatory cytokines and blood–brain barrier

Jie Yang[1,2†], Mingzi Ran[1,3†], Hongyu Li[1,2†], Ye Lin[4], Kui Ma[1], Yuguang Yang[2], Xiaobing Fu[1*] and Siming Yang[1,2*]

[1]Research Centre for Tissue Repair and Regeneration Affiliated to the Medical Innovation Research Department, PLA General Hospital, PLA Medical College, Beijing, China, [2]Department of Dermatology, 4th Medical Centre, PLA General Hospital, Beijing, China, [3]Department of Anaesthesiology, 4th Medical Centre, PLA General Hospital, Beijing, China, [4]Department of Neurology, The First Medical Centre, PLA General Hospital, Beijing, China

Neurological degeneration after neuroinflammation, such as that resulting from Alzheimer's disease (AD), stroke, multiple sclerosis (MS), and post-traumatic brain injury (TBI), is typically associated with high mortality and morbidity and with permanent cognitive dysfunction, which places a heavy economic burden on families and society. Diagnosing and curing these diseases in their early stages remains a challenge for clinical investigation and treatment. Recent insight into the onset and progression of these diseases highlights the permeability of the blood–brain barrier (BBB). The primary factor that influences BBB structure and function is inflammation, especially the main cytokines including IL-1β, TNFα, and IL-6, the mechanism on the disruption of which are critical component of the aforementioned diseases. Surprisingly, the main cytokines from systematic inflammation can also induce as much worse as from neurological diseases or injuries do. In this review, we will therefore discuss the physiological structure of BBB, the main cytokines including IL-1β, TNFα, IL-6, and their mechanism on the disruption of BBB and recent research about the main cytokines from systematic inflammation inducing the disruption of BBB and cognitive impairment, and we will eventually discuss the need to prevent the disruption of BBB.

KEYWORDS

inflammatory cytokines, blood-brain barrier, neurological degeneration, TNFα, IL-1β, IL-6

Introduction

Aging body is vulnerable to chronic inflammatory conditions that cause neurological degeneration in the central nervous system (CNS), such as Alzheimer's disease (AD) (Ju and Tam, 2022). These diseases are frequently associated with high mortality and morbidity and with permanent cognitive dysfunction, which are commonly considered

a significant economic burden on society and on the families of patients. The difficulties faced in resolving these clinical problems are related to the inability of the damaged and degenerated nerve cells to repair themselves (Ren et al., 2018). Although recent research indicates that necrotic foci can be replaced by proliferative neural stem cells (NSCs) (Kuhn and Svendsen, 1999), the number and scale of the NSCs cannot make up for the entire injury to the CNS, and strategies for curing neurological diseases in the clinic remain far off. Interestingly, recent research finds that these diseases share a key pathological feature, namely, the disruption of the blood–brain barrier (BBB) (Sweeney et al., 2019; Gold et al., 2021). The disruption of BBB can be detected before the onset of neurodegeneration, and the repairing of BBB after neurodegeneration can be beneficial for the disease (Liebner et al., 2018). Therefore, studying the biological and pathological features of BBB may be a useful target for future diagnosis and treatment.

A primary cause to disrupt the BBB is uncontrolled inflammation after injuries or diseases. Under this condition, the abnormal increasing pro-inflammatory cytokines such as TNFα (Chen et al., 2019), interleukin-1beta (IL-1β) (Hauptmann et al., 2020), interleukin-6 (IL-6) (Yang et al., 2017, Yang J. et al., 2020), interferon-γ (INF-γ) (Bonney et al., 2019), and inducible nitric oxide synthase (iNOS) (Smith et al., 2018) can compromise BBB permeability and induce or deteriorate neurological disorders which make the regulation of inflammation more difficult (Ren et al., 2020). In addition, although BBB structure becomes compromised with aging, leaving patients vulnerable to neurological diseases such as AD (Huang et al., 2020), the main inducer to disrupt the BBB is the abnormal increasing inflammatory cytokines after injuries or diseases.

Moreover, most research focus only on the primary diseases or injuries of the brain inducing the dysfunction of BBB and thus CNS impairment, but few on the peripheral injuries leading to that. Our previous studies indicated that peripheral burns and traumatic surgical wound could induce the dysfunction of BBB and thus cognitive impairment through IL-6 and IL-1β (Yang et al., 2017, Yang J. et al., 2020). As a result, regulating inflammatory factors from assaulting the BBB is crucial for curing neurological diseases. In this review, we will systematically discuss how these pro-inflammatory cytokines assaulting on BBB.

The structure and biomechanisms of blood–brain barrier

In contrast to the peripheral vasculature, the vessels in the brain possess a highly selectively permeable barrier, BBB, that protects the CNS from potential toxins, pathogens, and so on. Only small lipid-soluble molecules <400 Da and with fewer than nine hydrogen bonds can independently cross the BBB *via* lipid-mediated diffusion (Padden et al., 2007; Segarra et al., 2021). BBB comprises a tightly sealed monolayer of brain endothelial capillaries (Ohtsuki and Terasaki, 2007) containing cell types such as brain microvascular endothelial cells (BMECs), pericytes (PCs), astrocytes (ACs) end feet, microglia, and neurons (**Figures 1A,B**; Bazzoni and Dejana, 2004). Molecules between the blood circulation and the brain parenchyma through BBB by two ways include transcellular vesicular transport (transcytosis) and paracellular pathway. BMECs are connected to one another by tight junctions (TJs) and adherens junctions (AJs) (Hawkins and Davis, 2005), which regulate the paracellular permeability of BBB (Bazzoni and Dejana, 2004). TJs include the endothelial-specific claudin family member claudin-5 (Cldn5) and occludin (Ocln), which are linked to the cytoskeleton by members of the zonula occludens family (ZO-1, ZO-2, and ZO-3) (Brown and Davis, 2002). The interactions among these proteins are the primary factors regulating the paracellular barrier of BMECs (Sandoval and Witt, 2008; **Figure 1A**). AJs, which are formed by homophilic interactions between cadherins, such as vascular endothelial (VE)-cadherin (Cdh5, CD144) and N-cadherin, are considered a prerequisite for the establishment of TJs (**Figure 1A**). In BMECs, AJs intermingle with TJs to form junctional complexes that contribute to BBB stability (Dejana and Orsenigo, 2013). Another way, transcytosis, is mainly regulated by PCs, which are embedded along with vascular mural cells in the basement membrane of brain microvessels and abnormal PC function may lead to BBB dysfunction and neuroinflammation (Daneman et al., 2010; Dohgu and Banks, 2013; Ben-Zvi et al., 2014). Furthermore, recent research indicates that an important membrane protein, major facilitator superfamily domain containing 2a (Mfsd2a), on BMECs also plays an important role on transcytosis, and its expression may be regulated by PCs (Ben-Zvi et al., 2014) (**Figures 1A,B**). The reduced Mfsd2a after CNS diseases or injuries can increase the levels of transcellular vesicles including Cav-1, Nrf-2, and HO-1 on BMECs which may contain toxins, pathogens, or cytokines in brain, while upregulation of Mfsd2a will protect BBB from decreasing levels of the vesicles (Eser Ocak et al., 2020; **Figure 1C**).

Moreover, ACs are also the principal components of the BBB. ACs, whose end feet cover nearly the entire surface of BECs, have a critical effect on the BBB (Cheslow and Alvarez, 2016). Various AC proteins such as aquaporin-4 (Aqp4) and the Kir4.1 potassium channel localize to the end-foot membrane to regulate water homeostasis (Engelhardt and Liebner, 2014; **Figure 1A**). ACs function in BBB maintenance and induce the barrier properties of BMECs through various pathways such as Wnt (Guérit et al., 2021), Shh (Xing et al., 2020), and VE-PTP-dependent restoration of Tie2 signaling (Gurnik et al., 2016). The interaction between ACs and BMECs not only improves AC differentiation *via* the secretion of leukemia inhibitory factor 1 (LIF1) by BMECs but also maintains the development of the BBB through VE-PTP-dependent restoration of Tie2 signaling (Liebner et al., 2018). However, the relationship between PCs and ACs remains undetermined (**Figure 1A**).

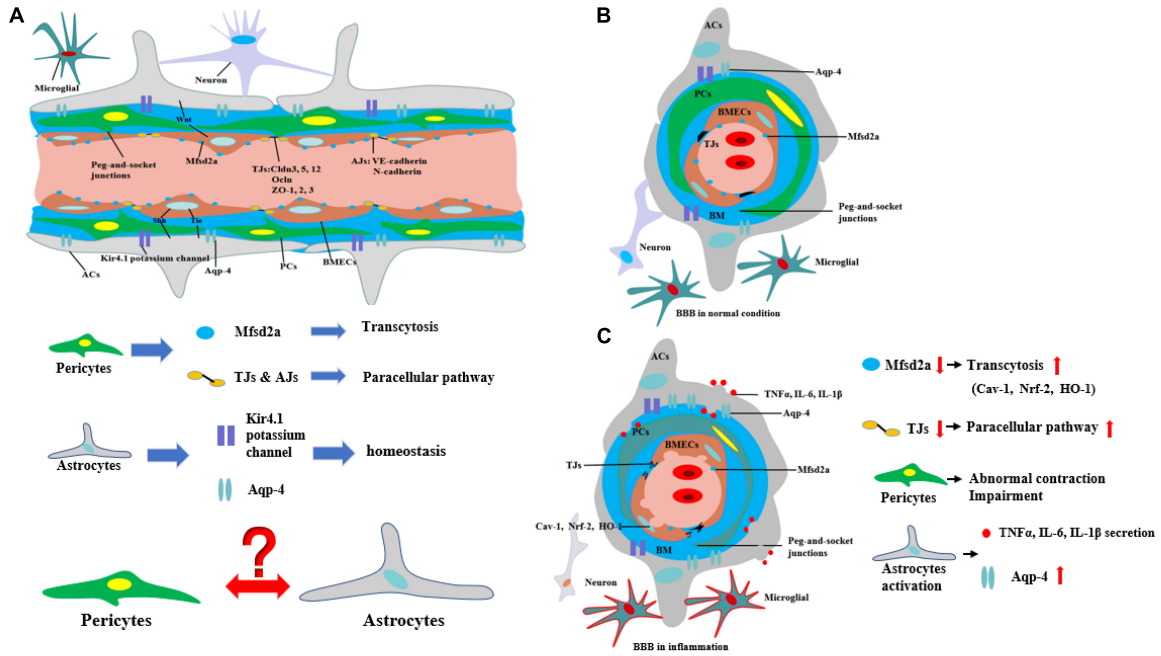

FIGURE 1
Structure and biomechanisms of blood–brain barrier during physical or inflammation. **(A)** The structure of BBB from longitudinal section during physical condition. PCs control the transcytosis and paracellular pathway of BBB by regulating the expression of Mfsd2a and TJs. The structure of potassium channel of Kir4.1 potassium channel and Aqp-4 on ACs regulates the homeostasis of CNS. However, the relationship between ACs and PCs is still unknown. **(B)** The structure of BBB from cross-section during physical condition. **(C)** The structure of BBB from cross-section during inflammation. During inflammation, the expression of Mfsd2a is decreasing, which is negatively correlated with transcytosis of BBB. The level of TJs is decreasing, which means the paracellular pathway of BBB is increasing. Moreover, PCs are abnormal contracted and impairment. In addition, ACs are activated to secrete pro-inflammatory cytokines and the level of Aqp-4 is increasing, which is correlated with the deterioration of CNS diseases or injuries.

Effects of inflammation on blood–brain barrier

During neurological diseases or injuries, immune cells inside the brain secrete pro-inflammatory cytokines, and the structure of BBB tends to be loosened, including the disruption of PCs, which regulate the transcytosis, and TJs, which regulate the paracellular pathway (Figure 1C). Immune cells from outside the brain, such as T cells, specifically target adhesion molecules on BBB, particularly intercellular adhesion molecule-1 (ICAM-1) and vascular cell adhesion molecule-1 (VCAM-1) (Carrano et al., 2012). Subsequently, immune cells, especially CD4 + T cells, pass through BMECs and into the CNS *via* the transcytosis, mediated by caveolae cluster adhesion molecules, and through the matrix membrane *via* matrix metalloproteins (MMPs) expression by neutrophils in the early stage. The cytokines secreted by immune cells disrupt TJs to open the paracellular pathway in the late stage, which allows more immune cells to cross the BBB, especially Th1 and Th17 cells (Liebner et al., 2018). Immune cell reactivity and cytokine/chemokine secretion, therefore, play critical roles in the functional and anatomical structure of BBB and brain during neuroinflammation. However, our previous work suggested that diseases or traumatic injuries outside the brain may also induce BBB disruption and eventually lead to neurological degeneration through immune cells and pro-inflammatory cytokines (Yang et al., 2017, Yang J. et al., 2020). Both excessive activities can lead to BBB permeability and neurodegeneration, thereby worsening the progression of neurological diseases, such as AD. Given the ongoing debate regarding how immune cells gain entry into the CNS and induce BBB impairment and eventually neurological degeneration, we will systematically discuss the major cytokines (e.g., TNFα, IL-1β, and IL-6) that are secreted by immune cells and their impact on BBB and CNS (Figure 2).

The effects of TNFα on blood–brain barrier and neurological degeneration

TNFα, the main homotrimeric transmembrane protein belonging to the TNF/TNFR ligand/receptor superfamily, plays an important role in neuroinflammation and BBB permeability (Table 1 and Figure 3). TNFα primarily acts by binding receptors on the cell surface as membrane-bound precursor (tmTNFα) and can also be secreted as a 51-kDa soluble

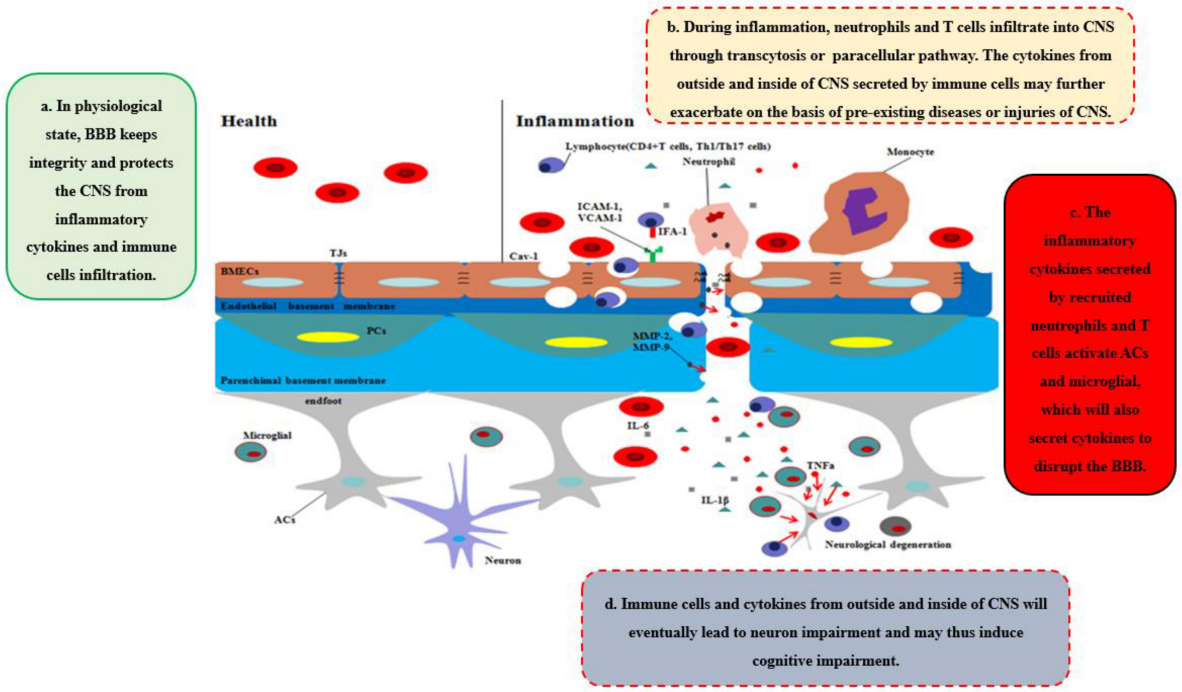

FIGURE 2
Disruption of BBB recruits the immune cells and cytokines into CNS. In healthy status, the integrity of BBB protects the CNS from toxins, pathogens, inflammatory cytokines, and immune cell infiltration. However, during inflammation, neutrophils and T cells from outside of CNS are recruited into CNS through transcytosis or paracellular pathway, which secrete pro-inflammatory cytokines and chemokines to further disrupt the integrity of BBB and deteriorate the CNS disease or injuries. Moreover, ACs and microglia are further activated by the cytokines, chemokines, and immune cells outside of CNS, which integrated with inflammatory factors outside of CNS will eventually lead to neurodegeneration and may induce cognitive impairment.

trimer soluble TNFα (sTNFα) *via* proteolytic cleavage by the TNFα-converting enzyme (TACE) (Tang et al., 1996). During neuroinflammation, TNFα is secreted by neurons (Janelsins et al., 2008), astrocytes (Lieberman et al., 1989), and microglia (Janelsins et al., 2005) and interacts with its cognate receptors, TNF receptor type-1 (TNFR-1, also known as CD120a, p55/60) and TNF receptor type-2 (TNFR-2, also known as CD120b, p75/80). TNFR-1, which is expressed by almost all cells in CNS and mainly integrated with sTNFα, contains an intracellular death domain (DD) that plays an important role in TNFα–mediated apoptosis and cytotoxicity (Locksley et al., 2001; Sedger and McDermott, 2014). At the onset of neurological diseases or injuries, transient TNFα-induced JNK pathway plays a cytoprotective role through TAK1-dependent phosphorylation (Sato et al., 2005), while continuous TNFα-induced JNK signal leads to caspase-dependent apoptosis through JNK phosphorylation by apoptosis signal-regulating kinase 1 (ASK1) (Tobiume et al., 2001). In contrast, TNFR-2 plays an easy biological role compared to TNFR-1 and is mainly expressed by BMECs. Recent research has found that TNFα integrates with TNFR-2 can have effects on both pro-survival pathway and pro-inflammation through the activation of the cellular inhibitor of apoptosis proteins 1 and 2 and nuclear factor κB (NF-κB) (Rothe et al., 1995). Moreover, TNFR-2 can enhance the association with TNFR-1 and sTNFα to perform pro-inflammatory role in CNS (Tartaglia et al., 1993). Recent studies have found that TNFα inhibition TNFR-1–IgG administration was able to control the effects of experimental autoimmune encephalomyelitis (EAE) by reducing activated immune cells, including inflammatory leukocytes and microglia (Korner et al., 1997a). Korner et al. reported that mice lacking TNFα also developed EAE to the same extent as wild-type (WT) mice, because TNF$^{-/-}$ mice were unable to form the typical mature perivascular cuffs observed in WT mice (Korner et al., 1997b). Neutralizing or knocking out TNFα has varying effects because the two types of TNFα receptor have different functions. It is the key that sustained sTNFα integrated with TNFR-1 plays a detrimental role in neurological diseases. To demonstrate this point, Suvannavejh et al. (2000) used TNFR-1/TNFR-2$^{-/-}$ and TNFR-2$^{-/-}$ mice and found that TNFR-1$^{-/-}$ mice were able to control EAE progression by reducing Th1 cells and immune cell infiltration while TNFR-2$^{-/-}$ mice have exacerbated the progression of EAE and the infiltration of immune cells (Suvannavejh et al., 2000). Sophie et al. found that a nanobody-based selective inhibitor of human TNFR1, TROS, was able to effectively delay disease onset, ameliorate symptoms,

and prevent further disease development in a murine model of MS, in which the researchers generated mice expressing human TNFR1 in a mouse TNFR1-knockout background.

Under normal inflammatory condition, TNFα can promote BMEC remodeling through PC proliferation and differentiation from α1 to α2 integrin (Tigges et al., 2013). When neuroinflammation cannot be controlled, sustained TNFα can alter BBB permeability and make the neurological diseases or injuries worsen. During neurological diseases or injuries, microglia-induced TNFα interacts with TNFR-1 disrupts TJs and leads to BMECs necroptosis, thereby allowing entry of toxins and pathogens into CNS (Chen et al., 2019). Aslam et al. (2012) found that TNFα can disrupt the TJ structure by reducing Cldn5 *via* activation of the NF-κB signaling pathway. Ni et al. (2017) used an immortalized human cerebral endothelial cell line (hCMEC/D3) to demonstrate that TNFα can disrupt TJs on BMECs, which can be largely inhibited by SB202190, an inhibitor of p38MAPK, and partly by U0126, a MEK1/2-ERK1/2 inhibitor, thus implicating both of these signaling pathways in BBB disruption. From the outside of CNS, during systemic inflammation, peripheral TNFα can directly cause BBB dysfunction through decreasing transcellular electrical resistance, cellular polarity, and activate BMECs and ACs to secrete pro-inflammatory chemokines, such as MCP-1 and IP-10, which are responsible for the recruitment of leukocyte. The situation can further disrupt TJs and induce an inflammatory milieu, as well as the adhesion molecule ICAM-1 and VCAM-1, which recruit leukocytes by increasing the transcellular permeability of the BBB (O'Carroll et al., 2015; Mantle and Lee, 2018). In addition, Ding et al. suggested that TNFα can upregulate the expression of MMP-9, a proteinase to disrupt TJs and basal membrane of BBB, through activation of Ca/CAMK II/ERK/NF-κB signaling pathway (Ding et al., 2019). Other potential mechanism about peripheral TNFα-induced BBB dysfunction includes cyclooxygenase (COX) pathway and iNOS released. By activation of COX pathway, TNFα can upregulate COX-2 to increase the levels of MMP-2, MMP-3, and MMP-9 and change the cytoskeletal structure of BMECs to disrupt the TJs. Another pathway is TNFα-induced iNOS release which can increase the BBB permeability by impairing BMECs, but the mechanism remains unknown (Liu et al., 2013). At last, sustained TNFα in blood can lead to AC dysfunction. In other situations, hypoxia, recent studies indicate that TNFα will inhibit the expression of erythropoietin (EPO), which is secreted by ACs and has an important neuroprotective role on CNS and BBB, thereby exacerbating the outcome of neurological injury in hypoxia (Nagaya et al., 2014). Kralingen et al. found that TNFα generates an inflammatory milieu that will induce a reduction of ACs (van Kralingen et al., 2013). In contrast, although TNFα can induce BBB disruption and TNFα inhibition can reduce CNS inflammation, representing a potentially promising target for treating neuroinflammation, TNFα may play a neuroprotective role in diseases, such as AD, having been shown to reduce cellular prion protein (PrPC) and Aβ protein levels in BMECs of mouse. The effects of TNFα on the BBB and CNS are well known (Yasutaka et al., 2015). After all, the underlying intercellular signaling pathways, as well as strategies for using these effects to save patients from diseases, such as neurodegeneration, are promising targets for future study.

The effects of IL-1β on blood–brain barrier and neurological degeneration

IL-1β, a member of the IL-1 family which includes seven agonist signaling ligands, three receptor antagonists, and IL-37, is largely responsible for the acute response and angiogenesis. During the initial inflammation, the inflammasome is synthesized in the cytoplasm which would assemble proteins made up mainly through the nucleotide binding and oligomerization domain (NOD)-like receptors (NLRs). This assembled inflammasome is specific for a set of cell damage-associated molecular patterns (DAMPs) or pathogen-associated microbial patterns (PAMP) according to the type of damage of body recognized by different NLR subtypes. Moreover, the inactive procaspase-1 molecules are recruited to the inflammasome complex to be activated (Nasti and Timares, 2012). IL-1β, primarily, occurs as a 31-kDa inactive precursor and would then be cleaved by the caspase-1 to yield the 17-kDa bioactive IL-1β (Netea et al., 2010). The low level of IL-1β in CNS performs an important biological and physiological role which controls sleep, appetite, hypothalamus–pituitary axis, neuroendocrine function (Liu and Quan, 2018), neurogenesis, and synaptic plasticity (Vezzani and Viviani, 2015). Furthermore, Goshen et al. found that blocking IL-1β signaling induced impaired hippocampal-independent memory and intact performance in adult mice (Cibelli et al., 2010). However, during neuroinflammation, sustained IL-1β integrated with toll-like receptor-4 (TLR-4) or IL-1 receptor (IL-1R) can promote the progression of diseases or injuries by activating ACs to secrete pro-inflammatory cytokines (IL-6, TNF), colony-stimulating factors, chemokines (CCL2, CXCL2, etc.), phospholipase A2, COX-2, prostaglandins and iNO *via* NF-κB and JNK pathways, and activator protein 1 (AP-1) (Blanco et al., 2005; Kitazawa et al., 2011; Musella et al., 2020). The activation of ACs can initiate microglia response to neuroinflammation by ACs-derived ATP as well (Bianco et al., 2005).

The ability of IL-1β to increase BBB permeability after CNS injuries and neurological degeneration is well established (**Table 1** and **Figure 4**). IL-1β disrupts BBB in two ways: First, IL-1β can activate ACs to disrupt BBB and exacerbate the progression of the neurological diseases or injuries. Recent work has shown that IL-1β induces the expression of hypoxia-inducible factor-1 (HIF-1) and its gene target, vascular

TABLE 1 Interaction between inflammatory cytokines and the BBB.

Inflammatory cytokines	Type	Effects on BBB
TNFα	TNFR-1, Pro-inflammatory effects	Disrupting TJs, especially Claudin-5 Chen et al., 2019
		Altered BBB morphology Ni et al., 2017
		Increased secretion of other pro-inflammatory cytokines Aslam et al., 2012
		Recruitment of leukocytes O'Carroll et al., 2015; Mantle and Lee, 2018
		Disrupting astrocytes van Kralingen et al., 2013
	TNFR-2, anti-inflammatory effects	Reduced recruitment of other pro-inflammatory cytokines Suvannavejh et al., 2000
		Promoting BBB recovery Madsen et al., 2020
IL-1β	Pro-inflammatory cytokine	Disrupting astrocyte
		Decreasing TEEB on the BMECs Argaw et al., 2006
		Increased secretion of other pro-inflammatory cytokines Labus et al., 2014
IL-6	sIL-6R, pro-inflammatory effects	Disrupting TJs Rosejohn and Heinrich, 1994
		Decreased β-catenin Yang et al., 2017
	mIL-6R, anti-inflammatory effects	Reduced recruitment of other pro-inflammatory cytokines
		Promoting BBB recovery Jones and Jenkins, 2018
HMGB1	Pro-inflammatory cytokine	Activating neuroinflammation
		BBB disruption O'Connor et al., 2003; Liesz et al., 2015
IL-10	Anti-inflammatory cytokine	Reduced BBB impairment
		Reduced down-regulation of Claudin-5 Couper et al., 2008; Lin et al., 2018

endothelial growth factor-A (VEGF-A), in human astrocytes, which in turn induces the breakdown of BBB and exacerbates the CNS degeneration, such as in MS (Argaw et al., 2006). Moynagh et al. (1994) suggested that cerebral IL-1β can activate NF-κB and increase the levels of VCAM-1 and ICAM-1 in ACs, which can recruit the leukocytes into CNS. Second, IL-1β promotes the secretion of other pro-inflammatory cytokines (IL-6 and TNFα) to disrupt the paracellular BBB pathway. Labus et al. used a transfected human brain microvascular endothelial cell (THBMEC)-based *in vitro* BBB model and found that IL-1β decreased TEER and induced the secretion of other pro-inflammatory cytokines, including IL-6 and TNFα, to increase the paracellular permeability of BBB. The increasing paracellular permeability will be more vulnerable to leukocytes and thus exacerbate neuroinflammation (Labus et al., 2014). Some studies have shown that increasing IL-1β or TNFα has similar effects on the secretion of inflammatory cytokines and the induction of ACs death (Netea et al., 2010). Ni et al. found that IL-1β may be a downstream target of TNFα, which can change the structure of Ocln, thereby changing BBB permeability, a smaller effect than that of TNFα through p38 MAPK and ERK1/2 in hCMEC/D3 cells (Ni et al., 2017). However, these effects are quite different from the effects of TNFα, as demonstrated by O'Carroll et al. who observed clear differences between the effects of TNFα and IL-1β on BBB permeability. IL-1β preferentially induces the cytokines sICAM-1, IL-6, sTNFRI, sTNFRII, GCSF, and GMCSF and the chemokine IP10, whereas TNFα is more likely to induce RANTES and IL-8 secretion (O'Carroll et al., 2015). As a result, the sustained IL-1β will impair the BBB and then induce neurological degeneration. The fact makes the inhibition of IL-1β a therapeutic target for attenuating neuroinflammatory and neurodegeneration (Cibelli et al., 2010).

Despite the evidence of IL-1β on disruption of BBB and then inducing the progression of neurological diseases discussed above, there are supplements of the role of IL-1β induced by systematic inflammation. Mario et al. (2010) have found that mice undergoing surgery of the tibia under general anesthesia have an extreme increasement of IL-1β in hippocampal and then inducing memory and cognitive impairment (Mario et al., 2010). Our research indicated that burn disrupted BBB both increasing the paracellular pathway and transcytosis through increasing the peripheral level of IL-1β and IL-6 (Yang J. et al., 2020). However, the potential mechanism of how it infiltrates into CNS is still unclear.

The effects of IL-6 on blood–brain barrier and neurological degeneration

The common receptor to bind IL-6 is receptor β-subunit, membrane glycoprotein 130 (gp130; also known as IL-6Rβ), which works with either a non-signaling receptor α-subunit or a signaling receptor β-subunit like gp130 to exert pleiotropy function (Heinrich et al., 2003). In addition to classical signaling pathway binding with gp130 on membrane, there is a soluble receptor mainly associated with IL-6(sIL-6R) which can bind circulating half-life IL-6 and expand its bioactivity in those cells without gp130 on their membrane. This signaling pathway is called trans-signaling pathway and is involved in numerous chronic inflammation and diseases

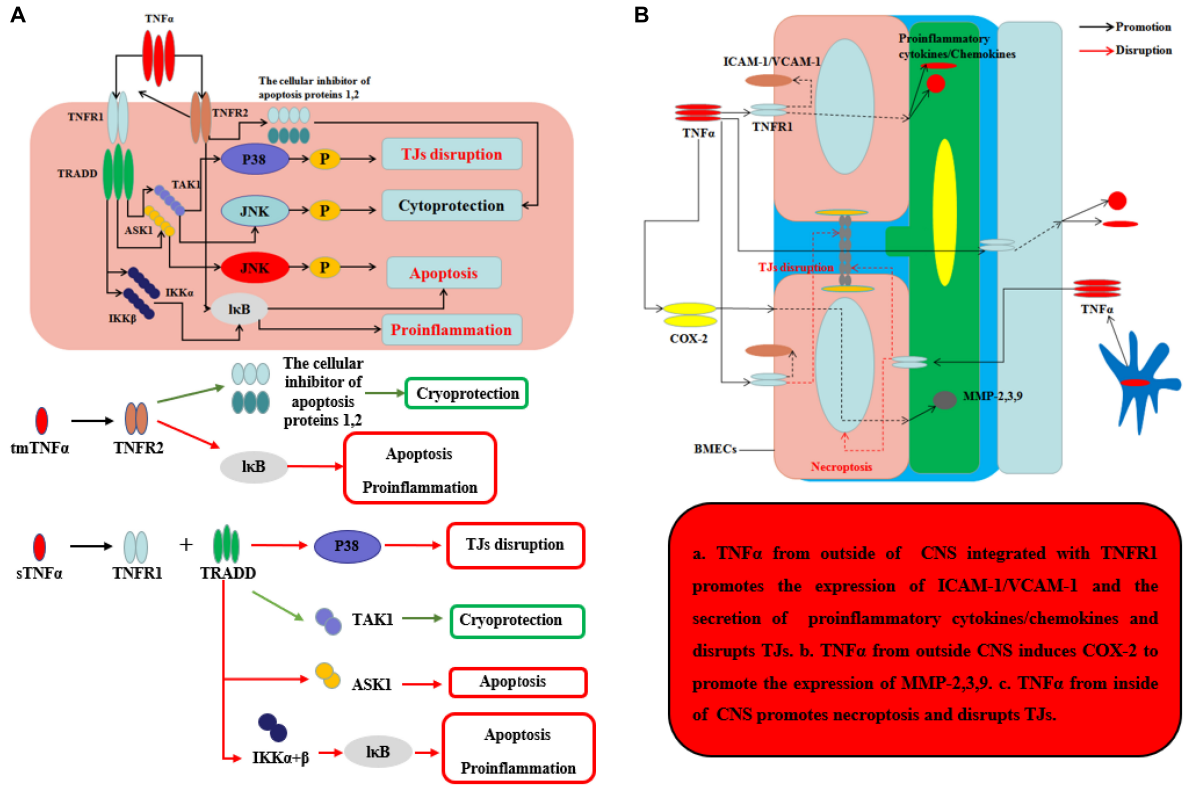

FIGURE 3
Effects of TNFα on BBB and neurological degeneration. **(A)** The mechanism of TNFα on CNS. The tmTNFα integrated with TNFR2 has two functions including promoting the expression of the cellular inhibitor of apoptosis proteins 1,2 to function as cryoprotection and integrating IκB to induce apoptosis and pro-inflammation. The sTNFα integrated with TNFR1 and TRADD can promote the expression of P38 to disrupt TJs and integrate with IKKα and β and further IκB to exert apoptosis and pro-inflammation. Moreover, the complex of sTNFα integrated with TNFR1 and TRADD can integrate TAK1 to exert cryoprotection through JNK in early stage, while the complex can integrate ASK1 to exert apoptosis through JNK in late stage. **(B)** The mechanism of TNFα on BBB from inside and outside of CNS. The sTNFα from outside CNS integrated with TNFR1 promotes the expression of ICAM-1/VCAM-1 on the membrane of BMECs and the secretion of pro-inflammatory cytokines and chemokines, which can disrupt the structure of TJs. Moreover, the complex of sTNFα with TNFR1 from outside CNS induces COX-2 to promote the expression of MMP-2,3,9 which can further disrupt the TJs and basement membrane. TNFα secreted mainly by ACs and microglia from inside CNS promotes necroptosis and disrupts TJs.

(Rosejohn and Heinrich, 1994) (**Table 1**; **Figure 5**). During neuroinflammation, normal level and biological function of IL-6 interacted with sIL-6R *via* trans-signaling pathway can induce repopulating microglia which has an important role on neurogenesis specifically by augmenting the survival of newborn neurons that directly support cognitive function (Willis et al., 2020). The level of IL-6 increases by the activation of ACs induced by TNF and IL-1β *via* NF-κB signaling pathway, while IL-6 is negatively regulated by Wnt signaling pathway (Edara et al., 2020). However, other research indicates that sustained IL-6 can lead to neuroinflammation and pain post-injury *via* signal transducer and activator of transcription 3 (STAT3) (Hu et al., 2020). Through STAT3, IL-6 can induce the demethylation of NeuroD1 (neurogenic differentiation 1) in neural stem cells (NSCs) to promote the neurogenesis in AD as well (Kong et al., 2019). Moreover, Escrig et al. found in mouse AD model that IL-6 trans-signaling induced increasing levels of amyloid plaques and neurofibrillary tangles and cognitive dysfunction (Escrig et al., 2019).

Recent research indicates that the peripheral levels of IL-6 are higher compared with those healthy people in those patients with neurological diseases or injuries (Robelin and Gonzalez De Aguilar, 2014; Yang et al., 2017, Yang J. et al., 2020). The disruption of BBB is mainly by the integration of complexes of sIL-6R and gp130 on the membrane of BMECs by trans-signaling pathway. The pathway can directly disrupt the TJs of BBB in one respect and indirectly increase the ICAM-1 and VCAM-1 to recruit neutrophils infiltrating into the inflammatory site in another. Rosejohn and Heinrich (1994) have found that blockage of the trans-signaling pathway can effectively reduce the leakage of BBB and then relieve the progression of neurological degeneration. As mentioned of TNFα and IL-1β, IL-6 can also induce the released pro-inflammatory cytokines/chemokines to deteriorate the progression in several neurological diseases or

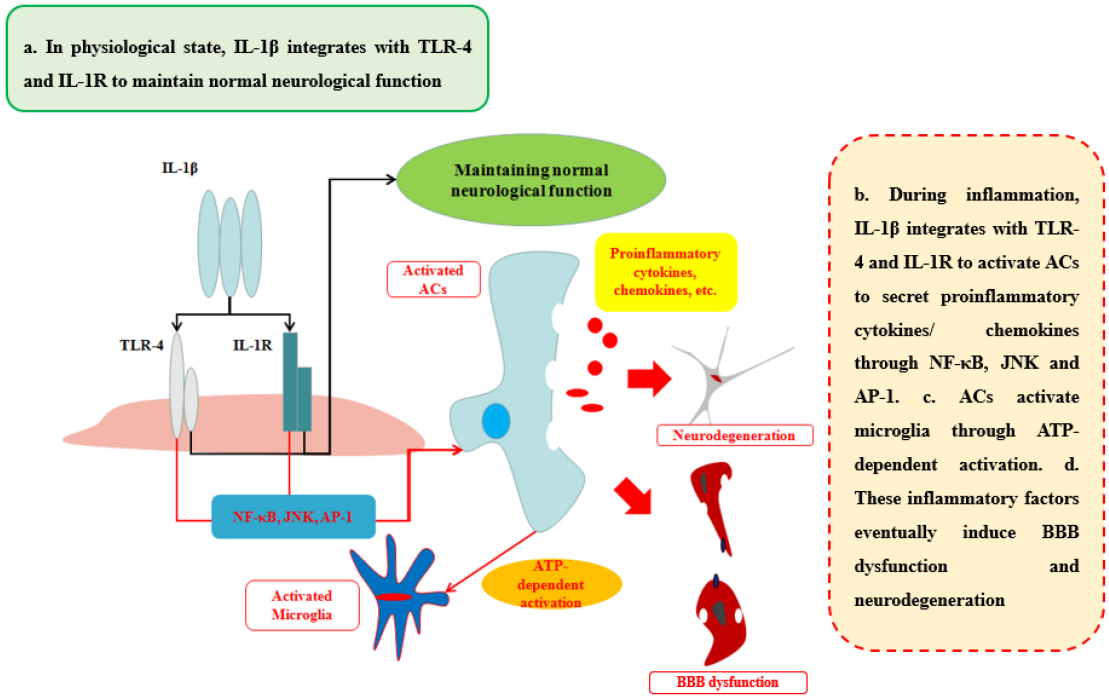

FIGURE 4
Effects of IL-1β on BBB and neurological degeneration. In healthy status, IL-1β integrates with TLR-4 and IL-1R to maintain normal neurological function in CNS. During inflammation, IL-1β integrates with TLR-4 and IL-1R to activate ACs to secrete pro-inflammatory cytokines and chemokines through NF-κB, JNK, and AP-1 pathways. In addition, ACs activate microglia through ATP-dependent activation. Finally, these inflammatory factors eventually induce BBB dysfunction and neurodegeneration.

injuries (Mantle and Lee, 2018). Zhang et al. (2015) found that peripheral IL-6 levels were increased during hypoxic-ischemic brain injury, thus disrupting BBB permeability, and that using neutralizing anti-IL-6 antibodies (anti-IL-6AB) decreased the disruption of TJs and controlled BBB permeability 24 h after ischemic injury. Emery et al. suggested that using an inhibitor of IL-6R can effectively control the progression of autoimmune diseases, such as amyotrophic lateral sclerosis (ALS), in a phase-three clinical trial (Emery et al., 2008).

Above all, most researches focus on the evidence that the inflammation caused by CNS diseases or injuries can induce neurodegeneration. However, peripheral IL-6 can also induce the BBB dysfunction. Our work using a murine surgery model revealed that surgical wounds can induce age-associated BBB dysfunction, and elevated serum IL-6 levels led to decreased TJs but had no effects on AJs (Yang et al., 2017). In addition, we used the mouse burn model which suggested that burn can increase the peripheral level of IL-6 and IL-1β and the level of MMP-9 to disrupt the integrity of BBB *via* paracellular pathway by decreasing TJs, and transcytosis by decreasing Mfsd2a (Yang J. et al., 2020). Other research indicates that the increasing peripheral level of IL-6 can disrupt the TJs to disrupt the BBB and cause neuroinflammation on one side (Furutama et al., 2020) and induce the increasing level of COX-2 to disrupt the BMECs (Eskilsson et al., 2014). Our previous study also found that increased peripheral IL-6 levels can induce decreased β-catenin levels, thereby activating the Wnt pathway, suggesting that the ability of IL-6 overexpression to disrupt the BBB may be related to Wnt signaling pathway (Yang et al., 2017). The study will provide a new insight how we should prevent the CNS injuries from the other site injuries or diseases.

The effects of other potential cytokines on the blood–brain barrier and neurological degeneration

Inflammation is controlled by a complex network of various pro-inflammatory cytokines and receptors (**Table 1**; Patin et al., 2016). However, the exact cytokines and receptors that participate in the neuroinflammation and how they produce their effects *via* signaling pathways remain unclear. In this section, we will try to elucidate the current possible factors and signaling pathways involved in BBB disruption. High-mobility group box 1 protein (HMGB1), which belongs to the damage-associated molecular pattern (DAMP) family (Chaudhry et al., 2018), is released from stressed and dying brain cells and is a potent neuroinflammatory mediator that is mainly regulated by post-translational redox modification. HMGB1 is a nuclear DNA-binding protein that contains two DNA-binding domains

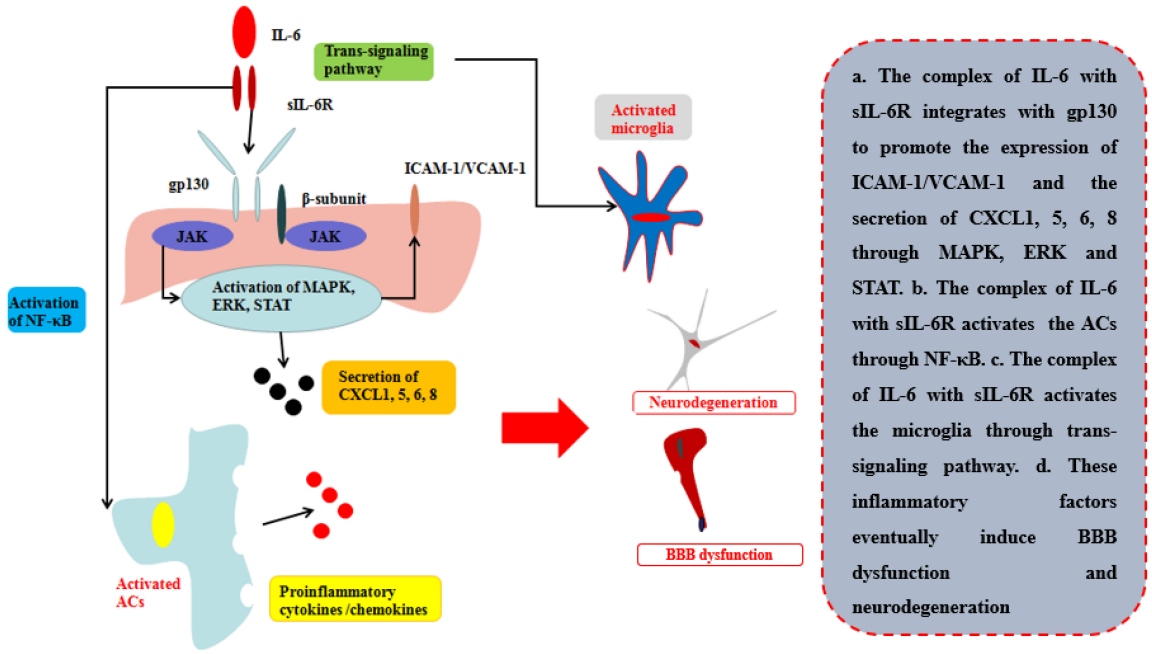

FIGURE 5
Effects of IL-6 on BBB and neurological degeneration. The complex of IL-6 with sIL-6R integrates with gp130 to promote the expression of ICAM-1 and VCAM-1 on BMECs and the secretion of CXCL1, 5, 6, 8 through MAPK, ERK, and STAT. Moreover, the complex of IL-6 with sIL-6R activates the ACs through NF-κB pathway to secrete pro-inflammatory cytokines and the microglia through trans-signaling pathway in CNS. Finally, these inflammatory factors eventually induce BBB dysfunction and neurodegeneration.

(boxes A and B) and a highly repetitive, negatively charged C-terminal tail (Thundyil and Lim, 2015). HMGB1 can disrupt the BBB and induce neurodegeneration by promoting the secretion of pro-inflammatory cytokines, such as TNFα, IL-1β, and IL-6, through the NF-κB signaling pathway and by activating the RAGE axis (O'Connor et al., 2003; Liesz et al., 2015). Moreover, intentionally blocking HMGB1 may improve the outcomes of neurological diseases and injuries such as stroke and TBI and protect the BBB from disruption (Zhang et al., 2011; Okuma et al., 2014).

In contrast, some cytokines play an important role on anti-inflammation and protect the permeability of BBB, including interleukin-10 (IL-10), which is an anti-inflammatory cytokine that is expressed by various leukocytes. The two main IL-10 receptors are IL-10Rα, which is specific to IL-10, and IL-10Rβ (Sanjabi et al., 2009). IL-10 mainly exerts its function by activating the STAT3 signaling pathway. The IL-10 gene promoter contains a STAT3 binding site, resulting in a feedback loop for this pathway. Interestingly, STAT3 plays an anti-inflammatory role when it is activated by IL-10 but plays a pro-inflammatory role with IL-6 (Mosser and Zhang, 2008). Regarding its effects on the BBB and CNS, Lin et al. suggested that IL-10 effectively reduced BMEC apoptosis induced by IL-6-activated STAT3 signaling during neuroinflammation and ameliorate the downregulation of Cldn5 expression in the BBB in a rat model, while *in vitro*, IL-10 protected BBB integrity against TNFα (Lin et al., 2018). Overall, IL-10 plays an important role in immune system homeostasis. Reduced IL-10 expression increases susceptibility to autoimmune inflammation, whereas IL-10 overexpression will impede the clearance of pathogens and induce a chronic inflammatory state (Couper et al., 2008). As a result, how to use IL-10 for clinical treatment requires further study.

In addition to major cytokines, such as TNFα, IL-1β, IL-6, and their receptors, other cytokines also play an important role in neuroinflammation and neurodegeneration and may provide some promising new targets for clinical application to treat neurological disease and injury. However, determining how these factors interact with each other and how the mechanisms of these effects change with age is of critical importance.

The effects of inflammatory cytokines on blood–brain barrier and central nervous system from primary neurological diseases or systematic inflammation

In primary neurological diseases including AD, MS, stroke, and TBI, inflammatory cytokines play an important role on

the promotion of the diseases healing or deteriorating the progression of the diseases in early or late stage, respectively. Rational regulation of inflammation will be the protection for the primary CNS diseases (Jayaraj et al., 2019). However, in neurological diseases, damage to the CNS may lead to a decrease in the control of inflammation, which will lead to inflammatory dysregulation (Lambertsen et al., 2019; Ren et al., 2020). Under this condition, the aberrant expression of inflammatory cytokines will induce the deterioration of neurological diseases and thus neurodegeneration, which may provide an effective target for future clinical treatment as well. Neurological diseases like AD, the secondary pro-inflammatory insults, trigger delirium and can accelerate cognitive decline. Lopez-Rodriguez et al. (2021) found that Aβ was surrounded with NLRP3-integrated inflammasome which recruited microglia to be primed and facilitated to secrete IL-1β using APP/PS1 mice. In addition, activated ACs were primed to pro-inflammatory chemokine responses induced by IL-1β. A CNS trauma like TBI (Kuwar et al., 2019) also found that the complexes of NLRP3-integrated inflammasome induced the expression of IL-1β which will subsequently induce the expression of TNFα and IL-6. On the other side, those pro-inflammatory cytokines secreted by the microglia and ACs can further induce the disruption of BBB through the pathway mentioned before. Furthermore, the expression of ICAM-1 and VCAM-1 and the disruption of TJs will subsequently recruit the peripheral immune cells and cytokines into CNS and thus accelerate the progression of primary diseases (Moynagh et al., 1994; Argaw et al., 2006; Labus et al., 2014; O'Carroll et al., 2015; Zhang et al., 2015; Mantle and Lee, 2018).

Nowadays, the CNS injury caused by peripheral trauma or surgery has gradually become a research hotspot which could also trigger delirium and accelerate cognitive decline on the basis of pre-existing diseases or with higher underlying risks of neurological diseases (Yang T. et al., 2020). Our research focused on the disruption of BBB and cognitive impairment induced by peripheral traumatic injuries. We used traumatic surgical model and burns model in mice and found that peripheral inflammatory cytokines, including IL-6 and IL-1β, were main factor leading to the disruption of BBB and thus cognitive impairment. In surgical model, we found that BBB was disrupted by the increasing level of IL-6 and thus induced cognitive impairment, especially in old mice with higher serum level of IL-6 than young mice with that (Yang et al., 2017). To fully understand the mechanism about the disruption of BBB induced by systematic inflammation, we further used burns model which had more serious inflammatory response than our previous study used surgical model. We found that the increasing permeability of BBB not only included paracellular pathway but also transcytosis induced by the increasing serum level of IL-1β and IL-6 (Yang J. et al., 2020). Unlike primary CNS disease, there are few inflammatory-mediated factors to specifically recruit the immune cells or inflammatory cytokines into CNS. From our studies, the potential mechanism about the disruption of BBB and thus CNS impairment induced by systematic inflammation may be caused by high amount and functional degeneration of immune cells and pro-inflammatory cytokines to identify the receptors in BMECs, the immune situation of which is more likely occur in aging or chronic diseases population (Sendama, 2020). However, new research associated with AD mentioned a potential mechanism that peripheral surgery inducing cognitive impairment may be through the disruption of nasal epithelium and olfactory receptor neurons by the increasing level of IL-6 after surgery (Zhang et al., 2022), but the sequence of disruption of nasal epithelium, olfactory receptor neurons, and cognitive impairment was not strictly discovered, which indicated that peripheral trauma inducing cognitive impairment through the disruption of BBB caused by systematic inflammation may still be the most probable theory in the field. Cognitive impairment and then neurological degeneration induced by systematic inflammation are our novel insight, which will need to pay attention to the protection of BBB in clinical treatment of peripheral diseases in future. However, the potential mechanism needs to be further studied.

Conclusion

The primary factors that disrupt the BBB to induce neurological degeneration are three inflammatory cytokines: TNFα, IL-1β, and IL-6. The basal functions of these cytokines are elucidated above. As an inflammatory network, these cytokines integrated with their special receptors can similarly disrupt TJs and TEER of the BBB without any impairment of AJs (Aslam et al., 2012; Labus et al., 2014), promote ACs apoptosis (Argaw et al., 2006; Nagaya et al., 2014), and recruit leukocytes into BBB (O'Carroll et al., 2015), thereby directly or indirectly inducing neurological degeneration. Other cytokines, including HMGB1 and IL-10, also play an important role in the BBB, as mentioned above. Cytokines such as TNFα and IL-6 bind their respective receptors and exert different functions, as discussed above (Locksley et al., 2001; McCoy and Tansey, 2008; Murakami and Hirano, 2012; Sedger and McDermott, 2014; Wolf et al., 2014). Currently, the pathways that may be involved in these processes include NF-κB (Bianco et al., 2005; Aslam et al., 2012; Edara et al., 2020), p38MAPK, and MEK1/2-ERK1/2 signaling pathway (Ni et al., 2017). However, the potential mechanisms by which cytokines attack the BBB are still unclear. Recent work has shown that blocking pro-inflammatory cytokines, including TNFα, IL-1β, and IL-6, can reduce the permeability of BBB and improve the outcomes of neurological diseases and injuries to a great extent. However, in some conditions, studies have found that cytokines such as TNFα, IL-1β, and IL-6 can also improve the outcome of diseases such as ADs and that neutralizing or knocking out

these cytokines can eventually attenuate the progression of neurological diseases or injuries (Goshen et al., 2007; Yasutaka et al., 2015; Han et al., 2016; Patin et al., 2016). Overall, neurological diseases or injuries present a substantial challenge to the medical field because they are difficult to diagnose and cure and are a social burden for families. Almost all neurological diseases and injuries have an important relationship with the BBB and inflammatory cytokines, which represent a new target for treating these diseases and injuries. As a result, the effects of these cytokines on the BBB and neurodegeneration must be investigated to develop new clinical treatments.

The most recent research has focused on local CNS diseases or injuries such as TBI, AD, and MS attacking BBB and inducing neurodegeneration (Owen et al., 2010; Vázquez-Rosa et al., 2020; Puthenparampil et al., 2021). However, our previous research has confirmed that systematic inflammation will also induce neurological degeneration. For example, after peripheral surgery, the concentration of IL-6 increases in peripheral blood and the structure of the BBB breakdown, thereby inducing cognitive impairment in mice. Older individuals (18-month-old mice) have a higher risk of such impairment. Using IL-6-neutralizing antibodies or gene IL-6 knockout protected the BBB from disruption (Yang et al., 2017). Furthermore, we use the mouse burn model to indicate that peripheral burn can also increase the level of IL-6 and IL-1β in serum which disrupt the integrity of BBB through paracellular pathway and transcytosis (Yang J. et al., 2020). Similar results have been observed in humans. Reichenberg et al. (2001) found that humans with Salmonella abortus equi endotoxin (0.8 ng/kg) presented with abnormal behavior compared with healthy individuals. The results revealed that even a small amount of inflammation can impair the BBB and induce cognitive impairments. As a result, with advancing age, people are more vulnerable to various diseases, and their body experiences chronic inflammation. This effect may continue to produce pro-inflammatory cytokines that disrupt the BBB and induce neurological degeneration. However, demonstrating these effects and illuminating the detailed mechanisms require substantial future research.

Current treatments for neurological degeneration are minimally effective. To date, most studies have found that inhibiting the overexpression of inflammatory cytokines is effective at improving the outcomes of neurological diseases and injuries and delaying the onset of neurodegeneration. However, the timing and mode of intervention are not ideal. As in our research, using anti-IL-6 antibody 18 h before surgery effectively reduced BBB disruption and cognitive impairment, whereas post-surgery treatment has no effect. In clinical settings, we cannot readily use protective interventions before injuries or diseases. Additional research has also found that mesenchymal stem cells (MSCs) effectively protect BBB integrity and that MSC intracranial transplantation may be a promising method for future treatment (Si et al., 2011). Tang et al. found that MSC intracranial transplantation protected BBB integrity, inhibited ACs apoptosis, and decreased Aqp4 expression, which reduced brain edema and impairment (Tang et al., 2014). Menge et al. (2012) suggested that the injection of MSCs can increase the level of tissue inhibitor of matrix metalloproteinase-3 (TIMP3) which can inhibit VEGF-A to protect the BBB from disruption. As mentioned before, injecting MSCs requires cerebral transplantation, which involves substantial risk, and the exact mechanism of how MSCs influence the BBB is poorly understood. Our previous study suggested that MSCs injecting through the tail of mice can effectively protect the integrity of BBB by decreasing peripheral inflammatory cytokines including IL-1β and IL-6, the level of MMP-9, and increasing the level of Mfsd2a (Yang J. et al., 2020). However, the mechanism by which MSCs prevent the BBB from pro-inflammatory cytokines attacking is still under discussed. As a result, additional studies are needed before this approach can be used in clinically.

Individuals with acute or chronic non-cerebral diseases account for a large proportion of patients in the world, and few treatments are available to protect the BBB. Especially, aging makes BBB more vulnerable to the disruption by inflammatory cytokines. The impairment of BBB is easy to recruit more immune cells and cytokines into brain parenchyma and then induce neurological degeneration (Boland et al., 2018). With an aging society coming, the medical care of aging people with neurological diseases is commonly considered a significant economic burden on society and on families (Chen, 2010; Gonneaud and Chételat, 2018; Fang et al., 2020; Pandya and Patani, 2021). As a result, whether the prevention of the disruption of BBB from non-cerebral injuries and diseases will delay the outset and improve the progression of neurological degeneration and this question requires urgent and massive future research to approve. As such, future studies should focus on the mechanisms and treatment of peripheral inflammation-induced BBB disruption. Regardless of cerebral or non-cerebral inflammation, protecting the BBB is a key to preventing neurological degeneration.

Author contributions

SY, JY, MR, YL, and XF conceived and designed the review. JY, YL, KM, and YY prepared the figures. JY, HL, SY, and XF wrote the manuscript. All authors contributed to the article and approved the submitted version.

Funding

This study was supported in part by the National Nature Science Foundation of China (81801909, 81830064, and

81721092) and the Military Medical Research and Development Projects (18-JCJQ-QT-020 and AWS17J005, 2019-126).

Conflict of interest

The authors declare that the research was conducted in the absence of any commercial or financial relationships that could be construed as a potential conflict of interest.

Publisher's note

References

Argaw, A. T., Zhang, Y., Snyder, B. J., Zhao, M. L., Kopp, N., Lee, S. C., et al. (2006). IL-1beta regulates blood-brain barrier permeability via reactivation of the hypoxia-angiogenesis program. *J. Immunol.* 177, 5574–5584. doi: 10.4049/jimmunol.177.8.5574

Aslam, M., Ahmad, N., Srivastava, R., and Hemmer, B. (2012). TNF-alpha induced NFkappaB signaling and p65 (RelA) overexpression repress Cldn5 promoter in mouse brain endothelial cells. *Cytokine* 57, 269–275. doi: 10.1016/j.cyto.2011.10.016

Bazzoni, G., and Dejana, E. (2004). Endothelial cell-to-cell junctions: Molecular organization and role in vascular homeostasis. *Physiol. Rev.* 84, 869–901. doi: 10.1152/physrev.00035.2003

Ben-Zvi, A., Lacoste, B., Kur, E., Andreone, B. J., Mayshar, Y., Yan, H., et al. (2014). Mfsd2a is critical for the formation and function of the blood-brain barrier. *Nature* 509, 507–511. doi: 10.1038/nature13324

Bianco, F., Pravettoni, E., Colombo, A., Schenk, U., Möller, T., Matteoli, M., et al. (2005). Astrocyte-derived ATP induces vesicle shedding and IL-1 beta release from microglia. *J. Immunol.* 174, 7268–7277. doi: 10.4049/jimmunol.174.11.7268

Blanco, A., Vallés, S., Pascual, M., and Guerri, C. (2005). Involvement of TLR4/type I IL-1 receptor signaling in the induction of inflammatory mediators and cell death induced by ethanol in cultured astrocytes. *J. Immunol.* 175, 6893–6899. doi: 10.4049/jimmunol.175.10.6893

Boland, B., Yu, W., Corti, O., Mollereau, B., Henriques, A., Bezard, E., et al. (2018). Promoting the clearance of neurotoxic proteins in neurodegenerative disorders of ageing. *Nat. Rev. Drug Discov.* 17, 660–688. doi: 10.1038/nrd.2018.109

Bonney, S., Seitz, S., Ryan, C., Jones, K., Clarke, P., Tyler, K., et al. (2019). Gamma interferon alters junctional integrity via rho kinase, resulting in blood-brain barrier leakage in experimental viral encephalitis. *mBio* 10:e01675-19. doi: 10.1128/mBio.01675-19

Brown, R., and Davis, T. (2002). Calcium modulation of adherens and tight junction function: A potential mechanism for blood-brain barrier disruption after stroke. *Stroke* 33, 1706–1711. doi: 10.1161/01.STR.0000016405.06729.83

Carrano, A., Hoozemans, J. J., van der Vies, S. M., van Horssen, J., de Vries, H. E., and Rozemuller, A. J. (2012). Neuroinflammation and blood-brain barrier changes in capillary amyloid angiopathy. *Neurodegener. Dis.* 10, 329–331. doi: 10.1159/000334916

Chaudhry, S. R., Hafez, A., Rezai Jahromi, B., Kinfe, T. M., Lamprecht, A., Niemela, M., et al. (2018). Role of damage associated molecular pattern molecules (DAMPs) in aneurysmal subarachnoid hemorrhage (aSAH). *Int. J. Mol. Sci.* 19:2035. doi: 10.3390/ijms19072035

Chen, A., Fang, Z., Chen, X., Yang, S., Zhou, Y., Mao, L., et al. (2019). Microglia-derived TNF-α mediates endothelial necroptosis aggravating blood brain-barrier disruption after ischemic stroke. *Cell Death Dis.* 10:487. doi: 10.1038/s41419-019-1716-9

Chen, L. (2010). Population ageing is a global phenomenon, which affects both Taiwan and China. Preface. *Ageing Res. Rev.* 9(Suppl. 1):S1. doi: 10.1016/j.arr.2010.04.006

Cheslow, L., and Alvarez, J. I. (2016). Glial-endothelial crosstalk regulates blood-brain barrier function. *Curr. Opin. Pharmacol.* 26, 39–46. doi: 10.1016/j.coph.2015.09.010

Cibelli, M., Fidalgo, A. R., Terrando, N., Ma, D., Monaco, C., Feldmann, M., et al. (2010). Role of interleukin-1beta in postoperative cognitive dysfunction. *Ann. Neurol.* 68, 360–368. doi: 10.1002/ana.22082

Couper, K. N., Blount, D. G., and Riley, E. M. (2008). IL-10: The master regulator of immunity to infection. *J. Immunol.* 180, 5771–5777. doi: 10.4049/jimmunol.180.9.5771

Daneman, R., Zhou, L., Kebede, A. A., and Barres, B. A. (2010). Pericytes are required for blood-brain barrier integrity during embryogenesis. *Nature* 468, 562–566. doi: 10.1038/nature09513

Dejana, E., and Orsenigo, F. (2013). Endothelial adherens junctions at a glance. *J. Cell Sci.* 126(Pt 12), 2545–2549. doi: 10.1242/jcs.124529

Ding, X., Sun, X., Shen, X., Lu, Y., Wang, J., Sun, Z., et al. (2019). Propofol attenuates TNF-α-induced MMP-9 expression in human cerebral microvascular endothelial cells by inhibiting Ca/CAMK II/ERK/NF-κB signaling pathway. *Acta Pharmacol. Sin.* 40, 1303–1313. doi: 10.1038/s41401-019-0258-0

Dohgu, S., and Banks, W. (2013). Brain pericytes increase the lipopolysaccharide-enhanced transcytosis of HIV-1 free virus across the in vitro blood-brain barrier: Evidence for cytokine-mediated pericyte-endothelial cell crosstalk. *Fluids Barriers CNS* 10:23. doi: 10.1186/2045-8118-10-23

Edara, V., Nooka, S., Proulx, J., Stacy, S., Ghorpade, A., and Borgmann, K. (2020). β-catenin regulates wound healing and IL-6 expression in activated human astrocytes. *Biomedicines* 8:479. doi: 10.3390/biomedicines8110479

Emery, P., Keystone, E., Tony, H. P., Cantagrel, A., van Vollenhoven, R., Sanchez, A., et al. (2008). IL-6 receptor inhibition with tocilizumab improves treatment outcomes in patients with rheumatoid arthritis refractory to anti-tumour necrosis factor biologicals: Results from a 24-week multicentre randomised placebo-controlled trial. *Ann. Rheum. Dis.* 67, 1516–1523. doi: 10.1136/ard.2008.092932

Engelhardt, B., and Liebner, S. (2014). Novel insights into the development and maintenance of the blood-brain barrier. *Cell Tissue Res.* 355, 687–699. doi: 10.1007/s00441-014-1811-2

Escrig, A., Canal, C., Sanchis, P., Fernández-Gayol, O., Montilla, A., Comes, G., et al. (2019). IL-6 trans-signaling in the brain influences the behavioral and physio-pathological phenotype of the Tg2576 and 3xTgAD mouse models of Alzheimer's disease. *Brain Behav. Immun.* 82, 145–159. doi: 10.1016/j.bbi.2019.08.005

Eser Ocak, P., Ocak, U., Sherchan, P., Gamdzyk, M., Tang, J., and Zhang, J. H. (2020). Overexpression of Mfsd2a attenuates blood brain barrier dysfunction via Cav-1/Keap-1/Nrf-2/HO-1 pathway in a rat model of surgical brain injury. *Exp. Neurol.* 326:113203. doi: 10.1016/j.expneurol.2020.113203

Eskilsson, A., Mirrasekhian, E., Dufour, S., Schwaninger, M., Engblom, D., and Blomqvist, A. (2014). Immune-induced fever is mediated by IL-6 receptors on brain endothelial cells coupled to STAT3-dependent induction of brain endothelial prostaglandin synthesis. *J. Neurosci.* 34, 15957–15961. doi: 10.1523/JNEUROSCI.3520-14.2014

Fang, E., Xie, C., Schenkel, J., Wu, C., Long, Q., Cui, H., et al. (2020). A research agenda for ageing in China in the 21st century (2nd edition): Focusing on basic and translational research, long-term care, policy and social networks. *Ageing Res. Rev.* 64:101174. doi: 10.1016/j.arr.2020.101174

Furutama, D., Matsuda, S., Yamawaki, Y., Hatano, S., Okanobu, A., Memida, T., et al. (2020). IL-6 induced by periodontal inflammation causes neuroinflammation and disrupts the blood-brain barrier. *Brain Sci.* 10:679. doi: 10.3390/brainsci10100679

Gold, B., Shao, X., Sudduth, T., Jicha, G., Wilcock, D., Seago, E., et al. (2021). Water exchange rate across the blood-brain barrier is associated with CSF amyloid-β 42 in healthy older adults. *Alzheimers Dement.* 17, 2020–2029. doi: 10.1002/alz.12357

Gonneaud, J., and Chételat, G. (2018). Which is to blame for cognitive decline in ageing: Amyloid deposition, neurodegeneration or both? *Brain* 141, 2237–2241. doi: 10.1093/brain/awy174

Goshen, I., Kreisel, T., Ounallah-Saad, H., Renbaum, P., Zalzstein, Y., Ben-Hur, T., et al. (2007). A dual role for interleukin-1 in hippocampal-dependent memory processes. *Psychoneuroendocrinology* 32, 1106–1115. doi: 10.1016/j.psyneuen.2007.09.004

Guérit, S., Fidan, E., Macas, J., Czupalla, C., Figueiredo, R., Vijikumar, A., et al. (2021). Astrocyte-derived Wnt growth factors are required for endothelial blood-brain barrier maintenance. *Prog. Neurobiol.* 199:101937. doi: 10.1016/j.pneurobio.2020.101937

Gurnik, S., Devraj, K., Macas, J., Yamaji, M., Starke, J., Scholz, A., et al. (2016). Angiopoietin-2-induced blood-brain barrier compromise and increased stroke size are rescued by VE-PTP-dependent restoration of Tie2 signaling. *Acta Neuropathol.* 131, 753–773. doi: 10.1007/s00401-016-1551-3

Han, Y., Ripley, B., Serada, S., Naka, T., and Fujimoto, M. (2016). Interleukin-6 deficiency does not affect motor neuron disease caused by superoxide dismutase 1 mutation. *PLoS One* 11:e0153399. doi: 10.1371/journal.pone.0153399

Hauptmann, J., Johann, L., Marini, F., Kitic, M., Colombo, E., Mufazalov, I., et al. (2020). Interleukin-1 promotes autoimmune neuroinflammation by suppressing endothelial heme oxygenase-1 at the blood-brain barrier. *Acta Neuropathol.* 140, 549–567. doi: 10.1007/s00401-020-02187-x

Hawkins, B. T., and Davis, T. P. (2005). The blood-brain barrier/neurovascular unit in health and disease. *Pharmacol. Rev.* 57, 173–185. doi: 10.1124/pr.57.2.4

Heinrich, P. C., Behrmann, I. S., Hermanns, H. M., Muller-Newen, G., and Schaper, F. (2003). Principles of interleukin (IL)-6-type cytokine signalling and its regulation [Review]. *Biochem. J.* 374(Pt 1), 1–20. doi: 10.1042/bj20030407

Hu, Z., Deng, N., Liu, K., Zhou, N., Sun, Y., and Zeng, W. (2020). CNTF-STAT3-IL-6 axis mediates neuroinflammatory cascade across Schwann cell-neuron-microglia. *Cell Rep.* 31:107657. doi: 10.1016/j.celrep.2020.107657

Huang, Z., Wong, L., Su, Y., Huang, X., Wang, N., Chen, H., et al. (2020). Blood-brain barrier integrity in the pathogenesis of Alzheimer's disease. *Front. Neuroendocrinol.* 59:100857. doi: 10.1016/j.yfrne.2020.100857

Janelsins, M. C., Mastrangelo, M. A., Oddo, S., LaFerla, F. M., Federoff, H. J., and Bowers, W. J. (2005). Early correlation of microglial activation with enhanced tumor necrosis factor-alpha and monocyte chemoattractant protein-1 expression specifically within the entorhinal cortex of triple transgenic Alzheimer's disease mice. *J. Neuroinflammation* 2:23. doi: 10.1186/1742-2094-2-23

Janelsins, M. C., Mastrangelo, M. A., Park, K. M., Sudol, K. L., Narrow, W. C., Oddo, S., et al. (2008). Chronic neuron-specific tumor necrosis factor-alpha expression enhances the local inflammatory environment ultimately leading to neuronal death in 3xTg-AD mice. *Am. J. Pathol.* 173, 1768–1782. doi: 10.2353/ajpath.2008.080528

Jayaraj, R. L., Azimullah, S., Beiram, R., Jalal, F. Y., and Rosenberg, G. A. (2019). Neuroinflammation: Friend and foe for ischemic stroke. *J. Neuroinflammation* 16:142. doi: 10.1186/s12974-019-1516-2

Jones, S. A., and Jenkins, B. J. (2018). Recent insights into targeting the IL-6 cytokine family in inflammatory diseases and cancer. *Nat. Rev. Immunol.* 18, 773–789. doi: 10.1038/s41577-018-0066-7

Ju, Y., and Tam, K. Y. (2022). Pathological mechanisms and therapeutic strategies for Alzheimer's disease. *Neural Regen. Res.* 17, 543–549. doi: 10.4103/1673-5374.320970

Kitazawa, M., Cheng, D., Tsukamoto, M., Koike, M., Wes, P., Vasilevko, V., et al. (2011). Blocking IL-1 signaling rescues cognition, attenuates tau pathology, and restores neuronal β-catenin pathway function in an Alzheimer's disease model. *J. Immunol.* 187, 6539–6549. doi: 10.4049/jimmunol.1100620

Kong, X., Gong, Z., Zhang, L., Sun, X., Ou, Z., Xu, B., et al. (2019). JAK2/STAT3 signaling mediates IL-6-inhibited neurogenesis of neural stem cells through DNA demethylation/methylation. *Brain Behav. Immun.* 79, 159–173. doi: 10.1016/j.bbi.2019.01.027

Korner, H., Lemckert, F. A., Chaudhri, G., Etteldorf, S., and Sedgwick, J. D. (1997a). Tumor necrosis factor blockade in actively induced experimental autoimmune encephalomyelitis prevents clinical disease despite activated T cell infiltration to the central nervous system. *Eur. J. Immunol.* 27, 1973–1981. doi: 10.1002/eji.1830270822

Korner, H., Riminton, D. S., Strickland, D. H., Lemckert, F. A., Pollard, J. D., and Sedgwick, J. D. (1997b). Critical points of tumor necrosis factor action in central nervous system autoimmune inflammation defined by gene targeting. *J. Exp. Med.* 186, 1585–1590. doi: 10.1084/jem.186.9.1585

Kuhn, H. G., and Svendsen, C. N. (1999). Origins, functions, and potential of adult neural stem cells. *BioEssays* 21, 625–630. doi: 10.1002/(SICI)1521-1878(199908)21:8<625::AID-BIES1>3.0.CO;2-6

Kuwar, R., Rolfe, A., Di, L., Xu, H., He, L., Jiang, Y., et al. (2019). A novel small molecular NLRP3 inflammasome inhibitor alleviates neuroinflammatory response following traumatic brain injury. *J. Neuroinflammation* 16:81. doi: 10.1186/s12974-019-1471-y

Labus, J., Hackel, S., Lucka, L., and Danker, K. (2014). Interleukin-1beta induces an inflammatory response and the breakdown of the endothelial cell layer in an improved human THBMEC-based in vitro blood-brain barrier model. *J. Neurosci. Methods* 228, 35–45. doi: 10.1016/j.jneumeth.2014.03.002

Lambertsen, K., Finsen, B., and Clausen, B. (2019). Post-stroke inflammation-target or tool for therapy? *Acta Neuropathol.* 137, 693–714. doi: 10.1007/s00401-018-1930-z

Lieberman, A. P., Pitha, P. M., Shin, H. S., and Shin, M. L. (1989). Production of tumor necrosis factor and other cytokines by astrocytes stimulated with lipopolysaccharide or a neurotropic virus. *Proc. Natl. Acad. Sci. U.S.A.* 86, 6348–6352. doi: 10.1073/pnas.86.16.6348

Liebner, S., Dijkhuizen, R. M., Reiss, Y., Plate, K. H., Agalliu, D., and Constantin, G. (2018). Functional morphology of the blood-brain barrier in health and disease. *Acta Neuropathol.* 135, 311–336.

Liesz, A., Dalpke, A., Mracsko, E., Antoine, D. J., Roth, S., Zhou, W., et al. (2015). DAMP signaling is a key pathway inducing immune modulation after brain injury. *J. Neurosci.* 35, 583–598. doi: 10.1523/JNEUROSCI.2439-14.2015

Lin, R., Chen, F., Wen, S., Teng, T., Pan, Y., and Huang, H. (2018). Interleukin-10 attenuates impairment of the blood-brain barrier in a severe acute pancreatitis rat model. *J. Inflammation* 15:4. doi: 10.1186/s12950-018-0180-0

Liu, H., Luiten, P., Eisel, U., Dejongste, M., and Schoemaker, R. (2013). Depression after myocardial infarction: TNF-α-induced alterations of the blood-brain barrier and its putative therapeutic implications. *Neurosci. Biobehav. Rev.* 37, 561–572. doi: 10.1016/j.neubiorev.2013.02.004

Liu, X., and Quan, N. (2018). Microglia and CNS interleukin-1: Beyond immunological concepts. *Front. Neurol.* 9:8. doi: 10.3389/fneur.2018.00008

Locksley, R. M., Killeen, N., and Lenardo, M. J. (2001). The TNF and TNF receptor superfamilies: Integrating mammalian biology. *Cell* 104, 487–501. doi: 10.1016/S0092-8674(01)00237-9

Lopez-Rodriguez, A., Hennessy, E., Murray, C., Nazmi, A., Delaney, H., Healy, D., et al. (2021). Acute systemic inflammation exacerbates neuroinflammation in Alzheimer's disease: IL-1β drives amplified responses in primed astrocytes and neuronal network dysfunction. *Alzheimers Dement.* 17, 1735–1755. doi: 10.1002/alz.12341

Madsen, P., Desu, H., de Rivero Vaccari, J., Florimon, Y., Ellman, D., Keane, R., et al. (2020). Oligodendrocytes modulate the immune-inflammatory response in EAE via TNFR2 signaling. *Brain Behav. Immun.* 84, 132–146. doi: 10.1016/j.bbi.2019.11.017

Mantle, J., and Lee, K. (2018). A differentiating neural stem cell-derived astrocytic population mitigates the inflammatory effects of TNF-α and IL-6 in an iPSC-based blood-brain barrier model. *Neurobiol. Dis.* 119, 113–120. doi: 10.1016/j.nbd.2018.07.030

Mario, C., Antonio Rei, F., Niccolò, T., Daqing, M., Claudia, M., Marc, F., et al. (2010). Role of interleukin-1beta in postoperative cognitive dysfunction. *Ann. Neurol.* 68, 360–368.

McCoy, M. K., and Tansey, M. G. (2008). TNF signaling inhibition in the CNS: Implications for normal brain function and neurodegenerative disease. *J. Neuroinflammation* 5:45. doi: 10.1186/1742-2094-5-45

Menge, T., Zhao, Y., Zhao, J., Wataha, K., Gerber, M., Zhang, J., et al. (2012). Mesenchymal stem cells regulate blood-brain barrier integrity through TIMP3 release after traumatic brain injury. *Sci. Transl. Med.* 4:161ra150. doi: 10.1126/scitranslmed.3004660

Mosser, D. M., and Zhang, X. (2008). Interleukin-10: New perspectives on an old cytokine. *Immunol. Rev.* 226, 205–218. doi: 10.1111/j.1600-065X.2008.00706.x

Moynagh, P., Williams, D., and O'Neill, L. (1994). Activation of NF-kappa B and induction of vascular cell adhesion molecule-1 and intracellular adhesion molecule-1 expression in human glial cells by IL-1. Modulation by antioxidants. *J. Immunol.* 153, 2681–2690.

Murakami, M., and Hirano, T. (2012). The pathological and physiological roles of IL-6 amplifier activation. *Int. J. Biol. Sci.* 8, 1267–1280. doi: 10.7150/ijbs.4828

Musella, A., Fresegna, D., Rizzo, F., Gentile, A., De Vito, F., Caioli, S., et al. (2020). 'Prototypical' proinflammatory cytokine (IL-1) in multiple sclerosis: Role in pathogenesis and therapeutic targeting. *Expert Opin. Ther. Targets* 24, 37–46. doi: 10.1080/14728222.2020.1709823

Nagaya, Y., Aoyama, M., Tamura, T., Kakita, H., Kato, S., Hida, H., et al. (2014). Inflammatory cytokine tumor necrosis factor alpha suppresses neuroprotective endogenous erythropoietin from astrocytes mediated by hypoxia-inducible factor-2alpha. *Eur. J. Neurosci.* 40, 3620–3626. doi: 10.1111/ejn.12747

Nasti, T. H., and Timares, L. (2012). Inflammasome activation of IL-1 family mediators in response to cutaneous photodamage. *Photochem. Photobiol.* 88, 1111–1125. doi: 10.1111/j.1751-1097.2012.01182.x

Netea, M. G., Simon, A., van de Veerdonk, F., Kullberg, B. J., Van der Meer, J. W., and Joosten, L. A. (2010). IL-1beta processing in host defense: Beyond the inflammasomes. *PLoS Pathog.* 6:e1000661. doi: 10.1371/journal.ppat.1000661

Ni, Y., Teng, T., Li, R., Simonyi, A., Sun, G. Y., and Lee, J. C. (2017). TNFalpha alters occludin and cerebral endothelial permeability: Role of p38MAPK. *PLoS One* 12:e0170346. doi: 10.1371/journal.pone.0170346

O'Carroll, S. J., Kho, D. T., Wiltshire, R., Nelson, V., Rotimi, O., Johnson, R., et al. (2015). Pro-inflammatory TNFalpha and IL-1beta differentially regulate the inflammatory phenotype of brain microvascular endothelial cells. *J. Neuroinflammation* 12:131. doi: 10.1186/s12974-015-0346-0

O'Connor, K. A., Hansen, M. K., Rachal Pugh, C., Deak, M. M., Biedenkapp, J. C., Milligan, E. D., et al. (2003). Further characterization of high mobility group box 1 (HMGB1) as a proinflammatory cytokine: Central nervous system effects. *Cytokine* 24, 254–265. doi: 10.1016/j.cyto.2003.08.001

Ohtsuki, S., and Terasaki, T. (2007). Contribution of carrier-mediated transport systems to the blood-brain barrier as a supporting and protecting interface for the brain; importance for CNS drug discovery and development. *Pharm. Res.* 24, 1745–1758. doi: 10.1007/s11095-007-9374-5

Okuma, Y., Date, I., and Nishibori, M. (2014). [Anti-high mobility group box-1 antibody therapy for traumatic brain injury]. *Yakugaku Zasshi* 134, 701–705. doi: 10.1248/yakushi.13-00255-2

Owen, J., Sultana, R., Aluise, C., Erickson, M., Price, T., Bu, G., et al. (2010). Oxidative modification to LDL receptor-related protein 1 in hippocampus from subjects with Alzheimer disease: Implications for Aβ accumulation in AD brain. *Free Radic. Biol. Med.* 49, 1798–1803. doi: 10.1016/j.freeradbiomed.2010.09.013

Padden, M., Leech, S., Craig, B., Kirk, J., Brankin, B., and McQuaid, S. (2007). Differences in expression of junctional adhesion molecule-A and beta-catenin in multiple sclerosis brain tissue: Increasing evidence for the role of tight junction pathology. *Acta Neuropathol.* 113, 177–186. doi: 10.1007/s00401-006-0145-x

Pandya, V., and Patani, R. (2021). Region-specific vulnerability in neurodegeneration: Lessons from normal ageing. *Ageing Res. Rev.* 67:101311. doi: 10.1016/j.arr.2021.101311

Patin, F., Baranek, T., Vourc'h, P., Nadal-Desbarats, L., Goossens, J. F., Marouillat, S., et al. (2016). Combined metabolomics and transcriptomics approaches to assess the IL-6 blockade as a therapeutic of ALS: Deleterious alteration of lipid metabolism. *Neurotherapeutics* 13, 905–917. doi: 10.1007/s13311-016-0461-3

Puthenparampil, M., Tomas-Ojer, P., Hornemann, T., Lutterotti, A., Jelcic, I., Ziegler, M., et al. (2021). Altered CSF albumin quotient links peripheral inflammation and brain damage in MS. *Neurol. Neuroimmunol. Neuroinflamm.* 8:e951. doi: 10.1212/NXI.0000000000000951

Reichenberg, A., Yirmiya, R., Schuld, A., Kraus, T., Haack, M., Morag, A., et al. (2001). Cytokine-associated emotional and cognitive disturbances in humans. *Arch. Gen. Psychiatry* 58, 445–452. doi: 10.1001/archpsyc.58.5.445

Ren, C., Yao, R. Q., Zhang, H., Feng, Y. W., and Yao, Y. M. (2020). Sepsis-associated encephalopathy: A vicious cycle of immunosuppression. *J. Neuroinflammation* 17:14. doi: 10.1186/s12974-020-1701-3

Ren, C., Yin, P., Ren, N., Wang, Z., Wang, J., Zhang, C., et al. (2018). Cerebrospinal fluid-stem cell interactions may pave the path for cell-based therapy in neurological diseases. *Stem Cell Res. Ther.* 9:66. doi: 10.1186/s13287-018-0807-3

Robelin, L., and Gonzalez De Aguilar, J. L. (2014). Blood biomarkers for amyotrophic lateral sclerosis: Myth or reality? *Biomed Res. Int.* 2014:525097. doi: 10.1155/2014/525097

Rosejohn, S., and Heinrich, P. C. (1994). Soluble receptors for cytokines and growth factors: Generation and biological function. *Biochem. J.* 300(Pt 2), 281–290. doi: 10.1042/bj3000281

Rothe, M., Pan, M., Henzel, W., Ayres, T., and Goeddel, D. (1995). The TNFR2-TRAF signaling complex contains two novel proteins related to baculoviral inhibitor of apoptosis proteins. *Cell* 83, 1243–1252. doi: 10.1016/0092-8674(95)90149-3

Sandoval, K., and Witt, K. (2008). Blood-brain barrier tight junction permeability and ischemic stroke. *Neurobiol. Dis.* 32, 200–219. doi: 10.1016/j.nbd.2008.08.005

Sanjabi, S., Zenewicz, L. A., Kamanaka, M., and Flavell, R. A. (2009). Anti-inflammatory and pro-inflammatory roles of TGF-beta, IL-10, and IL-22 in immunity and autoimmunity. *Curr. Opin. Pharmacol.* 9, 447–453. doi: 10.1016/j.coph.2009.04.008

Sato, S., Sanjo, H., Takeda, K., Ninomiya-Tsuji, J., Yamamoto, M., Kawai, T., et al. (2005). Essential function for the kinase TAK1 in innate and adaptive immune responses. *Nat. Immunol.* 6, 1087–1095. doi: 10.1038/ni1255

Sedger, L. M., and McDermott, M. F. (2014). TNF and TNF-receptors: From mediators of cell death and inflammation to therapeutic giants - past, present and future. *Cytokine Growth Factor Rev.* 25, 453–472. doi: 10.1016/j.cytogfr.2014.07.016

Segarra, M., Aburto, M., and Acker-Palmer, A. (2021). Blood-brain barrier dynamics to maintain brain homeostasis. *Trends Neurosci.* 44, 393–405. doi: 10.1016/j.tins.2020.12.002

Sendama, W. (2020). The effect of ageing on the resolution of inflammation. *Ageing Res. Rev.* 57:101000. doi: 10.1016/j.arr.2019.101000

Si, Y., Zhao, Y., Hao, H., Fu, X., and Han, W. (2011). MSCs: Biological characteristics, clinical applications and their outstanding concerns. *Ageing Res. Rev.* 10, 93–103. doi: 10.1016/j.arr.2010.08.005

Smith, N., Giacci, M., Gough, A., Bailey, C., McGonigle, T., Black, A., et al. (2018). Inflammation and blood-brain barrier breach remote from the primary injury following neurotrauma. *J. Neuroinflammation* 15:201. doi: 10.1186/s12974-018-1227-0

Suvannavejh, G. C., Lee, H. O., Padilla, J., Dal Canto, M. C., Barrett, T. A., and Miller, S. D. (2000). Divergent roles for p55 and p75 tumor necrosis factor receptors in the pathogenesis of MOG(35-55)-induced experimental autoimmune encephalomyelitis. *Cell. Immunol.* 205, 24–33. doi: 10.1006/cimm.2000.1706

Sweeney, M., Zhao, Z., Montagne, A., Nelson, A., and Zlokovic, B. (2019). Blood-brain barrier: From physiology to disease and back. *Physiol. Rev.* 99, 21–78. doi: 10.1152/physrev.00050.2017

Tang, G., Liu, Y., Zhang, Z., Lu, Y., Wang, Y., Huang, J., et al. (2014). Mesenchymal stem cells maintain blood-brain barrier integrity by inhibiting aquaporin-4 upregulation after cerebral ischemia. *Stem Cells* 32, 3150–3162. doi: 10.1002/stem.1808

Tang, P., Hung, M. C., and Klostergaard, J. (1996). Human pro-tumor necrosis factor is a homotrimer. *Biochemistry* 35, 8216–8225. doi: 10.1021/bi952182t

Tartaglia, L., Pennica, D., and Goeddel, D. (1993). Ligand passing: The 75-kDa tumor necrosis factor (TNF) receptor recruits TNF for signaling by the 55-kDa TNF receptor. *J. Biol. Chem.* 268, 18542–18548. doi: 10.1016/S0021-9258(17)46661-0

Thundyil, J., and Lim, K. L. (2015). DAMPs and neurodegeneration. *Ageing Res. Rev.* 24(Pt A), 17–28. doi: 10.1016/j.arr.2014.11.003

Tigges, U., Boroujerdi, A., Welser-Alves, J., and Milner, R. (2013). TNF-α promotes cerebral pericyte remodeling in vitro, via a switch from α1 to α2 integrins. *J. Neuroinflammation* 10:33. doi: 10.1186/1742-2094-10-33

Tobiume, K., Matsuzawa, A., Takahashi, T., Nishitoh, H., Morita, K., Takeda, K., et al. (2001). ASK1 is required for sustained activations of JNK/p38 MAP kinases and apoptosis. *EMBO Rep.* 2, 222–228. doi: 10.1093/embo-reports/kve046

van Kralingen, C., Kho, D. T., Costa, J., Angel, C. E., and Graham, E. S. (2013). Exposure to inflammatory cytokines IL-1beta and TNFalpha induces compromise and death of astrocytes; implications for chronic neuroinflammation. *PLoS One* 8:e84269. doi: 10.1371/journal.pone.0084269

Vázquez-Rosa, E., Shin, M., Dhar, M., Chaubey, K., Cintrón-Pérez, C., Tang, X., et al. (2020). P7C3-A20 treatment one year after TBI in mice repairs the blood-brain barrier, arrests chronic neurodegeneration, and restores cognition. *Proc. Natl. Acad. Sci. U.S.A.* 117, 27667–27675. doi: 10.1073/pnas.2010430117

Vezzani, A., and Viviani, B. (2015). Neuromodulatory properties of inflammatory cytokines and their impact on neuronal excitability. *Neuropharmacology* 96, 70–82. doi: 10.1016/j.neuropharm.2014.10.027

Willis, E., MacDonald, K., Nguyen, Q., Garrido, A., Gillespie, E., Harley, S., et al. (2020). Repopulating microglia promote brain repair in an IL-6-dependent manner. *Cell* 180, 833–846.e16. doi: 10.1016/j.cell.2020.02.013

Wolf, J., Rose-John, S., and Garbers, C. (2014). Interleukin-6 and its receptors: A highly regulated and dynamic system. *Cytokine* 70, 11–20. doi: 10.1016/j.cyto.2014.05.024

Xing, G., Zhao, T., Zhang, X., Li, H., Li, X., Cui, P., et al. (2020). Astrocytic sonic hedgehog alleviates intracerebral hemorrhagic brain injury *via* modulation of blood-brain barrier integrity. *Front. Cell. Neurosci.* 14:575690. doi: 10.3389/fncel.2020.575690

Yang, J., Ma, K., Zhang, C., Liu, Y., Liang, F., Hu, W., et al. (2020). Burns impair blood-brain barrier and mesenchymal stem cells can reverse the process in mice. *Front. Immunol.* 11:578879. doi: 10.3389/fimmu.2020.578879

Yang, S., Gu, C., Mandeville, E. T., Dong, Y., Esposito, E., Zhang, Y., et al. (2017). Anesthesia and surgery impair blood-brain barrier and cognitive function in mice. *Front. Immunol.* 8:902. doi: 10.3389/fimmu.2017.00902

Yang, T., Velagapudi, R., and Terrando, N. (2020). Neuroinflammation after surgery: From mechanisms to therapeutic targets. *Nat. Immunol.* 21, 1319–1326. doi: 10.1038/s41590-020-00812-1

Yasutaka, Y., Watanabe, T., Nakashima, A., Matsumoto, J., Futagami, K., Yamauchi, A., et al. (2015). Tumor necrosis factor-alpha reduces beta-amyloid accumulation primarily by lowering cellular prion protein levels in a brain endothelial cell line. *FEBS Lett.* 589, 263–268. doi: 10.1016/j.febslet.2014.12.007

Zhang, C., Han, Y., Liu, X., Tan, H., Dong, Y., Zhang, Y., et al. (2022). Odor enrichment attenuates the anesthesia/surgery-induced cognitive impairment. *Ann. Surg.* [Epub ahead of print]. doi: 10.1097/SLA.0000000000005599

Zhang, J., Sadowska, G. B., Chen, X., Park, S. Y., Kim, J. E., Bodge, C. A., et al. (2015). Anti-IL-6 neutralizing antibody modulates blood-brain barrier function in the ovine fetus. *FASEB J.* 29, 1739–1753. doi: 10.1096/fj.14-258822

Zhang, J., Takahashi, H. K., Liu, K., Wake, H., Liu, R., Maruo, T., et al. (2011). Anti-high mobility group box-1 monoclonal antibody protects the blood-brain barrier from ischemia-induced disruption in rats. *Stroke* 42, 1420–1428. doi: 10.1161/STROKEAHA.110.598334

Glossary

AD, Alzheimer's disease; MS, multiple sclerosis; TBI, post-traumatic brain injury; BBB, blood–brain barrier; CNS, central nervous system; NSCs, neural stem cells; TNFα, tumor necrosis factor α; IL-1β, interleukin-1beta; IL-6, interleukin-6; iNOS, inducible nitric oxide synthase; BECs, brain endothelial cells; PCs, pericytes; ACs, astrocytes; TJs, tight junctions; AJs, adherens junctions; Cldn5, claudin-5; Ocln, occludin; ZO, zonula occludens; VE, vascular endothelial; Aqp4, aquaporin-4; Kir4.1, inwardly rectifying 4.1; shh, sonic hedgehog; VE-PTP, vascular endothelial protein tyrosine phosphatase; Tie2, type I tyrosine kinase receptor 2; ECs, endothelial cells; ICAM-1, intercellular adhesion molecule-1; VCAM-1, vascular cell adhesion molecule-1; MMPs, matrix metalloproteinases; PD, Parkinson's disease; TACE, TNFα-converting enzyme; TNFR, tumor necrosis factor receptor; DD, death domain; NF-κB, nuclear factor κB; EAE, experimental autoimmune encephalomyelitis; WT, wild-type; hCMEC/D3, immortalized human cerebral endothelial cell line; EPO, erythropoietin; PrPC, cellular prion protein; MBEC4, mouse brain microvascular endothelial cell line; IL-37, interleukin-37; HIF-1, hypoxia-inducible factor-1; VEGF-A, vascular endothelial growth factor-A; THBMEC, transfected human brain microvascular endothelial cell; TEER, transendothelial electrical resistance; IL-11,interleukin-11; IL-27, interleukin-27; IL-31, interleukin-31; OSM, oncostatin M; LIF, leukemia inhibitory factor; CNTF, ciliary neurotrophic factor; CT-1, cardiotrophin 1; CLCF1, cardiotrophin-like cytokine factor 1; gp130, membrane glycoprotein 130; CXCL, CXC- chemokine ligand; HMGB1, high-mobility group box 1 protein; DAMP, damage-associated molecular pattern; MHC, major histocompatibility complex; RAGE, receptor for advanced glycation endproducts; STAT3, signal transducers and activators of transcription; MAPK, mitogen-activated protein kinase; IL-10, interleukin-10; MSCs, mesenchymal stem cells.

frontiers | Frontiers in Molecular Neuroscience

TYPE Original Research
PUBLISHED 24 November 2022
DOI 10.3389/fnmol.2022.1078854

OPEN ACCESS

EDITED BY
Andrei Surguchov,
University of Kansas Medical Center,
United States

REVIEWED BY
Irina G. Sourgoutcheva,
University of Kansas Medical Center,
United States
Vittorio Maglione,
Mediterranean Neurological Institute
Neuromed (IRCCS), Italy

*CORRESPONDENCE
Jay S. Schneider
jay.schneider@jefferson.edu

SPECIALTY SECTION
This article was submitted to
Brain Disease Mechanisms,
a section of the journal
Frontiers in Molecular Neuroscience

RECEIVED 24 October 2022
ACCEPTED 11 November 2022
PUBLISHED 24 November 2022

CITATION
Schneider JS and Singh G (2022)
Altered expression of
glycobiology-related genes in
Parkinson's disease brain.
Front. Mol. Neurosci. 15:1078854.
doi: 10.3389/fnmol.2022.1078854

Altered expression of glycobiology-related genes in Parkinson's disease brain

Jay S. Schneider* and Garima Singh

Department of Pathology, Anatomy and Cell Biology, Thomas Jefferson University, Philadelphia, PA, United States

The precise mechanisms initiating and perpetuating the cellular degeneration in Parkinson's disease (PD) remain unclear. There is decreased expression of the main brain gangliosides, and GM1 ganglioside in particular, in the PD brain along with decreased expression of the genes coding for the glycosyltranferase and the sialyltransferase responsible for the synthesis of these brain gangliosides. However, potentially important pathogenic mechanisms contributing to the neurodegeneration in PD may also include altered levels of expression of genes involved in glycosylation, sialylation and sphingolipid synthesis and metabolism. Although various studies have described pathological lipid and glycolipid changes in PD brain, there have been limited studies of expression of glycobiology-related genes in PD brain. The current study was performed as an initial attempt to gain new information regarding potential changes in glycoprotein and glycolipid-related genes in PD by investigating the gene expression status for select glycosyltransferases, sialyltransferases, sialidases, sphingosine kinases, and lysosomal enzymes in the substantia nigra and putamen from patients with PD and neurologically normal controls. Results showed altered expression of glycosyltransferase genes (*B3GALT2* and *B4GALT*1) potentially involved in microglial activation and neuroinflammation, sphingosine-1-phosphate (S1P) modulators (*SPHK1*, *SPHK2*, and *SGPL1*) involved in sphingolipid synthesis and metabolism, polysialyltransferase genes (*ST8SIA2* and *ST8SIA4*) that encode enzymes responsible for polysialic acid (polySia) biosynthesis, and the sialidase *NEU4*, expression of which has been linked to the clearance of storage materials from lysosomes. The data presented here underscore the complexity of the glycolipid/sphingolipid dysregulation in the PD brain and continued and expanded study of these processes may not only provide a greater understanding of the complex roles of aberrant glycosylation sialylation, and sphingolipid synthesis/metabolism in the pathophysiology of PD but may identify potential druggable targets for PD therapeutics.

KEYWORDS

Parkinson's disease, glycolipid, sphingolipid, substantia nigra, putamen, gene expression

Introduction

Parkinson's disease (PD) is a complex progressive neurodegenerative disorder primarily characterized by the loss of nigrostriatal dopamine-producing neurons in the substantia nigra. Although the majority of cases of PD are idiopathic in origin, several mechanisms have been proposed to explain the onset and progression of the neurodegeneration in PD including mitochondrial dysfunction, increased oxidative stress and oxidative damage, α-synuclein aggregation and associated toxicity, and lysosomal and autophagic dysfunction, among other potential contributing factors (Doria et al., 2016). In addition, various abnormalities in the content and composition of various lipids, including gangliosides, have been reported in PD brain [ex. (den Jager, 1969; Riekkinen et al., 1975; Seyfried et al., 2018)]. Recently, dysregulation of ceramide synthesis and metabolism have been suggested to play a role in PD-associated neurodegeneration (Plotegher et al., 2019) and lipdomic studies have reported PD-specific lipid alterations detected in brain and in plasma that have been suggested to promote PD-associated neurodegeneration at least in part through promoting α-synuclein aggregation, neuroinflammation, and dysfunction of autophagic processing [see Alecu and Bennett (2019) for review].

In addition to changes in lipid content and metabolism in the PD brain, some studies have also reported altered glycosylation and sialylation in PD brain (Videira and Castro-Caldas, 2018; Wilkinson et al., 2021). Altered levels of sialylation and fucosylation have also been reported in serum samples from PD patients and interestingly, mainly in male patients (Varadi et al., 2019). Additionally, many proteins are synthesized in the endoplasmic reticulum (ER) where many of them undergo glycoslylation and functionalization. ER stress has been suggested to be one of the pathological mechanisms contributing to PD (Mercado et al., 2013; Tsujii et al., 2015), and aberrant glycosylation has been suggested to contribute to an overload of the ER in PD brain with underglycosylated proteins (Videira and Castro-Caldas, 2018). Oxidative stress and inflammation have also been suggested to potentially trigger abnormal glycosylation in PD (Videira and Castro-Caldas, 2018).

Although various studies have described pathological lipid and glycolipid changes in PD brain, there have been limited studies of expression of glycobiology-related genes in PD brain (see (Alecu and Bennett, 2019) for review) and how dysregulation of the expression of these genes may contribute to PD-like neurodegeneration. In contrast, genes related to glycobiology have been examined in Huntington's disease (HD) transgenic mice as well as in the caudate nucleus from human HD subjects (Desplats et al., 2007) where a number of glycosyltransferases and sialyltransferases were found to be significantly changed compared to normal controls. In particular, ganglioside metabolism genes *ST3GAL5*, *ST8SIA3*, *B4GALNT1*, and *ST3GAL2* had significantly decreased expression in HD caudate compared to control caudate (Desplats et al., 2007). We previously described significantly decreased expression of gene *B3GALT4* and *ST3GAL2* in residual dopaminergic neurons in the PD substantia nigra (Schneider, 2018), consistent with an earlier finding of decreased expression of the main brain gangliosides (GM1, GD1a, GD1b, and GT1b) in PD substantia nigra (Seyfried et al., 2018). The current study was performed to gain additional information regarding potential changes in glycoprotein and glycolipid metabolism in PD by investigating the gene expression status for select glycosyltransferases (*B3GALT4, B4GALT1, B4GALNT1, and B4GALT5*), sialyltransferases (*ST6GALNAC4, ST8SIA2, ST8SIA4, and NCAM1* (substrate for *ST8SIA2, ST8SIA4*), sialidases (*NEU1, NEU3, and NEU4*), sphingosine kinases (S1P modulators) (*SPHK1, SPHK2, and SGPL1)* (S1P lyase), and lysosomal enzymes (*GBA* (β-glucocerebroside), *GLB1* (β-galactosidase)) in the substantia nigra and putamen in patients with PD and neurologically normal controls. These genes were chosen to expand upon limited previous preliminary data that suggested potential abnormal expression levels of some glycosyltransferases, sialyltransferases, sialidases, and S1P modulators in PD brain (Schneider and Singh, 2019).

Materials and methods

Human brain tissue collection

Coded/anonymous substantia nigra-containing tissue blocks were obtained through the NIH NeuroBioBank and sourced from the NICHD Brain and Tissue Bank for Developmental Disorders at the University of Maryland, Baltimore, MD, the Harvard Brain Tissue Resource Center, which is supported in part by HHSN-271-2013-00030C, and from the Human Brain and Spinal Fluid Resource Center, VA, West Los Angeles Healthcare Center, 11301 Wilshire Blvd., Los Angeles, CA, which is sponsored by NINDS/NIMH, the National Multiple Sclerosis Society, and the Department of Veterans Affairs. Coded/anonymous putamen samples were obtained solely from the Human Brain and Spinal Fluid Resource Center, VA, West Los Angeles Healthcare Center. The clinical diagnosis of Parkinson's disease was confirmed at autopsy by presence of gross depigmentation of the SN and microscopic confirmation of SN cell loss and presence of Lewy bodies in the SN and normal findings in other brain regions sampled. Frozen tissue blocks containing the SN were stored at −80°C and warmed to −20°C for dissection of samples. Dissected substantia nigra samples (containing the pars compacta region (SNc)) and dissected putamen samples (taken from dorsal putamen) were placed in sterile Eppendorf tubes and were rapidly refrozen in powdered dry ice. Standard BL2 procedures for handling human tissues were observed. Coded/anonymous non-neurological disease control tissues were obtained from the same sources mentioned above. Subject

characteristics are described in Table 1 regarding substantia nigra samples and Table 2 regarding putamen samples.

Ribonucleic acid isolation and quantitative real-time polymerase chain reaction

Ribonucleic acid (RNA) was extracted from the frozen SN and putamen samples using Zymo Direct-zol RNA miniprep Plus. During RNA isolation the DNase digestion step was performed with RNase-free DNase I (included in the kit) to eliminate genomic DNA contamination. To determine RNA quality, all the RNA samples were analyzed on an Agilent 2100 Bioanalyzer using the Agilent RNA 6000 Nano kit per the manufacturer's instructions. The RNA integrity (RIN) numbers for the samples are reported in Tables 1, 2. cDNA was prepared using NEB Protoscript II First strand cDNA synthesis, and Real-Time PCR was performed using a Roche LightCycler 480 with Roche LightCycler 480 SYBR Green I Mastermix. Real-Time PCR was carried out using commercially sourced and validated primers from GeneGlobe Qiagen against human genes *B3GALT2, B4GALT1, B4GALT5, B4GALNT1, GLB1, GBA, NCAM1, NEU1, NEU3, NEU4, SGPL1, SPHK1, SPHK2, ST6GALNAC4, ST8SIA2*, and *ST8SIA4* (GeneGlobe IDs are provided in Supplementary Table 1). The ΔΔCt method was used to calculate mRNA expression change relative to *GAPDH* (housekeeping gene) expression.

TABLE 1 Subject and tissue characteristics: Substantia nigra.

Control	Age (yrs)	Sex	PMI (hrs)	RIN
SN1	65	M	8.8	2.7
SN2	71	M	7	2.5
SN3	83	F	8.6	3.3
SN4	65	F	8.8	4.8
SN5	70	M	18.2	2.5
SN6	77	F	6	5.7
SN7	83	F	17.6	6.1
SN8	67	F	11.8	3.1
SN9	83	M	19.5	5.9
SN10	68	M	20.3	5.9
SN11	81	F	16.3	5.9
SN12	82	M	14	6.1
Control mean ± SEM	74.6 ± 2.2	6 M, 6 F	13.1 ± 1.5	4.5 ± 0.5
PD	**Age (yrs)**	**Sex**	**PMI (hrs)**	**RIN**
SN1	76	F	8.8	4.9
SN2	79	F	9.1	4
SN3	74	M	17	4.9
SN4	79	M	27	5.5
SN5	82	F	8	6
SN6	71	M	21.5	5.7
SN7	84	M	12.7	5.5
SN8	74	M	11.4	5.7
SN9	81	F	14.8	5.6
SN10	81	F	2	2.8
SN11	67	F	22.9	5.2
SN12	78	M	9.5	3
SN13	81	M	3.5	5.5
SN14	83	M	6.7	5.4
SN15	65	M	20.3	2.8
PD mean ± SEM	77.0 ± 1.5	9 M, 6 F	13.0 ± 1.9	4.8 ± 0.3

Statistical analyses

Raw data were subjected to outlier analysis using Grubbs test to identify and remove values that were significant outliers from the other values in each dataset. Statistical analyses were

TABLE 2 Subject and tissue characteristics: Putamen.

Control	Age (yrs)	Sex	PMI (hrs)	RIN
P1	53	M	15	6.1
P2	75	M	11.5	6.0
P3	76	M	11	6.2
P4	80	M	14	7.7
P5	61	F	26	6.2
P6	93	F	17	6.2
P7	52	M	19	5.6
P8	81	F	14.5	6.1
P9	75	F	15.4	7.3
P10	72	F	14	5.4
P11	70	M	12	5.9
P12	93	F	20.3	4.8
P13	57	M	12.6	5.0
Control mean ± SEM	72.2 ± 3.7	7 M, 6 F	15.6 ± 1.2	6.0 ± 0.2
PD	**Age (yrs)**	**Sex**	**PMI (hrs)**	**RIN**
P1	75	M	5.5	5.0
P2	72	M	5.5	4.1
P3	81	M	7	5.0
P4	75	M	5	7.1
P5	95	M	10	5.3
P6	72	F	14.7	5.7
P7	83	M	6.7	4.9
P8	67	M	9.8	6.8
P9	82	F	19	5.5
P10	70	M	22.5	5.7
P11	70	M	21.5	5.0
P12	71	M	17.5	5.2
P13	82	M	13.7	3.3
P14	81	F	12	3.0
P15	89	M	13.8	6.7
P16	73	M	30.6	5.4
P17	77	M	18.6	6.8
P18	71	M	21.5	5.3
PD mean ± SEM	77.0 ± 1.7	15 M, 3 F	14.2 ± 1.7	5.3 ± 0.3

then performed using unpaired *t*-test using GraphPad Prism software (v9) with significance for gene expression change set at $P < 0.05$ (GraphPad Software, San Diego, California USA). Data were converted to fold change relative to control for graphical presentation.

Results

Subjects and controls were well matched for age, post-mortem interval (PMI), and RNA integrity number (RIN) for both substantia nigra (Table 1) and putamen (Table 2) samples. There were no statistically significant differences between subjects and controls on any of these measures for either tissue type. Male/female ratios for substantia nigra samples were 50:50 for controls and 60:40 for subjects with PD. For putamen samples, male/female ratios were 54:46 for controls and 83:17 for subjects with PD. There were no significant sex-related differences in any of the gene expression data in either brain structure (data not shown).

Significant differences in gene expression were found in the substantia nigra from patients with PD compared to controls. Fold changes relative to control are shown in Figure 1 for the genes assayed. Gene expression for glycosyltransferases *B3GALT2* and *B4GALT1*, the S1P modulator *SGPL1*, and the lysosomal enzyme *GBA* were significantly upregulated in PD substantia nigra. Alternatively, gene expression for polysialyltransferases *ST8SIA2* and *ST8SIA4*, sialidase *NEU4*, and sphingosine kinases *SPHK1* and *SPHK2* were significantly downregulated in PD substantia nigra.

Gene expression data from the putamen were overall more variable than data from the substantia nigra. Although a number of genes trended toward being downregulated in the PD samples, none of these reached statistical significance compared to the controls (Figure 2). Only one gene, the lysosomal enzyme *GLB1*, was significantly upregulated in the PD putamen (Figure 2).

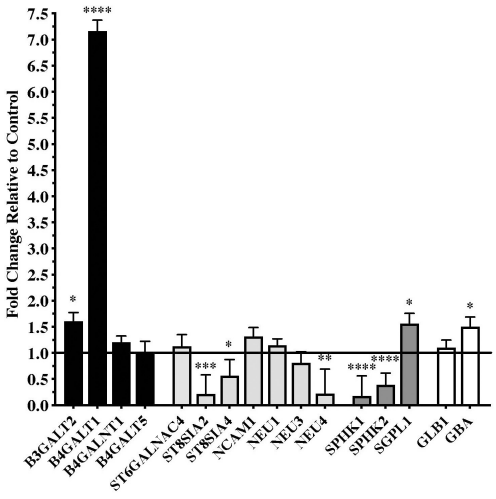

FIGURE 1
Gene expression changes in substantia nigra from patients with Parkinson's disease ($N = 15$) relative to normal, age-matched controls ($N = 12$). Data are presented as fold change relative to control. Gene expression for glycosyltransferases *B3GALT2* and *B4GALT1* was significantly higher in patients with PD than in normal controls, while polysialyltransferase genes *ST8SIA2* and *ST8SIA4* were significantly down-regulated in the PD substantia nigra along with the gene for sialidase *NEU4*. Genes involved with sphingodine-1-phosphate (S1P) metabolism were significantly dysregulated in PD substantia nigra with expression of sphingosine kinases necessary for S1P synthesis, *SPHK1* and *SPHK2*, significantly down-regulated and gene expression for S1P lyase, *SGPL1*, involved in the degradation of S1P, was significantly up-regulated. Gene expression for glucosidase beta acid 1 (*GBA*) was also significantly up-regulated in the PD substantia nigra. $^*P < 0.05$; $^{**}P < 0.01$; $^{***}P < 0.001$; $^{****}P < 0.0001$ vs. control.

Discussion

Over the last several years, there has been an increasing appreciation for the role that gangliosides and sphingolipids in general may play in the pathogenesis and progression of neurodegenerative diseases (Maglione et al., 2010; Di Pardo and Maglione, 2018; Lansbury, 2022) and PD in particular (Chiricozzi et al., 2020; Ledeen et al., 2022; Schneider, 2022). However, less attention has been paid to the roles that possible alterations in expression of genes involved in glycosylation, sialylation, and S1P regulation may play in the development and progression of PD. The current results show significant changes in gene expression of several key molecules involved in glycosylation, sialylation, and other process relevant to sphingolipid structure and function in the PD substantia nigra.

Glycosyltransferases

Glycosyltransferases are enzymes that catalyze the addition of polysaccharides to proteins, lipids, or nucleic acids to form glycoconjugates during glycosylation, a critical posttranslational process (Lv et al., 2017). Glycosyltransferases play important roles in the nervous system where they not only promote the development of neurons and glial cells and mediate the development of the myelin sheath (Angata et al., 2006; Lv et al., 2017) but are also critically involved in processes relevant to neurodegeneration including inflammation and microglial function, mitochondrial function, and autophagic processing (Chen et al., 2009; Videira and Castro-Caldas, 2018; Wang et al., 2020). There are various structural classes of glycosyltransferases that relate to their diverse biological functions. We previously showed that gene expression for the glycosyltransferase B3GALT4, an important enzyme in the synthesis of brain gangliosides GM1 and GD1b, was significantly

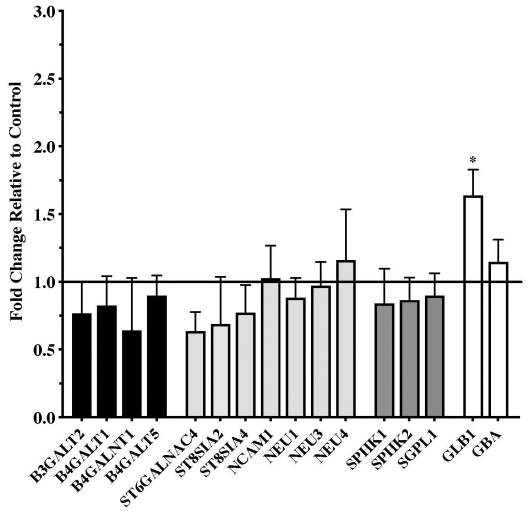

FIGURE 2
Gene expression changes in putamen from patients with Parkinson's disease (N = 18) relative to normal, age-matched controls (N = 13). Data are presented as fold change relative to control. In contrast to the numerous changes in gene expression observed in the PD substantia nigra, expression of only one of the genes examined, the lysosomal hydrolytic enzyme β-Galactosidase (*GLB1*), was significantly altered in the PD putamen. *$P < 0.05$ vs. control.

reduced in residual dopaminergic neurons in the PD substantia nigra (Schneider, 2018). Currently, we show that *B3GALT2* and *B4GALT1* gene expression is significantly increased in the PD substantia nigra, compared to age-matched controls. This may be potentially significant for the expression and potentiation of PD-related pathology as protein glycosylation regulated by B4Galt1 has been suggested to be related to microglial activation and neuroinflammatory responses (Yang et al., 2020), with increased expression of B4Galt1 related to increased microglial inflammatory responses (Yang et al., 2020). Increased levels of B3GALT2 are also associated with neuroinflammation and knockdown of *B3GALT2* reduced levels of inflammatory cytokines TNFα and IL-6 (Lv et al., 2017). This is significant as microglia activation and neuroinflammatory processes have been suggested to play important roles in the pathophysiology of PD (McGeer et al., 1988; Mogi et al., 1994; Ouchi et al., 2005; Gerhard et al., 2006; Zhang et al., 2017). Further, high levels of B4GALT1 have been suggested to suppress autophagic processes (Wang et al., 2020). Impaired autophagic processing is believed to play a significant role in the accumulation of toxic α-synuclein aggregates in dopaminergic neurons in the substantia nigra and the ensuing neurodegeneration (Karabiyik et al., 2017; Miki et al., 2018; Hou et al., 2020). In contrast to the significant changes observed in the substantia nigra, there were no significant changes in glycosyltransferase gene expression in the PD putamen.

Sialyltransferases and sialidases

Sialic acids are acidic sugars mostly found as terminal residues in glycan structures of glycoconjugates including glycoproteins and glycolipids (Rawal and Zhao, 2021). The highest levels of sialic acids are expressed in the brain where they regulate a diverse range of processes including neuronal sprouting, plasticity, myelination and myelin stability (Rawal and Zhao, 2021). Sialylation is the process mediated by sialytransferase enzymes, though which sialic acid is added to a glycoconjugate. Removal of sialic acid from sialoglycan is mediated by lysosomal, cytoplasmic, or plasma membrane bound sialidase enzymes (Schnaar et al., 2014; Rawal and Zhao, 2021). Gangliosides, sialylated glycosphingolipids that contain over 75% of the brain's sialic acid, are the most abundant sialoglycans in the nervous system (Schnaar et al., 2014). We previously showed that gene expression for the sialyltransferase *ST3GAL2*, the enzyme responsible for the synthesis of brain gangliosides GD1a from GM1 and GT1b from GD1b, was significantly reduced in residual dopaminergic neurons in the PD substantia nigra (Schneider, 2018).

The current study also shows that there are significantly decreased levels of gene expression for two polysialyltransferases, *ST8SIA2* and *ST8SIA4*, genes that encode enzymes responsible for polysialic acid (polySia) biosynthesis. PolySia plays important roles in brain development with neural cell adhesion molecule (NCAM) as the major polySia acceptor protein (Schnaar et al., 2014). While ST8SIA2 and ST8SIA4 are important for the addition of polySia to NCAM, gene expression for *NCAM1* was not altered in the PD substantia nigra. In developing and mature brains, polySia plays roles in modulating the function of neurotrophic factors including BDNF and FGF2, NMDA and AMPA receptors, and potentially also influences dopamine and norepinephrine neurotransmission through regulating the interactions of these transmitters with their receptors (Sato et al., 2016). In addition to these functions, polySia plays a role in inhibiting innate immunity reactions, inflammation, and microglia activation (Liao et al., 2021). Thus, abnormal polysialyation could play an important role in various physiological mechanisms of relevance to the development or progression of PD. The expression of polySia is highly correlated with gene expression of *ST8SIA2* and *ST8SIA4* (Sato and Hane, 2018). ST8SIA2 has been implicated in myelin formation and ST8SIA2 deficiency leads to myelin deficits, thinning axons, and age-related white matter degeneration (Szewczyk et al., 2017). Interestingly, *St8sia2*$^{-/-}$ mice have reduced polysialylation and display schizophrenic-like behaviors including cognitive and behavioral deficits and it was proposed that genetic variation in ST8SIA2 in humans may have the potential to confer a neurodevelopmental predisposition to schizophrenia (Krocher et al., 2015). It is not possible to know if the *ST8SIA2* gene down-regulation observed in the PD substantia nigra is a consequence of the disease

or whether defects in the polytransferase gene expressions detected in our study predispose to the development of PD. While both sialyltransferases are present in the adult brain albeit at relatively low levels, ST8SIA4 appears to be the predominant polysiayltransferase in the adult brain where it has been suggested to be important for neuronal plasticity (Curto et al., 2019), with ST8SIA4 deficiency related to memory deficits in mice (Nacher et al., 2010). While the functional significance of the decreased expression of *ST8SIA2* and *ST8SIA4* genes in the PD substantia nigra are not entirely clear at this time, their dysregulation may signal a more widespread impairment in sialo-conjugate metabolism that is worthy of further study.

In addition to the decreases in mRNA expression of the polysialyltransferases discussed above, sialylation could also be influenced by the decrease expression of the sialidase gene *NEU4*. There are four main mammalian sialidases, NEU1, NEU2, NEU3, and NEU4 (Glanz et al., 2019). NEU1 is a lysosomal sialidase that participates in lysosomal exocytosis, NEU2 is primarily a cytoplasmic sialidase and plays a role in neuronal differentiation, NEU3 is a plasma membrane sialidase involved in ganglioside metabolism and regulation of transmembrane signaling, and NEU4 is located to lysosomes, mitochondria, and endoplasmic reticulum, has broad substrate specificity against sialylated glycoconjugates, and its expression has been linked to the clearance of storage materials from lysosomes, among other functions (Miyagi and Yamaguchi, 2012). In the present study, *NEU4* gene expression was significantly decreased in PD substantia nigra. In *Neu4*$^{-/-}$ mice, NEU4 has been shown to be a ganglioside metabolizing enzyme, increasing relative amounts of GD1a ganglioside while substantially decreasing GM1 levels (Seyrantepe et al., 2008). Additionally, NEU4 has been suggested to regulate neuronal function through the degradation of polySia and may also play a role on immune function in microglia (Seyrantepe et al., 2008; Takahashi et al., 2012). Together, the data presented in the current paper suggest a dysregulation of sialylation in the PD substantia nigra that could have multiple negative influences on dopaminergic neuronal function and survival. In contrast to the significant changes observed in the substantia nigra, there were no significant changes in sialylation-related gene expression in the PD putamen.

Sphingosine-1-phosphate metabolism

Sphingosine-1-phosphate (S1P) is one the most potent signaling lipids, regulating several molecular events underlying cellular homeostasis and viability (Di Pardo and Maglione, 2018). S1P is normally synthesized by sphingosine kinase-1 and sphingosine kinase-2 (SPHK1 and SPHK2) and degraded by S1P phosphate phosphatase (SGPP) or S1P lyase (SGPL1). A balance between S1P synthesis and degradation is required for cellular homeostasis and normal cell functions (Di Pardo and Maglione, 2018). Decreased SPHK1/2 levels and increased SGPL1 levels are expected to decrease S1P levels, potentially impairing autophagic mechanisms, down-regulating pro-survival pathways, and promoting neurodegeneration (Di Pardo et al., 2019). Up-regulation of SGPL1 and reduced expression of SPHK1, with a subsequent decrease in S1P, has been associated with neurodegeneration in Alzheimer's disease (He et al., 2010; Ceccom et al., 2014; Couttas et al., 2014) and has also been described in animal models of Huntington's disease (HD) as well as in post-mortem brain tissues from patients with HD (Di Pardo et al., 2017). Interestingly, in HD transgenic mice, abnormally increased SGPL1 expression was observed at a very early stage of disease while SPHK1 and SPHK2 levels were not affected, suggesting that the process of dysregulation of S1P metabolism may begin very early in the disease process with alterations in expression SPHK1 and SPHK2 appearing as the disease progresses (Di Pardo et al., 2017). Importantly, pharmacological interventions aimed at modulating S1P metabolism were neuroprotective, suggesting modulation of S1P-metabolizing enzymes as potential druggable therapeutic targets for neuroprotection (Di Pardo et al., 2017). Although previous studies have demonstrated alterations in S1P metabolism using cellular and animal models of PD (Pyszko and Strosznajder, 2014; Sivasubramanian et al., 2015; Badawy et al., 2018; Motyl and Strosznajder, 2018; Zhang et al., 2018; Pepin et al., 2020) we believe the current report is the first to demonstrate this in post-mortem tissue from patients with PD. In contrast to the significant changes observed in the substantia nigra, there were no significant changes in expression of genes related to S1P metabolism in the PD putamen.

Lysosomal enzymes

Of the lysosomal-related genes examined, only *GBA* was affected in the PD substantia nigra and only *GLB1* was affected in the PD putamen. GBA encodes for the lysosomal hydrolase β-glucocerebrosidase (GCase), that catalyzes the conversion of glucosylceramide into glucose and ceramide. Our finding of increased expression of *GBA* mRNA in the PD substantia nigra was surprising as others have reported decreased *GBA* gene expression in the substantia nigra in patients with sporadic PD (Chiasserini et al., 2015) and reduced *GBA* gene expression in brain regions with and without pathological synuclein aggregates and in early and late-stage sporadic PD (Murphy et al., 2014). The activity of GBA can be a ceramide source (Giussani et al., 2014) and ceramides play important roles in modulating membrane protein dynamics and signaling as well as modulating processes related to autophagy and mitochondrial-mediated apoptosis (Ferrazza et al., 2016). However, it is a decrease in GBA activity that is typically associated with increased ceramide levels and inhibition of

autophagy and accumulation of synuclein. It is uncertain what the significance of an increase in GBA expression might be and how this may affect ceramide metabolism and accumulation as the relationship between GBA and ceramide levels is complex (Kurzawa-Akanbi et al., 2021).

β-Galactosidase (GLB1), a lysosomal hydrolytic enzyme, catalyzes the degradation of galactosylceramide to galactose and ceramide within the lysosome and *GLB1* mutation causes a deficiency in β-galactosidase-1 resulting in abnormal lysosomal accumulation of GM1 (GM1 gangliosidosis). GLB1 has not been studied extensively in PD and the significance of the increase in *GLB1* gene expression in the PD putamen is uncertain at this point.

Study limitations

There are some potential limitations of the current study. This study utilized whole tissue extracts of substantia nigra and putamen and thus interpretation of potential gene expression changes such as the ones observed in substantia nigra homogenates from PD brain could be complicated due to loss of dopaminergic neurons and signals from other cell types (i.e., microglia). While it is not possible to know in which cell types in the substantia nigra the observed gene expression changes originated, we observed both increases and decreases in expression of specific genes and thus our data are likely not attributed solely to neuronal loss in the PD substantia nigra. There was only one gene in the PD putamen that showed a significant change in expression. This may reflect the relative contributions of the genes assessed to the pathological process that occur in the substantia nigra and not in the putamen, although the putamen gene expression data were more variable than the data derived from the substantia nigra, potentially obscuring some significant gene expression changes in the putamen. The reasons for the higher level of variability in levels of gene expression in the putamen are not entirely clear but could relate at least in part to the anatomy of the putamen and the samples made available to us for this study. The human putamen is a very large structure and although we made an effort to take all samples from the dorsal putamen, the samples came from different rostro-caudal levels of the putamen and it is possible that there are sub-regionally specific patterns of expression of the genes examined in this study in different regions of the putamen. Regional heterogeneity in expression of various neuropeptides and in dopamine innervation and gradients of dopamine transporter loss in the PD putamen are well known and this regional heterogeneity may also apply to the expression of genes currently examined. Also, a relatively small number of patient samples were examined in the current study and only a relatively small number of genes were examined. Based on the consistency of the gene expression changes observed in the substantia nigra, it is unlikely that the data are related to a potentially different gene mutation status of different patients. However, additional studies using a larger number of cases with verified gene mutation status and examining a more extensive array of genes are indicated.

Conclusion

In summary, the current study shows significant changes in gene expression for several key molecules involved in glycosylation, sialylation, and S1P metabolism in the PD substantia nigra. Abnormal regulation of these processes has also been described in other neurodegenerative diseases including Alzheimer's disease and Huntington's disease, suggesting that dysregulation of processes involving glycosylation, sialylation, and sphingolipid metabolism such as those described here may transcend different brain disorders and neurodegenerative diseases.

Data availability statement

The raw data supporting the conclusions of this article will be made available by the authors, without undue reservation.

Ethics statement

Ethical review and approval was not required for the study on human participants in accordance with the local legislation and institutional requirements. Written informed consent for participation was not required for this study in accordance with the national legislation and the institutional requirements.

Author contributions

JS: conceptualization and writing—original draft. GS: collection of data. JS and GS: writing—review and editing and formal analyses. Both authors contributed to the article and approved the submitted version.

Funding

This study was supported by a grant from Qilu Pharmaceutical Co., Ltd. The funder had no role in the study design, data collection and analysis, decision to publish, or preparation of the manuscript.

Acknowledgments

The authors thank Vikrant Singh for initial work on the isolation of RNA from the clinical samples used in this study.

Conflict of interest

The authors declare that the research was conducted in the absence of any commercial or financial relationships that could be construed as a potential conflict of interest.

Publisher's note

All claims expressed in this article are solely those of the authors and do not necessarily represent those of their affiliated organizations, or those of the publisher, the editors and the reviewers. Any product that may be evaluated in this article, or claim that may be made by its manufacturer, is not guaranteed or endorsed by the publisher.

Supplementary material

The Supplementary Material for this article can be found online at: https://www.frontiersin.org/articles/10.3389/fnmol.2022.1078854/full#supplementary-material

References

Alecu, I., and Bennett, S. A. L. (2019). Dysregulated lipid metabolism and its role in alpha-synucleinopathy in Parkinson's disease. *Front. Neurosci.* 13:328. doi: 10.3389/fnins.2019.00328

Angata, K., Lee, W., Mitoma, J., Marth, J. D., and Fukuda, M. (2006). Cellular and molecular analysis of neural development of glycosyltransferase gene knockout mice. *Methods Enzymol.* 417, 25–37. doi: 10.1016/S0076-6879(06)17003-2

Badawy, S. M. M., Okada, T., Kajimoto, T., Hirase, M., Matovelo, S. A., Nakamura, S., et al. (2018). Extracellular alpha-synuclein drives sphingosine 1-phosphate receptor subtype 1 out of lipid rafts, leading to impaired inhibitory G-protein signaling. *J. Biol. Chem.* 293, 8208–8216. doi: 10.1074/jbc.RA118.001986

Ceccom, J., Loukh, N., Lauwers-Cances, V., Touriol, C., Nicaise, Y., Gentil, C., et al. (2014). Reduced sphingosine kinase-1 and enhanced sphingosine 1-phosphate lyase expression demonstrate deregulated sphingosine 1-phosphate signaling in Alzheimer's disease. *Acta Neuropathol. Commun.* 2:12. doi: 10.1186/2051-5960-2-12

Chen, J., Wang, H., Yang, H., Huang, X., Zhu, J., Hu, L., et al. (2009). Beta-1,4-galactosyltransferase-I participates in lipopolysaccharide induced reactive microgliosis. *Neurotoxicology* 30, 1107–1113. doi: 10.1016/j.neuro.2009.06.003

Chiasserini, D., Paciotti, S., Eusebi, P., Persichetti, E., Tasegian, A., Kurzawa-Akanbi, M., et al. (2015). Selective loss of glucocerebrosidase activity in sporadic Parkinson's disease and dementia with Lewy bodies. *Mol. Neurodegener.* 10:15. doi: 10.1186/s13024-015-0010-2

Chiricozzi, E., Lunghi, G., Di Biase, E., Fazzari, M., Sonnino, S., and Mauri, L. (2020). GM1 ganglioside is a key factor in maintaining the mammalian neuronal functions avoiding neurodegeneration. *Int. J. Mol. Sci.* 21:868. doi: 10.3390/ijms21030868

Couttas, T. A., Kain, N., Daniels, B., Lim, X. Y., Shepherd, C., Kril, J., et al. (2014). Loss of the neuroprotective factor sphingosine 1-phosphate early in Alzheimer's disease pathogenesis. *Acta Neuropathol. Commun.* 2:9. doi: 10.1186/2051-5960-2-9

Curto, Y., Alcaide, J., Rockle, I., Hildebrandt, H., and Nacher, J. (2019). Effects of the genetic depletion of polysialyltransferases on the structure and connectivity of interneurons in the adult prefrontal cortex. *Front. Neuroanat.* 13:6. doi: 10.3389/fnana.2019.00006

den Jager, W. A. (1969). Sphingomyelin in Lewy inclusion bodies in Parkinson's disease. *Arch. Neurol.* 21, 615–619. doi: 10.1001/archneur.1969.00480180071006

Desplats, P. A., Denny, C. A., Kass, K. E., Gilmartin, T., Head, S. R., Sutcliffe, J. G., et al. (2007). Glycolipid and ganglioside metabolism imbalances in Huntington's disease. *Neurobiol. Dis.* 27, 265–277. doi: 10.1016/j.nbd.2007.05.003

Di Pardo, A., Amico, E., Basit, A., Armirotti, A., Joshi, P., Neely, M. D., et al. (2017). Defective sphingosine-1-phosphate metabolism is a druggable target in Huntington's disease. *Sci. Rep.* 7:5280. doi: 10.1038/s41598-017-05709-y

Di Pardo, A., and Maglione, V. (2018). Sphingolipid metabolism: A New therapeutic opportunity for brain degenerative disorders. *Front. Neurosci.* 12:249. doi: 10.3389/fnins.2018.00249

Di Pardo, A., Pepe, G., Castaldo, S., Marracino, F., Capocci, L., Amico, E., et al. (2019). Stimulation of sphingosine kinase 1 (SPHK1) is beneficial in a Huntington's disease pre-clinical model. *Front. Mol. Neurosci.* 12:100. doi: 10.3389/fnmol.2019.00100

Doria, M., Maugest, L., Moreau, T., Lizard, G., and Vejux, A. (2016). Contribution of cholesterol and oxysterols to the pathophysiology of Parkinson's disease. *Free Radic. Biol. Med.* 101, 393–400. doi: 10.1016/j.freeradbiomed.2016.10.008

Ferrazza, R., Cogo, S., Melrose, H., Bubacco, L., Greggio, E., Guella, G., et al. (2016). LRRK2 deficiency impacts ceramide metabolism in brain. *Biochem. Biophys. Res. Commun.* 478, 1141–1146. doi: 10.1016/j.bbrc.2016.08.082

Gerhard, A., Pavese, N., Hotton, G., Turkheimer, F., Es, M., Hammers, A., et al. (2006). In vivo imaging of microglial activation with [11C](R)-PK11195 PET in idiopathic Parkinson's disease. *Neurobiol. Dis.* 21, 404–412. doi: 10.1016/j.nbd.2005.08.002

Giussani, P., Tringali, C., Riboni, L., Viani, P., and Venerando, B. (2014). Sphingolipids: Key regulators of apoptosis and pivotal players in cancer drug resistance. *Int. J. Mol. Sci.* 15, 4356–4392. doi: 10.3390/ijms15034356

Glanz, V. Y., Myasoedova, V. A., Grechko, A. V., and Orekhov, A. N. (2019). Sialidase activity in human pathologies. *Eur. J. Pharmacol.* 842, 345–350. doi: 10.1016/j.ejphar.2018.11.014

He, X., Huang, Y., Li, B., Gong, C. X., and Schuchman, E. H. (2010). Deregulation of sphingolipid metabolism in Alzheimer's disease. *Neurobiol. Aging* 31, 398–408. doi: 10.1016/j.neurobiolaging.2008.05.010

Hou, X., Watzlawik, J. O., Fiesel, F. C., and Springer, W. (2020). Autophagy in Parkinson's disease. *J. Mol. Biol.* 432, 2651–2672. doi: 10.1016/j.jmb.2020.01.037

Karabiyik, C., Lee, M. J., and Rubinsztein, D. C. (2017). Autophagy impairment in Parkinson's disease. *Essays Biochem.* 61, 711–720. doi: 10.1042/EBC20170023

Krocher, T., Malinovskaja, K., Jurgenson, M., Aonurm-Helm, A., Zharkovskaya, T., Kalda, A., et al. (2015). Schizophrenia-like phenotype of polysialyltransferase ST8SIA2-deficient mice. *Brain Struct. Funct.* 220, 71–83. doi: 10.1007/s00429-013-0638-z

Kurzawa-Akanbi, M., Tammireddy, S., Fabrik, I., Gliaudelyte, L., Doherty, M. K., Heap, R., et al. (2021). Altered ceramide metabolism is a feature in the extracellular vesicle-mediated spread of alpha-synuclein in Lewy body disorders. *Acta Neuropathol.* 142, 961–984. doi: 10.1007/s00401-021-02367-3

Lansbury, P. (2022). The sphingolipids clearly play a role in Parkinson's disease, but nature has made it complicated. *Mov. Disord.* 37, 1985–1989. doi: 10.1002/mds.29204

Ledeen, R., Chowdhury, S., Lu, Z. H., Chakraborty, M., and Wu, G. (2022). Systemic deficiency of GM1 ganglioside in Parkinson's disease tissues and its relation to the disease etiology. *Glycoconj. J.* 39, 75–82. doi: 10.1007/s10719-021-10025-9

Liao, H., Winkler, J., Wissfeld, J., Shahraz, A., Klaus, C., and Neumann, H. (2021). Low molecular weight polysialic acid prevents lipopolysaccharide-induced inflammatory dopaminergic neurodegeneration in humanized SIGLEC11 transgenic mice. *Glia* 69, 2845–2862. doi: 10.1002/glia.24073

Lv, Y., Ren, L., Fu, Y., Huang, K., and Bi, J. (2017). Role of beta-1,3-galactosyltransferase 2 in trigeminal neuronal sensitization induced by peripheral inflammation. *Neuroscience* 349, 17–26. doi: 10.1016/j.neuroscience.2017.02.043

Maglione, V., Marchi, P., Di Pardo, A., Lingrell, S., Horkey, M., Tidmarsh, E., et al. (2010). Impaired ganglioside metabolism in Huntington's disease and neuroprotective role of GM1. *J. Neurosci.* 30, 4072–4080. doi: 10.1523/JNEUROSCI.6348-09.2010

McGeer, P. L., Itagaki, S., Boyes, B. E., and McGeer, E. G. (1988). Reactive microglia are positive for HLA-DR in the substantia nigra of Parkinson's and Alzheimer's disease brains. *Neurology*38, 1285–1291. doi: 10.1212/wnl.38.8.1285

Mercado, G., Valdes, P., and Hetz, C. (2013). An ERcentric view of Parkinson's disease. *Trends Mol. Med.* 19, 165–175. doi: 10.1016/j.molmed.2012.12.005

Miki, Y., Shimoyama, S., Kon, T., Ueno, T., Hayakari, R., Tanji, K., et al. (2018). Alteration of autophagy-related proteins in peripheral blood mononuclear cells of patients with Parkinson's disease. *Neurobiol. Aging* 63, 33–43. doi: 10.1016/j.neurobiolaging.2017.11.006

Miyagi, T., and Yamaguchi, K. (2012). Mammalian sialidases: Physiological and pathological roles in cellular functions. *Glycobiology* 22, 880–896. doi: 10.1093/glycob/cws057

Mogi, M., Harada, M., Riederer, P., Narabayashi, H., Fujita, K., and Nagatsu, T. (1994). Tumor necrosis factor-alpha (TNF-alpha) increases both in the brain and in the cerebrospinal fluid from parkinsonian patients. *Neurosci. Lett.* 165, 208–210. doi: 10.1016/0304-3940(94)90746-3

Motyl, J., and Strosznajder, J. B. (2018). Sphingosine kinase 1/sphingosine-1-phosphate receptors dependent signalling in neurodegenerative diseases. The promising target for neuroprotection in Parkinson's disease. *Pharmacol. Rep.* 70, 1010–1014. doi: 10.1016/j.pharep.2018.05.002

Murphy, K. E., Gysbers, A. M., Abbott, S. K., Tayebi, N., Kim, W. S., Sidransky, E., et al. (2014). Reduced glucocerebrosidase is associated with increased alpha-synuclein in sporadic Parkinson's disease. *Brain* 137(Pt 3), 834–848. doi: 10.1093/brain/awt367

Nacher, J., Guirado, R., Varea, E., Alonso-Llosa, G., Rockle, I., and Hildebrandt, H. (2010). Divergent impact of the polysialyltransferases ST8SiaII and ST8SiaIV on polysialic acid expression in immature neurons and interneurons of the adult cerebral cortex. *Neuroscience* 167, 825–837. doi: 10.1016/j.neuroscience.2010.02.067

Ouchi, Y., Yoshikawa, E., Sekine, Y., Futatsubashi, M., Kanno, T., Ogusu, T., et al. (2005). Microglial activation and dopamine terminal loss in early Parkinson's disease. *Ann. Neurol.* 57, 168–175. doi: 10.1002/ana.20338

Pepin, E., Jalinier, T., Lemieux, G. L., Massicotte, G., and Cyr, M. (2020). Sphingosine-1-phosphate receptors modulators decrease signs of neuroinflammation and prevent Parkinson's disease symptoms in the 1-methyl-4-phenyl-1,2,3,6-tetrahydropyridine mouse model. *Front. Pharmacol.* 11:77. doi: 10.3389/fphar.2020.00077

Plotegher, N., Bubacco, L., Greggio, E., and Civiero, L. (2019). Ceramides in Parkinson's disease: From recent evidence to new hypotheses. *Front. Neurosci.* 13:330. doi: 10.3389/fnins.2019.00330

Pyszko, J. A., and Strosznajder, J. B. (2014). The key role of sphingosine kinases in the molecular mechanism of neuronal cell survival and death in an experimental model of Parkinson's disease. *Folia Neuropathol.* 52, 260–269. doi: 10.5114/fn.2014.45567

Rawal, P., and Zhao, L. (2021). Sialometabolism in brain health and Alzheimer's disease. *Front. Neurosci.* 15:648617. doi: 10.3389/fnins.2021.648617

Riekkinen, P., Rinne, U. K., Pelliniemi, T. T., and Sonninen, V. (1975). Interaction between dopamine and phospholipids. Studies of the substantia nigra in Parkinson disease patients. *Arch. Neurol.* 32, 25–27. doi: 10.1001/archneur.1975.00490430047006

Sato, C., and Hane, M. (2018). Mental disorders and an acidic glycan-from the perspective of polysialic acid (PSA/polySia) and the synthesizing enzyme, ST8SIA2. *Glycoconj. J.* 35, 353–373. doi: 10.1007/s10719-018-9832-9

Sato, C., Hane, M., and Kitajima, K. (2016). Relationship between ST8SIA2, polysialic acid and its binding molecules, and psychiatric disorders. *Biochim. Biophys. Acta* 1860, 1739–1752. doi: 10.1016/j.bbagen.2016.04.015

Schnaar, R. L., Gerardy-Schahn, R., and Hildebrandt, H. (2014). Sialic acids in the brain: Gangliosides and polysialic acid in nervous system development, stability, disease, and regeneration. *Physiol. Rev.* 94, 461–518. doi: 10.1152/physrev.00033.2013

Schneider, J. S. (2018). Altered expression of genes involved in ganglioside biosynthesis in substantia nigra neurons in Parkinson's disease. *PLoS One* 13:e0199189. doi: 10.1371/journal.pone.0199189

Schneider, J. S. (2022). A critical role for GM1 ganglioside in the pathophysiology and potential treatment of Parkinson's disease. *Glycoconj. J.* 39, 13–26. doi: 10.1007/s10719-021-10002-2

Schneider, J. S., and Singh, V. (2019). *Dysregulation of sphingolipid expression and metabolism and its role in the pathogenesis of Parkinson's disease. Society for neuroscience annual meeting.* Chicago, IL: Society for Neuroscience.

Seyfried, T. N., Choi, H., Chevalier, A., Hogan, D., Akgoc, Z., and Schneider, J. S. (2018). Sex-related abnormalities in substantia nigra lipids in Parkinson's disease. *ASN Neuro* 10:1759091418781889. doi: 10.1177/1759091418781889

Seyrantepe, V., Canuel, M., Carpentier, S., Landry, K., Durand, S., Liang, F., et al. (2008). Mice deficient in Neu4 sialidase exhibit abnormal ganglioside catabolism and lysosomal storage. *Hum. Mol. Genet.* 17, 1556–1568. doi: 10.1093/hmg/ddn043

Sivasubramanian, M., Kanagaraj, N., Dheen, S. T., and Tay, S. S. (2015). Sphingosine kinase 2 and sphingosine-1-phosphate promotes mitochondrial function in dopaminergic neurons of mouse model of Parkinson's disease and in MPP+ –treated MN9D cells in vitro. *Neuroscience* 290, 636–648. doi: 10.1016/j.neuroscience.2015.01.032

Szewczyk, L. M., Brozko, N., Nagalski, A., Rockle, I., Werneburg, S., Hildebrandt, H., et al. (2017). ST8SIA2 promotes oligodendrocyte differentiation and the integrity of myelin and axons. *Glia* 65, 34–49. doi: 10.1002/glia.23048

Takahashi, K., Mitoma, J., Hosono, M., Shiozaki, K., Sato, C., Yamaguchi, K., et al. (2012). Sialidase NEU4 hydrolyzes polysialic acids of neural cell adhesion molecules and negatively regulates neurite formation by hippocampal neurons. *J. Biol. Chem.* 287, 14816–14826. doi: 10.1074/jbc.M111.324186

Tsujii, S., Ishisaka, M., and Hara, H. (2015). Modulation of endoplasmic reticulum stress in Parkinson's disease. *Eur. J. Pharmacol.* 765, 154–156. doi: 10.1016/j.ejphar.2015.08.033

Varadi, C., Nehez, K., Hornyak, O., Viskolcz, B., and Bones, J. (2019). Serum N-glycosylation in Parkinson's disease: A novel approach for potential alterations. *Molecules* 24:2220. doi: 10.3390/molecules24122220

Videira, P. A. Q., and Castro-Caldas, M. (2018). Linking glycation and glycosylation with inflammation and mitochondrial dysfunction in Parkinson's disease. *Front. Neurosci.* 12:381. doi: 10.3389/fnins.2018.00381

Wang, P., Li, X., and Xie, Y. (2020). B4GalT1 regulates apoptosis and autophagy of glioblastoma in vitro and in vivo. *Technol. Cancer Res. Treat.* 19:1533033820980104. doi: 10.1177/1533033820980104

Wilkinson, H., Thomsson, K. A., Rebelo, A. L., Hilliard, M., Pandit, A., Rudd, P. M., et al. (2021). The O-glycome of human nigrostriatal tissue and its alteration in Parkinson's disease. *J. Proteome Res.* 20, 3913–3924. doi: 10.1021/acs.jproteome.1c00219

Yang, X., Li, Z. Y., Yuan, C. L., Tan, Y. F., Zhang, N. D., Liu, L. H., et al. (2020). Study on the role and mechanism of beta4GalT1 both in vivo and in vitro glioma. *Eur. Rev. Med. Pharmacol. Sci.* 24, 4368–4381. doi: 10.26355/eurrev_202004_21018

Zhang, L., Okada, T., Badawy, S. M. M., Hirai, C., Kajimoto, T., and Nakamura, S. I. (2018). Erratum: Extracellular alpha-synuclein induces sphingosine 1-phosphate receptor subtype 1 uncoupled from inhibitory G-protein leaving beta-arrestin signal intact. *Sci. Rep.* 8:46964. doi: 10.1038/srep46964

Zhang, Q. S., Heng, Y., Yuan, Y. H., and Chen, N. H. (2017). Pathological alpha-synuclein exacerbates the progression of Parkinson's disease through microglial activation. *Toxicol. Lett.* 265, 30–37. doi: 10.1016/j.toxlet.2016.11.002

frontiers | Frontiers in Molecular Neuroscience

TYPE Original Research
PUBLISHED 29 November 2022
DOI 10.3389/fnmol.2022.1029682

OPEN ACCESS

EDITED BY
Robert A. Nichols,
University of Hawaii at Manoa,
United States

REVIEWED BY
Enquan Xu,
Duke University,
United States
Evangelia Emmanouilidou,
National and Kapodistrian University of Athens, Greece

*CORRESPONDENCE
Sang-Yoon Lee
rchemist@gachon.ac.kr

SPECIALTY SECTION
This article was submitted to Molecular Signalling and Pathways, a section of the Frontiers in Molecular Neuroscience

RECEIVED 27 August 2022
ACCEPTED 27 October 2022
PUBLISHED 29 November 2022

CITATION
Suthar SK and Lee S-Y (2022) Ingenuity pathway analysis of α-synuclein predicts potential signaling pathways, network molecules, biological functions, and its role in neurological diseases.
Front. Mol. Neurosci. 15:1029682.
doi: 10.3389/fnmol.2022.1029682

Ingenuity pathway analysis of α-synuclein predicts potential signaling pathways, network molecules, biological functions, and its role in neurological diseases

Sharad Kumar Suthar[1] and Sang-Yoon Lee[1,2]*

[1]Neuroscience Research Institute, Gachon University, Incheon, South Korea, [2]Department of Neuroscience, College of Medicine, Gachon University, Incheon, South Korea

Despite the knowledge that mutation, multiplication, and anomalous function of α-synuclein cause progressive transformation of α-synuclein monomers into toxic amyloid fibrils in neurodegenerative diseases, the understanding of canonical signaling, interaction network molecules, biological functions, and role of α-synuclein remains ambiguous. The evolution of artificial intelligence and Bioinformatics tools have enabled us to analyze a vast pool of data to draw meaningful conclusions about the events occurring in complex biological systems. We have taken the advantage of such a Bioinformatics tool, ingenuity pathway analysis (IPA) to decipher the signaling pathways, interactome, biological functions, and role of α-synuclein. IPA of the α-synuclein NCBI gene dataset revealed neuroinflammation, Huntington's disease, TREM1, phagosome maturation, and sirtuin signaling as the key canonical signaling pathways. IPA further revealed Parkinson's disease (PD), sumoylation, and SNARE signaling pathways specific to the toxicity of α-synuclein. A frequency distribution analysis of α-synuclein-associated genes from the NCBI dataset that appeared in the predicted canonical pathways revealed that NFKB1 was the most populated gene across the predicted pathways followed by FOS, PRKCD, TNF, GSK3B, CDC42, IL6, MTOR, PLCB1, and IL1B. Overlapping of the predicted top-five canonical signaling pathways and the α-synuclein NCBI gene dataset divulged that neuroinflammation signaling was the most overlapped pathway, while NFKB1, TNF, and CASP1 were the most shared molecules among the pathways. The major diseases associated with α-synuclein were predicted to be neurological diseases, organismal injury and abnormalities, skeletal and muscular disorders, psychological disorders, and hereditary disorders. The molecule activity predictor (MAP) analysis of the principal interaction network of α-synuclein gene SNCA revealed that SNCA directly interacts with APP, CLU, and NEDD4, whereas it indirectly communicates with CALCA and SOD1. Besides, IPA also predicted amyloid plaque forming APP, cytokines/inflammatory mediators IL1B, TNF, MIF, PTGS2, TP53, and CCL2, and kinases of MAPK family Mek, ERK, and P38 MAPK as the top upstream regulators of α-synuclein signaling cascades. Taken together, the first IPA analysis of α-synuclein predicted PD as the key toxicity pathway, neurodegeneration as

the major pathological outcome, and inflammatory mediators as the critical interacting partners of α-synuclein.

KEYWORDS

α-synuclein, ingenuity pathway analysis, canonical signaling pathways, biological functions and diseases, regulators, interactome, toxicity, neuroinflammation

Introduction

Alpha-synuclein (α-synuclein) is 140 amino acids (Nakajo et al., 1993; Uéda et al., 1993), intrinsically disordered monomer protein in normal cellular conditions (Weinreb et al., 1996). Structurally, α-synuclein protein has three distinct regions; (i) N-terminal domain (1–95 residues), which binds to phospholipid membrane and upon binding, adopts α-helical conformation (Uéda et al., 1993; Davidson et al., 1998; Bussell and Eliezer, 2003; Bussell et al., 2005; Vamvaca et al., 2009; Zarbiv et al., 2014), (ii) Non-amyloid component region (61–95 residues), which is also called central hydrophobic region is responsible for α-synuclein aggregation by adopting β-sheet conformation (Uéda et al., 1993; Conway et al., 2000; Serpell et al., 2000; Giasson et al., 2001; Tuttle et al., 2016), and (iii) C-terminal domain (96–140 residues) is rich of acidic residues and a major site for phosphorylation activity (Fujiwara et al., 2002; Anderson et al., 2006; Figure 1A).

During cellular stress and pathological conditions, α-synuclein monomers trigger the formation of dimers *via* increased interaction with each other, which upon continuous interactions transformed into oligomers (Lashuel et al., 2013). These oligomers further recruit monomers to form protofibrils and finally β-sheet-rich insoluble amyloid fibrils (Waxman and Giasson, 2009; Lashuel et al., 2013), which are major components of Lewy bodies (LB) and Lewy neurites (LN) in Parkinson's disease (PD) and dementia with LB (DLB; Spillantini et al., 1997; Wakabayashi et al., 1997; Baba et al., 1998; Irizarry et al., 1998; Takeda et al., 1998; Trojanowski and Lee, 1998), and oligodendrocytes in multiple system atrophy (MSA; Arima et al., 1998; Spillantini et al., 1998; Tu et al., 1998; Wakabayashi et al., 1998; Figure 1B).

α-Synuclein acts as a chaperone for soluble NSF attachment protein receptor (SNARE)-complex assembly and upon recruitment to the SNARE-complex, facilitates the docking of synaptic vesicle onto the presynaptic plasma membrane. The fusion of synaptic vesicle to the presynaptic nerve terminals results in the release of neurotransmitters (Burré et al., 2010, 2014; Figure 1C). The deletion or knockout of α-synuclein in rodents promotes or exacerbates neurodegeneration, whereas the transgenic expression of α-synuclein rescued the animals from neurodegeneration (Chandra et al., 2005; Burré et al., 2010). Even though α-synuclein plays a critical role in neurodegeneration, its biological role in the initiation and progression of neurodegenerative diseases and disorders and the canonical signaling interactome remains elusive. Thus, the lack of information about α-synuclein's biological functions, role, signaling, and interaction cohorts weakens our understanding of the molecular mechanism behind neurodegeneration as well as limits the development of therapeutics for early diagnosis and treatment of neurodegenerative diseases and disorders. In this work, we have made an attempt to reveal the canonical signaling interactome and biological functions of α-synuclein using the ingenuity pathway analysis (IPA)-based bioinformatics approach.

Materials and methods

Preparation of the α-synuclein NCBI gene dataset

α-Synuclein and associated genes were searched in the National Center for Biotechnology Information (NCBI) database with a search query "Alpha-synuclein." The search was limited to the *Homo sapiens* genes only. A total of 215 α-synuclein-related genes available in the NCBI database till 26 August 2021 were downloaded as a text file (Supplementary Table S1; NCBI, 2021), which were subjected to analyzes on the IPA, QIAGEN.

IPA expression analysis of the α-synuclein NCBI gene dataset

A text file of α-synuclein and associated genes (Supplementary Table S1) obtained from the NCBI database was imported onto the IPA server for a new "core analysis." In the new core analysis, the "expression analysis" classification was selected. The default file format "flexible format" was chosen and the gene identification numbers (gene ID) were defined. For the population of genes to be considered for *P*-value calculations, the reference set was defined as the Ingenuity Knowledge Base genes only while for relationships that affect networks and upstream regulator analysis, both "direct and indirect relationships" were selected. For interaction networks, 35 molecules per network, 25 networks per analysis, and endogenous chemicals were selected while casual networks were predicted based on the score for master regulators for relationships to diseases, functions, genes, and chemicals. All node types, such as biological drugs, canonical pathways, all types of chemicals (endogenous, kinase, and protease inhibitors, drugs, toxic substances, and reagents), complexes, cytokines, diseases,

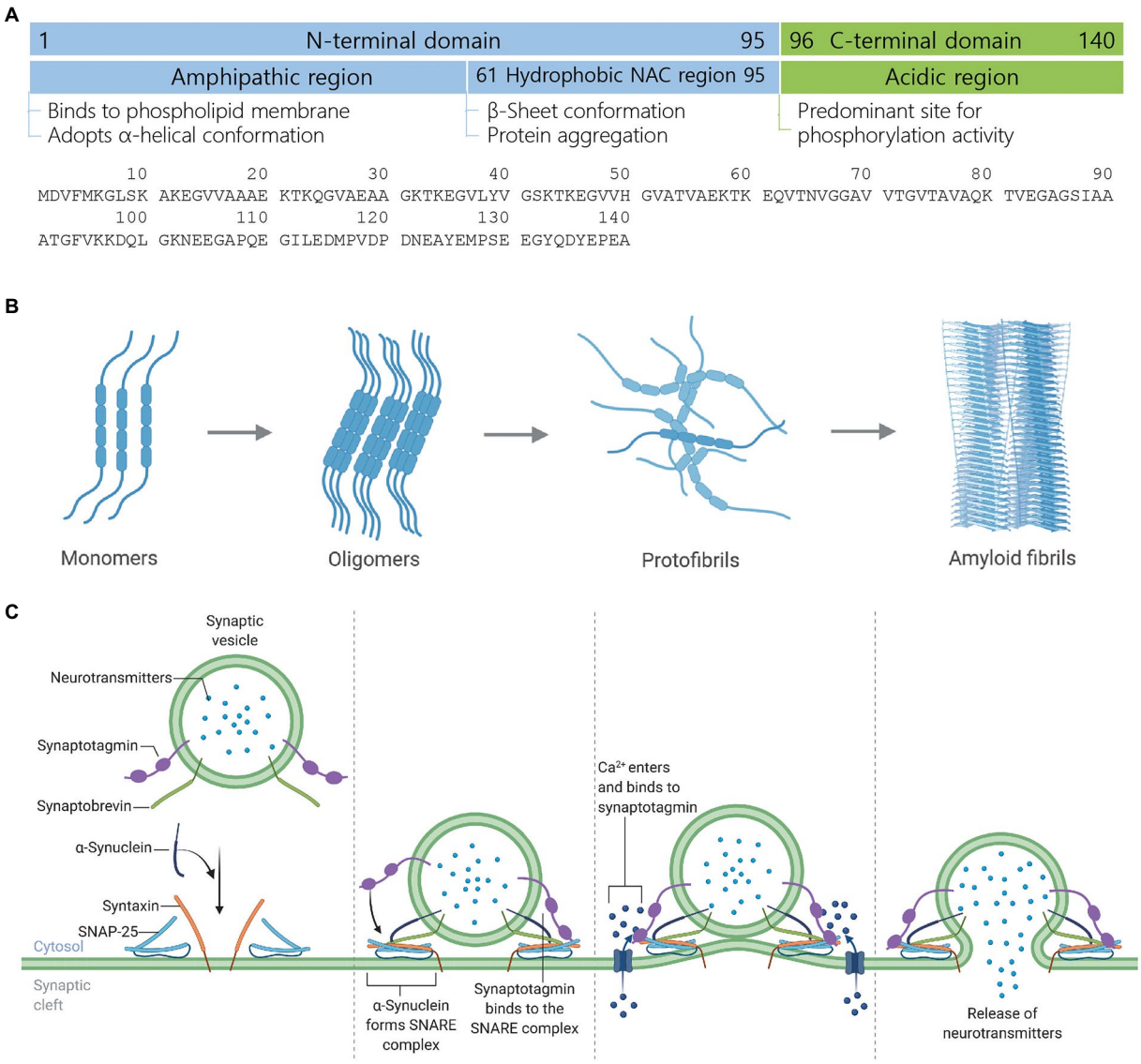

FIGURE 1
Structure, aggregate formation, and neurotransmission facilitation mechanism of α-synuclein. **(A)** Structure of α-synuclein highlighting different structural domains, their cardinal roles and an amino acid sequence. **(B)** Development of toxic α-synuclein aggregates. In the healthy brain, α-synuclein exists as a natively unfolded monomer. Upon mutation, multiplication, or unfavorable posttranslational modification, α-synuclein starts forming oligomers, which recruit further monomers and eventually form β-sheet-rich toxic amyloid fibrils. Amyloid fibrils form LB and LN, leading to neurodegeneration and cell death. **(C)** Mechanism of neurotransmission facilitation by α-synuclein. α-Synuclein is a presynaptic protein while synaptotagmin and synaptobrevin are synaptic vesicle membrane-associated proteins. During the docking of neurotransmitters-loaded synaptic vesicle onto the plasma membrane, α-synuclein binds to synaptobrevin while two other synaptic membrane proteins syntaxin and SNAP-25 are recruited to form the SNARE complex, which mediates vesicle priming. Action potential reaches the presynaptic terminal, calcium channel within the presynaptic plasma membrane opens, calcium ions enter into the cytosol, and bind to synaptotagmin, which leads to the exocytosis or release of neurotransmitters. Figure created with BioRender.com.

enzymes, etc., were marked for the core analysis. All data sources available on the IPA server were marked while the confidence of the prediction was limited to the experimentally observed values only. The species selection was restricted to humans only. For tissues and cells selection, tissues, cells, nervous system, organ systems, and other tissues and primary cells were marked. To observe the effect of possible mutations in IPA predictions, all types of mutations and effects, such as functional effect, inheritance mode, translation impact, unclassified mutations, zygosity, and wild type, were selected. The results were ranked based on Fisher's exact test, where the smaller *P*-value indicates the higher significance of predicted results (IPA, 2021; Suthar et al., 2021). GraphPad Prism 6 was used to plot the graphs at various stages of the study.

IPA toxicity analysis of α-synuclein, amyloid beta, tau, and Huntingtin

α-Synuclein, amyloid beta, tau, and Huntingtin *Homo sapiens* genes SNCA (gene ID 6622), APP (gene ID 351), MAPT (gene ID 4137), and HTT (gene ID 3064), respectively, were downloaded as an individual text file from the NCBI database (NCBI, 2022). IPA was performed by selecting the following options/parameters step-by-step available for selection on the IPA server (IPA, 2021); (i) the NCBI text file of the respective gene was imported onto the QIAGEN IPA server for a new core analysis, (ii) the imported text file was retained in the flexible format and the gene identification (GI) number of the SNCA/APP/MAPT/HTT was defined, (iii) IPA function "toxicity analysis" was chosen for the study, (iv) for the population of genes to be considered for *P*-value calculations, the reference set was limited to the Ingenuity Knowledge Base genes only, (v) for SNCA/APP/MAPT/HTT molecular network generation, we opted for molecules displaying both direct and indirect relationships in the network, (vi) furthermore, for SNCA/APP/MAPT/HTT molecular network generation, we opted for molecules exhibiting interaction networks as well as casual networks, (vii) an interaction network contained 35 molecules per network and 25 networks per analysis, (viii) the types of molecules to be included for network generation (referred to as node types), all node types, such as biological drugs, chemicals, complexes, cytokines, diseases, enzymes, etc. were selected, (ix) to consider the data sources for IPA predictions, all the data sources available on the IPA server were chosen, (x) to predict the relationships among the network molecules, the data sources with only experimentally observed molecular relationships were considered, (xi) IPA predictions were kept limited to the human species only, (xii) to opt for the data source experiments performed in the types of the organ system, tissues, and cell lines for IPA predictions, analysis was kept limited to the experimental results from tissues, cells, nervous system, and organ system only, (xiii) to consider the mutated molecules appearing in the network generation, all types of mutations, such as functional, inherited, translational, zygotic, and unclassified, were chosen, and (xiv) IPA prediction results were ranked based on the significance value (*P*-value) calculated by the right-tailed Fisher's exact test (Suthar et al., 2021).

Results

IPA expression analysis of the α-synuclein NCBI gene dataset

Prediction of α-synuclein canonical pathways, interaction network molecules, and pathological implications

IPA predicted 426 canonical signaling pathways for α-synuclein. Neuroinflammation (*P* 4.78 e-18) was the most prominent of the predicted signaling pathways for α-synuclein followed by Huntington's disease (*P* 4.34 e^{-11}), triggering receptor expressed on myeloid cells 1 (TREM1; *P* 1.28 e^{-10}), phagosome maturation (*P* 2.96 e^{-11}), and sirtuin signaling pathways (*P* 5.50 e^{-10}; Figure 2A). The major canonical signaling pathways of α-synuclein are presented in Supplementary Figures S1–S6. Next, we grouped α-synuclein and its interacting partner genes from the NCBI dataset that appeared across all the pathways together and performed a frequency distribution analysis. The analysis showed that 168 of 215 NCBI dataset genes appeared 1942 times across all the predicted canonical pathways. The analysis further revealed that nuclear factor-kappaB (NF-κB) protein subunit 1 gene (NFKB1) was the most populated gene (7.6%) across all the pathways followed by Fos proto-oncogene AP-1 transcription factor subunit (FOS; 5.1%), protein kinase C delta (PRKCD; 4.9%), tumor necrosis factor (TNF; 4.7%), glycogen synthase kinase 3 beta (GSK3B; 4.0%), cell division control protein 42 homolog (CDC42; 3.7%), interleukin 6 (IL6; 3.1%), mammalian target of rapamycin (MTOR; 3.1%), interleukin 1 beta (IL1B; 2.9%), and interferon-gamma (IFNG; 2.9%; Figure 2B; Supplementary Table S2). Thereafter, we overlapped the major canonical signaling pathways and the NCBI dataset genes expressed in those pathways, which divulged that neuroinflammation was the highest overlapped pathway with the molecules displaying a greater degree of overlapping with TREM1 and sirtuin signaling pathways. Huntington's disease displayed a relatively higher extent of overlapping with phagosome maturation signaling molecules while exhibiting the least overlapping with TREM1 signaling molecules. Furthermore, among the overlapped molecules, the molecules associated with inflammation, namely NFKB1, TNF, and caspase-1 (CASP1) displayed the highest prevalence across the overlapped pathways (Figure 2C). In our analysis of the pathological role of α-synuclein, it was highest implicated in neurological diseases (*P* 2.34 e^{-57}), followed by organismal injury and abnormalities (*P* 6.21 e^{-56}), skeletal and muscular disorders (*P* 4.55 e^{-53}), psychological disorders (*P* 1.96 e^{-47}), and hereditary disorders (*P* 6.27 e^{-43}; Figure 2D; Supplementary Figure S7).

Molecule activity predictor (MAP) analysis of the principal SNCA interaction network

The principal interaction network of the α-synuclein gene (SNCA) predicted that besides SNCA playing a key role in neuroinflammation and Huntington's disease, displayed direct interactions with amyloid beta precursor protein (APP), clusterin (CLU), and neural precursor cell expressed developmentally down-regulated protein 4 (also called NEDD4 E3 ubiquitin-protein ligase; NEDD4) genes, whereas it showed indirect relationships with calcitonin related polypeptide alpha (CALCA) and superoxide dismutase 1 (SOD1) genes (Figure 3A). Our attempt to predict the direct effect of the activation or inhibition of SNCA on the other genes of the

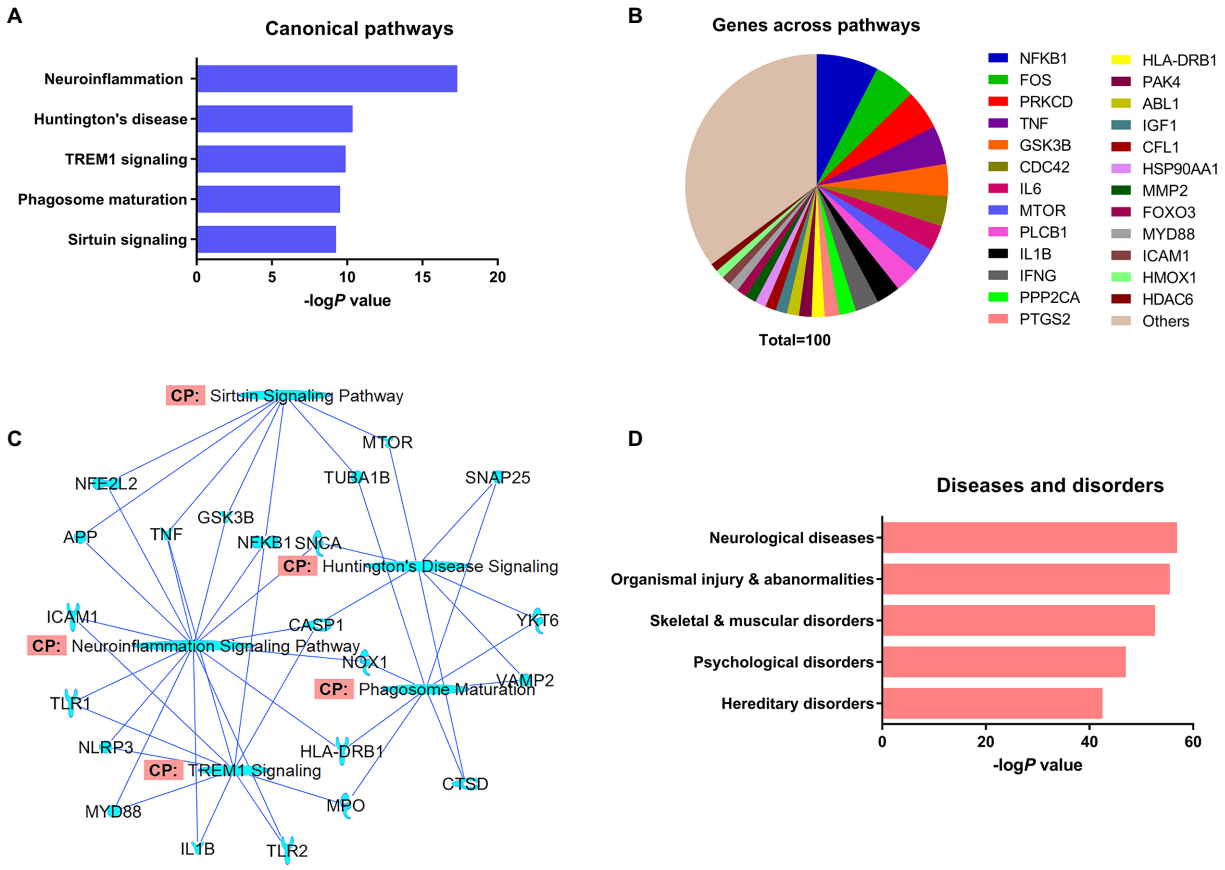

FIGURE 2
The expression analysis of differentially regulated α-synuclein and associated genes from the NCBI dataset by IPA. **(A)** Top-ranked canonical pathways of α-synuclein. **(B)** Significantly populated α-synuclein-associated genes from the NCBI dataset that appeared in the predicted canonical pathways. **(C)** Overlapping of the top-ranked canonical pathways of α-synuclein and α-synuclein-associated genes from the dataset. **(D)** Top-ranked diseases and disorders of α-synuclein.

principal interactome was not met with success. However, we observed that the increased activity of APP leads to the activation of pro-inflammatory genes IL1B and prostaglandin-endoperoxide synthase 2 (PTGS2; also known as cyclooxygenase-2 or COX-2) genes, which, in turn, activates the genes exhibiting the direct relationship with SNCA, namely CALCA and SOD1 (Figure 3B).

Prediction of upstream SNCA regulators

Along with the canonical pathways, interaction network, diseases, and biological functions, the core expression analysis of the α-synuclein NCBI gene dataset also predicted the upstream regulators of SNCA (Table 1). IL1B was the highest-ranked upstream regulator of SNCA followed by APP, TNF, macrophage migration inhibitory factor (MIF), and mitogen-activated protein kinase kinase 1 (MEK). Observation of the predicted top-thirty upstream regulators indicated that these molecules were associated with the protein aggregation (APP), inflammation and innate immunity (IL1B, TNF, MIF, PTGS2, CCL2, CD14, IL18, TLR4, CD163, IL27, lymphotoxin, IL33, NFKB, ADIPOQ, IGNG, STAT3, IgG, C5, and P2RX7), and neuronal cell growth, differentiation, and transcription regulation (Mek, ERK, P38 MAPK, MAP3K7, and HIF1A). Besides, molecules concerning the regulation of synaptic receptors (ARRB2), neurotransmission (TAC1), and post-transcriptional regulations (mir-155 and miR-155-5p) also appeared in the list of prominent upstream SNCA regulators.

IPA toxicity analysis of α-synuclein, amyloid beta, tau, and Huntingtin (HTT)

Prediction of α-synuclein, amyloid beta, tau, and Huntingtin toxicity signaling pathways

The core expression analysis of SNCA predicted canonical signaling pathways, upstream regulators, and interaction network molecules belonging to both physiological functions

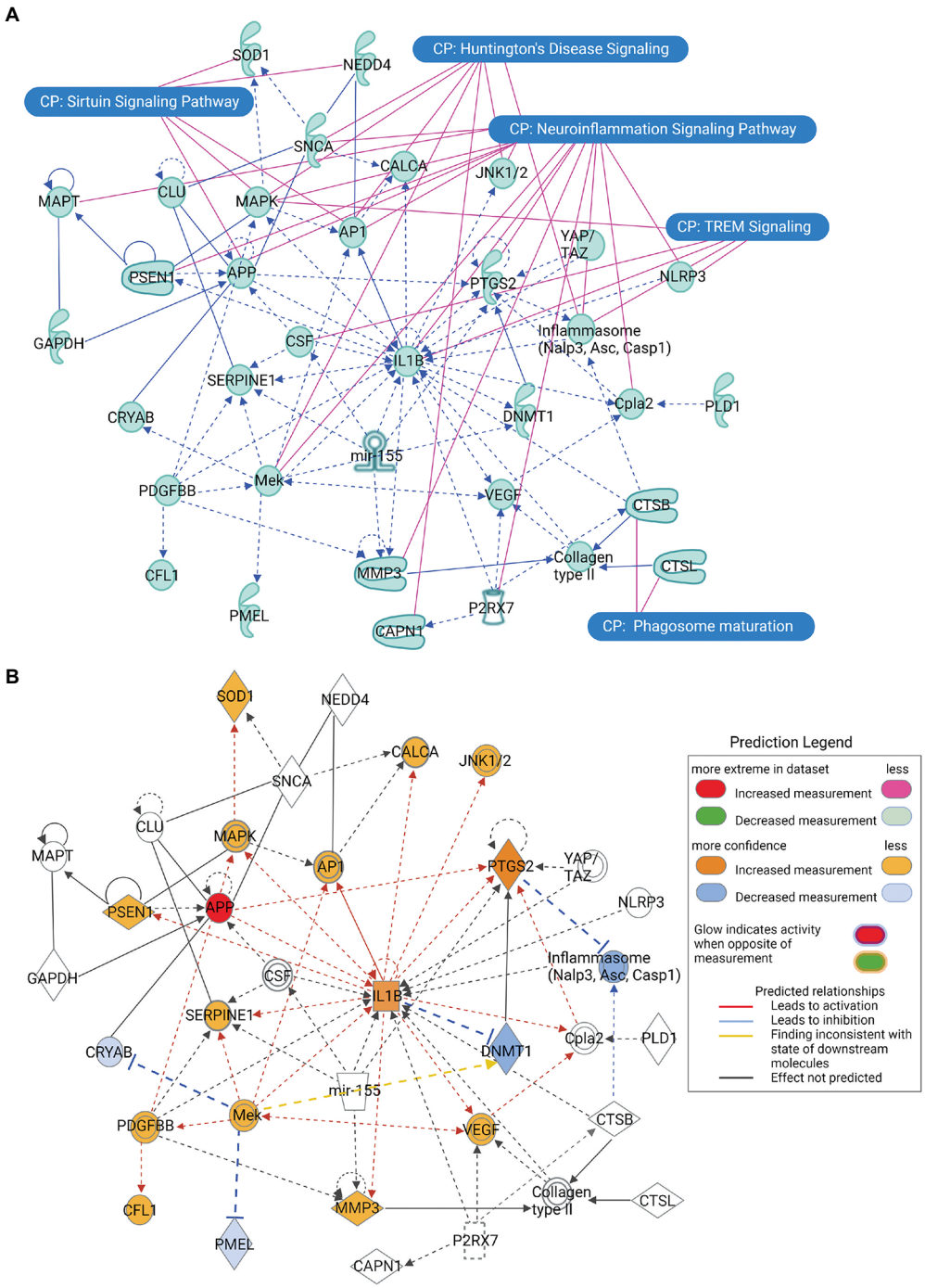

FIGURE 3
The principal interaction network of α-synuclein gene SNCA across all the predicted canonical signaling pathways. **(A)** The principal interaction network of SNCA revealed that SNCA directly interacts with APP, CLU, and NEDD4, whereas it interacts indirectly with CALCA and SOD1. Furthermore, the overlapping of the principal interaction network of α-synuclein and top-ranked canonical signaling pathways highlights a relationship between the interaction network genes and canonical pathways. **(B)** The molecule activity predictor (MAP) analysis of the principal interaction network of SNCA, depicting that increase in the activity of APP leads to a series of activation and inhibition of network genes. Figure created with BioRender.com.

and toxicity of α-synuclein. Therefore, to identify the pathways and network molecules specific to α-synuclein toxicity, we performed the toxicity analysis of α-synuclein. IPA toxicity analysis of SNCA predicted PD signaling (P 7.50 e^{-04}), sumoylation (P 4.73 e^{-03}), 14–3-3 (P 5.91 e^{-03}), SNARE (P 6.19 e^{-03}), mitochondrial dysfunction (P 7.74 e^{-03}), Huntington's

TABLE 1 The upstream regulators of α-synuclein (SNCA) predicted by expression analysis of the α-synuclein NCBI gene dataset using IPA.

Rank	Upstream regulator	Molecule type	*P*-value of overlap
1	IL1B	Cytokine	1.52 e^{-10}
2	APP	Other	1.81 e^{-10}
3	TNF	Cytokine	3.47 e^{-10}
4	MIF*	Cytokine	7.03 e^{-10}
5	Mek* (MAPK/ERK kinase 1)	Group	9.51 e^{-10}
6	ERK* (MAPK)	Group	1.04 e^{-09}
7	PTGS2 (COX2)	Enzyme	1.05 e^{-09}
8	TP53*	Transcription regulator	1.64 e^{-09}
9	P38 MAPK* (MAPK 14)	Group	1.97 e^{-09}
10	CCL2	Cytokine	2.17 e^{-09}
11	HIF1A*	Transcription regulator	3.87 e^{-09}
12	mir-155*	microRNA	4.17 e^{-09}
13	CD14*	Transmembrane receptor	7.55 e^{-09}
14	IL18	Cytokine	7.89 e^{-09}
15	TLR4	Transmembrane receptor	9.20 e^{-09}
16	CD163*	Transmembrane receptor	1.04 e^{-08}
17	IL27*	Cytokine	1.87 e^{-08}
18	Lymphotoxin* (TNFB)	Complex	4.55 e^{-08}
19	IL33*	Cytokine	6.69 e^{-08}
20	ARRB2*	Other	1.53 e^{-07}
21	TAC1*	Other	1.53 e^{-07}
22	NFKB	Complex	1.84 e^{-07}
23	MAP3K7	Kinase	1.92 e^{-07}
24	miR-155-5p* (miRNAs w/seed UAAUGCU)	Mature microRNA	2.00 e^{-07}
25	ADIPOQ* (Adiponectin C1Q)	Other	2.00 e^{-07}
26	IFNG	Cytokine	2.40 e^{-07}
27	STAT3*	Transcription regulator	2.58 e^{-07}
28	IgG*	Complex	2.83 e^{-07}
29	C5	Cytokine	2.86 e^{-07}
30	P2RX7	Ion channel	2.86 e^{-07}
31	COL18A1*	Other	3.45 e^{-07}
32	LILRB4*	Other	3.55 e^{-07}
33	ATF3	Transcription regulator	4.13 e^{-07}
34	CD40LG	Cytokine	6.07 e^{-07}
35	PI3K* (family)	Group	6.12 e^{-07}
36	IL1A	Cytokine	6.12 e^{-07}
37	DDX58*	Enzyme	7.96 e^{-07}
38	ABCA1	Transporter	1.04 e^{-06}
39	IL32	Cytokine	1.07 e^{-06}
40	Creb	Group	1.09 e^{-06}
41	TNFSF12*	Cytokine	1.26 e^{-06}
42	IL37	Cytokine	1.26 e^{-06}
43	Akt* (PKB)	Group	1.36 e^{-06}
44	CSF*	Group	1.36 e^{-06}
45	NAMPT	Cytokine	2.08 e^{-06}
46	PLG*	Peptidase	3.24 e^{-06}
47	BMP7*	Growth factor	3.46 e^{-06}
48	JUN	Transcription regulator	3.48 e^{-06}
49	CD44*	Other	3.76 e^{-06}
50	CASP1*	Peptidase	4.11 e^{-06}

*The predictions likely originated from the data obtained from cell culture studies. ABCA1; ATP binding cassette subfamily A member 1, ADIPOQ; Adiponectin C1Q, Akt; Serine/Threonine kinase 1/PKB, ARRB2; Arrestin beta-2, ATF3; Activating transcription factor 3, BMP7; Bone morphogenetic protein 7, C5; Complement component 5, CCL2; C-C motif chemokine ligand 2, CD14/163/40/44; Cluster of differentiation 14/163/40/44, CD40LG; CD40 ligand, COL18A1; Collagen type XVIII alpha 1 chain, Creb; cAMP-response element binding protein, CSF; Colony stimulating factor, DDX58; DExD/H-box helicase 58, ERK; Extracellular signal-regulated kinase/MAPK, HIF1A; Hypoxia inducible factor 1 subunit alpha, IgG; Immunoglobulin G, JUN; Jun proto-oncogene/AP1, LILRB4; Leukocyte immunoglobulin like receptor B4, Mek; Mitogen-activated protein kinase kinase 1/MAPK/ERK kinase 1, MIF; Macrophage migration inhibitory factor, mir-155 (miRNAs w/seed UAAUGCU); microRNA 155, NAMPT; Nicotinamide phosphoribosyltransferase, P2RX7; Purinergic receptor P2X 7, P38 MAPK; MAPK P38 alpha/MAPK 14, PI3K; Phosphoinositide 3-kinases, PLG; Plasminogen, STAT3; Signal transducer and activator of transcription 3, TAC1; Tachykinin precursor 1, TP53; Tumor protein P53.

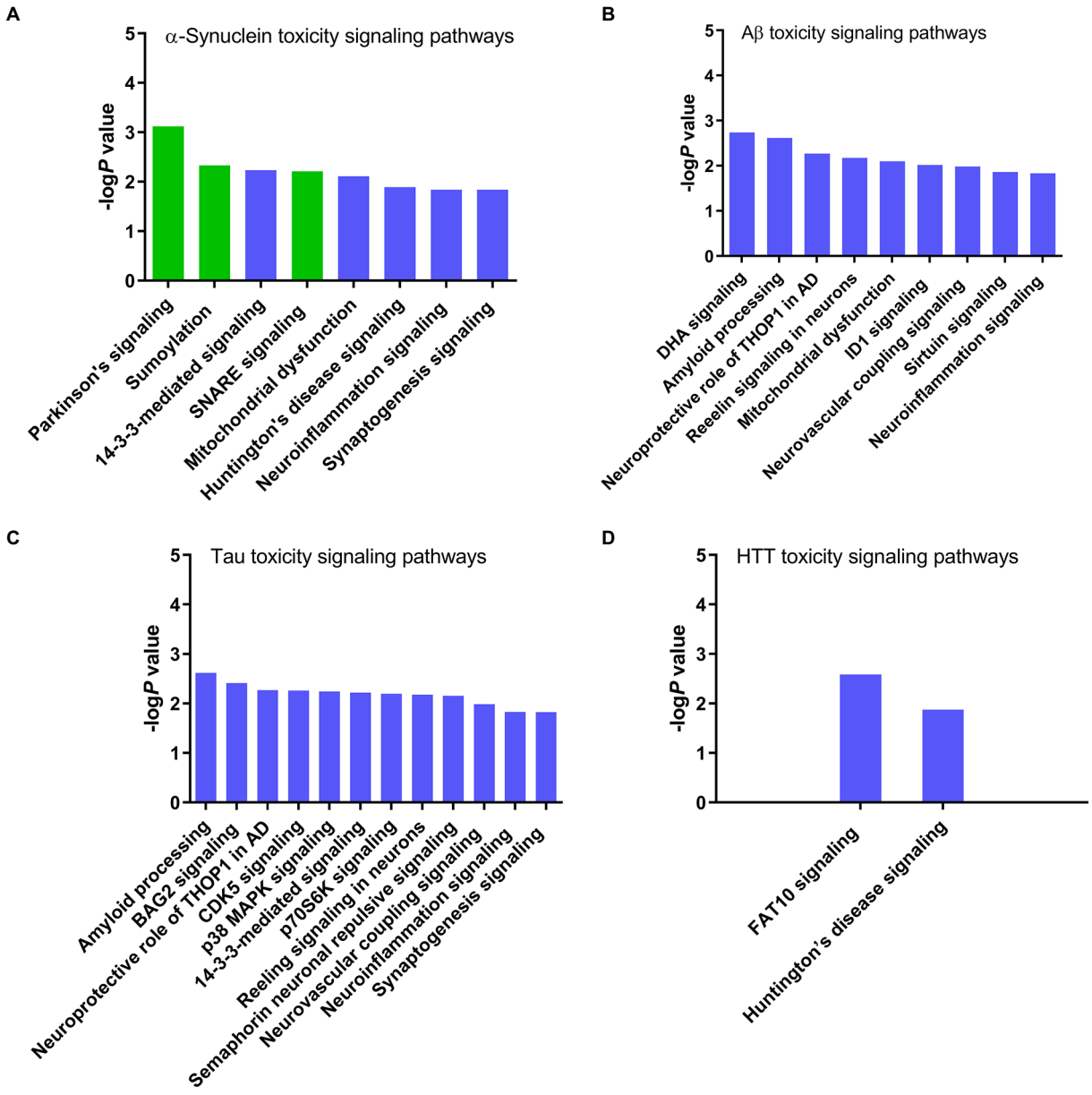

FIGURE 4
Canonical signaling pathways associated with the toxicity of neurodegenerative proteins predicted by IPA. **(A)** α-Synuclein, **(B)** Amyloid beta, **(C)** Tau, and **(D)** Huntingtin. IPA toxicity analysis identified Parkinson's, sumoylation, and SNARE signaling pathways specific to the α-synuclein toxicity. Conversely, α-synuclein shares 14–3-3, mitochondrial dysfunction, Huntington's disease, neuroinflammation, and synaptogenesis signaling pathways with other neurotoxic proteins amyloid beta, tau, and HTT, suggesting that these pathways are likely activated due to the host cell stress response or secondary non-specific response to the toxicity of α-synuclein.

disease (P 1.30 e^{-02}), neuroinflammation (P 1.44 e^{-02}), and synaptogenesis (P 1.46 e^{-02}) as the canonical signaling pathways of α-synuclein toxicity (Figure 4A). The role of α-synuclein in PD disease is illustrated in Figure 5 while the rest of the pathways concerning α-synuclein toxicity are depicted in Supplementary Figures S2, S3, S8–S12.

After exploring α-synuclein toxicity pathways, we also analyzed the toxicity profiles of similar pathogenic proteins, which cause neurodegeneration, such as amyloid beta, tau, and Huntingtin to rule out the α-synuclein toxicity pathways arising due to the host cell stress response or secondary non-specific response to the α-synuclein toxicity. The toxicity analysis of APP predicted docosahexaenoic acid (DHA) signaling (P 1.82 e^{-03}), amyloid processing (P 2.4 e^{-03}), neuroprotective role of thimet oligopeptidase (THOP1) in AD (P 5.37 e^{-03}), reelin signaling in neurons (P 6.62 e^{-03}),

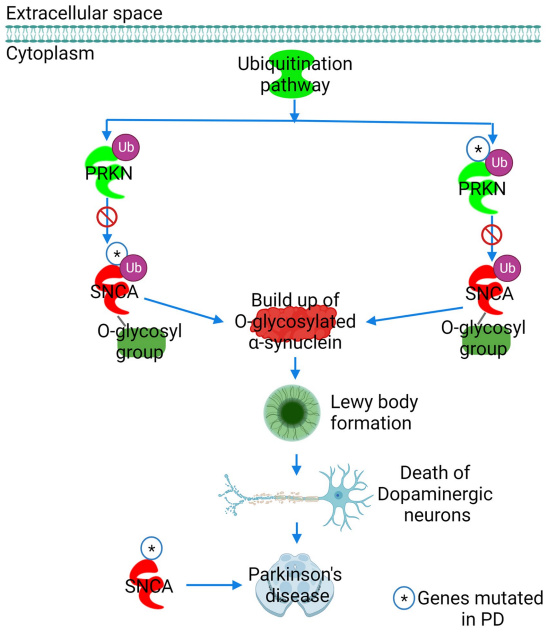

FIGURE 5
The role of α-synuclein in Parkinson's disease (PD) predicted by IPA. PD was ranked as the leading pathway of α-synuclein toxicity. The E3 ubiquitin ligase Parkin (PRKN) labels the glycosylated form of synuclein (SNCA) for proteasomal degradation. Mutation in either PRKN or SNCA precludes PRKN from binding to SNCA, preventing the proteasomal degradation of glycosylated α-synuclein. A build-up of glycosylated α-synuclein in neuronal cells results in the formation of Lewy bodies, leading to dopaminergic neuron death and PD. Figure created with BioRender.com.

mitochondrial dysfunction (P 7.91 e^{-03}), inhibitor of differentiation-1 (ID1 signaling (P 9.59 e^{-03}), neurovascular coupling signaling (P 1.03 e^{-02}), sirtuin signaling (P 1.37 e^{-02}), and neuroinflammation signaling (P 1.47 e^{-02}) pathways as the mediators of amyloid beta toxicity (Figure 4B). At the same time, the toxicity analysis of MAPT identified amyloid processing (P 2.4 e^{-03}), Bcl-2-associated athanogene 2 (BAG2) signaling (P 3.88 e^{-03}), neuroprotective role of THOP1 in AD (P 5.37 e^{-03}), CDK5 signaling (P 5.47 e^{-03}), p38 MAPK signaling (P 5.75 e^{-03}), 14–3-3-mediated signaling (P 6.04 e^{-03}), p70S6K signaling (P 6.38 e^{-03}), reelin signaling in neurons (P 6.62 e^{-03}), semaphorin neuronal repulsive signaling (P 6.95 e^{-03}), neurovascular coupling signaling (P 1.03 e^{-02}), neuroinflammation signaling (P 1.47 e^{-02}), and synaptogenesis signaling (P 1.49 e^{-02}) pathways as the architects of tau-induced toxicity in neurodegenerative diseases (Figure 4C). We also performed the toxicity analysis of HTT, which predicted human leukocyte antigen F-associated transcript10 (FAT10) signaling (P 2.59 e^{-03}) and Huntingtin's disease signaling (P 1.33 e^{-02}) pathways as the conveners of toxicity caused by Huntingtin's protein (Figure 4D).

Discussion

Prediction of α-synuclein canonical pathways

The core expression analysis of the α-synuclein NCBI gene dataset predicted 426 canonical pathways. These pathways were ranked based on Fisher's exact test P-values. Neuroinflammation signaling was predicted to be the foremost canonical pathway of α-synuclein followed by Huntington's disease, TREM1 signaling, phagosome maturation, and sirtuin signaling pathways (Figure 2A; Supplementary Figures S2–S6). Abnormal expression of SNCA forms LB in neuronal cells, which activates neuroinflammation signaling genes, like advanced glycosylation end-product specific receptor (AGER), toll-like receptor 2 (TLR2), and toll-like receptor 4 (TLR4). Activation of these genes triggers downstream inflammation marker genes activator protein 1 (AP1) and NFKB, which, in turn, stimulate a cascade of pro-inflammatory genes, like TNF, IL6, IL1B, and IFNG, etc., eventually resulting in neuronal cell death (Supplementary Figure S2). Activation of SNCA in Huntington's disease conveys an inhibitory effect on DnaJ heat shock protein family (Hsp40) member B1 (DNAJB1). The latter protein prevents the aggregation propensity of misfolded proteins *via* the activation of brain-derived neurotrophic factor (BDNF; Supplementary Figure S3). SNCA mediates innate immunity *via* TREM1 signaling. As the name indicates, TREM1 is expressed on myeloid or blood cells, like monocytes, eosinophils, neutrophils, basophils, and macrophages and its activation *via* inflammatory mediators amplifies immune response. TREM1-induced neuroinflammation is facilitated by common inflammatory mediators, such as NF-κB, TNF, IL6, IL1B, TLR1 and 2, NOD-like receptor pyrin domain-containing protein 3 (NLRP3), and intercellular adhesion molecule 1 (ICAM1; Supplementary Figure S4). α-Synuclein plays a vital role in the host defense mechanism, in the event of viral or bacterial infections (Alam et al., 2022). SNCA augments innate immunity through an interaction with Ras-related GTPases Rab5 and Rab7, cathepsins, and lysosomal-associated membrane protein 2 (LAMP2), which activates human leukocyte antigen—DR isotype (HLA-DR) or MHC class II cell surface receptor, resulting into phagolysosome of pathogens. During phagosome maturation, Rab5 interacts with SNARE proteins and vacuolar(H^+)-ATPase (V-ATPase) to impetus the maturation of the early endosome, whereas Rab7 is essential for the fusion of phagosome with the lysosome. V-ATPase acidifies phagosomes by translocation of H^+ ions, resulting in the suppression of microbial growth (Supplementary Figure S5). Acetylation is a key regulatory mechanism for the aggregation of α-synuclein. Sirtuins (SIRT) are histone deacetylases, which play an important role in inflammation, aging, and cancer (Supplementary Figure S6). Sirtuins, namely SIRT2, which is predominantly localized in the cytoplasm deacetylates α-synuclein, resulting in exacerbated α-synuclein toxicity and neurodegeneration. (Outeiro et al., 2007;

de Oliveira et al., 2017). Taken together, SNCA exercises its role in inflammation and immune response through inflammatory mediators *via* neuroinflammation and TREM1 signaling pathways and through cathepsin proteases *via* phagosome maturation pathways. Over-activation of SNCA exacerbates Huntingtin protein (HTT)-induced toxicity in Huntington's disease, while its deacetylation by sirtuins affects its aggregation propensity.

Analysis of SNCA-interacting NCBI dataset genes expressed in the predicted canonical pathways of α-synuclein

Ingenuity pathway expression analysis of the α-synuclein NCBI gene dataset predicted 426 canonical pathways for α-synuclein. A frequency distribution analysis of the α-synuclein dataset genes that appeared in the predicted canonical pathways revealed that 168 genes from the dataset of 215 genes appeared 1942 times across the predicted pathways. NFKB was the most frequently occurring interaction partner of SNCA with a prevalence of 7.6%. NFKB gene was followed by FOS (5.1%), PRKCD (4.9%), TNF (4.7%), GSK3B (4.0%), CDC42 (3.7%), IL6 (3.1%), MTOR (3.1%), IL1B (2.9%), and IFNG (2.9%). The major interaction partners of SNCA are presented in Figure 2B. The predominant presence of transcription factors NFKB and FOS, cytokines TNF, IFNG, IL-6, and IL1B, cell cycle regulator CDC42, cell growth, differentiation, and motility regulating kinases PRKCD and MTOR, and cytokine regulating kinase GSK3B in the SNCA interactome indicates that SNCA gene is an important mediator of neuroinflammation and neural cell growth and motility. Furthermore, MTOR and GSK3B are also being investigated as the potential targets for the therapeutic intervention of neurodegenerative diseases and aging. The increased MTOR signaling is associated with the build-up of Aβ (Caccamo et al., 2010) and α-synuclein plaques (Pérez-Revuelta et al., 2014), whereas GSK3B phosphorylates α-synuclein and tau proteins, which leads to accumulation and aggregate formation of these proteins (Credle et al., 2015). MTOR- and GSK3B-mediated increased α-synuclein activity modulates the level of CDC42, which affects neuronal outgrowth (Schnack et al., 2008). At the same time, α-synuclein aggregates upregulate PRKCD activity, leading to mitochondrial dysfunction, endoplasmic reticulum stress, and activation of inflammatory cascade mediated by NFKB, TNF, IL-6, and IL1B, etc. (Samidurai et al., 2021). In summary, molecules like MTOR and GSK3B induce α-synuclein aggregation, which, in turn, dysregulates the activity of PRKCD and CDC42, resulting in perturbed neuronal architecture and neuroinflammation.

Overlapping of the top-ranked canonical pathways and the α-synuclein NCBI gene dataset

Overlapping of IPA-predicted top canonical pathways and α-synuclein-associated genes could predict the common features of these pathways as well as reveal the otherwise unobserved molecular patterns of these pathways. Overlapping of the top-ranked canonical pathways and the α-synuclein NCBI gene dataset (Figure 2C) predicted that neuroinflammation signaling was the most overlapped pathway with 15 molecules displaying connections with the other pathways. Furthermore, neuroinflammation signaling shared the highest number of molecules with TREM1 signaling followed by sirtuin signaling pathways, indicating a plethora of cross-talks across these pathways. The presence of molecules, like ICAM1, TLR1/2, NLRP3, IL1B, NFKB1, and HLA-DRB1, and myeloid differentiation primary response 88 (MYD88) in both neuroinflammation and TREM1 signaling suggests the overwhelming role of neuroinflammation and immune response in TREM1 signaling. On the other hand, the occurrence of APP, GSK3B, nuclear factor (erythroid-derived 2)-like 2 (NFE2L2), TNF, and NFKB1 in both neuroinflammation and sirtuin signaling indicates shared functions of both the pathways in protein aggregation, oxidative stress, and neuroinflammation. Besides, Huntington's disease signaling molecules displayed the highest overlapping with the phagosome maturation signaling molecules. The presence of SNAP25, VAMP2, and YKT6 (synaptobrevin or V-SNARE homolog) in both the pathways points toward the shared role of both the signaling in exocytosis. As expected, SNCA was a mutual link between Huntington's disease and neuroinflammation signaling pathways. Coming to the molecules shared by all the overlapping pathways, the molecules related to inflammation and cell death, namely TNF, NFKB1, and CASP1 were markedly shared across the pathways. Taken together, the overlapping of IPA-predicted top-ranked canonical pathways and the α-synuclein NCBI gene dataset substantiate that neuroinflammation is the most prominent signaling pathway of α-synuclein.

Prediction of α-synuclein-associated diseases

Analysis of diseases and biological functions linked to α-synuclein predicted neurological diseases, organismal injury and abnormalities, skeletal and muscular disorders, psychological disorders, and hereditary disorders as the major pathological outcomes of SNCA gene anomalies (Figure 2D; Supplementary Figure S7). Among SNCA-linked diseases and disorders, PD, Alzheimer's disease (AD), tauopathy, degenerative dementia, progressive motor neuropathy, familial encephalopathy, hereditary and motor neuropathies, a disorder of basal ganglia, movement disorders, neuromuscular diseases, and other progressive neurological diseases were found to be the major diseases and disorders linked to SNCA gene. The recent research on α-synuclein associated diseases suggests that PD, DLB, and MSA, where the misfolding of α-synuclein monomers into oligomers followed by progressive transformation of oligomers into amyloid fibrils takes place, have become a central point of current synucleinopathy research (Oliveira et al., 2021). As a whole, abnormalities in α-synuclein expression primarily cause

aggregation of α-synuclein monomers into fibrils, which eventually form LB, LN, and glial cell inclusions—the pathological hallmarks of PD, DLB, and MSA.

MAP analysis of the principal SNCA interaction network

IPA predicted several interaction networks of SNCA and ranked them according to their statistical likelihood of molecules being appeared in the network by random chance. The top-ranked interaction network of SNCA (score 33) revealed that SNCA directly interacts with APP, CLU, and NEDD4, whereas it indirectly interacts with CALCA and SOD1 (Figure 3A). SNCA increases the activity of APP *via β-and γ*-secretase, leading to amyloid plaque formation (Roberts et al., 2017). Astrocytes play a vital role in the clearance of α-synuclein aggregates *via* the endolysosomal pathway. CLU directly binds to α-synuclein aggregates and limits their internalization into astrocytes; thus, contributing to the pathogenesis of PD (Filippini et al., 2021), whereas NEDD4 ligase ubiquitinates α-synuclein and clears α-synuclein aggregates *via* endolysosomal pathway; thereby protecting against α-synuclein-induced progressive neurodegeneration (Tofaris et al., 2011). CALCA potentiates the aggregation of α-synuclein and activates inflammation mediators, whereas inhibition of CALCA by a small molecule attenuates α-synuclein aggregation properties (Na et al., 2020). Mutations in SOD1 cause familial amyotrophic lateral sclerosis (ALS). α-Synuclein aggregates interact with SOD1 and promote its oligomerization and aggregation (Helferich et al., 2015). Altogether, APP, CLU, CALCA, and SOD1 may contribute to the α-synuclein-associated synucleinopathy, whereas NEDD4 by posttranslational modification protects against the formation of toxic α-synuclein inclusions.

We also performed the MAP analysis of the principal SNCA network to observe whether the increase or decrease in the activity of SNCA activates or inhibits the interacting genes (Figure 3B). Unfortunately, the MAP analysis of SNCA did not predict any activity pattern; therefore, we attempted MAP analysis of other genes which were directly interacting with SNCA, where the increase in the activity of APP was associated with the exacerbation of IL1B activity, which, in turn, activated a battery of molecules. APP-IL1B axis-mediated activation of catalytic subunit of γ-secretase (presenilin-1 or PSEN) breaks down APP, leading to the increased synthesis of A*β*. Proteolytic degradation of APP further activates protein kinases concerning cell death mitogen-activated protein kinase (Mapk) and C-Jun N-terminal kinase (JNK1/2), transcription factor Ap1, inflammatory mediators PTGS2 (COX2) and vascular endothelial growth factor (Vegf), cytosolic phospholipase A2 (Cpla2) for lipid biosynthesis, matrix metallopeptidase 3 (MMP3), innate immunity component serine proteinase (SERPINE1), and calcium regulating CALCA for potentiating aggregate formation, orchestrating a cascade of neuroinflammation and cell death. At the same time, the activation of IL1B by APP leads to the inhibition of DNA methyltransferase 1 (DNMT1), a molecule responsible for maintaining DNA methylation for epigenetic gene regulation. As a whole, the MAP analysis of the principal SNCA interaction network suggests that the aggregate formation of α-synuclein accompanies neuroinflammation, inevitably leading to cell death in neurodegenerative diseases.

Prediction of SNCA-upstream regulators

Besides, the predictions of canonical signaling pathways, interaction networks, and disease and biological functions, the core expression analysis of the α-synuclein NCBI gene dataset also predicted upstream regulators of SNCA (Table 1). The presence of APP in the list of revealed upstream regulators indicates that protein aggregation occurs during synucleinopathy. Since protein aggregation formation is always associated with neuroinflammation, the overwhelming presence of cytokines (IL1B, TNF, MIF, CCL2, IL18, IL27, lymphotoxin, IL33, IFNG, IgG, and C5), inflammatory mediator (PTGS2/COX2), transmembrane receptors mediating innate immunity (CD14, TLR4, and CD163), transcription regulators (TP53, HIF1A, NFKB, and STAT3), post-transcriptional gene regulators (mir-155 and miR-155-5p), and purinergic receptor for macrophage lysis (P2RX7) as the top-ranked upstream regulators substantiate that neuroinflammation is a hallmark of synucleinopathy in the brain. In addition, the presence of MEK, ERK, P38 MAPK, and MAP3K7 kinases as the upstream SNCA regulators suggests that stress and inflammatory cytokines induce the expression of MAPK signal transduction pathway members. Activated MAP kinases then collude with SNCA to cause synaptic dysfunction and neurodegeneration. As a whole, the upstream SNCA-regulating molecules underlie neuroinflammation and innate immune response as key events in α-synuclein pathology.

Analysis of SNCA, APP, MAPT, and HTT toxicity signaling pathways

IPA expression analysis of the α-synuclein NCBI gene dataset predicted canonical signaling pathways concerning physiological functions, toxicity, and host cell stress response to the toxicity of α-synuclein (Figure 2A; Supplementary Figure S1). Since with the expression analysis of SNCA and associated genes, we were not able to discriminate the canonical pathways specific to the physiological functions and toxicity of α-synuclein, we performed the toxicity analysis of SNCA to reveal the canonical signaling pathways specific to α-synuclein toxicity. The toxicity analysis of SNCA identified PD followed by sumoylation, 14–3-3, SNARE, mitochondrial dysfunction, Huntington's disease, neuroinflammation, and synaptogenesis as the canonical signaling pathways of α-synuclein-associated toxicity (Figure 4A). Here, we remind that the expression analysis of the α-synuclein NCBI gene dataset had predicted neuroinflammation, Huntington's disease, TREM1, phagosome maturation, and sirtuin signaling as the

major canonical pathways of α-synuclein (Figure 2A). As we can observe upon comparing the expression analysis- and toxicity analysis-predicted pathways that the top-ranked pathways of expression analysis, neuroinflammation and Huntingtin's disease also appeared in the list of pathways predicted by toxicity analysis of α-synuclein, suggesting that these pathways are likely associated with the toxicity of α-synuclein (Figures 2A, 4A). On the contrary, the absence of other top-ranked expression analysis-predicted pathways, such as TREM1, phagosome maturation, and sirtuin signaling in the list of pathways predicted through the toxicity analysis of α-synuclein, indicates that these pathways are more likely related to the physiological functions of α-synuclein than its toxicity. Thus, the comparison of the expression analysis-predicted pathways with the toxicity analysis-predicted pathways points out that the top-ranked pathways of expression analysis—neuroinflammation and Huntingtin's disease are likely associated with the abnormal expression of α-synuclein, whereas the rest of the three pathways such as TREM1, phagosome maturation, and sirtuin signaling pathways are likely related to the normal physiological functions of α-synuclein.

To gain further insight into the IPA-predicted toxicity pathways, and whether any of the predicted pathways is a result of the host cell stress response instead of α-synuclein pathogenicity, we compared the toxicity pathways of α-synuclein (Figure 4A) with that of other neurodegenerative proteins, such as amyloid beta (Figure 4B), tau (Figure 4C), and Huntingtin (Figure 4D). These proteins form toxic aggregates in a similar fashion to α-synuclein. IPA toxicity analysis of these proteins revealed that mitochondrial dysfunction and neuroinflammation signaling pathways were common to both α-synuclein and amyloid beta while 14–3-3, neuroinflammation, and synaptogenesis signaling pathways were common between α-synuclein and tau. Furthermore, the toxicity analysis of HTT identified Huntingtin's disease signaling as one of the major pathways and a common link between Huntingtin's protein and α-synuclein. Thus, the appearance of 14–3-3, mitochondrial dysfunction, Huntington's disease, neuroinflammation, and synaptogenesis signaling as the common toxicity pathways for α-synuclein and other neurotoxic proteins amyloid beta, tau, and Huntingtin suggest that these pathways are likely activated as a result of the host cell stress response or secondary non-specific response to the toxicity and immunogenicity of α-synuclein rather than as a direct consequence of the α-synuclein toxicity. Conversely, the revelation of PD, sumoylation, and SNARE signaling pathways exclusive to the toxicity of α-synuclein suggests that these pathways are likely an outcome of direct α-synuclein pathogenicity.

The appearance of the PD signaling pathway as the chief architect of α-synuclein-induced toxicity was expected as the mutation in the SNCA gene has been reported to cause familial PD (Figures 4A, 5). In normal cellular conditions, the glycosylated form of α-synuclein is a substrate for Parkin (PARK2), an E3 ubiquitin ligase, which marks α-synuclein for proteasomal degradation (Shimura et al., 2001). IPA predicted that due to mutations in either Parkin or α-synuclein gene (SNCA), Parkin fails to bind to the glycosylated α-synuclein. α-Synuclein in the glycosylated state then accumulates in the neuronal cells, forming LB, which causes the death of dopaminergic neurons and the progression of PD (Figure 5). IPA divulged that the sumoylation mechanism was the second-leading contributor to the α-synuclein-induced toxicity (Figure 4A; Supplementary Figure S8). Sumoylation is a posttranslational modification required for normal cellular functions, where a small ubiquitin-like modifier (SUMO) protein covalently binds to the target protein to perform mundane activities. Our study predicted that the sumoylation of α-synuclein by SUMO-conjugating E2 enzyme UBC9 (UBE2I) and E3 SUMO-protein ligase chromobox 4 (CBX4) promotes α-synuclein aggregation (Supplementary Figure S8). However, our finding that the sumoylation causes α-synuclein aggregation should be taken with caution because the fate of α-synuclein sumoylation depends upon the isoform and type of SUMO involved in the modification of α-synuclein, and many other studies have reported contrasting results. SNARE signaling was another pathway found to be explicit for α-synuclein toxicity and function (Figure 4A; Supplementary Figure S10). α-Synuclein is a presynaptic protein, which during the SNARE signaling binds to the synaptic vesicle-associated membrane protein synaptobrevin (VAMP2) and forms a SNARE complex in coordination with another synaptic vesicle protein synaptotagmin and the presynaptic plasma membrane proteins syntaxin-1 and SNAP25. The formation of the SNARE complex eventually leads to the exocytosis of synaptic vesicles, also referred to as the release of neurotransmitters (Supplementary Figure S10). Toxic α-synuclein inclusions disrupt the integrity of the synaptic vesicle membrane, leading to neurotoxicity.

Limitations of the study

The IPA predictions are affected by the gene dataset used for analysis. In due course, updates in NCBI dataset genes concerning α-synuclein may affect the IPA prediction about the biological roles and functions of α-synuclein. Furthermore, IPA predictions are derived from a dataset of context-dependent experimental outcomes, available on the IPA server. The future update in the IPA dataset or opting for different experimental contexts, either during the Bioinformatics predictions or while replicating the IPA predictions in the wet lab, like opting for different cells, tissues, organs, species, and experimental conditions, may diverge the IPA predictions. Furthermore, IPA predictions are derived from various data sources, including the data originating from RNA sequencing studies. IPA cannot classify if the α-synuclein used as an external reagent in some of those RNA sequencing studies was endotoxin contaminated, which might have affected IPA predictions. Besides, three different species of α-synuclein, oligomers, protofibrils, and amyloid fibrils, confer different levels of toxicity. The current version of the IPA cannot identify the species responsible for the predicted toxic effect.

Conclusion

To our knowledge, this work is the first report on the analysis of signaling pathways, network molecules, biological functions, and role of α-synuclein using the Bioinformatics tool, IPA. The expression and toxicity analyzes of α-synuclein identified TREM1, phagosome maturation, and sirtuin signaling pathways associated with the physiological functions of α-synuclein, whereas PD, sumoylation, and SNARE signaling pathways were identified as specific to the toxicity of α-synuclein. From the NCBI gene dataset used for IPA predictions of α-synuclein, NFKB1, FOS, PRKCD, TNF, GSK3B, CDC42, IL6, MTOR, PLCB1, and IL1B were the highest populated genes across the predicted canonical signaling pathways. According to the overlap of the top-ranked canonical pathways, neuroinflammation signaling was the most overlapped pathway while inflammatory mediators NFKB1, TNF, and CASP1 were the most shared molecules across the overlapped pathways. Neurological diseases were predicted to be the top pathological conditions associated with α-synuclein. A MAP analysis of the principal interaction network of SNCA revealed a direct relationship between SNCA and APP, suggesting that collusion between SNCA and APP likely produces neurotoxic effects. Besides, IPA predicted IL1B, APP, TNF, MIF, Mek, ERK, PTGS2, TP53, M38 MAPK, and CCL2 as the top upstream regulators of SNCA. The appearance of APP, a series of inflammatory mediators, and MAPK kinases as the upstream regulators indicate that the upstream SNCA regulators contribute to synucleinopathy. On the whole, IPA expression analysis of α-synuclein and associated genes reveals that α-synuclein is a key conspirator in protein aggregopathy and neuroinflammation, where the abnormal expression of α-synuclein activates cerebral amyloid peptide APP, a battery of cytokines, like NFKB1, TNF, IL1B, etc., and MAPK family kinases, like Mek, ERK, and P38 MAPK. Besides, our study provides an important piece of information for wet-lab researchers interested in further exploring signaling, molecular interaction networks, and biological functions of α-synuclein.

Data availability statement

The datasets presented in this study can be found in online repositories. The names of the repository/repositories and accession number(s) can be found in the article/Supplementary material.

Author contributions

SS conceived the idea, performed the analysis, and wrote and reviewed the manuscript. S-YL conceived the idea, provided suggestions, and reviewed the manuscript. All authors contributed to the article and approved the submitted version.

Funding

This work was supported by a Brain Pool research grant no. 2021H1D3A2A02044867 from the National Research Foundation (NRF) of Korea, and a research grant no. GCU-2018-0703 from the Gachon University.

Acknowledgments

The authors would like to thank Bharath Kumar Eriboina, QIAGEN, for proving the IPA trial version license.

Conflict of interest

The authors declare that the research was conducted in the absence of any commercial or financial relationships that could be construed as a potential conflict of interest.

Publisher's note

Supplementary material

The Supplementary material for this article can be found online at: https://www.frontiersin.org/articles/10.3389/fnmol.2022.1029682/full#supplementary-material

References

Alam, M. M., Yang, D., Li, X. Q., Liu, J., Back, T. C., Trivett, A., et al. (2022). Alpha synuclein, the culprit in Parkinson disease, is required for normal immune function. *Cell Rep.* 38:110090. doi: 10.1016/j.celrep.2021.110090

Anderson, J. P., Walker, D. E., Goldstein, J. M., de Laat, R., Banducci, K., Caccavello, R. J., et al. (2006). Phosphorylation of Ser-129 is the dominant pathological modification of α-synuclein in familial and sporadic Lewy body disease. *J. Biol. Chem.* 281, 29739–29752. doi: 10.1074/jbc.M600933200

Arima, K., Uéda, K., Sunohara, N., Arakawa, K., Hirai, S., Nakamura, M., et al. (1998). NACP/α-synuclein immunoreactivity in fibrillary components of neuronal

and oligodendroglial cytoplasmic inclusions in the pontine nuclei in multiple system atrophy. *Acta Neuropathol.* 96, 439–444. doi: 10.1007/s004010050917

Baba, M., Nakajo, S., Tu, P. H., Tomita, T., Nakaya, K., Lee, V. M., et al. (1998). Aggregation of α-synuclein in Lewy bodies of sporadic Parkinson's disease and dementia with Lewy bodies. *Am. J. Pathol.* 152, 879–884.

Burré, J., Sharma, M., and Südhof, T. C. (2014). α-Synuclein assembles into higher-order multimers upon membrane binding to promote SNARE complex formation. *Proc. Natl. Acad. Sci. U. S. A.* 111, E4274–E4283. doi: 10.1073/pnas.1416598111

Burré, J., Sharma, M., Tsetsenis, T., Buchman, V., Etherton, M. R., and Südhof, T. C. (2010). α-Synuclein promotes SNARE-complex assembly in vivo and in vitro. *Science* 329, 1663–1667. doi: 10.1126/science.1195227

Bussell, R., and Eliezer, D. (2003). A structural and functional role for 11-mer repeats in α-synuclein and other exchangeable lipid binding proteins. *J. Mol. Biol.* 329, 763–778. doi: 10.1016/s0022-2836(03)00520-5

Bussell, R., Ramlall, T. F., and Eliezer, D. (2005). Helix periodicity, topology, and dynamics of membrane-associated α-synuclein. *Protein Sci.* 14, 862–872. doi: 10.1110/ps.041255905

Caccamo, A., Majumder, S., Richardson, A., Strong, R., and Oddo, S. (2010). Molecular interplay between mammalian target of rapamycin (mTOR), amyloid-β, and tau. *J. Biol. Chem.* 285, 13107–13120. doi: 10.1074/jbc.M110.100420

Chandra, S., Gallardo, G., Fernández-Chacón, R., Schlüter, O. M., and Südhof, T. C. (2005). α-Synuclein cooperates with CSPα in preventing neurodegeneration. *Cells* 123, 383–396. doi: 10.1016/j.cell.2005.09.028

Conway, K. A., Harper, J. D., and Lansbury, P. T. (2000). Fibrils formed in vitro from α-synuclein and two mutant forms linked to Parkinson's disease are typical amyloid. *Biochemistry* 39, 2552–2563. doi: 10.1021/bi991447r

Credle, J. J., George, J. L., Wills, J., Duka, V., Shah, K., Lee, Y. C., et al. (2015). GSK-3β dysregulation contributes to Parkinson's-like pathophysiology with associated region-specific phosphorylation and accumulation of tau and α-synuclein. *Cell Death Differ.* 22, 838–851. doi: 10.1038/cdd.2014.179

Davidson, W. S., Jonas, A., Clayton, D. F., and George, J. M. (1998). Stabilization of α-synuclein secondary structure upon binding to synthetic membranes. *J. Biol. Chem.* 273, 9443–9449. doi: 10.1074/jbc.273.16.9443

de Oliveira, R. M., Miranda, H. V., Francelle, L., Pinho, R., Szegö, É. M., Martinho, R., et al. (2017). The mechanism of sirtuin 2-mediated exacerbation of α-synuclein toxicity in models of Parkinson disease. *PLoS Biol.* 15:e2000374. doi: 10.1371/journal.pbio.2000374

Filippini, A., Mutti, V., Faustini, G., Longhena, F., Ramazzina, I., Rizzi, F., et al. (2021). Extracellular clusterin limits the uptake of α-synuclein fibrils by murine and human astrocytes. *Glia* 69, 681–696. doi: 10.1002/glia.23920

Fujiwara, H., Hasegawa, M., Dohmae, N., Kawashima, A., Masliah, E., Goldberg, M. S., et al. (2002). α-Synuclein is phosphorylated in synucleinopathy lesions. *Nat. Cell Biol.* 4, 160–164. doi: 10.1038/ncb748

Giasson, B. I., Murray, I. V., Trojanowski, J. Q., and Lee, V. M. (2001). A hydrophobic stretch of 12 amino acid residues in the middle of α-synuclein is essential for filament assembly. *J. Biol. Chem.* 276, 2380–2386. doi: 10.1074/jbc.M008919200

Helferich, A. M., Ruf, W. P., Grozdanov, V., Freischmidt, A., Feiler, M. S., Zondler, L., et al. (2015). α-Synuclein interacts with SOD1 and promotes its oligomerization. *Mol. Neurodegener.* 10:66. doi: 10.1186/s13024-015-0062-3

IPA (2021). Ingenuity Pathway Analysis (IPA), Qiagen. Available at: https://digitalinsights.qiagen.com/products-overview/discovery-insights-portfolio/analysis-and-visualization/qiagen-ipa/ [Accessed August 26, 2021 & September 26, 2022].

Irizarry, M. C., Growdon, W., Gomez-Isla, T., Newell, K., George, J. M., Clayton, D. F., et al. (1998). Nigral and cortical Lewy bodies and dystrophic nigral neurites in Parkinson's disease and cortical Lewy body disease contain α-synuclein immunoreactivity. *J. Neuropathol. Exp. Neurol.* 57, 334–337. doi: 10.1097/00005072-199804000-00005

Lashuel, H. A., Overk, C. R., Oueslati, A., and Masliah, E. (2013). The many faces of α-synuclein: from structure and toxicity to therapeutic target. *Nat. Rev. Neurosci.* 14, 38–48. doi: 10.1038/nrn3406

Na, H., Gan, Q., Mcparland, L., Yang, J. B., Yao, H., Tian, H., et al. (2020). Characterization of the effects of calcitonin gene-related peptide receptor antagonist for Alzheimer's disease. *Neuropharmacology* 168:108017. doi: 10.1016/j.neuropharm.2020.108017

Nakajo, S., Tsukada, K., Omata, K., Nakamura, Y., and Nakaya, K. (1993). A new brain-specific 14-kDa protein is a phosphoprotein. Its complete amino acid sequence and evidence for phosphorylation. *Eur. J. Biochem.* 217, 1057–1063. doi: 10.1111/j.1432-1033.1993.tb18337.x

NCBI (2021). National Center for Biotechnology (NCBI). Available at: https://www.ncbi.nlm.nih.gov/gene/?term=Alpha-synuclein [Accessed August 26, 2021].

NCBI (2022). National Center for Biotechnology (NCBI). Available at: https://www.ncbi.nlm.nih.gov/gene [Accessed September 26, 2022].

Oliveira, L. M. A., Gasser, T., Edwards, R., Zweckstetter, M., Melki, R., Stefanis, L., et al. (2021). Alpha-synuclein research: defining strategic moves in the battle against Parkinson's disease. *NPJ Parkinsons Dis.* 7:65. doi: 10.1038/s41531-021-00203-9

Outeiro, T. F., Kontopoulos, E., Altmann, S. M., Kufareva, I., Strathearn, K. E., Amore, A. M., et al. (2007). Sirtuin 2 inhibitors rescue α-synuclein-mediated toxicity in models of Parkinson's disease. *Science* 317, 516–519. doi: 10.1126/science.1143780

Pérez-Revuelta, B. I., Hettich, M. M., Ciociaro, A., Rotermund, C., Kahle, P. J., Krauss, S., et al. (2014). Metformin lowers Ser-129 phosphorylated α-synuclein levels via mTOR-dependent protein phosphatase 2A activation. *Cell Death Dis.* 5:e1209. doi: 10.1038/cddis.2014.175

Roberts, H. L., Schneider, B. L., and Brown, D. R. (2017). α-Synuclein increases β-amyloid secretion by promoting β−/γ-secretase processing of APP. *PLoS One* 12:e0171925. doi: 10.1371/journal.pone.0171925

Samidurai, M., Palanisamy, B. N., Bargues-Carot, A., Hepker, M., Kondru, N., Manne, S., et al. (2021). PKC delta activation promotes endoplasmic reticulum stress (ERS) and NLR family pyrin domain-containing 3 (NLRP3) inflammasome activation subsequent to asynuclein-induced microglial activation: involvement of thioredoxin-interacting protein (TXNIP)/thioredoxin (Trx) redoxisome pathway. *Front. Aging Neurosci.* 13:661505. doi: 10.3389/fnagi.2021.661505

Schnack, C., Danzer, K. M., Hengerer, B., and Gillardon, F. (2008). Protein array analysis of oligomerization-induced changes in alpha-synuclein protein-protein interactions points to an interference with Cdc42 effector proteins. *Neuroscience* 154, 1450–1457. doi: 10.1016/j.neuroscience.2008.02.049

Serpell, L. C., Berriman, J., Jakes, R., Goedert, M., and Crowther, R. A. (2000). Fiber diffraction of synthetic α-synuclein filaments shows amyloid-like cross-β conformation. *Proc. Natl. Acad. Sci. U. S. A.* 97, 4897–4902. doi: 10.1073/pnas.97.9.4897

Shimura, H., Schlossmacher, M. G., Hattori, N., Frosch, M. P., Trockenbacher, A., Schneider, R., et al. (2001). Ubiquitination of a new form of α-synuclein by parkin from human brain: implications for Parkinson's disease. *Science* 293, 263–269. doi: 10.1126/science.1060627

Spillantini, M. G., Crowther, R. A., Jakes, R., Cairns, N. J., Lantos, P. L., and Goedert, M. (1998). Filamentous α-synuclein inclusions link multiple system atrophy with Parkinson's disease and dementia with Lewy bodies. *Neurosci. Lett.* 251, 205–208. doi: 10.1016/s0304-3940(98)00504-7

Spillantini, M. G., Schmidt, M. L., Lee, V. M., Trojanowski, J. Q., Jakes, R., and Goedert, M. (1997). α-Synuclein in Lewy bodies. *Nature* 388, 839–840. doi: 10.1038/42166

Suthar, S. K., Alam, M. M., Lee, J., Monga, J., Joseph, A., and Lee, S. Y. (2021). Bioinformatic analyses of canonical pathways of TSPOAP1 and its roles in human diseases. *Front. Mol. Biosci.* 8:667947. doi: 10.3389/fmolb.2021.667947

Takeda, A., Mallory, M., Sundsmo, M., Honer, W., Hansen, L., and Masliah, E. (1998). Abnormal accumulation of NACP/α-synuclein in neurodegenerative disorders. *Am. J. Pathol.* 152, 367–372.

Tofaris, G. K., Kim, H. T., Hourez, R., Jung, J. W., Kim, K. P., and Goldberg, A. L. (2011). Ubiquitin ligase Nedd4 promotes α-synuclein degradation by the endosomal-lysosomal pathway. *Proc. Natl. Acad. Sci. U. S. A.* 108, 17004–17009. doi: 10.1073/pnas.1109356108

Trojanowski, J. Q., and Lee, V. M. (1998). Aggregation of neurofilament and α-synuclein proteins in Lewy bodies: implications for the pathogenesis of Parkinson disease and Lewy body dementia. *Arch. Neurol.* 55, 151–152. doi: 10.1001/archneur.55.2.151

Tu, P. H., Galvin, J. E., Baba, M., Giasson, B., Tomita, T., Leight, S., et al. (1998). Glial cytoplasmic inclusions in white matter oligodendrocytes of multiple system atrophy brains contain insoluble α-synuclein. *Ann. Neurol.* 44, 415–422. doi: 10.1002/ana.410440324

Tuttle, M. D., Comellas, G., Nieuwkoop, A. J., Covell, D. J., Berthold, D. A., Kloepper, K. D., et al. (2016). Solid-state NMR structure of a pathogenic fibril of full-length human α-synuclein. *Nat. Struct. Mol. Biol.* 23, 409–415. doi: 10.1038/nsmb.3194

Uéda, K., Fukushima, H., Masliah, E., Xia, Y., Iwai, A., Yoshimoto, M., et al. (1993). Molecular cloning of cDNA encoding an unrecognized component of amyloid in Alzheimer disease. *Proc. Natl. Acad. Sci. U. S. A.* 90, 11282–11286. doi: 10.1073/pnas.90.23.11282

Vamvaca, K., Volles, M. J., and Lansbury, P. T. (2009). The first N-terminal amino acids of α-synuclein are essential for α-helical structure formation in vitro and membrane binding in yeast. *J. Mol. Biol.* 389, 413–424. doi: 10.1016/j.jmb.2009.03.021

Wakabayashi, K., Hayashi, S., Kakita, A., Yamada, M., Toyoshima, Y., Yoshimoto, M., et al. (1998). Accumulation of α-synuclein/NACP is a cytopathological feature common to Lewy body disease and multiple system atrophy. *Acta Neuropathol.* 96, 445–452. doi: 10.1007/s004010050918

Wakabayashi, K., Matsumoto, K., Takayama, K., Yoshimoto, M., and Takahashi, H. (1997). NACP, a presynaptic protein, immunoreactivity in Lewy bodies in Parkinson's disease. *Neurosci. Lett.* 239, 45–48. doi: 10.1016/s0304-3940(97)00891-4

Waxman, E. A., and Giasson, B. I. (2009). Molecular mechanisms of α-synuclein neurodegeneration. *Biochim. Biophys. Acta* 1792, 616–624. doi: 10.1016/j.bbadis.2008.09.013

Weinreb, P. H., Zhen, W., Poon, A. W., Conway, K. A., and Lansbury, P. T. (1996). NACP, a protein implicated in Alzheimer's disease and learning, is natively unfolded. *Biochemistry* 35, 13709–13715. doi: 10.1021/bi961799n

Zarbiv, Y., Simhi-Haham, D., Israeli, E., Elhadi, S. A., Grigoletto, J., and Sharon, R. (2014). Lysine residues at the first and second KTKEGV repeats mediate α-synuclein binding to membrane phospholipids. *Neurobiol. Dis.* 70, 90–98. doi: 10.1016/j.nbd.2014.05.031

frontiers | Frontiers in Molecular Neuroscience

TYPE Original Research
PUBLISHED 15 March 2023
DOI 10.3389/fnmol.2023.1048985

OPEN ACCESS

EDITED BY
Muddanna Sakkattu Rao,
Kuwait University,
Kuwait

REVIEWED BY
Manikandan Samidurai,
SENS Research Foundation,
United States
Bharathi Hattiangady,
Texas A&M University College of Medicine,
United States

*CORRESPONDENCE
Shupeng Li
✉ lisp@pku.edu.cn
Tao Li
✉ Litao050428@mail.xjtu.edu.cn

SPECIALTY SECTION
This article was submitted to
Brain Disease Mechanisms,
a section of the journal
Frontiers in Molecular Neuroscience

RECEIVED 20 September 2022
ACCEPTED 07 February 2023
PUBLISHED 15 March 2023

CITATION
Li A, Liu Z, Ali T, Gao R, Luo Y, Gong Q, Zheng C, Li W, Guo H, Liu X, Li S and Li T (2023) Roxadustat (FG-4592) abated lipopolysaccharides-induced depressive-like symptoms *via* PI3K signaling.
Front. Mol. Neurosci. 16:1048985.
doi: 10.3389/fnmol.2023.1048985

Roxadustat (FG-4592) abated lipopolysaccharides-induced depressive-like symptoms *via* PI3K signaling

Axiang Li[1,2,3], Zizhen Liu[3], Tahir Ali[3,4], Ruyan Gao[3], Yanhua Luo[3], Qichao Gong[3], Chenyou Zheng[3], Weifen Li[3], Hongling Guo[3], Xinshe Liu[1,2,5], Shupeng Li[3,4,6]* and Tao Li[1,2,5]*

[1]College of Forensic Medicine, Xi'an Jiaotong University Health Science Center, Xi'an, Shaanxi, China, [2]Institute of Forensic Injury, Institute of Forensic Bio-Evidence, Western China Science and Technology Innovation Harbor, Xi'an Jiaotong University, Xi'an, Shaanxi, China, [3]State Key Laboratory of Oncogenomics, School of Chemical Biology and Biotechnology, Peking University Shenzhen Graduate School, Shenzhen, China, [4]Shenzhen Bay Laboratory, Institute of Chemical Biology, Shenzhen, China, [5]NHC Key Laboratory of Forensic Science, College of Forensic Medicine, Xi'an Jiaotong University, Xi'an, Shaanxi, China, [6]Department of Psychiatry, University of Toronto, Toronto, ON, Canada

Background: Despite its role in inflammation and the redox system under hypoxia, the effects and molecular mechanisms of hypoxia-inducible factor (HIF) in neuroinflammation-associated depression are poorly explored. Furthermore, Prolyl hydroxylase domain-containing proteins (PHDs) regulate HIF-1; however, whether and how PHDs regulate depressive-like behaviors under Lipopolysaccharides (LPS)-induced stress conditions remain covered.

Methods: To highlight the roles and underlying mechanisms of PHDs-HIF-1 in depression, we employed behavioral, pharmacological, and biochemical analyses using the LPS-induced depression model.

Results: Lipopolysaccharides treatment induced depressive-like behaviors, as we found, increased immobility and decreased sucrose preference in the mice. Concurrently, we examined increased cytokine levels, HIF-1 expression, mRNA levels of PHD1/PHD2, and neuroinflammation upon LPS administration, which Roxadustat reduced. Furthermore, the PI3K inhibitor wortmannin reversed Roxadustat-induced changes. Additionally, Roxadustat treatment attenuated LPS-induced synaptic impairment and improved spine numbers, ameliorated by wortmannin.

Conclusion: Lipopolysaccharides-dysregulates HIF-PHDs signaling may contribute to neuroinflammation-coincides depression *via* PI3K signaling.

KEYWORDS

lipopolysaccharides, depression, Neuroinflammation, HIF-PHD/PI3K, roxadustat (FG-4592)

Introduction

Major depression disorder (MDD) is a global concern with increasing prevalence, expected to be a single leading cause among all disease burdens by 2030. Clinically, MMD is characterized by a lack of energy, persistent low mood, despairs, sleep disorders, and in severe cases, suicidal behaviors (Athira et al., 2020; Gutiérrez-Rojas et al., 2020; Abdoli

et al., 2022). Unfortunately, due to its complexity and heterogeneity as determined by genetic and environmental factors, the molecular mechanisms of MDD are enigmatic (Athira et al., 2020). The current hypothesis of depression focuses on the hypothalamus-pituitary–adrenal (HPA) axis, neuroplasticity, and monoamine neurotransmitter depletion (Brigitta, 2002; Hasler, 2010). However, the delayed effect of available antidepressants and lack of focus on cells other than neurons demonstrate the limitation of these specific pathological mechanisms (Andrade and Rao, 2010; Malhi et al., 2020). Thus， around one-third of MDD patients do not respond well to the existing treatments that demand the revitalization of psychiatric therapeutics with novel intervention options that engage non-monoaminergic molecular targets. In recent years, the inflammatory hypothesis has been proposed for depressive symptoms (Madeeh Hashmi et al., 2013; Gałecki and Talarowska, 2018) as an activated immune system has been founded in MMD patients (Cassano et al., 2017; Zou et al., 2018), which opened new avenues for depression investigation. We reported previously that lipopolysaccharides (LPS) could induce neuroinflammation and depressive-like behavior in mice. Besides, it modulated inflammatory signaling molecules, including NLRP3, NF-κB, p-p38, etc., accompanied by depressive symptoms such as immobility, decreased sucrose preferences in the mice, and synaptic defects (Ali et al., 2020b; Li et al., 2021b).

Mechanistically, LPS administration dysregulates PI3K/Akt/NF-kB signaling, which may lead to neuroinflammation. Concurrently, the altered neuroinflammatory response can coincide with synaptic defect *via* different signaling, including HDAC1 and Sirt3/HO-1 signaling (Li et al., 2019; Zhao et al., 2019; Ali et al., 2020a; Jamali-Raeufy et al., 2021; Li et al., 2021b). Similarly, LPS can initiate the transcription factor HIF-1 signaling, which may be mediated through the NF-kB signaling (Frede et al., 2006; Palladino et al., 2018), as NF-kB has a binding site on the promoter of the HIF-1 gene as a transcription factor (van Uden et al., 2008). However, it has also been reported that hypoxia-activated HIF-1 is synergistic with LPS in macrophages (Mi et al., 2008). Similarly, PI3K signaling could contribute to the translation of HIF-1 *via* mTOR (Xu et al., 2020), while its role in neuroinflammation and synaptic defects is not highlighted yet.

Roxadustat (FG-4592) is the reversible inhibitor of hypoxia-inducible factor prolyl hydroxylase (PHDs), a hypoxia-inducible factor (HIF-1) stabilizer, orally available and approved by the FDA. Initially, this drug was approved for treating anemia, including in China. FG-4592 showed considerable protection against other hypoxia-related disorders, including cancer, fibrosis, and chronic inflammation. Besides, in the sepsis animal model, Roxadustat-treatment significantly reduced the cytokines, including IL-1β, IL-6, and TNF-α (Akizawa et al., 2019; Liu et al., 2021; Zhu et al., 2022). Furthermore, prolyl hydroxylases (PHDs) regulate HIF-1 under different conditions (Appelhoff et al., 2004), whose underlying mechanisms have not been explored in LPS-induced stress conditions. Similarly, the HIF-1 anti-inflammatory consensus has not been currently elucidated (Zhu et al., 2022). Therefore, we aimed to determine whether LPS-altered HIF-1 signaling can affect depressive symptoms coinciding with neuroinflammation and synaptic defects. Surprisingly, our data showed that LPS lead to HIF-1 signaling impairment, neuroinflammation, synaptic defects, spine number modification, and depressive symptom, which PI3K-signaling could alter.

Materials and methods

Animals

C57BL/6J male mice (6–8 weeks) were obtained from the Guangdong Medical Laboratory Animal Centre, China. The experimental animals were housed at the Laboratory Animal Research Centre, Peking University Shenzhen Graduate School, under a 12 h light/12 h dark cycle at 18–22°C, *ad libitum* access to food and water throughout the study. The experimental procedures were set in such a way as to minimize mice suffering. The Animal Care and Use Committee of the Experimental Animal Center at Peking University, Shenzhen Graduate School, approved the animal experiments.

Lipopolysaccharides-induced depression is associated with inflammation (Ali et al., 2020a), and FG-4592 has shown anti-inflammatory action by reducing cytokine levels in the animal model (Akizawa et al., 2019; Liu et al., 2021; Zhu et al., 2022). Besides, the HIF-1 anti-inflammatory mechanism is largely unknown. Therefore, this was one reason for HIF-1 stabilizer selection for the LPS-induced neuroinflammation-coinciding depression. The rationale for the FG-4592 treatment for the depression model is unavailable; thus, we initially checked the dose-dependent action of the FG-4592 while performing OFT and SPT tests (Supplementary Figure S1A).

We performed the present study in two experiments. In the first experiment, animals were assigned to three groups (each group = 6–10): saline-treated group (Saline), LPS-treated group (1.5 mg/kg/day), Roxadustat: FG-4592 (Roxa; 5 mg/kg/day) plus LPS group (Roxa+LPS). LPS (0.1 ml/10 g mice) and Roxadustat (0.1 ml/10 g mice, were intraperitoneally administered to the mice. Besides, Roxadustat was treated 1 h before LPS administration. The drug treatment schedule is shown in Figure 1A. After 24 h of the final LPS administration, behavioral tests were performed. Finally, the mice were sacrificed, and tissues were collected and quickly stored at-80°C until further use. Notably, LPS (Sigma-Aldrich, #L2880) was dissolved with sterile water directly to its working concentration. Roxadustat was dissolved in 5% dimethyl-sulfoxide (DMSO) and was administrated 2 h before the behavior test.

In the second experiment, animals were again divided into three groups (8–15 mice/group): LPS group, Roxa+LPS group, and Roxa+LPS + Wort group (Wortmannin,1 mg/kg). Wortmannin (wort) was administered intraperitoneally for 2 days, before 2 h behavior tests (Figure 1C). Wortmannin was dissolved in 5% DMSO. The behavior and organ/tissues collection process were the same as above.

Open field test

Open field test (OFT) was performed according to previous protocols (Ali et al., 2020b). Briefly, mice were adapted to the experimental room for 1 h and then placed in a 45 × 45 × 30 cm chamber. Each mouse was started in the center of the chamber and was allowed to move freely for 5 min. The total distance traveled was recorded and analyzed using Smart v3.0 software.

10.3389/fnmol.2023.1048985

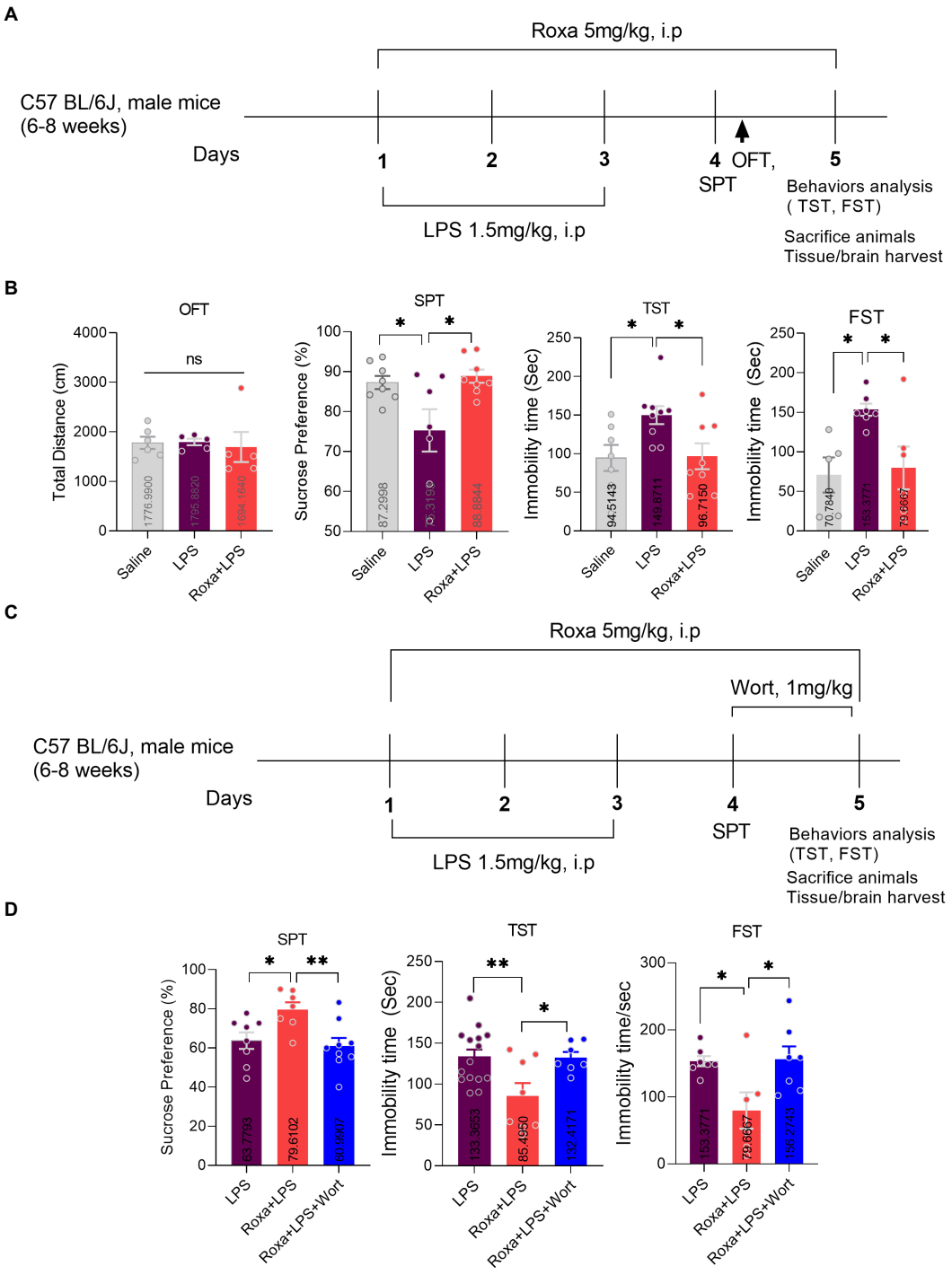

FIGURE 1
Roxadustat treatment reduced LPS-induced depressive-like behaviors *via* PI3K signaling. **(A)** Drugs treatment schedule, **(B)** open field test (OFT), forced swimming test (FST), and a sucrose preference test (SPT). **(C)** Drugs treatment schedule, **(D)** Sucrose preference Test (SPT), and tail suspension Test (TST). All the values are expressed as mean±SEM: ANOVA followed by *post hoc* analysis. p=<0.05 were considered significant *p<0.05, **p<0.01. ns: non-significant.

Sucrose preference test

A sucrose preference test was performed using a two-bottle free-choice paradigm (Liu et al., 2018). Initially, the mice were habituated for 48 h hrs with two drinking bottles (one containing 1% sucrose and the other water) in their home cage. Next, on the third day of the drug administration, the mice were deprived of water and food for 24 h. The next day, each mouse had free access to two bottles of either 1% sucrose solution or standard drinking water. The positions of the bottles were switched halfway through testing to prevent the possible effects of side preference on drinking behavior. Percentage preference for sucrose was calculated at the end of the test using the following

formula: Sucrose Preference = Sucrose consumption/ (Sucrose consumption + Water consumption) × 100%.

Tail suspension test

The tail suspension test was performed as described previously (Li et al., 2022). Mice were suspended by the tails to a rod about 45 cm above the floor by placing adhesive tape 1 cm from the tail tip. By the commonly accepted criteria, immobility was defined as the absence of movement of the animals' heads and bodies. The immobility time was recorded for 6 min in a dark room. Etho Vision XT software was used for TST recording and analysis.

Forced swimming test

The forced swimming test (FST) was performed as described previously. Animals were forced to swim in a Plexiglas cylinder (height: 70 cm, diameter: 30 cm) filled with water (23 ± 1°C) to a height of 30 cm. The video was recorded for 6 min, and the immobility time was analyzed during the last 5 min of the test. Mice were immobile when they remained motionless or only made movements necessary to keep their heads above the water's surface.

ELISA

According to the manufacturer's protocols, cytokines expression was quantified using ELISA kits (Elabscience). Briefly, a 100 μL standard or sample was added to the wells and incubated for 90 min at 37°C. The plates were then washed, and a Biotinylated Detection Ab working solution was added to each well. The plates were incubated for 1 h at 37°C. Next, 100ul HRP conjugate working solution was added for 30 min at 37°C. Finally, the reaction was stopped, and the optical density was measured.

Immunofluorescence

Immunofluorescence staining was performed according to described previously (Li et al., 2022). Briefly, mice were perfusion-fixed with 4% paraformaldehyde and soaked in PFA for 48 h, then brian was replaced with sucrose, and 30um brain tissue sections were prepared. Sections were washed with PBS for 15 min (5 min × 3). After washing, the sections were blocked with blocking buffer (10% normal goat serum in 0.3% Triton X-100 in PBS) for 1 h at room temperature and then incubated with primary antibodies overnight at 4°C, Rabbit anti-Iba1 (1: 1000, Wako,#019–19,741); Mouse anti-GFAP (1,1,000, Sigma-Aldrich, #MAB360). The next day, sections were incubated with secondary antibodies (Alexa Flour secondary antibodies, Thermo Fisher) at room temperature for 1 h; the hoechst was applied in the last 10 min. The sections were washed with PBS for 15 min (5 min × 3). After washing, sections were transferred onto glass slides, and glass coverslips were mounted using a mounting medium. Images were captured using a confocal microscope and were analyzed by ImageJ software.

Golgi staining

Golgi staining was performed according to Sami Zaqout's protocols (Li et al., 2021a). Impregnation step: the mice brain sample was kept in Golgi-Cox solution at room temperature in the dark; after 24 h, the sample was transferred into a new Golgi solution-containing bottle with the help of a histological cassette and kept settling at room temperature in the dark for 7–10 days. Tissue protection step: the brain sample is transferred from the Golgi-Cox impregnation solution to a new bottle with the tissue-protectant solution and kept at 4°C in the dark. After 24 h, the tissue-protectant solution is replaced by a new solution in a new bottle for 4–7 days. Sectioning step: the brain sample is embedded in 4% low melting point agarose. 150–200 um sections were prepared using a sliding microtome and mounted to gelatin-coated microscope slides. Then, the brain tissue was placed in a staining solution for 10 min and rinsed with double distilled water, followed by dehydration (sequential rinse 50,75, and 95% ethanol) and xylene treatment finally, examined under an inverted fluorescence microscope IX73 Olympus.

Real-time quantitative RT-PCR

Total RNA was isolated from the hippocampus with Trizol (Invitrogen, Germany) and reversed to cDNA using the Reverse Transcription System (Promega). Primers ordered with the following sequences: HIF-1, 5′-GAAACGACCACTGCTAAGGCA-3′(forward) and 5′-GGCAGACAGCTTAAGGCTCCT-3′(reverse); prolyl hydroxylase (PHD)1, 5′-GGCCAGTGGTAGCCAACATC-3′(forward) and 5′-GTGGCATAGGCTGGCTTCAC-3′(reverse); PHD2, 5′- TGACCACACCTCTCCAGCAA-3′ (forward) and 5′-CTGCCAACAATGCCAAACAG-3′ (reverse); and PHD3, 5′-GGTGGCTTGCTATCCAGGAA-3′(forward) and 5′-ATACAG CGGCCATCACCATT-3′(reverse).

Western blotting

Western blotting was also performed according to the standard protocol. Briefly, the protein sample was denatured by boiling at 95°C for 5 min and separated *via* SDS-PAGE. The separated protein was then transferred onto a nitrocellulose membrane. The membrane was blocked with non-fat milk in TBST (Tris-buffered saline, 0.1% Tween 20) and then incubated with primary antibody (1:1000) (Table 1) overnight at 4°C. The next day, the membranes were incubated with a secondary antibody (1:10000) for 1 h at room temperature. For detection, the ECL Super signal chemiluminescence kit was used according to the manufacturer's protocol. Blots were developed using ChemiDoc MP BIO-RAD. Densitometric analysis of the bands was performed using the Image Lab software. The stripping buffer was purchased from Thermo Scientific (LOT: WE32238 Scientific) blot stripping. Briefly, blots were washed with TBST 3 times. Immerse blot in stripping buffer, followed by incubating for 15-30 min at room temperature. Finally, removed the stripping buffer by washing it with TBST three times, followed by re-blocking the membrane for 1 h.

TABLE 1 List of antibodies.

Antibody	Company	Lot number	Dilute	Source
P-P38 (Thr180/Tyr182)	Cell signaling technology	4,511	1/1,00	Rabbit
P38	Cell signaling technology	9,212	1/1,000	Rabbit
P-PI3K (Tyr458)	Cell signaling technology	4,228	1/1,000	Rabbit
PI3K	Cell signaling technology	4,257	1/1,000	Rabbit
P-AKT (Ser473)	Cell signaling technology	4,060	1/1,000	Rabbit
AKT	Cell signaling technology	4,691	1/1,000	Rabbit
P-GSK3β(Ser9)	Cell signaling technology	5,558	1/1,000	Rabbit
GSK3β	Cell signaling technology	12,456	1/1,000	Rabbit
P-AMPKα(Thr172)	Cell signaling technology	2,535	1/1,000	Rabbit
AMPKα	Cell signaling technology	5,832	1/1,000	Rabbit
P-EEF2 (Thr56)	Cell signaling technology	2,331	1/1,000	Rabbit
EEF2	Abcam	Ab33523	1/1,000	Rabbit
Iba1	Cell signaling technology	17,198	1/1,000	Rabbit
GFAP	Cell signaling technology	3,670	1/1,000	Mouse
NLRP3	Cell signaling technology	15,101	1/1,000	Rabbit
Nrf2	Cell signaling technology	12,721	1/1,000	Rabbit
HO-1	Cell signaling technology	70,081	1/1,000	Rabbit
SOD2	Cell signaling technology	13,194	1/1,000	Rabbit
PSD95	Abcam	Ab18258	1/1,000	Rabbit
SNAP25	Cell signaling technology	5,308	1/1,000	Rabbit
SYNAPSIN1	Abcam	Ab254349	1/1,000	Rabbit
GAPDH	Cell signaling technology	5,174	1/1,000	Rabbit
β-Actin	Santa Cruz biotechnology	Sc-47,778	1/500	Mouse
HIF-1α	Cell signaling technology	14,179	1/1,000	Rabbit
PHD1	ABclonal	A3730	1/1,000	Rabbit
PHD2	ABclonal	A14557	1/1,000	Rabbit
PHD3	ABclonal	A0851	1/1,000	Rabbit

Statistical analysis

All the statistical analyses were performed using the GraphPad Prism 8 software. Data are presented as mean ± SEM. One-way analysis of variance (ANOVA) followed by *post hoc* Tukey/Bonferroni Multiple Comparison tests was performed to compare different groups. $p < 0.05$ was regarded as statistically significant.

Results

Roxadustat (FG-4592) reversed lipopolysaccharides-induced depressive symptoms

Lipopolysaccharides is a well-known inflammatory agent that can induce depressive-like behaviors in mice (Ali et al., 2020a). Similarly, our LPS-treated mice displayed depressive symptoms, as demonstrated by increased immobility during TST and FST, while decreased sucrose preference for 1% sucrose solution over normal water. However, Roxadustat (FG-4592) treatment significantly attenuated these LPS-induced depressive-like behaviors (Figures 1A,B).

PI3K Signaling mediated the effects of Roxadustat

Previous studies evidenced LPS-altered PI3K signaling (Saponaro et al., 2012; Zheng et al., 2018). However, its association with HIF-1 is enigmatic. Herein, we treated mice with wortmannin to determine the interplay among LPS, HIF-1, and PI3K signaling in depression. Surprisingly, PI3K antagonism significantly reversed Roxadustat anti-depressive effects in the presence of LPS, as it found that increased mice immobility decreased sucrose preference (Figures 1C,D). These findings suggested the involvement of HIF-1 and PI3K signaling in LPS-induced depressive symptoms. Moreover, we found an increase in HIF-1 expression, PHD1,2

10.3389/fnmol.2023.1048985

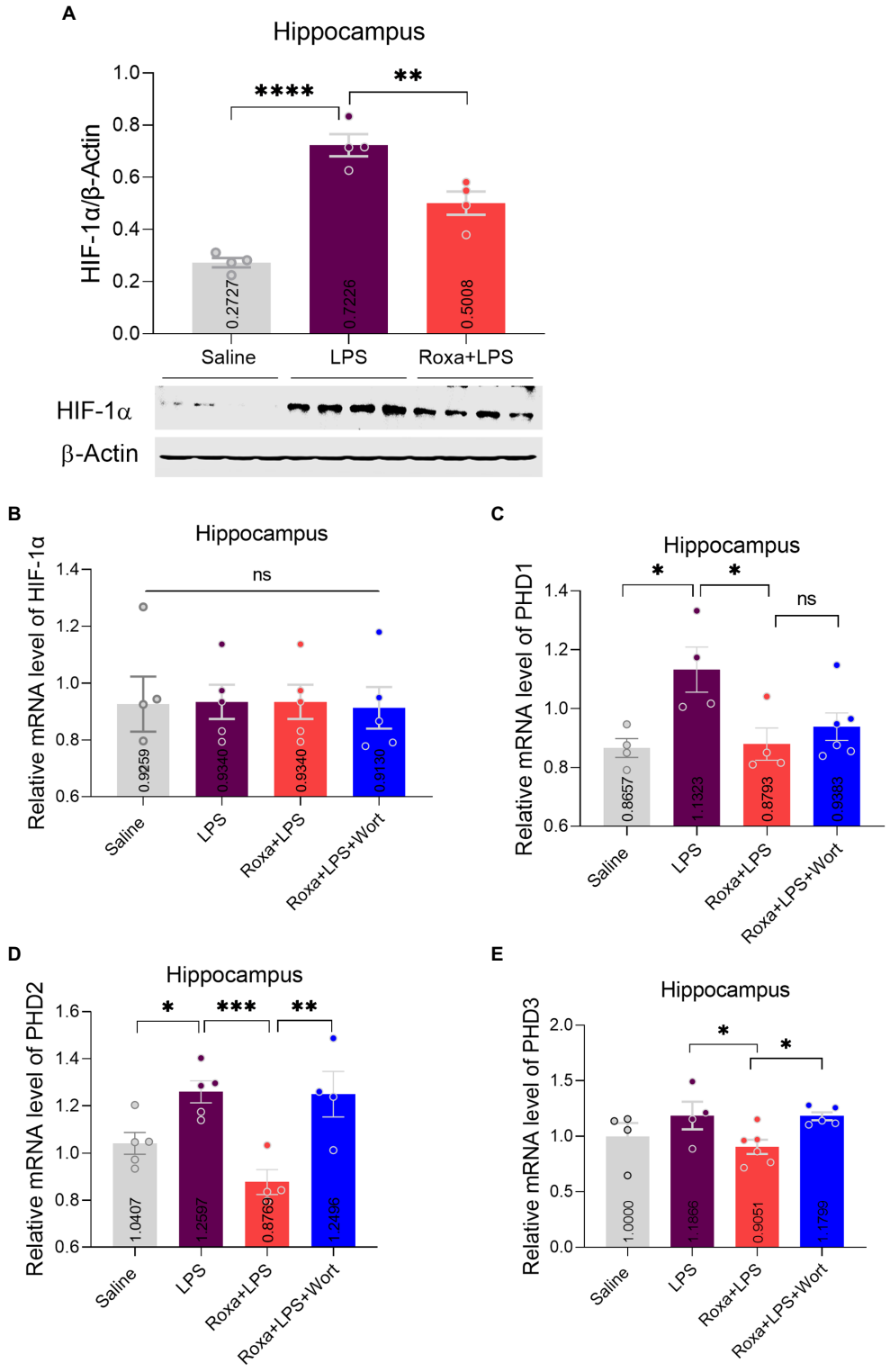

FIGURE 2
Roxadustat effects on HIF-1a and PHDs expression. **(A)** Representative immune blot images and average protein levels of HIF-1 levels were normalized with β-Actin. **(B–E)** Showing mRNA levels of HIF-1, PHD1, PHD2, and PHD3. Image lab software was used for quantitative blot analysis and was analyzed *via* GraphPad prism. Data were expressed as mean±SEM, One-way ANOVA, followed by *post hoc* analysis. p=<0.05 were considered significant. *p<0.05, **p<0.01, ***p<0.001, ****p<0.0001. ns: non-significant.

(mRNA), and PI3K phosphorylation upon LPS administration, which was reduced by Roxadustat treatment (Figure 2; Supplementary Figures S1B,C). As the PI3K-Akt signaling could be activated by LPS stimulus (Hemmings and Restuccia, 2012), we examined Akt and its downstream signaling changes in the hippocampus of LPS-treated mice. Notably, LPS administration

significantly enhanced Akt/GSK3β phosphorylation which was reduced by Roxadustat treatment.

Contrarily, Roxadustat treatment significantly increased AMPKα phosphorylation in the presence of LPS (Figure 3A), indicating a link between HIF-1 and AMPK singling under LPS-induced stress conditions. As reported, AMPK is involved in the Akt signaling activation (Han et al., 2018); its link to PI3K is largely unknown, particularly in LPS-initiated stress conditions. Thus, we examined AMPKα/Akt/GSK3b signaling changes upon PI3K antagonism in the presence of LPS. Except for Akt, wortmannin treatment significantly attenuated Roxadustat-induced p-AMPKα, GSK3b, and p-p38 expressional changes in the mice hippocampal tissues in the presence of LPS (Figure 3B). These findings indicated the interplay among AMPK/PI3K and HIF-1 signaling under LPS-induced stress conditions.

Roxadustat treatment attenuated lipopolysaccharides-induced neuroinflammation

Lipopolysaccharides-induced neuroinflammation played an integral role of depressive symptoms in mice (Li et al., 2017, 2021a). Here, we sought to determine whether LPS-induced neuroinflammation is linked to HIF-1 signaling. Our results indicated that Roxadustat significantly reduced IBA-1 and GFAP expression in the hippocampus (DG region) of the LPS-treated mice (Figures 4A,B). Similarly, Roxadustat treatment decreased cytokines, including IL-1b, IL-6, and TNF-a levels in the hippocampal tissue of the brain (Figure 4D). However, the anti-inflammatory effects of Roxadustat could be attenuated by wortmannin treatment (Figures 4A,C,D), suggesting PI3K signaling was involved in HIF-1 modulation of LPS-induced neuroinflammation. The cellular signaling changes associated with neuroinflammation were examined to validate these results further. Surprisingly, Roxadustat treatment significantly reduced LPS-elevated expression of NLRP3 in mice brains (Figure 5A), which could be increased by wortmannin (Figure 5B). As LPS-induced inflammation accompanies oxidative stress, we thus measured the expressions of anti-oxidative markers, including Nrf2, SOD2, and HO-1. However, no significant changes in NRF2, SOD2, and HO-1 Roxadustat and Wortmannin treatment could be defined (Figures 5A,B).

HIF-1-PHD antagonism by Roxadustat attenuated lipopolysaccharides-induced synaptic defects

Previous studies, including ours, showed that LPS administration could induce synaptic defects, which may underly the pathological processes of depression symptoms (Postnikova et al., 2020; Li et al., 2021a). Our results revealed dysregulated synaptic factors and reduced spins in hippocampal tissues (Figure 6C). Besides, the eEF2 phosphorylation level, which regulates synaptic plasticity, was also increased in LPS-treated mice but reversed by Roxadustat treatment (Figure 6A; Verpelli et al., 2010). Moreover, wortmannin attenuated the effects of Roxadustat and enhanced synaptic proteins, including PSD95, SNAP25, and Synapsin-1 (Figure 6B). These findings suggest that Roxadustat could alleviate dysregulated synaptic proteins induced by LPS *via* HIF-1/PI3K signaling.

Discussion

Results from our previous studies and other groups have documented the interplay between neuroinflammation and depressive-like behaviors (Li et al., 2017; Postnikova et al., 2020; Ali et al., 2020b; Li et al., 2021b), but its mechanistic link to HIF-1/PI3K signaling remains poorly explored. Here, we determined that LPS administration dysregulated HIF-1 *via* the PI3K pathway in the mice hippocampus, which underlined LPS elicited neuroinflammation and depressive-like behaviors. HIF-1-PHD inhibitor (Roxadustat) treatment attenuated LPS-mediated changes, which could be reversed by wortmannin, suggesting an etiological role of HIF-1 in neuroinflammation-associated depressive-like behaviors. However, conventional antidepressants show their effects slowly and may take about 2–3 weeks (Szegedi et al., 2009), immediate/quick antidepressant effects of several compounds/drugs (including Roxadustat treated here for 3 days) have also been documented in the LPS-induced model of depression (O'Connor et al., 2009; Cordeiro et al., 2019; Zhang et al., 2019).

As a transcriptional factor, HIF-1 controls the immune cell metabolism and function. Additionally, it plays a crucial role in regulating inflammatory functions in dendritic, mast, and epithelial cells (Imtiyaz and Simon, 2010). Besides, TNF-α and IL-1β can activate and increase HIF-1 expression/transcriptional *via* NF-kB (Jung et al., 2003; Zhou et al., 2003), indicating that HIF-1 could play an essential role in inflammation. Furthermore, it has also been reported that LPS can stimulate HIF-1 activities *via* several pathways, including NF-kB, ROS, and p42/p44 mitogen-activated protein kinases (MAPKs; Frede et al., 2006). In addition, in macrophages, LPS accumulates HIF-1 *via* decreasing PHD2 and PHD3 levels in a Toll-like receptor-4 (TLR-4) dependent manner (Peyssonnaux et al., 2007; Imtiyaz and Simon, 2010). This evidence supports our findings that LPS-induced neuroinflammation was reduced in the hippocampus of mice after Roxadustat treatment. However, it was more interesting to be identified here that PI3K inhibition reversed the effects of Roxadustat, indicating a link between HIF-1 and PI3K signaling in the presence of LPS. Previous studies have also demonstrated that PI3K/Akt signaling could regulate HIF-1 levels *via* mTOR signaling at the posttranslational level but not at the mRNA level (under hypoxic conditions; Zhang et al., 2018). Because PI3K inhibitor (LY294002) and Dual PI3K/mTOR inhibitor NVP-BEZ235 treatment suppressed Akt and HIF-1 activation and expression (Karar et al., 2012), respectively. These results indicated that the PI3K-Akt cascade is a highly conserved intracellular signaling pathway involved in the immune system's growth, motility, survival, metabolism, and coordinating defense mechanisms by transducing extracellular stimuli (Hemmings and Restuccia, 2012).

Studies demonstrate the beneficial effects of intermittent hypoxia on neurological disorders, including depression, by promoting neurogenesis *via* BDNF signaling (Ferrari et al., 2017; Meng et al., 2020); however, the mechanisms are not fully explored

10.3389/fnmol.2023.1048985

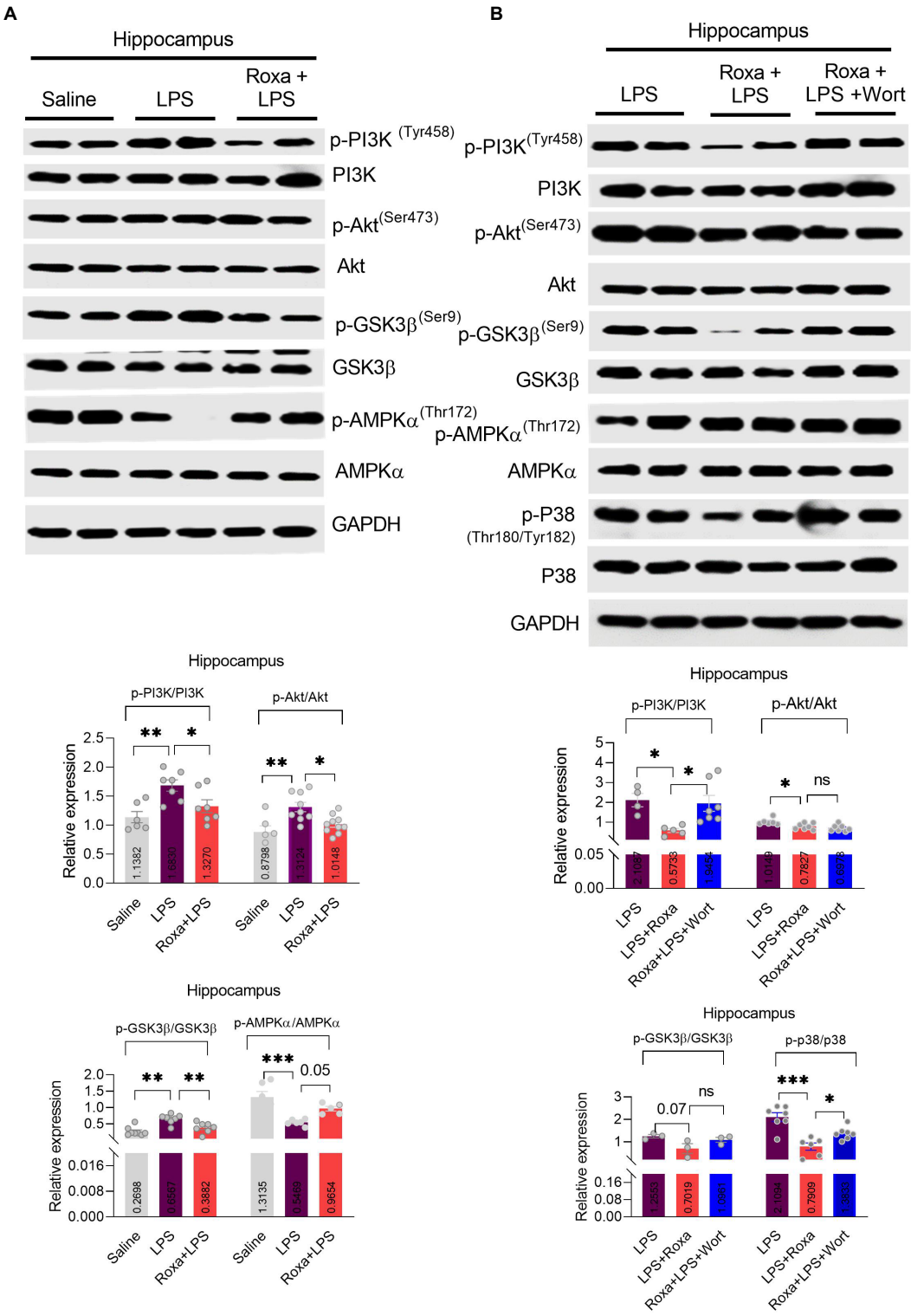

FIGURE 3
Roxadustat reduced LPS-induced PI3K and its associated signaling. **(A,B)** representative western blots of PI3K, Akt, GSK3β, APMKα, and P38 and quantitative column graphs for mice treated with LPS, Roxadustat and wortmannin. All the values were normalized with GAPDH. Image lab software was used for blots quantitative analysis and was analyzed *via* GraphPad prism. Data were expressed as mean±SEM, One-way ANOVA, followed by *post hoc* analysis. p=<0.05 were considered significant. *p<0.05, **p<0.01), ***p<0.001. ns: non-significant.

10.3389/fnmol.2023.1048985

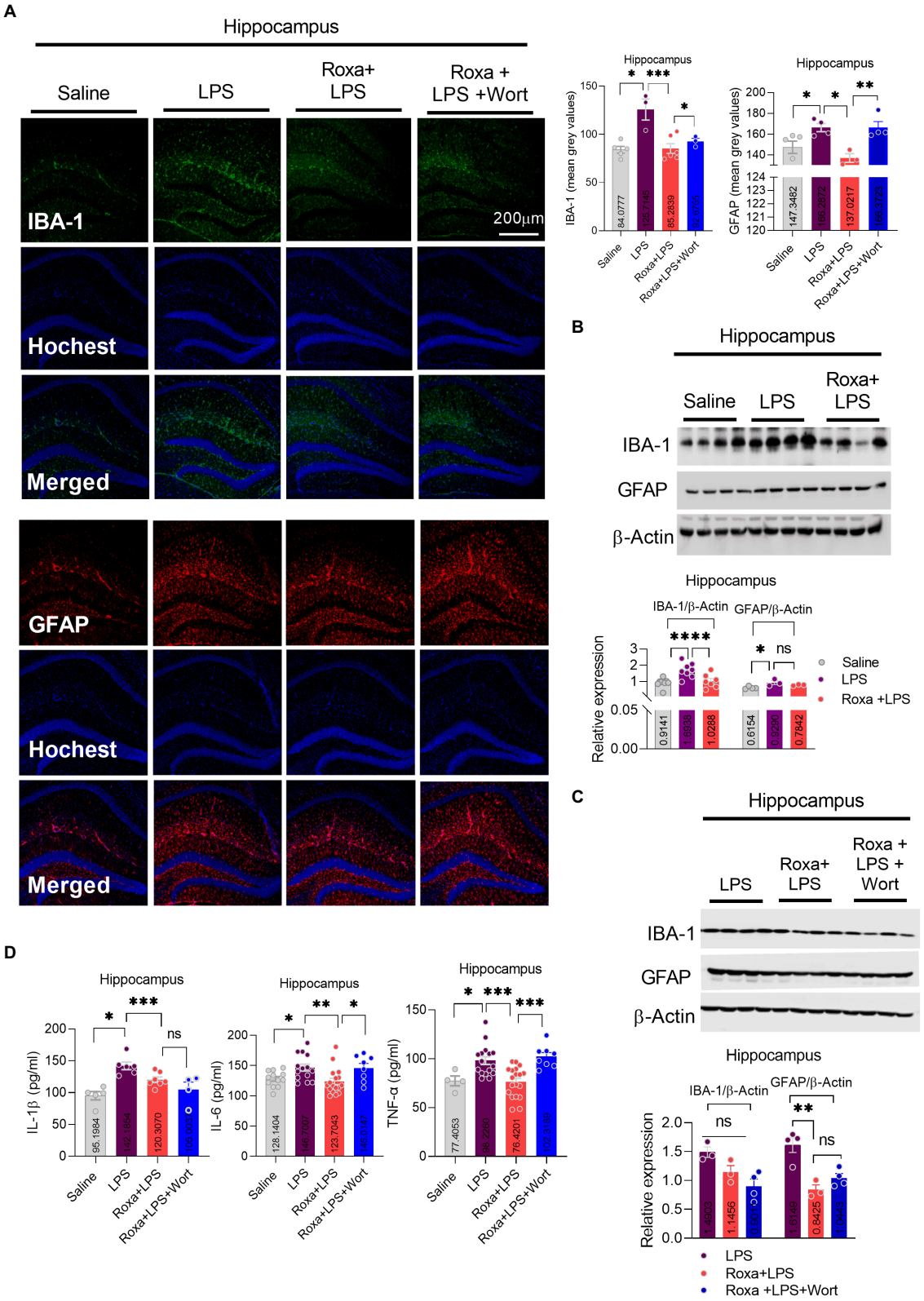

FIGURE 4
Roxadustat reduced LPS-induced neuroinflammation. **(A)** Microscopy results of Iba-1 expression in the different experimental groups of brain tissues, with respective bar graphs (n=6). Magnification 10x. The image data were collected from three independent experiments and were analyzed by ImageJ software. The differences are shown in the graphs. **(B,C)** Representative immune blots with individual level column graphs showing Iba-1 and GFAP expression n=3–6. All the values were normalized with β-Actin. **(D)** Bar graphs showing the expression level of IL-1β, IL-6, and TNF-α. Data were expressed as mean±SEM, One-way ANOVA, followed by *post hoc* analysis. p=<0.05 were considered significant. *p<0.05, **p<0.01, ***p<0.001, ****p<0.0001. ns: non-significant.

10.3389/fnmol.2023.1048985

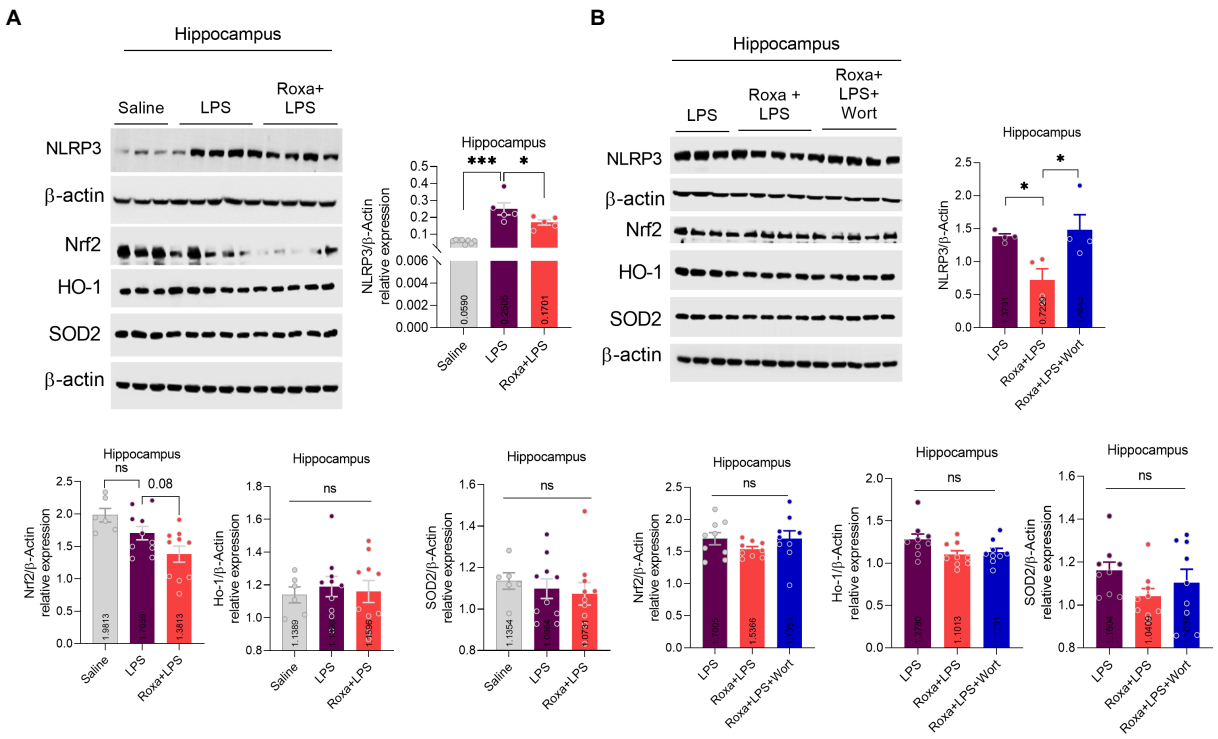

FIGURE 5
Roxadustat reduced NLRP3 level in the presence of LPS. **(A,B)** Representative immune blots images and bar graphs show the expression of NLRP3, Nrf2, HO-1, and SOD2. All the values were normalized with β-Actin. Image lab software was used for blots quantitative analysis and was analyzed *via* GraphPad prism. Data were expressed as mean±SEM, One-way ANOVA, followed by *post hoc* analysis. p=<0.05 were considered significant, *p<0.05, ***p<0.001. ns: non-significant.

as for the potential beneficial effects through the HIF-1 hypoxia responding factor. Our results showed that Roxadustat treatment rescued LPS-altered synaptic protein level and spin-altered morphology. Interestingly, similar neuroprotective roles of Roxadustat have been recently reported, while its link to LPS/PI3K signaling has not been explored. Our results further demonstrated that PI3K signalling-antagonism reversed the protective effects of Roxadustat, indicating that HIF-1/PI3K signaling mediated the LPS-induced neuroinflammation, synaptic deficits, and depressive symptoms.

In conclusion, HIF-1 contributed to inflammation and the redox system under hypoxia conditions; it also played a role in neuroinflammation-induced depression, which might be associated with PI3K-related signalings. Furthermore, Roxadustat showed potent anti-depressive effects *via* reducing neuroinflammation by stabilizing HIF-1 expression; however, the proper LPS-stimulated signaling cross-talk to HIF-1 under depression conditions is enigmatic, which is the limitation of the present study, and it needs further investigation.

Data availability statement

The original contributions presented in the study are included in the article/Supplementary material, further inquiries can be directed to the corresponding authors.

Ethics statement

The animal study was reviewed and approved by Institutional Animal Care and Use Committee of Peking University, Shenzhen Graduate School.

Author contributions

AL, TA, and SL: conceptualization. AL, ZL, RG, YL, QG, and HG: methodology. AL, ZL, CZ, WL, XL, and TL: investigation, analysis and funding support. TA and SL: writing. SL and TL: supervision. All authors reviewed and approved the manuscript.

Funding

This work was supported by the National Natural Science Foundation of CHINA (NSFC grant numbers: 82072112 and 81871530).

Acknowledgments

We thank Hong Kong Institute of Brain Science, Shenzhen and Shenzhen Fundamental Research Institutions, Shenzhen, China.

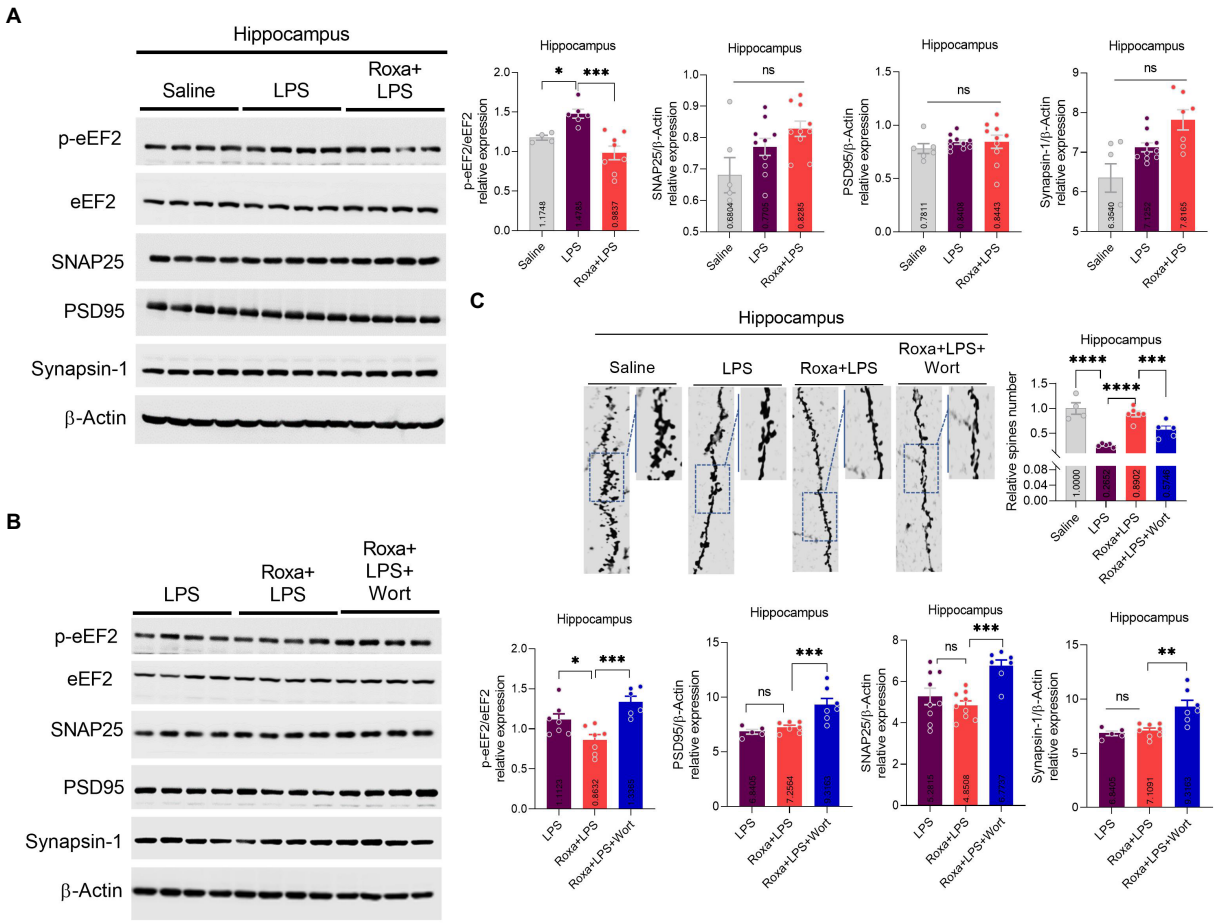

FIGURE 6
Changes in the expression of eEF2, SNAP25, PSD95, and Synapsin-1, and spine numbers after Roxa and LSP treatment. **(A,B)** Representative immune blots show the expression of p-eEF2, eEF2, SNAP25, PSD95, and Synapsin-1 levels in the hippocampus of subjects. All the values were normalized with β-Actin. **(C)** Golgi staining showing spine density and column graph showing spine numbers n=3–5. Image lab software was used for blots quantitative analysis and was analyzed *via* GraphPad prism. Data were expressed as mean±SEM, One-way ANOVA, followed by *post hoc* analysis. p=<0.05 were considered significant. *p<0.05, **p<0.01), ***p<0.001, ****p<0.0001. ns: non-significant.

Conflict of interest

The authors declare that the research was conducted in the absence of any commercial or financial relationships that could be construed as a potential conflict of interest.

Publisher's note

All claims expressed in this article are solely those of the authors and do not necessarily represent those of their affiliated organizations, or those of the publisher, the editors and the reviewers. Any product that may be evaluated in this article, or claim that may be made by its manufacturer, is not guaranteed or endorsed by the publisher.

Supplementary material

The Supplementary material for this article can be found online at: https://www.frontiersin.org/articles/10.3389/fnmol.2023.1048985/full#supplementary-material

References

Abdoli, N., Salari, N., Darvishi, N., Jafarpour, S., Solaymani, M., Mohammadi, M., et al. (2022). The global prevalence of major depressive disorder (MDD) among the elderly: a systematic review and meta-analysis. *Neurosci. Biobehav. Rev.* 132, 1067–1073. doi: 10.1016/j.neubiorev.2021.10.041

Akizawa, T., Iwasaki, M., Otsuka, T., Reusch, M., and Misumi, T. (2019). Roxadustat treatment of chronic kidney disease-associated anemia in Japanese patients not on dialysis: a phase 2, randomized, double-blind, placebo-controlled trial. *Adv. Ther.* 36, 1438–1454. doi: 10.1007/s12325-019-00943-4

Ali, T., Hao, Q., Ullah, N., Rahman, S. U., Shah, F. A., He, K., et al. (2020a). Melatonin act as an antidepressant via attenuation of Neuroinflammation by targeting Sirt1/Nrf2/HO-1 signaling. *Front. Mol. Neurosci.* 13:96. doi: 10.3389/fnmol.2020.00096

Ali, T., Rahman, S. U., Hao, Q., Li, W., Liu, Z., Ali Shah, F., et al. (2020b). Melatonin prevents neuroinflammation and relieves depression by attenuating autophagy impairment through FOXO3a regulation. *J. Pineal Res.* 69:e12667. doi: 10.1111/jpi.12667

Andrade, C., and Rao, N. S. (2010). How antidepressant drugs act: a primer on neuroplasticity as the eventual mediator of antidepressant efficacy. *Indian J. Psychiatry* 52, 378–386. doi: 10.4103/0019-5545.74318

Appelhoff, R. J., Tian, Y.-M., Raval, R. R., Turley, H., Harris, A. L., Pugh, C. W., et al. (2004). Differential function of the prolyl hydroxylases PHD1, PHD2, and PHD3 in the

regulation of hypoxia-inducible factor*. *J. Biol. Chem.* 279, 38458–38465. doi: 10.1074/jbc.M406026200

Athira, K. V., Bandopadhyay, S., Samudrala, P. K., Naidu, V. G. M., Lahkar, M., and Chakravarty, S. (2020). An overview of the heterogeneity of major depressive disorder: current knowledge and future prospective. *Curr. Neuropharmacol.* 18, 168–187. doi: 10.2174/1570159X17666191001142934

Brigitta, B. (2002). Pathophysiology of depression and mechanisms of treatment. *Dialogues Clin. Neurosci.* 4, 7–20. doi: 10.31887/DCNS.2002.4.1/bbondy

Cassano, P., Bui, E., Rogers, A. H., Walton, Z. E., Ross, R., Zeng, M., et al. (2017). Inflammatory cytokines in major depressive disorder: a case-control study. *Aust. N. Z. J. Psychiatry* 51, 23–31. doi: 10.1177/0004867416652736

Cordeiro, R. C., Chaves Filho, A. J. M., Gomes, N. S., Tomaz, V. D. S., Medeiros, C. D., Queiroz, A. I. D. G., et al. (2019). Leptin prevents lipopolysaccharide-induced depressive-like behaviors in mice: involvement of dopamine receptors. *Front. Psych.* 10:125. doi: 10.3389/fpsyt.2019.00125

Ferrari, M., Jain, I. H., Goldberger, O., Rezoagli, E., Thoonen, R., Cheng, K. H., et al. (2017). Hypoxia treatment reverses neurodegenerative disease in a mouse model of Leigh syndrome. *Proc. Natl. Acad. Sci. U. S. A.* 114, E4241–E4250. doi: 10.1073/pnas.1621511114

Frede, S., Stockmann, C., Freitag, P., and Fandrey, J. (2006). Bacterial lipopolysaccharide induces HIF-1 activation in human monocytes via p44/42 MAPK and NF-kappaB. *Biochem. J.* 396, 517–527. doi: 10.1042/BJ20051839

Gałecki, P., and Talarowska, M. (2018). Inflammatory theory of depression. *Psychiatr. Pol.* 52, 437–447. doi: 10.12740/PP/76863

Gutiérrez-Rojas, L., Porras-Segovia, A., Dunne, H., Andrade-González, N., and Cervilla, J. A. (2020). Prevalence and correlates of major depressive disorder: a systematic review. *Braz. J Psychiatry* 42, 657–672. doi: 10.1590/1516-4446-2020-0650

Han, F., Li, C.-F., Cai, Z., Zhang, X., Jin, G., Zhang, W.-N., et al. (2018). The critical role of AMPK in driving Akt activation under stress, tumorigenesis and drug resistance. *Nat. Commun.* 9:4728. doi: 10.1038/s41467-018-07188-9

Hasler, G. (2010). Pathophysiology of depression: do we have any solid evidence of interest to clinicians? *World Psychiatry* 9, 155–161. doi: 10.1002/j.2051-5545.2010.tb00298.x

Hemmings, B. A., and Restuccia, D. F. (2012). PI3K-PKB/Akt pathway. *Cold Spring Harb. Perspect. Biol.* 4:a011189. doi: 10.1101/cshperspect.a011189

Imtiyaz, H. Z., and Simon, M. C. (2010). Hypoxia-inducible factors as essential regulators of inflammation. *Curr. Top. Microbiol. Immunol.* 345, 105–120. doi: 10.1007/82_2010_74

Jamali-Raeufy, N., Alizadeh, F., Mehrabi, Z., Mehrabi, S., and Goudarzi, M. (2021). Acetyl-L-carnitine confers neuroprotection against lipopolysaccharide (LPS) -induced neuroinflammation by targeting TLR4/NFκB, autophagy, inflammation and oxidative stress. *Metab. Brain Dis.* 36, 1391–1401. doi: 10.1007/s11011-021-00715-6

Jung, Y. J., Isaacs, J. S., Lee, S., Trepel, J., and Neckers, L. (2003). IL-1beta-mediated up-regulation of HIF-1alpha via an NFkappaB/COX-2 pathway identifies HIF-1 as a critical link between inflammation and oncogenesis. *FASEB J.* 17, 2115–2117. doi: 10.1096/fj.03-0329fje

Karar, J., Cerniglia, G. J., Lindsten, T., Koumenis, C., and Maity, A. (2012). Dual PI3K/mTOR inhibitor NVP-BEZ235 suppresses hypoxia-inducible factor (HIF)-1α expression by blocking protein translation and increases cell death under hypoxia. *Cancer Biol. Ther.* 13, 1102–1111. doi: 10.4161/cbt.21144

Li, W., Ali, T., He, K., Liu, Z., Shah, F. A., Ren, Q., et al. (2021a). Ibrutinib alleviates LPS-induced neuroinflammation and synaptic defects in a mouse model of depression. *Brain Behav. Immun.* 92, 10–24. doi: 10.1016/j.bbi.2020.11.008

Li, W., Ali, T., Zheng, C., He, K., Liu, Z., Shah, F. A., et al. (2022). Anti-depressive-like behaviors of APN KO mice involve Trkb/BDNF signaling related neuroinflammatory changes. *Mol. Psychiatry* 27, 1047–1058. doi: 10.1038/s41380-021-01327-3

Li, W., Ali, T., Zheng, C., Liu, Z., He, K., Shah, F. A., et al. (2021b). Fluoxetine regulates eEF2 activity (phosphorylation) via HDAC1 inhibitory mechanism in an LPS-induced mouse model of depression. *J. Neuroinflammation* 18:38. doi: 10.1186/s12974-021-02091-5

Li, M., Li, C., Yu, H., Cai, X., Shen, X., Sun, X., et al. (2017). Lentivirus-mediated interleukin-1β (IL-1β) knock-down in the hippocampus alleviates lipopolysaccharide (LPS)-induced memory deficits and anxiety-and depression-like behaviors in mice. *J. Neuroinflammation* 14:190. doi: 10.1186/s12974-017-0964-9

Li, C., Zhao, B., Lin, C., Gong, Z., and An, X. (2019). TREM2 inhibits inflammatory responses in mouse microglia by suppressing the PI3K/NF-κB signaling. *Cell Biol. Int.* 43, 360–372. doi: 10.1002/cbin.10975

Liu, F., Wang, J., Ye, Q., Fu, H., and Mao, J. (2021). Roxadustat for renal anemia in ESRD from PKD patients: is it safe enough? *J. Am. Soc. Nephrol.* 32:1005. doi: 10.1681/ASN.2020111664

Liu, M. Y., Yin, C. Y., Zhu, L. J., Zhu, X. H., Xu, C., Luo, C. X., et al. (2018). Sucrose preference test for measurement of stress-induced anhedonia in mice. *Nat. Protoc.* 13, 1686–1698. doi: 10.1038/s41596-018-0011-z

Madeeh Hashmi, A., Awais Aftab, M., Mazhar, N., Umair, M., and Butt, Z. (2013). The fiery landscape of depression: a review of the inflammatory hypothesis. *Pak. J. Med. Sci.* 29, 877–884. doi: 10.12669/pjms.293.3357

Malhi, G. S., Bell, E., Morris, G., and Hamilton, A. (2020). The delay in response to antidepressant therapy: a window of opportunity? *Aust. N. Z. J. Psychiatry* 54, 127–129. doi: 10.1177/0004867419900313

Meng, S. X., Wang, B., and Li, W. T. (2020). Intermittent hypoxia improves cognition and reduces anxiety-related behavior in APP/PS1 mice. *Brain Behav.* 10:e01513. doi: 10.1002/brb3.1513

Mi, Z., Rapisarda, A., Taylor, L., Brooks, A., Creighton-Gutteridge, M., Melillo, G., et al. (2008). Synergystic induction of HIF-1alpha transcriptional activity by hypoxia and lipopolysaccharide in macrophages. *Cell Cycle* 7, 232–241. doi: 10.4161/cc.7.2.5193

O'connor, J. C., Lawson, M. A., André, C., Moreau, M., Lestage, J., Castanon, N., et al. (2009). Lipopolysaccharide-induced depressive-like behavior is mediated by indoleamine 2,3-dioxygenase activation in mice. *Mol. Psychiatry* 14, 511–522. doi: 10.1038/sj.mp.4002148

Palladino, M. A., Fasano, G. A., Patel, D., Dugan, C., and London, M. (2018). Effects of lipopolysaccharide-induced inflammation on hypoxia and inflammatory gene expression pathways of the rat testis. *Basic Clin. Androl.* 28:14. doi: 10.1186/s12610-018-0079-x

Peyssonnaux, C., Cejudo-Martin, P., Doedens, A., Zinkernagel, A. S., Johnson, R. S., and Nizet, V. (2007). Cutting edge: essential role of hypoxia inducible factor-1alpha in development of lipopolysaccharide-induced sepsis. *J. Immunol.* 178, 7516–7519. doi: 10.4049/jimmunol.178.12.7516

Postnikova, T. Y., Griflyuk, A. V., Ergina, J. L., Zubareva, O. E., and Zaitsev, A. V. (2020). Administration of Bacterial Lipopolysaccharide during early postnatal ontogenesis induces transient impairment of Long-term synaptic plasticity associated with behavioral abnormalities in young rats. *Pharmaceuticals* 13:48. doi: 10.3390/ph13030048

Saponaro, C., Cianciulli, A., Calvello, R., Dragone, T., Iacobazzi, F., and Panaro, M. A. (2012). The PI3K/Akt pathway is required for LPS activation of microglial cells. *Immunopharmacol. Immunotoxicol.* 34, 858–865. doi: 10.3109/08923973.2012.665461

Szegedi, A., Jansen, W. T., Van Willigenburg, A. P., Van Der Meulen, E., Stassen, H. H., and Thase, M. E. (2009). Early improvement in the first 2 weeks as a predictor of treatment outcome in patients with major depressive disorder: a meta-analysis including 6562 patients. *J. Clin. Psychiatry* 70, 344–353. doi: 10.4088/JCP.07m03780

Van Uden, P., Kenneth, N. S., and Rocha, S. (2008). Regulation of hypoxia-inducible factor-1alpha by NF-kappaB. *Biochem. J.* 412, 477–484. doi: 10.1042/BJ20080476

Verpelli, C., Piccoli, G., Zibetti, C., Zanchi, A., Gardoni, F., Huang, K., et al. (2010). Synaptic activity controls dendritic spine morphology by modulating eEF2-dependent BDNF synthesis. *J. Neurosci.* 30, 5830–5842. doi: 10.1523/JNEUROSCI.0119-10.2010

Xu, F., Na, L., Li, Y., and Chen, L. (2020). Roles of the PI3K/AKT/mTOR signalling pathways in neurodegenerative diseases and tumours. *Cell Biosci.* 10:54. doi: 10.1186/s13578-020-00416-0

Zhang, B., Wang, P. P., Hu, K. L., Li, L. N., Yu, X., Lu, Y., et al. (2019). Antidepressant-like effect and mechanism of action of Honokiol on the mouse lipopolysaccharide (LPS) depression model. *Molecules* 24:2035. doi: 10.3390/molecules24112035

Zhang, Z., Yao, L., Yang, J., Wang, Z., and Du, G. (2018). PI3K/Akt and HIF-1 signaling pathway in hypoxia-ischemia (review). *Mol. Med. Rep.* 18, 3547–3554. doi: 10.3892/mmr.2018.9375

Zhao, J., Bi, W., Xiao, S., Lan, X., Cheng, X., Zhang, J., et al. (2019). Neuroinflammation induced by lipopolysaccharide causes cognitive impairment in mice. *Sci. Rep.* 9:5790. doi: 10.1038/s41598-019-42286-8

Zheng, X., Zhang, W., and Hu, X. (2018). Different concentrations of lipopolysaccharide regulate barrier function through the PI3K/Akt signalling pathway in human pulmonary microvascular endothelial cells. *Sci. Rep.* 8:9963. doi: 10.1038/s41598-018-28089-3

Zhou, J., Schmid, T., and Brüne, B. (2003). Tumor necrosis factor-alpha causes accumulation of a ubiquitinated form of hypoxia inducible factor-1alpha through a nuclear factor-kappaB-dependent pathway. *Mol. Biol. Cell* 14, 2216–2225. doi: 10.1091/mbc.e02-09-0598

Zhu, X., Jiang, L., Wei, X., Long, M., and Du, Y. (2022). Roxadustat: not just for anemia. *Front. Pharmacol.* 13:971795. doi: 10.3389/fphar.2022.971795

Zou, W., Feng, R., and Yang, Y. (2018). Changes in the serum levels of inflammatory cytokines in antidepressant drug-naïve patients with major depression. *PLoS One* 13:e0197267. doi: 10.1371/journal.pone.0197267

frontiers | Frontiers in Molecular Neuroscience

TYPE Original Research
PUBLISHED 23 March 2023
DOI 10.3389/fnmol.2023.1133106

OPEN ACCESS

EDITED BY
Ildikó Rácz,
University Hospital Bonn,
Germany

REVIEWED BY
Homira Behbahani,
Karolinska Institutet (KI),
Sweden
Peng-Fei Zheng,
Hunan Provincial People's Hospital,
China
Li Chen,
Chinese Academy of Medical Sciences and Peking Union Medical College, China
Baojin Ding,
Louisiana State University Health Shreveport, United States

*CORRESPONDENCE
Menghua Chen
✉ xyicucmh@sina.com

†These authors share first authorship

SPECIALTY SECTION
This article was submitted to Molecular Signalling and Pathways, a section of the journal Frontiers in Molecular Neuroscience

RECEIVED 28 December 2022
ACCEPTED 22 February 2023
PUBLISHED 23 March 2023

CITATION
Su X, Xie L, Li J, Tian X, Lin B and Chen M (2023) Exploring molecular signatures related to the mechanism of aging in different brain regions by integrated bioinformatics. *Front. Mol. Neurosci.* 16:1133106. doi: 10.3389/fnmol.2023.1133106

Exploring molecular signatures related to the mechanism of aging in different brain regions by integrated bioinformatics

Xie Su[1†], Lu Xie[2†], Jing Li[2], Xinyue Tian[1], Bing Lin[1] and Menghua Chen[1*]

[1]Department of Intensive Care Unit, The Second Affiliated Hospital of Guangxi Medical University, Nanning, China, [2]Department of Physiology, Pre-Clinical Science, Guangxi Medical University, Nanning, China

The mechanism of brain aging is not fully understood. Few studies have attempted to identify molecular changes using bioinformatics at the subregional level in the aging brain. This study aimed to identify the molecular signatures and key genes involved in aging, depending on the brain region. Differentially expressed genes (DEGs) associated with aging of the cerebral cortex (CX), hippocampus (HC), and cerebellum (CB) were identified based on five datasets from the Gene Expression Omnibus (GEO). The molecular signatures of aging were explored using functional and pathway analyses. Hub genes of each brain region were determined by protein–protein interaction network analysis, and commonly expressed DEGs (co-DEGs) were also found. Gene–microRNAs (miRNAs) and gene–disease interactions were constructed using online databases. The expression levels and regional specificity of the hub genes and co-DEGs were validated using animal experiments. In total, 32, 293, and 141 DEGs were identified in aging CX, HC, and CB, respectively. Enrichment analysis indicated molecular changes related to leukocyte invasion, abnormal neurotransmission, and impaired neurogenesis due to inflammation as the major signatures of the CX, HC, and CB. Itgax is a hub gene of cortical aging. Zfp51 and Zfp62 were identified as hub genes involved in hippocampal aging. Itgax and Cxcl10 were identified as hub genes involved in cerebellar aging. S100a8 was the only co-DEG in all three regions. In addition, a series of molecular changes associated with inflammation was observed in all three brain regions. Several miRNAs interact with hub genes and S100a8. The change in gene levels was further validated in an animal experiment. Only the upregulation of Zfp51 and Zfp62 was restricted to the HC. The molecular signatures of aging exhibit regional differences in the brain and seem to be closely related to neuroinflammation. Itgax, Zfp51, Zfp62, Cxcl10, and S100a8 may be key genes and potential targets for the prevention of brain aging.

KEYWORDS

brain aging, brain regions, molecular signatures, neuroinflammation, bioinformatics, hub genes

Introduction

As an inevitable physiological phenomenon, brain aging leads to cognitive declines, including memory, learning ability, attention and processing speed, and neurodegenerative diseases, such as Alzheimer's disease (AD), dementia, and Parkinson's disease. These changes contribute to poor quality of life in elderly people and place a heavy burden on society. Currently, there are no

effective interventions for delaying the progression of brain aging. One of the important reasons for this dilemma is that the mechanism of brain aging remains unclear, despite tremendous efforts in recent years.

Mechanisms of brain aging generally include mitochondrial dysfunction, impaired DNA repair, aberrant neuronal network activity, stem cell exhaustion, glial cell activation and inflammation, and dysregulated neuronal calcium homeostasis (Yankner et al., 2008; Mattson and Arumugam, 2018). These mechanisms do not usually occur in isolation during the aging process and are highly interdependent and interactive. Therefore, these are common features of aging. However, the aging mechanism may be relatively independent and distinctive in specific brain regions because these regions differ in the proportion of nerve cell subtype and cellular communication. Each region has a specific biological function (Wyss-Coray, 2016). Magnetic resonance imaging has demonstrated that different brain regions did not age at the same pace (Jang et al., 2016; Marjańska et al., 2017). Regional differences in the rate of atrophy of brain tissues during the aging process have been described (Raz et al., 2010). Several biological changes in aging also have regional differences, such as DNA repair capacity, reactive oxygen species levels, metabolome atlas, lipofuscin deposition, and microglial phenotype (Oenzil et al., 1994; Strosznajder et al., 2000; Grabert et al., 2016; Stefanatos and Sanz, 2018; Ding et al., 2021). Therefore, we hypothesize that different brain regions may have different molecular signatures of aging. Exploring the key genes depending on the brain region instead of the whole brain may identify potential key genes of brain aging that may be productively targeted.

In this context, we used a bioinformatics analysis approach to explore molecular alterations in different brain regions. Given that the cerebral cortex (CX), hippocampus (HC), and cerebellum (CB) are associated with cognitive function (Bartsch and Wulff, 2015; Liang and Carlson, 2020; Upright and Baxter, 2021), we selected five datasets that include these three brain regions from the Gene Expression Omnibus (GEO) database for analysis. Differentially expressed genes (DEGs) between young and aged CX, HC, and CB groups were obtained. The DEGs were subjected to functional and pathway analyses to determine the molecular signatures of aging and subjected to R software (RGui) and online analysis to identify the hub genes. The commonly expressed DEGs (co-DEGs) of all three regions were identified to explore the basic and common molecular changes in the aging brain. Subsequently, we constructed the gene–microRNA (miRNA) interactions to explore the potential miRNAs involved in brain aging. Finally, real-time quantitative PCR (RT-qPCR) was used to validate the expression levels and regional specificity of the hub genes and co-DEGs. Overall, this study aimed to identify the molecular signatures and potential key genes involved in brain aging depending on the brain region. This knowledge may enhance the understanding of brain aging at a molecular level.

Materials and methods

Data processing

GSE75047, GSE34378, GSE48911, GSE62385, and GSE87102 were downloaded from the GEO database,[1] a public functional genomics data repository. In GSE75047 (platform GPL10787), samples of the CX and cerebellum CB from 2-month-old and 29-month-old wild-type mice were used for further analysis. Other samples were excluded. Similarly, in GSE34378 (platform GPL14996), CX samples from 3-month-old and 18-month-old mice were selected. In GSE48911 (platform GPL1261), samples of the HC from 4.5-month-old and 20-month-old wild-type mice were selected. In GSE62385 (platform GPL1261), HC samples from 1-month-old and 12-month-old mice from the control group were selected. In GSE87102 (platform GPL7202), samples of CB from 2 to 3-month-old and 21 to 23-month-old mice were selected. We reextracted the gene expression profiles from these datasets as described earlier. In total, 26 young brains and 27 aged brains from mice in these datasets were used for further analysis (Table 1). The expression matrices of the genes were downloaded and normalized using the BiocManager package (version 3.16.0) in the R software (version 4.2.1). After normalization, Sangerbox,[2] a comprehensive and interaction-friendly clinical bioinformatics analysis platform, was used to merge the matrices of

1 http://www.ncbi.nlm.nih.gov/geo
2 http://www.sangerbox.com

TABLE 1 Samples used in datasets.

Selected samples and ages	Datasets	Strain	Sample preparation	Sequencing method	Tissue type	Sample size
GSM1941427-1941430 (2Mo), GSM1941431-1941434 (29Mo)	GSE75047	C57Bl/6	untreated	GeneChip sequencing (GPL10787)	cortex	8
GSM847849-847851 (3Mo), GSM847858-847860 (18Mo)	GSE34378	C57BL/6J	untreated	GeneChIP sequencing (GPL14996)	cortex	6
GSM1186705-1186707 (4.5Mo), GSM1186723-1186725 (20Mo)	GSE48911	C57Bl/6	untreated	GeneChIP sequencing (GPL1261)	hippocampus	6
GSM1526451-1526453 (1Mo), GSM1526448-1526450 (12Mo),	GSE62385	C57BL/6J	untreated	GeneChIP sequencing (GPL1261)	hippocampus	6
GSM1941447-1941450 (2Mo), GSM1941451-1941454 (29Mo)	GSE75047	C57Bl/6	untreated	GeneChip sequencing (GPL10787)	cerebellum	8
GSM2322323-2322327 (2-3Mo), GSM2322338-2322341 (2-3Mo), GSM2322334-2322337 (21-23Mo), GSM2322344-2322349 (21-23Mo)	GSE87102	C57Bl/6 and BALB	untreated	GeneChip sequencing (GPL7202)	cerebellum	19

these datasets depending on the brain tissue type and batch differences were removed using the ComBat method (Zhang et al., 2020).

Identification of DEGs

DEGs between young (≤4.5 months old) and aged (≥12 months old) groups of CX, HC, and CB were identified by comparing the gene expression of the aged group to that of the young group. The Limma package (version 3.46.0) was used to identify DEGs for each brain region (Ritchie et al., 2015). The Benjamini–Hochberg method was used to adjust the false discovery rate. Genes with a Log2 fold change (FC) > 1 and an adjusted *p*-value of <0.05 were identified as DEGs. DEGs of each brain region were then visualized with a volcano plot created using the ggplot2 package in R software (RGui). A heatmap of DEGs was generated using the Pheatmap package in RGui. The co-DEGs of all three brain regions were also identified by taking the intersection of each set of DEGs using an online tool[3] and were visualized with a Venn diagram.

Gene ontology and Kyoto encyclopedia of genes and genomes pathway enrichment analyses

Gene ontology (GO) and Kyoto encyclopedia of genes and genomes (KEGG) enrichment analyses were performed for each set of DEGs using the clusterProfiler package (version 4.6.0) from the Bioconductor platform (Yu et al., 2012). The results were visualized using a bubble chart generated by RGui. The items in the bubble chart of GO enrichment were divided into three categories: biological processes (BP), cellular components (CC), and molecular functions (MF). Statistical significance was set at a *p*-value of <0.05. We performed GO and KEGG enrichment analyses using Metascape,[4] a powerful online tool for gene function annotation analysis (Xu et al., 2022). The criteria for the analysis were set as follows: minimum overlap = 3, *p*-value cut-off <0.05, and minimum enrichment = 1.5. To confirm the enrichment results, GO and KEGG analyses for DEGs were also performed using the Database for Annotation, Visualization, and Integrated Discovery (DAVID)[5] online bioinformatics analytical tool for public use, with the criterion of the *p*-value <0.05 (Dennis et al., 2003).

Protein–protein interaction network construction and identification of hub genes

Protein–protein interaction (PPI) networks of each set of DEGs were established by searching using STRING (version 11.5),[6] a public data resource used for network functional enrichment analysis of known and predicted PPI (Xu et al., 2022). The minimum required interaction score for network construction was set at <0.4 for the network construction. The disconnected nodes in the network were hidden. Then, RGui and Cytoscape (version 3.8.2)[7] were used for network analysis, network visualization, and hub gene identification (Xu et al., 2022). When RGui was applied, the hub genes were determined based on the number of gene connections in the networks. We applied Cytohubba in Cytoscape software to calculate the degree of genes using the maximal clique centrality method. Only the genes with the highest (or parallel highest) number of gene connections or degrees were considered hub genes. The results are visualized using bar plots and network diagrams.

Construction of potential gene–miRNA interactions

We used four online miRNA prediction tools, including six prediction methods. The four prediction tools used were miRBD,[8] TargetScan (version 8.0),[9] miRWALK(v 3.0),[10] and DIANA (including the microT-CDS, microT v4, and TarBase v7.0).[11] We used these tools to predict the potential miRNAs that could interact with hub genes and co-DEGs (S100a8). We identified three top alternative miRNAs based on the predictive scores for at least two prediction tools for each hub gene and co-DEG. The results are presented in the form of a table.

Exploring the relationships between aged-related nervous system disease and hub genes/co-DEGs

The Comparative Toxicogenomics Database (CTD)[12] is a robust, publicly available database that provides manually curated information about chemical–gene/protein interactions and gene–disease relationships (Davis et al., 2021). We used CTD to show the relationship between hub genes/co-DEGs (S100a8) and aging-related nervous system diseases, including neurodegenerative and cerebrovascular diseases.

Animal treatment

In total, 16 young mice (3 months old) and 16 aged mice (18 months old) were used for experimental validation. C57BL/6J mice were purchased from Changsha TianQin Biotechnology Technology Corporation Ltd. (Hunan China; animal license No: SCXK (Hunan) 2019-0014). The mice were housed in the Animal Experimental Center of Guangxi Medical University. The mice were housed under environmentally controlled standard indoor conditions (12/12 h light/dark cycle; room temperature, 21°C–24°C; humidity, 50%–70%) with *ad libitum* access to water and food. Mice were anesthetized *via*

3 http://bioinformatics.psb.ugent.be/webtools/Venn/
4 https://metascape.org/gp/index.html
5 https://david.ncifcrf.gov/tools.jsp
6 https://cn.string-db.org
7 https://cytoscape.org/
8 https://mirdb.org/
9 https://www.targetscan.org
10 http://mirwalk.umm.uni-heidelberg.de/
11 http://diana.imis.athena-innovation.gr/DianaTools/
12 http://ctdbase.org/

intraperitoneal injection of pentobarbital (50 mg/kg) and sacrificed by cervical dislocation. A total of 32 samples of CX, HC, and CB were obtained after rapid decapitation of half of the young and aged mice groups. All samples were used to validate gene expressions. Among these samples, seven young and seven aged samples of CX, HC, and CB were used to identify the regional specificity for each hub gene and co-DEG (S100a8). The animal procedures were approved by the Animal Care Welfare Committee of Guangxi Medical University.

RT-qPCR

The expression level of hub genes and co-DEGs was measured by RT-qPCR. Total RNA was extracted from CX, HC, and CB using the TRIzol reagent (Thermo Fisher Scientific, United States) according to the manufacturer's instructions. The mRNA was reverse transcribed to cDNA using the Revert Aid First Strand cDNA Synthesis kit (Thermo Fisher Scientific). PowerUp SYBR Green Premix (Thermo Fisher Scientific) was used for qPCR analysis. The cycling conditions were 50°C for 2 min and 95°C for 2 min in the holding stage followed by 40 cycles of 95°C for 15 s and 60°C for 1 min in the cycling stage. Gene expression was normalized to GADPH expression. Relative changes in mRNA levels among groups were determined with the $2^{-\triangle\triangle Ct}$ method. The primer sequences are listed in Table 2.

Statistical analyses

Statistical analysis was performed using IBM SPSS Statistics 26. Results were analyzed using an unpaired *t*-test (for normally distributed samples) or a Wilcoxon rank test (for non-normally distributed samples). In the RT-qPCR experiment, more than three wells were added to each sample. Results are expressed as the mean ± SEM. Statistical significance was set at a *p*-value of <0.05.

Results

Identification of DEGs

The procedures for this study are shown in Figure 1. After normalizing the matrices and removing the batch differences, the density distributions of gene expression for each dataset were fundamentally the same. The findings indicate that the data sources were reliable and can be used for further analysis (Figure 2). We identified 32 DEGs (27 upregulated genes and 5 downregulated genes), 293 DEGs (156 upregulated genes and 137 downregulated genes), and 141 DEGs (101 upregulated genes and 40 downregulated genes) between the young and aged CX, HC, and CB groups, respectively. The expression and distribution of DEGs are shown in volcano plots and heatmaps (Figures 3, 4). Co-DEGs responsible for brain aging were also identified. After taking the intersection of the three sets of DEGs, we found 10 co-DEGs between CX and CB, three between CX and HC, and one between HC and CB. S100a8 was the only co-DEG of all three brain regions and was upregulated in the DEGs (Figure 5).

Go and KEGG enrichment analyses of DEGs

The GO and KEGG enrichment results are shown in bubble plots (Figure 6). The GO terms for cortical aging were mainly neutrophil chemotaxis, granulocyte chemotaxis, neutrophil migration, granulocyte migration in BP, glial cell projection, cornified envelope, multivesicular body in CC, integrin binding, cell adhesion molecule binding, G protein-coupled receptor binding, and monocyte C-C motif chemokine receptor (CCR) chemokine receptor binding in MF (Figure 6A). The KEGG pathways of cortical aging included tuberculosis, complement and coagulation cascades, the interleukin (IL)-17 signaling pathway, and the Toll-like receptor signaling pathway (Figure 6B). The GO terms of hippocampal aging were mainly synaptic transmission, calcium ion regulation, α-amino-3-hydroxy-5-methyl-4-isoxazolepropionic acid (AMPA) receptor activity, myeloid cell differentiation, apoptotic process in BP, secretory granule, synaptic, and postsynaptic membrane in CC, and actin binding and actin filament binding in MF (Figure 6D). KEGG pathways of hippocampal aging included apoptosis (Figure 6E). GO terms of cerebellar aging were mainly leukocyte migration, leukocyte chemotaxis, neuron development, neuron differentiation in BP, secretory granule, presynaptic membrane in CC, cytokine activity, chemoattractant activity, chemokine activity, and hormone activity in MF (Figure 6G). The KEGG pathways of cerebellar aging included a series of inflammation-related signaling pathways (Figure 6H). The main parts of the networks of the enriched terms based on Metascape are shown in Figures 6C,F,I. We also applied DAVID to validate the enrichment analysis. The results are provided in the Supplementary material. These enrichment items indicate molecular signatures of aging in different brain regions.

TABLE 2 Primers used in qPCR.

Primers	Forward (5′-3′)	Reverse (5′-3′)
Itgax	AGCAGAGCCAGAACTTCCCA	ACTGATGCTACCCGAGCCAT
Zfp51	TCTCATGCAACCAACAGCCT	ACAGTGAGGCTTGAGGAGGT
Zfp62	TGCAGACTCTCAGTGCCCAA	AGTCACAAGTGTCACCGGTCTT
Cxcl10	TGCCGTCATTTTCTGCCTCATCC	TCCCTATGGCCCTCATTCTCACTG
S100a8	TCACCATGCCCTCTACAAGAATGAC	CCATCGCAAGGAACTCCTCGAAG
GADPH	GGTTGTCTCCTGCGACTTCA	TGGTCCAGGGTTTCTTACTCC

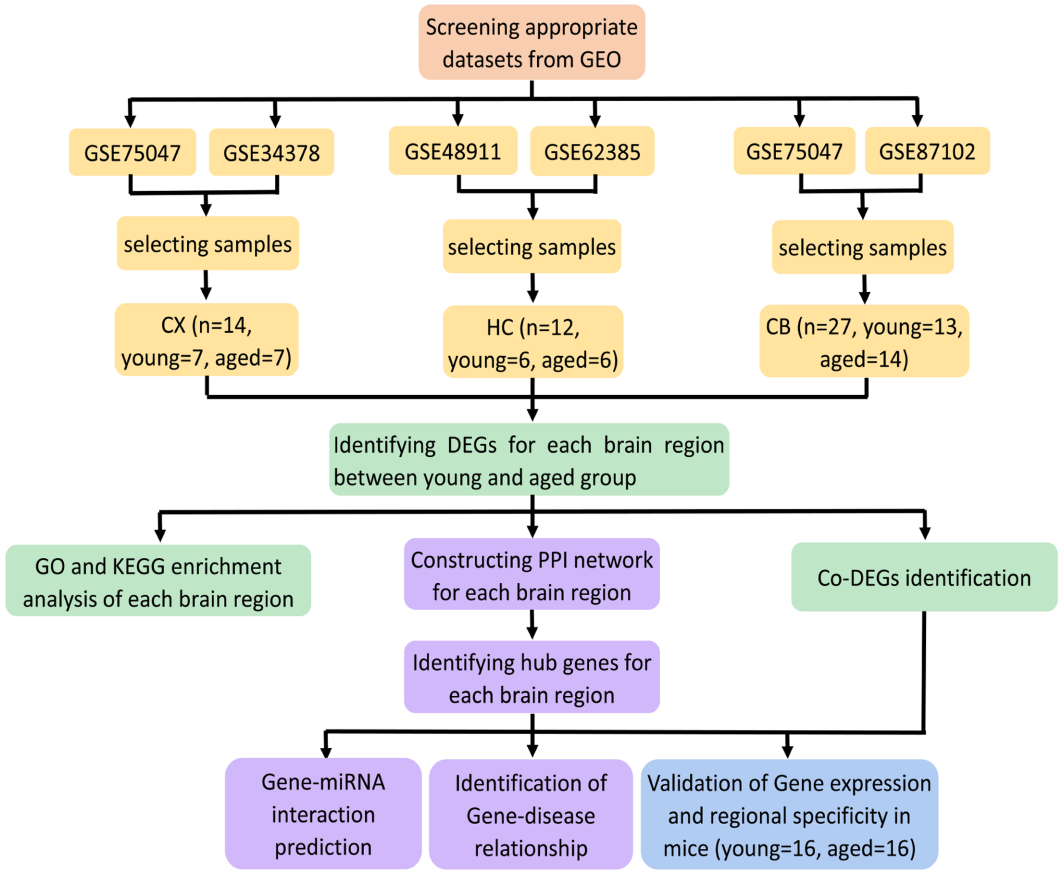

FIGURE 1
Flowchart of the study.

PPI network analysis and identification of hub genes

PPI networks were constructed using STRING and analyzed using RGui and Cytoscape. The cortical PPI network consisted of 19 nodes and 56 edges with an average node degree of 3.47 and an average clustering coefficient of 0.51. The hippocampal PPI network consisted of 121 nodes and 242 edges with an average node degree of 2.38 and an average clustering coefficient of 0.09. The cerebellar PPI network consisted of 94 nodes and 500 edges with an average node degree of 5.83 and an average clustering coefficient of 0.44. In the Cytoscape analysis, we obtained the hub genes depending on the degree of gene expression, and the results were visualized using Cytoscape. The network diagrams list only one-way edge results. Itgax is a hub gene involved in cerebral cortical aging (Figure 7A). Zfp52 and Zfp62 were hub genes involved in hippocampal aging (Figure 7B). Itgax and Cxcl10 were hub genes involved in cerebellar aging (Figure 7C). These four genes were all upregulated in the DEGs. The degrees of hub genes were as follows: Itgax: 20 (in the cortical network)/40 (in the cerebellar network); Zfp51 and Zfp62: 16; Cxcl10: 40. In RGui analysis, we obtained the same results for hub gene identification. The top 30 genes of each brain region are presented in a bar plot based on the number of gene connections in the PPI network (Figures 7D–F). The functional enrichment items and pathways that contain the hub genes or co-DEGs (S100a8) are also listed in Tables 2–4 (in which only the top three items according to *p*-values are listed). These results suggest that different brain regions may undergo different molecular changes during aging (Table 5).

Potential gene–miRNA interactions

The miRBD, TargetScan, miRWALK, and DIANA tools were used to identify the top three miRNAs targeting each hub gene and co-DEGs (S100a8) based on the predictive scores. The predicted miRNAs for Itgax are mmu-miR-185-3p, mmu-miR-7,048-5p, and mmu-miR-379-5p. The predicted miRNAs for Zfp51 are mmu-miR-23b-3p and mmu-miR-7,655-3p. The predicted miRNAs for Zfp62 are mmu-miR-181a-5p, mmu-miR-181b-5p, and mmu-miR-181c-5p. The predicted miRNAs for Cxcl10 are mmu-miR-101b-3p, mmu-miR-101a-3p, and mmu-miR-126b-5p (Table 6). These results implicate miRNAs in aging in different brain regions.

Relationship between aged-related nervous system disease and hub genes/S100a8

We used the CTD database to explore the relationship between age-related nervous system diseases and hub genes/co-DEGs (S100a8) based on the inference scores. The neurodegenerative diseases for the hub genes and S100a8 included dementia, Parkinson's disease,

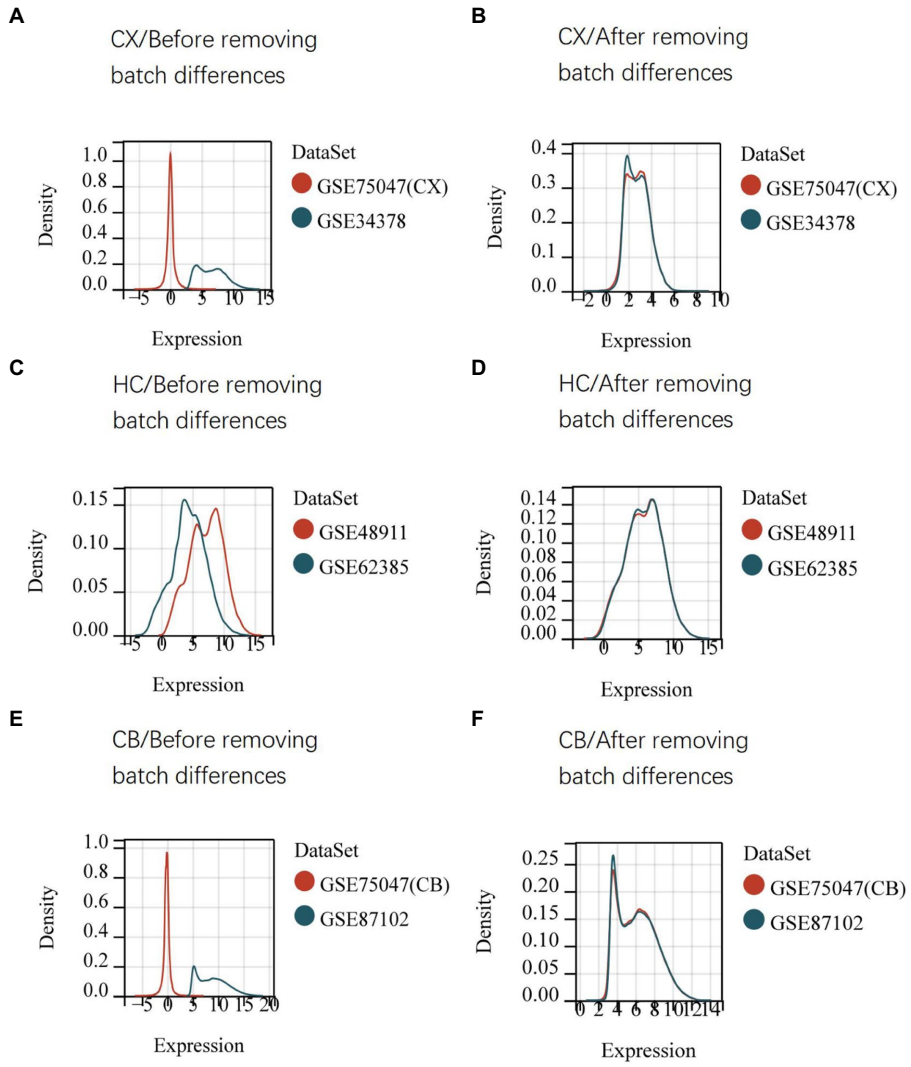

FIGURE 2
Density distribution map of gene expression in datasets before **(A,C,E)** and after **(B,D,F)** removing batch differences. The maps were generated by SangerBox using the ComBat method. The horizontal axis represents gene expression level and the vertical axis represents probability density. The higher curve overlap, the smaller batch differences. CX, cerebral cortex; HC, hippocampus; CB, cerebellum.

neurobehavioral abnormalities, memory disorders, learning disabilities, and Alzheimer's disease. The age-related cerebrovascular diseases for the hub genes and S100a8 included cerebrovascular disorders, stroke, brain ischemia, ischemic attack, cerebral infarction, cerebral hemorrhage, and intracranial hemorrhage (Figure 8).

Expression level and regional specificity of hub genes and S100a8

We used the qPCR method to validate gene expression levels. Consistent with the results of the bioinformatic analysis, the levels of Itgax, Zfp51, Zfp62, Cxcl10, and S100a8 were all significantly upregulated in the corresponding region of aged samples. Surprisingly, only the upregulation of Zfp51 and Zfp62 was restricted to the HC, whereas Itgax and Cxcl10 were significantly upregulated in all three regions in aged samples, similar to the co-DEGs (S100a8; Figure 9). This evidence further corroborates the level change of these genes in the aging of different brain regions and indicates the fundamental role of neuroinflammation in brain aging.

Discussion

The study findings reveal that the molecular changes and key genes involved in aging exhibit regional differences in the brain. Most of the changes seem to be closely related to neuroinflammation. Although several previous studies based on bioinformatics analyses have already focused on normal brain aging, none have explored the key genes of aging depending on the brain region and multiple online datasets (Li et al., 2018; Xu et al., 2022). Whether there are regional differences in molecular changes in the aging brain is unclear. Therefore, this study fills this gap to a certain extent.

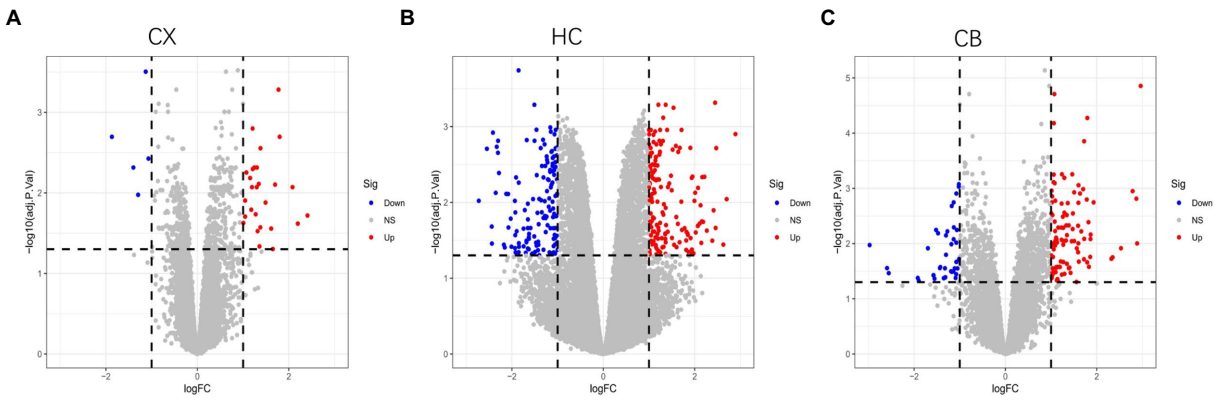

FIGURE 3
Volcano plots of DEGs between young and aged group in CX **(A)**, HC **(B)** and CB **(C)**. The Limma package was used to identify DEGs. Sample size: CX (Young: *n*=7, Aged: *n*=7); HC (Young: *n*=6, Aged: *n*=6); CB (Young: *n*=13, Aged: *n*=14). Red, blue, and gray nodes represent upregulated genes, downregulated genes and no significantly changed genes, respectively. The genes with |log FC|>1 and adjusted *p*<0.05 were identified as DEGs. CX, cerebral cortex; HC, hippocampus; CB, cerebellum.

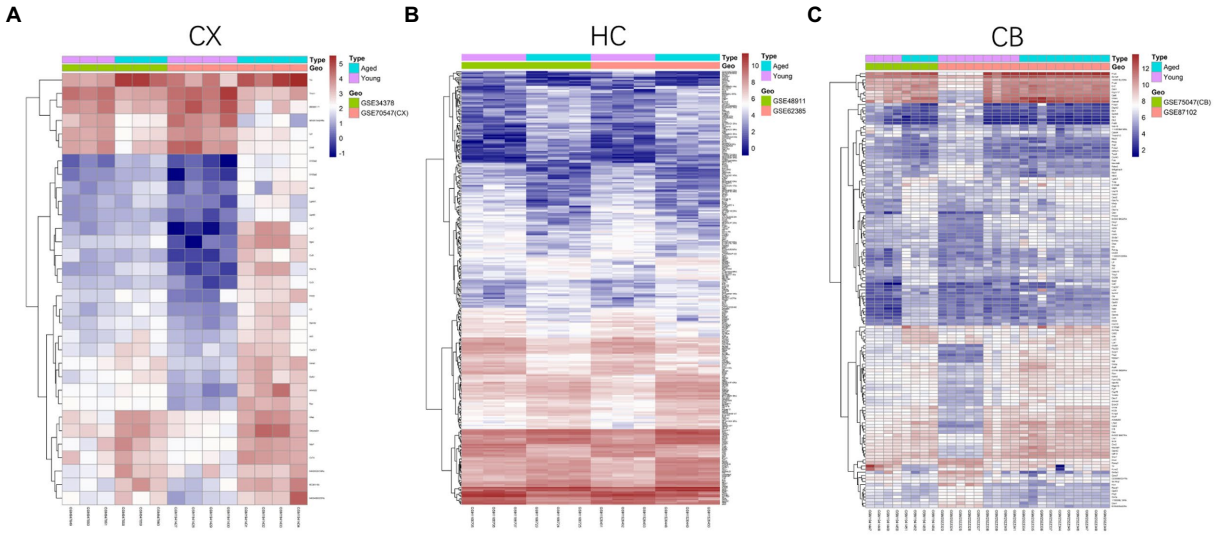

FIGURE 4
Heatmap of DEGs between young and aged groups of CX **(A)**, HC **(B)** and CB **(C)**. The heatmaps were generated using the Pheatmap package. The horizontal axis represents sample symbol and the vertical axis represents gene symbol. The depth of red (high value) and blue (low value) colors represent height of gene expression value. CX, cerebral cortex; HC, hippocampus; CB, cerebellum.

GO terms of cerebral cortical aging strongly suggest that leukocyte (especially neutrophils) chemotaxis and migration is an important change in cortical aging, and integrins (αβ-heterodimer CAMs), which are exclusively expressed on the surface of all leukocytes, play a key role in cerebral cortical aging (Wen et al., 2022). Previous studies have shown that aging increases blood–brain barrier permeability, which facilitates neutrophil invasion in the aging brain (Roy-O'Reilly et al., 2020). Integrin activation contributes to the slow rolling, adhesion, and recruitment of leukocytes during this invasion process, thus maintaining immune responses and inflammation levels (Sun et al., 2021). Chemokines are chemotactic agonists that regulate integrin activation through GPCRs, such as monocyte C-C motif chemokine receptor 2 (CCR2; Sun et al., 2021). Thus, the CCR may also be involved in leukocyte recruitment in aging CX. This is supported by evidence that GPCRs and CCR receptor levels are also altered in CX from aged rodents (Cartier et al., 2005; Gu et al., 2021). In addition, what can support the suggestion mentioned earlier is that the DEGs of cortical tissue were enriched in several inflammatory signaling pathways in the KEGG results. Coincidentally, integrin alpha x (Itgax) or CD11c (the latter has been already used in numerous studies) that encodes an integrin family protein was the hub gene of cerebral cortical aging in our results. Several studies have shown that the level of Itgax increases with age and is related to CX neuroinflammation (Hart et al., 2012; Raj et al., 2017; Kang et al., 2018; Sato-Hashimoto et al., 2019). In addition to its role in normal aging, Itgax participates in the pathological processes of neurodegenerative diseases such as AD (Rangaraju et al., 2018; Benmamar-Badel et al., 2020). Combined with this evidence, our results suggest that Itgax-mediated neutrophil invasion plays a key

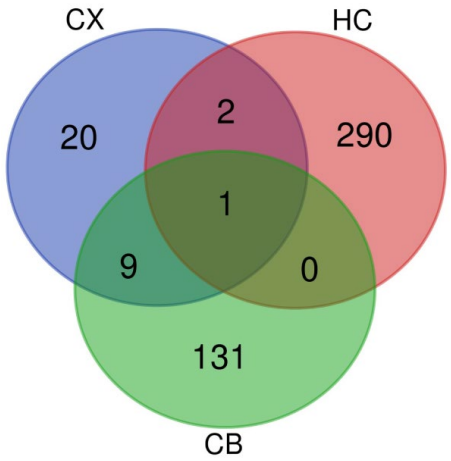

FIGURE 5
Venn diagram of DEGs. The intersections represent the co-DEGs between each brain region. CX, cerebral cortex; HC, hippocampus; CB, cerebellum.

role in cortical aging. However, despite inducing neuroinflammation, upregulation of Itgax enhances cellular phagocytosis and thus promotes the clearance of Aβ plaques, which is beneficial for the brain (Benmamar-Badel et al., 2020). Therefore, whether the increase in Itgax is an important factor in aging CX is unclear and requires further study.

The enrichment results for hippocampal aging appear more complex, but the abnormality of neurotransmitter transmission (especially excitatory neurotransmitters) seems to play a critical role. A decline in the level of excitatory neurotransmitters, such as glutamate, is a robust marker of brain aging (Roalf et al., 2020). Neurotransmitter transmission is regulated by calcium-dependent exocytosis (Wu et al., 2014). Actin cytoskeleton remodeling precisely controls exocytosis by actin filaments, thus ensuring normal granule transport in the synaptic cleft (Bader et al., 2004). Abnormal neurotransmission, oxidation of calcium channels, decrease in exocytosis, and levels of actin protein (for example, drebrin) have all been found in aging HC in previous studies (Lalo et al., 2014; Patel and Sesti, 2016; Willmes et al., 2017; Roalf et al., 2020; Tao et al., 2021). These alterations lead to impairment of long-term potentiation, which is directly responsible for cognitive decline (Kojima and Shirao, 2007; Ivanov et al., 2009; Jung et al., 2015). In addition, the enrichment results may also emphasize that neuroinflammation induced by microglia (a type of resident myeloid cells in the brain) and apoptosis are involved in hippocampal aging. Zfp51 and Zfp62 were identified as hub genes involved in hippocampal aging in our study. These two genes are zinc finger encoding genes and have the same evolutionarily conserved C2H2-link sequence. However, these two genes have not been thoroughly investigated. To the best of our knowledge, no study has focused on the relationship between these two genes and brain aging. Therefore, research on the role of these two genes in hippocampal aging is required.

CB appears to have a relatively slow rate of aging. The role of CB in cognitive decline is enigmatic. Therefore, it is not surprising that CB has been dismissed or even ignored in studies on brain aging. However, some recent studies have shown that pathological changes in CB may also be associated with neurodegenerative disorders, highlighting the significance of CB in normal aging (Liang and Carlson, 2020). Most GO items associated with cerebellar aging are related to neuronal development and differentiation. This suggests that impaired neurogenesis plays a fundamental role in cerebellar aging. As a compensatory mechanism for neuronal death, neurogenesis can restore the brain to a more youthful state during aging. However, neurogenesis in the CB is significantly impaired with age (Elkholy and Al-Gholam, 2018; Isaev et al., 2019). In addition, DEGs enriched for calcium ion transport provide further confirmation for this suggestion because calcium transport is indispensable for cell proliferation and neural differentiation in neurogenesis (Toth et al., 2016). However, during aging, the number of calcium channels necessary for transport decreases (Martini et al., 1994; Chung et al., 2001). A series of functions and pathways related to leukocyte reaction and inflammatory cytokine responses are consistent with the results that Itgax and Cxcl10 were the hub genes of cerebellar aging because these two genes are closely related to the inflammatory reaction. In addition to leukocyte-induced inflammation, Itgax is related to neurogenesis (Blau et al., 2012). Similar to Itgax, Cxcl10, a chemokine superfamily coding protein, is expressed in astrocytes, glial cells, dendritic cells, and neutrophils, and is closely related to neuroinflammation (Fazia et al., 2020). Cxcl10 is upregulated in aged brains (Hasegawa-Ishii et al., 2016; Palomera-Ávalos et al., 2017; Tennakoon et al., 2017; Hu et al., 2019). Expression of Cxcl10 can induce the release of the senescence-associated secretory phenotype, which consists of multiple inflammatory factors and promotes brain aging (Cardoso et al., 2018). The upregulation of inflammatory cytokines is usually accompanied by impaired neurogenesis (Kim et al., 2016). This evidence suggests that Itgax and Cxcl10-mediated neuroinflammation may be the driving force for the impairment of neurogenesis in CB and thus responsible for cerebellar aging.

Subsequently, we identified that S100a8 was the only co-DEG of all three brain regions. A previous study showed that the level of S100A8, the eponymous protein encoded by the S100a8 gene, is increased in the prefrontal cortex, hippocampus, and cerebellum of aged rats and plays a critical role in inflammatory regulation (Hamasaki et al., 2019). Similar results were obtained in aged mice and a mouse model of AD (Lodeiro et al., 2017). As the brain ages, some brain regions contain high levels of S100 proteins. Among these proteins, S100A8 has the highest staining intensity (Hoyaux et al., 2000). Most S100A8 proteins are aggregated around amyloid plaques neighboring activated microglia, which form a positive feedback loop between S100A8 and Aβproduction (Lodeiro et al., 2017). This may explain why amyloid deposition and neuroinflammation are common phenomena in the aging brain (Singh-Bains et al., 2019; Zhang et al., 2021). After gene identification, we were interested in determining whether the upregulation of hub genes had regional specificity. Therefore, we measured the level of each hub gene in each brain region. We were surprised to find that only the upregulation of Zfp51 and Zfp62 was restricted to the HC, whereas Itgax and Cxcl10 were significantly upregulated in all three regions of the aged brain, similar to S100a8. This suggests that Zfp51 and Zfp62 may be specific biomarkers of hippocampal aging, and neuroinflammation may be a common and basic mechanism of

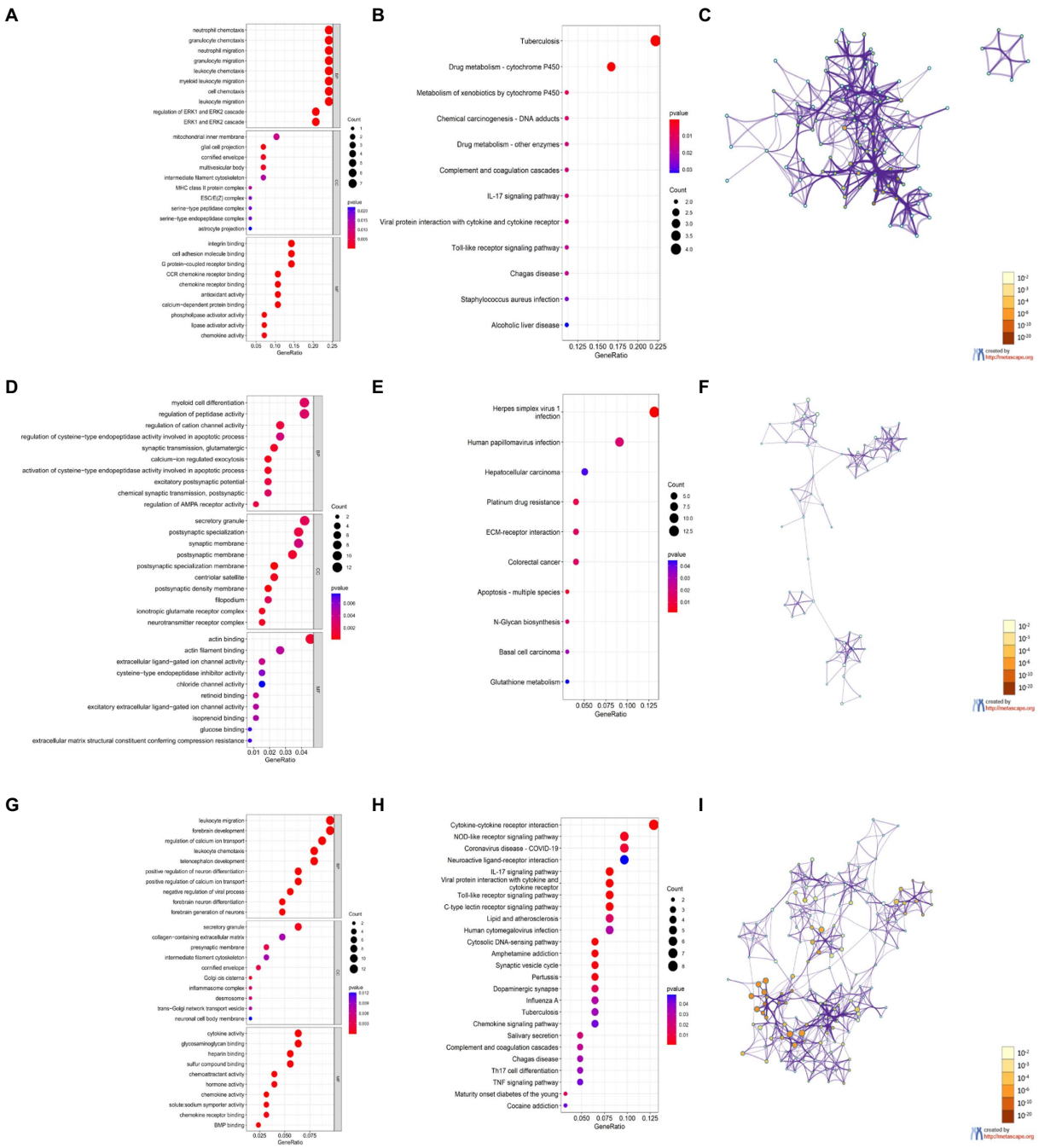

FIGURE 6
Enrichment analysis of DEGs based on R software and Metascape. **(A,D,G)** GO enrichment items of CX **(A)**, HC **(D)**, and CB **(G)**. **(B,E,H)** KEGG enrichment items of CX **(B)**, HC **(E)**, and CB **(H)**. **(C,F,I)** The main Networks of enrich terms of CX **(C)**, HC **(F)**, and CB **(I)**. **A,B,D,E,G,H** were generated by RGui using the clusterProfiler package. **C,F,I** were generated by Metascape. Statistical significance of enrichment item was set at $p<0.05$.

brain aging because the expression of Itgax, Cxcl10, and S100a8 are all strongly related to inflammatory reactions, as mentioned above.

Considering that the hub genes are also regulated by miRNA, we predicted the top three selected miRNAs that targeted each hub gene and S100a8 based on the predictive scores. Supporting evidence is also found for these predictions. In one study, miR-185-3p was related to aging and frailty in exosomes derived from plasma (Ipson et al., 2018). Jiang and colleagues described a decreased level of miR-23b-3p in HC from aged mice (Jiang et al., 2022). The authors also reported that upregulation of this miRNA attenuates cognition impairment. In another study, upregulation of miR-181a-5p was demonstrated in HC of AD mice (Rodriguez-Ortiz et al., 2020). The authors described that this upregulation negatively modulates synaptic plasticity, leading to memory impairment. Angiotensin II induces brain vascular smooth muscle

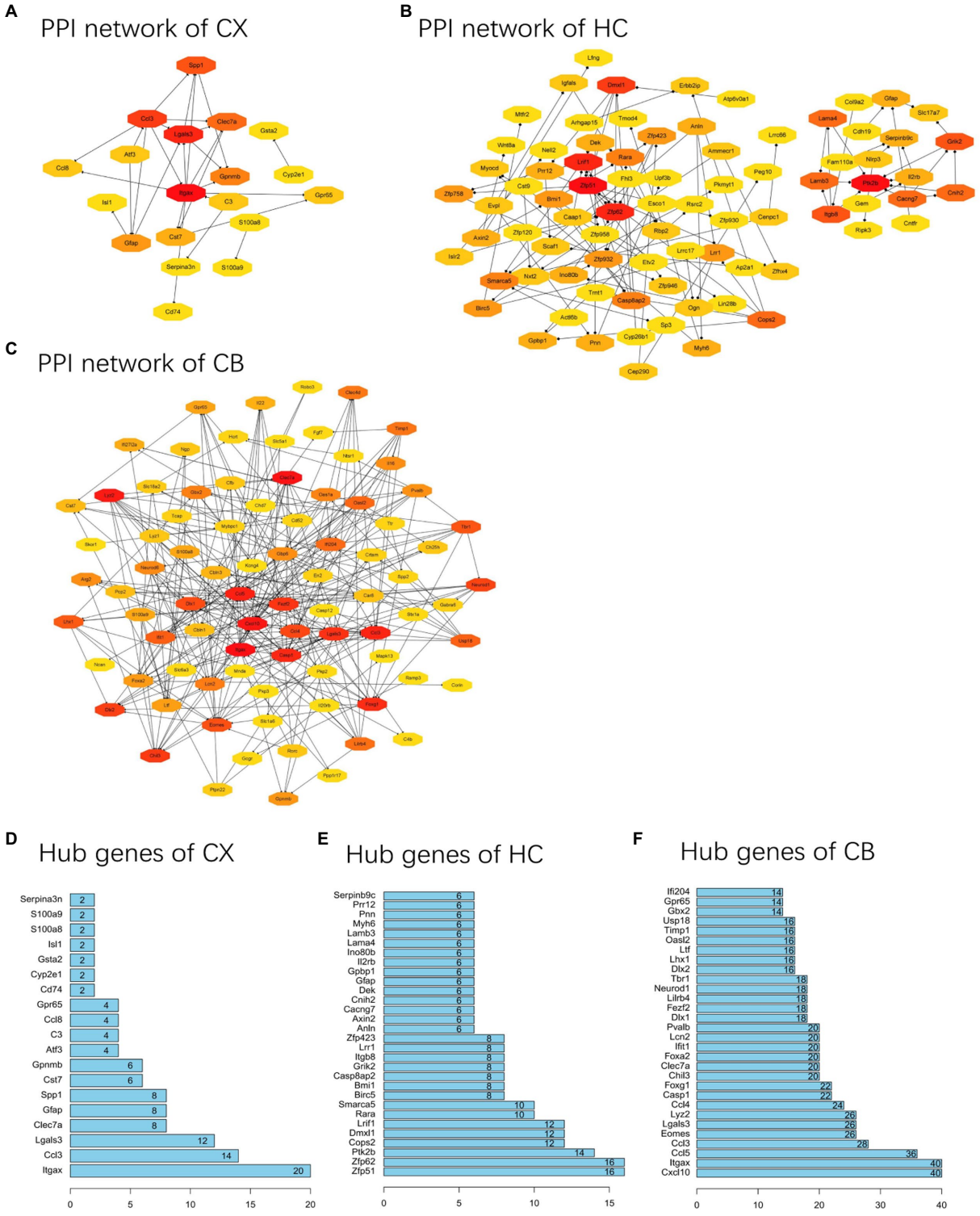

FIGURE 7
PPI networks and hub genes of DEGs. **(A-C)** The results of network analysis based on Cytoscape. The depth of color represents the degree of gene in network analysis. **(D-F)** The results of network analysis based on R software. The x-axis represents the number of gene connections in network. CX, cerebral cortex; HC, hippocampus; CB, cerebellum.

cell (BVSMC) senescence by negatively regulating miR-181b-5p (Li et al., 2019; Bai et al., 2021). Therefore, the downregulation of this miRNA in HC may be responsible for the aging of BVSMC. Microarray analysis has shown that miR-181c-5p is associated with hippocampal aging (Zhou et al., 2016). MiR-101b-3p controls neuronal plasticity, indicating a role in the impairment of neurogenesis in cerebellar aging (Codocedo and Inestrosa, 2016). This evidence functionally implicates miRNAs in

TABLE 3 GO and KEGG items.

Gene symbol	ID of GO/KEGG term	Description	GeneRatio	*p*-value
Itgax	GO:0005178	Integrin binding	4/28	1.61E-05
	GO:0050839	Cell adhesion molecule binding	4/28	0.00023
	mmu05152	Tuberculosis	4/18	0.00038
	mmu04610	Complement and coagulation cascades	2/18	0.01467
S100a8	GO:0030593	Neutrophil chemotaxis	7/29	8.87E-12
	GO:0071621	Granulocyte chemotaxis	7/29	4.16E-11
	GO:1990266	Neutrophil migration	7/29	4.64E-11
	mmu04657	IL-17 signaling pathway	2/18	0.01467

The top three items containing hub genes or S100a8 of CX according to *p*-values are listed if there are more than three items.

TABLE 4 GO and KEGG items.

Gene symbol	ID of GO/KEGG term	Description	GeneRatio	*p*-value
Zfp51	mmu05168	Herpes simplex virus 1 infection	13/99	0.00156
S100a8	GO:0006919	Activation of cysteine-type endopeptidase activity involved in apoptotic process	5/263	0.00075
	GO:0052547	Regulation of peptidase activity	11/263	0.00268
	GO:0030595	Regulation of cysteine-type endopeptidase activity involved in apoptotic process	7/263	0.00033

The top three items containing hub genes or S100a8 of HC according to *p*-values are listed if there are more than three items.

TABLE 5 GO and KEGG items.

Gene symbol	ID of GO/KEGG term	Description	GeneRatio	*p*-value
Itgax	mmu04610	Complement and coagulation cascades	3/62	0.02671
Cxcl10	GO:0051924	Regulation of calcium ion transport	11/126	5.83E-08
	GO:0030595	Leukocyte chemotaxis	10/126	6.83E-08
	GO:0050900	Leukocyte migration	12/126	1.18E-07
	mmu04657	IL-17 signaling pathway	5/62	0.00043
	mmu04061	Viral protein interaction with cytokine and cytokine receptor	5/62	0.00047
	mmu04620	Toll-like receptor signaling pathway	5/62	0.00060
S100a8	GO:0030595	Neutrophil chemotaxis	10/126	6.83E-08
	GO:0050900	Leukocyte migration	12/126	1.18E-07
	GO:0030593	Neutrophil chemotaxis	7/126	3.62E-07
	mmu04657	IL-17 signaling pathway	5/62	0.00043

The top three items containing hub genes or S100a8 of CB according to *p*-values are listed if there are more than three items.

TABLE 6 Interaction between hub genes and miRNA.

Brain region	Gene symbol	Predicted miRNA
CX	Itgax	mmu-miR-185-3p, mmu-miR-7,048-5p, mmu-miR-379-5p
HC	Zfp51	mmu-miR-23b-3p, mmu-miR-7,655-3p
	Zfp62	mmu-miR-181a-5p, mmu-miR-181b-5p, mmu-miR-181c-5p
CB	Cxcl10	mmu-miR-101b-3p, mmu-miR-101a-3p, mmu-miR-126b-5p

the aging brain. However, their relationship to hub genes and their effects on the aging of specific brain regions need to be confirmed. These four hub genes and S100a8 are all associated with the most common age-related nervous system diseases, and this further suggests that changes in the levels of these genes may play a critical role in cognitive decline and neurovascular aging; however, more animal and clinical studies are needed to confirm the biological role of these genes in normal brain aging.

This study has some limitations. First, this was a small sample study from the point of both bioinformatics analysis and animal experiments. In contrast, we only explored the potential mechanism at the gene expression level, but gene expression may not be directly

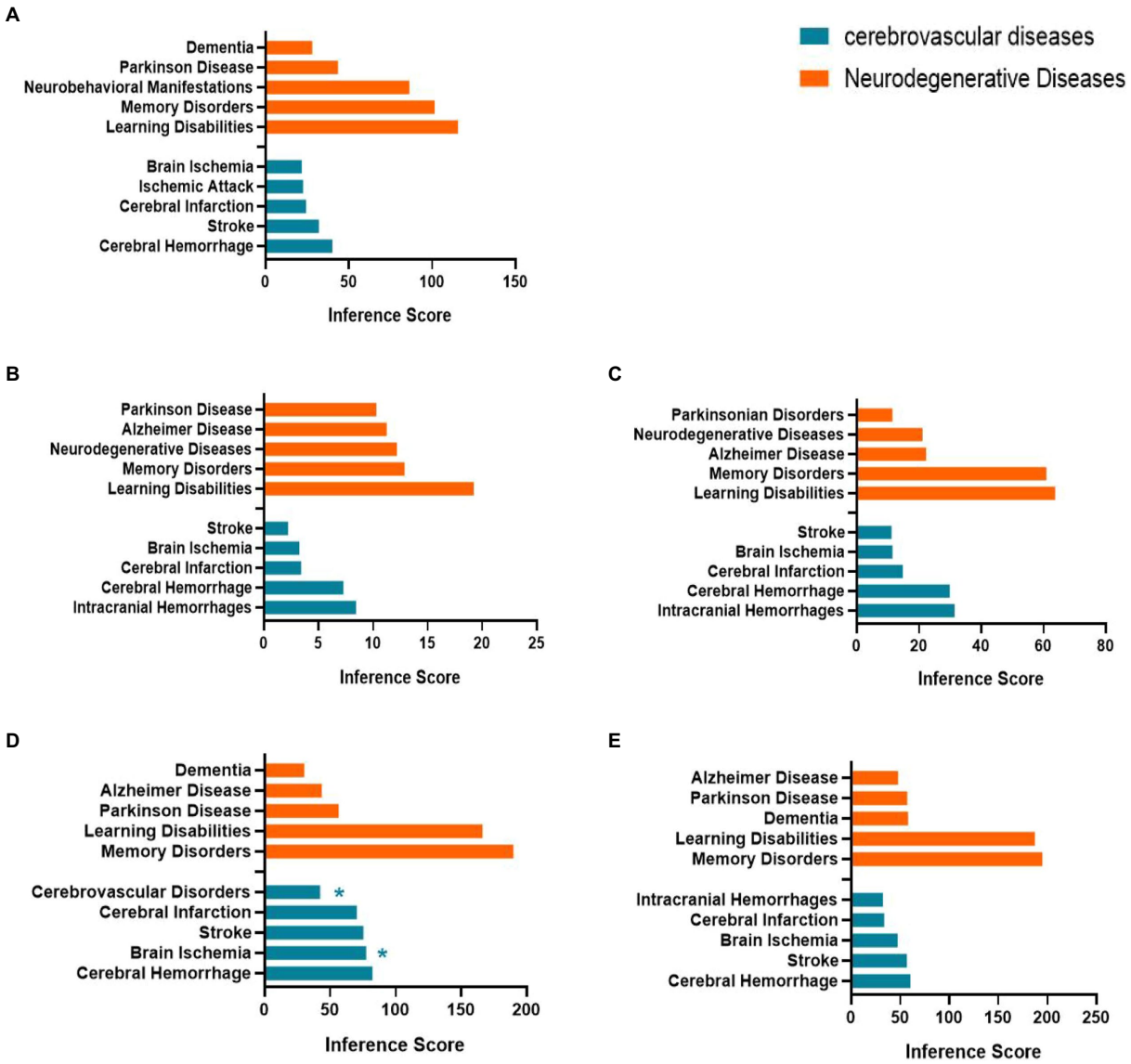

FIGURE 8
Relationship between Itgax **(A)**, Zfp51 **(B)**, Zfp62 **(C)**, Cxcl10 **(D)**, S100a8 **(E)** and aged related nervous system diseases. Data are from the Comparative Toxicogenomics Database. The top five of neurodegenerative diseases and age-related cerebrovascular diseases of each hub gene and S100a8 are listed in the bar charts based on the inference score. *, Direct evidence of marker or molecular change in this disease.

equivalent to protein expression and biological effects. Therefore, more animal and clinical studies are needed, other comprehensive databases of biometric information should be applied to bioinformatics analysis, and the results should be validated through different experimental methods.

Conclusion

This study revealed that the molecular signatures of aging exhibit regional differences in the brain and seem to be closely related to neuroinflammation. Integrin-mediated neutrophil invasion, abnormal synaptic transmission, and impaired neurogenesis due to inflammation may play key roles in the aging of CX, HC, and CB. Itgax, Zfp51, Zfp62, Cxcl10, and S100a8 are potential targets for preventing aging in the brain. Further studies are required to confirm these results.

Data availability statement

The original contributions presented in the study are included in the article/Supplementary material, further inquiries can be directed to the corresponding author.

Ethics statement

The animal study was approved by the Animal Care Welfare Committee of Guangxi Medical University.

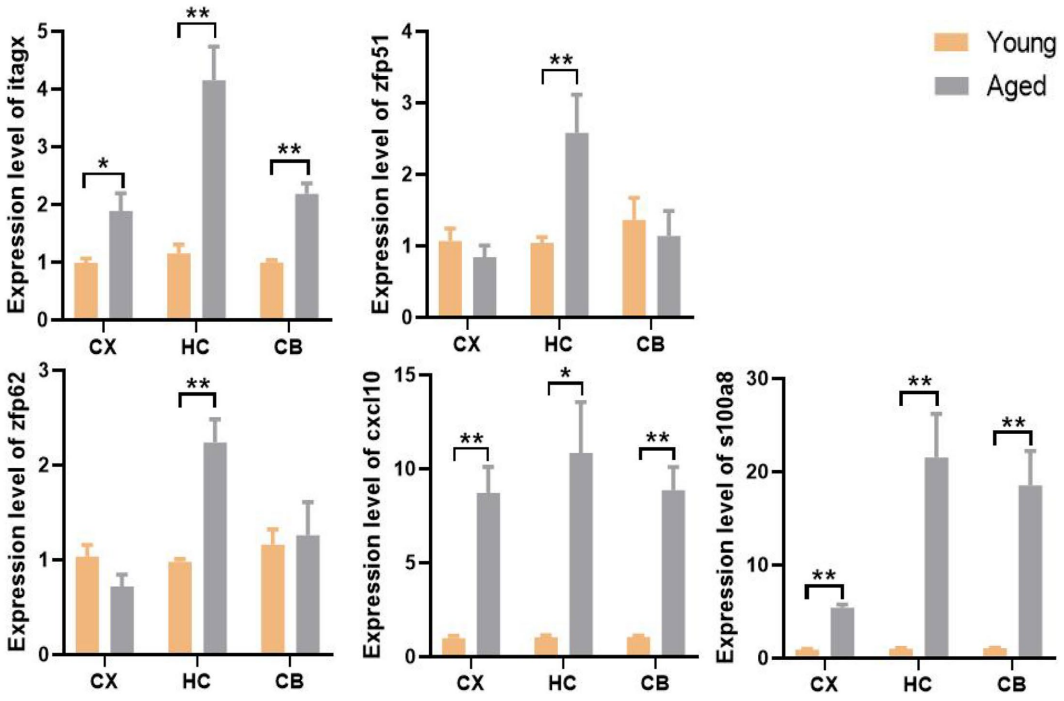

FIGURE 9
The expression level and regional specificity of the hub genes and S100a8 in mice (Measured by RT-qPCR method). Sample size (Young and aged samples account for half of each panel): Itgax (CX: *n*=32, HC: *n*=14. CB: *n*=32); Zfp51 (CX: *n*=14, HC: *n*=32. CB: *n*=14); Zfp62 (CX: *n*=14, HC: *n*=32. CB: *n*=14); Cxcl10 (CX: *n*=14, HC: *n*=14. CB: *n*=32); S100a8 (CX: *n*=32, HC: *n*=32. CB: *n*=32); *p*-values of Itgax of CX, Zfp51 of HC, S100a8 of HC and CB are calculated with Wilcoxon rank-sum test. *p*-value of other panel are calculated with t -test. Results are expressed as mean±SEM. CX, cerebral cortex; HC, hippocampus; CB, cerebellum. Y, young; A, aged; *$p<0.05$; **$p<0.01$.

Author contributions

XS and LX were responsible for the data acquisition, analysis, experimental operation, literature search, and writing of the manuscript. JL, XT, and BL curated the data and created the figures. MC designed the study and revised the manuscript. All authors contributed to the article and approved the submitted version.

Funding

This study was supported by the National Natural Science Foundation of China (grant numbers: 81860333, 82072128, and 82160372). The funders had no role in the study design, data collection and analysis, decision to publish, or manuscript preparation.

Acknowledgments

We are grateful to the team of Kaoru Mogushi from the Medical Research Institute, Tokyo Medical and Dental University, Tokyo; the team of Martijs Jonker from the Swammerdam Institute for Life Sciences, University of Amsterdam, Amsterdam; the team of Xinkun Wang from the Higuchi Biosciences Center, University of Kansas, Lawrence; the team of Akira Hirasawa from the Department of Genomic Drug Discovery Science, Kyoto University, Kyoto; and the team of Stephen J. Bonasera from the Division of Geriatrics, University of Nebraska Medical Center, Omaha for providing the datasets (GSE75047, GSE34378, GSE48911, GSE62385, and GSE87102).

Conflict of interest

The authors declare that the research was conducted in the absence of any commercial or financial relationships that could be construed as potential conflicts of interest.

Publisher's note

Supplementary material

The Supplementary material for this article can be found online at: https://www.frontiersin.org/articles/10.3389/fnmol.2023.1133106/full#supplementary-material

References

Bader, M. F., Doussau, F., Chasserot-Golaz, S., Vitale, N., and Gasman, S. (2004). Coupling actin and membrane dynamics during calcium-regulated exocytosis: a role for rho and ARF GTPases. *Biochim. Biophys. Acta* 1742, 37–49. doi: 10.1016/j.bbamcr.2004.09.028

Bai, H. Y., Min, L. J., Shan, B. S., Iwanami, J., Kan-No, H., Kanagawa, M., et al. (2021). Angiotensin II and amyloid-β synergistically induce brain vascular smooth muscle cell senescence. *Am. J. Hypertens.* 34, 552–562. doi: 10.1093/ajh/hpaa218

Bartsch, T., and Wulff, P. (2015). The hippocampus in aging and disease: from plasticity to vulnerability. *Neuroscience* 309, 1–16. doi: 10.1016/j.neuroscience.2015.07.084

Benmamar-Badel, A., Owens, T., and Wlodarczyk, A. (2020). Protective microglial subset in development, aging, and disease: lessons from transcriptomic studies. *Front. Immunol.* 11:430. doi: 10.3389/fimmu.2020.00430

Blau, C. W., Cowley, T. R., O'Sullivan, J., Grehan, B., Browne, T. C., Kelly, L., et al. (2012). The age-related deficit in LTP is associated with changes in perfusion and blood-brain barrier permeability. *Neurobiol. Aging* 33, 1005.e23–1005.e35. doi: 10.1016/j.neurobiolaging.2011.09.035

Cardoso, A. L., Fernandes, A., Aguilar-Pimentel, J. A., de Angelis, M. H., Guedes, J. R., Brito, M. A., et al. (2018). Towards frailty biomarkers: candidates from genes and pathways regulated in aging and age-related diseases. *Ageing Res. Rev.* 47, 214–277. doi: 10.1016/j.arr.2018.07.004

Cartier, L., Hartley, O., Dubois-Dauphin, M., and Krause, K. H. (2005). Chemokine receptors in the central nervous system: role in brain inflammation and neurodegenerative diseases. *Brain Res. Brain Res. Rev.* 48, 16–42. doi: 10.1016/j.brainresrev.2004.07.021

Chung, Y. H., Shin, C. M., Kim, M. J., Shin, D. H., Yoo, Y. B., and Cha, C. I. (2001). Differential alterations in the distribution of voltage-gated calcium channels in aged rat cerebellum. *Brain Res.* 903, 247–252. doi: 10.1016/s0006-8993(01)02392-7

Codocedo, J. F., and Inestrosa, N. C. (2016). Wnt-5a-regulated miR-101b controls COX2 expression in hippocampal neurons. *Biol. Res.* 49:9. doi: 10.1186/s40659-016-0071-x

Davis, A. P., Grondin, C. J., Johnson, R. J., Sciaky, D., Wiegers, J., Wiegers, T. C., et al. (2021). Comparative Toxicogenomics database (CTD): update 2021. *Nucleic Acids Res.* 49, D1138–D1143. doi: 10.1093/nar/gkaa891

Dennis, G. Jr., Sherman, B. T., Hosack, D. A., Yang, J., Gao, W., Lane, H. C., et al. (2003). DAVID: database for annotation, visualization, and integrated discovery. *Genome Biol.* 4:P3. doi: 10.1186/gb-2003-4-5-p3

Ding, J., Ji, J., Rabow, Z., Shen, T., Folz, J., Brydges, C. R., et al. (2021). A metabolome atlas of the aging mouse brain. *Nat. Commun.* 12:6021. doi: 10.1038/s41467-021-26310-y

Elkholy, W. B., and Al-Gholam, M. A. (2018). Role of medical ozone in attenuating age-related changes in the rat cerebellum. *Microscopy* 67, 214–221. doi: 10.1093/jmicro/dfy017

Fazia, T., Nova, A., Gentilini, D., Beecham, A., Piras, M., Saddi, V., et al. (2020). Investigating the causal effect of brain expression of CCL2, NFKB1, MAPK14, TNFRSF1A, CXCL10 genes on multiple sclerosis: a two-sample Mendelian randomization approach. *Front. Bioeng. Biotechnol.* 8:397. doi: 10.3389/fbioe.2020.00397

Grabert, K., Michoel, T., Karavolos, M. H., Clohisey, S., Baillie, J. K., Stevens, M. P., et al. (2016). Microglial brain region-dependent diversity and selective regional sensitivities to aging. *Nat. Neurosci.* 19, 504–516. doi: 10.1038/nn.4222

Gu, C., Chen, Y., Chen, Y., Liu, C. F., Zhu, Z., and Wang, M. (2021). Role of G protein-coupled receptors in microglial activation: implication in Parkinson's disease. *Front. Aging Neurosci.* 13:768156. doi: 10.3389/fnagi.2021.768156

Hamasaki, M. Y., Severino, P., Puga, R. D., Koike, M. K., Hernandes, C., Barbeiro, H. V., et al. (2019). Short-term effects of sepsis and the impact of aging on the transcriptional profile of different brain regions. *Inflammation* 42, 1023–1031. doi: 10.1007/s10753-019-00964-9

Hart, A. D., Wyttenbach, A., Perry, V. H., and Teeling, J. L. (2012). Age related changes in microglial phenotype vary between CNS regions: grey versus white matter differences. *Brain Behav. Immun.* 26, 754–765. doi: 10.1016/j.bbi.2011.11.006

Hasegawa-Ishii, S., Inaba, M., Li, M., Shi, M., Umegaki, H., Ikehara, S., et al. (2016). Increased recruitment of bone marrow-derived cells into the brain associated with altered brain cytokine profile in senescence-accelerated mice. *Brain Struct. Funct.* 221, 1513–1531. doi: 10.1007/s00429-014-0987-2

Hoyaux, D., Decaestecker, C., Heizmann, C. W., Vogl, T., Schäfer, B. W., Salmon, I., et al. (2000). S100 proteins in corpora amylacea from normal human brain. *Brain Res.* 867, 280–288. doi: 10.1016/s0006-8993(00)02393-3

Hu, W. T., Howell, J. C., Ozturk, T., Gangishetti, U., Kollhoff, A. L., Hatcher-Martin, J. M., et al. (2019). CSF cytokines in aging, multiple sclerosis, and dementia. *Front. Immunol.* 10:480. doi: 10.3389/fimmu.2019.00480

Ipson, B. R., Fletcher, M. B., Espinoza, S. E., and Fisher, A. L. (2018). Identifying exosome-derived MicroRNAs as candidate biomarkers of frailty. *J. Frailty Aging* 7, 100–103. doi: 10.14283/jfa.2017.45

Isaev, N. K., Stelmashook, E. V., and Genrikhs, E. E. (2019). Neurogenesis and brain aging. *Rev. Neurosci.* 30, 573–580. doi: 10.1515/revneuro-2018-0084

Ivanov, A., Esclapez, M., Pellegrino, C., Shirao, T., and Ferhat, L. (2009). Drebrin a regulates dendritic spine plasticity and synaptic function in mature cultured hippocampal neurons. *J. Cell Sci.* 122, 524–534. doi: 10.1242/jcs.033464

Jang, S. H., Kwon, Y. H., Lee, M. Y., Kim, J. R., and Seo, J. P. (2016). Aging of the cingulum in the human brain: preliminary study of a diffusion tensor imaging study. *Neurosci. Lett.* 610, 213–217. doi: 10.1016/j.neulet.2015.11.018

Jiang, H., Liu, J., Guo, S., Zeng, L., Cai, Z., Zhang, J., et al. (2022). miR-23b-3p rescues cognition in Alzheimer's disease by reducing tau phosphorylation and apoptosis via GSK-3β signaling pathways. *Mol Ther Nucleic Acids.* 28, 539–557. doi: 10.1016/j.omtn.2022.04.008

Jung, G., Kim, E. J., Cicvaric, A., Sase, S., Gröger, M., Höger, H., et al. (2015). Drebrin depletion alters neurotransmitter receptor levels in protein complexes, dendritic spine morphogenesis and memory-related synaptic plasticity in the mouse hippocampus. *J. Neurochem.* 134, 327–339. doi: 10.1111/jnc.13119

Kang, S. S., Ebbert, M. T. W., Baker, K. E., Cook, C., Wang, X., Sens, J. P., et al. (2018). Microglial translational profiling reveals a convergent APOE pathway from aging, amyloid, and tau. *J. Exp. Med.* 215, 2235–2245. doi: 10.1084/jem.20180653

Kim, Y. K., Na, K. S., Myint, A. M., and Leonard, B. E. (2016). The role of pro-inflammatory cytokines in neuroinflammation, neurogenesis and the neuroendocrine system in major depression. *Prog. Neuropsychopharmacol. Biol. Psychiatry* 64, 277–284. doi: 10.1016/j.pnpbp.2015.06.008

Kojima, N., and Shirao, T. (2007). Synaptic dysfunction and disruption of postsynaptic drebrin-actin complex: a study of neurological disorders accompanied by cognitive deficits. *Neurosci. Res.* 58, 1–5. doi: 10.1016/j.neures.2007.02.003

Lalo, U., Rasooli-Nejad, S., and Pankratov, Y. (2014). Exocytosis of gliotransmitters from cortical astrocytes: implications for synaptic plasticity and aging. *Biochem. Soc. Trans.* 42, 1275–1281. doi: 10.1042/BST20140163

Li, F. J., Zhang, C. L., Luo, X. J., Peng, J., and Yang, T. L. (2019). Involvement of the MiR-181b-5p/HMGB1 pathway in Ang II-induced phenotypic transformation of smooth muscle cells in hypertension. *Aging Dis.* 10, 231–248. doi: 10.14336/AD.2018.0510

Li, J., Zhou, Y., Du, G., Qin, X., and Gao, L. (2018). Bioinformatic analysis reveals key genes and pathways in aging brain of senescence-accelerated mouse P8 (SAMP8). *CNS Neurol. Disord. Drug Targets* 17, 712–722. doi: 10.2174/1871527317666180816094741

Liang, K. J., and Carlson, E. S. (2020). Resistance, vulnerability and resilience: a review of the cognitive cerebellum in aging and neurodegenerative diseases. *Neurobiol. Learn. Mem.* 170:106981. doi: 10.1016/j.nlm.2019.01.004

Lodeiro, M., Puerta, E., Ismail, M. A., Rodriguez-Rodriguez, P., Rönnbäck, A., Codita, A., et al. (2017). Aggregation of the inflammatory S100A8 precedes Aβ plaque formation in transgenic APP mice: positive feedback for S100A8 and Aβ productions. *J. Gerontol. A Biol. Sci. Med. Sci.* 72, glw073–glw328. doi: 10.1093/gerona/glw073

Marjańska, M., McCarten, J. R., Hodges, J., Hemmy, L. S., Grant, A., Deelchand, D. K., et al. (2017). Region-specific aging of the human brain as evidenced by neurochemical profiles measured noninvasively in the posterior cingulate cortex and the occipital lobe using (1)H magnetic resonance spectroscopy at 7 T. *Neuroscience* 354, 168–177. doi: 10.1016/j.neuroscience.2017.04.035

Martini, A., Battaini, F., Govoni, S., and Volpe, P. (1994). Inositol 1,4,5-trisphosphate receptor and ryanodine receptor in the aging brain of Wistar rats. *Neurobiol. Aging* 15, 203–206. doi: 10.1016/0197-4580(94)90113-9

Mattson, M. P., and Arumugam, T. V. (2018). Hallmarks of brain aging: adaptive and pathological modification by metabolic states. *Cell Metab.* 27, 1176–1199. doi: 10.1016/j.cmet.2018.05.011

Oenzil, F., Kishikawa, M., Mizuno, T., and Nakano, M. (1994). Age-related accumulation of lipofuscin in three different regions of rat brain. *Mech. Ageing Dev.* 76, 157–163. doi: 10.1016/0047-6374(94)91590-3

Palomera-Ávalos, V., Griñán-Ferré, C., Izquierdo, V., Camins, A., Sanfeliu, C., and Pallàs, M. (2017). Metabolic stress induces cognitive disturbances and inflammation in aged mice: protective role of resveratrol. *Rejuvenation Res.* 20, 202–217. doi: 10.1089/rej.2016.1885

Patel, R., and Sesti, F. (2016). Oxidation of ion channels in the aging nervous system. *Brain Res.* 1639, 174–185. doi: 10.1016/j.brainres.2016.02.046

Raj, D., Yin, Z., Breur, M., Doorduin, J., Holtman, I. R., Olah, M., et al. (2017). Increased white matter inflammation in aging- and Alzheimer's disease brain. *Front. Mol. Neurosci.* 10:206. doi: 10.3389/fnmol.2017.00206

Rangaraju, S., Raza, S. A., Li, N. X., Betarbet, R., Dammer, E. B., Duong, D., et al. (2018). Differential phagocytic properties of CD45low microglia and CD45high brain mononuclear phagocytes-activation and age-related effects. *Front. Immunol.* 9:405. doi: 10.3389/fimmu.2018.00405

Raz, N., Ghisletta, P., Rodrigue, K. M., Kennedy, K. M., and Lindenberger, U. (2010). Trajectories of brain aging in middle-aged and older adults: regional and individual differences. *Neuroimage* 51, 501–511. doi: 10.1016/j.neuroimage.2010.03.020

Ritchie, M. E., Phipson, B., Wu, D., Hu, Y., Law, C. W., Shi, W., et al. (2015). Limma powers differential expression analyses for RNA-sequencing and microarray studies. *Nucleic Acids Res.* 43:e47. doi: 10.1093/nar/gkv007

Roalf, D. R., Sydnor, V. J., Woods, M., Wolk, D. A., Scott, J. C., Reddy, R., et al. (2020). A quantitative meta-analysis of brain glutamate metabolites in aging. *Neurobiol. Aging* 95, 240–249. doi: 10.1016/j.neurobiolaging.2020.07.015

Rodriguez-Ortiz, C. J., Prieto, G. A., Martini, A. C., Forner, S., Trujillo-Estrada, L., LaFerla, F. M., et al. (2020). miR-181a negatively modulates synaptic plasticity in hippocampal cultures and its inhibition rescues memory deficits in a mouse model of Alzheimer's disease. *Aging Cell* 19:e13118. doi: 10.1111/acel.13118

Roy-O'Reilly, M. A., Ahnstedt, H., Spychala, M. S., Munshi, Y., Aronowski, J., Sansing, L. H., et al. (2020). Aging exacerbates neutrophil pathogenicity in ischemic stroke. *Aging* 12, 436–461. doi: 10.18632/aging.102632

Sato-Hashimoto, M., Nozu, T., Toriba, R., Horikoshi, A., Akaike, M., Kawamoto, K., et al. (2019). Microglial SIRPα regulates the emergence of CD11c(+) microglia and demyelination damage in white matter. *Elife* 8:e42025. doi: 10.7554/eLife.42025

Singh-Bains, M. K., Linke, V., Austria, M. D. R., Tan, A. Y. S., Scotter, E. L., Mehrabi, N. F., et al. (2019). Altered microglia and neurovasculature in the Alzheimer's disease cerebellum. *Neurobiol. Dis.* 132:104589. doi: 10.1016/j.nbd.2019.104589

Stefanatos, R., and Sanz, A. (2018). The role of mitochondrial ROS in the aging brain. *FEBS Lett.* 592, 743–758. doi: 10.1002/1873-3468.12902

Strosznajder, J. B., Jeśko, H., and Strosznajder, R. P. (2000). Age-related alteration of poly(ADP-ribose) polymerase activity in different parts of the brain. *Acta Biochim. Pol.* 47, 331–337. doi: 10.18388/abp.2000_4012

Sun, H., Hu, L., and Fan, Z. (2021). β2 integrin activation and signal transduction in leukocyte recruitment. *Am. J. Physiol. Cell Physiol.* 321, C308–c316. doi: 10.1152/ajpcell.00560.2020

Tao, W., Lee, J., Chen, X., Díaz-Alonso, J., Zhou, J., Pleasure, S., et al. (2021). Synaptic memory requires CaMKII. *Elife* 10. doi: 10.7554/eLife.60360

Tennakoon, A., Katharesan, V., and Johnson, I. P. (2017). Brainstem cytokine changes in healthy ageing and motor Neurone disease. *J. Neurol. Sci.* 381, 192–199. doi: 10.1016/j.jns.2017.08.013

Toth, A. B., Shum, A. K., and Prakriya, M. (2016). Regulation of neurogenesis by calcium signaling. *Cell Calcium* 59, 124–134. doi: 10.1016/j.ceca.2016.02.011

Upright, N. A., and Baxter, M. G. (2021). Prefrontal cortex and cognitive aging in macaque monkeys. *Am. J. Primatol.* 83:e23250. doi: 10.1002/ajp.23250

Wen, L., Moser, M., and Ley, K. (2022). Molecular mechanisms of leukocyte β2 integrin activation. *Blood* 139, 3480–3492. doi: 10.1182/blood.2021013500

Willmes, C. G., Mack, T. G., Ledderose, J., Schmitz, D., Wozny, C., and Eickholt, B. J. (2017). Investigation of hippocampal synaptic transmission and plasticity in mice deficient in the actin-binding protein Drebrin. *Sci. Rep.* 7:42652. doi: 10.1038/srep42652

Wu, L. G., Hamid, E., Shin, W., and Chiang, H. C. (2014). Exocytosis and endocytosis: modes, functions, and coupling mechanisms. *Annu. Rev. Physiol.* 76, 301–331. doi: 10.1146/annurev-physiol-021113-170305

Wyss-Coray, T. (2016). Ageing, neurodegeneration and brain rejuvenation. *Nature* 539, 180–186. doi: 10.1038/nature20411

Xu, J., Zhou, H., and Xiang, G. (2022). Identification of key biomarkers and pathways for maintaining cognitively Normal brain aging based on integrated bioinformatics analysis. *Front. Aging Neurosci.* 14:833402. doi: 10.3389/fnagi.2022.833402

Yankner, B. A., Lu, T., and Loerch, P. (2008). The aging brain. *Annu. Rev. Pathol.* 3, 41–66. doi: 10.1146/annurev.pathmechdis.2.010506.092044

Yu, G., Wang, L. G., Han, Y., and He, Q. Y. (2012). ClusterProfiler: an R package for comparing biological themes among gene clusters. *OMICS* 16, 284–287. doi: 10.1089/omi.2011.0118

Zhang, K., Mizuma, H., Zhang, X., Takahashi, K., Jin, C., Song, F., et al. (2021). PET imaging of neural activity, β-amyloid, and tau in normal brain aging. *Eur. J. Nucl. Med. Mol. Imaging* 48, 3859–3871. doi: 10.1007/s00259-021-05230-5

Zhang, Y., Parmigiani, G., and Johnson, W. E. (2020). ComBat-seq: batch effect adjustment for RNA-seq count data. *NAR Genom Bioinform.* 2:lqaa078. doi: 10.1093/nargab/lqaa078

Zhou, H., Zhang, R., Lu, K., Yu, W., Xie, B., Cui, D., et al. (2016). Deregulation of miRNA-181c potentially contributes to the pathogenesis of AD by targeting collapsin response mediator protein 2 in mice. *J. Neurol. Sci.* 367, 3–10. doi: 10.1016/j.jns.2016.05.038

Frontiers in
Molecular Neuroscience

Leading research into the brain's molecular structure, design and function

Part of the most cited neuroscience series, this journal explores and identifies key molecules underlying the structure, design and function of the brain across all levels.

Discover the latest Research Topics

See more →

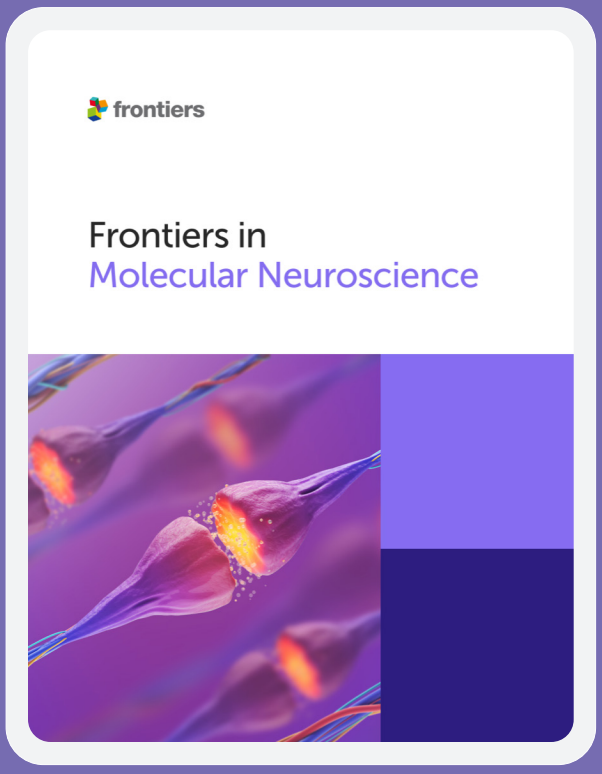

Frontiers

Avenue du Tribunal-Fédéral 34
1005 Lausanne, Switzerland
frontiersin.org

Contact us

+41 (0)21 510 17 00
frontiersin.org/about/contact